EMERGING INFECTIOUS DISEASES®

CDC
Centers for Disease Control and Prevention

Poxviruses

October 2022

Timothy Ivanov (1729–1802), *Inoculation of Catherine II and Her Son Paul against Smallpox, (c. 1700–1800)*. Copper, 2.5 in/64.7 mm, 6.1 oz/173 gm. Louvre Museum, Paris, France, Department of Art Objects of the Middle Ages, Renaissance and Modern Times. Permalink: https://collections.louvre.fr/en/ark:/53355/cl010366995.

EMERGING INFECTIOUS DISEASES®

Emerging Infectious Diseases is published monthly by the Centers for Disease Control and Prevention, 1600 Clifton Rd NE, Mailstop H16-2, Atlanta, GA 30329-4027, USA. Telephone 404-639-1960; email, eideditor@cdc.gov

EMERGING INFECTIOUS DISEASES®

Poxviruses **October 2022**

On the Cover

Timothy Ivanov (1729–1802), *Inoculation of Catherine II and Her Son Paul against Smallpox*, (c. 1700–1800). Copper, 2.5 in/64.7 mm, 6.1 oz/173 gm. Louvre Museum, Paris, France, Department of Art Objects of the Middle Ages, Renaissance and Modern Times. Permalink: https://collections.louvre.fr/en/ark:/53355/cl010366995.

About the Cover p. 2141

Medscape EDUCATION ACTIVITY

Synopses

Medscape EDUCATION ACTIVITY

Research

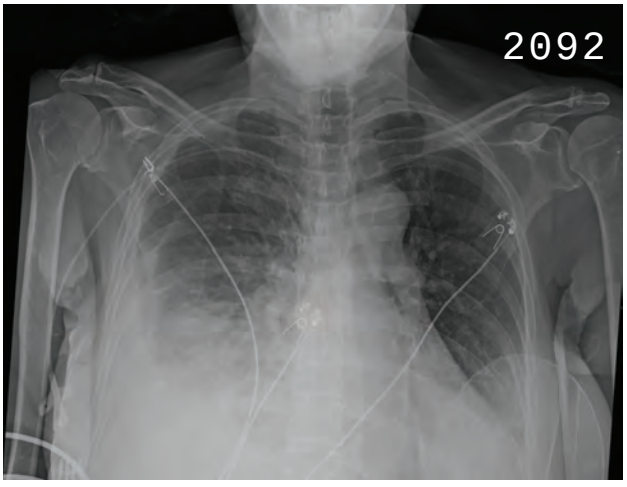

EMERGING INFECTIOUS DISEASES®
October 2022

Dispatches

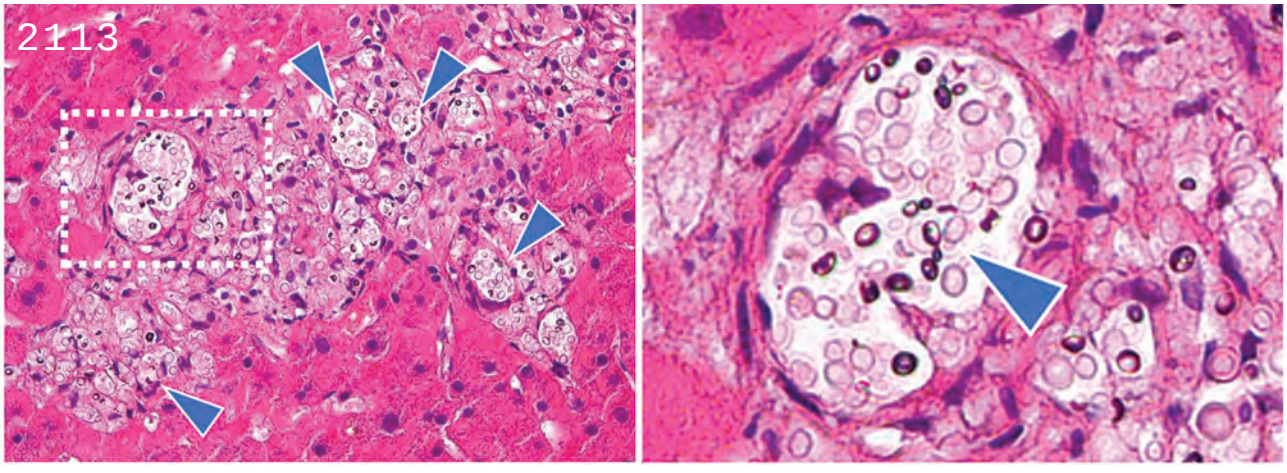

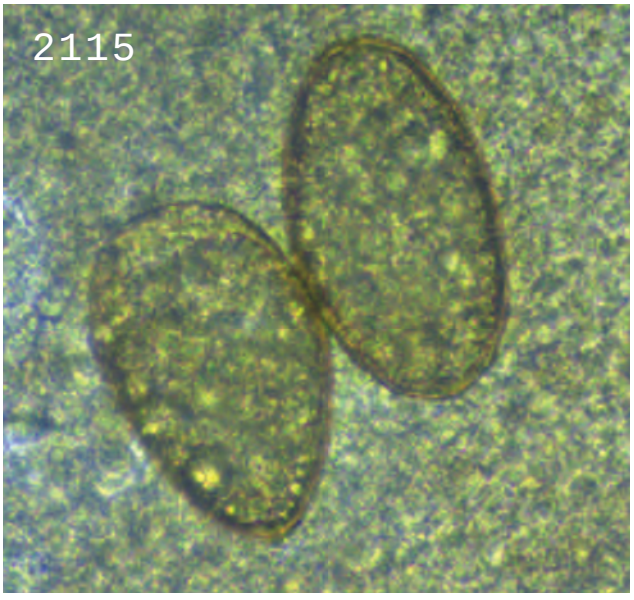

EMERGING INFECTIOUS DISEASES®
October 2022

Research Letters

Books and Media

About the Cover

Corrections

Vol. 27, No. 3
The name of author Tróndur Høgnason Mohr was misspelled in Epidemiology and Clinical Course of First Wave Coronavirus Disease Cases, Faroe Islands **2139**

Vol. 28, No. 8

The Figure legend has been corrected to refer to case counts by category in Incidence of Nontuberculous Mycobacterial Pulmonary Infection, by Ethnic Group, Hawaii, USA, 2005–2019 **2139**

Vol. 26, No. 9
The descriptions in the Acknowledgments have been expanded and updated for Sequestration and Destruction of Rinderpest Virus–Containing Material 10 Years after Eradication **2139**

COMING SOON

A special upcoming *EID* supplement highlights CDC's international response to COVID-19, how health systems and programs adapted during the pandemic, and lessons for future pandemics.

"A World United"
By Vasu Tolia, Detroit, Michigan

Systematic Review and Meta-analysis of Foodborne Tick-Borne Encephalitis, Europe, 1980–2021

Meital Elbaz, Avi Gadoth, Daniel Shepshelovich, David Shasha, Nir Rudoler, Yael Paran

Medscape EDUCATION ACTIVITY

In support of improving patient care, this activity has been planned and implemented by Medscape, LLC and Emerging Infectious Diseases. Medscape, LLC is jointly accredited by the Accreditation Council for Continuing Medical Education (ACCME), the Accreditation Council for Pharmacy Education (ACPE), and the American Nurses Credentialing Center (ANCC), to provide continuing education for the healthcare team.

Medscape, LLC designates this Journal-based CME activity for a maximum of 1.00 ***AMA PRA Category 1 Credit(s)™***. Physicians should claim only the credit commensurate with the extent of their participation in the activity.

Successful completion of this CME activity, which includes participation in the evaluation component, enables the participant to earn up to 1.0 MOC points in the American Board of Internal Medicine's (ABIM) Maintenance of Certification (MOC) program. Participants will earn MOC points equivalent to the amount of CME credits claimed for the activity. It is the CME activity provider's responsibility to submit participant completion information to ACCME for the purpose of granting ABIM MOC credit.

All other clinicians completing this activity will be issued a certificate of participation. To participate in this journal CME activity: (1) review the learning objectives and author disclosures; (2) study the education content; (3) take the post-test with a 75% minimum passing score and complete the evaluation at http://www.medscape.org/journal/eid; and (4) view/print certificate. For CME questions, see page 1147.

Release date: September 15, 2022; Expiration date: September 15, 2023

Learning Objectives

Upon completion of this activity, participants will be able to:

- Evaluate the epidemiological characteristics of foodborne tick-borne encephalitis in Europe in the last 4 decades, based on a systematic review and meta-analysis
- Assess the clinical characteristics and estimated attack rate of foodborne tick-borne encephalitis in Europe in the last 4 decades, based on a systematic review and meta-analysis
- Determine the clinical and public health implications of foodborne tick-borne encephalitis in Europe in the last 4 decades, based on a systematic review and meta-analysis

CME Editor

Amy J. Guinn, BA, MA, Technical Writer/Editor, Emerging Infectious Diseases. *Disclosure: Amy J. Guinn, BA, MA, has no relevant financial relationships.*

CME Author

Laurie Barclay, MD, freelance writer and reviewer, Medscape, LLC. *Disclosure: Laurie Barclay, MD, has the following relevant financial relationships: formerly owned stocks in AbbVie Inc.*

Authors

Meital Elbaz, MD; Avi Gadoth, MD; Daniel Shepshelovich, MD; David Shasha, MD; Nir Rudoler, DVM, MPH, PhD; *and* ***Yael Paran, MD.***

Author affiliations: Tel Aviv Sourasky Medical Center, Tel Aviv, Israel (M. Elbaz, A. Godath, D. Shepshelovich, D. Sasha, Y. Paran); Tel-Aviv University, Tel Aviv (A. Godath, D. Shepshelovich, D. Sasha, Y. Paran); Hebrew University, Jerusalem, Israel (N. Rudoler); Ministry of Health, Tel Aviv (N. Rudoler)

DOI: https://doi.org/10.3201/eid2810.220498

Tick-borne encephalitis (TBE) is a viral infection of the central nervous system that occurs in many parts of Europe and Asia. Humans mainly acquire TBE through tick bites, but TBE occasionally is contracted through consuming unpasteurized milk products from viremic livestock. We describe cases of TBE acquired through alimentary transmission in Europe during the past 4 decades. We conducted a systematic review and meta-analysis of 410 foodborne TBE cases, mostly from a region in central and eastern Europe. Most cases were reported during the warmer months (April–August) and were associated with ingesting unpasteurized dairy products from goats. The median incubation period was short, 3.5 days, and neuroinvasive disease was common (38.9%). The clinical attack rate was 14% (95% CI 12%–16%), and we noted major heterogeneity. Vaccination programs and public awareness campaigns could reduce the number of persons affected by this potentially severe disease.

Tick-borne encephalitis (TBE) is a viral infection of the central nervous system (CNS) caused by tick-borne encephalitis virus (TBEV). TBE occurs mainly in eastern, central, and northern Europe and in northern China, Mongolia, and Russia (*1*). Although vaccination can effectively prevent TBE, >3,000 cases were reported in Europe in 2019, and case-fatality was 0.7% (*2*). However, many mild and subclinical infections probably remain undiagnosed.

Humans acquire TBE mainly via tick bites, but TBEV can occasionally be transmitted through consumption of unpasteurized milk products from viremic livestock. The largest known outbreak of foodborne TBE (FB-TBE) occurred in 1954 in what was then Czechoslovakia, when TBE developed in >600 persons infected via TBEV-contaminated milk from cows and goats (*3*). During that period, the disease was termed biphasic milk fever. During the past 4 decades, repeated smaller outbreaks have been reported in association with TBEV transmission via contaminated milk in various countries in Europe and in Russia (*3*–*10*).

Despite the role of food as a transmission route, FB-TBE has not been systematically described until recently. Two recent published reviews summarized published reports (*11*,*12*), but those studies did not include meta-analysis of published data. We systematically describe cases of alimentary TBEV transmission in Europe during the past 4 decades, estimate the attack rate of FB-TBE, and describe the epidemiologic and clinical characteristics of FB-TBE.

Methods

We conducted a systematic review and meta-analysis according to guidelines of Preferred Reporting Items for Systematic Reviews and Meta-Analyses (PRISMA, http://www.prisma-statement.org) (*13*). We searched articles published during January 1, 1980–June 1, 2021, on PubMed (https://pubmed.ncbi.nlm.nih.gov) and Embase (https://www.embase.com) databases using the following key terms: ("tick-borne encephalitis" OR "TBE") AND ("food" OR "alimentary" OR "milk" OR "cheese" OR "dairy"). We excluded duplicate publications and articles without available abstracts. We screened all publications and selected those that met our eligibility criteria. We did not restrict inclusion by study type or minimum number of patients.

We only included original studies on human data for confirmed and probable cases of FB-TBE that were published in English. We reviewed and extracted data from articles meeting eligibility criteria. We collected data on the number of persons exposed to contaminated products, number of confirmed FB-TBE cases, laboratory testing, source of infection, geographic location, year and season of outbreak, incubation period, vaccination status, and clinical signs and symptoms of invasive central nervous system (CNS) disease, when reported.

Definitions

We defined a confirmed FB-TBE case as a positive laboratory test supporting TBEV infection in a person with or without symptoms of infection (Appendix Table, https://wwwnc.cdc.gov/EID/article/28/10/22-0498-App1.pdf) who also had a possible link to consumption of raw milk or cheese and did not recall having a tick bite. We defined a probable FB-TBE case as a person with symptoms compatible with TBE that was not tested for the virus but who was exposed to raw milk or cheese and did not recall a tick bite; probable cases were included only when a cluster of ≥2 exposed persons and virologic confirmation for TBE were reported.

We defined confirmed invasive CNS disease (meningitis, meningoencephalitis, or myelitis) when CNS neurologic symptoms (e.g., headache, vomiting, ataxia, altered consciousness, confusion, dysphasia, or hemiparesis) were reported and laboratory testing confirmed TBEV infection, including TBEV-positive cerebrospinal fluid (CSF) serology or CSF pleocytosis and other laboratory testing supporting TBEV infection. We defined probable invasive CNS disease as a combination of CNS neurologic symptoms and laboratory-confirmed TBEV infection in a patient who did not undergo lumbar puncture and CSF analysis.

Outcomes

For studies recording the number of persons exposed to TBEV-contaminated dairy products, we

calculated the FB-TBE clinical attack rate by dividing the number of symptomatic patients with confirmed and probable TBE by the number of persons exposed to the same dairy products. We also describe epidemiologic features, including country, season, and source of infection, and clinical characteristic including incubation period, vaccination status, and whether patients had biphasic disease or CNS involvement.

Statistical Methods

We pooled attack rates by using meta-analysis for untransformed proportion in a DerSimonian and Laird fixed-effects model. We assessed the level of heterogeneity (I^2) by visually examining the forest plot for nonoverlapping CIs and using χ^2 test. We considered $p<0.05$ statistically significant and I^2 >50% substantially heterogenic.

Results

Our search retrieved 61 articles, including 25 reporting the same outbreaks. Of the remaining 36 articles, 10 reported nonhuman outbreaks, 4 were in languages other than English or had no abstract available, and 3 overlapped with other studies. Ultimately, we included 19 studies meeting eligibility criteria, describing 410 patients across Europe: 384 (94%) with confirmed FB-TBE and 26 (6%) with probable FB-TBE. Countries reporting FB-TBE cases during 1980–2021 included Slovakia (*5*,*14*,*15*), the Czech Republic (*3*,*16*), Poland (*17*,*18*), Hungary (*10*,*19*), Estonia (*8*,*20*), Germany (*21*,*22*), Croatia (*23*,*24*), Austria (*9*,*25*), Russia (*6*), and Slovenia (*26*) (Table 1; Figure 1).

Of 273 patients with data regarding the season of infection, 243 (89%) were infected during April–August and 30 (11%) during September–November. Patient age distribution was wide, 1–85 years. Of the 120 FB-TBE patients for whom vaccination status was recorded, only 1 was vaccinated (*21*). The 1 exposed and vaccinated person had their last TBEV vaccination booster >15 years before infection; thus, the booster was >10 years overdue.

Among 232 (66%) patients, epidemiologic investigation revealed consumption of raw goat milk or cheese; consumption of raw sheep milk or cheese was reported in 88 (25%) cases, consumption of unpasteurized cow milk in 23 (7%) cases, and consumption of a mixture of unpasteurized dairy products in 7 cases (2%). For 124/138 (90%) patients for whom incubation period was reported, incubation was <2 weeks. Among 14 patients who reported the exact infection timeline, the median incubation period was 3.5 days (IQR 2–14 days).

Biphasic disease was reported in 49/64 (77%) patients for whom the disease course was described. Common symptoms of the first phase included nonspecific influenza-like symptoms, fever, vomiting, loose stools, headache, bilateral orbital pain, vertigo, sore throat, chills, bone pain, myalgia, and malaise.

Proven neuroinvasive disease was documented in 53/136 (39%) patients in the 13 studies that specifically reported on CNS disease (Table 2). Probable CNS invasive disease was reported in 24 additional cases, making the rate of probable and proven

Table 1. Foodborne and nonfoodborne TBE cases, Europe, 1980–2021*

Country, y (reference)	Total FB-TBE cases	No. FB-TBE/TBE cases (%)†
Slovakia (*5*,*14*,*15*)	177	
1993		7/NA
2012		15/32 (46.88)
2013		5/157 (3.18)
2014		11/115 (9.57)
2015		14/80 (17.50)
2016		65/169 (38.46)
2009–2016		60 additional cases not included in mentioned outbreaks‡
Czech Republic (*3*,*16*)	65	
1994		1/617 (0.16)
1997		2/415 (0.48)
1998		1/422 (0.24)
1999		28/489 (5.73)
2002		5/647 (0.77)
2003		6/606 (0.99)
2004		2/507 (0.39)
2005		8/643 (1.24)
2007		8/546 (1.47)
2008		4/631 (0.63)
Poland (*17*,*18*)	52	
1995		48/NA
2017		4/196 (2.04)
Hungary (*10*,*19*)	42	
2007		31/69 (44.93)
2011		11/43 (25.58)
Estonia (*8*,*20*)	28	
2005		27/164 (16.46)
2019		1/82 (1.22)
Germany (*21*,*22*)	16	
2016		2/348 (0.57)
2017		14/485 (2.89)
Croatia (*23*,*24*)	14	
2015		9/26 (34.62)
2019		5/13 (38.46)
Austria (*9*,*25*)	8	
1989		2/NA
2008		6/86 (6.98)
Russia (*6*)	5	
1991		5/NA
Slovenia (*26*)	3	
2012		3/164 (1.83)

*FB-TBE, foodborne tick-borne encephalitis; NA not available; TBE, tick-borne encephalitis.
†Number of TBE cases are from European Centre for Disease Prevention and Control annual report (*2*) and other reports (*27*,*28*).
‡From (*14*).

Figure 1. Geographic distribution of reported foodborne tick-borne encephalitis (FB-TBE) cases (blue shading), Europe, 1980–2021. A) The FB-TBE triangle in Europe. Russia had 5 cases in 1991 (not shown). Map created by using MapChart (https://mapchart.net). B) The tick-borne encephalitis belt, spanning from western Europe, across Russia, China, and Mongolia to Japan. Map from the Centers for Disease Control and Prevention (https://www.cdc.gov/tick-borne-encephalitis/geographic-distribution/index.html).

neuroinvasive disease 56% (77/136 patients). Among 23 patients for whom CNS syndrome was described, 13 (57%) patients had diagnosed meningoencephalitis, 9 (39%) had meningitis, and 1 (4%) had meningoencephalomyelitis. Diagnosis of proven CNS disease was made by positive CSF serology in 45 (87%) patients, and CSF pleocytosis and positive serum serology in 7 (13%) patients (Table 2).

We calculated attack rates for 10 outbreaks in which the number of exposed persons was reported (Table 3), representing a total of 907 exposed persons. We found a wide range of attack rates, from 6% in Germany in 2016 to 100% in Slovakia in 1993. The pooled attack rate was 15% (95% CI 13%–17%). Heterogeneity was significant (I^2 = 97.4%, 95% CI 96.5%–98.1%; p<0.01) but yielded inconsistent results, making I^2 an unreliable attack rate estimator (Table 3; Figure 2).

We applied an additional meta-analysis that included outbreaks with ≥10 reported cases, representing 7 outbreaks and a total of 889 exposed persons (Table 3). We still found a wide range in attack rates, from 6% in Germany in 2016 (*22*) to 90% in Croatia in 2015 (*23*). The pooled attack rate was 14% (95% CI 12%−16%) (Figure 2). Heterogeneity was significant (I^2 = 97.5%, 95% CI 96.3%–98.3%; p<0.01) but again yielded inconsistent results and demonstrated I^2 is an unreliable attack rate estimator.

Table 2. Neuroinvasive disease reported in cases of foodborne tick-borne encephalitis, Europe, 1980–2021*

Country (reference)	No. confirmed cases	No. CNS invasive disease	CNS invasive disease type	Blood serology	CSF serology
Austria (*9*)	6	4	4 ME cases	Positive IgG and IgM	Borderline IgM, positive IgG; borderline IgM, borderline IgG; positive IgM, positive IgG; positive IgM, borderline IgG
Croatia (*23*)	7	6 proven, 7 symptomatic	5 meningitis cases, 1 ME case; 1 case with fever and headache but LP not performed	Positive IgG and IgM	6 patients had CSF pleocytosis but negative IgG and IgM
Czech Republic (*16*)	1	1	ME, myelitis	Positive IgM	CSF pleocytosis
Estonia (*20*)	1	1	ME	Positive IgM and IgG	Positive serology
Germany (*22*)	2	2	ME in both cases	Positive IgG and IgM	Positive IgG and IgM
Hungary (*10*)	25	2 confirmed; 25 with neurologic symptoms but LP only performed on 3		Positive IgG and IgM	Positive IgG in 2 of 3 CSF samples
Hungary (*19*)	7	4	4 confirmed ME cases	In all 7 confirmed cases, positive IgM in blood or CSF	
Poland (*18*)	35	15		Positive IgM and IgG	Positive serology for 15 patients with neuroinfection
Poland (*29*)	4	4	4 meningitis cases	2 had elevated IgG and IgM. 1 had only elevated IgM. The fourth wasn't examined	All 4 had elevated IgG and IgM
Slovakia (*15*)	2 43	1 12		Positive IgM Positive IgM and IgG	Positive IgM 12 patients with IgM and IgG in CSF
Slovenia (*26*)	3	1	2 cases with symptoms of ME but LP only performed on 1	Positive IgG and IgM	CSF pleocytosis

*CNS, central nervous system; CSF, cerebrospinal fluid; LP, lumbar puncture; ME, meningoencephalitis.

For 26 outbreaks, we calculated the rate of FB-TBE out of all reported TBE cases in the country each year (Table 1; Figure 3). We calculated the median rate of FB-TBE only for outbreaks occurring after 2012, when TBE became a notifiable disease in the European Union (*30*). The median rate of FB-TBE per TBE cases was 6% (IQR 2%–36%).

Discussion

We report 410 cases of FB-TBE, most from a region in central and eastern Europe stretching from Croatia in the south to Poland and Germany in the north and an anecdotal report of 5 cases in Russia (*6*). This region represents an FB-TBE triangle (Figure 1, panel A). Most cases were reported during the warmer months of April–August and were associated with ingestion of unpasteurized dairy products from goats. None of the infected patients were vaccinated, except 1 patient who had their last TBE vaccination booster >15 years before infection. FB-TBE incubation period was short (median 3.5 days), and invasive CNS disease was common. The clinical attack rate was 14% (95% CI 12%−16%) for outbreaks with ≥10 reported cases and heterogeneity was significant (I^2 = 97.5%).

Table 3. Attack rates for foodborne tick-borne encephalitis, Europe, 1980–2021

Country (reference)	Year	No. persons exposed	Clinical attack rate, %	Source of dairy products
Slovakia (*5*)	1993	7	100	Goat
Poland (*18*)	1995	63	76.2	Goat
Hungary (*10*)	2007	154	20.1	Goat
Austria (*9*)	2008	7	57.1	Goat and cow
Hungary (*19*)	2011	103	10.7	Cow
Slovenia (*26*)	2012	4	75	Goat
Croatia (*23*)	2015	10	90	Goat
Germany (*22*)	2016	32	6.3	Goat
Slovakia (*15*)	2016	500	8.8	Sheep
Germany (*21*)	2017	27	51.9	Goat

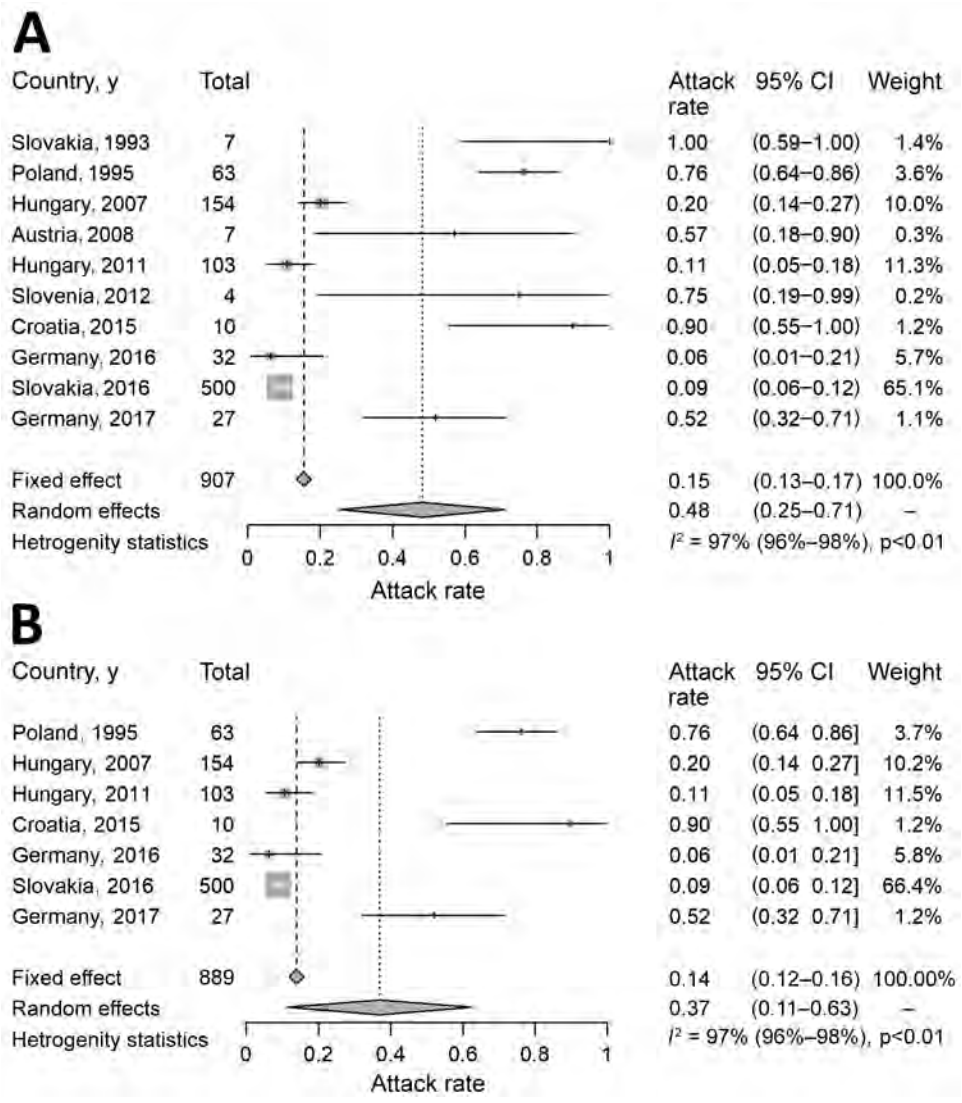

Figure 2. Analysis of clinical attack rate of foodborne tick-borne encephalitis, Europe, 1980–2021. A) Attack rate calculated for 10 outbreaks in which the number of exposed persons was reported. B) Attack rate calculated only for 7 outbreaks with ≥10 reported persons affected. I^2, level of heterogeneity.

Although TBE is a mandatory reportable disease in Europe (*30*,*31*) and cases of TBE are distributed along the southern part of the nontropical Eurasian Forest belt (Figure 1, panel B), we noted that nearly all FB-TBE cases occurred in a region we termed the FB-TBE triangle (Figure 1, panel A). This phenomenon might be explained by different habits of consumption of unpasteurized dairy products in different regions, but data on the frequency of unpasteurized dairy consumption in various parts of Europe is lacking. Of note, geographic distribution of brucellosis, a zoonosis caused by ingestion of unpasteurized milk, is not concordant with distribution of FB-TBE. One explanation for this discrepancy is that brucellosis is transmitted not only by raw dairy consumption but also by consuming undercooked meat and by contact with body fluids from farm animals. Moreover, brucellosis is a preventable disease by national eradication programs and vaccination of cattle in areas with high prevalence. For example, the Czech Republic has high FB-TBE rates but had no reported brucellosis cases during 2013–2017 (0.00 cases/100,000 population), according to a European Centre for Disease Prevention and Control annual report (*32*), likely resulting from a brucellosis eradication program among livestock, which was successfully completed in 1964.

TBEV has 3 subtypes: European (TBEV-Eu), Siberian (TBEV-Sib), and Far Eastern (TBEV-FE). The vector of TBEV-Eu is *Ixodes ricinus* ticks; *I. persulcatus* ticks are the vectors for the other 2 subtypes (*33*). *I. ricinus* ticks are seen in most of Europe, and their distribution extends to Turkey, northern Iran, and the Caucasus in the southeast (*34*). *I. persulcatus* ticks are found in the belt extending from eastern Europe to China and Japan. Both tick species circulate in a restricted area in northeastern Europe; northern areas

of the Republic of Karelia in Russia; St. Petersburg, Russia; eastern Estonia; and eastern Latvia (*35*,*36*). Consequently, all 3 TBEV subtypes have been recorded in these regions. In all the countries of the FB-TBE triangle, the TBEV-Eu subtype dominates, except in Estonia. Possible explanations could be underreporting of FB-TBE in the countries where the TBEV-Sib and TBEV-FE subtypes dominate due to unawareness of foodborne transmission or different habits of raw dairy consumption. Another explanation could be different capabilities for the vector or the virus to infect livestock or to survive in dairy products.

Recently, an outbreak of encephalitis and meningoencephalitis occurred in the Ain department of eastern France, where TBEV had not previously been detected (*37*). Epidemiologic investigation revealed that all but 1 of 43 TBE patients with encephalitis, meningoencephalitis, or influenza-like symptoms had consumed unpasteurized goat cheese from a single local producer. The researchers confirmed the alimentary origin of the TBE outbreak, and phylogenetic analyses found that the strain involved, TBEV_Ain_2020, belongs to the TBEV-Eu subtype (TBEV-Eu3) and is most closely related to TBEV strains recently isolated in bordering countries and eastern Europe. This finding emphasizes the role of foodborne transmission in TBE, even in areas where TBEV has never been detected. In addition, this finding is compatible with our observation of an association between the TBEV-Eu subtype and foodborne transmission.

We found that FB-TBE attack rates ranged widely. Possible explanations for the wide range could be underdiagnosis, underreporting, variations due to the low number of patients involved in some of the reports, and incomplete epidemiologic investigations. An alternative explanation might be the variability in the viral load in the infected dairy products because the exact TBEV dose required for human infection via the oral route is unknown and might be different from the viral load required for clinical infection through tick bites. Outbreaks with low attack rates might not have had high portions of milk or cheese that contained enough TBEV to cause human infection. In an analysis of cheese from the manufacturing and storage facilities of a dairy farm responsible for an outbreak, quantitative reverse transcription PCR and isolation results implied that the distribution of TBEV loads in infected goat cheese was heterogenous (*22*), which likely contributes to the variability in attack rate we observed.

Although alimentary transmission of TBE is uncommon, this transmission mode has the potential to cause outbreaks affecting many persons, making FB-TBE a major public health concern. Foodborne transmission could easily be eliminated through education campaigns that encourage persons to consume only pasteurized dairy products and through vaccination. Vaccination seems to be effective in preventing FB-TBE, not only disease caused by tick bites. In our cohort, among 120 FB-TBE patients for whom vaccination status was recorded, only 1 was vaccinated but did not receive an appropriate booster. Other observations regarding the effectiveness of the vaccine against alimentary transmission were made during a 2017 FB-TBE outbreak that included 27 exposed persons (*21*). Among 20 persons for whom medical information was available, 13 were infected and reported symptomatic disease. Among 6 exposed persons who were vaccinated, only 1 person developed disease, but that person was vaccinated >15 years prior to exposure. In contrast, among 14 unvaccinated exposed persons, 12 had TBE develop (*21*). Findings

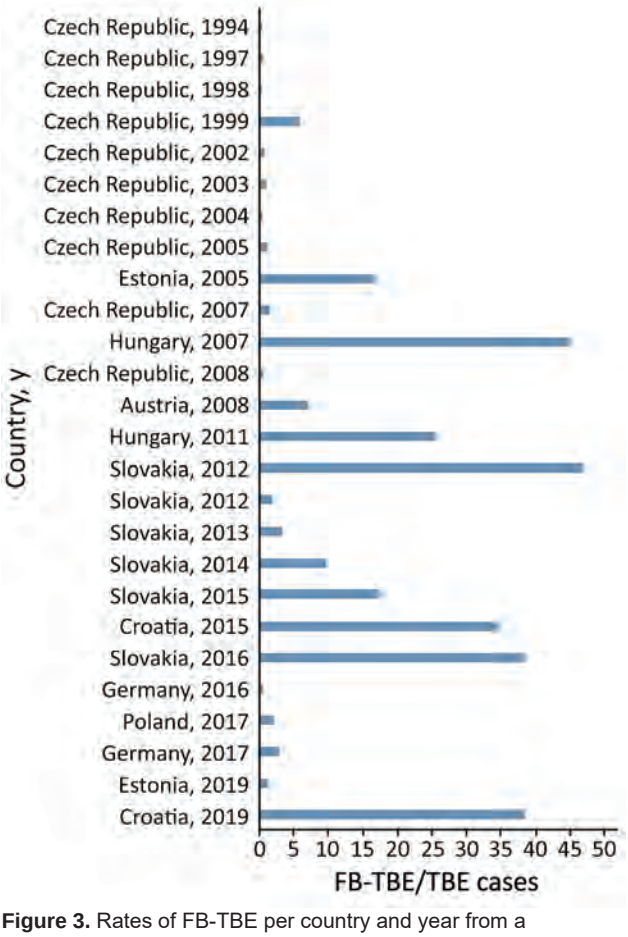

Figure 3. Rates of FB-TBE per country and year from a systematic review and meta-analysis, Europe, 1980–2021. Rates indicate FB-TBE per all TBE cases reported in the country, per year. Data are based on those reported in Table 1. FB-TBE, foodborne tick-borne encephalitis; TBE, tick-borne encephalitis.

from that outbreak suggest that vaccination also protects against alimentary TBEV transmission.

Most reported FB-TBE cases were documented in months that parallel tick season in Europe, even though transmission was through ingestion of contaminated dairy products. This finding probably implies that the infected livestock are most viremic during the peak of tick season.

We found the median incubation time for FB-TBE was shorter (median 3.5 days) than that for non–FB-TBE, which was reported to be 8 days (range 4–28) in 1 study (*1*). Another study reported a much longer incubation period, median 22 days, in 687 patients in Poland (*29*). We suggest that symptoms compatible with TBE in the context of recent exposure to raw dairy products should raise suspicion of FB-TBE, especially when symptoms develop in >1 patient exposed to the same source. This finding can assist clinicians and help guide epidemiologic investigation.

Although the transmission mode is different and the incubation period is shorter, FB-TBE has clinical manifestations similar to those for disease transmitted by ticks, and most symptomatic patients experience biphasic disease, as described (*1*,*38*). Among patients with CNS involvement, most had meningitis or meningoencephalitis, and myelitis was a rare manifestation, comparable with previous reports of TBE (*38*).

Typically, TBE is biphasic and 70% of patients experience neuroinvasive disease (*1*,*39*). We found lower rates of invasive disease in FB-TBE; only 39% of patients had neuroinvasive disease. Actual rates of neuroinvasive disease in TBE are challenging to assess because patients with mild symptoms and no CNS-specific symptoms are less likely to seek medical care; even for patients who do seek care, many will have diagnoses of nonspecific viral syndrome. FB-TBE outbreaks can help determine the actual rate of neuroinvasive disease because epidemiologic investigation of patients exposed to a common source can actively locate patients with only mild and nonspecific symptoms.

The first limitation of this study is that, although TBE is a reportable disease in many countries in Europe, many cases are not reported or are misdiagnosed by clinicians because most infected persons who experience clinical disease have only mild nonspecific symptoms, which could lead to underestimation of the true number of TBE cases. Moreover, ≈30%–50% of patients with diagnosed TBE do not recall a tick bite, but probably few are asked about consumption of unpasteurized dairy products, which could lead to underestimation of FB-TBE. Even in cases where epidemiologic investigations were conducted, many exposed persons might remain unidentified and untested for the reasons we mentioned, making the true attack rate higher than calculated here. Assessment of the attack rate was also limited by high variability between studies. Finally, we included only published articles and not reports from ProMED (https://promedmail.org) or other sources, and we almost certainly missed some FB-TBE cases.

In conclusion, FB-TBE in Europe is reported mostly in a well-defined geographic region during tick season, with a few reports from Russia and recently in France. We found a variable FB-TBE attack rate, which might be the result of many factors, including variability in the viral load in the infected dairy products, compatible with a previous report (*22*). Clinical features of FB-TBE are similar to those reported for TBE acquired through tick bites, and CNS-specific symptoms develop in nearly 40% of infected persons. Vaccination seems to be effective in preventing FB-TBE. Our findings could help raise awareness of FB-TBE among epidemiologists, clinicians, public health officials, and the public in endemic areas. Vaccination programs and public awareness campaigns could greatly reduce the number of patients affected by this potentially severe CNS infection.

About the Author

Dr. Elbaz is infectious disease fellow at Tel Aviv Sourasky Medical Center, Tel Aviv, Israel. Her primary research interests include fungal infection, antimicrobial resistance, and antibiotic stewardship.

References

1. Lindquist L, Vapalahti O. Tick-borne encephalitis. Lancet. 2008;371:1861–71. https://doi.org/10.1016/S0140-6736(08)60800-4
2. European Centre for Disease Prevention and Control. Tick borne encephalitis. In: Annual epidemiological report for 2019. Stockholm: The Centre; 2021.
3. Kríz B, Benes C, Daniel M. Alimentary transmission of tick-borne encephalitis in the Czech Republic (1997–2008). Epidemiol Mikrobiol Imunol. 2009;58:98–103.
4. Grešíková M, Sekeyová M, Stúpalová S, Necas S. Sheep milk–borne epidemic of tick-borne encephalitis in Slovakia. Intervirology. 1975;5:57–61. https://doi.org/10.1159/000149880
5. Kohl I, Kožuch O, Elecková E, Labuda M, Žaludko J. Family outbreak of alimentary tick-borne encephalitis in Slovakia associated with a natural focus of infection. Eur J Epidemiol. 1996;12:373–5. https://doi.org/10.1007/BF00145300
6. Vereta LA, Skorobrekha VZ, Nikolaeva SP, Aleksandrov VI, Tolstonogova VI, Zakharycheva TA, et al. The transmission of the tick-borne encephalitis virus via cow's milk [in Russian]. Med Parazitol (Mosk). 1991;3:54–6.
7. Juceviciene A, Vapalahti O, Laiskonis A, Čeplikien J, Leinikki P. Prevalence of tick-borne-encephalitis virus

antibodies in Lithuania. J Clin Virol. 2002;25:23–7. https://doi.org/10.1016/S1386-6532(01)00215-3
8. Kerbo N, Donchenko I, Kutsar K, Vasilenko V. Tick-borne encephalitis outbreak in Estonia linked to raw goat milk, May–June 2005. Euro Surveill. 2005;10:E050623.2. https://doi.org/10.2807/esw.10.25.02730-en
9. Holzmann H, Aberle SW, Stiasny K, Werner P, Mischak A, Zainer B, et al. Tick-borne encephalitis from eating goat cheese in a mountain region of Austria. Emerg Infect Dis. 2009;15:1671–3. https://doi.org/10.3201/eid1510.090743
10. Balogh Z, Ferenczi E, Szeles K, Stefanoff P, Gut W, Szomor KN, et al. Tick-borne encephalitis outbreak in Hungary due to consumption of raw goat milk. J Virol Methods. 2010;163:481–5. https://doi.org/10.1016/j.jviromet.2009.10.003
11. Ličková M, Fumačová Havlíková S, Sláviková M, Klempa B. Alimentary infections by tick-borne encephalitis virus. Viruses. 2021;14:56. https://doi.org/10.3390/v14010056
12. Buczek AM, Buczek W, Buczek A, Wysokińska-Miszczuk J. Food-borne transmission of tick-borne encephalitis virus—spread, consequences, and prophylaxis. Int J Environ Res Public Health. 2022;19:1812. https://doi.org/10.3390/ijerph19031812
13. Shamseer L, Moher D, Clarke M, Ghersi D, Liberati A, Petticrew M, et al.; PRISMA-P Group. Preferred reporting items for systematic review and meta-analysis protocols (PRISMA-P) 2015: elaboration and explanation. BMJ. 2015;350:g7647. https://doi.org/10.1136/bmj.g7647
14. Kerlik J, Avdičová M, Štefkovičová M, Tarkovská V, Pántiková Valachová M, Molčányi T, et al. Slovakia reports highest occurrence of alimentary tick-borne encephalitis in Europe: analysis of tick-borne encephalitis outbreaks in Slovakia during 2007–2016. Travel Med Infect Dis. 2018;26:37–42. https://doi.org/10.1016/j.tmaid.2018.07.001
15. Dorko E, Hockicko J, Rimárová K, Bušová A, Popaďák P, Popaďáková J, et al. Milk outbreaks of tick-borne encephalitis in Slovakia, 2012–2016. Cent Eur J Public Health. 2018;26:S47–50. https://doi.org/10.21101/cejph.a5272
16. Aendekerk RP, Schrivers AN, Koehler PJ. Tick-borne encephalitis complicated by a polio-like syndrome following a holiday in central Europe. Clin Neurol Neurosurg. 1996;98:262–4. https://doi.org/10.1016/0303-8467(96)00030-3
17. Król ME, Borawski B, Nowicka-Ciełuszecka A, Tarasiuk J, Zajkowska J. Outbreak of alimentary tick-borne encephalitis in Podlaskie voivodeship, Poland. Przegl Epidemiol. 2019;73:239–48. https://doi.org/10.32394/pe.73.01
18. Matuszczyk I, Tarnowska H, Zabicka J, Gut W. The outbreak of an epidemic of tick-borne encephalitis in Kielec province induced by milk ingestion [in Polish]. Przegl Epidemiol. 1997;51:381–8.
19. Caini S, Szomor K, Ferenczi E, Szekelyne Gaspar A, Csohan A, Krisztalovics K, et al. Tick-borne encephalitis transmitted by unpasteurised cow milk in western Hungary, September to October 2011. Euro Surveill. 2012;17:20128. https://doi.org/10.2807/ese.17.12.20128-en
20. Camprubí D, Moreno-García E, Almuedo-Riera A, Martinez MJ, Navarro A, Martinez-Hernandez E, et al. First imported case of tick-borne encephalitis in Spain—was it alimentary? Travel Med Infect Dis. 2020;37:101701. https://doi.org/10.1016/j.tmaid.2020.101701
21. Chitimia-Dobler L, Lindau A, Oehme R, Bestehorn-Willmann M, Antwerpen M, Drehmann M, et al. Tick-borne encephalitis vaccination protects from alimentary TBE infection: results from an alimentary outbreak. Microorganisms. 2021;9:889. https://doi.org/10.3390/microorganisms9050889
22. Brockmann SO, Oehme R, Buckenmaier T, Beer M, Jeffery-Smith A, Spannenkrebs M, et al. A cluster of two human cases of tick-borne encephalitis (TBE) transmitted by unpasteurised goat milk and cheese in Germany, May 2016. Euro Surveill. 2018;23:17-00336. https://doi.org/10.2807/1560-7917.ES.2018.23.15.17-00336
23. Markovinović L, Kosanović Ličina ML, Tešić V, Vojvodić D, Vladušić Lucić I, Kniewald T, et al. An outbreak of tick-borne encephalitis associated with raw goat milk and cheese consumption, Croatia, 2015. Infection. 2016;44:661–5. https://doi.org/10.1007/s15010-016-0917-8
24. Ilic M, Barbic L, Bogdanic M, Tabain I, Savic V, Kosanovic Licina ML, et al. Tick-borne encephalitis outbreak following raw goat milk consumption in a new micro-location, Croatia, June 2019. Ticks Tick Borne Dis. 2020;11:101513. https://doi.org/10.1016/j.ttbdis.2020.101513
25. Sixl W, Stünzner D, Withalm H, Köck M. Rare transmission mode of FSME (tick-borne encephalitis) by goat's milk. Geogr Med Suppl. 1989;2:11–4.
26. Hudopisk N, Korva M, Janet E, Simetinger M, Grgič-Vitek M, Gubenšek J, et al. Tick-borne encephalitis associated with consumption of raw goat milk, Slovenia, 2012. Emerg Infect Dis. 2013;19:806–8. https://doi.org/10.3201/eid1905.121442
27. Daniel M, Kríz B, Danielová V, Valter J, Kott I. Correlation between meteorological factors and tick-borne encephalitis incidence in the Czech Republic. Parasitol Res. 2008;103:S97–107. https://doi.org/10.1007/s00436-008-1061-x
28. Amicizia D, Domnich A, Panatto D, Lai PL, Cristina ML, Avio U, et al. Epidemiology of tick-borne encephalitis (TBE) in Europe and its prevention by available vaccines. Hum Vaccin Immunother. 2013;9:1163–71. https://doi.org/10.4161/hv.23802
29. Czupryna P, Moniuszko A, Pancewicz SA, Grygorczuk S, Kondrusik M, Zajkowska J. Tick-borne encephalitis in Poland in years 1993–2008—epidemiology and clinical presentation. A retrospective study of 687 patients. Eur J Neurol. 2011;18:673–9. https://doi.org/10.1111/j.1468-1331.2010.03278.x
30. Beauté J, Spiteri G, Warns-Petit E, Zeller H. Tick-borne encephalitis in Europe, 2012 to 2016. Euro Surveill. 2018;23:1800201. https://doi.org/10.2807/1560-7917.ES.2018.23.45.1800201
31. Korenberg EI, Gorban LY, Kovalevskii YV, Frizen VI, Karavanov AS. Risk for human tick-borne encephalitis, borrelioses, and double infection in the pre-Ural region of Russia. Emerg Infect Dis. 2001;7:459–62. https://doi.org/10.3201/eid0703.017319
32. European Centre for Disease Prevention and Control. Brucellosis—annual epidemiological report for 2017 [cited 2019 Jun 19]. https://www.ecdc.europa.eu/en/publications-data/brucellosis-annual-epidemiological-report-2017
33. Süss J. Epidemiology and ecology of TBE relevant to the production of effective vaccines. Vaccine. 2003;21(Suppl 1):S19–35. https://doi.org/10.1016/S0264-410X(02)00812-5
34. Jaenson TG, Tälleklint L, Lundqvist L, Olsen B, Chirico J, Mejlon H. Geographical distribution, host associations, and vector roles of ticks (Acari: Ixodidae, Argasidae) in Sweden. J Med Entomol. 1994;31:240–56. https://doi.org/10.1093/jmedent/31.2.240
35. Golovljova I, Vene S, Sjölander KB, Vasilenko V, Plyusnin A, Lundkvist A. Characterization of tick-borne encephalitis virus from Estonia. J Med Virol. 2004;74:580–8. https://doi.org/10.1002/jmv.20224

36. Haglund M, Vene S, Forsgren M, Günther G, Johansson B, Niedrig M, et al. Characterisation of human tick-borne encephalitis virus from Sweden. J Med Virol. 2003;71:610–21. https://doi.org/10.1002/jmv.10497
37. Gonzalez G, Bournez L, Moraes RA, Marine D, Galon C, Vorimore F, et al. A One-Health approach to investigating an outbreak of alimentary tick-borne encephalitis in a non-endemic area in France (Ain, Eastern France): a longitudinal serological study in livestock, detection in ticks, and the first tick-borne encephalitis virus isolation and molecular characterisation. Front Microbiol. 2022;13:863725. https://doi.org/10.3389/fmicb.2022.863725
38. Bogovic P, Strle F. Tick-borne encephalitis: a review of epidemiology, clinical characteristics, and management. World J Clin Cases. 2015;3:430–41. https://doi.org/10.12998/wjcc.v3.i5.430
39. Kaiser R. The clinical and epidemiological profile of tick-borne encephalitis in southern Germany 1994–98: a prospective study of 656 patients. Brain. 1999;122:2067–78. https://doi.org/10.1093/brain/122.11.2067

Address for correspondence: Meital Elbaz, Infectious Disease Unit, Tel Aviv Sourasky Medical Center, 6 Weizman St, Tel Aviv, Israel; email: meitale@tlvmc.gov.il

Demographic and Socioeconomic Factors Associated with Fungal Infection Risk, United States, 2019

Emily Rayens, Mary Kay Rayens, Karen A. Norris

Medscape EDUCATION ACTIVITY

In support of improving patient care, this activity has been planned and implemented by Medscape, LLC and Emerging Infectious Diseases. Medscape, LLC is jointly accredited by the Accreditation Council for Continuing Medical Education (ACCME), the Accreditation Council for Pharmacy Education (ACPE), and the American Nurses Credentialing Center (ANCC), to provide continuing education for the healthcare team.

Medscape, LLC designates this Journal-based CME activity for a maximum of 1.00 ***AMA PRA Category 1 Credit(s)™***. Physicians should claim only the credit commensurate with the extent of their participation in the activity.

Successful completion of this CME activity, which includes participation in the evaluation component, enables the participant to earn up to 1.0 MOC points in the American Board of Internal Medicine's (ABIM) Maintenance of Certification (MOC) program. Participants will earn MOC points equivalent to the amount of CME credits claimed for the activity. It is the CME activity provider's responsibility to submit participant completion information to ACCME for the purpose of granting ABIM MOC credit.

All other clinicians completing this activity will be issued a certificate of participation. To participate in this journal CME activity: (1) review the learning objectives and author disclosures; (2) study the education content; (3) take the post-test with a 75% minimum passing score and complete the evaluation at http://www.medscape.org/journal/eid; and (4) view/print certificate. For CME questions, see page 1148.

Release date: September 21, 2022; Expiration date: September 21, 2023

Learning Objectives

Upon completion of this activity, participants will be able to:

- Analyze the rate of hospitalizations with fungal infection, based on sex
- Distinguish sociodemographic risk factors for aspergillosis
- Evaluate patterns of fungal infections among hospitalized patients, based on race/ethnicity
- Assess age as a risk factor for fungal infections among inpatients

CME Editor

Amy J. Guinn, BA, MA, Technical Writer/Editor, Emerging Infectious Diseases. *Disclosure: Amy J. Guinn, BA, MA, has no relevant financial relationships.*

CME Author

Charles P. Vega, MD, Health Sciences Clinical Professor of Family Medicine, University of California, Irvine School of Medicine, Irvine, California. *Disclosure: Charles P. Vega, MD, has the following relevant financial relationships: served as a consultant or advisor for GlaxoSmithKline; Johnson & Johnson Pharmaceutical Research & Development, L.L.C.*

Authors

Emily Rayens, PhD, MPH; Mary Kay Rayens, PhD, MS; *and* ***Karen A. Norris, PhD.***

Author affiliations: University of Georgia, Athens, Georgia, USA (E. Rayens, K.A. Norris); University of Kentucky, Lexington, Kentucky, USA (M.K. Rayens)

DOI: https://doi.org/10.3201/eid2810.220391

Fungal infections cause substantial rates of illness and death. Interest in the association between demographic factors and fungal infections is increasing. We analyzed 2019 US hospital discharge data to assess factors associated with fungal infection diagnosis, including race and ethnicity and socioeconomic status. We found male patients were 1.5–3.5 times more likely to have invasive fungal infections diagnosed than were female patients. Compared with hospitalizations of non-Hispanic White patients, Black, Hispanic, and Native American patients had 1.4–5.9 times the rates of cryptococcosis, pneumocystosis, and coccidioidomycosis. Hospitalizations associated with lower-income areas had increased rates of all fungal infections, except aspergillosis. Compared with younger patients, fungal infection diagnosis rates, particularly for candidiasis, were elevated among persons ≥65 years of age. Our findings suggest that differences in fungal infection diagnostic rates are associated with demographic and socioeconomic factors and highlight an ongoing need for increased physician evaluation of risk for fungal infections.

Fungal pathogens cause millions of deaths and tens of millions of infections globally every year (*1*). Fungal infections are primarily opportunistic, causing moderate to severe disease in immunocompromised patients. Fungal infections also are associated with increased illness rates and substantial healthcare costs, resulting in $6.7 billion in hospitalization costs in the United States in 2018 (*2*). In addition, fungal infections doubled the average length and cost of hospital stays and risk for death among patients with ≥1 associated risk condition (*2*). Despite the considerable medical and economic burden of fungal infections, standardized diagnostic and treatment guidelines are lacking.

The risk for serious fungal infection continues to move away from HIV-associated infections (*3*), and increasingly affect patients with certain underlying conditions, including chronic obstructive pulmonary disease (COPD) (*4*), cirrhosis (*5*), cystic fibrosis (*6*), diabetes (*7*,*8*), influenza (*9*,*10*), and tuberculosis (*11*). Increased infection rates also have been reported among persons being treated for asthma (*12*,*13*), autoimmune disorders (*14*,*15*), and cancer (*16*), and among transplant recipients (*17*).

Interest in the effects of race and ethnicity and socioeconomic status on fungal infections and associated patient outcomes has increased (*18*,*19*), especially because diagnosed fungal infections have increased since 2010 (*3*). Previous studies documented the relationship between health disparities and fungal infections (*18*,*19*), but not as a main analytic focus, and studies across multiple fungal pathogens are lacking. We describe diagnosed fungal infections and associated risk conditions by key demographic variables, including race and ethnicity and socioeconomic status.

Methods

Data Sources

We used hospital discharge data from the National Inpatient Sample (NIS), Healthcare Cost and Utilization Project (HCUP), from the Agency for Healthcare Research and Quality (*20*). NIS is the largest database of US hospitalization data, covering >96% of the population (*20*). HCUP data comprise hospitalizations, rather than unique patients. We use the term patient to refer to inpatient status; we acknowledge that a specific patient might be included ≥1 time in our analyses. For total population per income quartile, we used 2006–2010 American Community Survey (*21*) results to estimate population percentages, then adjusted these to the 2019 population.

Element Descriptions

We used codes from the International Classification of Diseases, 10th Revision (ICD-10), to identify at-risk patients and invasive and noninvasive fungal infections, as previously described (*2*) (Table). We defined fungal infections and associated risk conditions when relevant ICD-10 codes were recorded as any diagnosis in the hospitalization record. Sex, race, and ethnicity data were provided by patient records in NIS. HCUP excludes the data for sex when the state level patient record identifies the patient as both nonfemale and nonmale. Ethnicity took precedence over race in the HCUP database when both were provided as distinct values in the patient record.

The HCUP dataset predefines each annual income quartile (Q) according to estimated median household income in US dollars of residents living within a patient's postal code. For 2019, Q1 was $1–$47,999, Q2 was $48,000–$60,999, Q3 was $61,000–$81,999, and Q4 was ≥$82,000. We defined insurance type by the expected primary payer type to which the hospital visit was billed in the HCUP NIS dataset.

We defined age groups as pediatric (0–17 years of age), adult (18–64 years of age), and senior (≥65 years of age). We defined urban-rural status, as previously described (*22*), and considered counties with >50,000 inhabitants as urban. We calculated rate ratios (RRs) and 95% CIs by using SAS version 9.4 (SAS Institute Inc., https://www.sas.com). We used Prism software (GraphPad Software Inc., https://www.graphpad.com) to create figures.

Table. Number of risk conditions and fungal infections diagnosed among hospitalized patients, United States, 2019*

Fungal infections and risk conditions	ICD-10 code	No. cases diagnosed
Fungal infections		
Aspergillosis	B44	17,825
Invasive	B44.0, B44.1, B44.7	8,875
Noninvasive	B44.2, B44.8	4,210
Candidiasis	B37	457,080
Invasive	B37.1, B37.5, B37.6, B37.7	19,920
Noninvasive	B37.0, B37.2, B37.3, B37.4, B37.8	396,765
Coccidioidomycosis	B38	8,990
Cryptococcosis	B45	4,900
Histoplasmosis	B39	4,880
Mucormycosis	B46	1,370
Pneumocystosis	B59	9,725
Other	B35, B36, B40–B43, B47, B48	145,925
Unspecified mycoses	B49	15,540
Risk conditions		
Asthma	J45–J46	2,273,360
Autoimmune conditions	G35, G70, K90, L93, M05, M35	483,850
Cancer	C00–C97	2,869,790
Chronic obstructive pulmonary disease	J44	4,402,564
Cirrhosis	K74	468,950
Cystic fibrosis	E84	29,465
Diabetes mellitus	E10–E14	8,376,979
End-stage renal disease	D17	32,665
HIV	B20–B24	109,180
Immunosuppressive disorders	D80–D89	224,100
Influenza	J09–J11	276,950
Myelodysplastic syndrome	D46	82,170
Neutropenia	D70	194,870
Osteomyelitis	M86	385,450
Pneumonia	J12–J18	2,552,504
Sepsis	A40–A41	2,820,729
Transplant history	Z94	266,580
Transplant complications	T86	145,540
Tuberculosis	A16–A19	3,690

*Data from ICD-10 codes listed in the Healthcare Cost and Utilization Project, 2019 (*20*). ICD-10, International Classification of Diseases, 10th Revision.

Results

Nearly 60,000 invasive fungal infections were reported during US hospitalizations in 2019, ≈10% of all diagnosed fungal infections among hospitalized patients. Another 391,000 noninvasive infections, primarily dermophyte, also were diagnosed.

Fungal Infections and Risk Conditions by Sex

Invasive fungal infections were diagnosed more frequently in male patients, at 1.4–3.4 times the rate for female patients (Figure 1, panel A; Appendix Table 1, https://wwnc.cdc.gov/EID/article/28/10/22-0391-App1.pdf). We observed the greatest differences between male and female patients in coccidioidomycosis (RR 2.0, 95% CI 1.9–2.1), pneumocystosis (RR 2.4, 95% CI 2.3–2.5), and cryptococcosis (RR 3.4, 95% CI 3.2–3.7) diagnoses. Noninvasive candidiasis, including vulvovaginal candidiasis, was the only diagnosis made more frequently in female patients, at 1.2 (95% CI 1.2–1.2) times the rate for male patients.

Male patients had ≥1 fungal-associated risk condition diagnosed at 1.2 (95% CI 1.2–1.2) times the rate for female patients (Figure 1, panel B). Of 19 risk conditions we analyzed, 16 were diagnosed more frequently in male patients. We observed the greatest differences in risk conditions between male and female patients for HIV (RR 3.1, 95% CI 3.0–3.1) and osteomyelitis (RR 2.7, 95% CI 2.7–2.7). Asthma (RR 1.7, 95% CI 1.7–1.7), autoimmune diseases (RR 1.9, 95% CI 1.9–1.9), and immunosuppressive disorders (RR 1.1, 95% CI 1.0–1.1) were diagnosed more frequently in female patients.

Fungal Infections and Risk Conditions by Race and Ethnicity

Overall, risk conditions and fungal infections were diagnosed among racial and ethnic subgroups at rates generally consistent with the current racial and ethnic composition of the United States; most (65.9%) cases were diagnosed in non-Hispanic White patients. However, we noted deviations that highlight racial and ethnic health disparities.

Among Black patients, cryptococcosis was diagnosed at 2.5 (95% CI 2.3–2.6) and pneumocystosis at 3.0 (95% CI 2.9–3.2) times the rates for non-Hispanic White patients (Figure 2, panel A). The transplant

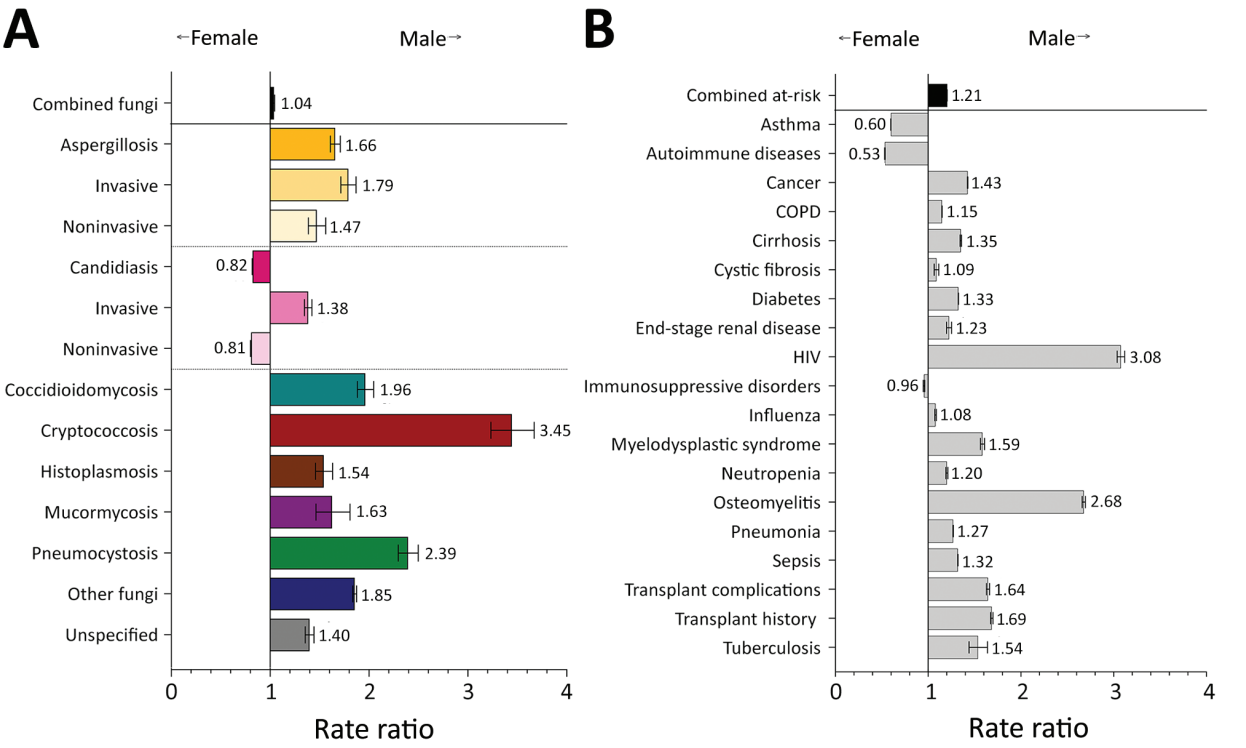

Figure 1. Comparison of rate ratios for fungal infections and risk conditions by sex among hospitalized patients, United States, 2019. A) Diagnosed fungal infections; B) risk conditions. Bars and numerals indicated rate ratios; error bars indicate 95% CIs. COPD, chronic obstructive pulmonary disease.

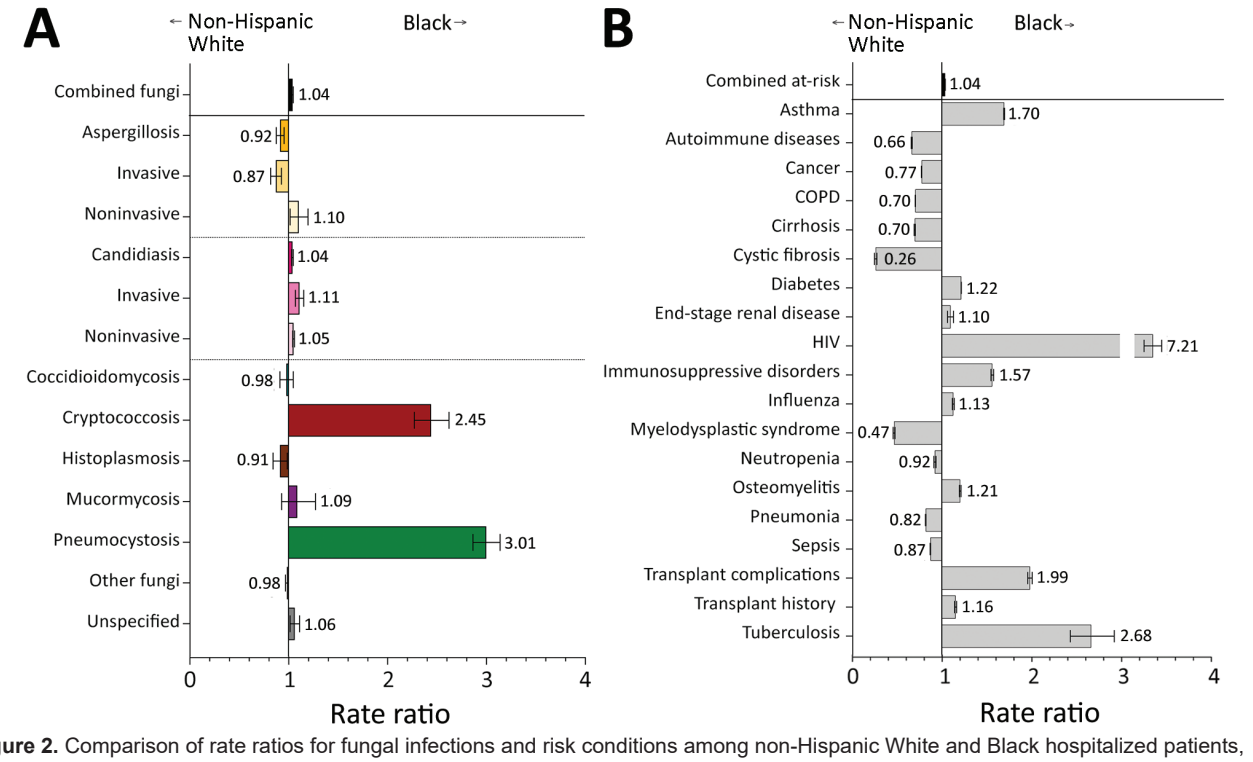

Figure 2. Comparison of rate ratios for fungal infections and risk conditions among non-Hispanic White and Black hospitalized patients, United States, 2019. A) Diagnosed fungal infections; B) risk conditions. Bars and numerals indicated rate ratios; error bars indicate 95% CIs. COPD, chronic obstructive pulmonary disease.

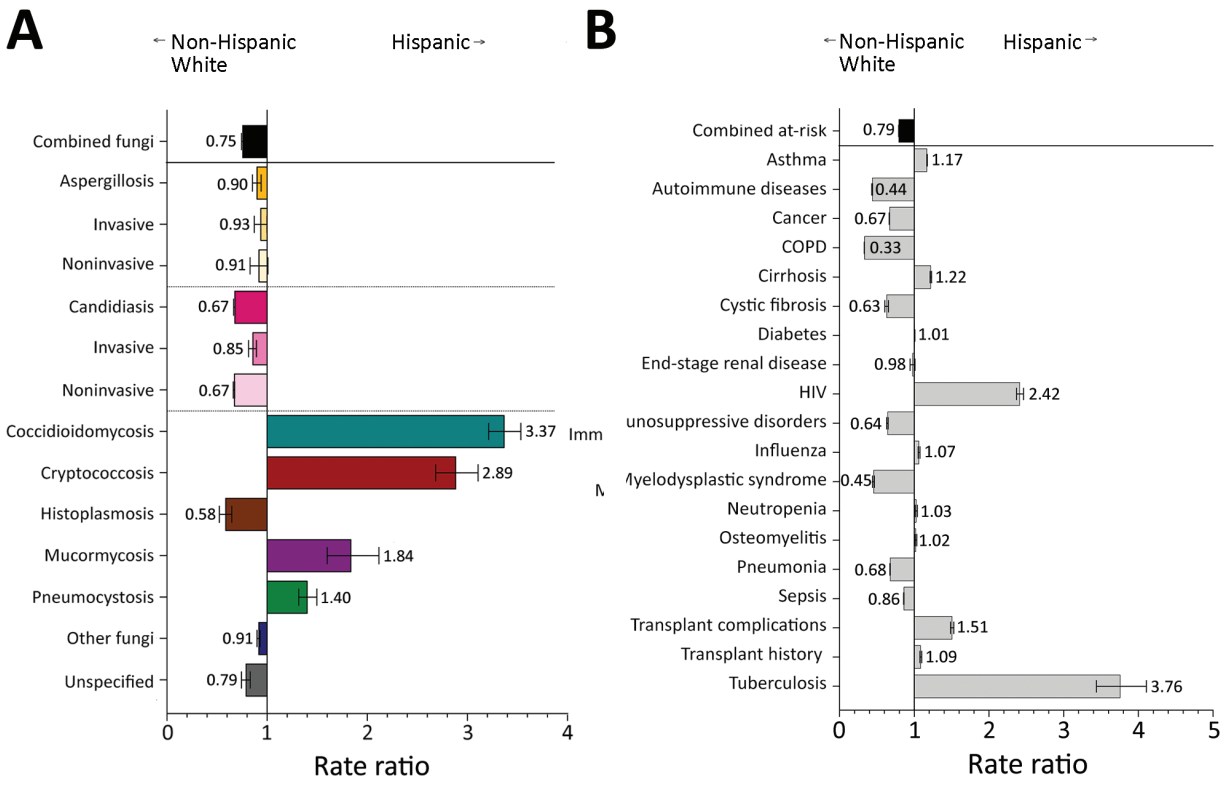

Figure 3. Comparison of rate ratios for fungal infections and risk conditions among hospitalized non-Hispanic White and Hispanic patients, United States, 2019. A) Diagnosed fungal infections; B) risk conditions. Bars and numerals indicated rate ratios; error bars indicate 95% CIs. COPD, chronic obstructive pulmonary disease.

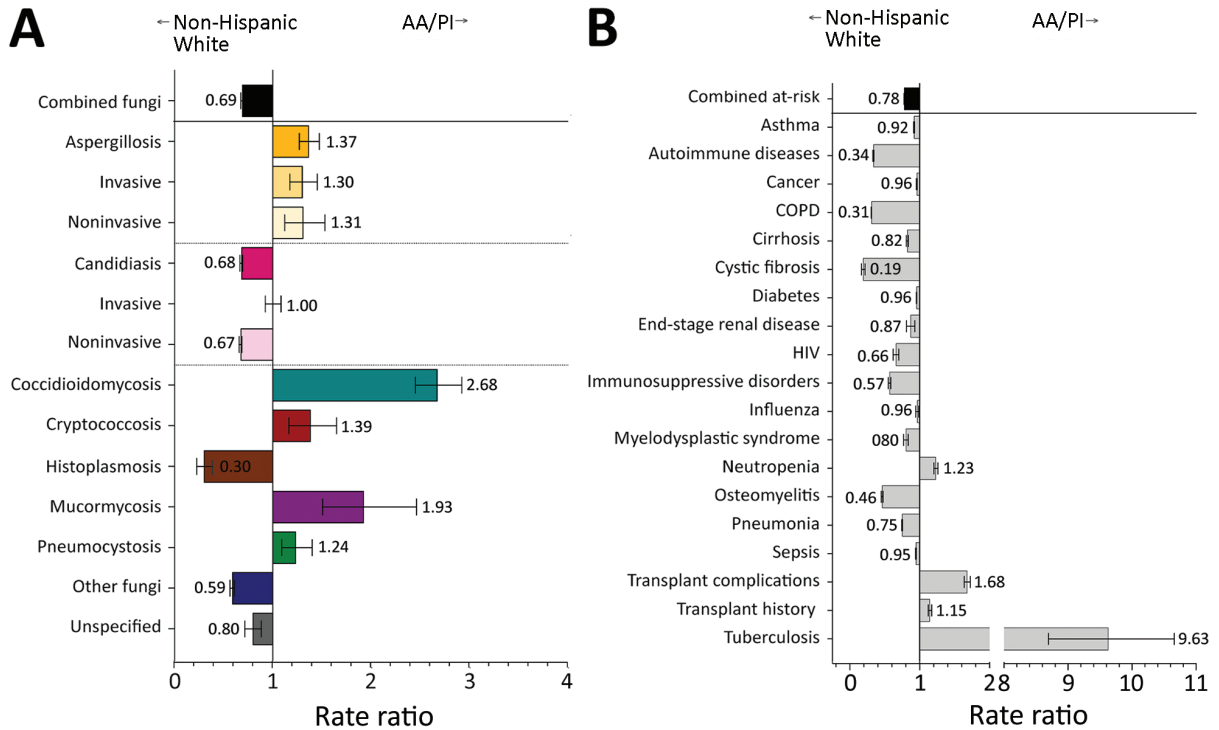

Figure 4. Comparison of rate ratios for fungal infections and risk conditions among hospitalized non-Hispanic White and AA/PI patients, United States, 2019. A) Diagnosed fungal infections; B) risk conditions. Bars and numerals indicated rate ratios; error bars indicate 95% CIs. AA/PI, Asian American/Pacific Islander; COPD, chronic obstructive pulmonary disease.

history rate appeared similar, but Black patients were twice as likely as non-Hispanic White patients to have transplant complications during hospitalization, particularly for heart and kidney transplants (Figure 2, panel B; Appendix Table 1). HIV was diagnosed among Black patients at 7.2 (95% CI 7.1–7.3) and tuberculosis at 2.7 (95% CI 2.4–2.9) times the rates for non-Hispanic White patients.

Hispanic patients had fungal infections diagnosed at 0.8 (95% CI 0.8–0.8) times the rate for non-Hispanic White patients; Hispanic patients had decreased rates of aspergillosis, candidiasis, and histoplasmosis (Figure 3, panel A). Rates for coccidioidomycosis (RR 3.4, 95% CI 3.2–3.5), cryptococcosis (RR 2.9, 95% CI 2.7–3.1), and pneumocystosis (RR 1.4, 95% CI 1.3–1.5) were higher among Hispanic than non-Hispanic White patients. HIV was diagnosed among Hispanic patients at 2.4 (95% CI 2.4–2.5) times and tuberculosis at 3.8 (95% CI 3.4–4.1) times the rates for non-Hispanic White patients (Figure 3, panel B). Transplant complications were also moderately elevated in the Hispanic patient cohort.

The overall rate of fungal infection diagnosis in Asian American and Pacific Islander (AA/PI) patients was reduced (RR 0.7, 95% CI 0.7–0.7) compared with non-Hispanic White patients (Figure 4, panel A). Aspergillosis (RR 1.4, 95% CI 1.3–1.5), coccidioidomycosis (RR 2.7, 95% CI 2.5–2.9), and mucormycosis (RR 1.9, 95% CI 1.5–2.5) rates were higher for AA/PI than for non-Hispanic White patients. AA/PI patients had ≥1 fungal-associated risk condition diagnosed at 0.8 (95% CI 0.8–0.8) times the rate for non-Hispanic White patients (Figure 4, panel B). Transplant complications were moderately elevated in the AA/PI cohort, but tuberculosis diagnoses were 9.6 (95% CI 8.7–10.7) times those for non-Hispanic White patients.

Native American patients had coccidioidomycosis diagnosed at 5.9 (95% CI 5.2–6.6) times the rate for non-Hispanic White patients (Figure 5, panel A). Native American patients also had higher rates of cryptococcosis (RR 2.5, 95% CI 1.9–3.3) than non-Hispanic White patients, but the rates of pneumocystosis did not differ between these 2 groups (RR 1.0, 95% CI 0.7–1.3). Rates of invasive aspergillosis and histoplasmosis were moderately reduced among Native American patients. For risk conditions, Native American patients had HIV diagnosed at 1.6 (95% CI 1.5–1.7), osteomyelitis at 1.8 (95% CI 1.8–1.9), and tuberculosis at 3.6 (95% CI 2.6–4.8) times the rates for non-Hispanic White patients (Figure 5, panel B).

Fungal Infections and Risk Conditions by Income

Of 35.5 million hospitalizations in 2019, nearly one third were associated with residence in lower income areas (Appendix Table 2). Patients from Q1 postal codes had 1.6 times the hospitalization rate as patients from Q4 areas. Fungal infections were diagnosed in patients from Q1 postal codes at 1.2 (95% CI 1.2–1.2) times the frequency of patients from Q4 postal codes (Figure 6, panel A; Appendix Table 2). Cryptococcosis was diagnosed at 2.0 (95% CI 1.8–2.1) and histoplasmosis at 1.7 (95% CI 1.5–1.8) times the rate in Q1 patients as in Q4 patients. The only fungal infection diagnosed more frequently in Q4 patients was aspergillosis (RR 1.3, 95% CI 1.2–1.4).

Q1 patients also had ≥1 fungal-associated risk condition diagnosed at 1.2 (95% CI 1.2–1.2) times the rate for Q4 patients (Figure 6, panel B). COPD, cirrhosis, diabetes, and HIV were diagnosed in Q1 patients at 1.4–2.8 times the rate for Q4 patients. In 2019, Q4 patients were admitted more frequently for conditions associated with higher healthcare costs, including cancer (RR 1.3, 95% CI 1.3–1.3), cystic fibrosis (RR 1.4, 95% CI 1.3–1.4), and organ transplants (RR 1.4, 95% CI 1.3–1.4).

Fungal Infections and Risk Conditions by Payer Type

Most (86.7%) persons covered by federally funded Medicare are ≥65 years of age (*23*). In hospitalizations billed to Medicare, fungal infections were diagnosed at 2.0 (95% CI 2.0–2.0) times the rate for hospitalizations billed to private insurance (Figure 7, panel A; Appendix Table 3). The diagnostic rates for aspergillosis (RR 1.4, 95% CI 1.4–1.5), candidiasis (RR 2.0, 95% CI 2.0–2.0), other fungi (RR 2.2, 95% CI 2.2–2.3), and unspecified fungal infections (RR 1.9, 95% CI 1.8–2.0) were particularly elevated among Medicare patients. Only pneumocystosis (RR 0.8, 95% CI 0.8–0.9) rates were notably lower among hospitalizations billed to Medicare than those billed to private insurance. Hospitalizations billed to Medicare had 2.1 (95% CI 2.1–2.1) times the rate of having ≥1 fungal-associated risk condition diagnoses as did hospitalizations billed to private insurance (Figure 7, panel B). Rates for 16 of the 19 risk conditions we investigated were elevated in hospitalizations billed to Medicare, and we noted differences in COPD (RR 4.6, 95% CI 2.6–2.6), cirrhosis (RR 2.5, 95% CI 2.4–2.5), diabetes mellitus (RR 2.5, 95% CI 2.5–2.6), myelodysplastic syndrome (RR 4.8, 95% CI 4.7–4.9), pneumonia (RR 2.7, 95% CI 2.7–2.7), and sepsis (RR 2.3, 95% CI 2.3–2.3). Conversely, cystic fibrosis was diagnosed at just over one third the frequency (RR 0.4, 95% CI 0.3–0.4) in hospitalizations billed to Medicare compared with those billed to private insurance.

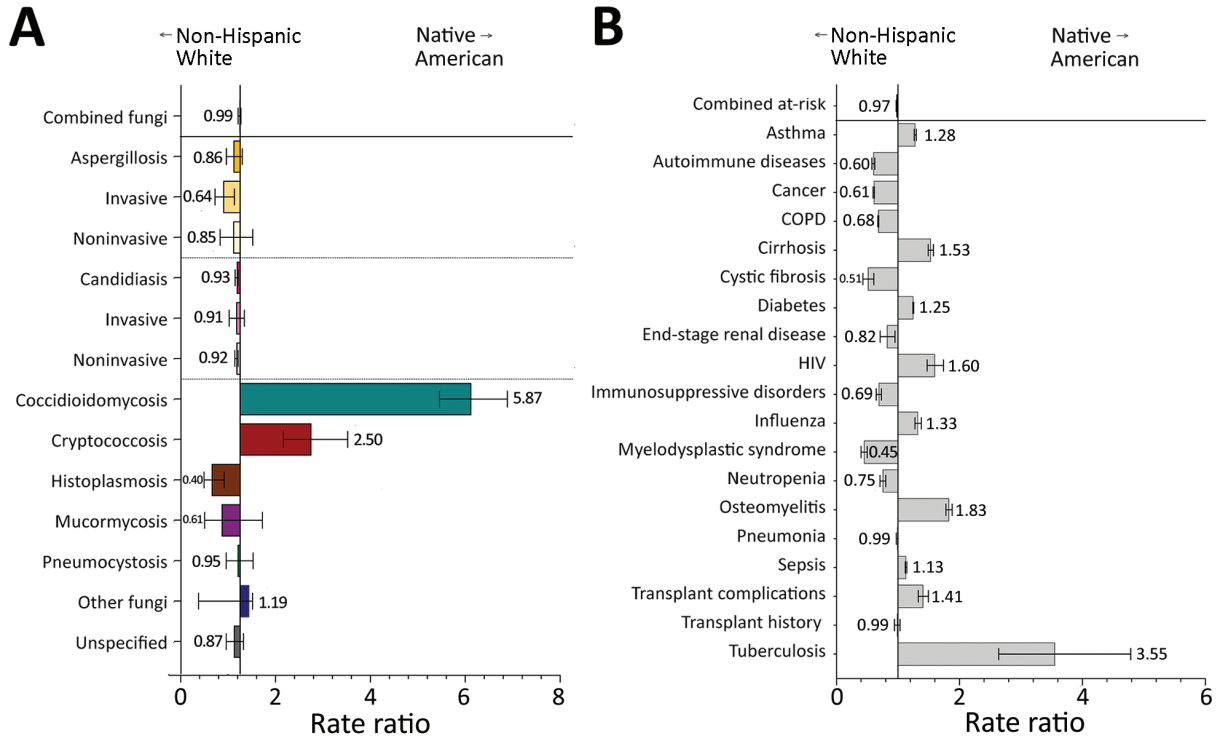

Figure 5. Comparison of rate ratios for fungal infections and risk conditions among hospitalized non-Hispanic White and Native American patients, United States, 2019. A) Diagnosed fungal infections; B) risk conditions. Bars and numerals indicated rate ratios; error bars indicate 95% CIs. COPD, chronic obstructive pulmonary disease.

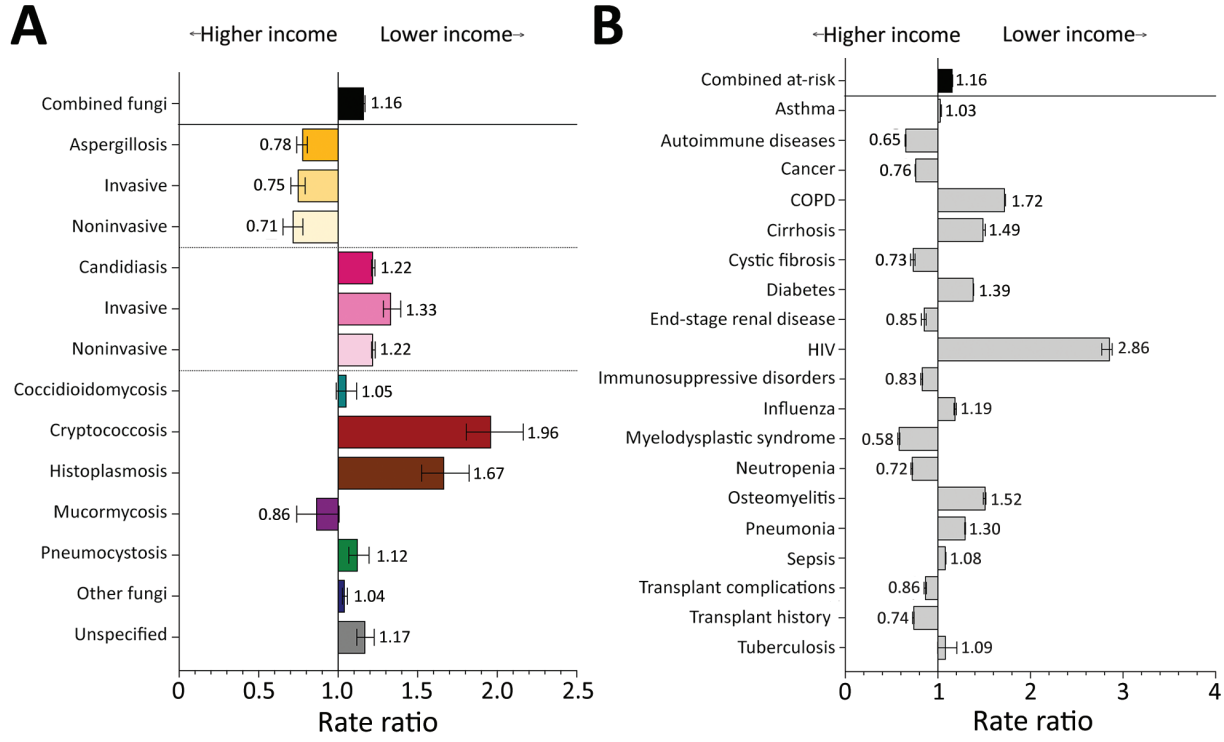

Figure 6. Comparison of rate ratios for fungal infections and risk conditions by income among hospitalized patients, United States, 2019. A) Diagnosed fungal infections; B) risk conditions. Income levels were determined by postal code; patients from postal codes with incomes in the highest quartile were compared with patients from postal codes with incomes in the lowest quartile. Bars and numerals indicated rate ratios; error bars indicate 95% CIs. COPD, chronic obstructive pulmonary disease.

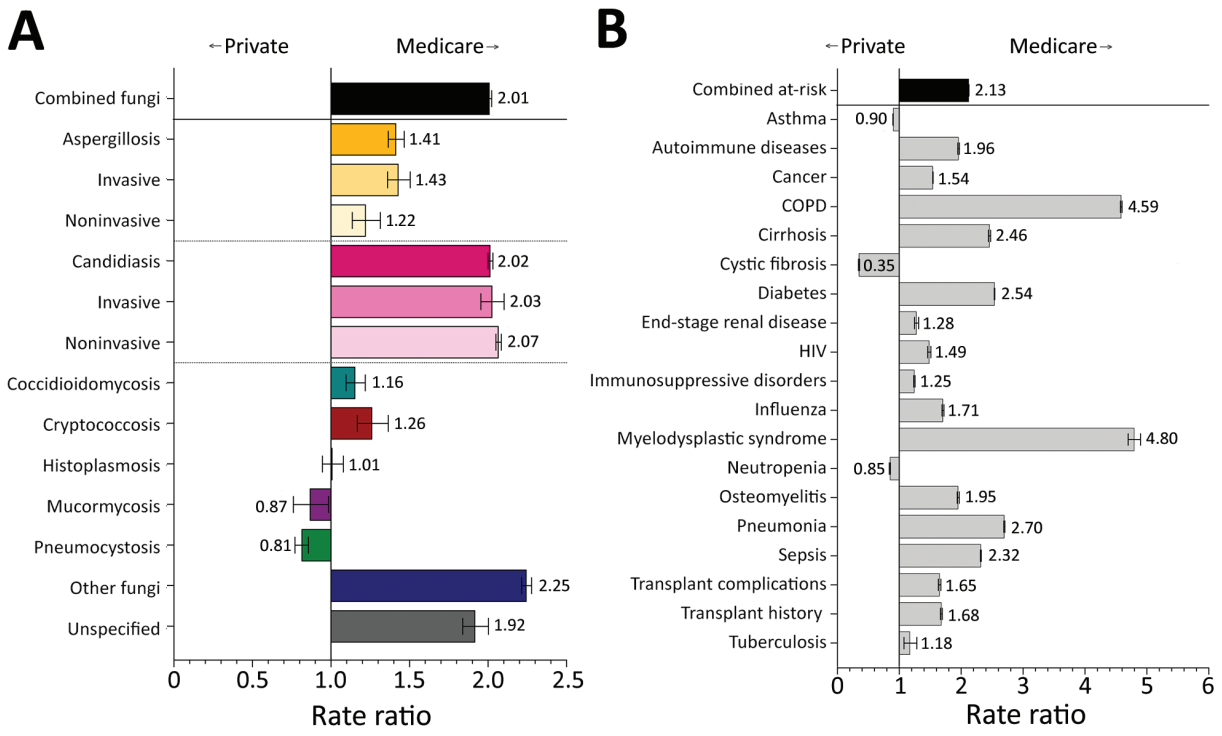

Figure 7. Comparison of rate ratios for fungal infections and risk conditions by billing type (private insurance vs. Medicare) among hospitalized patients, United States, 2019. A) Diagnosed fungal infections; B) risk conditions. Bars and numerals indicated rate ratios; error bars indicate 95% CIs. COPD, chronic obstructive pulmonary disease.

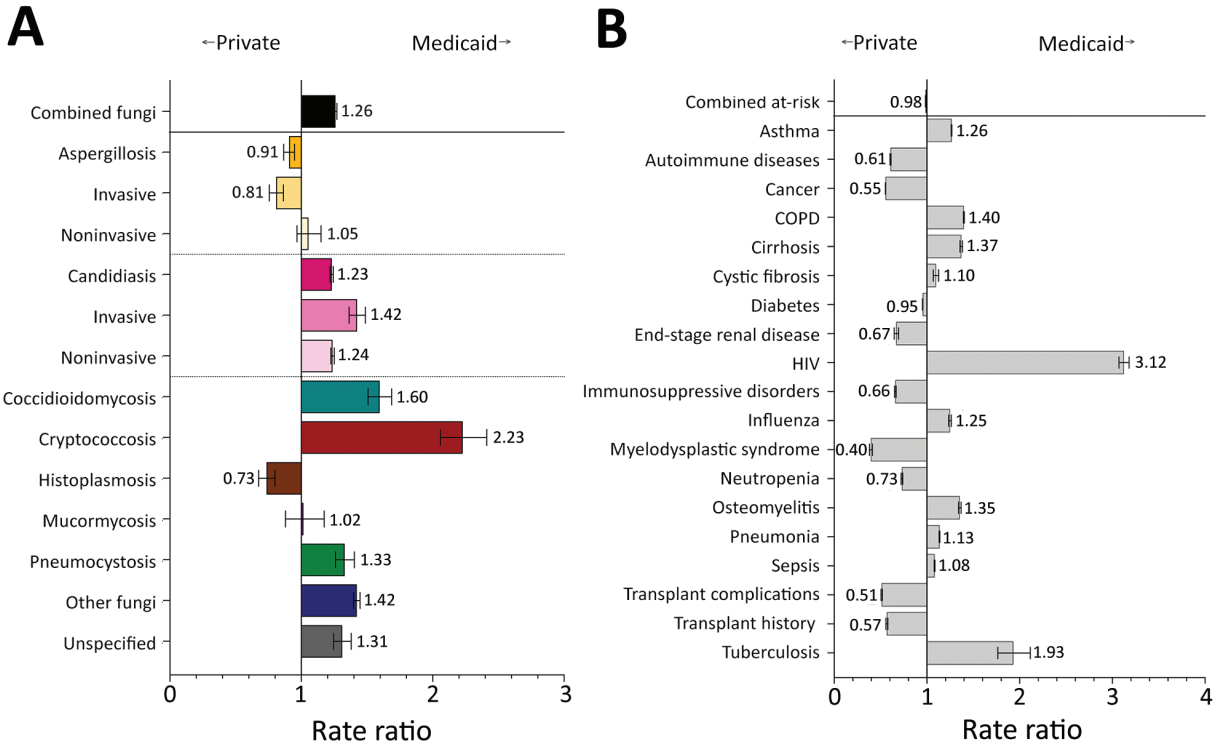

Figure 8. Comparison of rate ratios for fungal infections and risk conditions by billing type (private insurance vs. Medicaid) among hospitalized patients, United States, 2019. A) Diagnosed fungal infections; B) risk conditions. Bars and numerals indicated rate ratios; error bars indicate 95% CIs. COPD, chronic obstructive pulmonary disease.

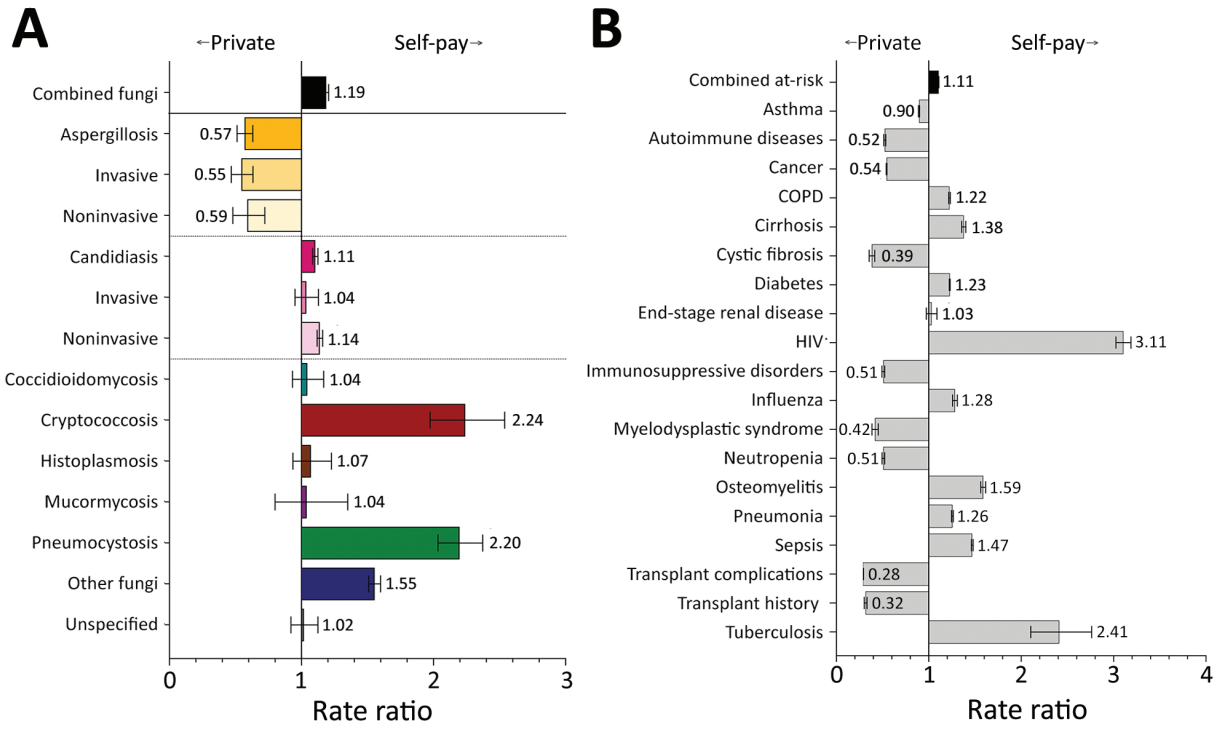

Figure 9. Comparison of rate ratios for fungal infections and risk conditions by billing type (private insurance vs. self-pay) among hospitalized patients, United States, 2019. A) Diagnosed fungal infections; B) risk conditions. Bars and numerals indicated rate ratios; error bars indicate 95% CIs. COPD, chronic obstructive pulmonary disease.

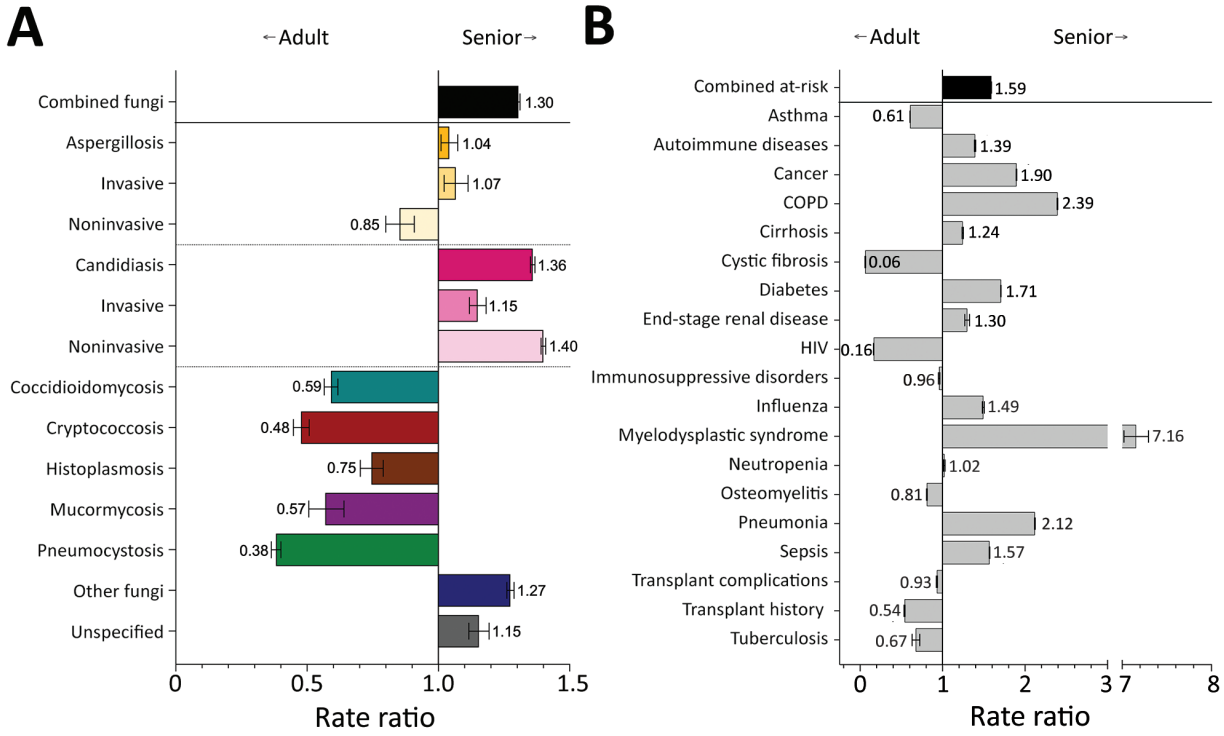

Figure 10. Comparison of rate ratios for fungal infections and risk conditions among adult and senior hospitalized patients, United States, 2019. A) Diagnosed fungal infections; B) risk conditions. Adult patients are persons 18–64 years of age; senior patients are ≥65 years of age. Bars and numerals indicated rate ratios; error bars indicate 95% CIs. COPD, chronic obstructive pulmonary disease.

Federal- and state-funded Medicaid provides free health insurance to persons with low incomes, disabilities, or both (*24*). Fungal infections were more frequent in hospitalizations billed to Medicaid than those billed to private insurance (Figure 8, panel A). In particular, invasive candidiasis (RR 1.4, 95% CI 1.4–1.5), coccidioidomycosis (RR 1.6, 95% CI 1.5–1.7), cryptococcosis (RR 2.2, 95% CI 2.1–2.4), pneumocystosis (RR 1.3, 95% CI 1.3–1.4), other fungi (RR 1.4, 95% CI 1.4–1.5), and unspecified fungal infections (RR 1.3, 95% CI 1.3–1.4) were diagnosed more frequently, and invasive aspergillosis (RR 0.8, 95% CI 0.8–0.9) and histoplasmosis (RR 0.7, 95% CI 0.7–0.8) were diagnosed less frequently for hospitalizations billed to Medicaid compared with those billed to private insurance. The rates of HIV (RR 3.1, 95% CI 3.1–3.2) and tuberculosis (RR 1.9, 95% CI 1.8–2.1) were higher in hospitalizations billed to Medicaid than those billed to private insurance (Figure 8, panel B). Risk conditions with fewer diagnoses billed to Medicaid than to private insurance included autoimmune diseases (RR 0.6, 95% CI 0.6–0.6), cancer (RR 0.6, 95% CI 0.6–0.6), immunosuppressive disorders (RR 0.7, 95% CI 0.7–0.7), myelodysplastic syndrome (RR 0.4, 95% CI 0.4–0.4), and transplant history (RR 0.5, 95% CI 0.5–0.5).

Hospitalizations billed as self-pay represent patients that are uninsured or underinsured (i.e., <30% estimated insurance coverage). These hospitalizations had a lower frequency of diagnoses for aspergillosis (RR 0.6, 95% CI 0.5–0.6) but elevated frequencies for cryptococcosis (RR 2.2, 95% CI 2.0–2.5) and pneumocystosis (RR 2.2, 95% CI 2.0–2.4) (Figure 9, panel A). Rates of HIV (RR 3.1, 95% CI 3.0–3.2) and tuberculosis (RR 2.4, 95% CI 2.1–2.8) were elevated in hospitalizations billed as self-pay compared with private insurance, but other risk conditions were reduced, including autoimmune diseases (RR 0.5, 95% CI 0.5–0.5), cancer (RR 0.5, 95% CI 0.5–0.5), immunosuppressive disorders (RR 0.5, 95% CI 0.5–0.5), myelodysplastic syndrome (RR 0.4, 95% CI 0.4–0.5), and transplant history (RR 0.3, 95% CI 0.3–0.3) (Figure 9, panel B).

Fungal Infections and Risk Conditions by Age

Fungal infection diagnosis rates among senior patients were 1.3 (95% CI 1.3–1.3) times that for adult patients. We noted moderate elevation in the rate of invasive aspergillosis diagnoses among senior patients, but noninvasive candidiasis was diagnosed more frequently (RR 1.4, 95% CI 1.4–1.4) among senior than adult patients (Figure 10, panel A; Appendix Table 4). Fungal infections diagnosed less frequently in senior than adult patients included coccidioidomycosis (RR 0.6, 95% CI 0.6–0.6), cryptococcosis (RR 0.5, 95% CI 0.5–0.5), histoplasmosis (RR 0.8, 95% CI 0.7–0.8), mucormycosis (RR 0.6, 95% CI 0.5–0.6), and pneumocystosis (RR 0.4, 95% CI 0.4–0.4). Senior patients had ≥1 fungal-associated risk condition diagnosed at 1.6 (95% CI 1.6–1.6) times the rate of adult patients (Figure 10, panel B). We also noted elevated rates of COPD (RR 2.4, 95% CI 2.4–2.4), myelodysplastic syndrome (RR 7.2, 95% CI 7.0–7.3), and pneumonia (RR 2.1, 95% CI 2.1–2.1) among senior patients compared with adult patients. Few senior patients had a cystic fibrosis diagnosis, and HIV (RR 0.2, 95% CI 0.2–0.2) diagnoses also were lower than among adult patients.

Despite representing 14.9% of hospitalizations in 2019, pediatric patients accounted for only 4.2% of diagnosed fungal infections and had one third the diagnostic rate (RR 0.3, 95% CI 0.3–0.3) of adult patients (Figure 11, panel A); rates of all fungal pathogens and manifestations were reduced. Pediatric patients had ≥1 fungal-associated risk condition diagnosed at 0.2 (95% CI 0.2–0.2) times the rate for adult patients (Figure 11, panel B). Only the diagnostic rate for cystic fibrosis (RR 1.3, 95% CI 1.2–1.3) was higher among pediatric than adult patients.

Fungal Infections and Risk Conditions by Rural or Urban Status

Among patients from urban areas, certain fungal infections were diagnosed more frequently, including coccidioidomycosis at 3.4 (95% CI 3.1–3.8), pneumocystosis at 1.9 (95% CI 1.8–2.0), and aspergillosis at 1.2 (95% CI 1.1–1.2) times the rates for patients from rural areas (Figure 12, panel A; Appendix Table 5). All aspergillosis infections were diagnosed more frequently in urban patients, but noninvasive aspergillosis (RR 1.8, 95% CI 1.6–2.0) had the greatest difference. Infections diagnosed more frequently among rural patients included candidiasis at 1.1 (95% CI 1.1–1.1) and histoplasmosis at 1.6 (95% CI 1.5–1.7) times the rate for urban patients.

Urban patients had much higher rates of HIV (RR 2.9, 95% CI 2.9–2.9) and tuberculosis (RR 2.0, 95% CI 1.8–2.3) than rural patients (Figure 12, panel B). Asthma (RR 1.4, 95% CI 1.4–1.4) and transplants (RR 1.2, 95% CI 1.2–1.2) also were more common among urban patients, consistent with previous reports (*25*). COPD (RR 1.4, 95% CI 1.4–1.4) and pneumonia (RR 1.3, 95% CI 1.3–1.4) were more frequent among rural patients.

Discussion

We analyzed rates of fungal infection diagnoses in hospitalizations on the basis of racial and ethnic

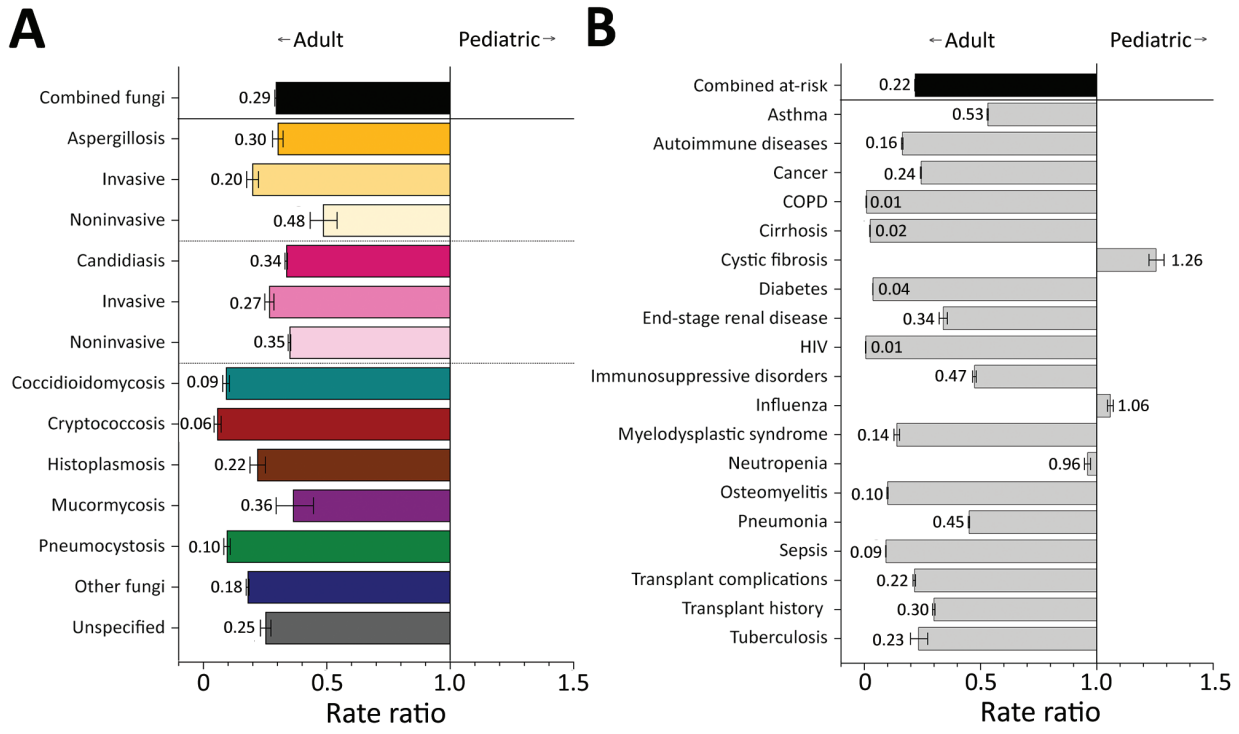

Figure 11. Comparison of rate ratios for fungal infections and risk conditions among adult and pediatric hospitalized patients, United States, 2019. A) Diagnosed fungal infections; B) risk conditions. Adult patients are persons 18–64 years of age; pediatric patients are ≤17 years of age. Bars and numerals indicated rate ratios; error bars indicate 95% CIs. COPD, chronic obstructive pulmonary disease.

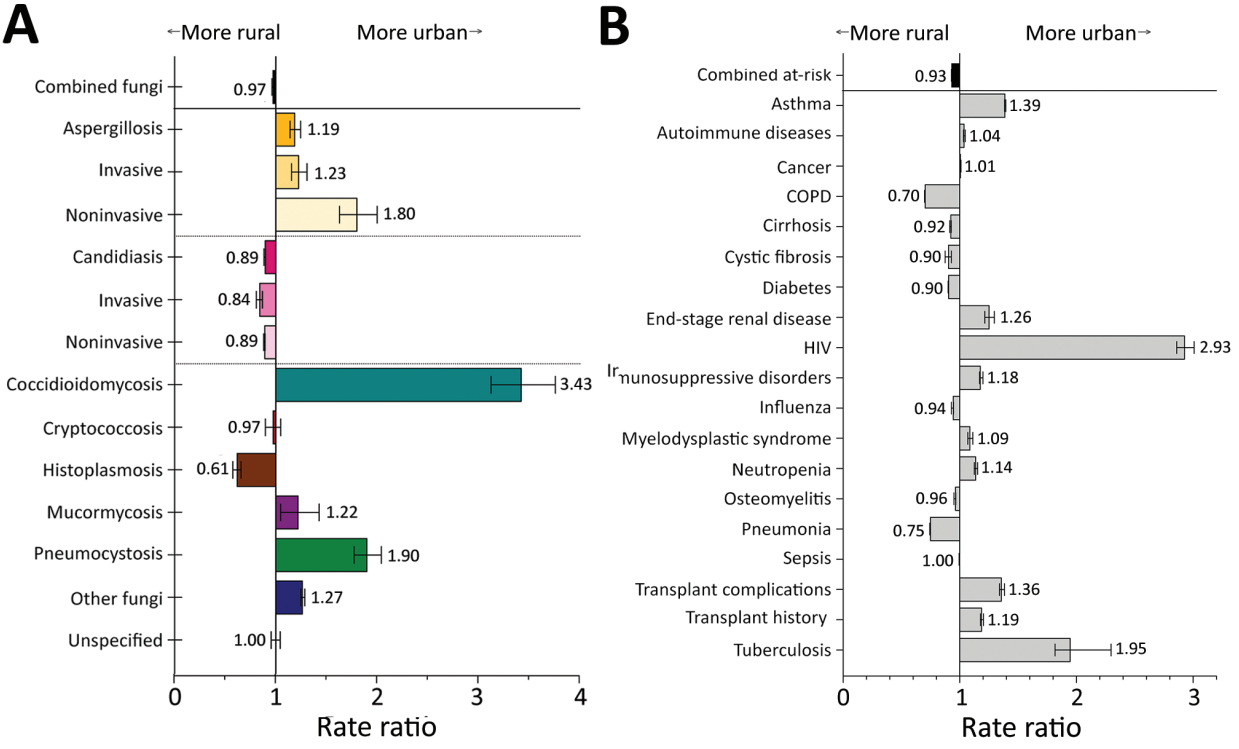

Figure 12. Comparison of rate ratios for fungal infections and risk conditions by residential location (urban vs. rural) among hospitalized patients, United States, 2019. A) Diagnosed fungal infections; B) risk conditions. Persons from more urban settings are considered those whose resident county has a population >50,000. Bars and numerals indicated rate ratios; error bars indicate 95% CIs. COPD, chronic obstructive pulmonary disease.

background and socioeconomic status. Our findings demonstrate that health disparities between racial, ethnic, and socioeconomic groups extend to fungal infections, especially for predisposing risk conditions.

In HCUP NIS, male patients had 1.4–3.5 times the rate of invasive fungal infection diagnoses as female patients, a finding supported by existing literature (*26*). The influence of genetic components by sex has been postulated, as have higher environmental exposure and behavioral risks (*26*,*27*). The relationship between sex and susceptibility is more complex than our analyses can capture, but ≥1 risk condition for fungal infection was more frequently diagnosed among male patients.

Aspergillosis was diagnosed more frequently in non-Hispanic White and AA/PI patients than in other racial and ethnic groups. As previously described (*3*), invasive aspergillosis is closely associated with stem cell and solid organ transplantation, and noninvasive manifestations, including allergic bronchopulmonary aspergillosis and chronic pulmonary aspergillosis, are more often diagnosed in cystic fibrosis and tuberculosis patients; AA/PI patients have >9 times the rate of tuberculosis diagnoses as non-Hispanic White patients (*28*). In addition, aspergillosis is the only fungal infection diagnosed more frequently in patients from higher income areas. Higher income is associated with higher probability of receiving a transplant (*29*,*30*) and improved patient outcomes in cystic fibrosis care (*31*), possibly because these patients have better access to healthcare facilities and the financial capacity for regular treatment. Aspergillosis likely is more frequently diagnosed in higher income patients because of their ability to continually seek treatment for associated risk factors. Income differences also could relate to cost of living because aspergillosis is more likely to be diagnosed in urban than rural patients (*32*).

Candidiasis was diagnosed more frequently in Black patients. Invasive candidiasis was more frequent in male patients, fitting with previous findings (*33*), but noninvasive candidiasis was more frequent in female patients. Increased rates of candidiasis among senior patients compared with adult patients also is consistent with prior findings (*33*). All candidiasis clinical manifestations were more frequent in patients from lower income areas. Assessments of the relationship of candidiasis and income are lacking, but these diagnoses might be related to the higher frequency of diabetes in patients from low-income areas (*7*). This finding also might be an artifact of the relationship between low income and increased frequency of repeat hospitalizations (*34*). All candidiasis clinical manifestations were diagnosed moderately more frequently in rural patients.

Coccidioidomycosis and histoplasmosis are endemic infections that can affect immunocompetent persons, but severe disease is more common in immunocompromised persons. Coccidioidomycosis is endemic in the US Southwest and histoplasmosis in the Ohio and Mississippi River Valley regions. Our analysis showed coccidioidomycosis was diagnosed more frequently in Hispanic, AA/PI, and Native American adult male patients than in non-Hispanic White or Black, senior, or female patients. Environmental exposure is key in coccidioidomycosis; workers performing soil-disturbing work or exposed to dusty conditions in endemic areas are at increased risk. Black and Hispanic persons are overrepresented in lower wage, more manual labor, and higher risk occupations, including occupations with frequent dust exposure (*35*,*36*). Previous reports noted higher frequencies of coccidioidomycosis in AA/PI and Hispanic male adults residing in urban areas, but older state-level data also indicated increased rates in Black compared with non-Hispanic White male persons (*36*–*38*).

Non-Hispanic White patients had up to 3 times the rate of histoplasmosis as other racial and ethnic groups. Histoplasmosis diagnoses were higher among adult, low-income, and rural patients. These results are supported by previous reports of histoplasmosis predominantly among middle-aged adult White male persons living in rural areas (*39*). These demographic variables likely capture persons with environmental or occupational exposure, including persons employed in construction, agriculture, and forestry industries (*40*).

Historically, cryptococcosis and pneumocystosis were closely tied to HIV, which continues to disproportionately affect Black and Hispanic/Latino populations (*41*). We found cryptococcosis and pneumocystosis were diagnosed in Black and Hispanic patients at 2–3 times the rate for non-Hispanic White patients. HIV, cryptococcosis, and pneumocystosis frequencies also were elevated in Q1 patients and were far more frequent in adult than senior patients, fitting with previous literature (*42*). HIV, cryptococcosis, and pneumocystosis rates were elevated in hospitalizations billed to Medicaid or self-pay and in urban patients.

Incidence of mucormycosis, a rare and often fatal infection, has been rising (*43*). We found mucormycosis diagnoses were more frequent among AA/PI and Hispanic patients than among non-Hispanic White patients. The most common underlying condition for

mucormycosis is diabetes mellitus (*43*), but diabetes was not diagnosed more frequently in AA/PI or Hispanic populations in our study. We noted no differences in mucormycosis rates by income or insurance type. Adult patients were more likely to have mucormycosis than senior patients, and we noted a slight elevation in diagnoses among urban patients.

Other fungal infections include primarily superficial cutaneous and mucosal infections, which were diagnosed more frequently in senior patients and in hospitalizations billed to Medicare, consistent with previous studies (*44*). Unspecified mycotic infections also were more frequently diagnosed in senior patients, which could reflect increased mortality and shorter survival times associated with an aging immune response failing to control invasive fungal infections, as previously described (*45*).

Our results are informative, but our data likely underrepresent the true burden of fungal disease in the United States. Evidence suggests that only half of invasive fungal infections are diagnosed before patient death (*46*). The sensitivity and specificity of many ICD-10 codes for fungal infections are unknown, and misclassification is possible. HCUP NIS enabled us to comprehensively study fungal infections; however, unique patients cannot be identified in NIS, so our data likely represent multiple hospitalizations per patient. Data collection also could be a limitation because race and ethnicity analyses are limited by single identifiers and failed to represent patients with multiracial or multiethnic identities. In addition, some previously studied racial and ethnic subgroups might not have been included for this variable in the NIS dataset. Finally, hospitals might have reported a private insurance payer type for patients covered by a Medicare-managed care program administered by a private insurance company, potentially underrepresenting differences between payer types.

In conclusion, we provide a comprehensive summary of fungal infections and associated risk conditions among hospitalized patients, including corresponding rate ratios by demographic and socioeconomic factors. These findings are based on bivariate analysis, but future studies could use a multivariable analysis of the potential predictive weight of demographic and socioeconomic risk factors and ≥1 comorbidity to measure evaluated risk for fungal infection by type. Our findings suggest that differences in fungal infection diagnostic rates are associated with demographic and socioeconomic factors. Because fungal infections increase mortality rates and healthcare costs, our results highlight an ongoing need for increased physician evaluation of risk for fungal infections, especially among minority and low-income populations that are disproportionately affected.

Acknowledgments

We thank the participating Healthcare Cost and Utilization Project (HCUP) Data Partners for the state-level data collection efforts involved in creating the National Inpatient Sample (https://www.hcup-us.ahrq.gov/db/hcupdatapartners.jsp).

This work was supported by National Institutes of Health (grant no. 1R01 AI148365-01A1 to K.A.N.), and endowments to K.A.N. from the Georgia Research Alliance and the University of Georgia Research Foundation.

About the Author

Dr. E. Rayens is a postdoctoral research associate at the University of Georgia, Athens, Georgia, USA. Her research interests include fungal disease immunology and epidemiology.

References

1. Bongomin F, Gago S, Oladele RO, Denning DW. Global and multi-national prevalence of fungal diseases–estimate precision. J Fungi (Basel). 2017;3:57. https://doi.org/10.3390/jof3040057
2. Rayens E, Norris KA. Prevalence and healthcare burden of fungal infections in the United States, 2018. Open Forum Infect Dis. 2022;9:ofab593. https://doi.org/10.1093/ofid/ofab593
3. Rayens E, Norris KA, Cordero JF. Mortality trends in risk conditions and invasive mycotic disease in the United States, 1999–2018. Clin Infect Dis. 2022;74:309–18. https://doi.org/10.1093/cid/ciab336
4. Morris A, Netravali M, Kling HM, Shipley T, Ross T, Sciurba FC, et al. Relationship of pneumocystis antibody response to severity of chronic obstructive pulmonary disease. Clin Infect Dis. 2008;47:e64–8. https://doi.org/10.1086/591701
5. Pilmis B, Puel A, Lortholary O, Lanternier F. New clinical phenotypes of fungal infections in special hosts. Clin Microbiol Infect. 2016;22:681–7. https://doi.org/10.1016/j.cmi.2016.05.016
6. Amin R, Dupuis A, Aaron SD, Ratjen F. The effect of chronic infection with *Aspergillus fumigatus* on lung function and hospitalization in patients with cystic fibrosis. Chest. 2010;137:171–6. https://doi.org/10.1378/chest.09-1103
7. Rodrigues CF, Rodrigues ME, Henriques M. *Candida* sp. infections in patients with diabetes mellitus. J Clin Med. 2019;8:76. https://doi.org/10.3390/jcm8010076
8. Ghanaat F, Tayek JA. Weight loss and diabetes are new risk factors for the development of invasive aspergillosis infection in non-immunocompromized humans. Clin Pract (Lond). 2017;14:296–301. https://doi.org/10.4172/clinical-practice.1000125
9. Vanderbeke L, Spriet I, Breynaert C, Rijnders BJA, Verweij PE, Wauters J. Invasive pulmonary aspergillosis

complicating severe influenza: epidemiology, diagnosis and treatment. Curr Opin Infect Dis. 2018;31:471–80. https://doi.org/10.1097/QCO.0000000000000504
10. Coste A, Frerou A, Raute A, Couturaud F, Morin J, Egreteau P-Y, et al. The Extent of aspergillosis in critically ill patients with severe influenza pneumonia: a multicenter cohort study. Crit Care Med. 2021;49:934–42. https://doi.org/10.1097/CCM.0000000000004861
11. Bongomin F. Post-tuberculosis chronic pulmonary aspergillosis: an emerging public health concern. PLoS Pathog. 2020;16:e1008742. https://doi.org/10.1371/journal.ppat.1008742
12. Denning DW, O'Driscoll BR, Hogaboam CM, Bowyer P, Niven RM. The link between fungi and severe asthma: a summary of the evidence. Eur Respir J. 2006;27:615–26. https://doi.org/10.1183/09031936.06.00074705
13. Rayens E, Noble B, Vicencio A, Goldman DL, Bunyavanich S, Norris KA. Relationship of *Pneumocystis* antibody responses to paediatric asthma severity. BMJ Open Respir Res. 2021; 8:e000842. https://doi.org/10.1136/bmjresp-2020-000842
14. Bishu S, Su EW, Wilkerson ER, Reckley KA, Jones DM, McGeachy MJ, et al. Rheumatoid arthritis patients exhibit impaired *Candida albicans*–specific Th17 responses. Arthritis Res Ther. 2014;16:R50. https://doi.org/10.1186/ar4480
15. Silva MF, Ferriani MP, Terreri MT, Pereira RM, Magalhães CS, Bonfá E, et al. A multicenter study of invasive fungal infections in patients with childhood-onset systemic lupus erythematosus. J Rheumatol. 2015;42:2296–303. https://doi.org/10.3899/jrheum.150142
16. Sipsas NV, Kontoyiannis DP. Invasive fungal infections in patients with cancer in the intensive care unit. Int J Antimicrob Agents. 2012;39:464–71. https://doi.org/10.1016/j.ijantimicag.2011.11.017
17. Pappas PG, Alexander BD, Andes DR, Hadley S, Kauffman CA, Freifeld A, et al. Invasive fungal infections among organ transplant recipients: results of the Transplant-Associated Infection Surveillance Network (TRANSNET). Clin Infect Dis. 2010;50:1101–11. https://doi.org/10.1086/651262
18. Anderson JL, Frost HM, King JP, Meece JK. Racial differences in clinical phenotype and hospitalization of blastomycosis patients. Open Forum Infect Dis. 2019;6:ofz438. https://doi.org/10.1093/ofid/ofz438
19. Boehme AK, McGwin G, Andes DR, Lyon GM, Chiller T, Pappas PG, et al. Race and invasive fungal infection in solid organ transplant recipients. Ethn Dis. 2014;24:382–5.
20. Agency for Healthcare Research and Quality. National Inpatient Sample (NIS), Healthcare Cost and Utilization Project (HCUP) [cited 2022 Jan 14]. https://www.hcup-us.ahrq.gov/nisoverview.jsp
21. US Census Bureau. American community survey data 2006–2010 [cited 2022 Jan 14]. https://www.census.gov/programs-surveys/acs/data.html
22. Stranges E, Holmquist L, Andrews RM; Agency for Healthcare Research and Quality. Inpatient stays in rural hospitals, 2007: statistical brief #85. Healthcare Cost and Utilization Project (HCUP) Statistical Briefs. Rockville (MD): The Agency; 2006.
23. El-Nahal W. An overview of Medicare for clinicians. J Gen Intern Med. 2020;35:3702–6. https://doi.org/10.1007/s11606-019-05327-6
24. Hill SC, Abdus S. The effects of Medicaid on access to care and adherence to recommended preventive services. Health Serv Res. 2021;56:84–94. https://doi.org/10.1111/1475-6773.13603
25. Rodriguez A, Brickley E, Rodrigues L, Normansell RA, Barreto M, Cooper PJ. Urbanisation and asthma in low-income and middle-income countries: a systematic review of the urban-rural differences in asthma prevalence. Thorax. 2019;74:1020–30. https://doi.org/10.1136/ thoraxjnl-2018-211793
26. Egger M, Hoenigl M, Thompson GR III, Carvalho A, Jenks JD. Let's talk about sex characteristics—as a risk factor for invasive fungal diseases. Mycoses. 2022;65:599–612. https://doi.org/10.1111/myc.13449
27. vom Steeg LG, Klein SL. SeXX matters in infectious disease pathogenesis. PLoS Pathog. 2016;12:e1005374. https://doi.org/10.1371/journal.ppat.1005374
28. Khan A, Marks S, Katz D, Morris SB, Lambert L, Magee E, et al. Changes in tuberculosis disparities at a time of decreasing tuberculosis incidence in the United States, 1994–2016. Am J Public Health. 2018;108:S321–6. https://doi.org/10.2105/AJPH.2018.304606
29. Wesselman H, Ford CG, Leyva Y, Li X, Chang CH, Dew MA, et al. Social determinants of health and race disparities in kidney transplant. Clin J Am Soc Nephrol. 2021;16:262–74. https://doi.org/10.2215/CJN.04860420
30. Hong S, Rybicki L, Abounader DM, Bolwell BJ, Dean R, Gerds AT, et al. Association of socioeconomic status with autologous hematopoietic cell transplantation outcomes for lymphoma. Bone Marrow Transplant. 2016;51:1191–6. https://doi.org/10.1038/bmt.2016.107
31. Kerem E, Cohen-Cymberknoh M. Disparities in cystic fibrosis care and outcome: socioeconomic status and beyond. Chest. 2016;149:298–300. https://doi.org/10.1016/j.chest.2015.08.021
32. Grehn C, Eschenhagen P, Temming S, Düesberg U, Neumann K, Schwarz C. Urban life as risk factor for aspergillosis. Front Cell Infect Microbiol. 2020;10:601834. https://doi.org/10.3389/fcimb.2020.601834
33. Strollo S, Lionakis MS, Adjemian J, Steiner CA, Prevots DR. Epidemiology of hospitalizations associated with invasive candidiasis, United States, 2002–2012. Emerg Infect Dis. 2016;23:7–13. https://doi.org/10.3201/eid2301.161198
34. Barnett ML, Hsu J, McWilliams JM. Patient characteristics and differences in hospital readmission rates. JAMA Intern Med. 2015;175:1803–12. https://doi.org/10.1001/jamainternmed.2015.4660
35. Stanbury M, Rosenman KD. Occupational health disparities: a state public health-based approach. Am J Ind Med. 2014;57:596–604. https://doi.org/10.1002/ajim.22292
36. McCurdy SA, Portillo-Silva C, Sipan CL, Bang H, Emery KW. Risk for coccidioidomycosis among Hispanic farm workers, California, USA, 2018. Emerg Infect Dis. 2020;26:1430–7. https://doi.org/10.3201/eid2607.200024
37. Kassis C, Durkin M, Holbrook E, Myers R, Wheat L. Advances in diagnosis of progressive pulmonary and disseminated coccidioidomycosis. Clin Infect Dis. 2021;72:968–75. https://doi.org/10.1093/cid/ciaa188
38. Kupferwasser D, Miller LG. Sociodemographic factors associated with patients hospitalised for coccidioidomycosis in California and Arizona, State Inpatient Database 2005–2011. Epidemiol Infect. 2020;149:e127. https://doi.org/10.1017/S0950268820002836
39. Armstrong PA, Jackson BR, Haselow D, Fields V, Ireland M, Austin C, et al. Multistate epidemiology of histoplasmosis, United States, 2011–2014. Emerg Infect Dis. 2018;24:425–31. https://doi.org/10.3201/eid2403.171258
40. Benedict K, McCracken S, Signs K, Ireland M, Amburgey V, Serrano JA, et al. Enhanced surveillance for histoplasmosis—9 states, 2018–2019. Open Forum Infect Dis. 2020;7:ofaa343. https://doi.org/10.1093/ofid/ofaa343

41. McCree DH, Williams AM, Chesson HW, Beer L, Jeffries WL IV, Lemons A, et al. Changes in disparities in estimated HIV incidence rates among Black, Hispanic/Latino, and White men who have sex with men (MSM) in the United States, 2010–2015. J Acquir Immune Defic Syndr. 2019;81:57–62. https://doi.org/10.1097/QAI.0000000000001977
42. George IA, Spec A, Powderly WG, Santos CAQ. Comparative epidemiology and outcomes of human immunodeficiency virus (HIV), non-HIV non-transplant, and solid organ transplant associated cryptococcosis: a population-based study. Clin Infect Dis. 2018;66:608–11. https://doi.org/10.1093/cid/cix867
43. Prakash H, Chakrabarti A. Global epidemiology of mucormycosis. J Fungi (Basel). 2019;5:26. https://doi.org/10.3390/jof5010026
44. Loo DS. Cutaneous fungal infections in the elderly. Dermatol Clin. 2004;22:33–50. https://doi.org/10.1016/S0733-8635(03)00109-8
45. Barchiesi F, Orsetti E, Mazzanti S, Trave F, Salvi A, Nitti C, et al. Candidemia in the elderly: What does it change? PLoS One. 2017;12:e0176576. https://doi.org/10.1371/journal.pone.0176576
46. Dignani MC. Epidemiology of invasive fungal diseases on the basis of autopsy reports. F1000Prime Rep. 2014;6:81. https://doi.org/10.12703/P6-81

Address for correspondence: Emily Rayens, University of Georgia, 119 Carlton St, Athens, GA 30605, USA; email: emily.rayens25@uga.edu

Seasonality of Common Human Coronaviruses, United States, 2014–2021[1]

Melisa M. Shah, Amber Winn, Rebecca M. Dahl, Krista L. Kniss, Benjamin J. Silk, Marie E. Killerby

The 4 common types of human coronaviruses (HCoVs)—2 alpha (HCoV-NL63 and HCoV-229E) and 2 beta (HCoV-HKU1 and HCoV-OC43)—generally cause mild upper respiratory illness. Seasonal patterns and annual variation in predominant types of HCoVs are known, but parameters of expected seasonality have not been defined. We defined seasonality of HCoVs during July 2014–November 2021 in the United States by using a retrospective method applied to National Respiratory and Enteric Virus Surveillance System data. In the 6 HCoV seasons before 2020–21, season onsets occurred October 21–November 12, peaks January 6–February 13, and offsets April 18–June 27; most (>93%) HCoV detection was within the defined seasonal onsets and offsets. The 2020–21 HCoV season onset was 11 weeks later than in prior seasons, probably associated with COVID-19 mitigation efforts. Better definitions of HCoV seasonality can be used for clinical preparedness and for determining expected patterns of emerging coronaviruses.

The 4 common human coronaviruses (HCoVs), 2 alpha (HCoV-NL63 and HCoV-229E) and 2 beta (HCoV-HKU1 and HCoV-OC43) types, generally cause mild upper respiratory illness. The HCoVs are endemic among humans, as evidenced by sustained, widespread, continuous transmission, unlike the betacoronaviruses SARS-CoV (detected in 2002) and Middle East respiratory syndrome coronavirus (detected in 2012). An additional betacoronavirus, SARS-CoV-2, emerged in the human population in late 2019 and has become widespread. HCoVs circulate annually in the United States with a seasonal pattern, generally peaking during December–March and with the predominant types varying each year (*1*).

Although HCoVs are known to have seasonal patterns, parameters of expected seasonality have not been defined. Given mitigation efforts and behavior changes resulting from the COVID-19 pandemic, national patterns of respiratory viruses, including influenza, differed during the 2020–21 season compared with previous seasons (*2*). Knowledge of changes to seasonal patterns in HCoV circulation is valuable for clinical and public health preparedness and may provide insight into transmission patterns for novel HCoVs. We analyzed circulation of 4 common HCoVs in the United States during July 2014–November 2021.

Methods

We analyzed circulation of HCoVs (HCoV-NL63, HCoV-229E, HCoV-HKU1, and HCoV-OC43, excluding SARS-CoV-2) by using data from the National Respiratory and Enteric Viruses Surveillance System (NREVSS, https://www.cdc.gov/surveillance/nrevss/labs/map.html), a passive surveillance system established by the Centers for Disease Control and Prevention (CDC) in the 1980s. NREVSS collects respiratory virus testing results from laboratories across the United States. Not all NREVSS laboratories submit results for all pathogen types, and ≈344 laboratories met the criteria for inclusion in our analysis. Clinical, public health, and commercial laboratories submit weekly aggregated numbers of tests performed and detections determined by reverse transcription PCR for the 4 common HCoV types. Although most NREVSS participants provide aggregated data, NREVSS also collects specimen-level data from a subset of 57 laboratories through the Public Health Laboratory Interoperability Project (PHLIP). Laboratories that submit data to NREVSS via PHLIP include information on patient age, administrative sex, and other respiratory virus test results.

Author affiliation: Centers for Disease Control and Prevention, Atlanta, Georgia, USA

DOI: https://doi.org/10.3201/eid2810.220396

[1]Preliminary results from this study were presented at the IDWeek Virtual Conference 2021, September 29–October 3, 2021.

The first week in the second surveillance year when common coronaviruses were surveyed in NREVSS ended on July 5, 2014. We included reports of specimens tested for HCoVs in NREVSS from the week ending July 5, 2014, through the week ending November 6, 2021. We excluded HCoV results without virus typing and data from laboratories that did not report any positive HCoV test results during the study period. We compiled total HCoV testing and positive detections by HCoV type, season, and US Census region. To characterize detections by patient age and sex, we used a subset of data submitted through PHLIP with specimens tested for all 4 HCoV types collected from June 29, 2014, through November 29, 2021 (because of data availability, we included a few additional weeks compared with NREVSS). We also examined codetection of HCoVs with other respiratory viruses in the PHLIP subset, including parainfluenza viruses, respiratory syncytial virus (RSV), human metapneumovirus, human adenovirus, rhinovirus/enterovirus, and influenza A and B viruses. We excluded specimens with panpositive results for codetections in the PHLIP subset.

We evaluated the onset and offset of seasons between MMWR week 31 (early August) through MMWR week 30 of the following year (https://ndc.services.cdc.gov/wp-content/uploads/MMWR_Week_overview.pdf) by using a method from NREVSS previously validated for RSV detection. This method (retrospective slope 10 method) is characterized by a centered, 5-week moving average of weekly detections with each seasonal peak normalized to 1,000 detections (*3*). We determined the absolute difference between normalized detections for each week and the previous week. We defined season onset as the second consecutive week with an absolute difference of ≥10 normalized detections and season offset as the last of 2 consecutive weeks when the number of normalized detections was greater than the number of normalized detections during the onset week. We determined seasonal characteristics nationally, including season onset, peak, and offset as well as season duration and percentage of annual detections that occurred within the season. We calculated the mean MMWR week for which seasonal inflections occurred by taking the mean of the MMWR weeks of the 6 seasons starting with 2014–15 and ending with 2019–20.

For our analyses, we used RStudio version 1.4.1106 (https://www.rstudio.com). This study was reviewed by CDC and conducted consistent with applicable federal law and CDC policy (45 C.F.R. part 46.102(l) (2), 21 C.F.R. part 56; 42 U.S.C. Sect. 241(d); 5 U.S.C. Sect. 552a; 44 U.S.C. Sect. 3501 et seq.).

Results

We detected an HCoV of any type in 104,911 (3.6%) of 2,878,479 specimens with results submitted to NREVSS during the week ending July 5, 2014, through November 6, 2021. Among these 104,911 specimens, 40.1% were positive for HCoV-OC43, 27.8% for HCoV-NL63, 19.9% for HCoV-HKU1, and 12.2% for HCoV-229E. Weekly testing volumes were higher during March 2020, the onset of the COVID-19 pandemic, than during any other week in July 2014 and November 2021 (Figure 1, panel A). The predominant common HCoV type fluctuated by surveillance year (Figure 1, panel B).

In the 6 HCoV seasons before the COVID-19 pandemic (i.e., excluding the 2020–21 season), seasonal onsets were during October–November, peaks during January–February, and seasonal offsets during April–June (Table 1; Figure 2). Specifically, the seasonal onset occurred on average during MMWR week 44 (range weeks 42–45), peak during week 4 (range weeks 1–6), and offset during week 19 (range weeks 17–25) (Table 1; Figure 3); 93.2% of all HCoV detections occurred between the onset and offset. The mean duration of the 6 seasons before the 2020–21 season was 25 weeks. The 2020–21 common HCoV season onset was delayed by 11 weeks compared with mean onset of prior seasons (Table 1; Figure 3). The number of days between onset and peak for the 2020–21 season (119 days) was longer than the mean observed for the prior 6 seasons (88 days). By November 2021, normalized values had not reached the requirement for offset for the 2020–21 season.

The predominant type of alpha HCoV was HCoV-NL63 during 4 of the 7 seasons (Figure 1, panel C). When positivity for either HCoV-229E or HCoV-NL63 was >4%, positivity for the other alpha HCoV was <1% (Figure 1, panel C). The predominant beta HCoV type was HCoV-OC43, in a biennial pattern alternating with HCoV-HKU1 (Figure 1, panel D) except for 2017–18, when they were co-dominant. When positivity for either beta HCoV peaked at >4%, the other beta HCoV circulated at low levels (<1% positivity), except for the 2015–16 season (Figure 1, panel D). Across US Census regions, patterns of the predominant HCoV type were similar to national patterns (Appendix Figure 1, https://wwwnc.cdc.gov/EID/article/28/10/22-0396-App1.pdf).

Among 82,768 specimens from PHLIP tested for the 4 HCoVs from June 29, 2014, through November 29, 2021, any HCoV was detected in 5,204 (6.3%) (Table 2). We excluded 3 specimens because their reports indicated positive results for all respiratory viruses. Among 80,574 PHLIP specimens with information on

patient sex, the percentage of specimens in which any HCoV was detected was similar among male (6.0%, 2,617/43,694) and female (6.2%, 2,284/36,880) patients. Of the 4 types of HCoV, detection of HCoV-OC43 was highest among children <1 years of age and adults 66–100 years of age (Table 2). HCoV-229E was detected in patients with the highest mean age and at the lowest percentages among children ≤5 years of age. Of specimens in which HCoV was detected, >1 type was detected in 64/5,204 (1.2%) and another respiratory virus was detected in 1,132/4,685 (24.2%); co-detection of influenza virus was most common (8.1%) (Table 3).

Discussion

During the 6 seasons of HCoV circulation before the COVID-19 pandemic in 2020–21, the relative consistency of timing of seasonal onsets, peaks, and offsets indicates expected patterns in the seasonality of HCoVs in the United States. The predominant type of HCoV varied from season to season, but at least 1 alpha HCoV and 1 beta HCoV circulated each season,

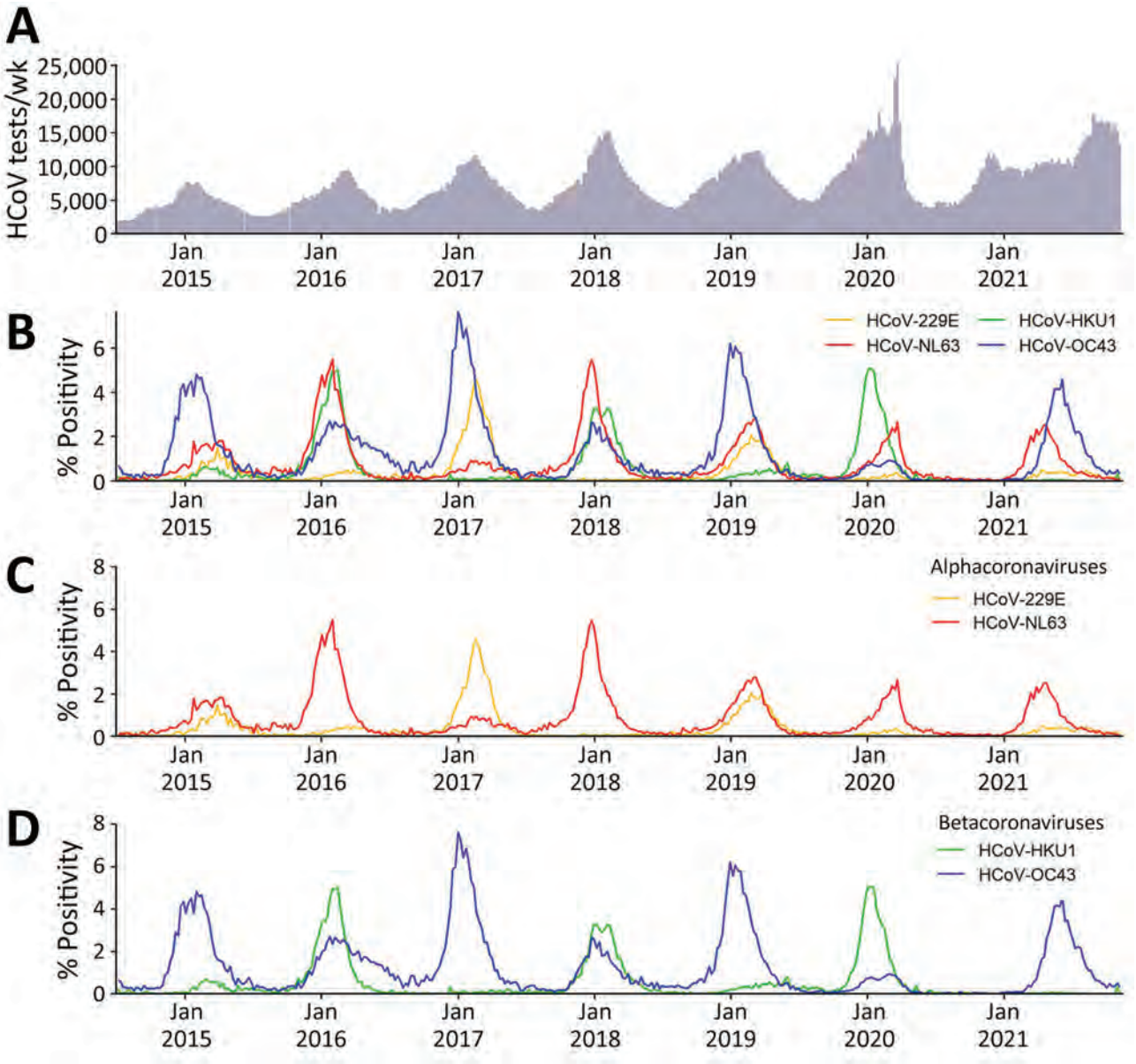

Figure 1. Total tests and percentage positivity of 4 common HCoVs from weekly aggregated data submitted to the National Respiratory and Enteric Virus Surveillance System, United States, July 2014–November 2021. A) Total specimens tested for all 4 HCoV types. B) Percentage positivity of the 4 HCoV types by week. C) Percentage positivity of the common alphacoronaviruses. D) Percentage positivity of the common betacoronaviruses. HCoVs, human coronaviruses.

Table 1. Onset, peak, and offset dates for 4 common HCoVs and percentage detection, by season, from weekly aggregated data submitted to the National Respiratory and Enteric Virus Surveillance System, United States, July 2014–November 2021*

	Date (MMWR wk)			HCoV, %			
Season (MMWR wk)	Onset	Peak	Offset	OC43	NL63	HKU1	229E
2014–15 (31–30)	2014 Nov 1 (44)	2015 Feb 7 (5)	2015 Jun 27 (25)	6.3	23.5	58.8	11.4
2015–16 (31–30)	2015 Nov 7 (44)	2016 Feb 13 (6)	2016 May 14 (19)	31.1	34.8	29.4	4.8
2016–17 (31–30)	2016 Nov 12 (45)	2017 Feb 4 (5)	2017 Apr 29 (17)	1.8	10.0	56.8	31.4
2017–18 (31–30)	2017 Oct 21 (42)	2018 Jan 6 (1)	2018 Apr 21 (16)	33.5	39.3	25.8	1.4
2018–19 (31–30)	2018 Nov 10 (45)	2019 Feb 9 (6)	2019 May 11 (19)	5.8	25.3	49.9	19.0
2019–20 (31–30)	2019 Nov 2 (44)	2020 Jan 18 (3)	2020 Apr 18 (16)	51.9	29.5	14.2	4.3
2020–21 (31–44)	2021 Jan 23 (03)	2021 May 22 (20)	Not reached†	1.6	31.6	55.8	10.9

*Dates for season onset, peak, and offset for all seasons are based on the retrospective slope 10 method, which uses a centered 5-week moving average of weekly detections with normalization to peak to define seasonal inflections. Seasons were defined as starting on MMWR week 31 (beginning of August) of each year through MMWR week 30 (end of July) of the following year (https://ndc.services.cdc.gov/wp-content/uploads/MMWR_Week_overview.pdf). For the last 2020–21 season, data were included from August 2021–November 2022 because of the delayed seasonal start. The percent of positive detections by each HCoV type by season (with the denominator being total positive detections of any HCoV type for that season) is included in the final 4 columns. HCoV, human coronavirus.
†By November of 2021, normalized values had not reached the requirement for offset for the 2020–21 season.

often in a biennial pattern, as in other northern latitude countries (*4*,*5*). This biennial pattern may reflect cross-immunity and waning population-level immunity to alpha and beta HCoVs from prior infections (*6*) because serologic and human studies suggest immunity to reinfection lasting ≈1 year (*7*,*8*).

Cross-reactive binding and neutralizing antibodies seem to be higher among common HCoV types within a genus (*9*). SARS-CoV-2 cross-reactive serum antibodies were present in serum before the COVID-19 pandemic, probably attributable to cross-immunity from prior HCoV infections, but they have not been shown to be protective against SARS-CoV-2 infection (*10*). Similarly, nonneutralizing antibodies to the common betacoronaviruses are boosted after SARS-CoV-2 infection (*10*), but potential effects of

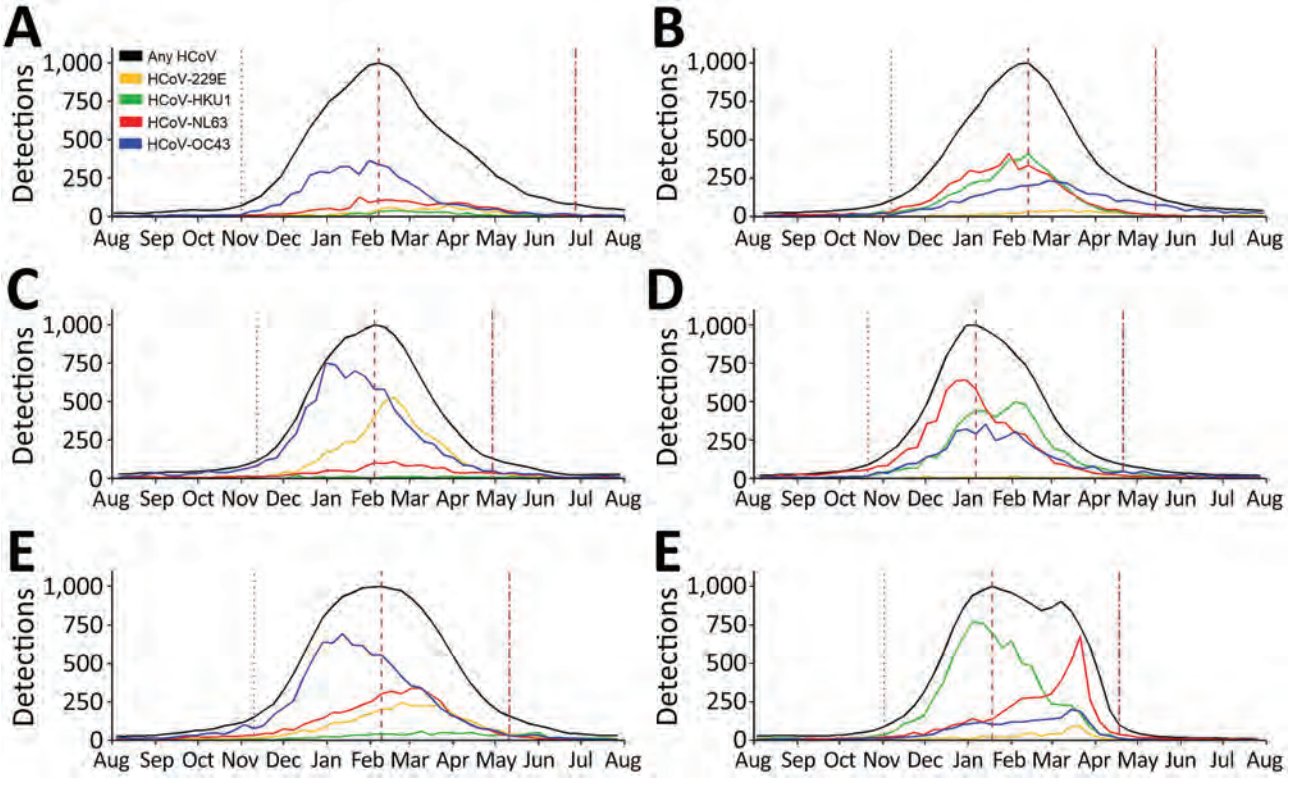

Figure 2. Total number of detections of the 4 common HCoVs, by week and season, from weekly aggregated data submitted to the National Respiratory and Enteric Virus Surveillance System, United States, July 2014–July 2020. The 3 vertical dotted lines, left to right, indicate the week of season onset, peak, and offset for all types combined (black line). These seasonal inflections were defined by using the retrospective slope 10 method, which uses a centered 5-week moving average of weekly detections with normalization to peak. The type-specific curves depict the actual number of detections; the black curve depicts specimens with any HCoV detections normalized to a peak of 1,000. HCoVs, human coronaviruses.

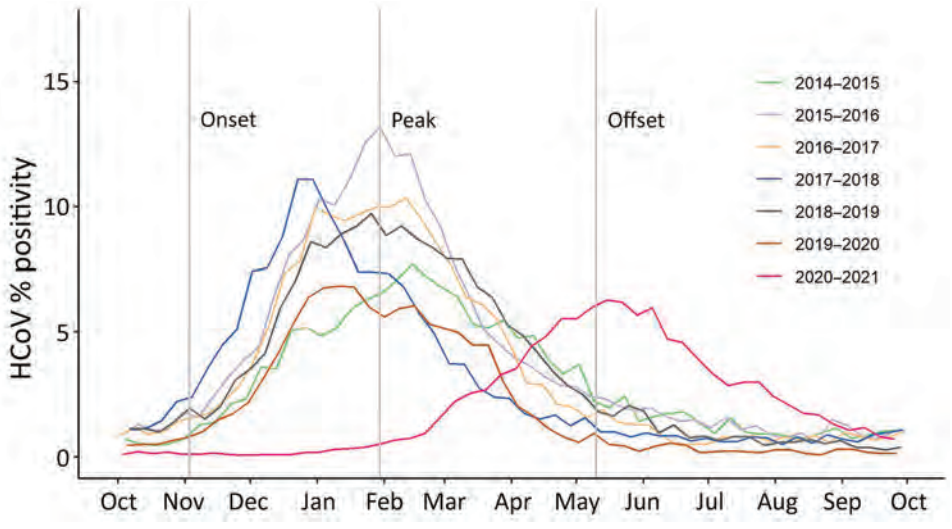

Figure 3. Percentage positivity and seasonal characteristics of common HCoVs, by season, from weekly aggregated data submitted to the National Respiratory and Enteric Virus Surveillance System, United States, October 2014–September 2021. Gray vertical lines indicate the mean starting week dates for season onset, peak, and offset for all seasons except 2020–21, based on the retrospective slope 10 method, which uses a centered 5-week moving average of weekly detections with normalization to peak to define seasonal inflections. The average onset week for the 6 seasons spanning 2014–2020 is MMWR week 44, average peak week is MMWR week 4, and the average offset week is MMWR week 19. For the 2020–21 season, the onset week is January 23 (MMWR week 3) and the peak week is May 22 (MMWR week 20) (not shown). HCoVs, human coronaviruses.

SARS-CoV-2 immunity on seasonal HCoV circulation remain unknown.

The seasonality of HCoVs probably results from a combination of viral, host, and environmental factors. In temperate climates, HCoVs circulate during the winter, aligned with cooler ambient temperature (*11*,*12*); seasonality is more varied and less predictable in tropical regions than in temperate regions (*4*,*13*). Colder temperatures are thought to improve the stability of enveloped viruses (*14*). In addition, lower temperatures lead to drying of airways and can increase host susceptibility to infection. Environmental factors can also lead to behavior change, which affects the spread of HCoVs, such as from more indoor human contact during winter (*14*). Similarly, other widespread behavior changes could alter the seasonality of HCoV circulation.

The pattern of HCoV circulation during the 2020–21 season differed from that during prior seasons; onset was delayed by 11 weeks compared with the mean of prior seasons, and duration to peak was extended. The 2020–21 season offset could not be determined because the number of detections had not fallen to low enough levels at the time of this analysis. In the United States, the seasonal starts of RSV and parainfluenza virus circulation were delayed during 2020–21, and influenza virus and human metapneumovirus circulation was attenuated (*2*,*15*). Activity of rhinovirus/enterovirus and human adenovirus was lower than usual at the beginning of the season, but activity increased to prepandemic levels later in the season. These changes are probably attributable in part to implementation of COVID-19 pandemic mitigation measures, such as decreased domestic and global travel, use of face masks, school and office closures, and physical distancing (*2*).

Certain clinical and phenotypic differences in the 4 seasonal HCOVs have been observed (e.g., distribution of patient sex and age and virus pathogenicity). HCoV-OC43 has been reported as the most prevalent

Table 2. Percentage positivity of the 4 common HCoVs, by patient sex and age categories, Public Health Laboratory Interoperability Project, United States, July 2014-November 2021

	HCoV, no. detected/no. tested (%)				
Patient category	Any	OC43	NL63	HKU1	229E
Total	5,204/82,768 (6.3)	2,056/82,768 (2.5)	1,519/82,768 (1.8)	962/8,276 (1.2)	732/82,768 (0.9)
Sex					
F	2,284/36,880 (6.2)	902/36,880 (2.4)	680/36,880 (1.8)	433/36,880 (1.2)	294/36,880 (0.8)
M	2,617/43,694 (6.0)	1,025/43,694 (2.3)	767/43,694 (1.8)	499/43,694 (1.1)	363/43,694 (0.8)
Age group, y*					
<1	578/4,788 (12.1)	271/4,788 (5.7)	144/4,788 (3.0)	110/4,788 (2.3)	62/4,788 (1.3)
1–5	795/9,501 (8.4)	349/9,501 (3.7)	271/9,501 (2.9)	146/9,501 (1.5)	47/9,501 (0.5)
6–17	517/9,568 (5.4)	147/9,568 (1.5)	207/9,568 (2.2)	92/9,568 (1.0)	77/9,568 (0.8)
18–65	2,738/50,240 (5.4)	994/50,240 (2.0)	781/50,240 (1.6)	566/50,240 (1.1)	425/50,240 (0.8)
>65	364/7,092 (5.1)	198/7,092 (2.8)	77/7,092 (1.1)	35/7,092 (0.5)	57/7,092 (0.8)

*Mean age (± SD), y: any, 25.8 (± 22.7); OC43, 27.3 (± 25.3); NL63, 22.9 (± 20.5); HKU1, 24.0 (± 19.8); 229E, 29.9 (± 21.8). HCoV, human coronavirus.

Table 3. Respiratory co-detections by common HCoV type, Public Health Laboratory Interoperability Project, July 2014–November 2021*

	HCoV, no. tested/no. detected (%)				
Virus co-detected	Any, n = 5,204	OC43, n = 2,056	NL63, n = 1,519	HKU1, n = 962	229E, n = 732
Any non-HCoV	1,132/4,685 (24.2)	447/1,831 (24.4)	289/1,357 (21.3)	217/893 (24.3)	161/657 (24.5)
Influenza virus	422/5,178 (8.1)	146/2,046 (7.1)	126/1,513 (8.3)	87/960 (9.1)	73/724 (10.1)
Rhinovirus/enterovirus	268/5,200 (5.2)	116/2,055 (5.6)	85/1,518 (5.6)	44/960 (4.6)	26/732 (3.6)
Respiratory syncytial virus	254/5,203 (4.9)	136/2,056 (6.6)	54/1,519 (3.6)	46/961 (4.8)	23/732 (3.1)
Respiratory adenovirus	158/5,202 (3.0)	80/2,054 (3.9)	38/1,519 (2.5)	28/962 (2.9)	16/732 (2.2)
Parainfluenza virus	99/5,204 (1.9)	43/2,056 (2.1)	19/1,519 (1.3)	19/962 (2.0)	20/732 (2.7)
Human metapneumovirus	95/5,204 (1.8)	29/2,056 (1.4)	27/1,519 (1.8)	26/962 (2.7)	15/732 (2.0)
HCoV co-detected					
≥2 HCoV types	64/5,204 (1.2)	40/2,056 (1.9)	45/1,519 (3.0)	26/962 (2.7)	18/732 (2.5)
OC43	2,056/5,204 (39.5)	NA	21/1,519 (1.4)	6/962 (0.6)	14/732 (1.9)
NL63	1,519/5,204 (29.2)	21/2,056 (1.0)	NA	20/962 (2.1)	5/732 (0.7)
HKU1	962/5,204 (18.5)	6/2,056 (0.3)	20/1,519 (1.3)	NA	0/732 (0)
229E	732/5,204 (14.1)	14/2,056 (0.7)	5/1,519 (0.3)	0/962 (0)	NA

*HCoV, human coronavirus; NA, not applicable.

of the 4 common HCoVs, consistent with our findings (*12*). A previous study reported male sex as being associated with higher odds of HCoV positivity (*16*), but in our study, likelihood of HCoV detection was not higher among male patients.

HCoVs circulate seasonally with other respiratory viruses, including RSV, influenza virus, and rhinoviruses; co-infections are not uncommon (*17*,*18*). We similarly show high levels of HCoV co-detections (24%), particularly with influenza virus, which is probably an underestimate because only influenza virus detections from respiratory panels are included in the PHLIP dataset. Further work is needed to understand mechanisms of viral interference and the role of virus co-infections in the pathophysiology of illness and circulation of respiratory viruses.

Among the limitations of this investigation, testing patterns for respiratory viruses changed during the 2020–21 season because of delayed routine healthcare and an emphasis on SARS-CoV-2 testing, which affects comparison with earlier seasons. The representativeness of co-detections reported (i.e., true burden of illness) could not be evaluated because this PHLIP platform does not include reasons for testing (e.g., symptomatic disease); positive detections may be more likely to be reported than negative detections. The NREVSS platform represents a geographically heterogenous subset of all US laboratories but may not be nationally or locally representative. Furthermore, types of laboratory participation and the process for obtaining the subset of specimen level data for PHLIP are not fully comparable with the overall NREVSS platform.

According to our analysis, a typical common HCoV season in the United States generally starts during October–November, peaks near the end of January, and ends during April–June. This knowledge of expected seasonal variation in HCoV circulation is useful for public health preparedness and clinical management of patients. Clinicians and the public health community should be aware that patterns of HCoV circulation changed during 2020–21 and that trends in future seasons may also deviate from trends before the COVID-19 pandemic.

Acknowledgment

We thank Phillip Salvatore for his assistance.

This work was supported by CDC.

About the Author

Dr. Shah is a recent graduate of the Epidemic Intelligence Service in the Respiratory Viruses Branch, Division of Viral Diseases, National Center for Immunization and Respiratory Diseases, CDC, and an infectious diseases physician. Her research interests include the circulation of viral diseases and the natural history of SARS-CoV-2.

References

1. Killerby ME, Biggs HM, Haynes A, Dahl RM, Mustaquim D, Gerber SI, et al. Human coronavirus circulation in the United States 2014–2017. J Clin Virol. 2018;101:52–6.
2. Olsen SJ, Winn AK, Budd AP, Prill MM, Steel J, Midgley CM, et al. Changes in influenza and other respiratory virus activity during the COVID-19 pandemic—United States, 2020–2021. MMWR Morb Mortal Wkly Rep. 2021;70:1013–9. https://doi.org/10.15585/mmwr.mm7029a1
3. Midgley CM, Haynes AK, Baumgardner JL, Chommanard C, Demas SW, Prill MM, et al. Determining the seasonality of respiratory syncytial virus in the United States: the impact of increased molecular testing. J Infect Dis. 2017;216:345–55. https://doi.org/10.1093/infdis/jix275
4. Li Y, Wang X, Nair H. Global seasonality of human seasonal coronaviruses: a clue for postpandemic circulating season of severe acute respiratory syndrome coronavirus 2? J Infect Dis. 2020;222:1090–7. https://doi.org/10.1093/infdis/jiaa436
5. Hawkes MT, Lee BE, Kanji JN, Zelyas N, Wong K, Barton M, et al. Seasonality of respiratory viruses at northern latitudes. JAMA Netw Open. 2021;4:e2124650. https://doi.org/10.1001/jamanetworkopen.2021.24650
6. Kissler SM, Tedijanto C, Goldstein E, Grad YH, Lipsitch MJS. Projecting the transmission dynamics of SARS-CoV-2

through the postpandemic period. Science. 2020;368:860–8.
7. Edridge AWD, Kaczorowska J, Hoste ACR, Bakker M, Klein M, Loens K, et al. Seasonal coronavirus protective immunity is short-lasting. Nat Med. 2020;26:1691–3. https://doi.org/10.1038/s41591-020-1083-1
8. Callow KA, Parry HF, Sergeant M, Tyrrell DA. The time course of the immune response to experimental coronavirus infection of man. Epidemiol Infect. 1990;105:435–46. https://doi.org/10.1017/S0950268800048019
9. Gorse GJ, Donovan MM, Patel GB. Antibodies to coronaviruses are higher in older compared with younger adults and binding antibodies are more sensitive than neutralizing antibodies in identifying coronavirus-associated illnesses. J Med Virol. 2020;92:512–7. https://doi.org/10.1002/jmv.25715
10. Anderson EM, Goodwin EC, Verma A, Arevalo CP, Bolton MJ, Weirick ME, et al.; UPenn COVID Processing Unit. Seasonal human coronavirus antibodies are boosted upon SARS-CoV-2 infection but not associated with protection. Cell. 2021;184:1858–1864.e10. https://doi.org/10.1016/j.cell.2021.02.010
11. Aldridge RW, Lewer D, Beale S, Johnson AM, Zambon M, Hayward AC, et al.; Flu Watch Group. Seasonality and immunity to laboratory-confirmed seasonal coronaviruses (HCoV-NL63, HCoV-OC43, and HCoV-229E): results from the Flu Watch cohort study. Wellcome Open Res. 2020;5:52. https://doi.org/10.12688/wellcomeopenres.15812.2
12. Nickbakhsh S, Ho A, Marques DFP, McMenamin J, Gunson RN, Murcia PR. Epidemiology of seasonal coronaviruses: establishing the context for the emergence of coronavirus disease 2019. J Infect Dis. 2020;222:17–25. https://doi.org/10.1093/infdis/jiaa185
13. Komabayashi K, Seto J, Matoba Y, Aoki Y, Tanaka S, Ikeda T, et al. Seasonality of human coronavirus OC43, NL63, HKU1, and 229E infection in Yamagata, Japan, 2010-2019. Jpn J Infect Dis. 2020;73:394–7. https://doi.org/10.7883/yoken.JJID.2020.525
14. Price RHM, Graham C, Ramalingam S. Association between viral seasonality and meteorological factors. Sci Rep. 2019;9:929. https://doi.org/10.1038/s41598-018-37481-y
15. Olsen SJ, Azziz-Baumgartner E, Budd AP, Brammer L, Sullivan S, Pineda RF, et al. Decreased influenza activity during the COVID-19 pandemic–United States, Australia, Chile, and South Africa, 2020. MMWR Morb Mortal Wkly Rep. 2020;69:1305–9. https://doi.org/10.15585/mmwr.mm6937a6
16. Dyrdak R, Hodcroft EB, Wahlund M, Neher RA, Albert J. Interactions between seasonal human coronaviruses and implications for the SARS-CoV-2 pandemic: a retrospective study in Stockholm, Sweden, 2009–2020. J Clin Virol. 2021; 136:104754.
17. Gaunt ER, Hardie A, Claas EC, Simmonds P, Templeton KE. Epidemiology and clinical presentations of the four human coronaviruses 229E, HKU1, NL63, and OC43 detected over 3 years using a novel multiplex real-time PCR method. J Clin Microbiol. 2010;48:2940–7. https://doi.org/10.1128/JCM.00636-10
18. Lu R, Yu X, Wang W, Duan X, Zhang L, Zhou W, et al. Characterization of human coronavirus etiology in Chinese adults with acute upper respiratory tract infection by real-time RT-PCR assays. PLoS One. 2012;7:e38638. https://doi.org/10.1371/journal.pone.0038638

Address for correspondence: Melisa M. Shah, Centers for Disease Control and Prevention, 1600 Clifton Rd NE, Mailstop H24-5, Atlanta, GA 30329-4027, USA; email: bgn3@cdc.gov

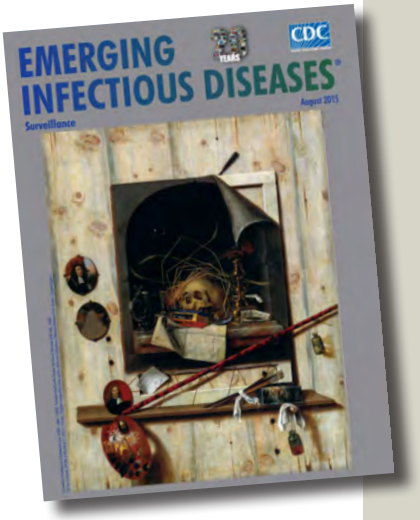

Originally published in August 2015

etymologia revisited

Escherichia coli

[esh″ə-rik′e-ə co′lī]

A gram-negative, facultatively anaerobic rod, *Escherichia coli* was named for Theodor Escherich, a German-Austrian pediatrician. Escherich isolated a variety of bacteria from infant fecal samples by using his own anaerobic culture methods and Hans Christian Gram's new staining technique. Escherich originally named the common colon bacillus *Bacterium coli commune*. Castellani and Chalmers proposed the name *E. coli* in 1919, but it was not officially recognized until 1958.

Sources:

1. Oberbauer BA. Theodor Escherich—Leben und Werk. Munich: Futuramed-Verlag; 1992.
2. Shulman ST, Friedmann HC, Sims RH. Theodor Escherich: the first pediatric infectious diseases physician? Clin Infect Dis. 2007;45:1025–9 .

https://wwwnc.cdc.gov/eid/article/21/8/et-2108_article

Rapid Increase in Suspected SARS-CoV-2 Reinfections, Clark County, Nevada, USA, December 2021

Jeanne Ruff, Ying Zhang, Matthew Kappel, Sfurti Rathi, Kellie Watkins, Lei Zhang, Cassius Lockett

Genetic differences between SARS-CoV-2 variants raise concerns about reinfection. Public health authorities monitored the incidence of suspected reinfection in Clark County, Nevada, USA, during March 2020–March 2022. Suspected reinfections, defined as a second positive PCR test collected ≥90 days after an initial positive test, were monitored through an electronic disease surveillance system. We calculated the proportion of all new cases per week that were suspected reinfections and rates per 1,000 previously infected persons by demographic groups. The rate of suspected reinfection remained ≤2.7% until December 2021, then increased to ≈11%, corresponding with local Omicron variant detection. Reinfection rates were higher among adults 18–50 years of age, women, and minority groups, especially persons identifying as American Indian/Alaska Native. Suspected reinfection became more common in Clark County after introduction of the Omicron variant, and some demographic groups are disproportionately affected. Public health surveillance could clarify the SARS-CoV-2 reinfection burden in communities.

The emergence of new SARS-CoV-2 variants with antibody-evading mutations raises concerns about variable levels of protection against infection after prior infection or vaccination (*1*). The Omicron variant is genetically divergent from previous variants, exacerbating these concerns (*1*). Reinfection with SARS-CoV-2 after previous infection has been demonstrated through a comparison of viral genomes collected from the same person (*2*). However, without genomic sequencing, reinfection can be difficult to distinguish from prolonged viral shedding. Available evidence suggests an interval of at least 90 days between positive tests is more likely to indicate reinfection than prolonged viral shedding (*3*).

Public health authorities at the Southern Nevada Health District (SNHD) conducted surveillance of suspected reinfections in Clark County, Nevada, USA, to determine whether previously infected persons were protected against reinfection with new variants and to estimate the proportion of COVID-19 cases that occurred among persons with previous SARS-CoV-2 infections. SNHD also compared rates of suspected reinfection between demographic groups to characterize the groups most affected by suspected reinfection in Clark County and determine whether any groups were disproportionately affected. We report findings from surveillance of suspected reinfection with SARS-CoV-2 and rates of suspected reinfection among demographic groups in Clark County during March 2020–March 2022.

Methods

Health care providers, medical facilities, laboratories, and other out-of-state health departments report positive SARS-CoV-2 PCR test results for residents of Clark County to SNHD. These results are collected in an electronic disease surveillance system. We calculated intervals between the specimen collection date from each person's initial positive PCR test and subsequent positive PCR tests. We considered a subsequent positive PCR test with specimen collection ≥90 days after specimen collection of the initial positive PCR test to be a suspected reinfection (*3*). Repeat positive PCR tests with specimen collection dates <90 days after the specimen collection of an initial positive PCR test were not considered suspected reinfections and were excluded from the analysis.

We calculated the proportion of new cases per week that were suspected reinfections by dividing the number of suspected reinfections by all new PCR-identified

Author affiliations: Centers for Disease Control and Prevention, Atlanta, Georgia, USA (J. Ruff); Southern Nevada Health District, Las Vegas, Nevada, USA (Y. Zhang, M. Kappel, S. Rathi, K. Watkins, L. Zhang, C. Lockett)

DOI: https://doi.org/10.3201/eid2810.221045

cases during the same week. We also identified suspected third infections, defined as a third positive PCR test collected at least 90 days after specimen collection of a second positive PCR test that met the above definition of suspected reinfection (*3*). Because of a small number of suspected third infections, we did not calculate the proportion of cases for suspected third infections.

We gathered demographic information from case investigation data. We calculated the rate of suspected reinfections per 1,000 previously infected persons by age group, sex, and race/ethnicity. We calculated odds ratio (OR), 95% CI, and p value by using logistic regression and performed all analyses in SAS version 9.4 (SAS Institute Inc., https://www.sas.com). This activity was reviewed by the US Centers for Disease Control and Prevention (CDC) and was conducted consistent with CDC policy and applicable federal law, including the following Code of Federal Regulations (CFR) and US Code (USC): 45 CFR part 46; 21 CFR part 56; 42 USC Section 241(d); 5 USC Section 552a; 44 USC Section 3501 et seq.

Results

During March 2020–April 2, 2022, SNHD identified 19,589 suspected reinfections in Clark County; reinfections began occurring in June 2020. The incidence of suspected reinfection remained <0.5% of new cases until February 2021 (Figure 1). During the last week of February 2021, the incidence increased to ≈2% of all new cases. This increase in suspected reinfections occurred after the Alpha variant (B.1.1.7) was detected in Clark County in late January 2021 (*4*). During March 2021–November 2021, incidence of suspected reinfection remained at 1%–2.7% of cases, even after the Delta variant was detected in Clark County in May 2021 (*5*). In December 2021, we observed a rapid increase in the incidence of suspected reinfection, from 2% during the week of December 5–11 to 11% during the week of December 19–25. This rapid increase corresponded with an unprecedented rise in first-time infections and detection of the Omicron variant, which was reported in Clark County on December 14, 2021 (*6*). Although the weekly number of both suspected reinfections and first-time infections decreased substantially after a peak during the first week of January 2022, the proportion of suspected reinfection cases remained elevated, near 11%, through March 2022.

The rate of suspected reinfection was highest among adults 18–49 years of age; rates were 49/1,000 cases for persons 18–24 years of age and 46/1,000 cases for persons 25–49 years of age (Table). The odds that children <5 years of age were reinfected (15/1,000 cases; OR 0.30, 95% CI 0.26–0.35) was 70% lower than that for adults 18–24 years of age. Adults ≥65 years of age had 58% lower odds of suspected reinfection (rate 21/1,000 cases; OR 0.42, 95% CI 0.40–0.45) than adults 18–24 years of age. Women had a higher suspected reinfection rate (44/1,000 cases) than men (33/1,000 cases) and had 36% higher odds of suspected reinfection compared with men (OR 1.36, 95% CI 1.32–1.40). Persons identifying as American Indian/Alaska Native had a higher rate of suspected reinfection (53/1,000 cases) than other racial and ethnic groups; persons identifying as Hispanic had rates of 48/1,000 cases, persons identifying as multiracial had 43/1,000 cases, and persons identifying as non-Hispanic Black had 40/1,000 cases. We observed lower suspected reinfection rates among persons identifying

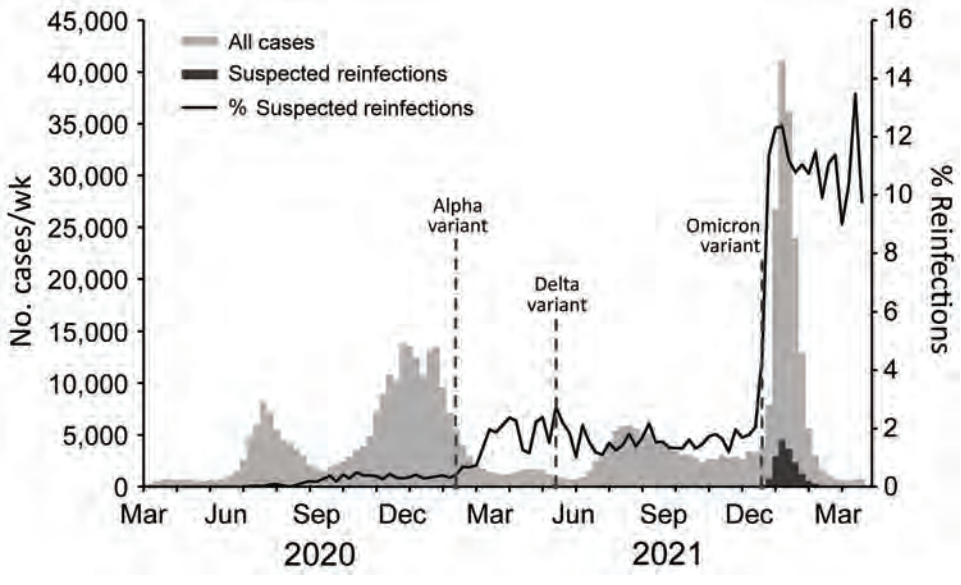

Figure 1. SARS-CoV-2 cases and suspected reinfections, Clark County, Nevada, USA, March 2020–March 2022. Dotted lines show timeframe for identification of Alpha, Delta, and Omicron SARS-CoV-2 variants in Clark County. New cases were defined as a first positive SARS-CoV-2 PCR test for a person. Suspected reinfections were defined as a second positive SARS-CoV-2 PCR test collected ≥90 days after a person's first positive PCR test.

Table. Characteristics of persons with suspected SARS-CoV-2 reinfections, Clark County, Nevada, USA, December 2021

Characteristics	Suspected reinfection rate per 1,000 primary cases	Odds ratio (95% CI)	p value
Age group, y			
0–4	15	0.30 (0.26–0.35)	<0.0001
5–17	29	0.58 (0.55–0.62)	<0.0001
18–24	49	Referent	Referent
25–49	46	0.95 (0.91–0.99)	0.0246
50–64	33	0.66 (0.63–0.69)	<0.0001
≥65 years	21	0.42 (0.40–0.45)	<0.0001
Sex			
F	44	1.36 (1.32–1.40)	<0.0001
M	33	Referent	Referent
Race/ethnicity*			
American Indian/Alaska Native	53	1.55 (1.10–2.19)	0.0116
Asian or Pacific Islander	38	1.08 (1.02–1.14)	0.0087
Black	40	1.17 (1.10–1.23)	<0.0001
Hispanic	48	1.40 (1.34–1.45)	<0.0001
Multiracial	43	1.26 (0.98–1.62)	0.0771
White	35	Referent	Referent

*Hispanic persons could be of any race; American Indian/Alaska Native, Asian or Pacific Islander, Black, White, and multiracial persons were non-Hispanic.

as Asian or Pacific Islander (38/1,000 cases) and non-Hispanic White (35/1,000 cases). We observed higher odds of suspected reinfection among all non-White racial and ethnic groups compared with non-Hispanic White, but we did not see statistically significant differences among persons identifying as multiracial (OR 1.26, 95% CI 0.98–1.62; p = 0.077) (Table).

From the beginning of March 2021 through April 2, 2022, we identified 161 suspected third infections among Clark County residents. Thirteen of those infections occurred sporadically from March 2021 through the week of December 12–18, 2021. Beginning the week of December 19–25, the rate rapidly increased, and 92% (148/161) of the suspected third infections occurred after the Omicron variant was detected. The number of suspected third infections declined during January–March 2022, mirroring trends in primary infections and suspected reinfections (Figure 2).

Discussion

This population-level analysis shows that suspected SARS-CoV-2 reinfections were relatively rare in Clark County before the Omicron variant was detected but that suspected reinfection accounted for a substantially higher proportion of COVID-19 cases during December 2021–March 2022. Although the weekly number of suspected reinfections fell in concert with the number of primary cases, the proportion of all cases that were suspected reinfections remained around peak levels of 11%. This trend is consistent with reports from other jurisdictions (*7*) and supports the hypothesis that prior infection might be less protective against infection with the Omicron variant than against previous SARS-CoV-2 variants (*1*,*8*). Suspected third infections were rare in Clark County but increased during December 2021 after the Omicron variant was detected, suggesting multiple SARS-CoV-2 infections might occur more frequently as genetically diverse variants are introduced.

Among previously infected persons, the incidence of suspected reinfection was highest among adults <50 years of age, women, and persons identifying as American Indian/Alaska Native. We also observed elevated incidence among persons identifying as Hispanic, multiracial, non-Hispanic Black, and Asian or Pacific Islander compared with persons identifying as non-Hispanic White. This finding might indicate a higher risk for repeated exposure among these groups. These disparities mirror disparities observed among primary cases in Clark County, except for a comparatively low rate of primary infection observed among persons identifying as American Indian/Alaska Native (*9*) but a comparatively high rate of suspected reinfection among this group. This discrepancy is notable; however, race and ethnicity data were missing for ≈26% of persons with primary infections and 21% of persons with suspected reinfection. We do not know whether this finding would persist if the data were more complete.

The first limitation of our study is that we only examined suspected reinfections meeting the 90-day interval criteria. We did not confirm reinfection by using viral genomic sequencing or other data, such as known COVID-19 exposure before a second occurrence or negative test between occurrences. We did not identify reinfection cases occurring within the 90-day interval, regardless of viral genomic sequencing or clinical suspicion of reinfection. Second, we did not match viral lineage data to specimens from suspected reinfections, so the rapid increase in suspected cases cannot definitively be linked to the Omicron variant. However,

by the week of December 19, 2021, 79% of sequenced samples from Clark County were the Omicron variant, and that proportion continued to increase through January 2022 (*10*). Finally, the large proportion of missing race and ethnicity data adds uncertainty to findings regarding the racial and ethnic groups most affected. By comparison, age and sex data were missing for <1% of persons. Some occupational or demographic groups, such as healthcare workers and college students, might undergo COVID-19 screening more frequently than others (*11*), which could lead to a disproportionate reduction of missed diagnoses among some groups and affect incidence estimates of primary infections and suspected reinfections.

Additional data of interest, including vaccination status, prior health status, and illness severity, were not available for this analysis. Other studies have observed reduced risk for severe illness during suspected reinfection compared with primary infection (*12*,*13*). As with primary infection, older age, male sex, and comorbidities have been described as risk factors for severe outcomes during reinfection (*12*).

COVID-19 vaccination has been associated with reduced risk for reinfection (*14*) and reduced risk for intensive care unit admission during reinfection (*12*). By the end of March 2022, ≈91% of Nevada residents ≥70 years of age had initiated COVID-19 vaccination, more than any other age group in the state (*15*). Vaccination might contribute to the relatively lower rates of suspected reinfection we observed among older persons in Clark County during this investigation. However, children <5 years of age were not eligible for COVID-19 vaccination until June 2022 (*16*), so vaccination rates do not explain the relatively lower rates of suspected reinfection we observed among young children. The proportion of other adult groups initiating vaccination in Nevada ranged from ≈61% for persons 20–29 years of age to ≈84% for persons 60–69 years of age (*15*). During the same timeframe, ≈54% of Nevada residents identifying as Asian or Pacific Islander had initiated COVID-19 vaccination, as had ≈53% of residents identifying as Hispanic and ≈44% of those identifying as non-Hispanic White (*15*). Vaccination initiation was lower among persons identifying as non-Hispanic Black (≈40%) and American Indian or Alaska Native (33%) (*15*). Lagging vaccination rates among racial and ethnic minority groups could be a contributing factor to the higher rates of suspected reinfection observed among these groups. However, the higher rates of vaccine initiation among Nevada residents and higher rates of suspected reinfection among Clark County residents identifying as Asian or Pacific Islander and Hispanic compared with those identifying as non-Hispanic White suggest a different factor driving risk for reinfection among these groups.

Reduced vaccine effectiveness (VE) against COVID-19–associated emergency department and urgent care encounters and hospitalizations has been observed during the Omicron wave compared with the Delta wave (*17*). However, VE against hospitalization was still high during the Omicron wave, especially among persons who received a second vaccine dose within 180 days before the healthcare encounter (VE 81%, 95% CI 65%–90%) and persons who received a third dose (VE 90%, 95% CI 80%–94%) (*17*). In our analysis, we did not know whether persons with suspected reinfection were vaccinated, the interval between vaccination and second positive test, or whether illness severity during reinfection was different between vaccinated and unvaccinated persons. Vaccination status is only one of many factors, including occupational and social exposures, that likely influence risk for reinfection.

Although formerly rare, suspected SARS-CoV-2 reinfection has occurred more frequently in Clark County after the emergence of the Omicron variant. Several factors might contribute to reduced protection

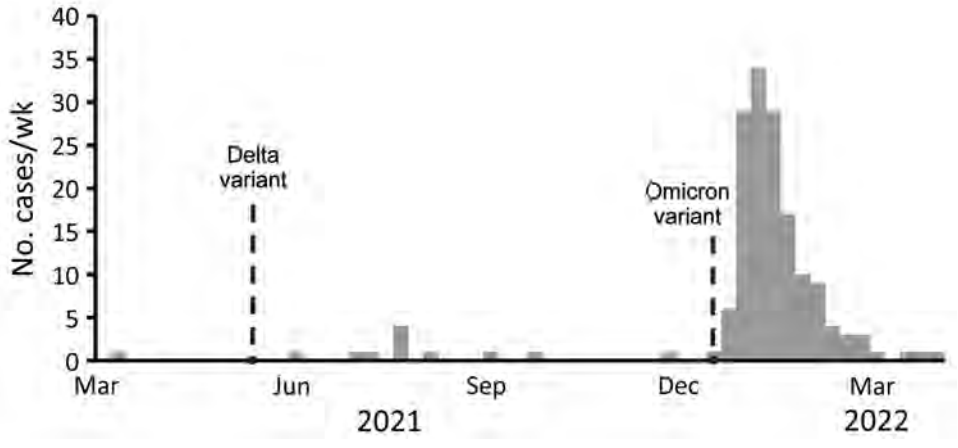

Figure 2. Suspected third SARS-CoV-2 infections, Clark County, Nevada, USA, March 2021–March 2022. Dotted lines show timeframe for identification of Delta and Omicron SARS-CoV-2 variants in Clark County. Suspected third infections were defined as a third positive PCR test collected ≥90 days after a second positive test collected ≥90 days after a person's initial positive PCR test.

against repeated infection, including the emergence of variants capable of immune evasion and waning immunity as the interval from initial infection or vaccination increases for many persons (*18*,*19*). Some demographic groups are disproportionately affected by suspected reinfection in Clark County. Further investigation into factors driving these disparities could inform prevention measures. Further investigation also might help determine impacts of these disparities, such as the burden of severe disease, the economic burden of repeated isolation and quarantine, and whether the same disparities are observed in other jurisdictions. Public health surveillance is necessary to clarify the burden of SARS-CoV-2 reinfection in communities. COVID-19 vaccination is one essential tool to help prevent SARS-CoV-2 reinfection and reduce disease severity when reinfection occurs, and vaccination efforts could help curb reinfection risk.

Acknowledgments

We extend our gratitude to Lynette Gumbleton for providing information regarding the prevalence of SARS-CoV-2 lineages in Clark County.

About the Author

Ms. Ruff was an Epidemic Intelligence Service Officer for the Centers for Disease Control and Prevention stationed at the Southern Nevada Health District, Las Vegas, Nevada, during this work. Her research interests include public health surveillance and environmental health.

References

1. Liu L, Iketani S, Guo Y, Chan JFW, Wang M, Liu L, et al. Striking antibody evasion manifested by the Omicron variant of SARS-CoV-2. Nature. 2022;602:676–81. https://doi.org/10.1038/s41586-021-04388-0
2. Tillett RL, Sevinsky JR, Hartley PD, Kerwin H, Crawford N, Gorzalski A, et al. Genomic evidence for reinfection with SARS-CoV-2: a case study. Lancet Infect Dis. 2021;21:52–8. https://doi.org/10.1016/S1473-3099(20)30764-7
3. Council of State and Territorial Epidemiologists. Update to the standardized surveillance case definition and national notification for 2019 novel coronavirus disease (COVID-19) [cited 2022 Feb 20]. https://cdn.ymaws.com/www.cste.org/resource/resmgr/ps/ps2021/21-ID-01_COVID-19_updated_Au.pdf
4. Southern Nevada Health District. New COVID-19 strain B.1.1.7 detected in Clark County [cited 2022 Jan 16]. https://www.southernnevadahealthdistrict.org/news-release/new-covid-19-strain-b-1-1-7-detected-in-clark-county
5. Southern Nevada Health District. B.1.617.2 variant detected in Clark County [cited 2022 Jan 16]. https://www.southernnevadahealthdistrict.org/news-release/b-1-617-2-variant-detected-in-clark-county/
6. Southern Nevada Health District. Southern Nevada Health District reports first Omicron case in Clark County resident [cited 2022 Jan 16]. https://www.southernnevadahealthdistrict.org/news-release/southern-nevada-health-district-reports-first-omicron-case-in-clark-county-resident
7. Washington State Department of Health. Reported COVID-19 reinfections in Washington state 2022 Feb. Report no. 421-024 [cited 2022 Jan 16]. https://www.doh.wa.gov/Portals/1/Documents/1600/coronavirus/data-tables/421-024-ReportedReinfections.pdf
8. Pulliam JRC, van Schalkwyk C, Govender N, von Gottberg A, Cohen C, Groome MJ, et al. Increased risk of SARS-CoV-2 reinfection associated with emergence of Omicron in South Africa. Science. 2022;36:eabn4947. https://doi.org/10.1126/science.abn4947
9. Southern Nevada Health District. Daily aggregate COVID-19 2022 April 1 [cited 2022 Apr 10]. https://media.southernnevadahealthdistrict.org/download/COVID-19/updates/2022/April/20220401-Daily-Aggregate-COVID19.pdf
10. Nevada State Public Health Laboratory. Genomic sequencing of SARS-CoV-2 in Nevada [cited 2022 Feb 23]. https://www.nvsarscov2variant.org/overview
11. Centers for Disease Control and Prevention. Overview of testing for SARS-CoV-2, the virus that causes COVID-19 [cited 2022 May 15]. https://www.cdc.gov/coronavirus/2019-ncov/hcp/testing-overview.html
12. Mensah AA, Lacy J, Stowe J, Seghezzo G, Sachdeva R, Simmons R, et al. Disease severity during SARS-COV-2 reinfection: a nationwide study. J Infect. 2022;84:542–50. https://doi.org/10.1016/j.jinf.2022.01.012
13. Abu-Raddad LJ, Chemaitelly H, Bertollini R; National Study Group for COVID-19 Epidemiology. Severity of SARS-CoV-2 reinfections as compared with primary infections. N Engl J Med. 2021;385:2487–9. https://doi.org/10.1056/NEJMc2108120
14. Cavanaugh AM, Spicer KB, Thoroughman D, Glick C, Winter K. Reduced risk of reinfection with SARS-CoV-2 after COVID-19 vaccination—Kentucky, May–June 2021. MMWR Morb Mortal Wkly Rep. 2021;70:1081–3. https://doi.org/10.15585/mmwr.mm7032e1
15. Nevada Health Response. COVID-19: demographics: vaccinations [cited 2022 Mar 30]. https://nvhealthresponse.nv.gov/#covid-data-tracker
16. Centers for Disease Control and Prevention. CDC recommends COVID-19 vaccines for young children [cited 2022 Jul 18]. https://www.cdc.gov/media/releases/2022/s0618-children-vaccine.html
17. Thompson MG, Natarajan K, Irving SA, Rowley EA, Griggs EP, Gaglani M, et al. Effectiveness of a third dose of mRNA vaccines against COVID-19–associated emergency department and urgent care encounters and hospitalizations among adults during periods of Delta and Omicron variant predominance—VISION Network, 10 states, August 2021–January 2022. MMWR Morb Mortal Wkly Rep. 2022;71:139–45. https://doi.org/10.15585/mmwr.mm7104e3
18. Hall V, Foulkes S, Insalata F, Kirwan P, Saei A, Atti A, et al.; SIREN Study Group. Protection against SARS-CoV-2 after Covid-19 vaccination and previous infection. N Engl J Med. 2022;386:1207–20. https://doi.org/10.1056/NEJMoa2118691
19. Centers for Disease Control and Prevention. Science brief: SARS-CoV-2 infection-induced and vaccine-induced immunity [cited 2022 May 19]. https://www.cdc.gov/coronavirus/2019-ncov/science/science-briefs/vaccine-induced-immunity.html#anchor_1635540136596

Address for correspondence: Jeanne Ruff, Nevada Division of Public and Behavioral Health, 3811 W Charleston Blvd #104, Las Vegas, NV 89102, USA; email: qdw5@cdc.gov

Environmental Persistence of Monkeypox Virus on Surfaces in Household of Person with Travel-Associated Infection, Dallas, Texas, USA, 2021

Clint N. Morgan, Florence Whitehill, Jeffrey B. Doty, Joann Schulte, Audrey Matheny, Joey Stringer, Lisa J. Delaney, Richard Esparza, Agam K. Rao, Andrea M. McCollum

In July 2021, we conducted environmental sampling at the residence of a person in Dallas, Texas, USA, who had travel-associated human West African monkeypox virus (MPXV-WA). Targeted environmental swab sampling was conducted 15 days after the person who had monkeypox left the household. Results indicate extensive MPXV-WA DNA contamination, and viable virus from 7 samples was successfully isolated in cell culture. There was no statistical difference (p = 0.94) between MPXV-WA PCR positivity of porous (9/10, 90%) vs. nonporous (19/21, 90.5%) surfaces, but there was a significant difference (p<0.01) between viable virus detected in cultures of porous (6/10, 60%) vs. nonporous (1/21, 5%) surfaces. These findings indicate that porous surfaces (e.g., bedding, clothing) may pose more of a MPXV exposure risk than nonporous surfaces (e.g., metal, plastic). Viable MPXV was detected on household surfaces after at least 15 days. However, low titers ($\leq 10^2$ PFU) indicate a limited potential for indirect transmission.

Monkeypox, a zoonotic infectious disease caused by monkeypox virus (MPXV; genus *Orthopoxvirus* [OPXV]), is endemic to West and Central Africa. After its discovery in 1958, the virus had not been reported in humans outside its endemic range until 2003, when a shipment of MPXV-infected small mammals was transported from Ghana to the United States, causing secondary animal and human infections (*1*). Genomic sequencing of isolates of MPXV across its endemic range indicates the existence of 2 clades: West African (WA) and Congo Basin; WA MPXV has a lower mortality rate (*2*).

Transmission is known to occur by direct contact with infectious lesion material or bodily fluids of an infected human or animal or by inhalation of respiratory secretions during prolonged, face-to-face contact (*3*,*4*). In addition, transmission might occur by direct contact with objects or materials contaminated with MPXV, although documented occurrences are rare (*5*,*6*). Poxvirus lesions, their exudates (vesicular or pustular fluid), and crusts contain viable virus (*3*,*4*). Poxvirus virions within lesion material shed during infection are known to be more resistant to desiccation than for other enveloped viruses (e.g., influenza viruses, rubella virus) because the virions are tightly bound with the fibrin matrices of the scab/crust material (*7*,*8*). This feature can lead to long-term environmental persistence of OPXVs.

Studies with variola (causative agent of smallpox) and vaccinia viruses demonstrated that if contaminated material is maintained in an environment that has low humidity, low temperature, and remains protected from UV radiation, the viral particles can remain viable for months to years (*9*,*10*). One study demonstrated the extreme longevity of variola virus in lesion scabs stored within an envelope in a cupboard; the virus remained viable for 13 years until the sample was used to completion (*11*). This longevity is striking; however, the infectivity of variola scabs alone is believed to be low based on epidemiologic and laboratory data (*11*–*14*). Vesicular fluid from OPXV lesions and other secretions generally have lower persistence in some laboratory studies than scabs (*15*,*16*). Outside of insights gained from other OPXVs, the

Author affiliations: Centers for Disease Control and Prevention, Atlanta, Georgia, USA (C.N. Morgan, F. Whitehill, J.B. Doty, A. Matheny, L.J. Delaney, A. K. Rao, A.M. McCollum; Dallas County Health and Human Services, Dallas, Texas, USA (J. Schulte, J. Stringer, R. Esparza)

DOI: https://doi.org/10.3201/eid2810.221047

longevity and environmental persistence of MPXV is largely unknown, including within a household environment. Considering the increasing frequency of monkeypox cases being exported from disease-endemic areas (*17*–*20*), and the concern for secondary infections among household contacts, there is a need for more specific information on transmission risks due to contaminated fomites in the household.

On July 16, 2021, the US Centers for Disease Control and Prevention (CDC) confirmed a WA MPXV infection in a man (US resident) who had recently traveled from Lagos, Nigeria, to Dallas, Texas, USA. This case was the first MPXV infection reported in the United States since the 2003 outbreak, prompting an immediate response and investigation. The person who had monkeypox arrived in Dallas on July 9 and stayed in a household, a 1-bedroom residence that had no other occupants, for 4 days before coming to the hospital for treatment (*17*). During these 4 days, the man was in the household and had a disseminated purulent rash (*17*). We conducted environmental sampling within the residence and assessed the viral load and viability of virus present on commonly used surfaces and objects within the household.

Methods

Site Information

Environmental sampling took place in July 2021, 15 days after the person who had monkeypox departed the residence for the hospital. The person was interviewed by CDC, Dallas County Health and Human Services, and hospital officials regarding condition of residence, activities within the household before hospital admittance, and locations of potentially soiled materials and high-touch objects. We recorded notes on specific location, soiled condition of surfaces, and light exposure for each sample collected.

Personal Protective Equipment

Personnel performing the household environmental sampling were vaccinated with ACAM2000 (Sanofi Pasteur, https://www.sanofi.com), in accordance with recommendations for personnel at risk for occupational exposure to OPXVs (*21*). Before entering the residence, the sampling team donned personal protective equipment, including Tyvek (DuPont, https://www.dupont.com) coverall with hood, inner and outer nitrile gloves, fit-tested N95 filtering facepiece respirator, and face shield. Because of the public setting, discretion was used when entering the residence, avoiding areas of high visibility, and personal protective equipment was donned at the exterior entrance immediately before entering.

Sample Collection

The sampling team collected swab samples from high-use objects and environmental surfaces within the household that would probably have had direct contact with the person who had monkeypox and objects that appeared visibly soiled. Individually wrapped sterile cotton-tipped applicator swabs (Puritan, https://www.puritanmedproducts.com) were removed from their packaging and prewetted by inserting into a corresponding labeled 2-mL cryotube (Sarstedt, https://www.sarstedt.com) filled with 300 μL of phosphate-buffered saline (PBS; pH 7.4). The swab was then immediately applied to the environmental surface and swabbed vigorously for 10 seconds while rotating the swab to ensure all sides of the swab contact the environmental surface. On all surfaces and objects, an approximate area of 2 in^2 was swabbed, and if soiled, the soiled area was targeted. Aseptic techniques were used, and outer gloves were changed between samples or if soiled. There is not a fully validated environmental sampling method for OPXVs, so the sampling procedure was adapted from similar studies with vaccinia virus and SARS-CoV-2 (*22*,*23*).

Sample Processing and PCR Testing

We stored all swab samples and shipped them in sealed 2-mL cryotubes containing ≈300 μL PBS and kept refrigerated (2°C–4°C) until processing. We transferred swabs and the 300 μL of sterile PBS within the tube to the swab extraction tube system (SETS; Roche, https://www.roche.com). We then centrifuged SETS tubes at 6,000 rpm for 1 min to collect the elute, after which we discarded inner SETS tubes and swabs. We aliquoted 100 μL of swab eluate and used it for DNA extraction; the remaining eluate was kept for viral titration. We extracted DNA from all samples by using the EZ1 DNA Tissue Kit and Biorobot System (QIAGEN, https://www.qiagen.com). We screened all samples for MPXV DNA by real-time PCR using the WA MPXV-specific assay (*24*) on the VIIA7 Real-Time PCR System (Applied Biosystems, https://www.thermofisher.com).

Virus Isolation and Titration

We put swab eluate from all samples into cell culture to attempt virus isolation and assess presence of viable virus. We added a 100-μL aliquot of swab eluate to BSC-40 cell monolayers (African green monkey kidney cell line) in T-25 cell culture flasks and incubated

at 35.5°C in an atmosphere of 6% CO_2, in Roswell Park Memorial Institute medium as described (*25*). We observed infected T-25 flasks daily for cytopathic effect (CPE), incubated for a maximum of 14 days or until positive. We harvested material from flasks if considered positive for viable virus (successful viral isolation attempt), when ≈100% of monolayer showed CPE activity. For an additional confirmation of the successful virus isolation attempt, we tested an aliquot of the harvested flasks material by using PCR.

Swabs collected from environmental surfaces might result in bacterial or fungal contamination during virus isolation attempts. To help mitigate bacterial or fungal overgrowth in T-25 flasks, we supplemented cell culture medium with penicillin/streptomycin, amphotericin B, and gentamicin. If either bacterial or fungal contamination was identified, 4 cycles of removing medium and adding fresh medium to wash monolayers was conducted as often as necessary to prevent overgrowth.

After PCR and attempt at virus isolation, samples from which virus was isolated were evaluated by using viral titration accords to methods described (*26*). Because of low sample volume, we added 50 µL of PBS diluent to 100 µL of swab eluate from each positive sample and serially diluted them in 2% Roswell Park Memorial Institute medium, and we added 650 µL of each dilution to 6-well plates in duplicate on BSC-40 cell monolayers. We incubated plates at 35.5°C in an atmosphere of 6% CO_2. After a 72-hour incubation period, we inactivated and stained plates with 2× formalinized crystal violet stain and then enumerated plaques. Titers are expressed as PFU/mL.

Statistical Analyses

We performed statistical analyses to compare PCR positivity, average cycle threshold (Ct) value, and viral culture positivity of environmental swab samples from porous and nonporous surface types collected in the household. We conducted statistical

Table 1. Objects and surfaces swabbed during environmental sampling of residence of a patient who had monkeypox, Texas, USA, 2021*

Object/surface	Room, specific location	Sample from visibly soiled surface	Sample exposed to UV	Surface type	Mean cycle threshold	Viral culture result, PFU/mL
Paper towels	Bedroom, on bed	Yes	Low	Porous	16.1	$<1 \times 10^2$
Underwear	Bedroom, on bed	Yes	No	Porous	17.9	$<1 \times 10^2$
Underwear	Bedroom, on bed	Yes	No	Porous	19.3	3.2×10^2
Blanket	Living room, on couch	Yes	Low	Porous	20.3	$<1 \times 10^2$
Towel	Living room, on couch	Yes	Low	Porous	20.3	$<1 \times 10^2$
Disinfectant wipes	Bedroom, bedside table	No	Low	Porous	21.9	–
Towel	Bedroom, on bed	Yes	Low	Porous	22.3	–
Mattress cover	Bedroom closet, in hamper	Yes	No	Porous	23.1	$<1 \times 10^2$
Towel	Bedroom, near bathroom	Yes	Low	Porous	36.7	–
Underwear	Bedroom, near bathroom	Yes	No	Porous	UND	–
Coffee table top	Living room, edge near couch	No	Low	Nonporous	21.6	$<1 \times 10^2$
Bedside table	Bedroom, at bedside	No	Low	Nonporous	21.7	–
Sink knobs	Bathroom, at sink near entry	No	Low	Nonporous	22.3	–
Bathtub drain	Bathroom, in bathtub	No	Low	Nonporous	24.4	–
Toilet seat	Bathroom, on toilet	Yes	Low	Nonporous	24.7	–
Light switch	Bathroom, at entrance above sink	Yes	Low	Nonporous	25.0	–
Closet doorknob	Outer knob of closet door in bedroom	No	Low	Nonporous	25.2	–
Dresser top	Bedroom, near entry	No	Low	Nonporous	25.9	–
Refrigerator handle	Kitchen, on refrigerator door	Yes	Low	Nonporous	26.7	–
Toilet handle	Bathroom, on toilet	No	Low	Nonporous	26.7	–
Bathtub faucet	Bathroom, in bathtub/shower unit	No	Low	Nonporous	26.9	–
Doorknob	Inner knob of bathroom door	No	Low	Nonporous	27.3	–
Freezer handle	Kitchen, on freezer door	No	Low	Nonporous	28.2	–
Cell phone	Living room, on coffee table	No	Low	Nonporous	28.3	–
Light switch	Bedroom, at entrance above dresser	No	Low	Nonporous	33.3	–
Light switch	Kitchen, on wall	No	Low	Nonporous	33.5	–
Light switch	Living room, near front door	No	Low	Nonporous	33.9	–
Power strip button	Bedroom, on floor along bed	No	Low	Nonporous	34.2	–
Television remote	Living room, on TV stand	No	Low	Nonporous	35.7	–
Microwave handle	Kitchen, on microwave	No	Low	Nonporous	UND	–
Closet light switch	Bedroom, next to closet door	No	Low	Nonporous	UND	–

*UND, undetermined (below detectable limit); –, negative.

Table 2. Characteristics of environmental swab samples from porous and non-porous surface types collected in household of a patient who had confirmed monkeypox, Texas, USA, 2021

Surface type	No. samples collected	Positive by PCR, no. (%)	p value*	Average cycle threshold (SD)	p value†	Viable virus cultured, no. (%)	p value*
Porous	10	9 (90)	0.94	22.0 (6.0)	<0.01	6 (60)	<0.01
Nonporous	21	19 (90)		27.7 (4.4)		1 (5)	

*By mid-p exact test.
†By 2-sample independent t-test.

analyses by using OpenEpi version 3.01 (https://www.OpenEpi.com).

Results

Site Information

We conducted interviews with the person who had monkeypox detailed limited activities within the household during the 4-day period between returning from travel and admittance to the hospital. The person reported sleeping/resting on the bed in the bedroom, spending prolonged time on 2 couches in the living room, showering, and retrieving food from the kitchen refrigerator. The person detailed the location of clothing items worn during travel, as well as other clothing worn while in the household. The heating, ventilation, and air conditioning system of the residence was turned off when the person left for the hospital. The exact environmental conditions within the residence for 15 days are unknown, although it is probable they were nearing the external environmental conditions; the mean temperature was 86°F (range 73°F–101°F) and mean relative humidity 63% (range 49%–76%) (*27*). Within the residence, we collected 31 environmental swab samples. Of these 31 samples, 10 (32%) were from items and surfaces made of porous material, such as cloth and paper, and 21 (68%) were from nonporous material, such as sealed wood and plastic (Table 1).

All windows were covered with closed blinds, enabling limited sunlight into the household. Sunlight (UV) exposure is denoted as no UV, indicating surface sampled was completed covered or kept in dark room, or low UV, indicating surface was uncovered and exposed to the low ambient light environment of the household (Table 1).

PCR Testing

Overall, 27 (87%) samples amplified MPXV-WA DNA, and the mean cycle threshold (Ct) value was 25.83 (range 16.14–36.74). Swabs collected from porous materials were 90% (9/10) PCR positive, and those collected from nonporous materials were 90.5% (19/21) PCR positive (p = 0.94) (Table 2). Porous materials had higher detectable levels of viral DNA (Ct 21.98) than did nonporous materials (Ct 27.65) (p<0.01) (Table 2). Among the PCR-positive swabs, detectable levels of viral DNA in each room within the household was, in order of highest to lowest: closet (Ct 23.08, n = 1); bedroom (Ct 24.96, n = 13); bathroom (Ct 25.33, n = 7); living room (Ct 26.66, n = 6); and kitchen (Ct 29.44, n = 4) (Table 1). Cell culture isolates considered positive were also tested by using PCR, and all were positive (Ct range 14.2–16.0).

Virus Isolation and Titration

Viral isolation was attempted from all 31 swab samples, and 7 (23%) contained viable virus (Table 1). Virus isolation was successful with 23% (3/11) of swabs from the bedroom, 50% (3/6) from the living room, and 1 sample collected from a used mattress cover in the closet. Overall, 60% (6/10) of porous materials contained viable virus, and only 5% (1/21) of nonporous materials contained viable virus (p<0.01) (Table 2). The appearance of the first signs of CPE in the successful virus isolation attempts ranged from 2 to 8 (mean 5) days postinfection. We harvested material from flasks when CPE affected 100% of the monolayer at 6–12 (mean 9) days postinfection. We observed limited bacterial or fungal contamination in this study; only 1 sample (bathtub faucet) required >3 monolayer washes to curtail bacterial overgrowth.

Of the 7 culture-positive swab specimens, 6 were below the detectable limit (2.1×10^2 PFU) of the titration assay (titers $<1 \times 10^2$ PFU/mL). Only sample TX-23 had a quantifiable titer of 3.2×10^2 PFU/mL.

Discussion

In this real-world setting, targeted sampling of high-use surfaces and objects was effective at detecting MPXV DNA and viable virus. MPXV DNA was found throughout the household, indicating extensive spread of viral material, probably a result of the man having an extensive purulent rash develop. Our study demonstrated the ability of MPXV to persist in a household environment for at least 15 days. Previous studies with vaccinia and variola viruses demonstrate the capability of OPXVs to persist in the environment much longer than 15 days (months or years), so potentially the virus sampled in this household could have remained viable for a longer period (*10*,*15*,*16*). A similar investigation had been conducted with a household case of eczema vaccinatum (vaccinia

virus), in which household contamination was a concern because of extensive rash (*22*). That study reported less extensive viral DNA dissemination around the household than what we detected and viable virus from 1 cloth item and 2 nonporous items at 10 days after removal of an infected person (*22*).

In a household environment, myriad physical, chemical, and biologic factors could affect the persistence of OPXVs (Appendix Table, https://wwwnc.cdc.gov/EID/article/28/10/22-1047-App1.xlsx). Most viruses exhibit greater persistence on nonporous surfaces; however, OPXVs typically have higher persistence on porous surfaces and show a high resistance to drying (*28*,*29*). In this study, we detected viable virus on multiple substrate types, including cellulose fiber sheets (paper towels), cotton and cotton/synthetic blended fabrics (towel, blanket, underwear, mattress cover), and sealed wood veneer (coffee tabletop). Items considered porous had increased detectable levels of viral DNA, and viable virus was only detected from 1 nonporous surface.

Despite the hardiness of OPXVs, it is probable there was some degree of viral decay of MPXV before sampling. This decay could have occurred either because of environmental and physical properties of the residence and surface types or contact with a disinfectant or soap. For example, 4 culture-negative samples had MPXV-WA Ct values higher than that of the mattress cover, which was culture positive. One of these samples was collected from dried disinfectant wipes (Clorox, https://www.thecloroxcompany.com), which probably successfully inactivated the virus. In addition, no viable virus was detected in the 7 samples collected from the bathroom, even though the person who had monkeypox spent much time in this room; this result could also be the result of contact with disinfectant or soap. The bathroom samples, if not inactivated by contact with disinfectants, could possibly have been culture negative because of the nonporous surfaces and higher humidity that would occur in the bathroom during showering or sink use. It is useful in studies assessing environmental persistence or contamination of MPXV to attempt viral isolation from PCR-positive samples. In environmental sampling studies, low Ct values should not be used as a proxy for viable virus because many factors and environmental conditions might lead to complete viral decay on contaminated surfaces.

Interviews with the person who had monkeypox in this study showed that most of the time in the residence was spent lying down or resting. As a probable result, it was only items on or near the bed and couches from which viable virus was detected. The results of this study demonstrate the need to take special precautions when handling bedding, clothing, or towels of a person who has monkeypox. When there are other occupants in a household, or visitors, persons who have monkeypox should not share bedding, clothing, towels, or sleeping and living spaces.

During 2018, a healthcare worker in the United Kingdom became infected, probably as a result of handling the bedding of a person who had monkeypox without using respiratory protection (*30*). The persistence of the virus in the environment depends largely on the viral load and type of infectious material initially deposited, environmental conditions, and physical/chemical properties of the contaminated objects. Furthermore, if fomites in the environment have sufficient amounts of viable virus, the capability of these materials to cause secondary infection is probably dependent on route of exposure, including opportunistic contact or transfer to mucous membranes, or preexisting immunity.

The only culture-positive swab sample with sufficient viral load to reach the detectable limits of our titration assay was from an article of clothing that had prolonged, direct contact with purulent lesions; the titer was 3.2×10^2 PFU/mL (detection limit 2.1×10^2 PFU/mL). There are few data on the infectious dose necessary to cause infection in humans. However, these data can be inferred from laboratory challenge studies with the prairie dog animal model. Virus titers of 10^4 and 10^3 PFU in most cases cause infection, and in 1 study, 1 of 4 prairie dogs infected with 6×10^2 PFU MPXV-WA became infected and showed development of disseminated lesions (*26*,*31*). This result might indicate that in otherwise healthy persons, a viral load on the order of 10^2 PFU is the lower threshold for infection, and at these levels the innate immune system can potentially clear the virus.

It is unknown how long the culture-positive materials in this study would remain viable with MPXV because viral titers will decrease over time until undetectable by viral culture. Subsequently, as viral titers decrease, infectivity (capacity to cause secondary infection) would also decrease. In comparable studies of OPXV persistence (Appendix Table), under slightly lower heat and humidity conditions, the maximum duration that virus remained detectable on fabrics ranged from 28 to 70 days (*16*,*32*). Considering the low titers observed ($\leq 3.2 \times 10^2$ PFU/mL) and the high heat and moderate humidity environment, it is probable that maximum persistence of viable virus on the items sampled would fall into a similar range.

This study was conducted alongside a public health response, and priorities were identifying

potential high transmission risk areas and objects and confirming presence/absence of viable virus. These results are merely representative of the conditions of each specific item at 1 point in time and not representative of the total potential for fomite transmission within the household from items not sampled. A more robust sampling method would be recommended for future studies, including multiple sampling time points and recording the environmental conditions in the household over time. Household disinfection is recommended for any household occupied by a person confirmed to have monkeypox. A disinfectant registered with the Environmental Protection Agency should be used, such as a disinfectant that has an emerging viral pathogens claim, in accordance with the manufacturer's instructions (*33*). Specific recommendations for household disinfection can be found on the CDC monkeypox web page (*34*).

After this case in July 2021, two additional travel-associated cases were detected in the United States and the United Kingdom (*19*,*20*), and in May 2022, an unprecedented number of monkeypox cases were identified from multiple clusters worldwide (*35*,*36*). Current outbreaks of human monkeypox cases in endemic and nonendemic regions, and the increasing frequency of which travel-associated cases are occurring, necessitate a further need to understand transmission dynamics within a household setting. Since the 2022 outbreak began, an additional study on monkeypox contamination within a household has been published and detected comparable levels of viral contamination despite differences in sampling and processing methods (*37*). In that study, samples were collected 3 days after the patient was last in the residence, and similar to our study, virus was isolated mostly from porous surfaces. However, the authors reported successful MPXV isolation from 40% (2/5) of nonporous surfaces sampled from which isolation was attempted (door handle and handheld electronic device). Because we report isolation of MPXV from just 5% (1/21) of nonporous surface sampled after 15 days, this finding potentially indicates that MPXV decay occurs more rapidly on nonporous than porous surfaces, as was reported for other OPXVs (*28*,*29*).

Future studies should develop a validated environmental sampling protocol for OPXVs and explore additional sample collection methods, comparing multiple applicator types and transport media because they might affect viral recovery during processing and overall viral yield (*38*,*39*). Additional studies on household transmission risks should be conducted to inform public health responses and cleaning and disinfection protocols, and to provide specific recommendations to at-risk communities and persons. Furthermore, documenting the risk potential of object-specific fomites and materials within a household will inform recommendations for infection prevention strategies and cleaning and disinfecting efforts.

Acknowledgments

We thank the Dallas County Health and Human Services Public Health Laboratory for assistance with the study and facilitating coordination with local and state agencies, Whitni Davidson for providing laboratory support and assistance, Theodora Khan for providing assistance compiling relevant literature, and the Poxvirus and Rabies Branch at CDC for collaboration.

A.M. was supported in part by an appointment to the Research Participation Program at the Centers for Disease Control and Prevention, administered by the Oak Ridge Institute for Science and Education through an interagency agreement between the US Department of Energy and CDC.

About the Author

Mr. Morgan is a biologist in the Poxvirus and Rabies Branch, Division of High-Consequence Pathogens and Pathology, National Center for Emerging and Zoonotic Infectious Diseases, Centers for Disease Control and Prevention, Atlanta, GA. His primary research interests include virus–host interactions of orthopoxviruses and lyssaviruses in the natural environment, and the ecologies of their host systems.

References

1. Reed KD, Melski JW, Graham MB, Regnery RL, Sotir MJ, Wegner MV, et al. The detection of monkeypox in humans in the Western Hemisphere. N Engl J Med. 2004;350:342–50. https://doi.org/10.1056/NEJMoa032299
2. Likos AM, Sammons SA, Olson VA, Frace AM, Li Y, Olsen-Rasmussen M, et al. A tale of two clades: monkeypox viruses. J Gen Virol. 2005;86:2661–72. https://doi.org/10.1099/vir.0.81215-0
3. Parker S, Nuara A, Buller RM, Schultz DA. Human monkeypox: an emerging zoonotic disease. Future Microbiol. 2007;2:17–34. https://doi.org/10.2217/17460913.2.1.17
4. Brown K, Leggat PA. Human monkeypox: current state of knowledge and implications for the future. Trop Med Infect Dis. 2016;1:8. https://doi.org/10.3390/tropicalmed1010008
5. Jezek Z, Grab B, Szczeniowski MV, Paluku KM, Mutombo M. Human monkeypox: secondary attack rates. Bull World Health Organ. 1988;66:465–70.
6. Learned LA, Reynolds MG, Wassa DW, Li Y, Olson VA, Karem K, et al. Extended interhuman transmission of monkeypox in a hospital community in the Republic of the Congo, 2003. Am J Trop Med Hyg. 2005;73:428–34. https://doi.org/10.4269/ajtmh.2005.73.428
7. Nolen LD, Osadebe L, Katomba J, Likofata J, Mukadi D, Monroe B, et al. Introduction of monkeypox into a

community and household: risk factors and zoonotic reservoirs in the Democratic Republic of the Congo. Am J Trop Med Hyg. 2015;93:410–5. https://doi.org/10.4269/ajtmh.15-0168
8. Hutson CL, Carroll DS, Gallardo-Romero N, Weiss S, Clemmons C, Hughes CM, et al. Monkeypox disease transmission in an experimental setting: prairie dog animal model. PLoS One. 2011;6:e28295. https://doi.org/10.1371/journal.pone.0028295
9. Henderson DA, Inglesby TV, Bartlett JG, Ascher MS, Eitzen E, Jahrling PB, et al.; Working Group on Civilian Biodefense. Smallpox as a biological weapon: medical and public health management. JAMA. 1999;281:2127–37. https://doi.org/10.1001/jama.281.22.2127
10. McCollum AM, Li Y, Wilkins K, Karem KL, Davidson WB, Paddock CD, et al. Poxvirus viability and signatures in historical relics. Emerg Infect Dis. 2014;20:177–84. https://doi.org/10.3201/eid2002.131098
11. Wolff HL, Croon JJ. The survival of smallpox virus (variola minor) in natural circumstances. Bull World Health Organ. 1968;38:492–3.
12. Harper GJ. Airborne micro-organisms: survival tests with four viruses. J Hyg (Lond). 1961;59:479–86.
13. Wood JP, Choi YW, Wendling MQ, Rogers JV, Chappie DJ. Environmental persistence of vaccinia virus on materials. Lett Appl Microbiol. 2013;57:399–404. https://doi.org/10.1111/lam.12126
14. McDevitt JJ, Lai KM, Rudnick SN, Houseman EA, First MW, Milton DK. Characterization of UVC light sensitivity of vaccinia virus. Appl Environ Microbiol. 2007;73:5760–6. https://doi.org/10.1128/AEM.00110-07
15. MacCallum FO, McDonald JR. Survival of variola virus in raw cotton. Bull World Health Organ. 1957;16:247–54.
16. Rao AR. Infected inanimate objects (fomites) and their role in transmission of smallpox. World Health Organization. May 1, 1972 [cited 2022 Jun 1]. https://apps.who.int/iris/bitstream/handle/10665/67501/WHO_SE_72.40.pdf
17. Rao AK, Schulte J, Chen T-H, Hughes CM, Davidson W, Neff JM, et al.; July 2021 Monkeypox Response Team. Monkeypox in a traveler returning from Nigeria—Dallas, Texas, July 2021. MMWR Morb Mortal Wkly Rep. 2022;71:509–16. https://doi.org/10.15585/mmwr.mm7114a1
18. Mauldin MR, McCollum AM, Nakazawa YJ, Mandra A, Whitehouse ER, Davidson W, et al. Exportation of monkeypox virus from the African continent. J Infect Dis. 2022;225:1367–76. https://doi.org/10.1093/infdis/jiaa559
19. Costello V, Sowash M, Gaur A, Cardis M, Pasieka H, Wortmann G, et al. Imported monkeypox from international traveler, Maryland, USA, 2021. Emerg Infect Dis. 2022;28:1002–5. https://doi.org/10.3201/eid2805.220292
20. Hobson G, Adamson J, Adler H, Firth R, Gould S, Houlihan C, et al. Family cluster of three cases of monkeypox imported from Nigeria to the United Kingdom, May 2021. Euro Surveill. 2021;26:2100745. https://doi.org/10.2807/1560-7917.ES.2021.26.32.2100745
21. Petersen BW, Harms TJ, Reynolds MG, Harrison LH. Use of vaccinia virus smallpox vaccine in laboratory and health care personnel at risk for occupational exposure to orthopoxviruses: Recommendations of the Advisory Committee on Immunization Practices (ACIP), 2015. MMWR Morb Mortal Wkly Rep. 2016;65:257–62. https://doi.org/10.15585/mmwr.mm6510a2
22. Lederman E, Miramontes R, Openshaw J, Olson VA, Karem KL, Marcinak J, et al. Eczema vaccinatum resulting from the transmission of vaccinia virus from a smallpox vaccinee: an investigation of potential fomites in the home environment. Vaccine. 2009;27:375–7. https://doi.org/10.1016/j.vaccine.2008.11.019
23. Marcenac P, Park GW, Duca LM, Lewis NM, Dietrich EA, Barclay L, et al. Detection of SARS-CoV-2 on surfaces in households of persons with COVID-19. Int J Environ Res Public Health. 2021;18:8184. https://doi.org/10.3390/ijerph18158184
24. Li Y, Zhao H, Wilkins K, Hughes C, Damon IK. Real-time PCR assays for the specific detection of monkeypox virus West African and Congo Basin strain DNA. J Virol Methods. 2010;169:223–7. https://doi.org/10.1016/j.jviromet.2010.07.012
25. Hughes CM, Liu L, Davidson WB, Radford KW, Wilkins K, Monroe B, et al. A tale of two viruses: coinfections of monkeypox and varicella zoster virus in the Democratic Republic of Congo. Am J Trop Med Hyg. 2020;104:604–11. https://doi.org/10.4269/ajtmh.20-0589
26. Hutson CL, Gallardo-Romero N, Carroll DS, Clemmons C, Salzer JS, Nagy T, et al. Transmissibility of the monkeypox virus clades via respiratory transmission: investigation using the prairie dog-monkeypox virus challenge system. PLoS One. 2013;8:e55488. https://doi.org/10.1371/journal.pone.0055488
27. National Oceanic and Atmospheric Administration National Climatic Data Center. Climate data online. 2022 [cited 2022 May 4]. https://www.ncdc.noaa.gov/cdo-web/datasets/LCD/stations/WBAN:13960/detail
28. Rakowska PD, Tiddia M, Faruqui N, Bankier C, Pei Y, Pollard AJ, et al. Antiviral surfaces and coatings and their mechanisms of action. Communications Materials. 2021;2:53. https://doi.org/10.1038/s43246-021-00153-y
29. Rheinbaben F, Gebel J, Exner M, Schmidt A. Environmental resistance, disinfection, and sterilization of poxviruses. In: Mercer AA, Schmidt A, Weber O, editors. Poxviruses. Basel (Switzerland). Birkhäuser; 2007. p. 397–405.
30. Vaughan A, Aarons E, Astbury J, Brooks T, Chand M, Flegg P, et al. Human-to-human transmission of monkeypox virus, United Kingdom, October 2018. Emerg Infect Dis. 2020;26:782–5. https://doi.org/10.3201/eid2604.191164
31. Hutson CL, Carroll DS, Self J, Weiss S, Hughes CM, Braden Z, et al. Dosage comparison of Congo Basin and West African strains of monkeypox virus using a prairie dog animal model of systemic orthopoxvirus disease. Virology. 2010;402:72–82. https://doi.org/10.1016/j.virol.2010.03.012
32. Sidwell RW, Dixon GJ, McNeil E. Quantitative studies on fabrics as disseminators of viruses. I. Persistence of vaccinia virus on cotton and wool fabrics. Appl Microbiol. 1966;14:55–9. https://doi.org/10.1128/am.14.1.55-59.1966
33. US Environmental Protection Agency. Disinfectants for emerging viral pathogens (EVPs): list Q. June 2, 2022 [cited 2022 Jun 15]. https://www.epa.gov/pesticide-registration/disinfectants-emerging-viral-pathogens-evps-list-q
34. Centers for Disease Control and Prevention. Disinfection of the home and non-healthcare settings. June 6, 2022 [cited 2022 Jun 15]. https://www.cdc.gov/poxvirus/monkeypox/pdf/Monkeypox-Interim-Guidance-for-Household-Disinfection-508.pdf
35. Centers for Disease Control and Prevention. 2022 US monkeypox outbreak. July 28, 2022 [cited 2022 Aug 1]. https://www.cdc.gov/poxvirus/monkeypox/response/2022/index.html
36. Luo Q, Han J. Preparedness for a monkeypox outbreak. Infect Med. 2022. https://doi.org/10.1016/j.imj.2022.07.001
37. Atkinson B, Burton C, Pottage T, Thompson KA, Ngabo D, Crook A, et al. Infection-competent monkeypox virus

contamination identified in domestic settings following an imported case of monkeypox into the UK. Environ Microbiol. 2022; (Jul):1–9. https://doi.org/10.1111/1462-2920.16129

38. Garnett L, Bello A, Tran KN, Audet J, Leung A, Schiffman Z, et al. Comparison analysis of different swabs and transport mediums suitable for SARS-CoV-2 testing following shortages. J Virol Methods. 2020;285:113947. https://doi.org/10.1016/j.jviromet.2020.113947

39. Bruijns BB, Tiggelaar RM, Gardeniers H. The extraction and recovery efficiency of pure DNA for different types of swabs. J Forensic Sci. 2018;63:1492–9. https://doi.org/10.1111/1556-4029.13837

Address for correspondence: Clint N. Morgan, Centers for Disease Control and Prevention, 1600 Clifton Rd NE, Atlanta, GA 30327-4029, USA; email: cnmorgan@cdc.gov

SARS-CoV-2 Vaccine Breakthrough by Omicron and Delta Variants, New York, USA

Alexander C. Keyel, Alexis Russell, Jonathan Plitnick, Jemma V. Rowlands, Daryl M. Lamson, Eli Rosenberg, Kirsten St. George

Recently emerged SARS-CoV-2 variants have greater potential than earlier variants to cause vaccine breakthrough infections. During emergence of the Delta and Omicron variants, a matched case–control analysis used a viral genomic sequence dataset linked with demographic and vaccination information from New York, USA, to examine associations between virus lineage and patient vaccination status, patient age, vaccine type, and time since vaccination. Case-patients were persons infected with the emerging virus lineage, and controls were persons infected with any other virus lineage. Infections in fully vaccinated and boosted persons were significantly associated with the Omicron lineage. Odds of infection with Omicron relative to Delta generally decreased with increasing patient age. A similar pattern was observed with vaccination status during Delta emergence but was not significant. Vaccines offered less protection against Omicron, thereby increasing the number of potential hosts for emerging variants.

As of August 10, 2022, the SARS-CoV-2 pandemic had claimed >6.4 million human lives globally, >1 million in the United States, and >70,000 in New York state (*1*). Virus evolution and adaptation have been observed in persistently infected immunocompromised persons (*2*) and animal reservoirs (*3*,*4*), leading to the potential for new, highly adapted variants.

Novel variants of SARS-CoV-2 have shown increased rates of transmission and immune evasion (*5*,*6*). In particular, Omicron has evolved a suite of unique mutations, which have greatly increased its infectiousness (*7*), increased its ability to evade current vaccines (*5*,*6*), and decreased the effectiveness of convalescent plasma transfusions and monoclonal antibody treatments (*8*,*9*). To a lesser degree, the Delta variant showed some of these same patterns of increased infectiousness (*10*) and potential for immune evasion compared with earlier strains that preceded Delta (*11*).

Prior literature has also shown differences in vaccine effectiveness for SARS-CoV-2 lineages associated with variation in vaccine type, time since vaccination, and patient age. Before emergence of the Delta and Omicron variants, data showed reduced neutralizing antibody protection for the Janssen vaccine (Johnson & Johnson, https://www.jnj.com) compared with the Pfizer (Pfizer-BioNTech, https://www.pfizer.com) and Moderna (https://www.modernatx.com) vaccines (*12*) and slightly stronger protection for Moderna compared with Pfizer vaccines (*12*). An effect of time since vaccination has been demonstrated for the Delta variant (*11*). Younger persons were found to be more likely to be infected with Omicron (*13*,*14*).

To test the associations between vaccination status, vaccine type, and time since vaccination with lineage identity during the emergence of new variants of SARS-CoV-2, we conducted a matched case–control study. We performed analyses for the emergence of the Omicron and Delta variants in New York, USA. The study was waived by the New York State Department of Health (NYSDOH) Institutional Review Board for Human Subjects Research review.

Methods

Data Analysis

Omicron Emergence Analysis

We analyzed emergence of the SARS-CoV-2 Omicron variant from November 28, 2021, through January 24, 2022 (Figure 1). We matched persons infected with Omicron (case-patients) to persons infected with any other virus lineage (controls). Case-patients (n = 1,439) included infection with B.1.1.529 and all BA

Author affiliations: New York State Department of Health, Albany, New York, USA (A.C. Keyel, A. Russell, J. Plitnick, J.V. Rowlands, D.M. Lamson, E. Rosenberg, K. St. George); State University of New York, Albany (E. Rosenberg, K. St. George)

DOI: https://doi.org/10.3201/eid2810.221058

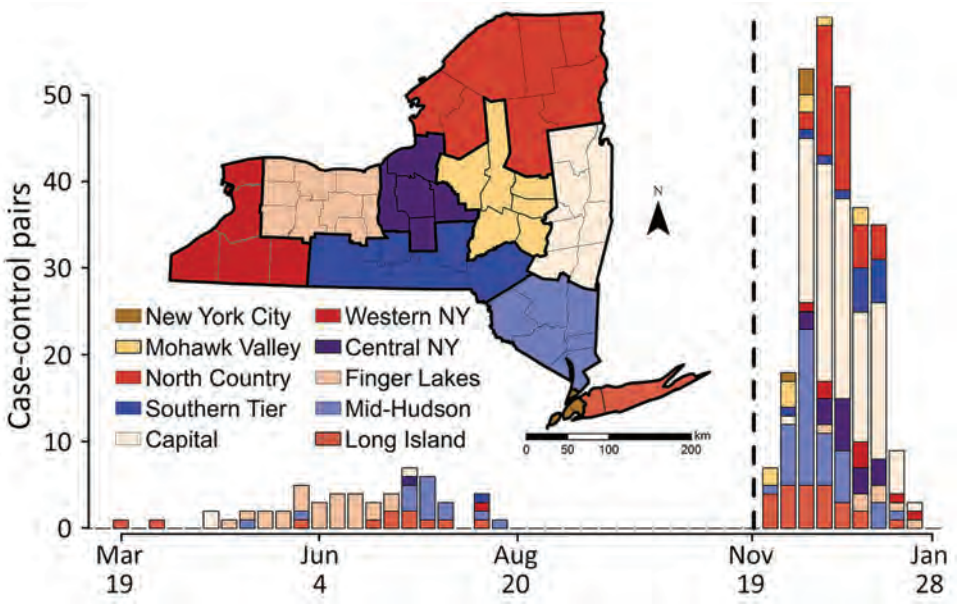

Figure 1. Matched case–control pairs used in the conditional logistic regression by analysis for the SARS-CoV-2 Delta variant (March 19, 2021–August 15, 2021) and the Omicron variant (November 28, 2021–January 24, 2022) emergence periods, by economic region (map), New York, USA. The bars correspond to the order given in the legend; New York City is on top when present and Long Island on bottom when present. The dashed line separates the 2 datasets used in the analyses; the Delta emergence period is on the left and the Omicron emergence period on the right. Map base layer was derived from a combination of 2 public domain layers (US Census data, https://www.census.gov/geo/maps-data/data/tiger-line.html) and Natural Earth Administrative boundaries (https://www.naturalearthdata.com/downloads/50m-cultural-vectors/50m-admin-1-states-provinces).

sublineages (at the time of the analysis, none were classified as BA.2 through BA.5). Controls (n = 728) were persons infected with all other SARS-CoV-2 lineages circulating during the period of Omicron emergence (all sequenced control samples in the matched dataset were Delta variant, B.1.617.2 or AY sublineages). We defined the start of the Omicron emergence period as the first detection in the genomic surveillance dataset (although Omicron was present in the state before that date). The emergence period ended when the last non-Omicron case was detected in the surveillance dataset. One additional case of infection with Delta was identified >14 days after the last date in the surveillance dataset but was excluded because the sensitivity analysis indicated that it would not substantively change the analysis results. We matched case-patients to controls on the basis of specimen collection date (± 6 days), location (using New York state economic regions [Figure 1]), patient age, and patient sex. We matched age according to age groups: 0–4, 5–11, 12–17, 18–29, 30–49, 50–69, 70–89, and ≥90 years. If an exact match could not be found, we allowed mismatches for sex. We used 1-to-1 matching, without replacement (i.e., each case-patient was matched to a unique control). We performed matching in 2 stages. In the first stage, we considered all possible matches for each case-patient. To maximize the sample size, we then sorted case-patients such that the case-patients with the fewest possible matches would be matched to controls first. To estimate odds ratios (ORs) and 95% CIs, we performed 3 sets of conditional logistic regressions.

In analysis 1, we included vaccinated and unvaccinated persons. Key variables tested were vaccination status (binary: yes/no), booster status (yes/no), vaccine type (none, Pfizer, Moderna, Janssen), time since last vaccination or booster (3 factor levels: unvaccinated, vaccinated <90 days, vaccinated ≥90 days). We explored time since completion of initial vaccination and time since booster but found these factors were less predictive and overlapped strongly with the combined time since last vaccination or booster variable and therefore excluded them.

In analysis 2, we examined the association between patient age and virus lineage and therefore removed age as a matching criterion. We performed a conditional logistic regression using age, other main variables for context, and interactions. For this analysis, we did not perform sorting before matching. We examined age in 2 ways: with each age group treated as a factor and with each age group treated as a continuous predictor. Model exploration revealed that a mixture of categorical and continuous predictors best described the underlying data structure (Appendix Table 1, https://wwwnc.cdc.gov/EID/article/28/10/22-1058-App1.pdf).

In analysis 3, we again matched case-patients to controls on the basis of age, but we excluded unvaccinated persons to allow time since last dose (vaccination series or booster) to be treated as continuous

variables. Unvaccinated persons could not be included in this analysis because assigning them NA (not applicable) would cause these values to be excluded, and 0 would be an unrealistic value.

We tested leverage by removing each case–control pair sequentially, refitting the model and noting the change in the OR. We selected models by using Akaike information criterion (AIC) scores (*15*,*16*). Models with lower AIC scores have more model support, and models with ΔAIC >2 are generally considered less likely models. Because a more complicated nested model can be within ΔAIC of 2, nested models were required to be within 2 × no. model parameters to be considered tied (*17*). Of note, AIC provides a relative ranking of models but provides no information on the absolute fit of the model. We examined the fit of each model by considering its statistical significance and the OR estimates. When test results were not significant, we examined the magnitude of the OR. More research was deemed necessary if the estimated OR was large enough to be a public health concern but 95% CIs included 1.

We performed all analyses in R 4.1.2 (*18*) by using the package survival for conditional logistic regressions code (https://www.github.com/akeyel/CLR) (*19*,*20*). We created the New York state map in ArcGIS 10.6 (ESRI, https://www.esri.com) by using a 2017 Tiger Shapefile from the US Census Bureau (*21*) and Admin 1 States, provinces 50-m cultural vector shapefile from Natural Earth Data (as of March 18, 2022) (https://www.naturalearthdata.com/downloads/50m-cultural-vectors).

Delta Emergence Analysis

We analyzed emergence of the SARS-CoV-2 Delta variant during March 19, 2021–August 15, 2021 (Figure 1). The Delta analyses followed the same methods used for the Omicron analyses but with focal virus lineages (603 case-patients) including B.1.617.2 and all AY sublineages. Nonfocal virus lineages (1,816 controls) were all other lineages circulating during the period of Delta emergence (62% B.1.1.7 and Q.4 Alpha, 20% B.1.526 Iota, 3.5% P.1.X Gamma, 1% B.1.351.X Beta); none of the other non–variant of concern strains (13.7% combined) exceeded 5%. We excluded booster-associated variables because booster doses were not available (Appendix Figure 3). We omitted the vaccinated-only analysis because of low statistical power (n = 12 pairs).

Power Analysis

Statistical power for conditional logistic regression is nonlinear and depends on estimated probabilities. Although we used multiple conditional logistic regression for the analyses described above, to make the power analyses easier to set up and interpret, we calculated statistical power for univariate logistic regression by using the WebPower package (*22*,*23*) as a simplifying assumption. We examined statistical power to detect an OR of 2 with a sample size of 110 for a range of probability values (0.1–0.9 for the upper probability); we adjusted lower probability to give an OR of 2. We then used the upper probability value with the highest power (0.7) to assess statistical power for ORs of 2, 3, and 4 for sample sizes of 50–350 by increments of 50.

Data Sources

Respiratory swab specimens that were positive for SARS-CoV-2 by real-time reverse transcription PCR were sent from clinical laboratories across the state for whole-genome sequencing at the NYSDOH Wadsworth Center as part of an enhanced genomic surveillance program. Samples were selected for sequencing on the basis of cycle threshold value and region of patient residence; the goal was full geographic coverage across the state. Sample selection criteria did not change over the course of the study period. We matched samples to demographics in the Communicable Disease Electronic Surveillance System and vaccination records in the New York State Immunization Information System. For persons from whom multiple samples were collected, we included only the earliest collected sample with genome available.

Vaccination status for each person was based on dates of sample collection and administration of vaccines. A person was considered unvaccinated if the sample was collected before any vaccination, vaccinated if the sample was collected >14 days after completion of vaccination (first dose of Janssen, second dose of Pfizer or Moderna vaccine), and boosted if the sample was collected any time after receiving a booster of any vaccine type. We removed from the study persons who were partially vaccinated (sample collected between initial dose and 14 days after vaccination completion, n = 261 [90 with Moderna and 171 with Pfizer vaccine]) and persons who received a greater number of vaccinations than normal. This study does not apply to persons who received a third dose as part of their vaccination series (e.g., potentially immunocompromised persons); these persons were removed from the dataset because of different vaccination history and low sample sizes (58 persons who received a third dose <135 days after their second dose were removed).

Sequencing Methods

We performed whole-genome amplicon sequencing of SARS-CoV-2 by using a modified version of the Illumina ARTIC protocol (https://artic.network/ncov-2019) with ARTIC V3 primers in the Applied Genomics Technology Core at the Wadsworth Center, as previously described (*24*), and amplified later samples with ARTIC V4 primers. We sequenced samples with particularly low virus titers by using AmpliSeq chemistry on the Ion Torrent S5XL sequencer, as previously described (*25*).

GISAID (https://www.gisaid.org) accession numbers for sequences are available from https://github.com/akeyel/CLR/blob/main/GISAID_accession_IDs.csv. In that chart, the first column shows the GISAID accession number, and the subsequent columns indicate whether the identification number was used in the respective analyses. Data are coded such that –1 indicates records that were removed before analysis, 0 indicates records that met the basic overall study criteria but were not matched for a particular analysis, and 1 indicates that the record was included in the analysis.

Results

Omicron Emergence

In analysis 1, >80% of 272 case-patient/control pairs were 18–69 years of age; most were from the Capital and Mid-Hudson regions (Table 1; Figure 1). Among controls, 8% had received a booster, and among case-patients, 22% had received a booster. Among controls, 56.6% were unvaccinated; among case-patients, 30% were unvaccinated (Table 1). Sample sizes were 177 for Pfizer, 109 for Moderna, and 22 for Janssen vaccine recipients. The variables most associated with an Omicron lineage identity were vaccination (OR 3.1, 95% CI 2.0–4.9; p<0.001) and booster status (OR 6.7, 95% CI 3.4–13.0; p <0.001) (Table 2, Figure 2).

Table 1. Descriptive statistics for matched case-patients and controls for the conditional logistic regression model for study of SARS-CoV-2 vaccine breakthrough during the emergence period of the Omicron variant, New York, USA*

	No. (%)					
	Analysis 1, main		Analysis 2, by age		Analysis 3, vaccinated only	
Demographic group	Controls	Case-patients	Controls	Case-patients	Controls	Case-patients
Age, y						
0–4	4 (1.5)	4 (1.5)	9 (2.9)	4 (1.3)	0	0
5–11	4 (1.5)	4 (1.5)	7 (2.3)	9 (2.9)	0	0
12–17	11 (4)	11 (4.0)	15 (4.9)	16 (5.2)	3 (2.3)	3 (2.3)
18–29	55 (20.2)	55 (20.2)	39 (12.6)	85 (27.5)	23 (17.8)	23 (17.8)
30–49	95 (34.9)	95 (34.9)	85 (27.5)	95 (30.7)	49 (38.0)	49 (38.0)
50–69	71 (26.1)	71 (26.1)	96 (31.1)	69 (22.3)	40 (31.0)	40 (31.0)
70–89	31 (11.4)	31 (11.4)	52 (16.8)	30 (9.7)	14 (10.9)	14 (10.9)
≥90	1 (0.4)	1 (0.4)	6 (1.9)	1 (0.3)	0	0
Sex						
M	141 (51.8)	147 (54.0)	155 (50.2)	153 (49.5)	65 (50.4)	77 (59.7)
F	129 (47.4)	123 (45.2)	152 (49.2)	155 (50.2)	63 (48.8)	52 (40.3)
Unknown	2 (0.7)	2 (0.7)	2 (0.6)	1 (0.3)	1 (0.8)	0
Region						
Capital	107 (39.3)	107 (39.3)	121 (39.2)	121 (39.2)	47 (36.4)	47 (36.4)
Central New York	17 (6.2)	17 (6.2)	18 (5.8)	18 (5.8)	10 (7.8)	10 (7.8)
Finger Lakes	7 (2.6)	7 (2.6)	9 (2.9)	9 (2.9)	3 (2.3)	3 (2.3)
Long Island	25 (9.2)	25 (9.2)	27 (8.7)	27 (8.7)	12 (9.3)	12 (9.3)
Mid-Hudson	42 (15.4)	42 (15.4)	47 (15.2)	47 (15.2)	26 (20.2)	26 (20.2)
Mohawk Valley	10 (3.7)	10 (3.7)	18 (5.8)	18 (5.8)	4 (3.1)	4 (3.1)
New York City	4 (1.5)	4 (1.5)	6 (1.9)	6 (1.9)	1 (0.8)	1 (0.8)
North Country	38 (14.0)	38 (14.0)	39 (12.6)	39 (12.6)	20 (15.5)	20 (15.5)
Southern Tier	14 (5.1)	14 (5.1)	16 (5.2)	16 (5.2)	2 (1.6)	2 (1.6)
Western New York	8 (2.9)	8 (2.9)	8 (2.6)	8 (2.6)	4 (3.1)	4 (3.1)
Vaccination status						
Unvaccinated	154 (56.6)	82 (30.1)	175 (56.6)	78 (25.2)	0	0
Vaccinated <90 d	3 (1.1)	4 (1.5)	3 (1.0)	5 (1.6)	2 (1.6)	2 (1.6)
Vaccinated >90 d	115 (42.3)	186 (68.4)	131 (42.4)	226 (73.1)	127 (98.4)	127 (98.4)
Pfizer vaccine	64 (23.5)	113 (41.5)	69 (22.3)	135 (43.7)	64 (49.6)	82 (63.6)
Moderna vaccine	43 (15.8)	66 (24.3)	49 (15.9)	82 (26.5)	48 (37.2)	41 (31.8)
Janssen vaccine	11 (4)	11 (4.0)	16 (5.2)	14 (4.5)	17 (13.2)	6 (4.7)
Unboosted	250 (91.9)	211 (77.6)	281 (90.9)	210 (68.0)	108 (83.7)	88 (68.2)
Boosted <90 d	18 (6.6)	49 (18.0)	25 (8.1)	76 (24.6)	18 (14)	37 (28.7)
Boosted ≥90 d	2 (0.7)	9 (3.3)	2 (0.6)	20 (6.5)	1 (0.8)	3 (2.3)
Pfizer booster	11 (4.8)	41 (15.4)	13 (4.5)	68 (22.7)	10 (7.8)	33 (25.6)
Moderna booster	9 (3.3)	17 (7)	14 (4.5)	281 (9.4)	9 (7.0)	7 (5.4)

*Presence (case-patient) or absence (control) of Omicron was used as the basis for matching. Janssen vaccine, Janssen/Johnson & Johnson (https://www.jnj.com); Pfizer vaccine/booster, Pfizer-BioNTech (https://www.pfizer.com); Moderna

Table 2. Variables most associated with an Omicron variant in 3 analyses of SARS-CoV-2 vaccine breakthrough during the emergence period of the Omicron variant, New York, USA*

Model	ΔAIC	Odds ratio (95% CI)		
		Parameter 1	Parameter 2	Parameter 3
Main analysis				
Vaccination status	0	Vaccinated: 3.1 (2.0–4.9)†	Vaccinated + boosted: 6.7 (3.4–13.0)†	
Vaccine type	3.33	Pfizer	Moderna	Janssen
Without booster		3.3 (1.9–5.6)†	3.6 (2.0–6.7)†	2.0 (0.8–5.1)
With booster		10.4 (4.3–25.2)†	3.8 (1.5–9.3)‡	
Age analysis				
Vaccination status + age + age groups	0.00	Vaccinated: 4.8 (2.8–8.1)†	Vaccinated + boosted: 38.5 (15.9–93.2)†	Age, linear: 0.964 (0.950–0.978);† age 0–4 y: 0.250 (0.059–1.051); age 18–29 y: 2.0 (1.1–3.7)§
Vaccination status + age	7.41	Vaccinated: 5.0 (3.0–8.3)†	Vaccinated + boosted: 34.1 (14.6–79.5)†	Age: 0.962 (0.950–0.974)†
Vaccination-only analysis				
Janssen + days after dose	0.00	Janssen, relative to mRNA vaccine: 0.388 (0.149–1.009)		Days after last dose, booster or primary series: 0.996 (0.993–0.999)‡
Vaccine type + days after dose	1.18	Moderna, relative to Pfizer: 0.776 (0.448–1.344)	Janssen, relative to Pfizer: 0.351 (0.132–0.935)§	Days after last dose, booster or primary series:0.996 (0.993–0.999)‡

*Only 1 boosted person had received an initial dose of Janssen vaccine, so for statistical reasons, this person was pooled with the unboosted Janssen recipients. When fit separately, the odds ratio for unboosted Janssen recipients was 1.9 (0.8–4.9) with a parameter p value of 0.20, and the parameter estimate for the single boosted Janssen individual was unreliable. Janssen vaccine, Janssen/Johnson & Johnson (https://www.jnj.com); Pfizer vaccine, Pfizer-BioNTech (https://www.pfizer.com); Moderna vaccine, Moderna (https://www.modernatx.com). ΔAIC, change in Akaike information criterion.
†p<0.001.
‡p<0.01.
§p<0.05.

In analysis 2 (309 pairs), when patient age was removed as a matching criterion, younger age was also predictive of an Omicron infection; log-odds of infection with Omicron generally decreased as age increased (OR 0.962, 95% CI 0.950–0.974) (Table 2). Significant patterns beyond this log-linear age effect were found for persons in 2 age groups. log-odds of infection with Omicron were lower for persons 0–4 years of age than predicted by a log-linear age effect alone (Figure 2) and higher for persons 18–29 years of age than predicted by a log-linear age term alone; risk was highest for those 18–29 years of age (Figure 2). OR estimates for vaccination status (OR 4.8, 95% CI 2.8–8.1) and booster status (OR 38.5, 95% CI 15.9–93.2) were higher than in the analysis that used age as a matching criterion (Table 2).

In analysis 3 (vaccinated-only persons, 129 pairs), the probability of infection with Omicron decreased with an increased number of days after the last vaccine dose (OR 0.996, 95% CI 0.993–0.999) (Table 2). Vaccine type was also included in the top statistical models (Appendix Table 1) and the trend toward reduced odds of Omicron infection after vaccination with the Janssen vaccine was borderline significant (OR 0.351, 95% CI 0.132–0.935, relative to Pfizer vaccine; OR 0.388, 95% CI 0.149–1.009, relative to any mRNA vaccine) (Table 2).

Delta Emergence

In analysis 1 (55 pairs), 75% were 18–69 years of age; 89% of case-patients/controls were from the Finger Lakes, Long Island, and the Mid-Hudson regions (Table 3). A total of 74.5% of controls and 61.8% of case-patients were unvaccinated (Table 3). Vaccine type, time from last vaccination, and an interaction of the 2 were not significantly associated with an increased likelihood of infection with Delta than any other virus lineage in the fully matched conditional logistic regression (Table 4). Vaccination status was the top model (OR 2.4, 95% CI 0.8–6.8; p = 0.08). Vaccine type had no significant effect (p = 0.12), but estimated ORs were 2.9 (95% CI 0.9–8.9) for Pfizer, 0.38 (95% CI 0.04–4.2) for Moderna, and 2.0 (95% CI 0.17–23.6) for Janssen.

The power analysis showed that a sample size of 110 (55 pairs) would have a 15%–45% chance of obtaining a significant result for an OR of 2 under the simulated probability distributions. A sample size of ≥255 would be needed to have ≥80% power for an OR of 2. A sample size of 110 could have ≤78% power to detect an OR of 3 and 93% power to detect an OR of 4. A sample size of 24 could detect an OR of 22 with 80% power but would only have 36% power to detect an OR of 4.

When case-patients and controls were no longer matched on the basis of age (66 pairs), vaccine type was the top model (Appendix Table 2), suggesting that odds of being infected with Delta rather than any other virus lineage increased by a factor of 7.3 (2.0–26.7) for those receiving the Pfizer vaccine

relative to unvaccinated persons. Effects for Moderna (2.0, 95% CI 0.25–17.1) and Janssen (0.46, 95% CI 0.04–4.76) vaccines were substantial but not individually significant.

Discussion

Our exploration of vaccine breakthrough, vaccination status, and time since vaccination in this matched case–control study adds to the body of evidence supporting immune escape of SARS-CoV-2. Some results may seem counterintuitive because of the study design. For example, although a booster increases protection against infection with Omicron compared with absence of a booster (*13*,*26*), history of a booster was associated with Omicron (the emergent strain) and not Delta (the established strain) infection. This finding is consistent with evidence that suggests that having a booster is less effective for preventing infection with Omicron than with Delta (*6*,*13*). Similarly, vaccine effectiveness has been shown to wane with time (*11*); therefore, we hypothesized that increased time after vaccination would decrease the odds of being infected with the emergent strain.

Our analysis of New York state genomic surveillance data yielded results that are consistent with previous research showing an increased probability of breakthrough for Omicron compared with other variants for both vaccinated and boosted persons (*6*,*8*). In a similar study in Connecticut, USA, comparing odds of infection with Omicron versus Delta (*6*), an OR of ≈2 (95% CI 1.5–3.7 or 1.5–2.2, depending on time after vaccination) was found for vaccinated persons and ≈3 (95% CI 1.8–4.9) for boosted persons. These estimates are lower than the estimates from our study of 3.1 (95% CI 2.0–4.9) for vaccinated persons and 6.7 (95% CI 3.4–13.0) for unvaccinated persons, but the 95% CIs overlap between the 2 studies. A strong pattern of the emergent strain shows increased ability for vaccine breakthrough compared with other strains circulating at the time. Studies of prior variants of concern have found significant vaccine breakthrough in emergent variants. For example, Kustin et al. found that vaccine breakthrough for Alpha (B.1.1.7) was more likely compared with prior strains (*27*). Similarly, Tartof et al. found evidence for increased rates of vaccine breakthrough by Delta (B.1.617.2), although waning vaccine immunity was also a factor in that study (*11*). In addition, Rosenberg et al. showed increased breakthrough during the Delta emergence period and suggested that this effect was independent of waning immunity (*28*).

When we restricted the analysis to vaccinated persons only, time after vaccination was a statistically significant factor; probability of Omicron infection decreased with increased time after vaccination. The time-after-vaccination variable combined persons who had recently received a booster with those who had recently completed their primary series. Adding a variable to indicate booster status did not improve the model fit (Appendix Table 1). Of note, most persons in this study were >3 months past completion of their initial vaccination series. Boosters were more recent, and therefore vaccination status and booster status probably encoded much of the same information as a time-after-last-dose variable. No time-after-vaccination effect was detected if the data were coarsely divided into persons who had and had not received boosters, suggesting that more examination of this variable may be necessary. This variable was not found among the top models in the Delta emergence analysis.

Younger persons were more likely to be infected with Omicron than with Delta during the Omicron emergence period, although the data in this study cannot be used to distinguish a physiological basis from a behavioral basis for these age effects. Kahn et al. found Delta and Omicron infection be equally distributed by age among unvaccinated persons but to shift strongly toward younger persons among vaccinated persons (*14*); however, Accorsi et al. found

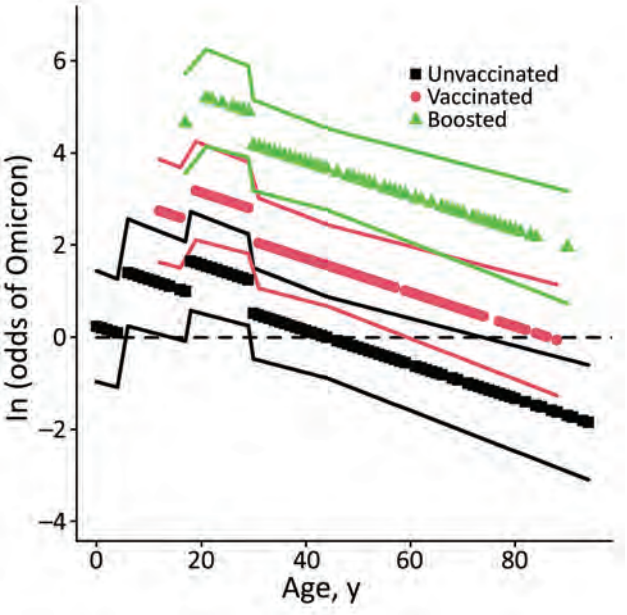

Figure 2. Visualization of the fixed effects from the second Omicron emergence analysis on a log-odds scale (without age matching) in a study of SARS-CoV-2 vaccine breakthrough by Omicron and Delta variants, New York, USA. Odds scale in Appendix (https://wwwnc.cdc.gov/EID/article/28/10/22-1058-App1.pdf). Stratum-specific effects were often strong but were excluded for visual clarity. Increased values indicate an increased probability of infection with Omicron instead of Delta. Lines show ± 1 SE.

Table 3. Descriptive statistics for matched case-patients and controls for the conditional logistic regression model for study of SARS-CoV-2 vaccine breakthrough during the emergence period of the Delta variant, New York, USA*

	No. (%)			
	Analysis 1, main		Analysis 2, age	
Demographic group	Controls	Case-patients	Controls	Case-patients
Age, y				
0–4	0	0	3 (4.5)	0
5–11	3 (5.5)	3 (5.5)	5 (7.6)	0
12–17	5 (9.1)	5 (9.1)	3 (4.5)	4 (6.1)
18–29	11 (20)	11 (20)	12 (18.2)	10 (15.2)
30–49	26 (47.3)	26 (47.3)	23 (34.8)	30 (45.5)
50–69	6 (10.9)	6 (10.9)	14 (21.2)	17 (25.8)
70–89	4 (7.3)	4 (7.3)	6 (9.1)	5 (7.6)
≥90	0	0	0	0
Sex				
M	26 (47.3)	25 (45.5)	28 (42.4)	30 (45.5)
F	29 (52.7)	29 (52.7)	38 (57.6)	35 (53)
Unknown	0	1 (1.8)	0	1 (1.5)
Region				
Capital Region	3 (5.5)	3 (5.5)	4 (6.1)	4 (6.1)
Central New York	1 (1.8)	1 (1.8)	1 (1.5)	1 (1.5)
Finger Lakes	24 (43.6)	24 (43.6)	27 (40.9)	27 (40.9)
Long Island	11 (20)	11 (20)	15 (22.7)	15 (22.7)
Mid-Hudson	14 (25.5)	14 (25.5)	16 (24.2)	16 (24.2)
New York City	0	0	1 (1.5)	1 (1.5)
North Country	0	0	0	0
Southern Tier	1 (1.8)	1 (1.8)	1 (1.5)	1 (1.5)
Western New York	1 (1.8)	1 (1.8)	1 (1.5)	1 (1.5)
Vaccination status				
Unvaccinated	41 (74.5)	34 (61.8)	48 (72.7)	35 (53)
Vaccinated <90 d	7 (12.7)	9 (16.4)	9 (13.6)	9 (13.6)
Vaccinated ≥90 d	7 (12.7)	12 (21.8)	9 (13.6)	22 (33.3)
Pfizer vaccine	10 (18.2)	18 (32.7)	11 (16.7)	28 (42.4)
Moderna vaccine	5 (9.1)	2 (3.6)	4 (6.1)	3 (4.5)
Janssen vaccine	1 (1.8)	3 (5.5)	3 (4.5)	1 (1.5)

*Presence (case-patient) or absence (control) of Omicron was used as the basis for matching. Janssen vaccine, Janssen/Johnson & Johnson (https://www.jnj.com); Pfizer vaccine, Pfizer-BioNTech (https://www.pfizer.com); Moderna vaccine, Moderna (https://www.modernatx.com).

elevated rates of Omicron infection among vaccinated and unvaccinated persons (*13*). It is possible that the age group effects are the result of a greater degree of socialization and other behavioral risk factors among persons 18–29 years of age. In 2020, college campus re-openings were associated with increased transmission of SARS-CoV-2 (*29*). Because Omicron infections can break through vaccinations, college campuses may have increased the likelihood of persons in this age group being infected with SARS-CoV-2 (*30*). The age group effect for preschool children (0–4 years of age) may represent a reduced level of socialization for this group. This effect, although included in the top model identified by the information theoretic approach here, was not statistically significant, so it also may be an artifact of low sample sizes for this age group. Other research has found that vaccines were not equally effective among age groups (V. Dorabawila, unpub. data, https://www.medrxiv.org/content/10.1101/2022.02.25.22271454v1). Vaccine effectiveness in New York was very low for persons 5–11 years of age, who received a lower dose (10 μg) of the Pfizer vaccine than for vaccinated persons ≥12 years of age who received a 30-μg dose (V. Dorabawila, unpub. data, https://www.medrxiv.org/content/10.1101/2022.02.25.2

Table 4. Variables most associated with a Delta variant infection in 2 analyses of SARS-CoV-2 vaccine breakthrough during the emergence period of the Delta variant, New York, USA*

Model	ΔAIC	Parameter 1	Parameter 2	Parameter 3
Main analysis				
Vaccination status	0.00	Vaccinated: 2.4 (0.8–6.8)		
Vaccine type	1.05	Pfizer: 2.86 (0.92–8.94)	Moderna: 0.38 (0.04–4.20)	Janssen: 1.97 (0.17–23.57)
Age analysis				
Vaccine type	0.02	Pfizer: 7.3 (2.0–26.7)†	Moderna: 2.0 (0.25–17.1)	Janssen: 0.46 (0.04–4.76)

*None of the main analysis models were statistically significant because all 95% CIs for odds ratio estimates overlapped 1. Janssen vaccine, Janssen/Johnson & Johnson (https://www.jnj.com); Pfizer vaccine, Pfizer-BioNTech (https://www.pfizer.com); Moderna vaccine, Moderna (https://www.modernatx.com). ΔAIC, change in Akaike information criterion.
†p<0.01.

2271454v1). However, the log-linear age effect detected here was not driven by children <12 years of age. When children <12 years of age were removed from the analysis, the estimated OR changed from 0.962 to 0.957 (95% CI 0.944–0.971), suggesting that the magnitude of the effect is greater when young children were removed from the analysis. Larger estimates for vaccination status and booster status were also greater when children <12 years of age were removed from the analysis (vaccination status OR 5.4, 95% CI 3.1–9.7; vaccination plus booster status OR 43.0, 95% CI 17.1–108.5). Vaccination rates and booster rates changed substantially during the study periods as well (Appendix Figures 2, 3), but any resulting biases were probably controlled for by the case–control study design.

Sample sizes were generally too small to detect robust vaccine type effects. The Janssen vaccine showed borderline significantly reduced OR for infection with Omicron relative to the Pfizer vaccine in 1 statistical model (Table 2; Appendix Table 1). This result would be consistent with improved performance against Omicron infection or with worse performance of this vaccine against Delta infection, as has been observed (*28*). Otherwise, OR estimates showed the potential for substantial differences, but overlapping 95% CIs prevent drawing robust conclusions (Table 2; Appendix Table 1).

Statistical power was constrained by the limited emergence periods and the relatively small percentage of viruses from COVID-19 case-patients that were sequenced. For Delta, the emergence period occurred during a time of reduced sequencing, because of low overall incidence during the summer of 2021, when Delta displaced previous strains (Figure 1). For Omicron, a larger sequencing effort was made, but the emergence period was considerably shorter because of the rapid dominance of the Omicron variant (Figure 1). Sample sizes could potentially be increased by expanding the regional scope of the study or incorporating sequencing results from other research laboratories.

We used only 1 matched set for each analysis. However, because case-patients were randomly matched to controls, other matches were possible. This limitation could be overcome by assessing significance with Monte Carlo simulation over the range of possible matches. That said, visual examination of leverage plots based on removing a single pair suggested that the results were generally unlikely to change with the removal of any single data point. The exception is the Delta analysis, in which a change of 1–2 data points would change the overall statistical significance of the results (Appendix Figure 1) without much change in the estimated OR.

In conclusion, this analysis of the emergence of the Omicron and Delta variants in New York, USA, based on sequenced virus identity broadly supports the results of prior studies (*5*–*8*). Vaccines offered less protection against Omicron infection, thereby increasing the number of potential hosts for emerging variants.

This article was preprinted at https://www.medrxiv.org/content/10.1101/2022.06.24.22276709v1.

Acknowledgments

We thank the Wadsworth Center Virology Laboratory for processing specimens, the Advanced Genomic Technologies Core for performing next-generation sequencing, and the Bioinformatics Core for sequence analysis. We thank Kathleen McDonough for constructive feedback on the project. We also thank the New York state clinical laboratories that submitted SARS-CoV-2–positive specimens to Wadsworth for sequencing, as well as all originating and submitting laboratories for their SARS-CoV-2 sequence contributions to the GISAID database.

Initial funding for sequencing was generously provided by the New York Community Trust. The work for this publication was also supported by Cooperative Agreement no. NU50CK000516, funded by the Centers for Disease Control and Prevention.

A.C.K., A.R., J.P., J.V.R., E.R., and D.M.L. declare no conflicts of interest. K.S.G. receives research support from ThermoFisher for the evaluation of new assays for the diagnosis and characterization of viruses and has a royalty generating collaborative agreement with Zeptometrix.

About the Author

Dr. Keyel is a research scientist at the NYSDOH Wadsworth Center. His expertise is in Geographic Information Systems, scripting in R and Python, and ecological modeling.

References

1. Johns Hopkins University of Medicine. Johns Hopkins Coronavirus Resource Center [cited 2022 Aug 10]. https://coronavirus.jhu.edu
2. Borges V, Isidro J, Cunha M, Cochicho D, Martins L, Banha L, et al. Long-term evolution of SARS-CoV-2 in an immunocompromised patient with non-Hodgkin lymphoma. MSphere. 2021;6:e0024421. https://doi.org/10.1128/mSphere.00244-21
3. Hale VL, Dennis PM, McBride DS, Nolting JM, Madden C, Huey D, et al. SARS-CoV-2 infection in free-ranging white-tailed deer. Nature. 2022;602:481–6. https://doi.org/10.1038/s41586-021-04353-x

4. Bashor L, Gagne RB, Bosco-Lauth AM, Bowen RA, Stenglein M, VandeWoude S. SARS-CoV-2 evolution in animals suggests mechanisms for rapid variant selection. Proc Natl Acad Sci U S A. 2021;118:e2105253118. https://doi.org/10.1073/pnas.2105253118
5. Collie S, Champion J, Moultrie H, Bekker LG, Gray G. Effectiveness of BNT162b2 vaccine against Omicron variant in South Africa. N Engl J Med. 2022;386:494–6. https://doi.org/10.1056/NEJMc2119270
6. Chaguza C, Coppi A, Earnest R, Ferguson D, Kerantzas N, Warner F, et al. Rapid emergence of SARS-CoV-2 Omicron variant is associated with an infection advantage over Delta in vaccinated persons. Med (N Y). 2022;3:325–334.e4. https://doi.org/10.1016/j.medj.2022.03.010
7. Chen J, Wang R, Gilby NB, Wei GW. Omicron variant (B.1.1.529): infectivity, vaccine breakthrough, and antibody resistance. J Chem Inf Model. 2022;62:412–22. https://doi.org/10.1021/acs.jcim.1c01451
8. Liu L, Iketani S, Guo Y, Chan JFW, Wang M, Liu L, et al. Striking antibody evasion manifested by the Omicron variant of SARS-CoV-2. Nature. 2022;602:676–81. https://doi.org/10.1038/s41586-021-04388-0
9. Hoffmann M, Krüger N, Schulz S, Cossmann A, Rocha C, Kempf A, et al. The Omicron variant is highly resistant against antibody-mediated neutralization: Implications for control of the COVID-19 pandemic. Cell. 2022;185:447–456.e11. https://doi.org/10.1016/j.cell.2021.12.032
10. Li B, Deng A, Li K, Hu Y, Li Z, Shi Y, et al. Viral infection and transmission in a large, well-traced outbreak caused by the SARS-CoV-2 Delta variant. Nat Commun. 2022;13:460. https://doi.org/10.1038/s41467-022-28089-y
11. Tartof SY, Slezak JM, Fischer H, Hong V, Ackerson BK, Ranasinghe ON, et al. Effectiveness of mRNA BNT162b2 COVID-19 vaccine up to 6 months in a large integrated health system in the USA: a retrospective cohort study. Lancet. 2021;398:1407–16. https://doi.org/10.1016/S0140-6736(21)02183-8
12. Atmar RL, Lyke KE, Deming ME, Jackson LA, Branche AR, El Sahly HM, et al.; DMID 21-0012 Study Group. Homologous and heterologous Covid-19 booster vaccinations.N Engl J Med. 2022;386:1046–57. https://doi.org/10.1056/NEJMoa2116414
13. Accorsi EK, Britton A, Fleming-Dutra KE, Smith ZR, Shang N, Derado G, et al. Association between 3 Doses of mRNA COVID-19 vaccine and symptomatic infection caused by the SARS-CoV-2 Omicron and Delta variants. JAMA. 2022;327:639–51. https://doi.org/10.1001/jama.2022.0470
14. Kahn F, Bonander C, Moghaddassi M, Rasmussen M, Malmqvist U, Inghammar M, et al. Risk of severe COVID-19 from the Delta and Omicron variants in relation to vaccination status, sex, age and comorbidities—surveillance results from southern Sweden, July 2021 to January 2022. Euro Surveill. 2022;27:2200121. https://doi.org/10.2807/1560-7917.ES.2022.27.9.2200121
15. Akaike H. A new look at the statistical model identification. IEEE Trans Automat Contr. 1974;19:716–23. https://doi.org/10.1109/TAC.1974.1100705
16. Burnham KP, Anderson DR. Model Selection and Multimodel inference. New York: Springer-Verlag; 2002. p. 1–488.
17. Arnold TW. Uninformative parameters and model selection using Akaike's Information Criterion. J Wildl Manage. 2010;74:1175–8. https://doi.org/10.1111/j.1937-2817.2010.tb01236.x
18. R Core Team. R: A language and environment for statistical computing. R Foundation for Statistical Computing. Vienna (Austria); 2021 [cited 2022 Aug 10]. https://www.R-project.org
19. Therneau T. A package for survival analysis in R [cited 2022 Aug 10]. https://CRAN.R-project.org/package=survival
20. Therneau TM, Grambsch PM. Modeling Survival Data: Extending the Cox Model. New York: Springer; 2000.
21. US Census Bureau. TIGER/Line Shapefiles [cited 2021 Nov 23]. https://www.census.gov/geo/maps-data/data/tiger-line.html
22. Zhang Z, Mai Y. WebPower: basic and advanced statistical power analysis. R package version 0.7 [cited 2022 Aug 10]. https://CRAN.R-project.org/package=WebPower
23. Demidenko E. Sample size determination for logistic regression revisited. Stat Med. 2007;26:3385–97. https://doi.org/10.1002/sim.2771
24. Alpert T, Brito AF, Lasek-Nesselquist E, Rothman J, Valesano AL, MacKay MJ, et al. Early introductions and transmission of SARS-CoV-2 variant B.1.1.7 in the United States. Cell. 2021;184:2595–2604.e13. https://doi.org/10.1016/j.cell.2021.03.061
25. Plitnick J, Griesemer S, Lasek-Nesselquist E, Singh N, Lamson DM, St George K. Whole-genome sequencing of SARS-CoV-2: assessment of the Ion Torrent AmpliSeq panel and comparison with the Illumina MiSeq ARTIC protocol. J Clin Microbiol. 2021;59:e0064921. https://doi.org/10.1128/JCM.00649-21
26. Nyberg T, Ferguson NM, Nash SG, Webster HH, Flaxman S, Andrews N, et al.; COVID-19 Genomics UK (COG-UK) consortium. Comparative analysis of the risks of hospitalisation and death associated with SARS-CoV-2 omicron (B.1.1.529) and delta (B.1.617.2) variants in England: a cohort study. Lancet. 2022;399:1303–12. https://doi.org/10.1016/S0140-6736(22)00462-7
27. Kustin T, Harel N, Finkel U, Perchik S, Harari S, Tahor M, et al. Evidence for increased breakthrough rates of SARS-CoV-2 variants of concern in BNT162b2-mRNA-vaccinated individuals. Nat Med. 2021;27:1379–84. https://doi.org/10.1038/s41591-021-01413-7
28. Rosenberg ES, Dorabawila V, Easton D, Bauer UE, Kumar J, Hoen R, et al. Covid-19 vaccine effectiveness in New York State. N Engl J Med. 2022;386:116–27. https://doi.org/10.1056/NEJMoa2116063
29. Yamey G, Walensky RP. Covid-19: re-opening universities is high risk. BMJ. 2020;370:m3365. https://doi.org/10.1136/bmj.m3365
30. Meredith GR, Diel DG, Frazier PI, Henderson SG, Koretzky GA, Wan J, et al. Routine surveillance and vaccination on a university campus during the spread of the SARS-CoV-2 Omicron variant. JAMA Netw Open. 2022;5:e2212906. https://doi.org/10.1001/jamanetworkopen.2022.12906

Address for correspondence: Alexander C. Keyel, New York State Department of Health, Division of Infectious Diseases, David Axelrod Institute, 120 New Scotland Rd, Albany, NY 12208, USA; email: alexander.keyel@health.ny.gov

SARS-CoV-2 Secondary Attack Rates in Vaccinated and Unvaccinated Household Contacts during Replacement of Delta with Omicron Variant, Spain

Israel López-Muñoz, Ariadna Torrella, Olga Pérez-Quílez, Amaia Castillo-Zuza, Elisa Martró, Antoni E. Bordoy, Verónica Saludes, Ignacio Blanco, Laura Soldevila, Oriol Estrada, Lluís Valerio, Sílvia Roure, Xavier Vallès

We performed a prospective, cross-sectional study of household contacts of symptomatic index case-patients with SARS-CoV-2 infection during the shift from Delta- to Omicron-dominant variants in Spain. We included 466 household contacts from 227 index cases. The secondary attack rate was 58.2% (95% CI 49.1%–62.6%) during the Delta-dominant period and 80.9% (95% CI 75.0%–86.9%) during the Omicron-dominant period. During the Delta-dominant period, unvaccinated contacts had higher probability of infection than vaccinated contacts (odds ratio 5.42, 95% CI 1.6–18.6), but this effect disappeared at ≈20 weeks after vaccination. Contacts showed a higher relative risk of infection (9.16, 95% CI 3.4–25.0) in the Omicron-dominant than Delta-dominant period when vaccinated within the previous 20 weeks. Our data suggest vaccine evasion might be a cause of rapid spread of the Omicron variant. We recommend a focus on developing vaccines with long-lasting protection against severe disease, rather than only against infectivity.

The mass vaccination against SARS-CoV-2 that began at the end of 2020 reduced COVID-19-related mortality and severity in countries where substantial vaccine coverage was achieved (*1*,*2*). The vaccines also had a protective effect against the most recent variants (*3*,*4*). However, expectations that vaccines would stop community transmission of SARS-CoV-2 through herd immunity were quickly dampened by the early observation of infection and re-infection among vaccinated persons; waning vaccine effectiveness against transmission (VET) over time was observed (*1*,*3*) and confirmed in a large systematic literature review (*5*). Despite these results, protective effects of vaccination against infection among contacts have been reported (*6*). The vaccination status of index case-patients was also shown to play a role (*6*), underscoring the importance of vaccination for reducing the circulation of SARS-CoV-2. Nonetheless, the emergence of new variants of concern (VOC) with increased infectivity is an ongoing challenge for VET of currently licensed vaccines; early reports have shown a substantially lower VET for the Delta variant (B.1.617.2) compared with previous VOCs (*7*). Furthermore, rapid replacement of the Delta variant by Omicron (B.1.1.529) began in late 2021; the Omicron variant showed a transmission advantage because of its shorter generation time (S. Abbott et al., unpub. data, https://www.medrxiv.org/content/10.1101/2022.01.08.22268920v1).

Evaluating both variant virulence and SARS-CoV-2 VET under high vaccine coverage levels has major epidemiologic, social, and policy implications. We report the results of an observational study of household contacts of SARS-CoV-2–infected index case-patients during a Delta variant–dominant period from September to December 2021 and an Omicron variant–dominant period during January 2022 in a north-metropolitan area of Barcelona, Spain. We

Author affiliations: North Metropolitan International Health Program, Catalan Institute of Health (PROSICS), Badalona, Spain (I. López-Muñoz, A. Torrella, O. Pérez-Quílez, A. Castillo-Zuza, L. Soldevila, L. Valerio, S. Roure, X. Vallès); Hospital Universitari Germans Trias i Pujol, Badalona (E. Martró, A.E. Bordoy, V. Saludes, I. Blanco, L. Soldevila, S. Roure); Center for Biomedical Research in Epidemiology and Public Health (CIBEREPS), Instituto de Salud Carlos III, Madrid, Spain (E. Martró, A.E. Bordoy, V. Saludes); Institut d'Investigació en Ciències de la Salut Germans Trias i Pujol, Badalona (E. Martró, A.E. Bordoy, V. Saludes, I. Blanco, O. Estrada, X. Vallès); Fundació Lluita contra la Sida i les Malalties Transmissibles, Badalona (L. Soldevila, S. Roure, X. Vallès)

DOI: https://doi.org/10.3201/eid2810.220494

evaluated the protective effects of vaccination status, time elapsed since vaccine administration, absolute and relative infectiousness of both variants, overall VET, and VET relative to vaccination status for index case-patients and contacts during both periods. The study was approved by the Ethics Board of the Hospital Universitari Germans Trias i Pujol, Badalona, Catalonia, Spain (reference no. PI-20-228) and conducted in accordance with the principles of the Declaration of Helsinki. Oral informed consent was obtained from all individual participants included in the study.

Materials and Methods

Study Population

The study population catchment area was the northern part of the greater metropolitan area of Barcelona in Catalonia, Spain. The area has ≈800,000 inhabitants and comprises a mixture of urban and semirural municipalities. During the study period, SARS-CoV-2 screening was readily available at no cost to persons with suspected COVID-19 and their contacts at health centers serving the respective primary care catchment areas. The smallest administrative area of the public healthcare system in Catalonia typically covers 15,000–25,000 inhabitants.

Study Design

We performed a prospective cross-sectional study of household contacts of symptomatic index case-patients who had SARS-CoV-2 infection during September 21, 2021–February 7, 2022. Infection was determined in primary health centers by using either reverse transcription PCR (RT-PCR) or rapid antigen detection tests (Ag-RDT). The cutoff date between the Delta and Omicron dominant periods was December 21, 2021, which was determined on the basis of data from the epidemiologic surveillance system operating in the study area (Figure 1) (*8*). To evaluate differences between Delta and Omicron clusters, we estimated the relative risk (RR) of infection for contacts between the first tertile of the study period, when the Delta variant was clearly dominant, and the last tertile, when Omicron was clearly dominant.

Symptoms of SARS-CoV-2 infection were fever or clinical signs of upper respiratory tract infection. Index case-patients were those who first showed clinical symptoms of infection in a specific household and sought diagnosis or treatment at a primary healthcare center. The patient and COVID-19 epidemiologic surveillance system were notified after infection was confirmed. Index cases were included consecutively after notification but randomly chosen for subsequent data collection. We included only the index case-patients who provided ≥1 household contacts.

We followed up and screened contacts according to standard procedures implemented in the study region. In brief, after confirmation of a positive case by either SARS-CoV-2–specific RT-PCR or Ag-RDT, a health officer began a systematic contact tracing study. Contacts were defined as persons who had spent >15 min with the index case-patient in an indoor space without nonpharmaceutical intervention measures during the 48 hours before COVID-19 diagnosis was confirmed for the index case-patient. This category included all housemates who were living with the index case-patient. For contacts, we performed an Ag-RDT test if the person was

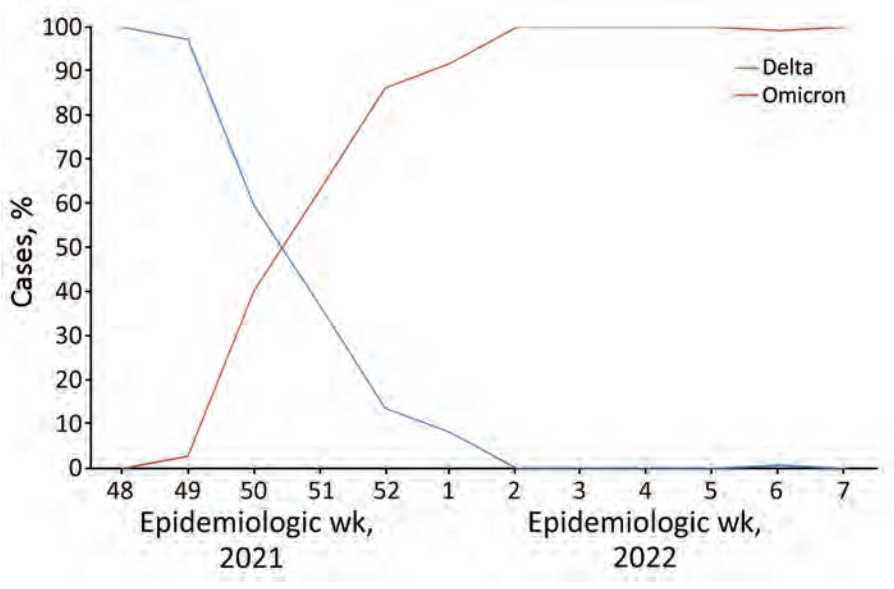

Figure 1. Dominance of infection with SARS-CoV-2 Delta and Omicron variants in a study of secondary attack rates in vaccinated and unvaccinated household contacts, Spain. The study population was located in the northern part of the greater metropolitan area of Barcelona, Spain. Genotyping of 1,554 samples from patients with SARS-CoV-2 infections was conducted during November 23, 2020–February 8, 2021 to identify the dominant variant infecting the population. The cutoff date between the Delta and Omicron predominance periods was December 21, 2021.

symptomatic at the time of the contact tracing study. We subsequently tested all contacts with a negative Ag-RDT test by RT-PCR from 3 to 7 days after the notification of the index case-patient, irrespective of the presence of symptoms. We excluded persons without available laboratory test results and those for whom RT-PCR was not performed after a negative Ag-RDT result (Figure 2). Clinical data and test results were recorded in the healthcare system's electronic database.

Diagnosis of SARS-CoV-2 Infection

Clinical samples collected through nasopharyngeal swabs were shipped to the referral laboratory (Microbiology Services, Metropolitan Clinical Laboratory, Hospital Universitari Germans Trias i Pujol), where they were stored at 4°C before chemical inactivation using lysis buffer. SARS-CoV-2 infection was diagnosed by using either the Novaplex SARS-CoV-2/FluA/FluB/RSV RT-PCR Assay (Seegene Inc., https://www.seegene.com) or Aptima SARS-CoV-2 assay (Hologic, https://www.hologic.com) according to the manufacturers' instructions. Panbio Ag-RDT kits (Abbott, https://www.abbott.com) were used in situ at primary healthcare centers according to the manufacturer's instructions.

Data Management and Statistical Analysis

We collected data from the public health system's electronic records and obtained additional sociodemographic data from contacts or close informants through telephone interviews. Data included RT-PCR and Ag-RDT results for contacts, presence of symptoms, background of previous COVID-19 diagnosis (defined as a previous positive SARS-CoV-2 RT-PCR test or Ag-RDT), age, sex, vaccination status against SARS-CoV-2, vaccine brand if applicable, number of vaccine doses administered (1–3), date of vaccine inoculations, and number of housemates. The vaccines licensed in our study setting were AZD1222 (ChAdOx1 nCoV-19; AstraZeneca, https://www.astrazeneca.com), BNT162b2 (Pfizer-BioNTech, https://www.pfizer.com), mRNA-1273 (Moderna, https://www.modernatx.com), and JNJ-78436735/Ad26.COV2.S (Janssen/Johnson & Johnson, https://www.jnj.com). Contacts were considered positive COVID-19 cases if either RT-PCR or Ag-RDT was positive for SARS-CoV-2 during the contact tracing period from 48 hours before to 7 days after notifying the index case-patient. For contacts, we used 2 definitions for vaccination status: vaccinated with any dose or stratified according to the number of doses received. Full vaccination was considered to be 2 or 3 doses.

We analyzed data using Stata version 14.0 (StataCorp LLC, https://www.stata.com) and R version 4.1.2 (The R Project for Statistical Computing, https://www.r-project.org) software. For descriptive analysis, we used medians and interquartile ranges (IQRs) for continuous variables and proportions and 95% CIs for categorical variables. For univariate analysis, we used the χ^2 test to compare categorical variables and for trends, when appropriate, and Student *t*-test for continuous variables after testing for normality (skewness and kurtosis tests) or nonparametric Fisher or Wilcoxon tests, when necessary. We performed logistic regression for multivariate analysis and estimated crude odds ratios (ORs), RRs, adjusted ORs (aORs), or adjusted RRs for study variables, including age of contacts and index-patients, sex, vaccination status, and number of housemates. We performed regression analysis to compare continuous variables, calculated crude ORs and aORs, and estimated 95% CIs and p values. We considered a p value <0.05 significant.

Results

Study Sample

We included 227 symptomatic index case-patients who reported a total of 466 household contacts; median number of contacts was 2 (IQR 2–3, range 1–7). The Delta-dominant period had 123 index cases and 251 contacts, and the Omicron-dominant period had 104 index cases and 215 contacts (Figure 2). The median age for the entire sample of 693 participants (index patients plus contacts) was 38.0 (IQR 15.0–49.5, range 1–91) years; 347 participants (50.1%) were female, and 511 (73.7%, 95% CI 70.3%–77.0%) were vaccinated (Appendix Table, https://wwwnc.cdc.gov/EID/article/28/10/22-0494-App1.pdf). Vaccination levels increased to 89.9% (491/546, 95% CI 87.1%–92.3%) when we excluded children <12 years of age, for whom vaccination was not implemented until mid-December 2021. Among vaccinated persons, 12.9% (66/511, 95% CI 10.1%–16.1%) were vaccinated with ≥1 dose of ChAdOx1-S vaccine, 3.9% (20/511, 95% CI 2.4%–6.0%) with JNJ-78436735/Ad26.COV2.S, 20.0% (102/511, 95% CI 16.6%–23.7%) with mRNA-1273, and 71.8% (367/511, 95% CI 67.7%–65.7%) with BNT162b2 (Appendix Table). Unvaccinated persons tended to be younger (median 10 [IQR 6.0–21.0] years of age) compared with those who were vaccinated (median 43.0 [IQR 27.0–53.0] years of age), mainly because of the overrepresentation of children in the unvaccinated group (p<0.001). Overall, 87.5% (447/511, 95% CI 84.3%–90.2%) of vaccinated adults

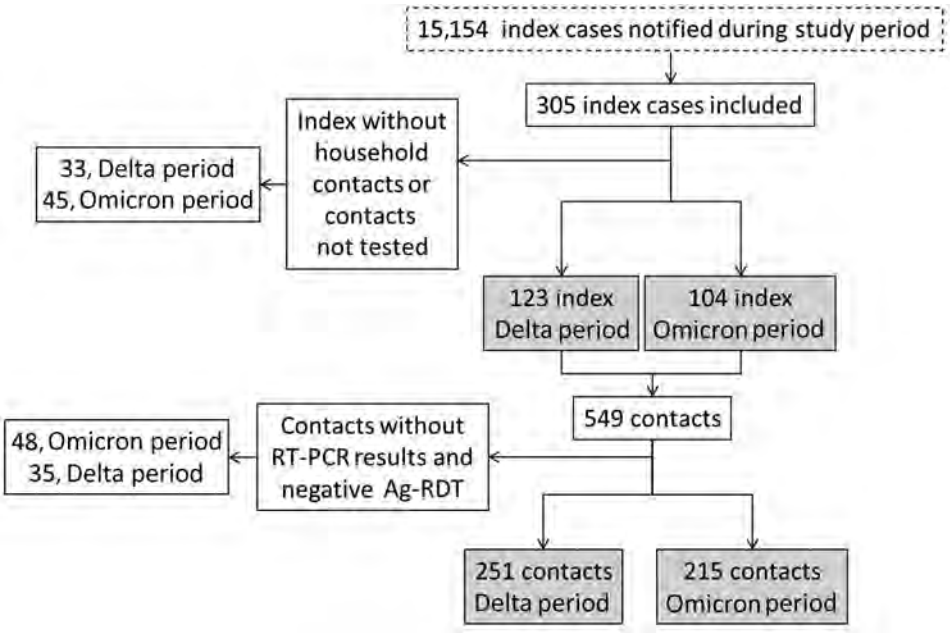

Figure 2. Selection process of participants in a study of SARS-CoV-2 secondary attack rates in vaccinated and unvaccinated household contacts during replacement of Delta with Omicron variant, Spain. Index case-patients were those who first showed clinical symptoms of infection in a specific household and sought diagnosis or treatment at a primary healthcare center. Contacts were defined as persons who had spent >15 min with the index case-patient in an indoor space without intervention measures, such as masks, during the 48 hours before COVID-19 diagnosis was confirmed for the index case-patient. Contacts with no RT-PCR results and negative Ag-RDT were excluded from the study. Ag-RDT, rapid antigen detection tests; RT-PCR, reverse transcription PCR.

had received a full vaccine course, most often 2 doses of BNT162b2 (295/511, 57.7%, 95% CI 53.3%–62.1%). The median time from the index case report date to the administration of the last vaccine dose among contacts was 20.4 (IQR 14.3–25.0, range 0.1–46) weeks. Index case-patients from the Omicron-dominant period tended to be younger (39.0 [IQR 19.3–48.0] years of age) than those from the Delta-dominant period (43.0 [IQR 25.0–55.0] years of age; p = 0.03). Contacts from the Omicron-dominant period had a higher prevalence of symptoms (57.1%, 95% CI 50.0%–64.0%) than those from the Delta-dominant period (46.4%, 95% CI 34.9%–53.0%; p = 0.03). The overall vaccination coverage was higher among persons during the Omicron-dominant period (79.3%, 95% CI 64.0%–73.6%) than during the Delta-dominant period (69.0%, 95% CI 74.4%–83.6%; p = 0.002). The secondary attack rate (SAR) was higher in contacts during the Omicron-dominant period (58.2%, 95% CI 51.8%–64.3%) than during the Delta-dominant period (80.9%, 95% CI 75.0%–86.9%; p<0.001) (Appendix Table).

Risk Factors for Infection among Contacts

During the Delta-dominant period, independent risk factors associated with infection were unvaccinated status (aOR 5.42, 95% CI 1.6–18.6), elapsed time since last vaccine dose (pooled aOR 1.63, 95% CI 1.1–2.4), and older age (pooled aOR 1.48, 95% CI 1.1–1.9) (Table 1). We observed a protective association between unvaccinated status of index cases and infection risk of contacts (aOR 0.30, 95% CI 0.1–0.8) in the Delta-dominant period (Table 1). We did not observe any associations between study variables and infection risk for contacts during the Omicron period (Table 2). Only 1 of 9 contacts with a previous SARS-CoV-2 infection was re-infected during the Delta-dominant period (p = 0.002), but we did not observe this effect during the Omicron-dominant period (Tables 1, 2).

Infection Risk for Contacts during Delta- versus Omicron-Dominant Periods

The adjusted RR of infection among contacts was 3.87-fold (95% CI 2.4–6.2-fold) higher during the Omicron-dominant period than the Delta-dominant period. Analysis of RR of infection was restricted to the first and last tertiles of the study period for vaccinated and unvaccinated contacts and index case-patients (Table 3). Contacts during the Omicron-dominant period showed a higher RR of infection than those in the Delta-dominant period for all strata studied. However, this effect was more prominent among contacts who were vaccinated <20 weeks before contact with the index-case patient (RR 9.16, 95% CI 3.4–25.0) compared with those who were vaccinated >20 weeks before contact with the index-case patient (RR 2.91, 95% CI 0.8-10.2).

To explore the time lag effect since vaccine administration, we stratified the group of vaccinated contacts according to the IQR and number of weeks that elapsed since their last vaccination dose and compared each group with unvaccinated contacts. We found a protective effect for VET in vaccinated

compared with unvaccinated persons in the first 2 strata that were closer to the vaccination date during the Delta-dominant period after adjusting for age (OR 0.21, 95% CI 0.1–0.7, p = 0.007, and OR 0.26, 95% CI 0.1–0.9, p = 0.03), but not for the Omicron-dominant period (Figure 3). This protective effect disappeared during the Delta-dominant period, in the upper IQR strata (>20 weeks) (Figure 3).

We observed no significant differences for age of contacts in all time lag strata. We reassessed these results using only data for contacts who had received 2 or 3 vaccine doses and observed similar results. We plotted age against time elapsed since vaccination after stratifying according to the infection status of contacts and used linear regression analysis to visualize the effects of age on infection risk during the 2 study periods (Appendix Figure 1).

Discussion

Our results show a high SAR among household contacts for both the Delta-dominant (58.2%) and Omicron-dominant (80.9%) periods; we found a 2- to 6-fold higher risk of infection for household contacts of symptomatic index case-patients during the Omicron-dominant period. SARs in our study were higher than that observed in a previous study conducted in the same geographic area in 2020, which showed a secondary infection rate of 48.3% when the ancestral SARS-CoV-2 strain responsible for the first infection wave was predominant (*9*). This previous study (*9*) classified hospitalized persons as index case-patients, and the mapping of those index cases demonstrated clear clustering in geographic areas with lower socioeconomic status. In our study, we did not observe geographic aggregation of index case-patients and

Table 1. Crude and adjusted risk factors for infection among contacts in the Delta-dominant period in a study of SARS-CoV-2 secondary attack rates in vaccinated and unvaccinated household contacts during replacement of Delta with Omicron variant, Spain*

		Crude OR		Adjusted OR‡	
Variable	No. patients†	OR (95% CI)	p value	OR (95% CI)	p value
Vaccination status, contacts					
Vaccinated	88/167	Referent		Referent	
Unvaccinated	58/84	2.00 (1.2–3.5)	0.01	5.42 (1.6–18.6)	0.007
1 dose	8/17	Referent		Referent	
2 doses	77/146	1.25 (0.5–3.4)	0.7	1.26 (0.4–3.8)	0.7
3 doses	3/4	3.37 (0.3–39.3)	0.3	2.12 (0.2–27.2)	0.5
Time since vaccination, wk					
1–13	11/31	Referent		Referent	
14–20	20/50	1.21 (0.5–3.1)	0.7	0.98 (0.4–2.7)	0.9
21–25	32/54	2.64 (1.1–6.6)	0.04	1.74 (0.6–5.0)	0.3
>25	25/31	7.58 (2.4–24.1)	0.001	4.17 (1.1–15.3)	0.03
Missing data	0/1				
Pooled		1.96 (1.4–2.8)	<0.001	1.63 (1.1–2.4)	0.01
Age of contacts, y					
0–12	45/70	Referent		Referent	
13–18	7/18	0.35 (0.1–1.0)	0.06	1.50 (0.3–6.8)	0.6
19–35	14/32	0.43 (0.2–1.0)	0.05	1.62 (0.4–6.4)	0.5
36–45	24/46	0.61 (0.3–1.3)	0.2	2.68 (0.7–10.1)	0.1
>45	53/81	1.05 (0.5–2.1)	0.9	4.45 (1.1–18.3)	0.04
Missing data	3/4	1.7 (0.2–16.9)	0.5		
Pooled		1.03 (0.9–1.2)	0.7	1.48 (1.1–1.9)	0.003
Vaccination status, index patients					
Vaccinated	114/180	Referent		Referent	
Unvaccinated	32/71	0.48 (0.3–0.8)	0.009	0.30 (0.1–0.8)	0.02
Age of index patients, y					
0–12	21/48	Referent		Referent	
13–18	4/6	2.57 (0.4–15.4)	0.3	0.54 (0.1–4.6)	0.6
19–35	20/38	1.43 (0.6–3.4)	0.4	0.40 (0.1–1.4)	0.1
36–45	46/69	2.57 (1.2–5.5)	0.02	0.71 (0.2–2.3)	0.6
>45	55/90	2.02 (1.0–4.1)	0.05	0.57 (0.2–1.9)	0.4
Pooled		1.20 (1.0–1.4)	0.03	0.94 (0.7–1.2)	0.6
Number of housemates					
≤2	70/104	Referent		Referent	
>2	58/116	0.52 (0.3–0.9)	0.01	0.63 (0.3–1.2)	0.1
Sex					
M	79/132	Referent		Referent	
F	67/118	1.13 (0.7–1.9)	0.6	1.03 (0.6–1.8)	0.9
Missing data	0/1				

*OR, odds ratio.
†Values are number infected/total number of patients in each strata.
‡Adjusted analysis only included participants who had all data available.

Table 2. Crude and adjusted risk factors for infection among contacts in the Omicron-dominant period in a study of SARS-CoV-2 secondary attack rates in vaccinated and unvaccinated household contacts during replacement of Delta with Omicron variant, Spain*

Variable	No. patients†	Crude OR		Adjusted OR‡	
		OR (95% CI)	p value	OR (95% CI)	p value
Vaccination status, contacts					
Vaccinated	135/170	Referent		Referent	
Unvaccinated	39/45	1.69 (0.7–4.3)	0.3	1.86 (0.6–6.2)	0.3
1 dose	25/29	Referent		Referent	
2 doses	90/113	0.63 (0.2–2.0)	0.4	0.75 (0.2–2.9)	0.7
3 doses	19/27	0.38 (0.1–1.5)	0.2	0.36 (0.1–1.9)	0.2
Missing data	1/1				
Time since vaccination, wk					
1–13	36/48	Referent		Referent	
14–20	28/35	1.33 (0.5–3.8)	0.6	2.17 (0.5–9.3)	0.3
21–25	34/41	1.62 (0.6–4.6)	0.4	2.41 (0.7–7.8)	0.1
>25	36/45	1.33 (0.5–3.6)	0.6	1.91 (0.6–5.7)	0.2
Missing data	1/1				
Pooled		1.12 (0.8–1.5)	0.5	1.26 (0.9–1.8)	0.2
Age of contacts, y					
0–12	36/42	Referent		Referent	
13/18	22/27	0.73 (0.2–2.7)	0.6	0.99 (0.2–4.4)	0.9
19/35	38/47	0.70 (0.2–2.2)	0.5	0.94 (0.2–3.8)	0.9
36/45	33/42	0.61 (0.2–1.9)	0.4	0.83 (0.2–3.3)	0.8
>45	45/57	0.63 (0.2–1.8)	0.4	0.82 (0.2–3.2)	0.8
Pooled		0.90 (0.7–1.1)	0.4	0.94 (0.7–1.2)	0.6
Vaccination status, index patients					
Vaccinated	134/161	Referent		Referent	
Unvaccinated	40/54	0.56 (0.3–1.2)	0.1	0.98 (0.2–3.9)	0.9
Age of index patients, y					
0–12	36/50	Referent		Referent	
13–18	13/15	2.53 (0.5–12.7)	0.3	2.79 (0.4–20.4)	0.3
19–35	35/44	1.51 (0.6–3.9)	0.4	1.47 (0.4–5.8)	0.6
36–45	51/59	2.48 (0.9–6.5)	0.07	2.27 (0.5–10.5)	0.3
>45	39/47	1.90 (0.7–5.0)	0.2	1.84 (0.4–8.8)	0.4
Pooled		1.20 (0.9–1.5)	0.1	1.09 (0.8–1.5)	0.6
Number of housemates					
≤2	60/70	Referent		Referent	
>2	114/145	0.61 (0.3–1.3)	0.2	0.62 (0.3–1.4)	0.3
Sex					
M	93/115	Referent		Referent	
F	81/100	1.13 (0.7–1.9)	0.6	0.97 (0.5–2.0)	0.9

*OR, odds ratio.
†Values are number infected/total number of patients in each strata.
‡Adjusted analysis only included participants who had all data available.

contacts in either variant-dominant period, which might indicate intrinsically higher infectious capacity and community penetrance of the Delta and Omicron variants compared with previous variants and explain their markedly high SAR. Despite high vaccine coverage, infection during the Delta- and Omicron-dominant periods occurred regardless of other socioeconomic factors previously observed, such as the number of housemates (*10*). Furthermore, for the Delta variant, the SAR observed in our study was higher than those reported among household contacts in England (25%) (*11*), Denmark (21%) (F.P. Lyngse et al., unpub. data, https://www.medrxiv.org/content/10.1101/2021.12.27.21268278v1), Japan (25.2%) (*12*), Northern Spain (24%) (*13*), and those published in a systematic review and meta-analysis (22.5%) (*14*) but was similar to the 43.1% SAR reported in South Korea (*15*). For the Omicron variant, the SAR in our study was higher than those reported in Denmark (31%) (F.P. Lyngse et al., unpub. data), Japan (31.8%) (*12*), and the United States (52.7%) (*16*), and an overall rate of 42.7% (*14*). In our study, we included only symptomatic index case-patients. Symptomatic SARS-CoV-2–infected patients might be more efficient transmitters of the virus (*17*) because they maintain higher viral loads for a longer period (*18*) and might spread the infection more efficiently through sneezing or coughing (*19*). The higher SARs in our study might also reflect a low level of compliance with isolation measures among index case-patients within households or different testing and inclusion strategies. Nevertheless, our results indicate that the Omicron variant and, to a lesser extent, the Delta variant have an extremely high transmission capacity among close contacts, irrespective of vaccination status and other co-factors.

Vaccine evasion might be a contributor to the higher transmissibility of the Omicron variant in areas with high vaccine coverage (F.P. Lyngse et al., unpub. data). This conclusion is supported by the substantial RR of SARS-CoV-2 infection in contacts during the Omicron-dominant period who were vaccinated within 20 weeks before infection by the index case-patients but not in contacts vaccinated at >20 weeks before infection (Table 3). These observations are consistent with the reduction of neutralizing antibodies against Omicron observed in experimental studies (*20*,*21*) and a notable duration of infectious shedding of the Omicron virus in vaccinated persons (*22*). The protective effect of vaccination against SARS-CoV-2 infection in the Delta-dominant period was consistent with previous reports on the Delta VOC, which had similar but limited results (*6*,*21*,*23*–*26*). However, we could not ascertain if the booster dose was effective for reducing transmission, likely because of the low sample size (only 46 contacts had booster vaccines administered during the Delta-dominant period). The protective effect against the Delta variant diminished as the time since vaccination increased, which has also been previously reported (*5*,*24*,*26*). Our estimates suggest a nonlinear trend for reduction of vaccine protection, culminating at ≈20 weeks after vaccination. The underlying mechanisms might include a rapid decline of vaccine-induced peak IgA, which is a mucosal antibody with more potent neutralizing activity than IgG (*27*) against the spike protein (*28*). A substantial reduction of IgA was also observed 3 months following natural infection (*29*), which is compatible with our results, considering that IgA remains longer in mucosal fluids than serum (*29*).

We cannot conclude that the vaccination status of the index case-patients provided protection against infection for their contacts. However, we suggest that a complex relationship exists between vaccination status, immunity, and age. Children, who have shown a lower susceptibility to SARS-CoV-2 infection (*30*), might have a lower ability to transmit the infection (*31*–*33*) and tended to be unvaccinated in our sample. However, older persons tend to have better vaccine coverage but lose vaccine-induced immunity more rapidly than younger persons (*34*,*35*) and develop symptoms (*36*). Finally, vaccinated persons might have a lower inclination to practice social distancing than unvaccinated persons (*37*). Overall, these factors might explain the protective association against infection between unvaccinated index case-patients and their contacts during the Delta-dominant period. These interactions could have implications for vaccination strategy and deserve further examination; however, they might have had little or no effect during the Omicron-dominant period. Risk factors related to infection with the Omicron variant might only be ascertained with a larger sample size of Omicron-infected households. A recent large cohort study conducted in Spain found that booster mRNA vaccine doses were moderately effective in preventing infection with the SARS-CoV-2 Omicron variant for >1 month after administration, after which protection rapidly diminished compared with the protection observed against the Delta variant (*38*).

Our study's first limitation is that we relied on the assumption that the classification of 2 periods on the basis of molecular epidemiologic surveillance of SARS-CoV-2 variants was an acceptable proxy to compare the epidemiologic behavior of the Omicron and Delta variants. However, a misclassification of the Delta and Omicron variant clusters might have occurred, especially during the middle tertile of our study period, when variants within the population overlapped. We overcame this limitation by restricting data analysis to the first and last tertiles (Table 3); however, we used all data for the remaining analyses to maintain statistical power of the study. Second, we could not confirm which persons were the true index case-patients and,

Table 3. Risk of infection among contacts relative to vaccination status in a study of SARS-CoV-2 secondary attack rates in vaccinated and unvaccinated household contacts during replacement of Delta with Omicron variant, Spain*

	Delta-dominant period		Omicron-dominant period			
Variable	Patients†	p value‡	Patients†	p value‡	RR§ (95% CI)	p value
Vaccination status, contacts						
Vaccinated	50/101 (49.5)	0.1	112/124 (90.3)	0.3	6.48 (3.0–13.8)	<0.001
Unvaccinated	35/56 (62.5)		28/29 (96.6)		10.4 (1.2–82.5)	0.03
Vaccinated, <20 wk	23/62 (37.1)	0.002	59/65 (90.8)	0.8	9.16 (3.4–25.0)	<0.001
Vaccinated, >20 wk	27/39 (69.3)		52/58 (89.7)		2.91 (0.8–10.2)	0.1
Vaccination status, index						
Vaccinated	67/112 (59.8)	0.02	108/120 (90.0)	0.2	3.99 (2.0–8.1)	<0.001
Unvaccinated	18/45 (40.0)		32/33 (97.0)		43.5 (5.1–369.9)	0.001

*RR, relative risk
†Values are no. infected/total no. (%) patients in each strata.
‡p values for differences between vaccinated and unvaccinated groups.
§RR between Omicron vs. Delta variant, adjusted by age of contact.

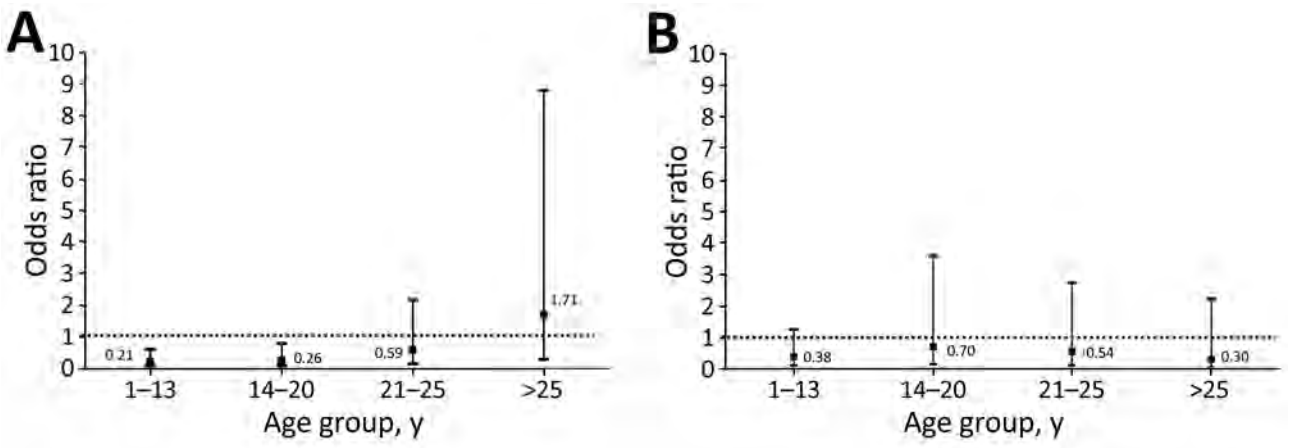

Figure 3. Association between time elapsed since the last vaccination and infection risk in a study of SARS-CoV-2 secondary attack rates in vaccinated and unvaccinated household contacts during replacement of Delta with Omicron variant, Spain. Odds ratios for infection risk of contacts were calculated for each age group in the Delta-dominant period (A) and Omicron-dominant period (B). Data were stratified according to interquartile range distribution of vaccinated contacts and number of weeks that elapsed since their last vaccination dose. Unvaccinated contacts were used as the control group for comparison. Dashed lines indicate the no-association threshold (odds ratio = 1).

therefore, some misclassification of index cases versus contacts may have occurred. In this regard, the effects of the variables studied, such as index and contact vaccination effects, might have been diluted in the study. Third, we cannot exclude the possibility that, in some households, contacts were not infected by the same index case-patient or were infected elsewhere in the community, which might again dilute the factors associated with contacts. Finally, the percentages of infected contacts in the excluded group (14% of contacts during the Delta-dominant period and 22% during the Omicron-dominant period) were lower than those for the cohort included in the study, which might have skewed the results by increasing the estimated SAR during both periods. Ultimately, full confirmation of our findings will require a longitudinal study that includes a long-term follow-up of participants and household-level genotyping results.

Our results underscore the need for continuous community-based surveillance studies to characterize the epidemiologic phenotypes of SARS-CoV-2 variants in vaccine-covered populations, especially considering the emergence of new variants, such as Omicron subvariants BA.4 and BA.5 (Appendix Figure 2). Given the increased infectiousness of the Omicron variant compared with previous VOCs, we should focus on developing vaccines with long-lasting protection against severe disease rather than only infectivity. Sustained public health measures focused on the most vulnerable populations, such as the consistent use of masks in public settings to limit infection of SARS-CoV-2, should remain a cornerstone of pandemic management. The results from this study could help healthcare policy makers formulate effective prevention policies for newly emerging VOCs.

Acknowledgments

We thank the primary care teams who carried out the contact tracing in the field, all microbiologists and laboratory technicians at the Microbiology Service of Hospital Germans Trias i Pujol for their contributions to the generation of SARS-CoV-2 RT-PCR diagnostics data, and all members of the Can Ruti Sequencing Hub for their efforts in generating SARS-CoV-2 genotyping data. Finally, we thank the CERCA Programme/Generalitat de Catalunya for their support of the Germans Trias i Pujol Research Institute.

The authors declare that no funds, grants, or other support were received during the preparation of this manuscript. The authors have no relevant financial or nonfinancial interests to disclose.

About the Author

Mr. López-Muñoz is a nurse and social scientist whose research interests include the control and prevention of emerging and imported diseases, pandemic preparedness, and outbreak controls in the Northern Metropolitan Health area of Barcelona, Spain.

References

1. Saban M, Myers V, Wilf-Miron R. Changes in infectivity, severity and vaccine effectiveness against delta COVID-19 variant ten months into the vaccination program: the Israeli case. Prev Med. 2022;154:106890. https://doi.org/10.1016/j.ypmed.2021.106890

2. McNamara LA, Wiegand RE, Burke RM, Sharma AJ, Sheppard M, Adjemian J, et al. Estimating the early impact of the US COVID-19 vaccination programme on COVID-19 cases, emergency department visits, hospital admissions, and deaths among adults aged 65 years and older: an ecological analysis of national surveillance data. Lancet. 2022;399:152–60. https://doi.org/10.1016/S0140-6736(21)02226-1
3. Andrews N, Tessier E, Stowe J, Gower C, Kirsebom F, Simmons R, et al. Duration of protection against mild and severe disease by COVID-19 vaccines. N Engl J Med. 2022;386:340–50. https://doi.org/10.1056/NEJMoa2115481
4. Lopez Bernal J, Andrews N, Gower C, Gallagher E, Simmons R, Thelwall S, et al. Effectiveness of COVID-19 vaccines against the B.1.617.2 (Delta) variant. N Engl J Med. 2021;385:585–94. https://doi.org/10.1056/NEJMoa2108891
5. Feikin DR, Higdon MM, Abu-Raddad LJ, Andrews N, Araos R, Goldberg Y, et al. Duration of effectiveness of vaccines against SARS-CoV-2 infection and COVID-19 disease: results of a systematic review and meta-regression. Lancet. 2022;399:924–44. https://doi.org/10.1016/S0140-6736(22)00152-0
6. Harris RJ, Hall JA, Zaidi A, Andrews NJ, Dunbar JK, Dabrera G. Effect of vaccination on household transmission of SARS-CoV-2 in England. N Engl J Med. 2021;385:759–60. https://doi.org/10.1056/NEJMc2107717
7. Nanduri S, Pilishvili T, Derado G, Soe MM, Dollard P, Wu H, et al. Effectiveness of Pfizer-BioNTech and Moderna vaccines in preventing SARS-CoV-2 infection among nursing home residents before and during widespread circulation of the SARS-CoV-2 B.1.617.2 (Delta) variant—National Healthcare Safety Network, March 1–August 1, 2021. MMWR Morb Mortal Wkly Rep. 2021;70:1163–6. https://doi.org/10.15585/mmwr.mm7034e3
8. Generalitat de Catalunya, Departament de Salut. Vigilància de noves variants de SARS-CoV-2: integració de la seqüència genòmica del SARS-CoV-2 al Sistema de Vigilància de Catalunya, 2021 [cited Feb 2022]. https://scientiasalut.gencat.cat/handle/11351/5782
9. Vallès X, Roure S, Valerio L, López-Muñoz I, Pérez-Quílez O, Soldevila L, et al. SARS-CoV-2 contact tracing among disadvantaged populations during epidemic intervals should be a priority strategy: results from a pilot experiment in Barcelona. Public Health. 2021;195:132–4. https://doi.org/10.1016/j.puhe.2021.04.027
10. Madewell ZJ, Yang Y, Longini IM Jr, Halloran ME, Dean NE. Factors associated with household transmission of SARS-CoV-2: an updated systematic review and meta-analysis .JAMA Netw Open. 2021;4:e2122240. https://doi.org/10.1001/jamanetworkopen.2021.22240
11. Singanayagam A, Hakki S, Dunning J, Madon KJ, Crone MA, Koycheva A et al. Community transmission and viral load kinetics of the SARS-CoV-2 delta (B.1.617.2) variant in vaccinated and unvaccinated individuals in the UK: a prospective, longitudinal, cohort study. Lancet Infect Dis. 2022;22:183–95. https://doi.org/10.1016/S1473-3099(21)00648-4
12. Ogata T, Tanaka H, Tanaka E, Osaki N, Noguchi E, Osaki Y, et al. Increased secondary attack rates among the household contacts of patients with the Omicron variant of the coronavirus disease 2019 in Japan. Int J Environ Res Public Health. 2022;19:8068. https://doi.org/10.3390/ijerph19138068
13. Martínez-Baz I, Trobajo-Sanmartín C, Miqueleiz A, Guevara M, Fernández-Huerta M, Burgui C, et al.; Working Group for the Study of COVID-19 in Navarre; Investigators, other members of the Working Group for the Study of COVID-19 in Navarre. Product-specific COVID-19 vaccine effectiveness against secondary infection in close contacts, Navarre, Spain, April to August 2021. Euro Surveill. 2021;26:2100894. https://doi.org/10.2807/1560-7917.ES.2021.26.39.2100894
14. Madewell ZJ, Yang Y, Longini IM Jr, Halloran ME, Dean NE. Household secondary attack rates of SARS-CoV-2 by variant and vaccination status: an updated systematic review and meta-analysis. JAMA Netw Open. 2022;5:e229317. https://doi.org/10.1001/jamanetworkopen.2022.9317
15. Yi S, Kim JM, Choe YJ, Hong S, Choi S, Ahn SB, et al. SARS-CoV-2 Delta variant breakthrough infection and onward secondary transmission in household. J Korean Med Sci. 2022;37:e12. https://doi.org/10.3346/jkms.2022.37.e12
16. Baker JM, Nakayama JY, O'Hegarty M, McGowan A, Teran RA, Bart SM, et al. SARS-CoV-2 B.1.1.529 (Omicron) variant transmission within households—four U.S. jurisdictions, November 2021–February 2022. MMWR Morb Mortal Wkly Rep. 2022;71:341–6. https://doi.org/10.15585/mmwr.mm7109e1
17. Ge Y, Martinez L, Sun S, Chen Z, Zhang F, Li F, et al. COVID-19 transmission dynamics among close contacts of index patients with COVID-19: a population-based cohort study in Zhejiang Province, China. JAMA Intern Med. 2021;181:1343–50. https://doi.org/10.1001/jamainternmed.2021.4686
18. Walsh KA, Jordan K, Clyne B, Rohde D, Drummond L, Byrne P, et al. SARS-CoV-2 detection, viral load and infectivity over the course of an infection. J Infect. 2020;81:357–71. https://doi.org/10.1016/j.jinf.2020.06.067
19. Mostaghimi D, Valdez CN, Larson HT, Kalinich CC, Iwasaki A. Prevention of host-to-host transmission by SARS-CoV-2 vaccines. Lancet Infect Dis. 2022;22:e52–8. https://doi.org/10.1016/S1473-3099(21)00472-2
20. Cele S, Jackson L, Khoury DS, Khan K, Moyo-Gwete T, Tegally H, et al.; NGS-SA; COMMIT-KZN Team. Omicron extensively but incompletely escapes Pfizer BNT162b2 neutralization. Nature. 2022;602:654–6. https://doi.org/10.1038/s41586-021-04387-1
21. Ai J, Zhang H, Zhang Y, Lin K, Zhang Y, Wu J, et al. Omicron variant showed lower neutralizing sensitivity than other SARS-CoV-2 variants to immune sera elicited by vaccines after boost. Emerg Microbes Infect. 2022;11:337–43. https://doi.org/10.1080/22221751.2021.2022440
22. Takahashi K, Ishikane M, Ujiie M, Iwamoto N, Okumura N, Sato T, et al. Duration of infectious virus shedding by SARS-CoV-2 Omicron variant–infected vaccinees. Emerg Infect Dis. 2022;28:998–1001. https://doi.org/10.3201/eid2805.220197
23. Del Cura-Bilbao A, López-Mendoza H, Chaure-Pardos A, Vergara-Ugarriza A, Guimbao-Bescós J. Effectiveness of 3 COVID-19 vaccines in preventing SARS-CoV-2 infections, January–May 2021, Aragon, Spain. Emerg Infect Dis. 2022;28:591–8. https://doi.org/10.3201/eid2803.212027
24. Chemaitelly H, Tang P, Hasan MR, AlMukdad S, Yassine HM, Benslimane FM, et al. Waning of BNT162b2 vaccine protection against SARS-CoV-2 infection in Qatar. N Engl J Med. 2021;385:e83. https://doi.org/10.1056/NEJMoa2114114
25. Tseng HF, Ackerson BK, Luo Y, Sy LS, Talarico CA, Tian Y, et al. Effectiveness of mRNA-1273 against SARS-CoV-2 Omicron and Delta variants. Nat Med. 2022;28:1063–71. https://doi.org/10.1038/s41591-022-01753-y
26. Bramante CT, Proper JL, Boulware DR, Karger AB, Murray T, Rao V et al. Vaccination against SARS-CoV-2 is associated with a lower viral load and likelihood of systemic symptoms. Open Forum Infect Dis. 2022;9:ofac066. https://doi.org/10.1093/ofid/ofac066
27. Sterlin D, Mathian A, Miyara M, Mohr A, Anna F, Claër L, et al. IgA dominates the early neutralizing antibody response

to SARS-CoV-2. Sci Transl Med. 2021;13:eabd2223. https://doi.org/10.1126/scitranslmed.abd2223
28. Wisnewski AV, Campillo Luna J, Redlich CA. Human IgG and IgA responses to COVID-19 mRNA vaccines. PLoS One. 2021;16:e0249499. https://doi.org/10.1371/journal.pone.0249499
29. Moncunill G, Mayor A, Santano R, Jiménez A, Vidal M, Tortajada M, et al. SARS-CoV-2 seroprevalence and antibody kinetics among health care workers in a Spanish hospital after 3 months of follow-up. J Infect Dis. 2021;223:62–71. https://doi.org/10.1093/infdis/jiaa696
30. Viner RM, Mytton OT, Bonell C, Melendez-Torres GJ, Ward J, Hudson L, et al. Susceptibility to SARS-CoV-2 infection among children and adolescents compared with adults: a systematic review and meta-analysis. JAMA Pediatr. 2021;175:143–56. https://doi.org/10.1001/jamapediatrics.2020.4573
31. Heavey L, Casey G, Kelly C, Kelly D, McDarby G. No evidence of secondary transmission of COVID-19 from children attending school in Ireland, 2020. Euro Surveill. 2020;25:2000903. https://doi.org/10.2807/1560-7917.ES.2020.25.21.2000903
32. Fontanet A, Tondeur L, Grant R, Temmam S, Madec Y, Bigot T, et al. SARS-CoV-2 infection in schools in a northern French city: a retrospective serological cohort study in an area of high transmission, France, January to April 2020. Euro Surveill. 2021;26:2001695. https://doi.org/10.2807/1560-7917.ES.2021.26.15.2001695
33. Stich M, Elling R, Renk H, Janda A, Garbade SF, Müller B, et al. Transmission of severe acute respiratory syndrome coronavirus 2 in households with children, southwest Germany, May–August 2020. Emerg Infect Dis. 2021;27:3009–19. https://doi.org/10.3201/eid2712.210978
34. Brockman MA, Mwimanzi F, Lapointe HR, Sang Y, Agafitei O, Cheung PK, et al. Reduced magnitude and durability of humoral immune responses to COVID-19 mRNA vaccines among older adults. J Infect Dis. 2022;225:1129–40. https://doi.org/10.1093/infdis/jiab592
35. Bajaj V, Gadi N, Spihlman AP, Wu SC, Choi CH, Moulton VR. Aging, immunity, and COVID-19: how age influences the host immune response to coronavirus infections? Front Physiol. 2021;11:571416. https://doi.org/10.3389/fphys.2020.571416
36. Poletti P, Tirani M, Cereda D, Trentini F, Guzzetta G, Sabatino G, et al.; ATS Lombardy COVID-19 Task Force. Association of age with likelihood of developing symptoms and critical disease among close contacts exposed to patients with confirmed SARS-CoV-2 infection in Italy. JAMA Netw Open. 2021;4:e211085. https://doi.org/10.1001/jamanetworkopen.2021.1085
37. Andersson O, Campos-Mercade P, Meier AN, Wengström E. Anticipation of COVID-19 vaccines reduces willingness to socially distance. J Health Econ. 2021;80:102530. https://doi.org/10.1016/j.jhealeco.2021.102530
38. Monge S, Rojas-Benedicto A, Olmedo C, Mazagatos C, José Sierra M, Limia A et al.; IBERCovid. Effectiveness of mRNA vaccine boosters against infection with the SARS-CoV-2 omicron (B.1.1.529) variant in Spain: a nationwide cohort study. Lancet Infect Dis. 2022 Jun 2 [Epub ahead of print]. https://doi.org/10.1016/S1473-3099(22)00292-4

Address for correspondence: Xavier Vallès, Institut Fundació per la recerca en Ciències de la Salut Germans Trias i Pujol, C/Canyet s/n, Badalona, Catalonia 08016, Spain; email: xvallesc.mn.ics@gencat.cat

Novel Zoonotic Avian Influenza A(H3N8) Virus in Chicken, Hong Kong, China

Thomas H.C. Sit, Wanying Sun, Anne C.N. Tse, Christopher J. Brackman, Samuel M.S. Cheng, Amy W. Yan Tang, Jonathan T.L Cheung, Malik Peiris,[1] Leo L.M. Poon[1]

Zoonotic and pandemic influenza continue to pose threats to global public health. Pandemics arise when novel influenza A viruses, derived in whole or in part from animal or avian influenza viruses, adapt to transmit efficiently in a human population that has little population immunity to contain its onward transmission. Viruses of previous pandemic concern, such as influenza A(H7N9), arose from influenza A(H9N2) viruses established in domestic poultry acquiring a hemagglutinin and neuraminidase from influenza A viruses of aquatic waterfowl. We report a novel influenza A(H3N8) virus in chicken that has emerged in a similar manner and that has been recently reported to cause zoonotic disease. Although they are H3 subtype, these avian viruses are antigenically distant from contemporary human influenza A(H3N2) viruses, and there is little cross-reactive immunity in the human population. It is essential to heighten surveillance for these avian A(H3N8) viruses in poultry and in humans.

Diverse influenza A viruses are found in aquatic waterfowl, poultry, swine, horses, aquatic mammals, bats, and domestic pets such as cats and dogs. Although there is a diversity of virus hemagglutinin (H1–H16) and neuraminidase (N1–N9) subtypes in aquatic birds, more restricted numbers of virus subtypes are established in other species, including chicken (*1*). The high mutation rates associated with an error-prone virus replication complex and the presence of a segmented genome enables genetic reassortment of gene segments of viruses of different species and interspecies transmission and adaptation to new hosts.

Influenza A virus subtypes H9 and H6 have formed established lineages in domestic chicken and game birds (quail, pheasant) farmed for consumption in Asia (*2*). The internal gene constellation of H9N2 viruses contains hemagglutinin (HA) and neuraminidase (NA) genes acquired from aquatic waterfowl to generate H5N1, H5N6, H7N9, and H10N8 viruses through genetic reassortment, and many of these viruses also became established in poultry, subsequently posing zoonotic and pandemic threats (*3*–*5*). A novel influenza A(H3N8) virus has been recently reported to cause zoonotic infection in Henan Province, China (*6*).

In this context, we report detection of novel H3N8 viruses recently identified in chicken in live poultry markets and chicken farms in Hong Kong, China, that are genetically similar to the zoonotic H3N8 viruses reported in mainland China (*6*). We also report that these recent H3N8 viruses have arisen in a manner akin to zoonotic H5N1, H7N9, and H10N8 viruses and that there is little cross-reactive immunity in the human population to these chicken H3N8 viruses.

Methods

Influenza A Virus Surveillance and Virologic Testing of Poultry Farms

The Department of Agriculture, Fisheries and Conservation in Hong Kong routinely conducts virologic surveillance on each batch of chickens from local farms before release for sale. The surveillance is conducted on 30 unvaccinated sentinel chickens cohoused with each chicken flock. During December 14, 2021–January 21, 2022, we obtained oropharyngeal and cloacal swab samples from 30 chickens on each of 28 poultry farms. We combined samples into pools of 6 and placed each pool into a vial of virus transport medium (medium 199 plus antimicrobial drugs).

In a follow-up investigation of 4 farms found positive for H3N8 virus, we conducted more intensive

Author affiliations: Government of the Hong Kong Special Administrative Region, Hong Kong, China (T.H.C. Sit, A.C.N. Tse, C.J. Brackman); The University of Hong Kong, Hong Kong (W. Sun, S.M.S. Cheng, A.W. Yan Tang, J.T.L. Cheung, M. Peiris, L.L.M. Poon)

DOI: https://doi.org/10.3201/eid2810.221067

[1]These authors contributed equally to this article.

Table 1. Virologic results for local farm chickens positive for avian influenza A(H3N8) virus under active surveillance, Hong Kong, China*

Farm	Date sample collected	No. vials	No. (%) positive by RT-PCR		No. (%) positive by virus isolation	
			H9	H3	H9	H3
A	2021 Dec 14	10	0	6 (60)	0	6 (60)
B	2022 Dec 28	10	0	6 (60)	0	3 (30)
	2022 Feb 21	10	0	0	0	1 (10)
	2022 Mar 7	10	0	6 (60)	0	5 (50)
	2022 Mar 21	10	0	1 (10)	0	1 (10)
C	2022 Jan 12	10	0	6 (60)	0	6 (60)
D	2022 Jan 21	10	0	6 (60)	0	6 (60)

*No other influenza virus subtypes were detected. RT-PCR, reverse transcription PCR.

surveillance during May 2022 to check for any continuing evidence of on-farm viral circulation. We sampled a total of 50 chickens by using oropharyngeal and cloacal swabbing, again in pools containing 6 specimens.

Influenza A Surveillance in Live Poultry Markets

The School of Public Health of The University of Hong Kong routinely conducts surveillance in live poultry market stalls in Hong Kong (n = 116) by sampling from each stall fecal droppings (n = 10), drinking water in poultry cages (n = 2), and chopping boards and the inner wall and outer surface of defeathering machines used (n = 3) in preparation of slaughtered poultry for sale (*7*). All 116 poultry stalls were sampled every 3 months. Samples were individually collected and placed into vials of virus transport medium (medium 199 plus antimicrobial drugs), and samples were kept in cool packs for transport to the laboratory.

Real-Time Reverse Transcription PCR for Detection of Influenza A Viruses

We extracted viral RNA from chicken oropharyngeal and cloacal swab specimens by using the MagNA Pure 96 DNA and Viral NA Small Volume Kit (Roche, https://lifescience.roche.com) according to the manufacturer's instructions. We tested eluted specimen RNA by using real-time reverse transcription PCR (RT-PCR) for the influenza A virus matrix (M) gene as described (*8*).

We tested swab specimen supernatants of all influenza A virus M gene–positive swab specimens by RT-PCR for H5, H7, and H9 (*9*) and for virus isolation. We identified virus subtype of M gene–positive swab specimens negative for H5, H7, and H9 by using genetic sequencing of the virus isolate or directly from the swab specimen.

Virus Isolation

We inoculated 0.2 mL of swab specimen supernatant of all influenza A virus M gene–positive swab specimens into the allantoic cavity of three 9–11-day-old specific pathogen–free embryonated eggs and incubated at them at 36°C (± 2°C) for 4 days. We candled the eggs daily, and harvested allantoic fluid. We subtyped virus isolates by using hemagglutination inhibition (HI) tests and reference panels of antiserum to a range of influenza virus A subtypes (*7*).

Genetic Sequencing of Virus Isolates and Phylogenetic Analysis

We deduced near full-length genomes from virus grown in allantoic fluid samples by using an Illumina Sequencing Protocol (https://www.illumina.com) as described (*5,10–12*). We removed low-quality base pairs in the raw data by using Fastp (*13*) and selected reference sequence by using SPAdes (*11*) and BLAST (*14*). We generated consensus sequences by using BWA (http://arxiv.org/abs/1303.3997) and Pilon (*15*) and aligned sequences by using MUSCLE (*16*) and public sequences from GenBank and GISAID (https://www.gisaid.org) (Appendix Table, https://wwwnc.cdc.gov/EID/article/28/10/22-1067-App1.pdf). We constructed phylogenic trees by using IQtree (*17*) with the general time-reversible plus gamma model and 1,000 bootstrap replicates.

DNA Bar Coding

We conducted PCR amplification of the mitochondrial cytochrome oxidase I gene for host-species-

Table 2. Retrospective seroprevalence of antibodies to A/chicken/Hong Kong/22-10782/2022 influenza A(H3N8) virus in chicken serum samples collected from affected farms, Hong Kong, China*

Farm	Date samples collected	No.	H3N8 HI titer ≥1:16, no. (%)	H3N8 GMT (95% CI)
A	2022 Feb 16	30	26 (86.7)	28.51 (20.01–40.61)
B	2022 Feb 9	30	2 (6.7)	1.35 (0.96–1.91)
C	2022 Feb 16	30	29 (96.7)	46.31 (31.97–67.09)
D	2022 Feb 24	30	26 (86.7)	16 (10.25–24.99)

*Serologic study was conducted on 28 farms in January–February 2022. Only data for 4 farms positive for H3N8 virus are shown. GMT, geometric mean titer; HI, hemagglutination inhibition.

Table 3. Follow-up virologic results for local chicken farms previously positive for avian influenza A(H3N8) virus, Hong Kong, China*

Farm	Date samples collected	No. samples†	No. (%) positive by RT-PCR		No. (%) positive by virus isolation	
			H9	H3	H9	H3
A	2022 May 10	50	0	0	0	0
B	2022 May 11	50	0	0	0	0
C	2022 May 10	50	2 (4)	0	0	0
D	2022 May 11	50	0	0	0	0

*RT-PCR, reverse transcription PCR.
†Includes oropharyngeal and cloacal samples.

identification as described (*18*). We sequenced the amplified ≈700-bp PCR fragment of the cytochrome oxidase I gene by using the 3730xl DNA Analyzer (Applied Biosystems, https://www.thermofisher.com) and analyzed by using the barcoding software bold, which provides a taxonomic assignment to the query sequence by using a linear search to collect nearest neighbors (lowest percentage divergence) from a global alignment of all reference sequences (19).

Serologic Analysis

We used the HI test to detect the seroprevalence to 1 of the novel H3N8 viruses, A/chicken/Hong Kong/MKT-AB13cp/2022, and human seasonal virus A/Switzerland/8060/2017 (H3N2) in a panel of age-stratified blood donor serum samples collected during 2019–2020. The study protocol was approved by the University of Hong Kong. We also tested HI titers of a World Health Organization reference antiserum to A/Switzerland/8060/2017 against A/chicken/MKT-AB13cp/2020 H3N8 virus (original serum dilution provided was 1:128) in comparison with the homologous virus A/Switzerland/8060/2017. The HI tests were conducted as described (*20,21*). We analyzed the effect of age-stratified seroprevalence on the reproduction number (R_0) and population immunity as described (*22*).

Results

During routine virologic surveillance on chicken farms, H3N8 viruses were first identified on samples collected from 2 broiler farms (farms A and B) in December 2021 and subsequently detected on 2 other broiler farms in January 2022 (farms C and D) (Table 1). On 1 of the farms (B), H3N8 virus was detected on 3 other occasions during February and March 2022.

Of the 4 chicken farms that had positive virologic results, all had serologic evidence (HI titers ≥16) of past influenza A(H3N8) virus infection; 3 of 4 farms had ≥26 of 30 birds sampled on each farm in February 2022 test serologically positive (Table 2). Chicken producers were subsequently advised to conduct thorough disinfection and strengthen farm biosecurity to prevent further spread and eliminate the virus.

Follow-up virologic testing in May 2022 of 150 chickens from each of the 4 positive farms yielded negative results (Table 3). As of the end of June 2022, there has been no additional detection of H3N8 on any farms.

During January 2022–June 2022, we collected and tested 3,525 environmental swab samples of fecal droppings, drinking water in poultry cages, and chopping boards and defeathering machines in live poultry markets and stalls sampled (Table 4). An environmental swab specimen collected from a chicken defeathering machine on January 12 and a swab specimen collected from a poultry chopping board on January 20 from 2 different live poultry markets were positive for influenza A(H3N8) viruses. The second market only sells chicken, and the first market additionally sells chilled dressed duck slaughtered elsewhere. The species of origin from both swab specimens was determined by DNA bar coding to be domestic chicken (*Gallus domesticus*).

We sequenced 7 H3N8 viruses in this study and submitted them to GISAID (Table 5). Phylogenetic analysis of the full-genome sequence of poultry H3N8 viruses showed that the chicken H3N8 viruses from farms and poultry markets are closely related to

Table 4. Samples tested in live poultry markets and those positive for influenza A virus, Hong Kong, China, 2022*

Month	No. swabs tested	No. markets sampled	No. stalls sampled	No. (%) positive by RT-PCR			No. (%) positive by virus isolation		
				H9	H6	H3	H9	H6	H3
Jan	555	25	37		0	2 (0.36)	0	0	2 (0.36)
Feb	435	16	29	6 (1.38)	2 (0.46)	0	4 (0.92)	1 (0.23)	0
Mar	705	34	47	4 (0.57)	0	0	1 (0.14)	0	0
Apr	585	27	39	2 (0.34)	0	0	0	0	0
May	630	25	42	0	0	0	0	0	0
Jun	615	32	41	2 (0.33)	0	0	2 (0.33)	0	0
Total	3,525	159	235	14 (0.40)	2 (0.06)	2 (0.06)	7 (0.20)	1 (0.03)	2 (0.06)

*No other influenza A virus subtypes were detected. RT-PCR, reverse transcription PCR

Table 5. Influenza A (H3N8) viruses genetically sequenced in from chicken farms, live poultry markets, and the Mai Po Wetlands, Hong Kong, China

Virus name	Date of collection	Place and site of collection	DNA barcoding	GISAID accession no.*
A/chicken/Hong Kong/21-17040/2021 (H3N8)	2021 Dec 13	Farm A	Not relevant	ON909094-ON909101
A/chicken/Hong Kong/21-17632/2021 (H3N8)	2021 Dec 28	Farm B	Not relevant	ON909102-ON909109
A/Env/Hong_Kong/MKT_TYEB_13d2/2022 (H3N8)	2022 Jan 12	Live poultry market, defeathering machine	*gallus*	EPI_ISL_13566013
A/Env/Hong_Kong/MKT_AB_13cp/2022 (H3N8)	2022 Jan 20	Live poultry market, chopping board	*gallus*	EPI_ISL_13566014
A/Env/HongKong/MP16_1834/2016 (H3N8)	2016 Dec 21	Mai Po wetlands	*Anas acuta*	EPI_ISL_13566015
A/Env/HongKong/MP18_0131/2018 (H3N8)	2018 Nov 14	Mai Po Wetlands	*Anas clypeata*	EPI_ISL_13566016
A/Env/HongKong/MP18_0135/2018 (H3N8)	2018 Nov 14	Mai Po Wetlands	*Anas clypeata*	EPI_ISL_13566017

*GISAID, https://www.gisaid.org.

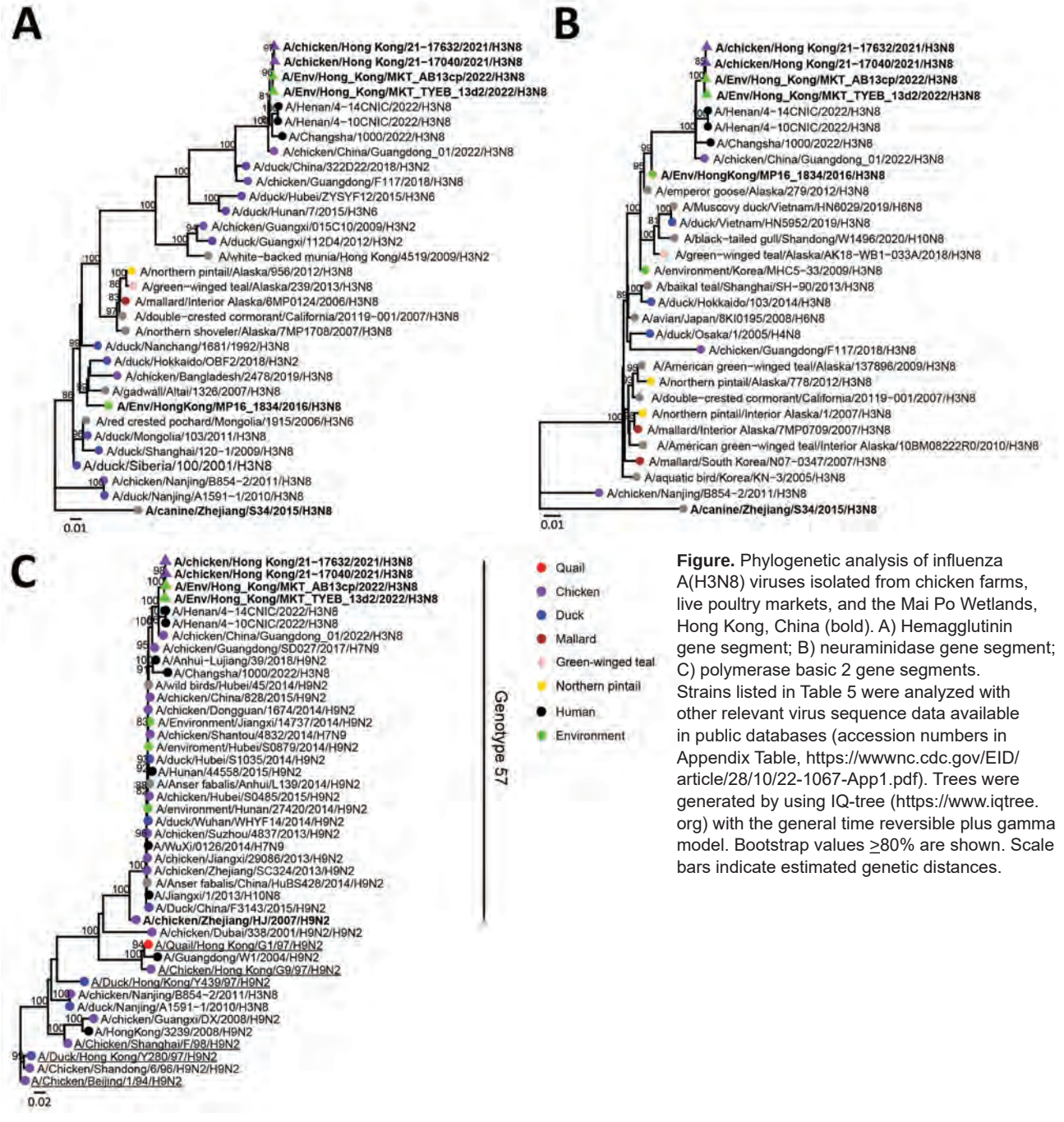

Figure. Phylogenetic analysis of influenza A(H3N8) viruses isolated from chicken farms, live poultry markets, and the Mai Po Wetlands, Hong Kong, China (bold). A) Hemagglutinin gene segment; B) neuraminidase gene segment; C) polymerase basic 2 gene segments. Strains listed in Table 5 were analyzed with other relevant virus sequence data available in public databases (accession numbers in Appendix Table, https://wwwnc.cdc.gov/EID/article/28/10/22-1067-App1.pdf). Trees were generated by using IQ-tree (https://www.iqtree.org) with the general time reversible plus gamma model. Bootstrap values ≥80% are shown. Scale bars indicate estimated genetic distances.

Table 6. Seroprevalence of antibodies to human seasonal influenza virus A/Switzerland/8060/2017 (H3N2) and A/chicken/Hong Kong/MKT-AB13cp/2022 (H3N8) virus in age-stratified human serum samples from blood donors, Hong Kong, China, 2020*

		H3N2 HI titers, no. (%)		H3N8 HI titer, no. (%)			
Age group, y	No.	≥1:10	≥1:40	≥1:10	≥1:40	H3N2 GMT (95% CI)	H3N8 GMT (95% CI)
10–19	10	10 (100)	9 (90)	0	0	183.8 (74.8–451.7)	5 (5–5)
20–29	10	7 (70)	7 (70)	0	0	37.32 (11.8–118.6)	5 (5–5)
30–39	10	5 (50)	5 (50)	0	0	20 (6.7–59.9)	5 (5–5)
40–49	10	8 (80)	6 (60)	3 (30)	1 (10)	30.31 (12.6–73.1)	7.071 (4.4–11.5)
50–59	10	3 (30)	0	2 (20)	0	7.1 (4.6–10.8)	5.743 (4.7–7.1)
60–69	10	9 (90)	9 (90)	1 (10)	1 (10)	56.6 (25.8–123.9)	6.156 (3.9–9.9)
70–79	3	1 (33)	1 (3)	0	0	12.6 (0.2–671.9)	5 (5–5)
Total	63	43 (68.3)	37 (58.7)	6 (9.5)	2 (3.2)	32.8 (22.1–48.8)	5.6 (5.1–6.2)

*GMT, geometric mean titer; HI, hemagglutination inhibition.

each other and to an H3N8 virus associated with zoonotic disease in mainland China (Figure; Appendix Figure). The polymerase basic 1, polymerase basic 2, polymerase acidic, NA, nonstructural protein, and M gene segments were derived from the G57 sublineage of influenza A(H9N2) viruses commonly found in mainland China (*23*), whereas the HA gene sequences belong to the Eurasian avian H3 lineage, which has been detected in ducks and other wild birds (*24*).

The NA gene sequences of the poultry A(H3N8) viruses belonged to the North American lineage, but a closely related N8 NA sequence had previously been detected in A/Env/Hong_Kong/MP16_1834/2016 (H3N8), a virus isolated on December 21, 2018, from the Mai Po Wetlands, Hong Kong, in 2018, obtained from a fecal specimen identified by DNA bar coding to be derived from a Northern pintail duck (*Anas acuta*) (Table 5). Two other H3N8 viruses isolated from fecal droppings collected from the Mai Po Wetlands on November 14, 2018, identified to be from a Northern shoveler duck (*Anus clypeata*) were genetically unrelated in all gene segments to the chicken H3N8 viruses. The N8 gene segment sequence also is closely related to other aquatic wild bird H3 viruses from mainland China. Other than for the N8 NA gene segment, none of the other gene segments of the poultry H3N8 viruses were derived from the wild bird H3N8 viruses detected in the Mai Po Wetlands of Hong Kong. These viruses were distinct from chicken H3N8 viruses previously reported in mainland China (*25*). However, 1 sequence of a virus from chicken similar in all 8 gene segments to our Hong Kong H3N8 viruses is available in virus genetic sequence databases (Figure).

The HI titer of the World Health Organization reference antiserum to human seasonal H3N2 virus A/Switzerland/8060/2017 against the homologous virus antigen was 1:128, and the titer against A/chicken/Hong Kong/MKT-AB13cp/2022 was <1:10, suggesting limited antigenic cross-reactivity of current human seasonal H3N2 viruses with these novel avian H3N8 viruses. The overall seroprevalence (HI titer ≥1:40) to A/chicken/Hong Kong/MKT-AB-13cp/2022 (H3N8) in age-stratified human serum samples was 3.2% (Table 6). In contrast, as expected, we found high (58.7%) seroprevalence to a recent human seasonal A/Switzerland/8060/2017 (H3N2) virus in this same panel of serum samples.

Human population immunity to a potentially zoonotic virus is a major parameter that is included in the risk assessment of animal viruses for a pandemic threat. We have described an approach to assess that risk by estimating the effect of age-stratified immunity in the human population by using HI tests on R_0 of such a virus if it were to become transmissible in humans (*22*). We found that the observed seroprevalence in humans would provide little or no resistance to such a virus, if it were to acquire other factors required for transmission between humans (Table 7).

Discussion

We report detection of chicken influenza A(H3N8) viruses from live poultry markets and farms in Hong Kong. These viruses were genetically similar to each other and to a recently reported zoonotic H3N8 virus in mainland China (*6*). The viruses were novel reassortants that have virus internal gene segments

Table 7. Estimates of effect of observed seroprevalence on human population immunity and reproductive numbers needed to cause a pandemic for novel zoonotic avian influenza virus A(H3N8) virus in chicken, Hong Kong, China*

	Estimate (95% CI)		
Virus used	Proportion of population immune	Relative reduction in reproduction number	Smallest reproductive number needed to cause a pandemic
A/Switzerland/8060/2017(H3N2)	0.393 (0.337–0.446)	0.375 (0.317–0.43)	1.601 (1.464–1.755)
A/chicken/Hong Kong/MKT0AB13cp.2022 (H3N8)	0.029 (0.012–0.058)	0.032 (0.013–0.061)	1.033 (1.013–1.066)

*See Nguyen et al. (*17*) for the methods used.

derived from H9N2 lineage genotype 57 viruses (A/chicken/Zhejiang/HJ/2007-like) established in poultry in mainland China, but the H3 and N8 gene segments were derived from wild aquatic bird influenza A viruses. The H9N2 virus internal gene cassette was previously reported to facilitate the emergence of reassortant influenza A viruses of zoonotic potential (*26*). These chicken H3N8 viruses in Hong Kong were distinct from H3N8 viruses reported from poultry in mainland China (*25*), but a A/chicken/China/Guangdong_01/2022 (H3N8) virus genetically similar to these viruses in all 8 gene segments is reported in public databases (Appendix Table). These H3N8 viruses were also distinct from H3N8 viruses reported in horses, dogs and cats (*27*–*29*).

These novel H3N8 viruses appear to have arisen in a manner analogous to the emergence of previous zoonotic H7N9 and H10N8 viruses, in which the H9N2 viruses enzootic in chicken and other game birds in China acquired HA and NA gene segments from wild, aquatic bird viruses. Wild aquatic birds share ecosystems with domestic ducks, and it is inevitable that influenza viruses will also be shared in such ecosystems. Subsequent trade systems in which domestic ducks and chickens (and other game birds) are mixed in close proximity within wholesale and retail poultry markets provide the opportunity for H9N2 viruses in chicken to acquire HA and NA gene segments from domestic ducks, as has been postulated in the emergence of H7N9 and H10N8 viruses (*4*).

Pandemics emerge when influenza viruses of birds, swine, or other mammals adapt to transmission between humans and when the human population lacks immunity to the hemagglutinin of the newly emerged virus. Cross-reactive immunity in humans is 1 parameter that is considered when risk assessing the pandemic threat from a newly emerged animal influenza virus (*30*). Our data suggest that there is little antigenic cross-reactivity between contemporary seasonal H3N2 viruses and the H3N8 virus. The overall HI test seroprevalence at a titer $\geq$1:40 to H3N8 in age-stratified serum samples collected from blood donors in Hong Kong was 3.2%, and the estimated proportion of the population immune (weighted for age structure) was 2.9% (95% CI 1.2%–5.8%). We estimated that if this H3N8 virus acquired transmissibility between humans and acquired an $R_0 \geq 1.033$, cross-reactive population immunity would fail to impede its onward transmission in the human population. For comparison, similar estimation of the minimal R_0 required for the 2009 pandemic H1N1 virus to spread in face of population immunity before its emergence and spread in 2009 was 1.231 (95% CI 1.185–1.292), a markedly higher threshold to cross (*22*).

In conclusion, we report the emergence of a novel influenza A(H3N8) virus in chickens in Hong Kong. This virus might have major zoonotic and pandemic potential. Our results indicate the need to enhance surveillance for this virus in poultry, carry out comprehensive risk assessment of such a virus, and prepare pandemic seed vaccine strains if justified by such risk assessment.

Acknowledgments

We thank Les Sims for providing technical advice on farm surveillance methods, Candy Lau for gene sequence analysis of the farm H3N8 viruses, and the World Health Organization Collaborating Centre for Reference and Research on Influenza (Melbourne, Victoria, Australia) for providing antiserum to A/Switzerland/8060/2017.

This study was supported by the Research Grants Committee of the Hong Kong Special Administrative region (T11-712/19-N) and the National Institute of Allergy and Infectious Diseases, National Institutes of Health (contract no. U01AI151810 to M.P. and L.L.M.P.).

About the Author

Dr. Sit is the chief veterinary officer and assistant director of the Agriculture, Fisheries, and Conservation Department of the Government of the Hong Kong Special Administrative Region, Hong Kong, China. His primary research interest is veterinary public health.

References

1. Krammer F, Smith GJ, Fouchier RA, Peiris M, Kedzierska K, Doherty PC, et al. Influenza. Nat Rev Dis Primers. 2018;4:3. https://doi.org/10.1038/s41572-018-0002-y
2. Fouchier RA, Guan Y. Ecology and evolution of influenza viruses in wild and domestic birds. In: Webster RG, Monto AS, Braciale TJ, Lamb RA, editors. Textbook of influenza, 2nd ed. Hoboken (NJ): John Wiley and Sons; 2013. p. 175–89.
3. Guan Y, Shortridge KF, Krauss S, Webster RG. Molecular characterization of H9N2 influenza viruses: were they the donors of the "internal" genes of H5N1 viruses in Hong Kong? Proc Natl Acad Sci U S A. 1999;96:9363–7. https://doi.org/10.1073/pnas.96.16.9363
4. Lam TT, Zhou B, Wang J, Chai Y, Shen Y, Chen X, et al. Dissemination, divergence and establishment of H7N9 influenza viruses in China. Nature. 2015;522:102–5. https://doi.org/10.1038/nature14348
5. Ma C, Lam TT, Chai Y, Wang J, Fan X, Hong W, et al. Emergence and evolution of H10 subtype influenza viruses in poultry in China. J Virol. 2015;89:3534–41. https://doi.org/10.1128/JVI.03167-14
6. World Health Organization. May 9, 2022. Disease outbreak news; avian influenza A (H3N8), China. 2022 [cited 2022 Jul 2].

https://www.who.int/emergencies/disease-outbreak-news/item/2022-DON378
7. Leung YH, Zhang LJ, Chow CK, Tsang CL, Ng CF, Wong CK, et al. Poultry drinking water used for avian influenza surveillance. Emerg Infect Dis. 2007;13:1380–2. https://doi.org/10.3201/eid1309.070517
8. Munster VJ, Baas C, Lexmond P, Bestebroer TM, Guldemeester J, Beyer WE, et al. Practical considerations for high-throughput influenza A virus surveillance studies of wild birds by use of molecular diagnostic tests. J Clin Microbiol. 2009;47:666–73. https://doi.org/10.1128/JCM.01625-08
9. Elizalde M, Agüero M, Buitrago D, Yuste M, Arias ML, Muñoz MJ, et al. Rapid molecular haemagglutinin subtyping of avian influenza isolates by specific real-time RT-PCR tests. J Virol Methods. 2014;196:71–81. https://doi.org/10.1016/j.jviromet.2013.10.031
10. Lee HK, Lee CK, Tang JW, Loh TP, Koay ES. Contamination-controlled high-throughput whole genome sequencing for influenza A viruses using the MiSeq sequencer. Sci Rep. 2016;6:33318. https://doi.org/10.1038/srep33318
11. Bankevich A, Nurk S, Antipov D, Gurevich AA, Dvorkin M, Kulikov AS, et al. SPAdes: a new genome assembly algorithm and its applications to single-cell sequencing. J Comput Biol. 2012;19:455–77. https://doi.org/10.1089/cmb.2012.0021
12. Grubaugh ND, Gangavarapu K, Quick J, Matteson NL, De Jesus JG, Main BJ, et al. An amplicon-based sequencing framework for accurately measuring intrahost virus diversity using PrimalSeq and iVar. Genome Biol. 2019;20:8. https://doi.org/10.1186/s13059-018-1618-7
13. Chen S, Zhou Y, Chen Y, Gu J. fastp: an ultra-fast all-in-one FASTQ preprocessor. Bioinformatics. 2018;34:i884–90. https://doi.org/10.1093/bioinformatics/bty560
14. Camacho C, Coulouris G, Avagyan V, Ma N, Papadopoulos J, Bealer K, et al. BLAST+: architecture and applications. BMC Bioinformatics. 2009;10:421. https://doi.org/10.1186/1471-2105-10-421
15. Walker BJ, Abeel T, Shea T, Priest M, Abouelliel A, Sakthikumar S, et al. Pilon: an integrated tool for comprehensive microbial variant detection and genome assembly improvement. PLoS One. 2014;9:e112963. https://doi.org/10.1371/journal.pone.0112963
16. Edgar RC. MUSCLE: multiple sequence alignment with high accuracy and high throughput. Nucleic Acids Res. 2004;32:1792–7. https://doi.org/10.1093/nar/gkh340
17. Nguyen LT, Schmidt HA, von Haeseler A, Minh BQ. IQ-TREE: a fast and effective stochastic algorithm for estimating maximum-likelihood phylogenies. Mol Biol Evol. 2015;32:268–74. https://doi.org/10.1093/molbev/msu300
18. Cheung PP, Leung YH, Chow CK, Ng CF, Tsang CL, Wu YO, et al. Identifying the species-origin of faecal droppings used for avian influenza virus surveillance in wild-birds. J Clin Virol. 2009;46:90–3. https://doi.org/10.1016/j.jcv.2009.06.016
19. Ratnasingham S, Hebert PD. bold: the barcode of life data system (http://www.barcodinglife.org). Mol Ecol Notes. 2007;7:355–64. https://doi.org/10.1111/j.1471-8286.2007.01678.x
20. World Health Organization. WHO manual on animal influenza diagnosis and surveillance, 2002 [cited 2022 Jul 2]. http://www.who.int/csr/resources/publications/influenza/en/whocdscsrncs20025rev.pdf
21. World Organisation for Animal Health.. Avian influenza. In: Terrestrial manual, 2018. p. 830–1 [cited 2022 Aug 11]. https://www.woah.org/en/what-we-do/standards/codes-and-manuals/terrestrial-manual-online-access</eref
22. Cheung JT, Tsang TK, Yen HL, Perera RA, Mok CK, Lin YP, et al. Determining existing human population immunity as part of assessing influenza pandemic risk. Emerg Infect Dis. 2022;28:977–85. https://doi.org/10.3201/eid2805.211965
23. Wang J, Jin X, Hu J, Wu Y, Zhang M, Li X, et al. Genetic evolution characteristics of genotype G57 virus, a dominant genotype of H9N2 avian influenza virus. Front Microbiol. 2021;12:633835. https://doi.org/10.3389/fmicb.2021.633835
24. Yang D, Liu J, Ju H, Ge F, Wang J, Li X, et al. Genetic analysis of H3N2 avian influenza viruses isolated from live poultry markets and poultry slaughterhouses in Shanghai, China in 2013. Virus Genes. 2015;51:25–32. https://doi.org/10.1007/s11262-015-1198-5
25. Cui H, Shi Y, Ruan T, Li X, Teng Q, Chen H, et al. Phylogenetic analysis and pathogenicity of H3 subtype avian influenza viruses isolated from live poultry markets in China. Sci Rep. 2016;6:27360. https://doi.org/10.1038/srep27360
26. Pu J, Wang S, Yin Y, Zhang G, Carter RA, Wang J, et al. Evolution of the H9N2 influenza genotype that facilitated the genesis of the novel H7N9 virus. Proc Natl Acad Sci U S A. 2015;112:548–53. https://doi.org/10.1073/pnas.1422456112
27. Payungporn S, Crawford PC, Kouo TS, Chen LM, Pompey J, Castleman WL, et al. Influenza A virus (H3N8) in dogs with respiratory disease, Florida. Emerg Infect Dis. 2008;14:902–8. https://doi.org/10.3201/eid1406.071270
28. Chambers TM. Equine influenza. Cold Spring Harb Perspect Med. 2022;12:a038331. https://doi.org/10.1101/cshperspect.a038331
29. Wasik BR, Voorhees IE, Parrish CR. Canine and feline influenza. Cold Spring Harb Perspect Med. 2021;11:a038562. https://doi.org/10.1101/cshperspect.a038562
30. Cox NJ, Trock SC, Burke SA. Pandemic preparedness and the influenza risk assessment tool (IRAT). Curr Top Microbiol Immunol. 2014;385:119–36. https://doi.org/10.1007/82_2014_419

Address for correspondence: Malik Peiris, School of Public Health, The University of Hong Kong, No. 7 Sassoon Rd, Pokfulam, Hong Kong Special Administrative Region, Hong Kong, China; email: malik@hku.hk

Improving Estimates of Social Contact Patterns for Airborne Transmission of Respiratory Pathogens

Nicky McCreesh, Mbali Mohlamonyane, Anita Edwards, Stephen Olivier, Keabetswe Dikgale, Njabulo Dayi, Dickman Gareta, Robin Wood, Alison D. Grant, Richard G. White, Keren Middelkoop

Data on social contact patterns are widely used to parameterize age-mixing matrices in mathematical models of infectious diseases. Most studies focus on close contacts only (i.e., persons spoken with face-to-face). This focus may be appropriate for studies of droplet and short-range aerosol transmission but neglects casual or shared air contacts, who may be at risk from airborne transmission. Using data from 2 provinces in South Africa, we estimated age mixing patterns relevant for droplet transmission, nonsaturating airborne transmission, and *Mycobacterium tuberculosis* transmission, an airborne infection where saturation of household contacts occurs. Estimated contact patterns by age did not vary greatly between the infection types, indicating that widespread use of close contact data may not be resulting in major inaccuracies. However, contact in persons ≥50 years of age was lower when we considered casual contacts, and therefore the contribution of older age groups to airborne transmission may be overestimated.

Mathematical models of infectious disease transmission are widely used to help develop infectious disease policy, estimate the potential effect of interventions, and provide insight into disease dynamics and natural history. Many models incorporate patterns of mixing between different sections of the population, most commonly between different age groups. Simulated mixing patterns can have a considerable effect on model dynamics (*1*), underscoring the importance of simulating realistic mixing patterns. Mixing patterns are frequently shaped by social contact data (i.e., empirical data collected from respondents about the persons with whom they had contact during a set period) (*2*).

Most social contact data collection has focused on close contacts, using a definition of contacts that required a 2-way face-to-face conversation of ≥3 words, close proximity (e.g., within 2 meters), physical contact, or some combination of those criteria (*2*). Those types of contact may approximate reasonably well the types of contact that are relevant for infections that are transmitted primarily through direct contact, short range aerosols, droplets, or some combination of these modes. For obligate, preferential, or opportunistic airborne infections such as measles, *Mycobacterium tuberculosis*, and SARS-CoV-2, however, this definition probably excludes many potentially effective contacts because transmission of airborne infections can occur between anybody sharing air in inadequately ventilated indoor spaces, regardless of whether conversation occurs, and over distances >2 meters (*3*). For airborne infections, estimates of casual contact time may therefore be more appropriate, calculated as the time spent in indoor locations multiplied by the number of other persons present.

Tuberculosis also differs from most respiratory infections in terms of the long periods during which persons are potentially infectious; an estimated 9–36 months elapses between disease development and diagnosis (or notification) in 11 countries with high tuberculosis incidences (*4*). Therefore, transmission to repeated contacts can partially saturate (even allowing for reinfection), making the relationship between contact time and infection risk nonlinear (*5*). This effect is most pronounced for contact between

Author affiliations: London School of Hygiene and Tropical Medicine TB Centre, London, UK (N. McCreesh, A.D. Grant, R.G. White); The Desmond Tutu HIV Centre, University of Cape Town, Cape Town, South Africa (M. Mohlamonyane, R. Wood, K. Middelkoop); University of KwaZulu-Natal Africa Health Research Institute, Durban, South Africa (A. Edwards, A.D. Grant); Africa Health Research Institute, Durban (S. Olivier, K. Dikgale, N. Dayi, D. Gareta); University of Cape Town Department of Medicine, Cape Town (R. Wood, K. Middelkoop); University of the Witwatersrand School of Public Health, Johannesburg, South Africa (A.D. Grant)

DOI: https://doi.org/10.3201/eid2810.212567

household members (*5*). Household membership and repeated contacts are rarely explicitly simulated in mathematical models, and therefore the effects of contact saturation need to be incorporated into the mixing matrices used to parameterize the models.

In this article, we describe methods for estimating age-mixing patterns relevant for nonsaturating airborne transmission and *M. tuberculosis* transmission by using a novel weighted approach to incorporate the effects of household contact saturation into our estimates for *M. tuberculosis*. We generate estimates of age mixing using data on close and casual contacts from 2 communities in South Africa and compare the estimated mixing patterns with those typically used in mathematical modeling studies (i.e., generated using close contact numbers, and more suitable for droplet or short range aerosol transmission).

Methods

We collected social contact data in 2 study communities in South Africa: 1 in KwaZulu-Natal Province and 1 in Western Cape Province. Both communities have high rates of unemployment, high prevalence of HIV, and high incidence of tuberculosis compared with the other provinces as a whole. The study community in KwaZulu-Natal consisted of a population of ≈46,000, living in the predominantly rural and peri-urban areas in the catchment areas of 2 primary care clinics and within a demographic surveillance area (DSA). The study community in Western Cape was a peri-urban community of ≈27,000 and was an established research site with biennial censuses.

Data Collection

We collected the KwaZulu-Natal data during March–December 2019. We sampled 3,093 adults (≥18 years of age) at random from an estimated population of 33,288, stratified by residential area (small-scale divisions with ≈350 households per area) and with probability proportional to the number of eligible persons in each area, based on the most recent DSA census conducted before area entry. We made up to 3 attempts to contact sampled persons.

We collected the Western Cape data during May–October 2019. In total, we selected 1,530 adults (≥15 years of age) from an estimated population of 20,633, by using age- and sex-stratified random sampling, based on a census conducted in the study population in February and March 2019. We made up to 5 attempts to contact selected persons on different days of the week (including weekends).

For both surveys, we conducted interviews face-to-face at the respondents' homes, by using interview administered questionnaires on tablet computers. We conducted interviews in isiZulu in KwaZulu-Natal and in English or isiXhosa in Western Cape. We asked respondents about their movements on a randomly assigned day during the preceding week in KwaZulu-Natal, and on the day before the interview in Western Cape. To allow casual contact time (defined as time spent "sharing air" indoors or on transport) to be estimated, we asked respondents to list the places they had visited (including their own home) and transport they had used. For each location, questions asked included:

- What type of location was it? (Appendix Figure 5, https://wwwnc.cdc.gov/EID/article/28/10/21-2567-App1.pdf)
- How long did you spend there? (recorded in hours and minutes)
- How many persons were there halfway through the time you were there?

We did not ask respondents for the ages of persons present because it was thought that respondents would not be able to accurately remember and estimate the ages of all persons present in all indoor locations visited and transport used. We also asked respondents about their close contacts, defined as persons with whom the respondent had a face-to-face conversation. We first asked respondents to make a numbered list of all their contacts, with help from the interviewer. We then asked respondents questions about 10 contacts (selected at random by number by the tablet computers) or all of their contacts if they reported <10. Questions included:

- Is this contact a member of your household?
- How old do you think they are?
- How much time did you spend with them in total?

We also collected respondents' basic demographic information. For the KwaZulu-Natal community, we obtained data on household size and residency (i.e., urban, peri-urban, or rural) from the most recent DSA census. We collected all other data directly from the respondents.

Data Analysis

We estimated close contact numbers and times by using data on persons with whom the respondents reported having a face-to-face conversation. We generated 95% plausible intervals for the age-mixing matrices by using bootstrapping.

We estimated casual contact time in a location as the duration of time the respondent reported

spending there multiplied by the reported number of persons present. We generated central estimates for casual contact time age-mixing matrices by using the method outlined in McCreesh et al (*6*). In brief, because data were collected on numbers of total persons and children present in indoor locations only, and not the ages of adults, we need to estimate the age distribution of adult casual contacts. We therefore assumed that the age distribution of adult contacts in each location type matched the weighted age distribution of respondents who reported visiting locations of that type. Again, we generated 95% plausible ranges by using bootstrapping.

We adjusted the age-mixing matrices to be symmetric by using the study community age structures. We used data on adult contact numbers and time with children to estimate child contact numbers and time with adults, assuming that overall contact numbers and time between children and adults in each age group is equal to overall contact numbers and time between adults in each age group and children. To enable comparison between the 2 study communities, the lowest respondent age group was set at 15–19 years for both surveys. Because persons 15–17 years of age were not interviewed in KwaZulu-Natal, we assumed that contact patterns in persons 18–19 years of age were representative of contact patterns in all persons 15–19 years of age (Appendix).

Generating Age-Mixing Matrices for Droplet and Nonsaturating Airborne Transmission and *Mycobacteria tuberculosis*

We set age-mixing matrices relevant for droplet transmission to be equal to age-mixing matrices calculated using close contact numbers (Figure 1). We set age-mixing matrices relevant for nonsaturating airborne transmission to be equal to the unweighted sum of the household close contact time matrices and the nonhousehold casual contact time matrices. We used close contact time between household members for household estimates, as opposed to casual contact time occurring in households. We did so because most contact between household members is likely to meet the definition of close contact, and because this approach enabled the age structures of households to be more accurately reflected in the age-mixing matrices. We set age-mixing matrices relevant for *M. tuberculosis* transmission to be equal to the sum of the household close contact number matrices and the nonhousehold casual contact time matrices. We weighted these matrices to reflect empirical estimates of the proportion of tuberculosis that results from household transmission (central estimate 12% [range 8%–16%]) (*5*).

To enable direct comparisons to be made between the different age-mixing matrices, we adjusted the matrices for nonsaturating airborne transmission and *M. tuberculosis* transmission to give the same mean contact intensity between adults as the matrices for droplet transmission. We used bootstrapping to generate plausible ranges (Appendix).

Results

Recruitment

Of the 3,093 persons sampled in KwaZulu-Natal, 1,723 (56%) were successfully contacted, 299 (10%) were dead or reported to have out-migrated, and

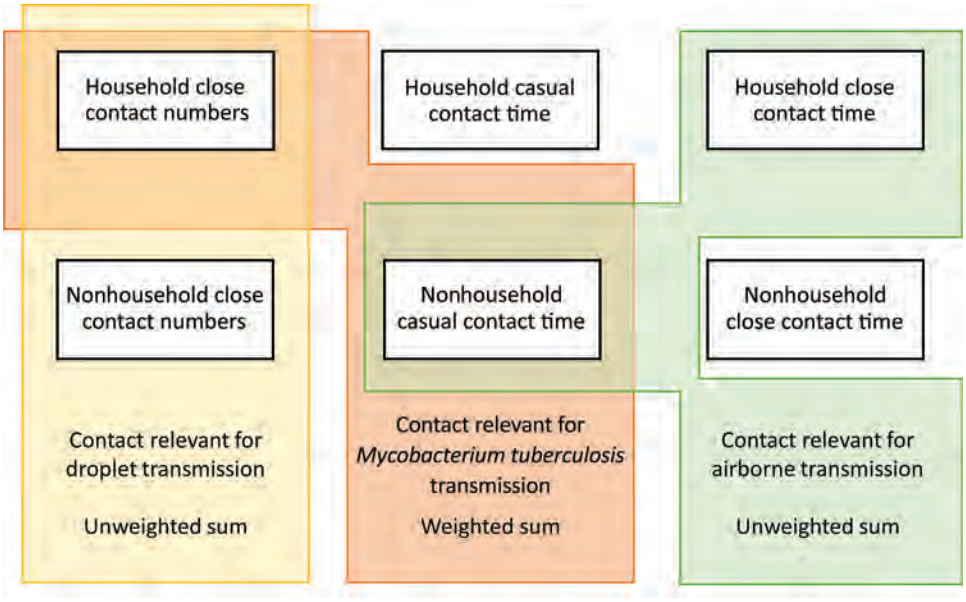

Figure 1. Summary of data used to estimate age-mixing matrices for a study of social contact patterns for airborne transmission of respiratory pathogens, KwaZulu Natal and Western Cape Provinces, South Africa, 2019. Diagram showing how age-mixing matrices relevant for the transmission of droplet infections, airborne infections, and *Mycobacterium tuberculosis* were estimated using empirical data on close contact numbers, close contact time, and casual contact time.

Table. Characteristics of respondents and target population for study of social contact patterns for airborne transmission of respiratory pathogens, KwaZulu Natal and Western Cape Provinces, South Africa, 2019

Characteristic	KwaZulu Natal		Western Cape	
	Sample, no. (%)	Target population, %*	Sample, no. (%)	Target population, %*
Sex				
M	751 (44)	41	553 (50)	52
F	953 (56)	59	562 (50)	48
Age group, y				
15–17	0	9.1	56 (5)	4.5
18–19	118 (6.9)	5.6	84 (7.5)	4.5
20–29	495 (29)	26	412 (37)	33
30–39	308 (18)	21	358 (32)	37
40–49	227 (13)	13	142 (13)	15
≥50	556 (33)	25	63 (5.7)	6.5
Residence				
Rural	867 (51)	59	0	0
Peri-urban	716 (42)	33	1,115 (100)	100
Urban	121 (7.1)	8	0	0
Monthly household income, South African rands				
<1,000	416 (24)		111 (10)	
1,000–2,500	785 (46)		261 (23)	
2,500–5,000	302 (18)		374 (34)	
5,000–10,000	125 (7.3)		179 (16)	
>10,000	65 (3.8)		61 (5.5)	
Unknown/missing	11 (0.65)		129 (12)	
Employment				
Full-time	329 (19)		403 (36)	
Part-time/casual	68 (4)		213 (19)	
None	1299 (76)		492 (44)	
Missing	8 (0.5)		7 (0.6)	
Household size				
1	115 (6.7)	4.1	203 (18)	19
2–4	287 (17)	26	683 (61)	66
5–7	488 (29)	33	195 (17)	13
8–10	375 (22)	20	26 (2.3)	1.6
≥11	439 (26)	17	8 (0.72)	0.4
Day reported				
Monday	239 (14)		203 (18)	
Tuesday	242 (14)		202 (18)	
Wednesday	239 (14)		187 (17)	
Thursday	251 (15)		138 (12)	
Friday	261 (15)		80 (7.2)	
Saturday	245 (14)		98 (8.8)	
Sunday	227 (13)		207 (19)	
Total	1,704	33,288	1,115	20,633

*Target population refers to persons in the populations ≥15 years of age.
†In KwaZulu-Natal, urban is defined as KwaMsane Municipality, peri-urban as other areas with a population density ≥400/km^2, and rural as areas with a population density <400/km^2.

1,071 (35%) could not be contacted. Of those successfully contacted, 1,704 (99%) completed an interview.

Of the 1,530 persons sampled in Western Cape, 1,214 (93%) were successfully contacted, 117 (8%) had moved or died, 193 (13%) had had incorrect information listed in the census, and 6 were uncontactable. Of the 1,214 persons contacted, 77 (6%) refused to be interviewed and 14 were ineligible (because of disability or lack of fluency with English and isiXhosa). Of 1,123 persons interviewed, unexplained technical issues meant that data from 8 interviews were lost between collection and transfer to the database, leaving 1,115 (92%) completed interviews.

For both populations, the recruited sample was a reasonable match to the target population in terms of sex, age, and residence type (urban, peri-urban, or rural) (Table). Respondents in Kwa-Zulu-Natal also were a close match to the target population in terms of employment status (Appendix). No data on employment status for the target population were available for Western Cape.

Contact Numbers and Time

We stratified household and nonhousehold close contact numbers and time and casual contact time in KwaZulu-Natal and Western Cape, by sex, age, and household size (Figure 2, 3; Appendix Tables 1–6). Overall, close contact numbers and time, as well as casual contact time, were higher for women than for men in both communities; however, the

differences were generally not large (close contact time 46% higher for women in KwaZulu-Natal and 8%–22% higher for other contact measures and settings) and not significant for close contact numbers or casual contact time in Western Cape. We observed a tendency for casual contact time to decrease slightly with age in both communities, and close contact numbers and time were substantially higher in persons 15–19 years of age than in older age groups in Western Cape only (Western Cape close contact numbers: 11 in persons 15–19 years of age, 7.7–8.7 in older age groups [p<0.001]; close contact time: 80 hours in persons 15–19 years of age, 49–63 in older age groups [p<0.001]). Close contact numbers and time, as well as casual contact time, increased with increasing household size in both communities, driven by increases in contact with household members. Contact between household members made up a higher proportion of total contact in KwaZulu-Natal than in Western Cape for all types of contact (close contact numbers: 62% in KwaZulu-Natal, 27% in Western Cape; close contact time: 79% in KwaZulu-Natal, 60% in Western Cape; casual contact time: 55% in KwaZulu-Natal, 31% in Western Cape).

Age Mixing

We generated estimated age-mixing matrices for droplet transmission non-saturating airborne transmission, and *M. tuberculosis* transmission for KwaZulu-Natal and Western Cape (Figure 4, 5). We also

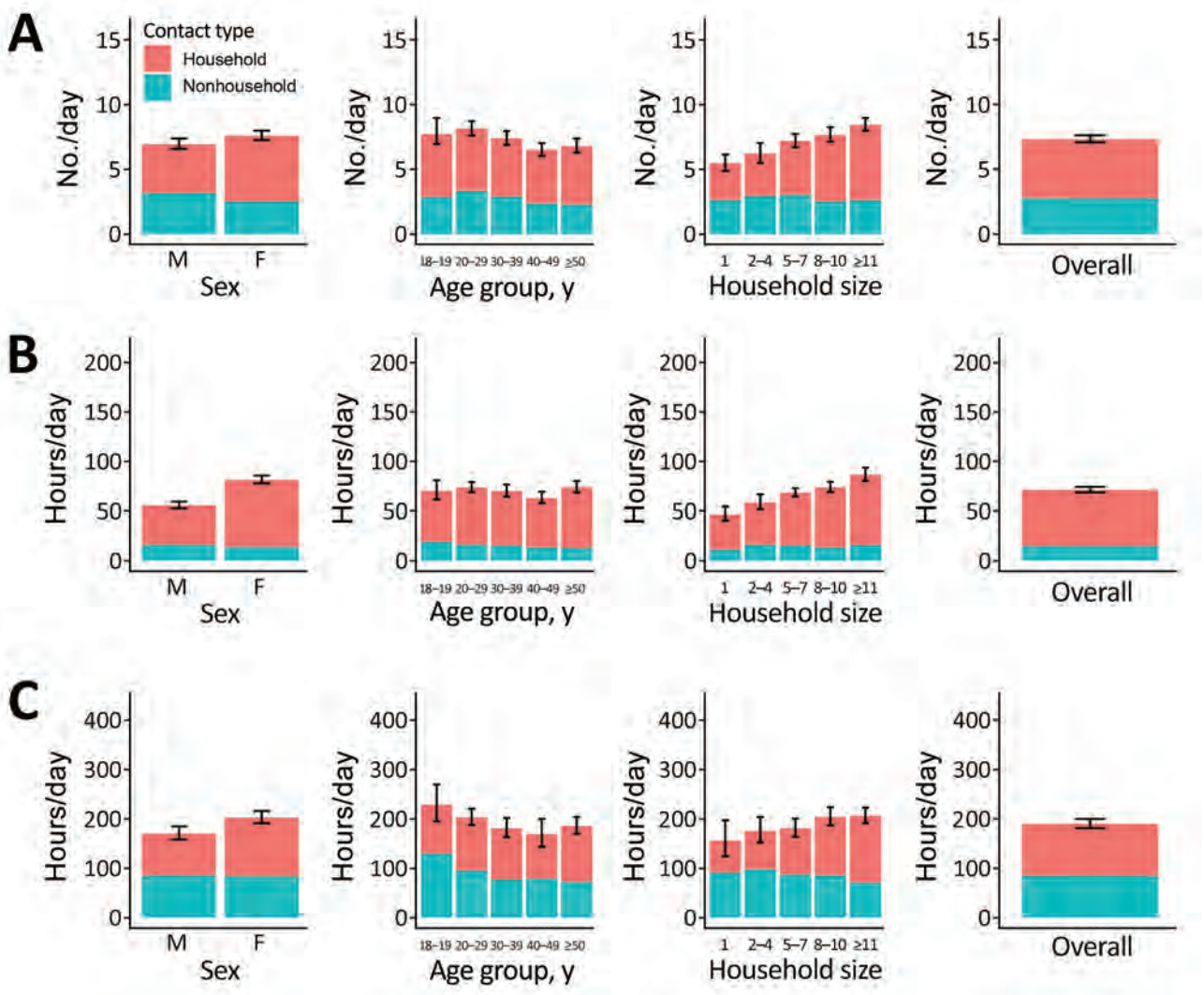

Figure 2. Household and nonhousehold close contact numbers (A), close contact time (B), and casual contact time (C) for study of social contact patterns for airborne transmission of respiratory pathogens, KwaZulu-Natal Province, South Africa, by sex, age group, and household size. Error bars show 95% CIs for total contact numbers or time. For KwaZulu-Natal, household size data were taken from census data and did not always correspond exactly with respondents' views of who they considered to be household members. For this reason, some contact with household members was reported by respondents who we recorded as having a household size of 1.

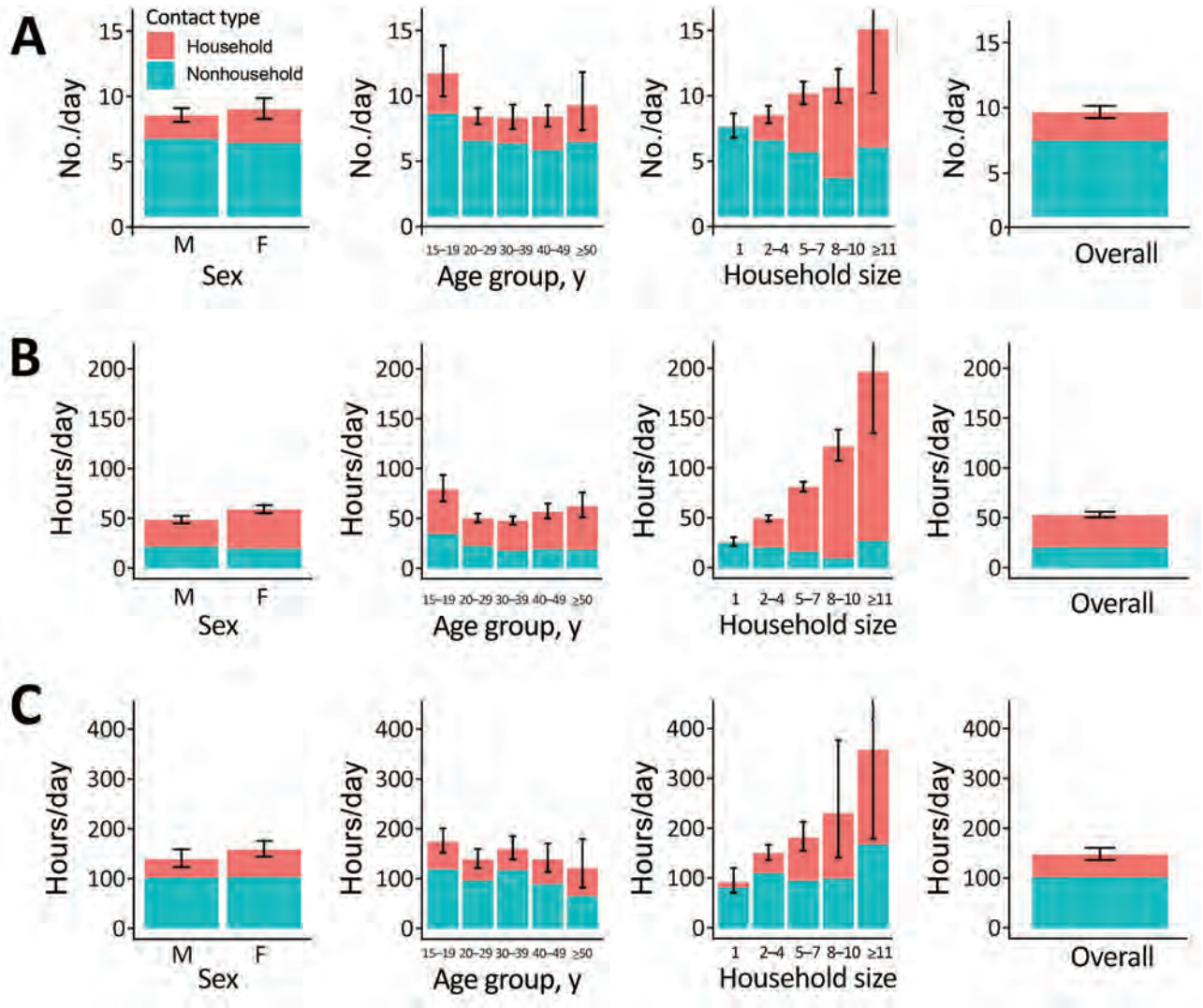

Figure 3. Household and nonhousehold close contact numbers (A), close contact time (B), and casual contact time (C) in Western Cape Province, South Africa, by sex, age, and household size, for study of social contact patterns for airborne transmission of respiratory pathogens. Error bars show 95% CIs for total contact numbers or time. In Western Cape, contact with household members was reported by a small proportion of respondents who had reported having no household members, most likely reflecting errors in the data.

generated 95% plausible ranges for these matrices (Appendix Figure 1, 2).

Estimated contact patterns by age did not vary greatly between the infection types in either community. However, age-mixing patterns were less assortative in the nonsaturating airborne and *M. tuberculosis* matrices compared with the droplet matrices in both communities (Appendix). The exception to this pattern was contact between persons 15–19 years of age in KwaZulu-Natal, which was more intense in the nonsaturating airborne and *M. tuberculosis* matrices than the droplet matrices. In both communities, relative to other adult age groups, overall contact intensities were lower in persons ≥50 years of age when considering contact relevant for nonsaturating airborne transmission or the transmission of *M. tuberculosis* compared with contact relevant for droplet transmission.

Discussion

Using data from 2 provinces in South Africa, we estimated contact and age-mixing patterns relevant for the transmission of droplet infections, nonsaturating airborne infections, and *M. tuberculosis*. In our communities, contact patterns did not vary greatly between contacts relevant for droplet infections and those relevant for nonsaturating airborne or *M. tuberculosis* transmission. However, using close contact data in models of the transmission of *M. tuberculosis* or other airborne infections in our study communities

may mean that the importance of adults ≥50 years of age to transmission is overestimated.

Very few data are available on casual contact patterns from any setting. Previous studies in the same community in Western Cape have found greater drops in casual contact time than in close contact numbers in older age groups (*6*) and decreases in indoor casual contact numbers with age (*7*). Another study in the same community found high levels of age-assortative mixing with respect to casual contact time in schools and workplaces (*8*). More data are needed on casual contact patterns, and age-mixing

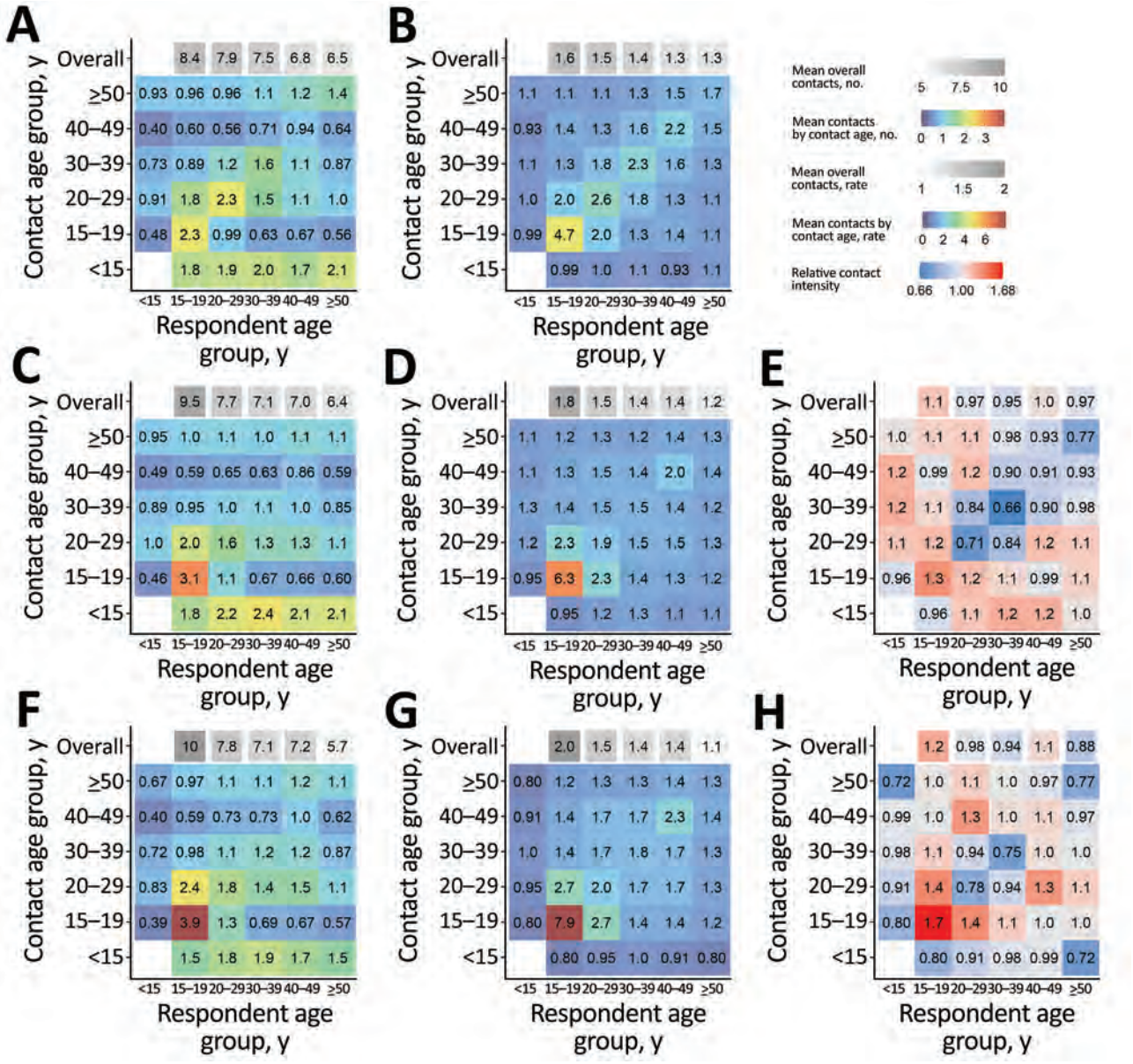

Figure 4. Age-mixing matrices relevant for droplet transmission (A, B), nonsaturating airborne transmission (C, D), and *Mycobacterium tuberculosis* transmission (F, G) for study of social contact patterns for airborne transmission of respiratory pathogens, KwaZulu-Natal Province, South Africa. Panels A, C, and F show absolute contact intensities between respondents and contacts in each age group; panels B, D, and G show intensities of contact between each member of each age group; panels E and H show intensities for airborne infections and *M. tuberculosis* compared with intensities for droplet infections, respectively. Numbers shown in panel A are the mean number of contacts respondents in each age group have with contacts in each age group per day. Numbers shown in panel B are the rate of contact between each person in the population per day, expressed as rates × 10^5. Numbers and rates in panels C, D, F, and G are standardized so that the mean overall contact intensity by reported by adult respondents is the same as the mean number of overall close contacts reported by adult respondents (panel A). Contact numbers between child respondents and contacts in each age group were estimated from data on contact between adult respondents and child contacts.

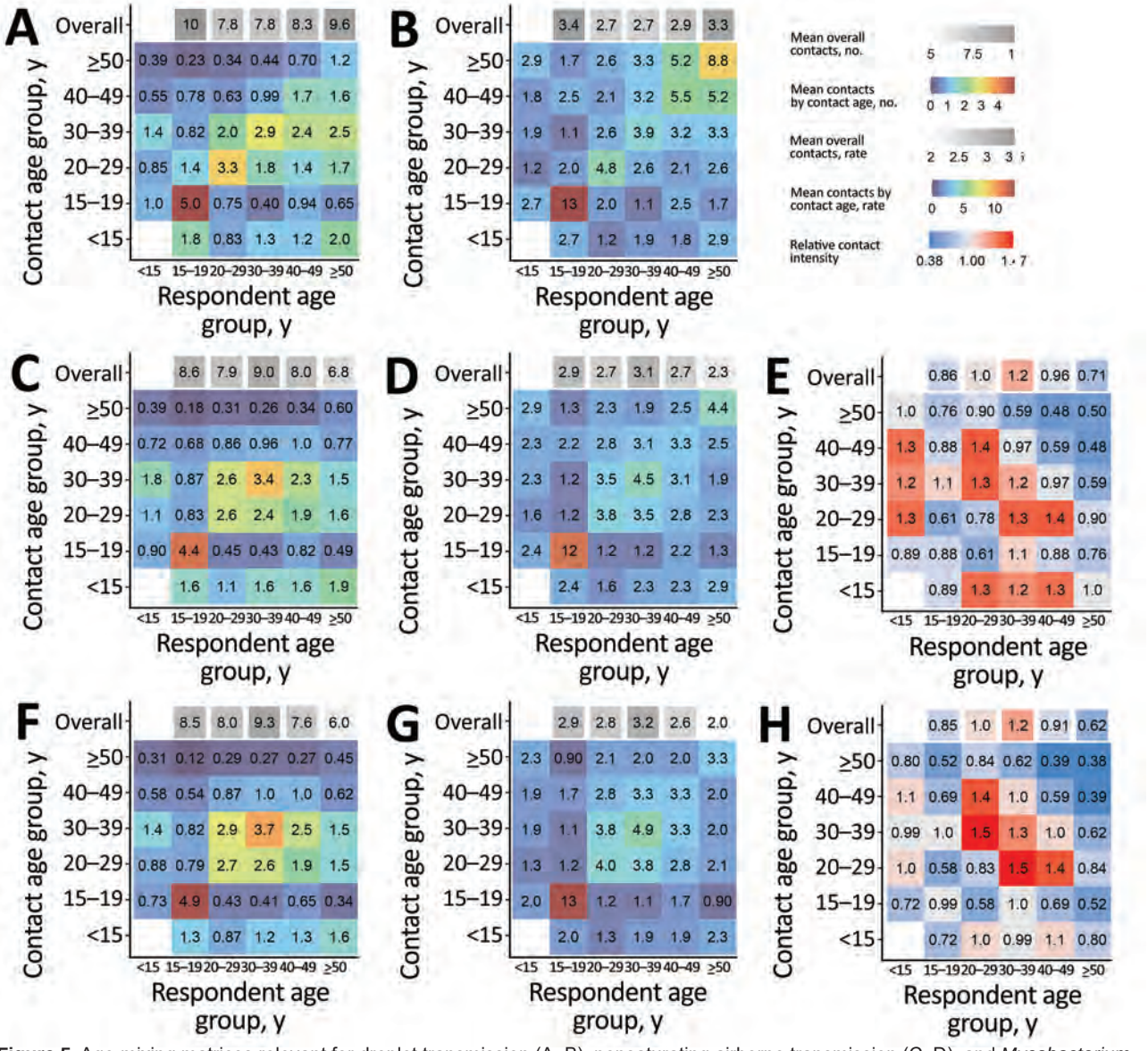

Figure 5. Age-mixing matrices relevant for droplet transmission (A, B), nonsaturating airborne transmission (C, D), and *Mycobacterium tuberculosis* transmission (F,G) for study of social contact patterns for airborne transmission of respiratory pathogens, Western Cape Province, South Africa. Panels A, C, and F show absolute contact intensities between respondents and contacts in each age group; panels B, D, and G show intensities of contact between each member of each age group; panels E and H show intensities for airborne infections and *Mycobacterium tuberculosis* compared with intensities for droplet infections, respectively. Numbers shown in panel A are the mean number of contacts respondents in each age group have with contacts in each age group per day. Numbers shown in panel B are the rate of contact between each person in the population per day, expressed as rates × 10^5. Numbers and rates in panels C, D, F, and G are standardized so that the mean overall contact intensity by reported by adult respondents is the same as the mean number of overall close contacts reported by adult respondents (panel A). Contact numbers between child respondents and contacts in each age group were estimated from data on contact between adult respondents and child contacts.

patterns in particular, to determine whether the findings of this study are generalizable to other settings and to improve the predictions from mathematical models of the transmission of *M. tuberculosis* and other airborne infections.

Our approaches to generating the separate droplet and airborne transmission matrices are necessarily simplifications, and many infections will not fit neatly into these 2 categories. In addition, considerable uncertainty exists about the role of different transmission routes to the spread of many infections. Droplets have traditionally been considered to be the main transmission route for most respiratory viruses; however, there is evidence that airborne transmission

can occur for a wide range of pathogens, including influenza, respiratory syncytial virus, Middle East respiratory syndrome coronavirus, and SARS-CoV-2 (*9*). One model using data on household transmission of influenza A suggested that airborne transmission was responsible for about half of infections (*10*). For infections where both airborne and droplet or short range aerosol transmission are thought to play an important role in transmission, an intermediate matrix may be preferable.

There are 2 main differences between our droplet and airborne or *M. tuberculosis* age-mixing matrices. The first is the type of nonhousehold contacts considered: close (face-to-face conversation) or casual (sharing space indoors). The second is that the airborne and (nonhousehold component of the) *M. tuberculosis* matrices are based on contact time, rather than unique contact numbers. The primary reason for using contact time for casual contacts is that respondents are unlikely to be able to estimate unique casual contact numbers for many locations they visit, necessitating the use of contact time or assumptions about the rate of turnover of unique persons in a location. For our droplet transmission matrices, we chose to use unique contact numbers in a 24-hour period because that is the most commonly used method (*2*) and therefore enables comparisons to be made with what is typically done. However, we should note that both the choice of a 24-hour time period and the lack of any weighting or restrictions by contact duration or other measures of closeness are relatively arbitrary choices.

Robust evidence as to the types of contact most relevant to transmission are limited for respiratory infections. Several studies have compared the fit to data on varicella, parvovirus B19, or influenza A seroprevalence by age of models parameterized by using contact patterns generated from close contact data in a range of different ways (*11*–*13*). Overall, those studies suggest that analysis methods that give greater weight to more intimate contacts may be preferable in some circumstances; for instance, restricting what counts as a contact to those involving physical touch or a minimum contact duration or using contact time rather than contact numbers. Approaches based on contact numbers may be more suitable for more highly transmissible infections such as measles, where only a short duration of contact is needed for transmission, whereas approaches based on contact time may be more suitable for less transmissible infections, where repeated or longer contacts are needed (*14*).

Fewer studies have considered expanding the pool of contacts beyond close contacts only, to also include casual contacts. However, a study that had paired individual-level contact data and pandemic influenza A serologic data found that models that included a variable for number of locations visited were strongly supported over those that only included variables for age and close contact numbers (*15*). This finding suggests that airborne transmission may play a role in the spread of influenza A, or that the standard close contact definition misses a substantial proportion of contacts at risk for droplet transmission.

Other factors may also influence airborne and *M. tuberculosis* transmission risk, which are not accounted for in the analyses. Ventilation rates play a large role in determining airborne infection risk (*16*), and giving less weight to contact occurring in better ventilated settings would improve our airborne and *M. tuberculosis* matrices. Unfortunately, few data on ventilation rates by location type are available, and they show large amounts of variation between locations and between the same location on different days (*17*). Saturation of contacts may occur for infections other than *M. tuberculosis*, particularly highly transmissible pathogens such as measles virus. An approach based on casual contact numbers may be preferable for these infections but would be highly dependent on assumptions made about how unique contact numbers are related to estimates of cross-sectional numbers of persons present.

There are several limitations when using casual contact data to estimate mixing patterns. First, estimates of contact time in places where large numbers of persons are present are likely to be less reliable because a person's estimates of the number of persons present are likely to be poor and because the assumption that a risk for transmission exists between all persons present in the space may not be true in larger spaces. Estimates may be poorer when asking about a random day in the past week (as we did in KwaZulu-Natal) than when asking about the day before the interview (as we did in Western Cape). In our main analysis, when estimating contact time, we cap the number of persons at risk for transmission at 100. In our sensitivity analyses, we show that using a cap of 20 persons or not capping the numbers of persons has a moderate effect on casual contact time age-mixing matrices (Appendix). Conducting similar sensitivity analyses may be necessary when using age-mixing matrices calculated using casual contact time in mathematical models.

A second limitation is that the approach we use to determining the ages of adults present in locations other than respondents' own homes is indirect and relies on the assumption that the age distribution of adults present in a location type reflects the duration

of time respondents of different ages reported spending in that location type. This assumption may not always be reasonable if different age groups tend to visit different locations of the same type (or at different times) or substantial mixing occurs with persons from outside the study community. These issues are discussed further in McCreesh et al. (*6*).

An additional limitation of our estimates for KwaZulu-Natal only is that we did not recruit persons 15–17 years of age and instead assumed in the analysis that contact by persons 18–19 years of age was representative of contact by all persons 15–19 years of age. This assumption is unlikely to be true given that contacts by persons 15–17 and 18–19 years of age differ greatly in Western Cape (Appendix Figure 9). For this reason, our estimates for persons 15–19 years of age in KwaZulu-Natal should be treated with caution.

To conclude, our estimated age-mixing matrices for droplet transmission, nonsaturating airborne transmission, and *M. tuberculosis* transmission were not substantially different from each other for either community. This finding provides some reassurance that the widespread use of close contact data to parameterize age-mixing matrices for transmission models of airborne infections may not be resulting in major inaccuracies. Some differences were observed, however, particularly in the oldest age group, and our data were from 2 communities in South Africa only. We recommend that future social contact surveys collect data on casual contacts as well as close contacts to determine whether the similarity between different types of contact pattern is true across other settings. We would also urge mathematical modelers to consider whether unique close contact numbers in a 24-hour period are the most appropriate contacts for the infection and scenario they are simulating and to consider performing sensitivity analyses when uncertainty exists as to the most appropriate contact definition.

Acknowledgments

We thank the social contact survey respondents and all of the fieldworkers involved in the data collection (in KwaZulu-Natal: Nkosingiphile Buthelezi, Zilethile Khumalo, Sifundesihle Malembe, Zodwa Mkwanazi, Sanele Mthiyane; in Western Cape: Sinayo Dyubhele, Mzukisa Diniso, Olwethu Kemele, Zilungile Majola Nyembezi, Nomonde Vungama & Nontyatyambo Bangani).

This research is jointly funded by the UK Medical Research Council (MRC) and the UK Department for International Development under an MRC/Department for International Development concordat (agreement no MR/P002404/1). The support of the Economic and Social Research Council is gratefully acknowledged. The project is partly funded by the Antimicrobial Resistance Cross Council Initiative supported by the 7 research councils in partnership with other funders, including support from the Global Challenges Research Fund (grant no. ES/P008011/1). N.M. is additionally funded by the Wellcome Trust (218261/Z/19/Z). R.G.W. is funded by the Wellcome Trust (grant no. 218261/Z/19/Z), the US National Institutes of Health (grant no. 1R01AI147321-01), the European and Developing Countries Clinical Trials Partnership (grant no. RIA208D-2505B), UK MRC (grant no. CCF17-7779 through Bloomsbury SET), the Economic and Social Research Council (grant no. ES/P008011/1), the Bill and Melinda Gates Foundation (grant nos. OPP1084276, OPP1135288, and INV-001754), and the World Health Organization (grant no. 2020/985800-0).

Analysis code and data are available at https://github.com/NickyMcC/CasualAgeMixing.

About the Author

Dr. McCreesh is an assistant professor in Infectious Disease Modelling at the London School of Hygiene and Tropical Medicine. Her research interests include using social contact data and mathematical modelling to understand the transmission patterns of, and inform the control of, tuberculosis and other infectious diseases.

References

1. Prem K, Cook AR, Jit M. Projecting social contact matrices in 152 countries using contact surveys and demographic data. PLOS Comput Biol. 2017;13:e1005697. https://doi.org/10.1371/journal.pcbi.1005697
2. Van Hoang T, Coletti P, Melegaro A, Wallinga J, Grijalva C, Edmunds J, et al. A systematic review of social contact surveys to inform transmission models of close contact infections. Epidemiology. 2019;30:723–36.
3. Raffalli J, Sepkowitz KA, Armstrong D. Community-based outbreaks of tuberculosis. Arch Intern Med. 1996;156:1053–60. https://doi.org/10.1001/archinte.1996.00040041053002
4. Ku C-C, MacPherson P, Khundi M, Nzawa R, Feasey HR, Nliwasa M, et al. Estimated durations of asymptomatic, symptomatic, and care-seeking phases of tuberculosis disease. BMC Med. 2021;19:298. https://doi.org/10.1186/s12916-021-02128-9
5. McCreesh N, White RG. An explanation for the low proportion of tuberculosis that results from transmission between household and known social contacts. Sci Rep. 2018;8:5382. https://doi.org/10.1038/s41598-018-23797-2
6. McCreesh N, Morrow C, Middelkoop K, Wood R, White RG. Estimating age-mixing patterns relevant for the transmission of airborne infections. Epidemics. 2019;28:100339. https://doi.org/10.1016/j.epidem.2019.03.005
7. Wood R, Racow K, Bekker L-G, Morrow C, Middelkoop K, Mark D, et al. Indoor social networks in a South African township: potential contribution of location to tuberculosis

transmission. PLoS One. 2012;7:e39246. https://doi.org/10.1371/journal.pone.0039246
8. Andrews JR, Morrow C, Walensky RP, Wood R. Integrating social contact and environmental data in evaluating tuberculosis transmission in a South African township. J Infect Dis. 2014;210:597–603. https://doi.org/10.1093/infdis/jiu138
9. Wang CC, Prather KA, Sznitman J, Jimenez JL, Lakdawala SS, Tufekci Z, et al. Airborne transmission of respiratory viruses. Science. 2021;373:eabd9149. https://doi.org/10.1126/science.abd9149
10. Cowling BJ, Ip DKM, Fang VJ, Suntarattiwong P, Olsen SJ, Levy J, et al. Aerosol transmission is an important mode of influenza A virus spread. Nat Commun. 2013;4:1935. https://doi.org/10.1038/ncomms2922
11. Ogunjimi B, Hens N, Goeyvaerts N, Aerts M, Van Damme P, Beutels P. Using empirical social contact data to model person to person infectious disease transmission: an illustration for varicella. Math Biosci. 2009;218:80–7. https://doi.org/10.1016/j.mbs.2008.12.009
12. Melegaro A, Jit M, Gay N, Zagheni E, Edmunds WJ. What types of contacts are important for the spread of infections?: using contact survey data to explore European mixing patterns. Epidemics. 2011;3:143–51. https://doi.org/10.1016/j.epidem.2011.04.001
13. Kucharski AJ, Kwok KO, Wei VWI, Cowling BJ, Read JM, Lessler J, et al. The contribution of social behaviour to the transmission of influenza A in a human population. PLoS Pathog. 2014;10:e1004206. https://doi.org/10.1371/journal.ppat.1004206
14. Iozzi F, Trusiano F, Chinazzi M, Billari FC, Zagheni E, Merler S, et al. Little Italy: an agent-based approach to the estimation of contact patterns—fitting predicted matrices to serological data. PLOS Comput Biol. 2010;6:e1001021. https://doi.org/10.1371/journal.pcbi.1001021
15. Kwok KO, Cowling BJ, Wei VW, Wu KM, Read JM, Lessler J, et al. Social contacts and the locations in which they occur as risk factors for influenza infection. Proc Biol Sci. 2014;281:20140709.
16. Li Y, Leung GM, Tang JW, Yang X, Chao CY, Lin JZ, et al. Role of ventilation in airborne transmission of infectious agents in the built environment—a multidisciplinary systematic review. Indoor Air. 2007;17:2–18. https://doi.org/10.1111/j.1600-0668.2006.00445.x
17. Taylor JG, Yates TA, Mthethwa M, Tanser F, Abubakar I, Altamirano H. Measuring ventilation and modelling *M. tuberculosis* transmission in indoor congregate settings, rural KwaZulu-Natal. Int J Tuberc Lung Dis. 2016;20:1155–61. https://doi.org/10.5588/ijtld.16.0085

Address for correspondence: Nicky McCreesh, London School of Hygiene & Tropical Medicine, Keppel St, London WC1E 7HT, UK; email: nicky.mccreesh@lshtm.ac.uk

Importation and Circulation of Vaccine-Derived Poliovirus Serotype 2, Senegal, 2020–2021

Martin Faye, Ousmane Kébé, Boly Diop, NDack Ndiaye, Annick Dosseh, Abdoulaye Sam, Aliou Diallo, Hamet Dia, Jean Pierre Diallo, Ndongo Dia, Davy Evrard Kiori, Ousmane Madiagne Diop, Amadou Alpha Sall, Ousmane Faye

Environmental surveillance for poliovirus is increasingly used in poliovirus eradication efforts as a supplement to acute flaccid paralysis (AFP) surveillance. Environmental surveillance was officially established in 2017 in Senegal, where no poliovirus had been detected since 2010. We tested sewage samples from 2 sites in Dakar monthly for polioviruses. We identified a vaccine-derived poliovirus serotype 2 on January 19, 2021, from a sample collected on December 24, 2020; by December 31, 2021, we had detected 70 vaccine-derived poliovirus serotype 2 isolates circulating in 7 of 14 regions in Senegal. Sources included 18 AFP cases, 20 direct contacts, 17 contacts in the community, and 15 sewage samples. Phylogenetic analysis revealed the circulation of 2 clusters and provided evidence on the virus introduction from Guinea. Because novel oral polio vaccine serotype 2 was used for response activities throughout Senegal, we recommend expanding environmental surveillance into other regions.

Human enteroviruses (HEVs) are ubiquitous and responsible for a spectrum of acute diseases in humans, including aseptic meningitis, encephalitis, acute flaccid paralysis, myocarditis, type 1 diabetes, and neonatal enteroviral sepsis through fecal-oral transmission (*1*,*2*). Belonging to the *Picornaviridae* family, HEVs are classified into 4 species (HEV-A, HEV-B, HEV-C, and HEV-D) covering >116 serotypes, including the polioviruses, members of the HEV-C species, which are divided into 3 serotypes named PV1, PV2, and PV3 (*3*).

Author affiliations: Institut Pasteur de Dakar, Dakar, Senegal (M. Faye, O. Kébé, H. Dia, N. Dia, D.E. Kiori, A.A. Sall, O. Faye); Ministry of Health and Social Actions, Dakar (B. Diop, A. Sam, J.P. Diallo); World Health Organization Inter-Country Support Team for Western Africa, Ouagadougou, Burkina Faso (A. Dosseh); World Health Organization Senegal Country Office, Dakar (A. Diallo); World Health Organization, Geneva, Switzerland (O.M. Diop)

DOI: https://doi.org/10.3201/eid2810.220847

The World Health Organization (WHO) recommended clinical surveillance of polioviruses by investigating cases of acute flaccid paralysis (AFP) in children <15 years of age, an age group considered high risk for infection. The last confirmed wild poliovirus (WPV) case in Senegal was reported in the Kaolack health district; the patient experienced AFP on April 30, 2010. The last supplementary immunization activities using the trivalent oral polio vaccine (OPV) took place in April 2016 in the Dakar region after identification of an ambiguous vaccine-derived poliovirus (VDPV) serotype 2 (aVDPV2) (*4*).

The Global Polio Eradication Initiative (GPEI) has established the testing of environmental or raw sewage samples to detect VDPV and WPV to complement AFP surveillance in children <15 years of age in polio-free countries in Africa (*5*–*7*). The reason for this surveillance is that 99% of poliovirus infections are asymptomatic and therefore not detected by AFP surveillance, but the virus is shed for weeks in the feces of infected persons. Environmental surveillance has played a pivotal role in detecting VDPVs in raw sewage samples and has provided meaningful data on the presence of polioviruses in communities (*7*,*8*). As of October 2021, the GPEI has initiated environmental surveillance in 309 sites from 36 countries (*6*,*9*,*10*), which enabled the identification of polioviruses in sewage and helped WHO to initiate investigations in the communities and confirm an outbreak of VDPV serotype 2 (VDPV2) in a low vaccination coverage area (*11*).

In Senegal, scarce data were collected during 2007–2015 through surveillance projects carried out at Institut Pasteur de Dakar (*12*). In 2017, environmental surveillance for polioviruses was initiated as part of a collaboration between the Prevention Office at the Senegalese Ministry of Health and Social Action (MoHSAS), the Dakar Medical Region, Institut Pasteur de Dakar, the National Office of

Sanitization in Senegal, and WHO. Sewage samples were collected monthly from 2 sites located in the city of Dakar (Khourounar lifting station and Cambérène sewage treatment site). A circulating VDPV2 (cVDPV2) isolate was detected in a sewage sample collected at the Khourounar site on December 24, 2020 (*13*). Data received from the reference sequencing laboratory for polio at the US Centers for Disease Control and Prevention (Atlanta, GA, USA) suggested an introduction of the cVDPV2 from the Ratoma district in Guinea (*13*). This notification alerted the MoHSAS to the occurrence of a poliomyelitis outbreak caused by cVDPV2; investigations were initiated in the communities.

We describe the data from a 7-year AFP and environmental surveillance program in Senegal for early detection of cVDPV2 and provide insights into virus circulation through the country since December 2020. As part of the GPEI, our study did not directly involve human participants but included stool samples and cell-culture isolates from AFP cases collected as part of routine surveillance for polio for public health purposes in Senegal. WHO and the national ethical committee at the Ministry of Health and Social Actions approved and supervised our study, considering all applicable national regulations governing the protection of human subjects. We obtained cleared oral consent from all patients or their parents or relatives.

Methods

Stool Sample Collection

In Senegal, AFP cases are ascertained either by surveillance focal points in medical districts that send notification to the Epidemiologic Surveillance Unit at MoHSAS within 72 hours of identification (*4*). As recommended by WHO, we collected 2 fecal specimens for laboratory investigations ≥24 hours apart and ≤14 days from the onset of paralysis from cases of AFP to identify the causative enterovirus agent. Specimens were tested in the intercountry WHO-accredited laboratory at Institut Pasteur de Dakar. We reported laboratory data from AFP cases in children to MoHSAS and WHO country and African Region (AFRO) offices each week.

Sewage Sample Collection

We collected sewage samples monthly from 2 sites by grab method as described in WHO guidelines for environmental surveillance (*11*,*12*,*14*). In brief, we collected 1 liter of sewage sample using a bucket, with strict compliance to safety requirements. We transferred sewage samples to the laboratory within 2–4 hours under cold chain container maintained at 4°C and transported to the WHO Intercountry Reference Laboratory for Poliomyelitis at Institut Pasteur de Dakar for processing. We reported data to MoHSAS and the WHO country and AFRO offices each week.

Sewage Sample Processing

We processed sewage samples by polyethylene glycol precipitation method as previously described (*11*). We performed virus isolation using 3 flasks (25 cm^2) of L20B and 2 flasks of rhabdomyosarcoma (RD) cell line, in accordance with standard WHO protocols (*15*,*16*). We monitored the inoculated cell lines for development of cytopathic effect (CPE) for 5 days. If CPE appeared in any cell line, we performed cross-passage to the opposite cell line. If no effect appeared, we performed a blind passage in the same cell line and monitored cells for cytopathic effect for 5 additional days. Samples with no CPE in both cell lines, even after the blind passage, were considered negative, whereas RD-positive and L20B-negative samples were classified as nonpolio enterovirus. We classified L20B-positive isolates as suspected poliovirus and subjected them to real-time reverse transcription-PCR using a qScript XLT qPCR Toughmix system kit (Quantabio, https://www.quantabio.com) with the intratypic differentiation kit (version 5.2) as recommended for identification of a poliovirus strain (*17*). The kit included primers for panenterovirus, panpoliovirus (pan-PV), Duplex wild poliovirus type 1 (WPV1), African wild poliovirus type 3 (AFR WPV3), and South Asian wild poliovirus type 3 (SOAS WPV3).

Sequencing

We spotted the PV2-positive isolates on FTA cards and sent to the CDC reference sequencing laboratory for polio. Samples were later processed for high-throughput RNA sequencing; complete sequences of the poliovirus viral protein (VP) 1 genomic region, which contains a major neutralizing antibody binding site, were generated (*18*,*19*). The number of mutations within the VP1 region of the live attenuated OPV strain was determined; genetically divergent VDPV strains had been classified as cVDPV2. In addition, a phylogenetic analysis was conducted to determine the poliovirus sequence most likely related to the virus (*19*).

Phylogenetic Tree Inference

We performed Bayesian phylogenetic analysis for estimation of data quality and selection of the best-

fit nucleotide substitution model using ModelFinder test (*20*) on the IQ-TREE version 1.6.3 web server (http://iqtree.cibiv.univie.ac.at) (*21*). We constructed a maximum-likelihood tree with sequences of VP1 using FastTree version 2.1.7 (*22*) with the best-fit nucleotide substitution model to our sequence dataset. We labeled nodes with local support values, which were computed with the Shimodaira-Hasegawa test (for 5,000 replications, and visualized the topology with FigTree version 1.4.2 (http://tree.bio.ed.ac.uk/software/figtree).

Results

Temporal Distribution of Isolated Enteroviruses

During 2015–2021, we received a total of 2,971 stool samples and 281 sewage samples from the AFP and environmental surveillance in Senegal. The AFP surveillance includes all human specimens (AFP cases, close contacts, and community contacts). No wild or VDPV serotype 1 or 3 were isolated in Senegal during this surveillance period; 1 VDPV2 was isolated from a sewage sample collected on December 24, 2020 and later classified as cVDPV2. In 2021, we identified a total of 79 cVDPV2-positive isolates in 14 laboratory-confirmed sewage samples and 65 stool samples from 18 AFP cases, 20 direct contacts, and 17 contacts in the community. During this 7-year surveillance period, we detected a total of 28 Sabin-like (SL) polioviruses (12 SL1, 2 SL2, and 15 SL3) from AFP surveillance and 63 (21 SL1, 16 SL2 and 26 SL3) from environmental surveillance (Appendix Table, https://wwwnc.cdc.gov/EID/article/28/10/22-0847-App1.pdf). We recorded the highest prevalence of SL polioviruses in 2015–2016, with a total of 17 isolates from AFP surveillance in 2015 and 33 isolates from environmental surveillance in 2016. In addition, we detected 469 nonpolio enterovirus from AFP surveillance and 152 from environmental surveillance. Of interest, the highest number of nonpolio enterovirus isolates, 206, was identified from AFP surveillance in 2021. We detected 12 mixtures from AFP surveillance during 2015–2017 and 7 from environmental surveillance in 2021 (Figure 1). No homotypic mixture has been found. However, from AFP surveillance, we detected 2 trivalent mixtures (SL1+SL2+SL3) in 2015–2016 and detected a total of 10 bivalent mixtures (5 SL1+SL2 and 2 SL1+SL3 in 2015, 2 SL1+SL2 in 2016,

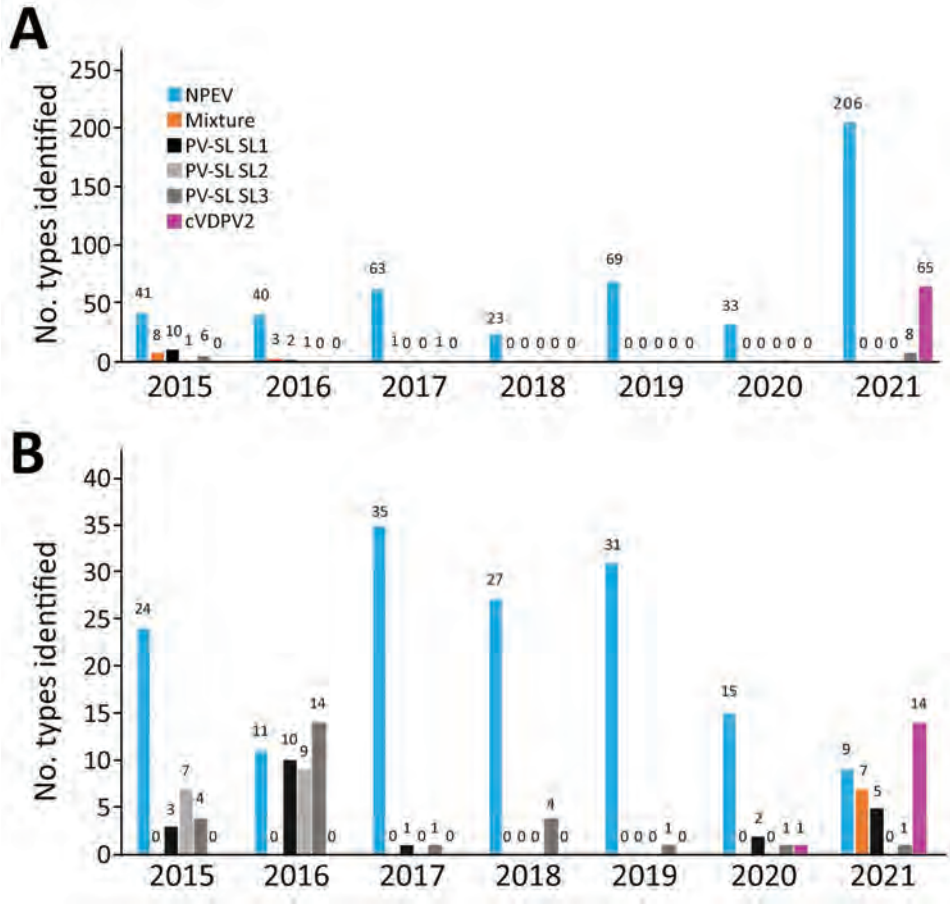

Figure 1. Temporal distribution of enterovirus isolates detected in Senegal during 2015–2021. A) Enteroviruses detected from acute flaccid paralysis surveillance, including all human specimens (cases, close contacts, and community contacts). B) Enteroviruses detected from environmental surveillance. cVDPV2, circulating vaccine-derived poliovirus serotype 2; NPEV, nonpolio enterovirus; PV-SL, Sabin-like poliovirus.

and 1 SL1+SL3 in 2017). Seven bivalent mixtures (5 SL1+cVDPV2, 1 SL1+SL3, and 1 SL3+cVDPV2) were detected from environmental surveillance.

Geographic Distribution of cVDPV2 in Senegal

As of December 31, 2021, a total of 70 cVDPV2 sequences were recorded from Senegal, including 18 AFP cases, 20 direct contacts, 17 contacts in the community, and 15 from sewage samples. One of the positive sewage samples collected in the Dakar region on May 6, 2021, was a mixture of cVDPV2 and VDPV1. The VDPV1 from Senegal has 10 nt differences from the VP1 sequence of Sabin 1 and was not genetically linked to any previously sequenced VDPV1s (data not shown). We identified cVDPV2 in 7 of 14 regions in Senegal: 24 isolates from Diourbel, 17 from Dakar, 11 from Thiès, 8 from Fatick, 6 from Matam, 2 from Louga, and 2 from Kaolack (Appendix Figure).

Phylogenetic Analyses

We submitted sequences to GenBank (accession nos. ON604861–950). The general time-reversible with a gamma distribution of 4 categories rate was the best nucleotide substitution model for our sequences dataset. We inferred maximum-likelihood trees in FastTree version 2.1.7 (*22*); phylogenetic analysis revealed that these new characterized cVDPV2 sequences from Senegal belonged to the NIE-JIS poliovirus lineage, which emerged from Nigeria in 2005 (*23*) and clustered closely with isolates sampled in neighboring countries such as Guinea, The Gambia, and Mauritania in 2021 (Figure 2).

Since its first introduction into Senegal in December 2020, VDPV has separated into 2 phylogenetic clades. Clade 1 comprised only the isolates from Dakar, Thiès, Fatick, Kaolack, and Matam. However, clade 2 comprised sequences from Dakar, Diourbel, Thiès, and Louga and grouped with isolates from Guinea, Mauritania, and The Gambia. Of interest, sequences from Mauritania were related to the isolates from the Thiès region, and sequences from The Gambia were related to the isolates from the Dakar region, whereas the isolates from Guinea emerged before those from the Dakar and Matam regions. The phylogenetic data confirm the epidemiologic data received from the CDC reference sequencing laboratory for polio regarding the introduction of cVDPV2 in Senegal from Guinea and the virus spread from Senegal to The Gambia (Figure 2).

Discussion

WHO has included environmental surveillance as a supplement to AFP surveillance in the strategic plan of the Global Polio Eradication Initiative. Examining sewage samples has been shown to be a more sensitive method to detect low-level circulation of WPV and VDPV; combining this environmental surveillance for polioviruses with enhanced AFP surveillance is expected to support eradication (*7*,*9*).

Excretion of poliovirus may contaminate surface-water sources for drinking water, recreational activities, aquaculture, and irrigation. The amount of virus so excreted can reach 10^7 infectious dose/day/person (*8*); such an environment could lead to reintroduction of poliovirus in certified polio-free areas, especially in population groups with low immunization coverage. Oral poliovirus vaccine strains, VDPV, and even WPV strains may remain infectious for as long as 2 months in sewage depending upon environmental factors, including inactivation by sunlight and high temperatures (*7*,*8*). Circulation of enteroviruses in sewage is a proven indicator of their presence in some communities (*5*,*8*). Environmental surveillance can provide valuable information on virus circulation or reintroduction, particularly in urban populations with no active surveillance (*6*,*7*,*9*).

Since 2017, several genetically-distinct cVDPV2 outbreaks continue to be reported across the WHO AFRO area; the virus emerged in 28 countries in Africa, including Senegal, during January 2020–June 2021 (*24*–*26*). Through GPEI programs, WHO has implemented outbreak response measures in 21 countries, including Senegal, in response to the ongoing cVDPV2 outbreak (*25*).

The detection of cVDPV2 from sewage in Senegal in December 2020 led to a major public health investigation that identified the source as a virus imported from Guinea. Thereafter, the virus was detected in sewage, in the community, and from AFP cases. The epidemiologic data showed that 2 additional independent introductions have been recorded during this 2020–2021 cVDPV2 outbreak and the virus circulated in 7 of the 14 regions in Senegal. The second introduction was reported on February 18, 2021, in the Diourbel region from Mali, and the third one was recorded in August 2, 2021, in the Thiès region from Côte d'Ivoire (*13*). In addition, epidemiologic data showed an evidence of virus spread from the Dakar region in Senegal to The Gambia in June 2021 and Bissau Guinea in October 2021 (data not shown).

Our data demonstrated not only the importance of environmental surveillance to complement AFP surveillance, but also its sensitivity to detect all serotypes of poliovirus, as previously reported (*7*,*27*). Mass vaccination using a vaccine based on the inactivated poliovirus vaccine (*28*) was ruled out as a public-health

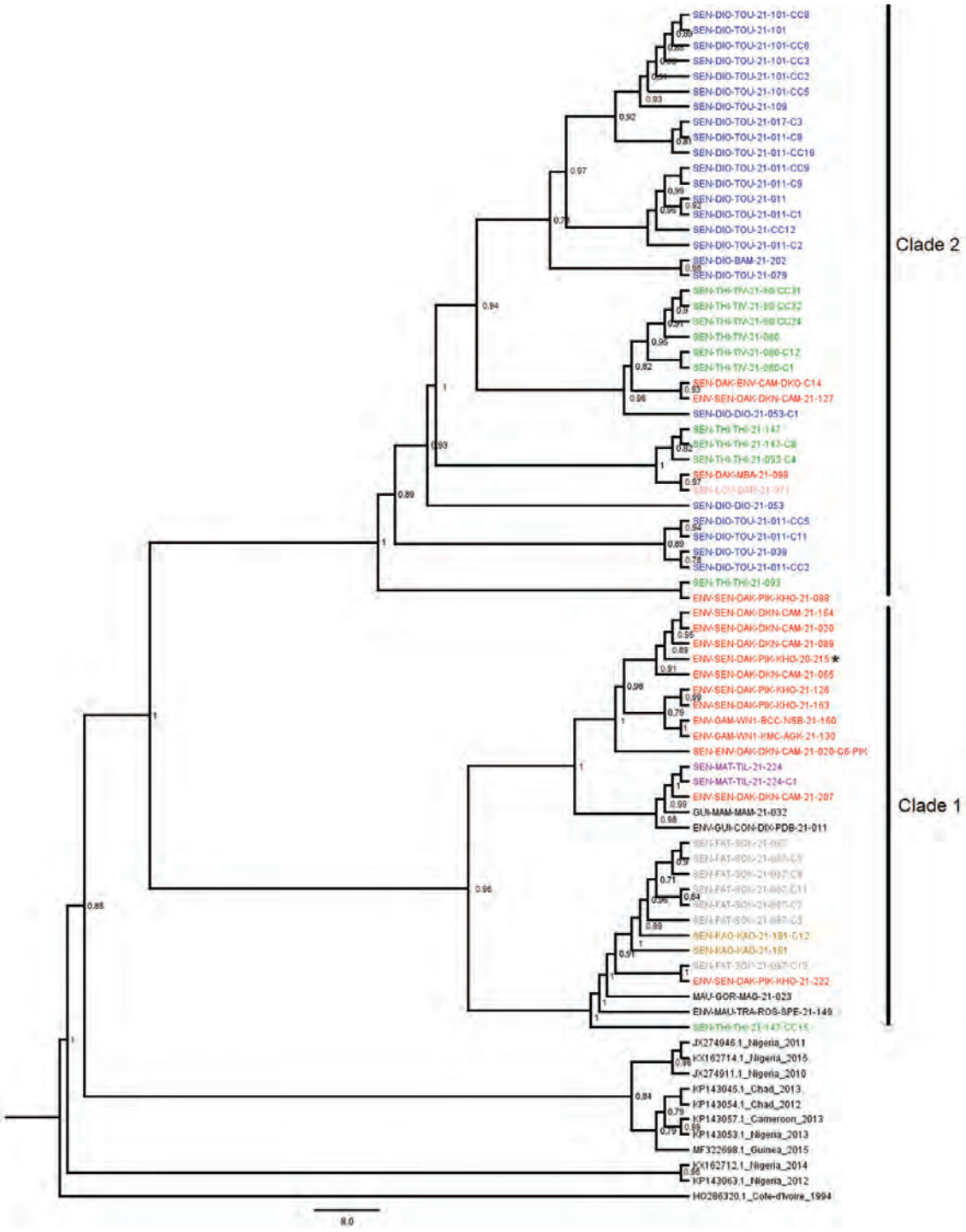

Figure 2. Maximum-likelihood tree based on complete viral protein 1 sequences of cVDPV2 isolates circulating in Senegal during 2020–2021. The tree is midpoint-rooted; nodes are labeled with local support values computed using the Shimodaira-Hasegawa test for 5,000 bootstrap replications. Strain identifiers are designated as follows: SEN-XXX-XXX-21-xxx indicates an isolate from an acute flaccid paralysis (AFP) cases; SEN-XXX-XXX-21-xxx-Cx, close contact of an AFP case; SEN-XXX-XXX-21-xxx-CCxx, community contact of an AFP case; ENV-XXX-XXX-XXX-XXX-21-xxx, isolate from a sewage sample; SEN-ENV-XXX-XXX-XXX-21-Cx-XXX, community contact around a positive environmental site. Isolate names are color-coded as follows: dark blue, new characterized isolates from the Diourbel region (SEN-DIO); green, the Thiès region (SEN-THI); red, the Dakar region (SEN-DAK); pink, the Louga region (SEN-LOU); purple, the Matam region (SEN-MAT); gray, the Fatick region (SEN-FAK); brown, the Kaolack region (SEN-KAO); black, Guinea (GUI), Mauritania (MAU), and The Gambia (GAM), and previous sequences of cVDPV2 from West Africa countries. Asterisk * indicates the first sequence isolated from sewage in Senegal in December 2020. cVDPV2, circulating vaccine-derived poliovirus serotype 2.

response in the Touba district, Diourbel region in June 2021 because no dose of the improved novel oral polio vaccine serotype 2 (nOPV2) was available in the country at that time (*29*). Fortunately, the immunizations done on a smaller scale have highly contributed to reduce the number of confirmed cVDPV2 cases in that region. However, the virus successively emerged in new places including the Dakar, Thiès, Fatick, Kaolack, Louga, and Matam regions; 2 mass vaccination response campaigns based on the nOPV2 that contains a genetically stabilized serotype 2 strain less prone to reversion (*30*) were implemented at country level on December 17–19, 2021, and February 25–29, 2022 (*31*). These 2 mass vaccination response campaigns based on the nOPV2 (*29*) have contributed to interrupt cVDPV2 transmission in Senegal since the last cVDPV2 confirmed contact was identified on November 19, 2021, in the Matam region (*13*). Because serotype 2 immunity could decline in the years following vaccination campaigns, further seroepidemiologic studies would provide a quantitative basis for supporting decisions on the magnitude of future vaccination response when new detections are identified, particularly in countries that do not have environmental surveillance program (*6*).

Environmental surveillance in Senegal is restricted to the Dakar region. The probable silent circulation of these cVDPV2 isolates for several months before the first isolation in Dakar in December 2020 could have been caused by the lack of surveillance in the other 13 regions, which had limitations, such as logistics issues, for sample transportation and difficulty finding convergent sewage effluent from sufficiently large catchment populations. Actions such as increasing the number of sewage collection sites, ensuring regular environmental testing and expanding the testing to other geographic regions, especially those with high incidence of polio circulation, would support investigation of cVDPV2 circulation in Senegal and monitor the rollout of nOPV2 (*6*).

The phylogenetic data have demonstrated virus introduction to Senegal from Guinea, likely caused by population movement across the borders. The virus spread within Senegal could have been caused by the absence of immunity against poliovirus serotype 2 in most children born after the global vaccine switch (*12*). The sequences generated in this study could serve in further phylodynamics studies and could include complete VP1 sequences from more West Africa countries to determine the circulation dynamics of the virus and the number of introduction events in each country during this cDVPV2 outbreak. They could be also useful in analyses targeting the exact period of divergence of these Senegal isolates from their most recent common ancestor. Sequences of cVDPV2 from other neighboring countries such as Mali, Bissau-Guinea, and Côte d'Ivoire are not publicly available at this time.

Because the international spread of VDPV continues to be a public health emergency of international concern, the GPEI should reinforce capacity of countries involved in both clinical and public health functions including surveillance, diagnosis, prevention, treatment, community immunization response, and research and health promotion targeting particularly the immunocompromised children, who can excrete the virus for several months, to limit its global transmission (*32*). Considering the introduction in Malawi and Mozambique of serotype 1 wild poliovirus imported from Pakistan (*33*,*34*), GPEI should implement urgent measures to forestall its spread such as routine immunization for members of the susceptible population who were missed or were only partially protected, to complement routine immunization and regular supplemental immunization activity in polio-free countries to prevent introduction of WPV and minimize the risk of circulating VDPV (*35*,*36*).

Acknowledgments

The authors acknowledge staff involved in the polio surveillance in Senegal, including those involved in the collection and processing of specimens, and coordination by the prevention office at the Senegalese Ministry of Health and Social Actions and the WHO country office and AFRO. We thank colleagues from Guinea, Mauritania, and The Gambia for collection of specimens, and CDC laboratory colleagues at Atlanta for sharing sequencing data.

This research was supported by the WHO AFRO for surveillance of polioviruses in West Africa countries.

About the Author

Dr. Faye is a virologist and the head of the Inter-country Reference Center for Poliomyelitis at the Institut Pasteur de Dakar, Senegal. His primary research interests include infectious disease epidemiology and public-health microbiology.

References

1. Pallansch M, Roos R. Enteroviruses: polioviruses, coxsackieviruses, echoviruses, and newer enteroviruses. In: Knipe DM, Howley PM, Griffin DE, Lamb RA, Martin MA, Roizman B, editors. Fields virology, 5th edition. Philadelphia: Lippincott Williams & Wilkins; 2007. p. 839–93.
2. Khetsuriani N, Parashar UD. Enteric viral infections. In: Dale DC, Federman DD, editors. Scientific American medicine. New York: Web MD, Inc.; 2003. p. 1758–66.

3. Walker PJ, Siddell SG, Lefkowitz EJ, Mushegian AR, Adriaenssens EM, Alfenas-Zerbini P, et al. Changes to virus taxonomy and to the International Code of Virus Classification and Nomenclature ratified by the International Committee on Taxonomy of Viruses (2021). Arch Virol. 2021;166:2633–48. https://doi.org/10.1007/s00705-021-05156-1
4. The Senegalese Ministry of Health and Social Action (MoHSAS): Technical guide for integrated disease monitoring of disease and response [In French]. June 2018 [cited 2021 Dec 28]. https://www.sante.gouv.sn/sites/default/files/gudie%20national%20de%20la%20surveillance_1.pdf
5. Gast C, Bandyopadhyay AS, Sáez-Llorens X, De Leon T, DeAntonio R, , Jimeno J, et al. Fecal shedding of 2 novel live attenuated oral poliovirus type 2 vaccine candidates by healthy infants administered bivalent oral poliovirus vaccine/inactivated poliovirus vaccine: 2 randomized clinical trials. J Infect Dis. 2021 [Epub 2021 Oct 5]. https://doi.org/10.1093/infdis/jiab507
6. Gumede N, Okeibunor J, Diop O, Baba M, Barnor J, Mbaye S, et al. Progress on the implementation of environmental surveillance in the African Region, 2011–2016. J Immunol Sci. 2018;:24–30.
7. Fischer TK, Simmonds P, Harvala H. The importance of enterovirus surveillance in a post-polio world. Lancet Infect Dis. 2022;22:e35–40. https://doi.org/10.1016/S1473-3099(20)30852-5
8. Pethani AS, Kazi Z, Nayyar U, Shafiq-Ur-Rehman M, Yousafzai MT, Ondrej M, et al. Poliovirus excretion among children with primary immune deficiency in Pakistan: a pilot surveillance study protocol. BMJ Open. 2021;11:e045904. https://doi.org/10.1136/bmjopen-2020-045904
9. Gardner TJ, Diop OM, Jorba J, Chavan S, Ahmed J, Anand A. Surveillance to track progress toward polio eradication—worldwide, 2016–2017. MMWR Morb Mortal Wkly Rep. 2018;67:418–23. https://doi.org/10.15585/mmwr.mm6714a3
10. Jorba J, Diop OM, Iber J, Henderson E, Zhao K, Quddus A, et al. Update on vaccine-derived poliovirus outbreaks—worldwide, January 2018–June 2019. MMWR Morb Mortal Wkly Rep. 2019;68:1024–8. https://doi.org/10.15585/mmwr.mm6845a4
11. World Health Organization. Guidelines for environmental surveillance of poliovirus circulation. WHO/V&B/03.03. 2003 [cited 2021 Dec 28]. https://apps.who.int/iris/handle/10665/67854
12. Ndiaye AK, Diop PAM, Diop OM. Environmental surveillance of poliovirus and non-polio enterovirus in urban sewage in Dakar, Senegal (2007–2013). Pan Afr Med J. 2014;19:243. https://doi.org/10.11604/pamj.2014.19.243.3538
13. World Health Organization. Country office in Senegal: Senegal—virus tracking 2021–2022. Weekly report number 16: April 19, 2022. Dakar: The Organization; 2022.
14. WHO/Module3-Polio. Surveillance guide for vaccine-preventable diseases in the WHO South-East Asia Region [cited 2021 Oct 24]. https://apps.who.int/iris/handle/10665/277459
15. Kaundal N, Sarkate P, Prakash C, Rishi N. Environmental surveillance of polioviruses with special reference to L20B cell line. Virusdisease. 2017;28:383–9. https://doi.org/10.1007/s13337-017-0409-1
16. World Health Organization. Polio Laboratory Manual. Website Department of Vaccines and Biologicals 2004 [cited 2021 Dec 12]. https://apps.who.int/iris/handle/10665/68762
17. Kilpatrick DR, Yang CF, Ching K, Vincent A, Iber J, Campagnoli R, et al. Rapid group-, serotype-, and vaccine strain-specific identification of poliovirus isolates by real-time reverse transcription-PCR using degenerate primers and probes containing deoxyinosine residues. J Clin Microbiol. 2009;47:1939–41. https://doi.org/10.1128/JCM.00702-09
18. Yang CF, Naguib T, Yang SJ, Nasr E, Jorba J, Ahmed N, et al. Circulation of endemic type 2 vaccine-derived poliovirus in Egypt from 1983 to 1993. J Virol. 2003;77:8366–77. https://doi.org/10.1128/JVI.77.15.8366-8377.2003
19. Stewardson AJ, Roberts JA, Beckett CL, Prime HT, Loh PS, Thorley BR, et al. Imported case of poliomyelitis, Melbourne, Australia, 2007. Emerg Infect Dis. 2009;15:63–5. https://doi.org/10.3201/eid1501.080791
20. Kalyaanamoorthy S, Minh BQ, Wong TKF, von Haeseler A, Jermiin LS. ModelFinder: fast model selection for accurate phylogenetic estimates. Nat Methods. 2017;14:587–9. https://doi.org/10.1038/nmeth.4285
21. Trifinopoulos J, Nguyen LT, von Haeseler A, Minh BQ. W-IQ-TREE: a fast online phylogenetic tool for maximum likelihood analysis. Nucleic Acids Res. 2016;44(W1):W232–5. https://doi.org/10.1093/nar/gkw256
22. Price MN, Dehal PS, Arkin AP. FastTree 2—approximately maximum-likelihood trees for large alignments. PLoS One. 2010;5:e9490. https://doi.org/10.1371/journal.pone.0009490
23. Burns CC, Shaw J, Jorba J, Bukbuk D, Adu F, Gumede N, et al. Multiple independent emergences of type 2 vaccine-derived polioviruses during a large outbreak in northern Nigeria. J Virol. 2013;87:4907–22. https://doi.org/10.1128/JVI.02954-12
24. World Health Organization (WHO). Circulating vaccine-derived poliovirus type 2—global update. 26 March 2021 [cited 2021 Oct 28]. https://www.who.int/emergencies/disease-outbreak-news/item/circulating-vaccine-derived-poliovirus-type-2-global-update
25. Global Polio Eradication Initiative. Circulating vaccine-derived polioviruses [cited 2021 Nov 2]. https://polioeradication.org/polio-today/polio-now/this-week/circulating-vaccine-derived-poliovirus
26. Alleman MM, Jorba J, Henderson E, Diop OM, Shaukat S, Traoré MA, et al. Update on vaccine-derived poliovirus outbreaks—worldwide, January 2020–June 2021. MMWR Morb Mortal Wkly Rep. 2021;70:1691–9. https://doi.org/10.15585/mmwr.mm7049a1
27. Maes EF, Diop OM, Jorba J, Chavan S, Tangermann RH, Wassilak SG. Surveillance systems to track progress toward polio eradication—worldwide, 2015–2016. MMWR Morb Mortal Wkly Rep. 2017;66:359–65. https://doi.org/10.15585/mmwr.mm6613a3
28. John J, Giri S, Karthikeyan AS, Iturriza-Gomara M, Muliyil J, Abraham A, et al. Effect of a single inactivated poliovirus vaccine dose on intestinal immunity against poliovirus in children previously given oral vaccine: an open-label, randomised controlled trial. Lancet. 2014; 384:1505–12. https://doi.org/10.1016/S0140-6736(14)60934-X
29. Global Polio Eradication Initiative. Novel oral polio vaccine type 2 (nOPV2) granted EUL recommendation. 2020 [cited 2022 Feb 2]. https://polioeradication.org/news-post/novel-oral-polio-vaccine-type-2-nopv2-granted-interim-emergency-use-listing-recommendation
30. Van Damme P, De Coster I, Bandyopadhyay AS, Revets H, Withanage K, De Smedt P, et al. The safety and immunogenicity of two novel live attenuated monovalent

(serotype 2) oral poliovirus vaccines in healthy adults: a double-blind, single-centre phase 1 study. Lancet. 2019; 394:148–58. https://doi.org/10.1016/S0140-6736(19)31279-6
31. UNICEF. Kicking polio out of Senegal. 2022 Feb 2 [cited 2022 Aug 30]. https://www.unicef.org/senegal/recits/bouter-la-polio-hors-du-s%C3%A9n%C3%A9gal.
32. Gumede N, Coulibaly SO, Yahaya AA, Ndihokubwayo JB, Nsubuga P, Okeibunor J, et al. Polio Eradication Initiative (PEI) contribution in strengthening public health laboratories systems in the African region. Vaccine. 2016;34:5164–9. https://doi.org/10.1016/j.vaccine.2016.05.055
33. World Health Organization Africa. Malawi declares polio outbreak. 17 February 2022 [cited 2022 Feb 18]. https://www.afro.who.int/news/malawi-declares-polio-outbreak
34. Global Polio Eradication Initiative. This week: 18 May 2022 [cited 2022 May 20]. https://polioeradication.org/polio-today/polio-now/this-week
35. Mohammed A, Tomori O, Nkengasong JN. Lessons from the elimination of poliomyelitis in Africa. Nat Rev Immunol. 2021;21:823–8. https://doi.org/10.1038/s41577-021-00640-w
36. Deressa W, Kayembe P, Neel AH, Mafuta E, Seme A, Alonge O.Lessons learned from the polio eradication initiative in the Democratic Republic of Congo and Ethiopia: analysis of implementation barriers and strategies. BMC Public Health. 2020;20(Suppl 4):1807. https://doi.org/10.1186/s12889-020-09879-9

Address for correspondence: Martin Faye, Virology Department, Institut Pasteur de Dakar, 36 Avenue Pasteur, 220 Dakar, Senegal; email: martin.faye@pasteur.sn

Shortening Duration of Swine Exhibitions to Reduce Risk for Zoonotic Transmission of Influenza A Virus

Dillon S. McBride, Jacqueline M. Nolting, Sarah W. Nelson, Michele M. Spurck, Nola T. Bliss, Eben Kenah, Susan C. Trock, Andrew S. Bowman

Reducing zoonotic influenza A virus (IAV) risk in the United States necessitates mitigation of IAV in exhibition swine. We evaluated the effectiveness of shortening swine exhibitions to ≤72 hours to reduce IAV risk. We longitudinally sampled every pig daily for the full duration of 16 county fairs during 2014–2015 (39,768 nasal wipes from 6,768 pigs). In addition, we estimated IAV prevalence at 195 fairs during 2018–2019 to test the hypothesis that ≤72-hour swine exhibitions would have lower IAV prevalence. In both studies, we found that shortening duration drastically reduces IAV prevalence in exhibition swine at county fairs. Reduction of viral load in the barn within a county fair is critical to reduce the risk for interspecies IAV transmission and pandemic potential. Therefore, we encourage fair organizers to shorten swine shows to protect the health of both animals and humans.

Swine are critical hosts for influenza A viruses (IAV) because they can be co-infected with IAV from multiple host species (*1*). Swine also have close proximity with humans through agricultural interfaces, making them a focus as a reassortment vessel for IAV with pandemic potential (*1*,*2*). The origin of the 2009 influenza A(H1N1) pandemic is attributed to North American swine, highlighting the effect of this host species on novel IAV emergence (*3*–*5*).

Swine-origin IAV that infects humans, also known as variant IAV, is reportable to the Centers for Disease Control and Prevention in the United States. Since 2011, >475 confirmed variant IAV cases have been reported in the United States (*6*). Most of these variant cases have reported swine contact at agricultural fairs before infection (*7*–*13*). At local county fairs, hundreds of pigs may commingle in the same barn for >1 week. When only a few pigs arrive at the fair infected with IAV, ample time has passed by the end of the fair for viral amplification, and we detected very high prevalence in the swine (*14*,*15*). The time afforded for infection to spread throughout exhibition swine within a single fair, probably drives the high viral load in the barn, which can increase the risk for zoonosis.

In the United States, although commercial swine operations often have a higher level of biosecurity than their exhibition swine counterparts, diverse lineages of IAV originating from commercial swine are annually found in exhibition swine (*16*,*17*). These viruses move with the exhibition swine as they travel within complex networks of shows across the country (*13*,*18*). This commingling with hundreds to thousands of other pigs leads to viral reassortment, dissemination, and ultimately interspecies transmission of IAV (*13*,*18*). This system provides a unique human–animal interface as a conduit for zoonotic emergence of IAV.

Variant cases of IAV are most often reported in association with fairs that have very high IAV prevalence within their exhibition swine population (*8*,*9*). Accordingly, zoonotic transmission mitigation strategies should target reduction of IAV prevalence in swine. Previous risk assessment for IAV mitigation at agricultural fairs had shown that exhibitions with >200 pigs had a greater risk for having IAV-positive pigs; therefore, fewer pigs commingling in the barn together at any one time was hypothesized to decrease the prevalence of viral shedding, but few other risk factors were identified (*19*).

Author affiliations: The Ohio State University, Columbus, Ohio, USA (D.S. McBride, J.M. Nolting, S.W. Nelson, M.M. Spurck, N.T. Bliss, E. Kenah, A.S. Bowman); Centers for Disease Control and Prevention, Atlanta, Georgia, USA (S.C. Trock)

DOI: https://doi.org/10.3201/eid2810.220649

In an effort to prevent zoonotic transmission from occurring between swine and humans at agricultural exhibitions, the Swine Exhibitions Zoonotic Influenza Working Group, consisting of animal and public health officials, drafted Measures to Minimize Influenza Transmission at Swine Exhibitions, 2013 (*20*), which has been updated in subsequent years. The measures are divided into practices for use by exhibition organizers and exhibitors before, during, and after the swine exhibition period. Those measures include, but are not limited to, becoming familiar with clinical signs of illness in both pigs and humans, reporting observed clinical signs to the proper authorities, practicing common hygiene practices (e.g., handwashing), using a 7-day downtime between swine exhibitions, and shortening the duration of exhibitions to 72 hours. Recommendations, including the 72-hour recommendation, had been outlined previously by the Indiana State Board of Animal Health (*21*). Although those practices are based on common public and animal health theories, most of the measures were not based on existing scientific evidence for preventing swine-to-human IAV transmission.

We sought to evaluate the recommendation to limit swine exhibitions to ≤72 hours. During 2014 and 2015, we conducted daily IAV testing at 8 agricultural fairs in the United States, in which we sampled all exhibition swine every day to measure changes in prevalence longitudinally during the exhibitions. We then evaluated IAV in swine at agricultural fairs that had implemented the shortened, 72-hour recommendation for swine exhibitions compared with fairs that did not during 2018 and 2019.

Materials and Methods

Longitudinal Study (2014 and 2015)

We enrolled 8 agricultural fairs (4 in Ohio and 4 in Indiana) to participate in the study on the basis of 3 factors: >350 swine typically being exhibited; previous IAV recovery in pigs, humans, or both associated with the exhibition; and the fair organizer's willingness to participate. Investigators coordinated with each fair organizer to determine the most accommodating schedule to collect samples at 24-hour intervals. The sample collection start time varied across the exhibitions in relation to hours after arrival of swine.

We collected nasal wipes from swine as previously described and in accordance with The Ohio State University Institutional Animal Care and Use Committee protocol (no. 2009A0134) (*22*,*23*). We recorded individual pig identification numbers. Origin time for each fair corresponds with the first time pigs could be identified, were required to be in place in the swine barn, or both. Four of the sampled fair events (fairs A and B in 2014 and 2015) included a weigh-in event shortly after the swine arrived on the fairgrounds. Origin time for those fairs is the weigh-in time and for all other fairs is the arrival deadline for swine. We preserved samples on dry ice for transportation to the laboratory, where we kept them in long-term storage at −80°C.

We screened samples collected from the first and last days of the exhibitions with real-time reverse transcription PCR (rRT-PCR). We used MagBind Viral DNA/RNA (Omega Bio-Tek, Norcross, https://www.omegabiotek.com) according to manufacturer's protocol for RNA extraction. We also used DiaControlRNA (Diagenode Diagnostics, https://www.diagenodediagnostics.com) as an internal positive control to ensure validity of our extraction and PCR. We used National Veterinary Services Laboratory PCR primer protocol (no. SOP-BPA-9034.04) with SuperScript One-Step RT-PCR (Invitrogen, https://www.thermofisher.com) according to the manufacturer's protocol. If samples collected on the first or last days of the fair were positive for IAV, we screened all remaining samples by using the same technique. We completed virus isolation attempts on select rRT-PCR–positive samples collected on the first and last day of individual exhibitions, as previously described (*14*). Any fairs from which we were not able to isolate any IAV in MDCK cell culture we considered to be negative.

One fair (2015 D) had 5 rRT-PCR–positive samples, none of which resulted in successful culture of IAV. We attributed these rRT-PCR positives to probably be carryover from previous infection or contamination from home-farm environment and not reflective of a productive IAV infection in the pigs at that fair.

We calculated the estimated hazard of IAV infection by using the time from the origin of each fair until the detection of IAV infection or censoring in each pig. We did not consider swine to be at risk until the first sampling after weigh-in for fairs that included a weigh-in as described previously. For each fair, we smoothed the increments of the Nelson–Aalen cumulative hazard estimate by using an Epanechnikov kernel function, which is the default in Stata version 14 (StataCorp LLC, https://www.stata.com).

72-hour Recommendation (2018 and 2019)

After our longitudinal study in 2014 and 2015, some fairs began to adopt the recommendation to reduce swine shows to ≤72 hours. As a part of our ongoing

surveillance program in 2018 and 2019, we collected ≥20 nasal samples per fair as described previously (*15*,*22*). We collected samples from exhibition swine at 195 individual fair events on the last day of the fair and selected pigs for sampling to evenly represent all spatial areas of the barn. This sampling scheme was designed to maximize detection of any IAV present in exhibition swine, which primarily have subclinical infections (*15*). We tested samples for IAV with the VetMAX-Gold SIV Detection rRT-PCR Kit (Life Technologies, https://www.thermofisher.com) and conducted virus isolation (MDCK cells) to estimate prevalence at each fair as previously described (*18*). We used virus isolation to estimate prevalence at these fairs because we expected it to reflect animals actively shedding IAV, which is the risk factor of concern regarding interspecies transmission. We calculated swine exhibition duration on the basis of the number of days between arrival and our sample collection. We classified levels of implementation into 3 categories: fairs that did not reduce duration to ≤72 hours, fairs that released any portion of their pigs at ≤72 hours, and fairs that released or sold all swine before 72 hours. To evaluate differences in IAV prevalence between the different 72-hour implementation categories, we used a Kruskal–Wallis test followed by Dunn's test for pairwise comparisons, applying the Benjamini–Hochberg method to control the false-discovery rate. We used Stata version 14.2 for statistical analyses.

Results

Longitudinal Surveillance within Fairs

During 2014 and 2015, we collected 39,768 nasal wipes from 6,768 individual pigs exhibited at 8 agricultural fairs (16 total fair events) (Table 1). We collected samples from all pigs present on each day of the fair; however, not all pigs remain present for the full duration of the fair. Many pigs were removed before the formal end of the fair, resulting in fewer pigs still at the fair on the last day compared with the beginning (Appendix Table 1, https://wwwnc.cdc.gov/EID/article/28/10/22-0649-App1.pdf). On the basis of fair structure, we expected this right censoring would be unrelated to health status of individual pigs.

We recovered IAV isolates from swine at 4 fairs in 2014 and 2 fairs in 2015, for a total of 6 IAV–positive fair events, at which we collected 15,162 samples; of those, 2,514 (16.6%) tested positive for IAV by rRT-PCR across all sampling times. Examining the rRT-PCR prevalence at each fair over time, we observed a clear increasing trend, providing strong evidence that these fair events had active IAV outbreaks ongoing in the exhibition swine population (Figure 1). IAV prevalence in all 6 fairs was relatively low through the first several 24-hour timepoints but increased dramatically by the end of the fair events as the outbreak spread throughout the swine barn. The exception to this trend was fair 2014 E. Although fair 2014 E did have an increasing trend in prevalence, it ended with only 6 rRT-PCR–positive samples of the 309 collected on the last day.

By the end of fair 2014 B, we observed the highest IAV prevalences, 98.7% by rRT-PCR and 77.5% by virus isolation (Figure 1; Appendix Table 1). Also at fair 2014 B, using rRT-PCR, we detected IAV in only 16 (3.8%) of samples 15 hours after arrival at the second sampling, which highlights how critical the duration of swine shows can be as a factor in an IAV outbreak at any individual county fair. As expected in a growing outbreak, the estimated hazard increased with time (Figure 2). Visible in the increasing prevalence (Figure 1) and hazard estimates (Figure 2), very little leveling off occurred. The risk for IAV infection in swine continued to rise throughout the duration of the fairs. Given enough time, we

Table 1. Longitudinal sampling efforts of swine at 16 agricultural fairs included in study of IAV transmission, Ohio and Indiana, USA, 2014 and 2015*

	2014			2015		
Fair	No. swine exhibited at fair	No. samples collected	HA–NA subtypes	No. swine exhibited at fair	No. samples collected	HA–NA subtypes
Fair A	377	1,927	H1N1, H3N2, mixed	400	2,092	H1N2, H3N2, mixed
Fair B	424	2,741	H1N1, H3N2, mixed	414	2,719	H3N2
Fair C	274	1,200	Negative	281	1,233	Negative
Fair D	367	2,858	Negative	349	2,732	Negative
Fair E	465	2,568	H1N1	434	2,525	Negative
Fair F	286	1,339	Negative	325	2,099	Negative
Fair G	597	3,813	Negative	659	3,258	Negative
Fair H	523	3,115	H3N2	593	3,549	Negative
Total	3,313	19,561		3,455	20,207	

*The number of swine exhibited at fair refers to the total number of individual pigs enrolled in the study. The number of samples collected is the total number of nasal wipes collected during the entire fair. The HA-NA subtypes we isolated are included for the IAV-positive fairs. HA, hemagglutinin; IAV, influenza A virus; NA, neuraminidase.

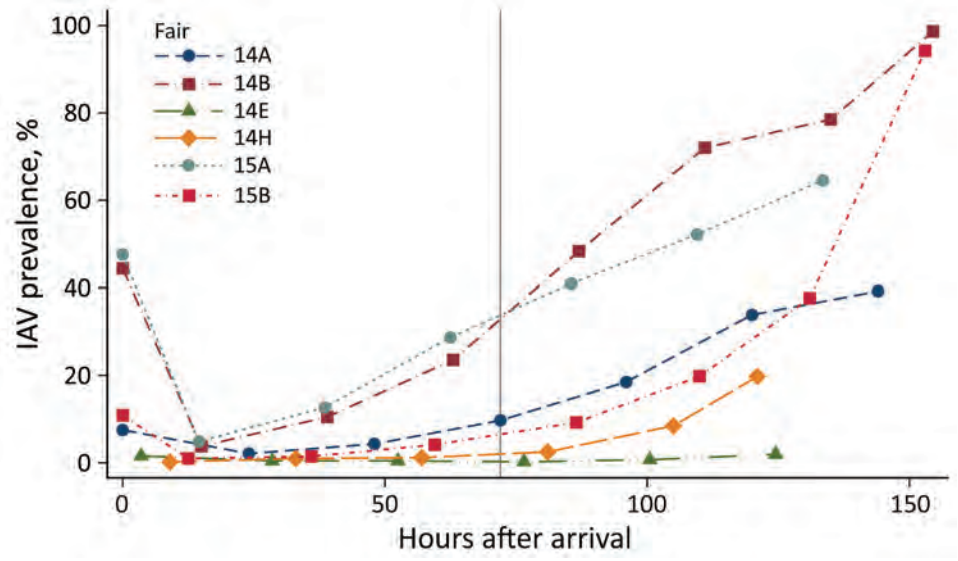

Figure 1. Percentage of pigs that tested positive for IAV by real-time reverse transcription PCR at 6 IAV-positive agricultural fairs, Ohio and Indiana, USA, 2014 and 2015. Each data point represents the prevalence at that sampling timepoint connected with colored lines to indicate trend over time for each individual fair. IAV prevalence rises steeply through the latter half of each fair, indicating the strong role of lengthy show duration in increased viral amplification in each swine population. The reference line shows the recommended 72-hour cutoff for swine show duration. IAV, influenza A virus.

found that most of the swine at a fair become infected with IAV, resulting in high viral load within the barn that could lead to zoonotic transmission to humans. These data provide strong support for the recommendation to limit the amount of time swine spend at a fair to curtail the interspecies transmission of IAV at county fairs.

Acceptance of the 72-hour Limitation

We collected surveillance samples from 195 county fairs during the summers of 2018 and 2019. Based on the date of entry for swine, 144 of those fairs had not released swine before 72 hours. We sampled 38 fairs whose organizers stated that they released a portion of their swine before 72 hours onsite. In addition, 13 of the fairs at which we sampled had fully implemented the 72-hour recommendation and released all of their swine in ≤72 hours. Although the recommendation to shorten swine exhibitions had been around for ≥5 years, the adoption of this recommendation was still quite limited at the county fairs at which we collected samples. We compiled and categorized additional characteristics for the 195 county fairs sampled, including state, size, month, and IAV vaccine requirement (Appendix Table 2).

Among 2018 and 2019 county fairs that tested positive for IAV, those that did not apply the 72-hour recommendation had the highest average estimated prevalence (Table 2). The overall Kruskal–Wallis test ($p = 0.0425$) indicated that estimated prevalence is not the same across fairs that applied the 72-hour recommendation at the 3 different levels. Pairwise tests revealed that fairs that released all pigs before 72 hours had significantly lower prevalence estimates compared with fairs that did not release any pigs ($p = 0.0176$) (Table 2). Although fairs that released some

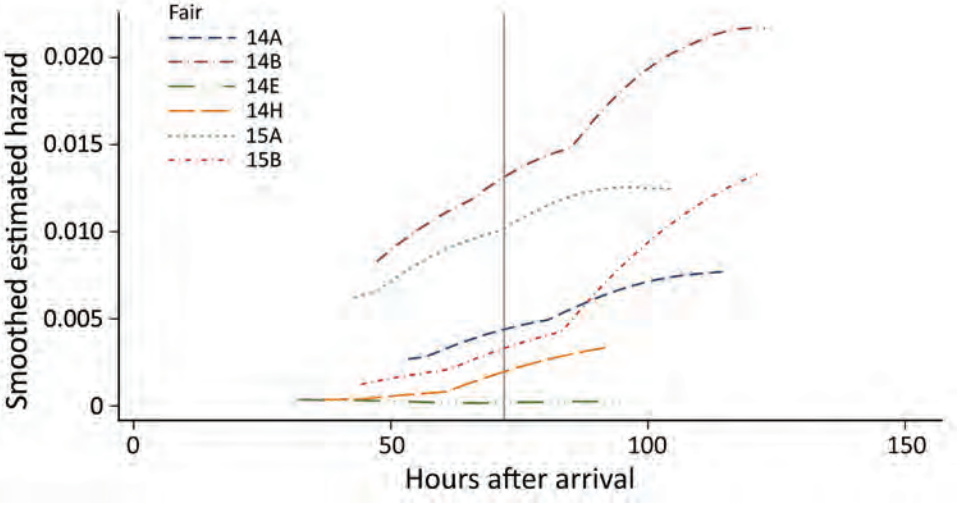

Figure 2. Estimated smoothed hazard of IAV infection over the number of hours since the origin of the fair for individual pigs at risk at 6 IAV-positive agricultural fairs, Ohio and Indiana, USA, 2014 and 2015. All 6 IAV-positive fairs from our longitudinal study are shown individually. Overall, hazard estimates increase throughout the duration of the fair. The exceptionally low hazards for fair 14E correspond to the low incidence of IAV documented in Figure 1 and Appendix Table 1

Table 2. Number of county fairs sampled and number of fairs with swine testing positive for IAV, by categorical level at which the 72-hour recommendation was implemented, Ohio, Indiana, and Michigan, USA, 2018 and 2019*

Categorical level of implementation of 72-hour recommendation	Total no. fairs	No. IAV-positive fairs	Mean estimated IAV prevalence, %†	p value‡
No implementation	144	26	40.9	Referent
Some swine released	38	10	33.2	0.3346
All swine released	13	3	6.1	0.0176

*Number of county fairs sampled and number of fairs that tested IAV-positive in 2018 and 2019 are shown by the categorical level at which the 72-hour recommendation was implemented. IAV, influenza A virus.
†Mean estimated IAV prevalence among the IAV-positive county fairs was estimated by using virus isolation data.
‡By Dunn's test. Pairwise comparisons were completed by using "no implementation" as the reference category.

pigs before 72 hours had lower prevalence estimates on average, we did not detect a significant difference between those fairs and fairs that did not release any pigs early (p = 0.3346) (Table 2). In addition, the only other fair characteristic found to be associated with IAV prevalence among IAV-positive fairs was that Indiana fairs had lower IAV prevalence compared with those in Ohio (Appendix Table 3).

Discussion

Through 2 active IAV field surveillance efforts, we found strong evidence that shortening the duration of swine exhibitions greatly reduces IAV prevalence in swine. In our longitudinal study sampling every pig every day, the IAV prevalence and hazard estimate at each IAV-positive fair rose consistently with increasing time at the fair, as we expected in the case of a growing infectious disease outbreak. Accordingly, if fairs had shortened their swine exhibitions, the maximum prevalence by the end of the fair would have been greatly reduced. For example, fair 2014 H and fair 2015 B displayed relatively parallel growth curves (Figure 1), and both had a PCR prevalence of 19.8% at the sixth sampling interval (121 hours after arrival at fair 2014 H and 110 hours after arrival at fair 2015 B). A critical difference between the 2 fairs, however, is that 2014 H ended after that sampling, resulting in the second-lowest end-of-fair prevalence in our study. In stark contrast, 2015 B had pigs on site through 153 hours and ended with 94.2% IAV PCR prevalence, the study's second-highest peak prevalence. Despite a rise in IAV-positive samples through the first 6 days, in ending ≈2 days earlier, IAV prevalence at 2014 H never exceeded 20%, greatly reducing the viral load in the barn at the end of the fair and reducing the risk for zoonotic transmission.

Among the 6 fairs that tested IAV-positive, we found considerable variation in the rate at which the outbreaks grew. Only fair 2014 E maintained very low IAV prevalence, never exceeding 2% prevalence. The reason this fair's prevalence remained so low compared with the other IAV-positive shows is unclear, but identification of management practices within fairs that can effectively flatten IAV spread in the swine barn should be an area of ongoing research. Reducing the transmission rate of IAV within fairs is a mitigation strategy for keeping IAV prevalence low, in addition to reducing the duration of fairs. A previous survey of swine exhibitors at jackpot shows found that most of those exhibitors supported many of the recommendations to minimize IAV risk (*24*). However, an advantage of mitigation measures like the 72-hour cutoff is that they can be applied at the fair level and do not require individual exhibitor compliance. For example, the effectiveness of the recommendation to not show any pigs with clinical signs of IAV infection is highly dependent on individual exhibitor education, awareness, and acceptance. As a result, we expect that, to varying degrees, pigs are likely to arrive infected with IAV (*14*). Therefore, recommendations that limit spread of IAV once it has been introduced to a county fair and can be put in place by fair organizers is a critical step toward reducing IAV prevalence in swine and the risk for zoonotic transmission of IAV.

Another control measure commonly recommended is vaccinating swine against IAV. Fair B tested positive in both 2014 and 2015 and had extraordinarily high peak IAV prevalence (98.7% in 2015 and 94.2% in 2015). Despite similarly high viral loads by the end, in 2015 the growth curve was flatter, crossing the 72-hour threshold at <10% IAV prevalence compared with >30% in 2014. In 2015, fair B added a required influenza vaccine for swine. Although we can only speculate as to whether the slower spread was attributable to vaccination, this finding would be consistent with previous work demonstrating that vaccination against IAV resulted in a shorter period of virus shedding and lower peak nasal titers in swine challenged with a heterologous IAV (*25*). Combining vaccination against IAV with reduced show duration could prove to be highly effective in reducing the risk for zoonotic transmission of IAV.

In all 4 fair events with a weigh-in upon arrival, the first sampling timepoint had a much higher PCR prevalence than did the second timepoint. Infected swine deposit IAV onto shared surfaces during these weigh-in events, which can lead to mass exposure of

noninfected swine as they arrive (*26*). Because the nasal wipe samples primarily collected nasal secretions from the exterior of the nostrils, we detected numerous contaminations through PCR upon first sampling. It is improbable that all of those swine were actively shedding IAV while arriving at the fair, especially considering the drastic drop in prevalence for the following days, when we sampled the same pigs at their individual pens in the barn. However, this pattern illustrates that ≥50% of the pigs at some fairs are exposed to IAV almost immediately after arrival. In these cases, ending the fair before 72 hours is not necessarily preventing IAV infection in exposed pigs. Rather, by not affording ample time for infection and amplification, the shortening eliminates the concentration of swine at the fair and thereby does not expose fairgoers to the high IAV viral load that could be present if the pigs remained in the barn. In addition to shortening the time pigs are at the fair, we recommend that fair organizers alter the structure of their weigh-in events to reduce infectious disease transmission. In addition to the washing and disinfecting procedures previously recommended (*26*), using owner-declared pig weights or open scales available for use in the barn over longer periods of time could also limit the effect of weigh-in on IAV transmission.

In our investigation in 2018 and 2019, we found extremely limited implementation of the 72-hour rule. We detected IAV at only 3 county fairs that had fully implemented the 72-hour rule in 2018 and 2019, which reduced our statistical power to detect differences. However, the downward trend in prevalence at fairs that release swine before 72 hours (Table 2) provides strong evidence that the recommendation results in fewer swine actively shedding IAV by the end of a fair and therefore reduces the risk for zoonotic IAV transmission. Although we saw a dramatic decrease in IAV prevalence for the 3 IAV-positive fairs that released all swine before 72 hours, the effect was less pronounced and not statistically significant for the 10 fairs that only released some pigs. We did not have enough IAV-positive fairs in this sample to build a model adjusting for other risk factors associated with fair prevalence. However, we did not identify any additional risk factors associated with IAV prevalence (Appendix Table 3). The only exception was fairs in Indiana, which had significantly lower IAV prevalence compared with Ohio despite a high proportion of fairs testing IAV-positive in Indiana (*18*). Because Indiana encouraged its county fairs to implement the 72-hour recommendation compared with other states, the 72-hour swine release is more proximate in the causal pathway explaining IAV prevalence in this system.

Although we do expect population size and density to play a role in infectious disease outbreak growth (*27*), we also expect contact network structure to strongly influence transmission dynamics (*28*). On the basis of the findings at weigh-in, many arriving swine are exposed to IAV early during a fair. If swine are often infected before 72 hours but do not begin actively shedding virus until closer to the end of the fair, then reducing the population density will have limited influence on outbreak spread. Because aerosolized IAV is shed into the air at county fairs (*29*), the reduced number of swine shedding IAV in the barn still reduces the overall viral load and therefore zoonotic transmission risk associated with that fair. Animals that return home early may already be exposed to IAV and introduce infection to the home farm. These animals are still infected but are no longer on public display, which reduces public health risk at the fair but can still result in pathogen dissemination and complicates home–farm transmission and downstream network implications when swine attend additional shows (*13*,*18*). Although our study is limited to IAV surveillance data, other agriculturally relevant pathogens have been detected in exhibition swine and are probably also affected by these transmission mechanisms (*30*,*31*).

Culturally, agricultural exhibitions are imperative to attracting the interest of and training the next generation of agriculturalists, upon whom we rely for safe and secure food sources. However, contracting IAV from swine at agricultural exhibitions not only poses a local and global public health risk but could also deter youth exhibitors and undermine the public image of and confidence in agriculture and food production. Because IAV is consistently introduced to county fairs from upstream sources (*13*–*15*,*17*,*18*), it is imperative that we provide measures to reduce IAV risk within an individual fair. Shortening the duration of swine exhibitions at county fairs reduces IAV prevalence in exhibition swine and the subsequent risk for harmful zoonotic emergence.

Acknowledgments

We thank our collaborators from the participating agricultural fairs. We also thank Alexa Edmunson, Elise Gerken, Amber Kihm, Grant Price, Christine Szablewski, Jeffrey Workman, Sarah Lauterbach, Nick Bortoloni, Christie Hammons, Alison Martin, and Josh Lorbach for their assistance in sample collection.

Graduate student stipend and support was provided by the US Department of Agriculture's National Bio and Agro-Defense Facility Scientist Training Program

(to D.S.M.). This work was supported in part with federal funds from the Centers for Disease Control and Prevention (cooperative agreement no. U38OT000143) and from the Centers of Excellence for Influenza Research and Surveillance, National Institute of Allergy and Infectious Diseases, National Institutes of Health (contract no. HHSN272201400006C).

About the Author

Mr. McBride is a fellow at the US Department of Agriculture's National Bio and Agro-Defense Facility Scientist Training Program and a PhD candidate in the Department of Veterinary Preventive Medicine, The Ohio State University, Columbus, Ohio. His research interests include epidemiology and evolution of emerging zoonotic diseases.

References

1. Webster RG, Bean WJ, Gorman OT, Chambers TM, Kawaoka Y. Evolution and ecology of influenza A viruses. Microbiol Rev. 1992;56:152–79. https://doi.org/10.1128/mr.56.1.152-179.1992
2. Ma W, Kahn RE, Richt JA. The pig as a mixing vessel for influenza viruses: Human and veterinary implications. J Mol Genet Med. 2008;3:158–66.
3. Smith GJD, Vijaykrishna D, Bahl J, Lycett SJ, Worobey M, Pybus OG, et al. Origins and evolutionary genomics of the 2009 swine-origin H1N1 influenza A epidemic. Nature. 2009;459:1122–5. https://doi.org/10.1038/nature08182
4. Vijaykrishna D, Poon LLM, Zhu HC, Ma SK, Li OTW, Cheung CL, et al. Reassortment of pandemic H1N1/2009 influenza A virus in swine. Science. 2010;328:1529. https://doi.org/10.1126/science.1189132
5. Mena I, Nelson MI, Quezada-Monroy F, Dutta J, Cortes-Fernández R, Lara-Puente JH, et al. Origins of the 2009 H1N1 influenza pandemic in swine in Mexico. eLife. 2016;5:e16777. https://doi.org/10.7554/eLife.16777
6. Centers for Disease Control and Prevention. Reported infections with variant influenza viruses in the United States. 2018 Nov [cited 2020 Feb 21]. https://www.cdc.gov/flu/swineflu/variant-cases-us.htm
7. Bowman AS, Sreevatsan S, Killian ML, Page SL, Nelson SW, Nolting JM, et al. Molecular evidence for interspecies transmission of H3N2pM/H3N2v influenza A viruses at an Ohio agricultural fair, July 2012. Emerg Microbes Infect. 2012;1:e33. https://doi.org/10.1038/emi.2012.33
8. Bowman AS, Walia RR, Nolting JM, Vincent AL, Killian ML, Zentkovich MM, et al. Influenza A(H3N2) virus in swine at agricultural fairs and transmission to humans, Michigan and Ohio, USA, 2016. Emerg Infect Dis. 2017;23:1551–5. https://doi.org/10.3201/eid2309.170847
9. Bowman AS, Nelson SW, Page SL, Nolting JM, Killian ML, Sreevatsan S, et al. Swine-to-human transmission of influenza A(H3N2) virus at agricultural fairs, Ohio, USA, 2012. Emerg Infect Dis. 2014;20:1472–80. https://doi.org/10.3201/eid2009.131082
10. Epperson S, Jhung M, Richards S, Quinlisk P, Ball L, Moll M, et al.; Influenza A (H3N2)v Virus Investigation Team. Human infections with influenza A(H3N2) variant virus in the United States, 2011–2012. Clin Infect Dis. 2013;57(Suppl 1):S4–11. https://doi.org/10.1093/cid/cit272
11. Jhung MA, Epperson S, Biggerstaff M, Allen D, Balish A, Barnes N, et al. Outbreak of variant influenza A(H3N2) virus in the United States. Clin Infect Dis. 2013;57:1703–12. https://doi.org/10.1093/cid/cit649
12. Killian ML, Swenson SL, Vincent AL, Landgraf JG, Shu B, Lindstrom S, et al. Simultaneous infection of pigs and people with triple-reassortant swine influenza virus H1N1 at a U.S. county fair. Zoonoses Public Health. 2013;60:196–201. https://doi.org/10.1111/j.1863-2378.2012.01508.x
13. Nelson MI, Perofsky A, McBride DS, Rambo-Martin BL, Wilson MM, Barnes JR, et al. A heterogenous swine show circuit drives zoonotic transmission of influenza A viruses in the United States. J Virol. 2020;94:e01453–20. https://doi.org/10.1128/JVI.01453-20
14. Bliss N, Nelson SW, Nolting JM, Bowman AS. Prevalence of influenza A virus in exhibition swine during arrival at agricultural fairs. Zoonoses Public Health. 2016;63:477–85. https://doi.org/10.1111/zph.12252
15. Bowman AS, Nolting JM, Nelson SW, Slemons RD. Subclinical influenza virus A infections in pigs exhibited at agricultural fairs, Ohio, USA, 2009-2011. Emerg Infect Dis. 2012;18:1945–50. https://doi.org/10.3201/eid1812.121116
16. Bliss N, Stull JW, Moeller SJ, Rajala-Schultz PJ, Bowman AS. Movement patterns of exhibition swine and associations of influenza A virus infection with swine management practices. J Am Vet Med Assoc. 2017;251:706–13. https://doi.org/10.2460/javma.251.6.706
17. Nelson MI, Wentworth DE, Das SR, Sreevatsan S, Killian ML, Nolting JM, et al. Evolutionary dynamics of influenza A viruses in US exhibition swine. J Infect Dis. 2016;213:173–82. https://doi.org/10.1093/infdis/jiv399
18. McBride DS, Perofsky AC, Nolting JM, Nelson MI, Bowman AS. Tracing the source of influenza A virus zoonoses in interconnected circuits of swine exhibitions. J Infect Dis. 2021;224:458–68. https://doi.org/10.1093/infdis/jiab122
19. Bowman AS, Workman JD, Nolting JM, Nelson SW, Slemons RD. Exploration of risk factors contributing to the presence of influenza A virus in swine at agricultural fairs. Emerg Microbes Infect. 2014;3:e5. https://doi.org/10.1038/emi.2014.5
20. National Association of State Public Health Veterinarians. Measures to minimize influenza transmission at swine exhibitions. 2018 [cited 2020 Jun 4]. https://www.nasphv.org/Documents/InfluenzaTransmissionAtSwineExhibitions2018.pdf
21. Indiana State Board of Animal Health. Disease risk management recommendations for swine exhibitions. 2012 Oct [cited 2020 Jun 9]. https://www.in.gov/boah/files/Swine_Exhibition_Recommendations_(BOAH_10-11-2012)(Final).pdf
22. Edwards JL, Nelson SW, Workman JD, Slemons RD, Szablewski CM, Nolting JM, et al. Utility of snout wipe samples for influenza A virus surveillance in exhibition swine populations. Influenza Other Respir Viruses. 2014;8:574–9. https://doi.org/10.1111/irv.12270
23. Nolting JM, Szablewski CM, Edwards JL, Nelson SW, Bowman AS. Nasal wipes for influenza A virus detection and isolation from swine. J Vis Exp. 2015;106:e53313. https://doi.org/10.3791/53313
24. Nolting JM, Scheer SD, Bowman AS. Perceptions and attitudes of swine exhibitors towards recommendations for reducing zoonotic transmission of influenza A viruses. Zoonoses Public Health. 2019;66:401–5. https://doi.org/10.1111/zph.12574
25. Lorbach JN, Nelson SW, Lauterbach SE, Nolting JM, Kenah E, McBride DS, et al. Influenza vaccination of swine

reduces public health risk at the swine–human interface. MSphere. 2021;6:e0117020. https://doi.org/10.1128/mSphere.01170-20
26. Lauterbach SE, Zentkovich MM, Nelson SW, Nolting JM, Bowman AS. Environmental surfaces used in entry-day corralling likely contribute to the spread of influenza A virus in swine at agricultural fairs. Emerg Microbes Infect. 2017;6:e10. https://doi.org/10.1038/emi.2016.138
27. Kermack WO, McKendrick AG. Contributions to the mathematical theory of epidemics—I. 1927. Bull Math Biol. 1991;53:33–55.
28. Ferrari MJ, Perkins SE, Pomeroy LW, Bjørnstad ON. Pathogens, social networks, and the paradox of transmission scaling. Interdiscip Perspect Infect Dis. 2011;2011:267049. https://doi.org/10.1155/2011/267049
29. Lauterbach SE, Wright CM, Zentkovich MM, Nelson SW, Lorbach JN, Bliss NT, et al. Detection of influenza A virus from agricultural fair environment: Air and surfaces. Prev Vet Med. 2018;153:24–9. https://doi.org/10.1016/j.prevetmed.2018.02.019
30. Lauterbach SE, Nelson SW, Robinson ME, Lorbach JN, Nolting JM, Bowman AS. Assessing exhibition swine as potential disseminators of infectious disease through the detection of five respiratory pathogens at agricultural exhibitions. Vet Res (Faisalabad). 2019;50:63. https://doi.org/10.1186/s13567-019-0684-5
31. Lorbach JN, Wang L, Nolting JM, Benjamin MG, Killian ML, Zhang Y, et al. Porcine hemagglutinating encephalomyelitis virus and respiratory disease in exhibition swine, Michigan, USA, 2015. Emerg Infect Dis. 2017;23:1168–71. https://doi.org/10.3201/eid2307.170019

Address for correspondence: Andrew S. Bowman, The Ohio State University, 1920 Coffey Rd, Sisson Hall A100B, Columbus, OH 43210, USA; email: bowman.214@osu.edu

Plasmodium falciparum pfhrp2 and *pfhrp3* Gene Deletions and Relatedness to Other Global Isolates, Djibouti, 2019–2020

Eric Rogier,[1] Jessica N. McCaffery,[1] Mohamed Ali Mohamed, Camelia Herman, Doug Nace, Rachel Daniels, Naomi Lucchi, Sophie Jones, Ira Goldman, Michael Aidoo, Qin Cheng, Edie A. Kemenang, Venkatachalam Udhayakumar, Jane Cunningham

Deletions of *pfhrp2* and paralogue *pfhrp3* (*pfhrp2/3*) genes threaten *Plasmodium falciparum* diagnosis by rapid diagnostic test. We examined 1,002 samples from suspected malaria patients in Djibouti City, Djibouti, to investigate *pfhrp2/3* deletions. We performed assays for *Plasmodium* antigen carriage, *pfhrp2/3* genotyping, and sequencing for 7 neutral microsatellites to assess relatedness. By PCR assay, 311 (31.0%) samples tested positive for *P. falciparum* infection, and 296 (95.2%) were successfully genotyped; 37 (12.5%) samples were *pfhrp2*+/*pfhrp3*+, 51 (17.2%) were *pfhrp2*+/*pfhrp3*–, 5 (1.7%) were *pfhrp2*–/*pfhrp3*+, and 203 (68.6%) were *pfhrp2*–/*pfhrp3*–. Histidine-rich protein 2/3 antigen concentrations were reduced with corresponding gene deletions. Djibouti *P. falciparum* is closely related to Ethiopia and Eritrea parasites (pairwise G_{ST} 0.68 [Ethiopia] and 0.77 [Eritrea]). *P. falciparum* with deletions in *pfhrp2/3* genes were highly prevalent in Djibouti City in 2019–2020; they appear to have arisen de novo within the Horn of Africa and have not been imported.

Diagnosis and appropriate case management of *Plasmodium falciparum* infection has greatly improved in many malaria-endemic settings through the use of rapid diagnostic tests (RDTs) that detect the histidine-rich protein 2 (HRP2) antigen (*1*). As the only *Plasmodium* species infecting humans to produce this antigen, the *P. falciparum* parasite expresses HRP2 in abundance and releases it into the bloodstream during blood-stage infection, making this marker a very sensitive and specific target for falciparum malaria (*1*,*2*). The *pfhrp2* gene is located on chromosome 8 of the parasite genome, and a paralogous gene (*pfhrp3*) is located on chromosome 13. The 2 protein products share common epitopes for diagnostic antibodies, enabling the HRP3 antigen to also be detected to some extent by HRP2-based RDTs (*3*–*6*).

P. falciparum produces large quantities of these antigens during human blood-stage infection, but their biologic functions are not well elucidated, and *pfhrp2*-deleted and *pfhrp3*-deleted parasites still complete the human–mosquito lifecycle successfully (*7*). Reports of these gene deletions have increased over the past decade from multiple countries in Africa, South America, and Asia (https://apps.who.int/malaria/maps/threats) (*8*). For countries that rely on HRP2-based RDTs for diagnosis of *P. falciparum* infection, those reports affirm the need to monitor the performance of this tool because deleted parasites could emerge and elicit false-negative results.

P. falciparum infection represents ≈99.7% of all malaria cases in sub-Saharan Africa, and ≈300 million HRP2-based RDTs are used in this region annually (*9*). Studies in the east Africa countries of Eritrea (*10*) and Ethiopia (*11*,*12*) have found high prevalence of *pfhrp2/pfhrp3* deletions, forcing changes away from HRP2-based RDTs to accurately diagnose *P. falci-*

Author affiliations: Centers for Disease Control and Prevention, Atlanta, Georgia, USA (E. Rogier, J.N. McCaffery, C. Herman, D. Nace, N. Lucchi, S. Jones, I. Goldman, M. Aidoo, V. Udhayakumar); Oak Ridge Institute for Science and Education, Oak Ridge, Tennessee, USA (J.N. McCaffery); Hôpital Général Peltier, Djibouti City, Djibouti (M.A. Mohamed); Harvard T.H. Chan School of Public Health, Boston, Massachusetts, USA (R. Daniels); Broad Institute, Cambridge, Massachusetts, USA (R. Daniels); Australian Defence Force Malaria and Infectious Disease Institute, Brisbane, Queensland, Australia (Q. Cheng); World Health Organization, Geneva, Switzerland (E.A. Kemenang, J. Cunningham)

DOI: https://doi.org/10.3201/eid2810.220695

[1]These authors contributed equally to this article.

parum infections in these countries. Furthermore, it is unknown whether these deleted genotypes are a result of importation and expansion or whether de novo deletions are arising from local *P. falciparum* lineages. A recent report from Djibouti, which borders both Eritrea and Ethiopia, investigated 79 *P. falciparum*–infected patients and found ≈80% of parasites were lacking both *pfhrp2* and *pfhrp3* genes (*13*). Triggered by health workers' reports of false-negative RDT results, we report data from an investigation of 1,002 suspected malaria patients enrolled in Djibouti City during December 2019–March 2020. Data were generated for infection-causing *Plasmodium* species, *pfhrp2/3* genotype, concordance with laboratory antigen detection, and relatedness to other global *P. falciparum* parasites.

Materials and Methods

Patient Enrollment and Ethics Statement

This activity was considered by the Ministry of Health of Djibouti, the World Health Organization (WHO) Ethical Review Committee, and Centers for Disease Control and Prevention (CDC) human subjects office as nonresearch and as public health surveillance (0900f3eb81abbef6). In December 2020, a study was initiated to investigate presence of *pfhrp2/3* deletions in Djibouti because of 4 specimens that tested negative by HRP2-based RDT (CareStart Malaria Combo RDT; Access Bio, https://accessbio.net) but were positive for *P. falciparum* lactate dehydrogenase (pf-LDH) (Bioline Malaria Ag Pf [HRP2/pLDH] Test; Abbott, https://www.abbott.com) and also confirmed for *P. falciparum* infection by microscopy. During January 29–March 11, 2020, consecutive patients of varying ages experiencing symptoms of malaria who sought care at Général Peltier Hospital, Djibouti City, were tested by malaria RDT with the First Response Malaria Ag (pLDH/HRP2) Combo Card Test (Premier Medical Corporation, https://www.premiermedcorp.com) and routine venipuncture for hematologic and electrolyte profiling.

Dried Blood Spot Creation

Dried blood spots (DBS) were prepared from remaining venous blood with 50–75 μL of remnant in EDTA tubes spotted on Whatman Protein Saver cards 903 or Whatmann 3M filter paper (Cytiva Life Sciences, https://www.cytivalifesciences.com). The spots were dried for ≥4 hours at room temperature and then stored with desiccant in sealable bags and shipped to the CDC (Atlanta, GA, USA).

Plasmodium Antigen Detection by Laboratory Multiplex Assay

DBS processing and testing for *Plasmodium* antigens were performed at CDC as described previously (*14*,*15*). A 6-mm punch was taken from each DBS for elution in blocking buffer (final whole blood dilution of 1:20) for the bead-based multiplex antigen detection assay of pan-*Plasmodium* aldolase and lactate dehydrogenase (LDH), HRP2 (and HRP3), and *P. vivax* LDH (PvLDH). Assay plates were run on a MAGPIX machine (Luminex Corp., https://www.luminexcorp.com) with a target of 50 beads per region.

Plasmodium Species Identification by PCR and *pfhrp2* and *pfhrp3* Genotyping

We selected DBS samples positive for any *Plasmodium* antigens for DNA extraction (DNA Mini Kit; QIAGEN, https://www.qiagen.com) and *Plasmodium* species–specific photo-induced electron transfer (PET) PCR and quantification of DNA (*16*). Samples positive for *P. falciparum* DNA had nested PCR reactions for single-copy *pfmsp1* and *pfmsp2* genes as quality control for DNA quantity and integrity (*17*,*18*). We further assayed only those samples amplifying both control genes to determine presence or absence of *pfhrp2* and *pfhrp3* genes. Genotyping for *pfhrp2* was performed by a single-step PCR amplifying *pfhrp2* inclusive of both exons (*19*), and genotyping for *pfhrp3* was through 2 nested PCR reactions with primers specific for exon 1–2 and exon 2 regions (*17*,*18*). All genotyping reactions were run by 2 independent operators on different days and by a third operator if amplification results were discordant.

Genetic Haplotypes through Neutral Microsatellites

To assess multiplicity of infection and relatedness of *P. falciparum* parasites, we selected 7 neutral microsatellite (NMS) genetic markers: TA1 on chromosome 6, poly-α on chromosome 4, PfPK2 on chromosome 12, 2490 on chromosome 10, C2M34–313 on chromosome 2, C3M69–383 on chromosome 3, and TA109 on chromosome 6 (*10*,*20*). We determined the sizes of the amplification products by capillary electrophoresis on an Applied Biosystems 3130xl Genetic Analyzer (ThermoFisher Scientific, https://www.thermofisher.com) and analyzed data by using GeneMarker version 3.0.0 (SoftGenetics, https://softgenetics.com). We considered infections monoclonal if all 7 NMS had only 1 allele call. We used NMS data from previous studies to compare Djibouti results to *P. falciparum* parasites from other countries (Appendix Table 1, https://wwwnc.cdc.gov/EID/article/28/10/22-0695-App1.pdf).

Statistical Analysis

We compared lognormal means for HRP2/3 antigen concentration by genotype by using the 2-tailed Student *t* test with equal variance. For secondary analyses, we divided antigen assay signals for the entire sample set into low and high HRP2/3 antigen levels by comparing them with levels of the pLDH and pAldolase antigens as described previously (*21*). In brief, if blood samples were positive for pan-*Plasmodium* LDH or aldolase and negative for HRP2/3 antigens or had atypically low amounts of HRP2/3 relative to the pan-*Plasmodium* targets, we selected them as high-priority specimens with phenotypic evidence for *pfhrp2/3* gene deletions (Appendix Figure 1).

We assessed NMS data and measures of relatedness by using the PopGenReport package in R (R Foundation for Statistical Computing, https://www.r-project.org) (*22*). For all countries, we used monoclonal infections and polyclonal infections with distinct haplotypes or dominant haplotypes for the relatedness and principal component analysis.

Results

During January 29–March 20, 2020, of the suspected malaria cases registered at Général Peltier Hospital, 998 DBS were collected; an additional 4 samples previously collected in December 2019 were included in the sample set because they were identified as highly suspicious of *pfhrp2/3* deletions on the basis of RDT results (Figure 1). Laboratory antigen screening revealed 630 (62.9%) samples were negative for all antigens; those samples were not investigated further because there was no suspicion of *Plasmodium* spp. infection.

We extracted DNA from the remaining 372 (37.1%) *Plasmodium* antigen–positive samples for further molecular investigation. Of those 372 samples, detectable *Plasmodium* DNA was absent in 17 (4.6%) samples, and 44 samples (11.8%) were found to be *P. vivax* single-species infections; samples within these 2 groups were not considered further for *pfhrp2/3* deletion reporting. Of the remaining 311 samples containing *P. falciparum* DNA, 15 (4.8%) did not amplify both *pfmsp1* and *pfmsp2* single-copy genes and were not eligible for reporting of *pfhrp2/3* genotypes. Of the 296 *P. falciparum* infections that qualified for reporting genotyping, 37 (12.5%) were a genotype of *pfhrp2+/pfhrp3+*, 51 (17.2%) were *pfhrp2+/pfhrp3–*, 5 (1.7%) were *pfhrp2–/pfhrp3+*, and 203 (68.6%) were a double-deletion genotype of *pfhrp2–/pfhrp3–* (Figure 1). For all 296 samples of *P. falciparum* infections successfully genotyped, 208 (70.3%) demonstrated a *P. falciparum* infection with *pfhrp2* deletion and 254 (85.8%) showed deletion in the *pfhrp3* gene.

Using the hypothetical selection method (see Methods) based on levels of pan-*Plasmodium* antigens compared with HRP2/3 antigens, of the 372 antigen-positive samples, 241 (64.8%) had a complete absence of HRP2/3 assay signal, 20 (5.4%) had an atypically low amount of HRP2/3 relative to other pan-*Plasmodium* antigens, and 111 (29.8%) had high levels of HRP2/3 relative to other pan-*Plasmodium* antigens (Appendix Figure 1). Of all 241 samples negative for HRP2/3 signal, 183 (75.9%) were appropriate for *pfhrp2/3* genotyping, and all demonstrated a *pfhrp2* deletion. When categorized into the low HRP2/3 category, of the 18 samples that qualified for genotyping, 6 (33.3%) showed a deletion of the *pfhrp2* gene. If categorized into the high HRP2/3 category, of 90 samples that qualified for genotyping, the *pfhrp2* gene was amplified in most (74 [82.2%]).

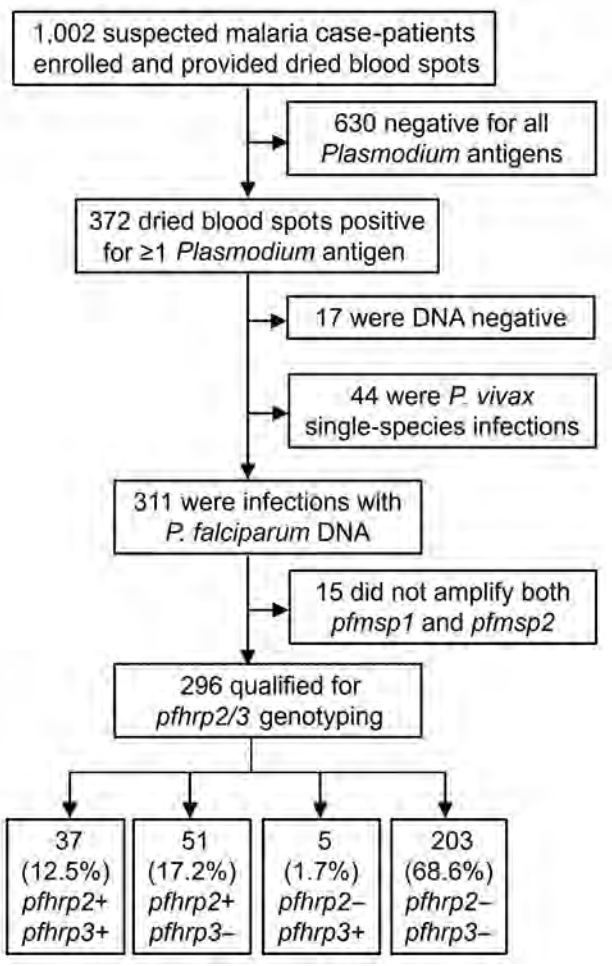

Figure 1. Flow diagram for reporting *pfhrp2* and *pfhrp3* genotype for all specimens in study of *Plasmodium falciparum* parasites with *pfhrp2* and *pfhrp3* deletions, Djibouti, 2019–2020. Terminal boxes display number of samples successfully genotyped for *pfhrp2/3*.

We found that concentrations of the HRP2 antigen (with potential supplemented signal from HRP3) were strongly associated with the different *pfhrp2/3* genotypes (Figure 2). With the exception of 1 specimen, all samples found to be positive for the *pfhrp2* gene (n = 88) showed high concentrations of the HRP2/3 antigen; the *pfhrp2+/pfhrp3+* genotype samples showed a log-normal mean concentration of 10,794 pg/mL, and the *pfhrp2+/pfhrp3–* genotype samples showed a log-normal mean concentration of 18,017 pg/mL (Figure 2, panel A). Blood samples from infections with *P. falciparum* parasites lacking the *pfhrp2* gene showed, on average, much lower concentrations of HRP2/3 antigens: log-normal mean of 421 pg/mL in *pfhrp2–/pfhrp3+* samples and log-normal mean of 2.0 pg/mL in *pfhrp2–/pfhrp3–* samples. Concentration was significantly lower in the blood samples from *pfhrp2–/pfhrp3–* parasite infections than in *pfhrp2+/pfhrp3+* ($p<0.001$), *pfhrp2+/pfhrp3–* ($p<0.001$), and *pfhrp2–/pfhrp3+* ($p = 0.049$) parasite infections. Of the 5 infections with *pfhrp2–/pfhrp3+* parasites, 2 (40.0%) showed an absence of HRP2/3 antigen signal, compared with 185/203 (91.1%) of *pfhrp2–/pfhrp3–* infections. Density plots of HRP2/3 antigen concentration by infecting parasite genotype illustrate these trends by genotype category (Figure 2, panel B).

In total, 65 of the Djibouti infections were chosen for NMS sequencing: 20 *pfhrp2+/pfhrp3+*, 20 *pfhrp2+/pfhrp3–*, 5 *pfhrp2–/pfhrp3+*, and 20 *pfhrp2–/pfhrp3–*. Of those, 52/65 (80.0%) were found to be monoclonal infections, and this finding did not differ significantly by genotype: *pfhrp2+/pfhrp3+* (16/20 [80.0%]), *pfhrp2+/pfhrp3–* (15/20 [75.0%]), *pfhrp2–/pfhrp3+* (4/5 [80.0%]), *pfhrp2–/pfhrp3–* (17/20 [85.5%]). Three of the genotypes (all except for *pfhrp2–/pfhrp3+*) showed a high degree of independent clustering by principal component analysis (Figure 3). Both the Jost pairwise D and Hendricks pairwise G_{ST} measures of gene differentiation found the *pfhrp2–/pfhrp3–* genotype to be most related to *pfhrp2–/pfhrp3+* parasites (Appendix Table 2).

Comparing relatedness of *P. falciparum* by country (regardless of *pfhrp2/3* genotype) found distinct clustering by the area of the world in which the parasites originated (Figure 4, panel A). Both Jost pairwise D and Hendricks pairwise G_{ST} found parasites from Djibouti and other parts of Africa more related to each other than to isolates from South America or Asia (Appendix Table 3, Figure 2). When repeating the analysis with only parasites from Africa, Djibouti and Ethiopia parasites were found to be most related in comparison with *P. falciparum* from the other 5 African countries (Appendix Figure 3). For global isolates with *pfhrp2* deletions, South America and Africa parasites were not strongly related to each other; Peru and Suriname parasites had the highest principal component 1 values as well as highest Jost pairwise D and Hendricks pairwise G_{ST} in comparison with African *pfhrp2*-deleted parasites (Table; Figure 4, panel B). The *pfhrp2* deleted parasites from Sudan, Eritrea, Ethiopia, and Djibouti showed relatively similar principal component 1 values, and Ethiopia and Djibouti *pfhrp2*-deleted genotypes demonstrated the closest overall clustering. Among these deleted parasites, Djibouti *P. falciparum* was most closely related to Ethiopia (pairwise G_{ST} 0.68) *pfhrp2*-deleted *P. falciparum*, followed by Eritrea (0.77), Sudan (0.97), Peru (0.98), and Suriname (0.99). If assessing relatedness among parasites lacking only the *pfhrp3* gene, we noted similar findings; the highest degree of relatedness was seen among the Djibouti and Ethiopia parasites (Appendix Figure 4).

Discussion

Confirmatory diagnosis of *P. falciparum* malaria through testing for the presence of HRP2 antigen by RDT has been a substantial improvement for providing appropriate case management in many malaria-endemic countries. Discovery of *pfhrp2* gene deletions in natural *P. falciparum* populations has led to doubts

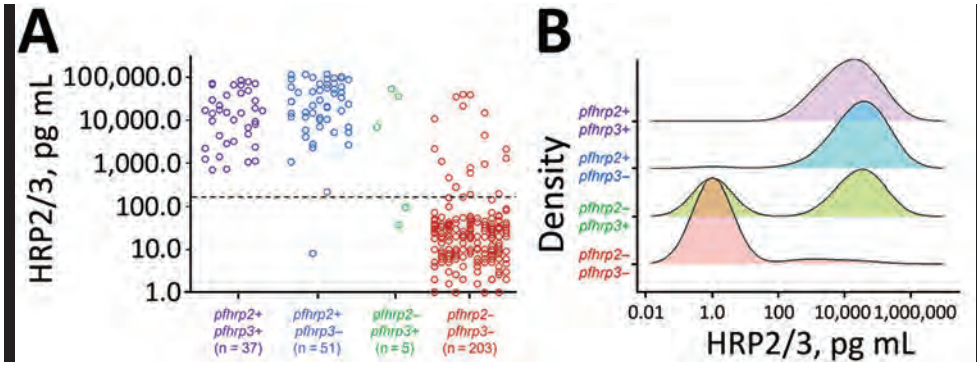

Figure 2. Distributions of HRP2/HRP3 antigen concentrations by *pfhrp2* and *pfhrp3* genotype for specimens in study of *Plasmodium falciparum* parasites with *pfhrp2* and *pfhrp3* deletions, Djibouti 2019–2020. A) Individual antigen concentrations for all 296 samples successfully genotyped for *pfhrp2/3.* Dashed line denotes the assay level of quantitation. B) Smoothed kernel density plots for log-transformed HRP2/3 concentration by the four *pfhrp2/3* genotypes. HRP2/3, histidine-rich protein 2/3.

about the sustained use of this antigen for diagnostic purposes (*1*). To date, most *P. falciparum*–endemic settings that rely heavily on RDTs for routine diagnostics have been found to have populations of parasites that express high amounts of HRP2 and HRP3 antigens (*8*,*15*,*18*,*21*,*23*,*24*). The ability to evade HRP2-based diagnostics (and subsequent treatment) might lead to a selective advantage for parasites with gene deletions (*25*). Routine surveillance of *P. falciparum*–endemic populations is required to ensure that primary diagnostic tools are still accurate.

Multiple recent studies in the Horn of Africa have demonstrated a high proportion of *P. falciparum* in the region with *pfhrp2* gene deletions and that most isolates also have *pfhrp3* deletions. A 2016 Eritrea health facility survey found 62.0% of *P. falciparum* infections consisted of parasites with both *pfhrp2* and *pfhrp3* deletions, all of which were also HRP2-negative by RDT (*10*). Of persons enrolled in health facility surveys during 2017–2018 in northern Ethiopia, *pfhrp2* deletions were responsible for between 11.5%–14.9% of false-negative HRP2-RDT results (*12*). A survey of 3 health facilities in Djibouti in early 2019 also found these concerning results: in a small sample set of 79 *P. falciparum* PCR-positive patients, 86.5% demonstrated *pfhrp2/3* deletions (*13*).

In light of previous findings, this 2019–2020 study was designed to assess the prevalence of *pfhrp2/3* deletions in Djibouti City, relatedness of Djibouti *P. falciparum* to other global isolates, and overall relatedness of *P. falciparum* within the Horn of Africa compared with other global sites. Most (63%) of the 1,002 DBS samples collected from persons with malaria-like symptoms were negative for any *Plasmodium* antigens and did not undergo molecular assays because *Plasmodium* infection was not suspected. The bead-based antigen assay has been shown to detect *Plasmodium* infection at approximately the same level as standard PCR assays at ≈2 parasites/uL blood (*15*). Among the remaining 372 *Plasmodium*-positive samples, only 111 (29.8%) displayed moderate to high levels of HRP2/3 antigen profile indicative of *P. falciparum* with functional *pfhrp2* or *pfhrp3* genes. By those *Plasmodium* antigen data alone, the pervasiveness of low or absent HRP2 levels in 70% of samples from symptomatic *Plasmodium*-infected persons raised sus-

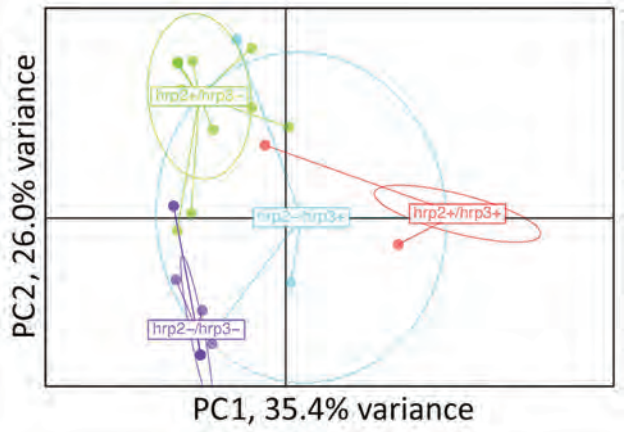

Figure 3. Relatedness of *Plasmodium falciparum* parasites from Djibouti, 2019–2020, with different *pfhrp2* and *pfhrp3* genotypes. Cluster PC analysis shown for 7 neutral microsatellite data for monogenomic infections by subpopulations: *pfhrp2+/pfhrp3+* (n = 16), *pfhrp2+/pfhrp3–* (n = 15), *pfhrp2–/pfhrp3+* (n = 4), *pfhrp2–/pfhrp3–* (n = 17). Plot shown with PC1 on x-axis and PC2 on y-axis with 95% confidence ellipses. PC, principal component.

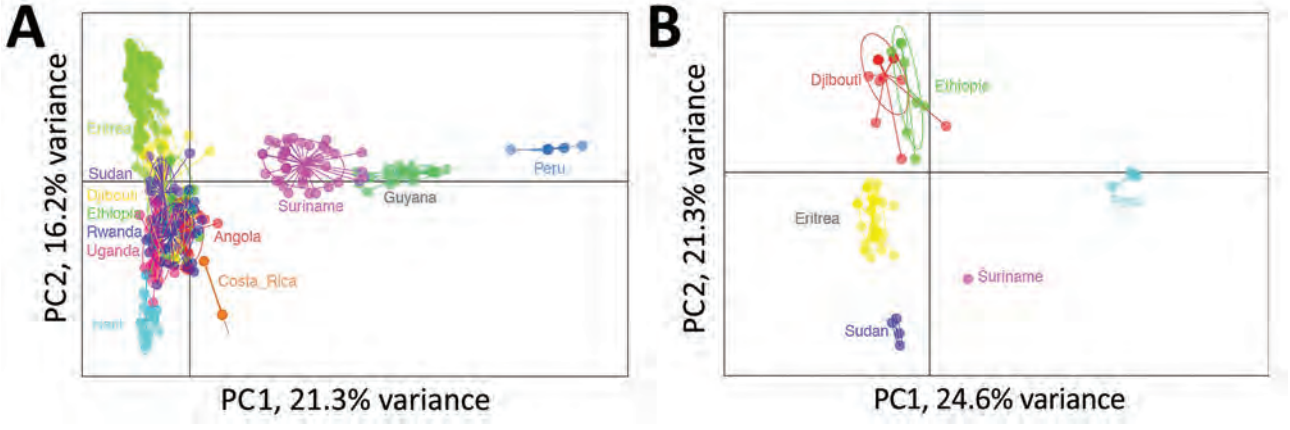

Figure 4. Relatedness of *Plasmodium falciparum* parasites from Djibouti, 2019–2020 with other global isolates. A) Cluster PC analysis shown for neutral microsatellite data for monogenomic infections by collection from different countries: Angola (n = 32), Costa Rica (n = 14), Djibouti (n = 52), Eritrea (n = 187), Ethiopia (n = 20), Guyana (n = 27), Haiti (n = 86), Peru (n = 18), Rwanda (n = 42), Sudan (n = 37), Suriname (n = 44), Uganda (n = 25). B) Cluster PC analysis shown for neutral microsatellite data for monogenomic infections containing *pfhrp2* deletions by collection from different countries: Djibouti (n = 21), Eritrea (n = 43), Peru (n = 18), Ethiopia (n = 8), Sudan (n = 4), and Suriname (n = 1). Plots shown with PC1 on x-axis and PC2 on y-axis and 95% confidence ellipses. PC, principal component.

Table. Genetic relatedness of *pfhrp2*-deleted *Plasmodium falciparum* parasites from Djibouti, 2019–2020, compared with those from other countries*

Comparison	Country	Djibouti	Eritrea	Ethiopia	Peru	Sudan
Jost D pairwise	Djibouti					
	Eritrea	0.530				
	Ethiopia	0.444	0.704			
	Peru	0.873	0.888	0.846		
	Sudan	0.920	0.817	0.879	0.994	
	Suriname	0.987	0.831	1.00	0.795	0.962
Hendrick pairwise G_{ST}	Djibouti					
	Eritrea	0.772				
	Ethiopia	0.679	0.843			
	Peru	0.977	0.972	0.953		
	Sudan	0.972	0.917	0.941	0.999	
	Suriname	0.998	0.949	1.000	0.991	0.990

*Darker shading indicates higher level of relatedness.

picion of either a high frequency of non–*P. falciparum* infections or high prevalence of *P. falciparum* isolates with the *pfhrp2/3* genes deleted; both scenarios were found to be true in Djibouti. Of the 355 samples with detectable *Plasmodium* DNA by PET-PCR, 44 (12.4%) were single-species *P. vivax* infections; this finding is in line with previous reports of *P. vivax* in Djibouti, as well as in neighboring Ethiopia and Eritrea (*9*,*26*). Most (95%) of the 311 samples with *P. falciparum* DNA were successfully genotyped for single-copy control genes (*17*), reflecting high-density infections in the symptomatic study population. Of the 296 *P. falciparum* infections with reportable genotyping results, only 37 (12.5%) contained wild-type parasites with both *pfhrp2* and *pfhrp3* genes amplified. Only *pfhrp3* was deleted in 17.2% of parasites, only *pfhrp2* was deleted in 1.7%, and more than two thirds of all infections (68.6%) were from *P. falciparum* lacking both genes. The 68.6% prevalence of double-deleted parasites in Djibouti City is lower than the 86.5% previously reported by Iriart et al. (*13*). This high prevalence of *pfhrp2/3* dual-deleted infections, coupled with our finding that most infections are monoclonal (80%), suggests that a high percentage of *P. falciparum* infections in Djibouti City would not be detected by HRP2-based RDTs. This level is well beyond the 5% threshold recommended by the WHO to consider a replacement of exclusive HRP2-based diagnostics for detecting *P. falciparum* (*27*), and the findings from our study have already been shared with the Djibouti Ministry of Health and WHO regional partners.

Regarding relatedness to other global isolates, the parasites found in Djibouti (regardless of genotype) clustered closely with *P. falciparum* haplotypes from Africa and showed greater distance to *P. falciparum* from the New World and Asia. Djibouti City is a large port city located on the east central coast and is home to approximately half the country's population. Because Djibouti City is a large center of trade and population movement, some enrolled patients might have contracted *P. falciparum* infection in a country other than Djibouti, but travel history for participants was unavailable for this study. However, the objective genetic data show that even if some infections were acquired outside Djibouti, they all appear to be Africa-derived from more proximal countries. High relatedness (low diversity) of *P. falciparum* within Djibouti has been previously observed for isolates collected throughout the country within individual surveys and without substantial differences among multiple years of collection (*28*), although genotyping for *pfhrp2/3* deletions was not performed. The relatedness of Djibouti and Ethiopia *pfhrp2*-deleted parasites observed in this study was closer when compared with Eritrea or Sudan isolates and very distant from *pfhrp2*-deleted *P. falciparum* from Peru and Suriname. The same finding was noted for *pfhrp3*-only deleted parasites, where Djibouti and Ethiopia populations practically overlie each other. This evidence points to de novo gene deletions and expansion of these deleted *P. falciparum* populations in the Horn of Africa rather than importation of deleted parasites from other areas of the world. Specifically for the Horn of Africa, close background lineages by NMS data for *pfhrp2*- and *pfhrp3*-deleted parasites from Djibouti and Ethiopia points to an expansion of common gene-deleted populations that exist in these adjacent countries. Eritrea parasite lineages from both wild-type and deleted *P. falciparum* appear to be differentiated from the Ethiopia/Djibouti lines, suggesting separate *pfhrp2/3* deletion events on unique *P. falciparum* strains and a more distant common ancestor.

This study and its findings are subject to limitations. Though many patients exhibiting malaria symptoms were enrolled in Djibouti City, no other areas of the country are represented by this sample set, so these conclusions and estimates could not necessarily be applied nationwide. However, Djibouti

City accounts for 95% of the country's malaria case load and Général Peltier Hospital is the largest hospital in the region, and previous reports have found *P. falciparum* in Djibouti to be of overall low diversity (*28*,*29*). Furthermore, the Djibouti Ministry of Health considered these results sufficiently representative to mandate a nationwide RDT policy change. Without the recent travel history of enrolled participants, we cannot state all *P. falciparum* parasites analyzed in this study originated in Djibouti. Quality microscopy could not be performed uniformly on these blood samples, so we were unable to obtain visual confirmation of *P. falciparum*. In addition, because of laboratory workflow, RDT results from enrollment could not be reliably linked with venous blood samples and therefore were not compared directly with laboratory data. However, the 4 samples collected in December 2019 that triggered this investigation demonstrated *pfhrp2/3* deletions causing known false-negative results by HRP2-based RDT.

In conclusion, results from both antigen detection and *pfhrp2/3* molecular genotyping provide evidence of a high prevalence of symptomatic malaria cases in Djibouti caused by *P. falciparum* lacking functional *pfhrp2/3* genes. These findings, coupled with high occurrence of monoclonal infections and single *pfhrp2*-deleted infections, suggest that nearly 70% of HRP2-based RDTs would return negative results for *P. falciparum* infection in Djibouti, which is expected to have serious negative health impacts on the community. Djibouti *P. falciparum* parasites with gene deletions are most closely related to other parasites in the Horn of Africa with a recent common ancestor or routine importation from Ethiopia. Gene-deleted haplotypes show no evidence of importation from South America.

Acknowledgments

We thank the staff of Général Peltier Hospital and Ghosem Zamani, who greatly assisted with this investigation.

The Bill and Melinda Gates Foundation and Centers for Disease Control and Prevention provided funding for this study.

About the Author

Dr. Rogier is a microbiologist in the Malaria Branch, Division of Parasitic Diseases and Malaria, Center for Global Health, Centers for Disease Control and Prevention. His laboratory develops multiplex serologic assays for the detection of antibodies and antigens against infectious diseases and works to interpret this serologic data for making assumptions about population-level epidemiology and disease transmission.

References

1. Poti KE, Sullivan DJ, Dondorp AM, Woodrow CJ. HRP2: transforming malaria diagnosis, but with caveats. Trends Parasitol. 2020;36:112–26. https://doi.org/10.1016/j.pt.2019.12.004
2. Rogier E, Hamre KES, Joseph V, Plucinski MM, Presume J, Romilus I, et al. Conventional and high-sensitivity malaria rapid diagnostic test performance in 2 transmission settings: Haiti 2017. J Infect Dis. 2020;221:786–95.
3. Lee N, Gatton ML, Pelecanos A, Bubb M, Gonzalez I, Bell D, et al. Identification of optimal epitopes for *Plasmodium falciparum* rapid diagnostic tests that target histidine-rich proteins 2 and 3. J Clin Microbiol. 2012;50:1397–405. https://doi.org/10.1128/JCM.06533-11
4. Baker J, Ho MF, Pelecanos A, Gatton M, Chen N, Abdullah S, et al. Global sequence variation in the histidine-rich proteins 2 and 3 of *Plasmodium falciparum*: implications for the performance of malaria rapid diagnostic tests. Malar J. 2010;9:129. https://doi.org/10.1186/1475-2875-9-129
5. World Health Organization. Malaria rapid diagnostic test performance: results of WHO product testing of malaria RDTs: round 8 (2016–2018). Geneva: The Organization; 2018.
6. Kong A, Wilson SA, Ah Y, Nace D, Rogier E, Aidoo M. HRP2 and HRP3 cross-reactivity and implications for HRP2-based RDT use in regions with *Plasmodium falciparum* hrp2 gene deletions. Malar J. 2021;20:207. https://doi.org/10.1186/s12936-021-03739-6
7. Gamboa D, Ho MF, Bendezu J, Torres K, Chiodini PL, Barnwell JW, et al. A large proportion of *P. falciparum* isolates in the Amazon region of Peru lack *pfhrp2* and *pfhrp3*: implications for malaria rapid diagnostic tests. PLoS One. 2010;5:e8091. https://doi.org/10.1371/journal.pone.0008091
8. Thomson R, Parr JB, Cheng Q, Chenet S, Perkins M, Cunningham J. Prevalence of *Plasmodium falciparum* lacking histidine-rich proteins 2 and 3: a systematic review. Bull World Health Organ. 2020;98:558–568F. https://doi.org/10.2471/BLT.20.250621
9. World Health Organization. World malaria report 2019. Geneva: The Organization; 2019.
10. Berhane A, Anderson K, Mihreteab S, Gresty K, Rogier E, Mohamed S, et al. Major threat to malaria control programs by *Plasmodium falciparum* lacking histidine-rich protein 2, Eritrea. Emerg Infect Dis. 2018;24:462–70. https://doi.org/10.3201/eid2403.171723
11. Girma S, Cheaveau J, Mohon AN, Marasinghe D, Legese R, Balasingam N, et al. Prevalence and epidemiological characteristics of asymptomatic malaria based on ultrasensitive diagnostics: a cross-sectional study. Clin Infect Dis. 2019;69:1003–10. https://doi.org/10.1093/cid/ciy1005
12. Feleke SM, Reichert EN, Mohammed H, Brhane BG, Mekete K, Mamo H, et al. *Plasmodium falciparum* is evolving to escape malaria rapid diagnostic tests in Ethiopia. Nat Microbiol. 2021;6:1289–99. https://doi.org/10.1038/s41564-021-00962-4
13. Iriart X, Menard S, Chauvin P, Mohamed HS, Charpentier E, Mohamed MA, et al. Misdiagnosis of imported *falciparum* malaria from African areas due to an increased prevalence of *pfhrp2/pfhrp3* gene deletion: the Djibouti case. Emerg Microbes Infect. 2020;9:1984–7. https://doi.org/10.1080/22221751.2020.1815590
14. Rogier E, Nace D, Ljolje D, Lucchi NW, Udhayakumar V, Aidoo M. Capture and Detection of *Plasmodium vivax* Lactate Dehydrogenase in a Bead-Based Multiplex Immunoassay. Am J Trop Med Hyg. 2020;102:1064–7. https://doi.org/10.4269/ajtmh.19-0772
15. Plucinski MM, Herman C, Jones S, Dimbu R, Fortes F, Ljolje D, et al. Screening for Pfhrp2/3-deleted *Plasmodium*

falciparum, non-falciparum, and low-density malaria infections by a multiplex antigen assay. J Infect Dis. 2019;219:437–47. https://doi.org/10.1093/infdis/jiy525
16. Lucchi NW, Narayanan J, Karell MA, Xayavong M, Kariuki S, DaSilva AJ, et al. Molecular diagnosis of malaria by photo-induced electron transfer fluorogenic primers: PET-PCR. PLoS One. 2013;8:e56677. https://doi.org/10.1371/journal.pone.0056677
17. Abdallah JF, Okoth SA, Fontecha GA, Torres RE, Banegas EI, Matute ML, et al. Prevalence of pfhrp2 and pfhrp3 gene deletions in Puerto Lempira, Honduras. Malar J. 2015;14:19. https://doi.org/10.1186/s12936-014-0537-7
18. Bharti PK, Chandel HS, Ahmad A, Krishna S, Udhayakumar V, Singh N. Prevalence of pfhrp2 and/or pfhrp3 gene deletion in *Plasmodium falciparum* population in eight highly endemic states in India. PLoS One. 2016;11:e0157949. https://doi.org/10.1371/journal.pone.0157949
19. Jones S, Subramaniam G, Plucinski MM, Patel D, Padilla J, Aidoo M, et al. One-step PCR: a novel protocol for determination of pfhrp2 deletion status in *Plasmodium falciparum*. PLoS One. 2020;15:e0236369. https://doi org/10.1371/journal.pone.0236369
20. Uwimana A, Umulisa N, Venkatesan M, Svigel SS, Zhou Z, Munyaneza T, et al. Association of *Plasmodium falciparum* kelch13 R561H genotypes with delayed parasite clearance in Rwanda: an open-label, single-arm, multicentre, therapeutic efficacy study. Lancet Infect Dis. 2021;21:1120–8. https://doi.org/10.1016/S1473-3099(21)00142-0
21. Bakari C, Jones S, Subramaniam G, Mandara CI, Chiduo MG, Rumisha S, et al. Community-based surveys for *Plasmodium falciparum* pfhrp2 and pfhrp3 gene deletions in selected regions of mainland Tanzania. Malar J. 2020;19:391. https://doi.org/10.1186/s12936-020-03459-3
22. Daniels RF, Chenet S, Rogier E, Lucchi N, Herman C, Pierre B, et al. Genetic analysis reveals unique characteristics of *Plasmodium falciparum* parasite populations in Haiti. Malar J. 2020;19:379. https://doi.org/10.1186/s12936-020-03439-7
23. Parr JB, Kieto E, Phanzu F, Mansiangi P, Mwandagalirwa K, Mvuama N, et al. Analysis of false-negative rapid diagnostic tests for symptomatic malaria in the Democratic Republic of the Congo. Sci Rep. 2021;11:6495. https://doi.org/10.1038/s41598-021-85913-z
24. Herman C, Huber CS, Jones S, Steinhardt L, Plucinski MM, Lemoine JF, et al. Multiplex malaria antigen detection by bead-based assay and molecular confirmation by PCR shows no evidence of Pfhrp2 and Pfhrp3 deletion in Haiti. Malar J. 2019;18:380. https://doi.org/10.1186/s12936-019-3010-9
25. Gatton ML, Dunn J, Chaudhry A, Ciketic S, Cunningham J, Cheng Q. Implications of parasites lacking *Plasmodium falciparum* histidine-rich protein 2 on malaria morbidity and control when rapid diagnostic tests are used for diagnosis. J Infect Dis. 2017;215:1156–66. https://doi.org/10.1093/infdis/jix094
26. de Santi VP, Khaireh BA, Chiniard T, Pradines B, Taudon N, Larréché S, et al. Role of *Anopheles stephensi* mosquitoes in malaria outbreak, Djibouti, 2019. Emerg Infect Dis. 2021;27:1697–700. https://doi.org/10.3201/eid2706.204557
27. World Health Organization. Response plan to pfhrp2 gene deletions. Geneva: The Organization; 2019.
28. Khaireh BA, Assefa A, Guessod HH, Basco LK, Khaireh MA, Pascual A, et al. Population genetics analysis during the elimination process of *Plasmodium falciparum* in Djibouti. Malar J. 2013;12:201. https://doi.org/10.1186/1475-2875-12-201
29. Rogier C, Pradines B, Bogreau H, Koeck JL, Kamil MA, Mercereau-Puijalon O. Malaria epidemic and drug resistance, Djibouti. Emerg Infect Dis. 2005;11:317–21. https://doi.org/10.3201/eid1102.040108

Address for correspondence: Eric Rogier, Centers for Disease Control and Prevention, 1600 Clifton Rd NE, Mailstop D67, Atlanta, GA, 30329-4027, USA; email: erogier@cdc.gov

Transmission Dynamics and Effectiveness of Control Measures during COVID-19 Surge, Taiwan, April–August 2021

Andrei R. Akhmetzhanov, Hao-Yuan Cheng, Natalie M. Linton, Luis Ponce, Shu-Wan Jian, Hsien-Ho Lin

An unprecedented surge of COVID-19 cases in Taiwan in May 2021 led the government to implement strict nationwide control measures beginning May 15. During the surge, the government was able to bring the epidemic under control without a complete lockdown despite the cumulative case count reaching >14,400 and ≥780 deaths. We investigated the effectiveness of the public health and social measures instituted by the Taiwan government by quantifying the change in the effective reproduction number, which is a summary measure of the ability of the pathogen to spread through the population. The control measures that were instituted reduced the effective reproduction number from 2.0–3.3 to 0.6–0.7. This decrease was correlated with changes in mobility patterns in Taiwan, demonstrating that public compliance, active case finding, and contact tracing were effective measures in preventing further spread of the disease.

SARS-CoV-2, the pathogen causing COVID-19, began infecting humans in Wuhan, China, in December 2019. Within 1 year, SARS-CoV-2 spread to nearly all countries, and >178 million infections and 3.7 million deaths were reported by April 2021. Taiwan, an island with 23.8 million inhabitants, reported only slightly more than 1,000 cases by April 2021, despite being located close to the original epicenter of the COVID-19 outbreak. At that time, most infections confirmed in Taiwan were acquired abroad, and <10% were acquired locally.

The subsequent emergence of more transmissible SARS-CoV-2 variants led to multiple introductions from those traveling to and from Taiwan, initiating cryptic transmissions in the capital city of Taipei and its surroundings in April 2021. Newly detected clusters of the virus led to an explosive growth in cases, and daily reported case numbers reached 200 by mid-May. The sudden increase in cases prompted the government to implement stricter control measures to prevent disease spread, and those measures proved effective in bringing the epidemic under control by the end of July. Those preventive measures included restricting public movement, enforcing compulsory shortening of business hours, implementing work-from-home for nonessential businesses, banning in-restaurant dining, and canceling social and religious gatherings. By October 2021, Taiwan was again reporting 0 cases daily.

The initial clusters of infections in 2021 were linked to international pilots and flight crew members, but the major epidemic hotspots were identified as owners and visitors of tea houses, which are landmarks in some districts of Taipei. Although tea houses in Taipei typically offer tea and other refreshments during the day, some also conduct business in the evening, when the potential for activities that increase risk for the transmission of SARS-CoV-2 (e.g., close physical contact) is greater and timely detection of infections can be hindered (*1*–*3*). In nightlife districts across the city, patrons and staff of tea houses and other establishments often are unwilling to share contact and travel histories with public health officials. Outside of Taipei and New Taipei City, clusters of infections were frequently linked to factories or other production sites, affecting vulnerable social groups such as migrant workers. Some initial clusters were linked to local markets and initiated by vendors traveling to the Taipei area for commercial purposes.

Author affiliations: National Taiwan University College of Public Health, Taipei, Taiwan (A.R. Akhmetzhanov, L. Ponce, H.-H. Lin); Taiwan Centers for Disease Control, Epidemic Intelligence Center, Taipei (H.-Y. Cheng, S.-W. Jian); Hokkaido University Graduate School of Medicine, Sapporo, Japan (N.M. Linton)

DOI: http://doi.org/10.3201/eid2810.220456

The effective reproduction number, R_t, has played a pivotal role in evaluating the effectiveness of various public health and social measures (PHSMs) during the COVID-19 pandemic (*4*–*6*). R_t is defined as the average number of secondary transmissions caused by a primary case at a given time while interventions, existing immunity, or other mediating factors are present. During the pandemic, R_t was used frequently as a data point to inform decision- and policy-making processes, because the value of R_t relative to the threshold value of 1 can be interpreted as an indicator for when PHSMs should be implemented, strengthened, or relaxed (*7*,*8*). Among the various PHSMs that might be used, stay-at-home orders, cancelling leisure activities, and restaurant-based interventions were found to be largely ineffective in curbing COVID-19 transmission in the United States (*9*). In contrast, strong social distancing, school closures, and widespread mask-wearing were found to be quite effective in mitigating the spread of COVID-19 in both the United States and elsewhere (*10*–*12*). One study found that only strict (complete) lockdowns could curb the spread of infections and reduce R_t to <1 (*5*). However, responses to the virus in Taiwan and Japan demonstrate that less extreme measures (i.e., without the implementation of a complete lockdown) were sufficient in preventing a wide, rampant spread of COVID-19 during the epidemic and returning daily counts to an acceptable level (<10 cases). The government's response to the surge of COVID-19 cases in Taiwan that began in May 2021 presents a striking example of how public compliance with such less extreme preventive measures successfully quelled a burgeoning epidemic wave.

Among various possible ways to estimate R_t, the instantaneous reproduction number based on the method of Cori et al. (*13*) has often been used during the COVID-19 pandemic to describe current epidemiologic situations (*14*,*15*) or to forecast future incidence (*16*). Predicting the real-time R_t value and accounting for covariates has been recognized as an important step toward the future real-time monitoring of disease spread in different countries (*17*–*21*).

Taiwan reported extremely low numbers of confirmed COVID-19 cases in 2020, offering an example of a relatively efficient prevention strategy against the spread of SARS-CoV-2 (*22*). The government instituted a 4-level system to efficiently contain and mitigate COVID-19 epidemics (Appendix Table 1, https://wwwnc.cdc.gov/EID/article/28/10/22-0456-App1.pdf). Before April 2021, the largest cluster of locally acquired infections had only 22 confirmed cases (*23*). Of the various factors contributing to Taiwan's early pandemic success, the key components were strict border control, public compliance with untargeted PHSMs (e.g., mask-wearing, proactive case finding, and contact tracing), and use of digital technologies, such as QR codes (*24*). However, the increased transmissibility of subsequent SARS-CoV-2 variants and low levels of vaccine coverage posed significant challenges for COVID-19 containment in Taiwan in 2021. We investigated the effectiveness of the public health and social measures instituted by the Taiwan government during the 2021 COVID-19 surge by quantifying the change in R_t.

Methods

Data Collection

We retrieved line list data from publicly available sources and Taiwan Centers for Disease Control reports (*25*). The combined dataset from these sources contained de-identified case records, including information on symptom onset date (when available), case confirmation date, confirmed date of death, level of severity of the infection (asymptomatic/mild, moderate, severe), and information on residency. The 3 categories of disease severity (mild, moderate, severe) were assigned in accordance with the World Health Organization definition (*26*). We extracted mobility metrics from community reports provided by Google (*27*). The 6 metrics used fell into the following categories: "grocery and pharmacy," "parks," "residential," "retail and recreation," "transit stations," and "workplaces." We quantified each metric by a daily change in the median mobility when compared with the baseline median for the 5-week period January 3–February 6, 2020.

Estimating Epidemiologic Parameters

We fitted time intervals from symptom onset to case confirmation, onset to severe disease, onset to death, and onset to report of death (as well as from death to report of death) to a mixture of 3 distributions (gamma, Weibull, and log-normal) (*23*). We then fitted the serial interval distribution to left-shifted gamma, Weibull, and log-normal distributions (to account for negative values). We estimated all parameters within a Bayesian framework, using a doubly censored likelihood with right truncation and Markov chain Monte Carlo simulations (*28*,*29*). To improve convergence of the mixture model, we set the mean and SDs to be common to the 3 distributions, as has been proposed for Bayesian model averaging (M. Keller et al., unpub. data, https://doi.org/10.48550/arXiv.1711.10016). We estimated the reporting delay, which is the time from symptom onset to

case confirmation, under 2 scenarios: when the distribution was unchanged over time, and when the parameters of the distribution were varied in time (*30*).

We estimated R_t using date of symptom onset and date of infection (*13*,*31*). When R_t was classified by date of symptom onset, the expected case count on day t was proportional to R_t and a convolution of case counts on previous days with the serial interval distribution. When R_t was classified by date of infection, the formula had a more complicated form and contained a double convolution, involving the incubation period and profile of infectiousness (*31*,*32*) (Appendix). Because some case records did not contain information on symptom onset date, we back-projected those cases from the date the case was confirmed to a presumptive date of symptom onset, using a time-varied distribution of the reporting delay.

Results

Epidemiologic Situation

Little to no local transmission of SARS-CoV-2 was reported in Taiwan before April 2021. Vaccine coverage was also arbitrarily low (<1%) at that time. There were, however, multiple clusters of infections during the latter half of April 2021, followed by a wave of COVID-19 cases at the beginning of May 2021 (Figure 1, panel A). A total of 14,442 cases associated with the epidemic wave were confirmed by August 25, 2021, including 5,029 (34.8%) persons who were asymptomatic at the time of testing and 3,093 (21.4%) persons recognized as having severe disease. Among patients requiring hospitalization, 238 (1.6%) had nonsevere pneumonia, 2414 (16.7%) had severe pneumonia, and 441 (3.1%) had acute respiratory distress syndrome (Table). A total of 779 persons (5.4%) died during the epidemic wave. Most (701, 90%) of the deceased patients had known underlying chronic conditions. Eight additional deaths among patients in the study population were unrelated to SARS-CoV-2 infection.

The median age of persons with confirmed cases was 51 years; 23.9% were ≥65 years of age, 51.9% 45–64 years of age, 18.3% 18–44 years of age, and 5.9% <18 years of age. Only 0.4% of patients <18 years were categorized as having moderate disease, and half (50.3%) of these younger patients were reported as asymptomatic at the time of testing. In contrast, 46.6% of those ≥65 years of age experienced moderate symptoms, and 22.3% were asymptomatic at the time of testing. The median age of patients who died was 72 years, and 79.8% of deaths were reported among those ≥65 years of age. Men accounted for most deaths (63.5%). Geographically, a substantial portion of the infections (1,874 cases, 13.0% of the total) were confirmed among residents of Wanhua District in Taipei (Figure 1, panel B).

The median time from date of symptom onset to date of case confirmation was estimated at 3.0 days (95% CI 0.7–11.9 days). The time required for disease progression from symptom onset to severe disease was an average of 7.7 days (95% CI 2.1–28.5 days). Death was observed, on average, 13.3 days after symptom onset (95% CI 1.1–92.4 days). Deaths were reported an average of 3.5 days thereafter (95% CI 1.0–12.3 days).

R_t and Efficiency of PHSMs

When quantifying R_t by date of symptom onset, we noted that the value remained relatively stable, with values of ≈2–3 before the surge of COVID-19 cases reported around May 10, 2021 (Figure 2, panel A). We estimated the median posterior value of R_t to exceed 3 during the first week of May, likely because of cryptic community transmission; confirmed cases with symptom onset in the first week of May had prolonged reporting delays of nearly 10 days (Figure 2, panel B, orange line), and later cases generally had shorter reporting delays of ≈3–4 days. The reporting delay quantified by date of case confirmation peaked around May 16 (Figure 2, panel B, gray line). The test-positivity rate for SARS-CoV-2 also reached its highest around the same dates (Figure 2, panel B, blue line). These results indicate that cases with earlier symptom onset dates had longer reporting delays compared with subsequent cases and serve as an indicator of persistent cryptic transmission of SARS-CoV-2 in the community between the end of April and the beginning of May 2021.

Next, we quantified the effective reproduction number by infection date and tied it to PHSMs (Figure 2, panels C, D). Taiwan adopted a 4-tier system of restrictions ranging from level 1 at the lowest to level 4 at the highest (Appendix Table 1). Level 2 restrictions began on May 11, 2021; level 3 restrictions began in Taipei and New Taipei City on May 15 and then expanded to the rest of Taiwan on May 19. Level 3 measures were further strengthened on May 29. We estimated the posterior mean R_t in the early stage of the epidemic—before level 2 restrictions began—at 2.85 (95% CI 2.51–3.26). Implementation of level 2 measures on May 11 was followed by a slightly decreased mean of 2.40 (95% CI 1.99–2.86), and level 3 measures in Taipei City and New Taipei City on May 15 further decreased the mean value to 1.59 (95% CI 1.30–1.90). Nonetheless, these measures were insufficient to bring the R_t consistently below 1. Only

after level 3 measures were expanded to all of Taiwan on May 19 did the mean R_t decrease to below 1 (0.86 [95% CI 0.76–0.95]). R_t then dropped even further when those measures were strengthened on May 29 by prohibiting dine-in services and setting up a work-from-home order (0.65 [95% CI 0.57–0.74]).

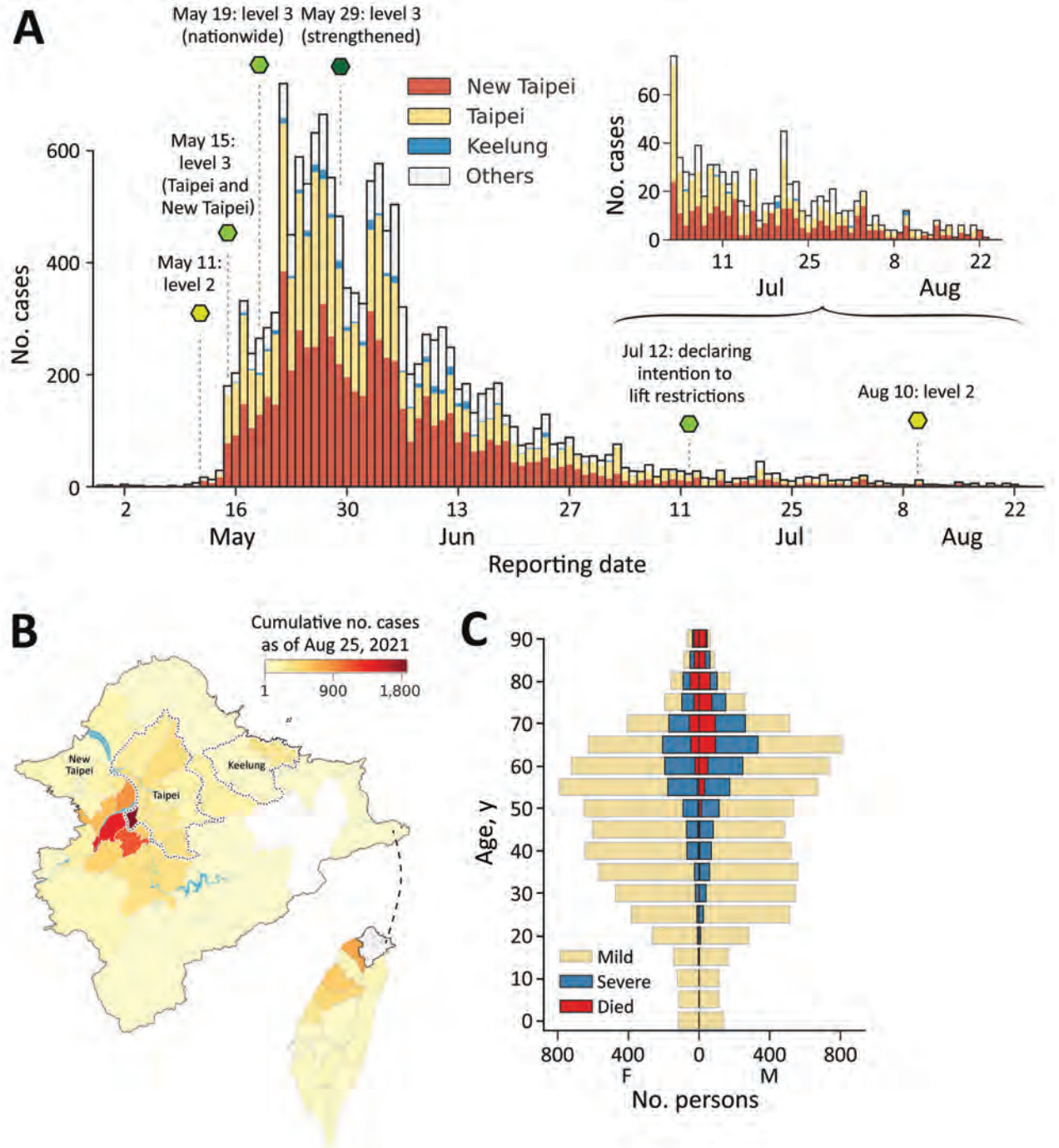

Figure 1. Epidemic wave of COVID-19 in Taiwan, April–August 2021. A) Epidemiologic curve of confirmed COVID-19 cases by reporting date, stratified by geographic area. Dashed lines and hexagons indicate timing and description of major public health and social measures; variation in hexagon colors shows relative strictness of measures, ranging from light to dark green. B) Geographic distribution of cases. The colormap indicates the cumulative number of cases confirmed by August 25, 2021, at district level for Taipei, New Taipei City, and Keelung and at county level for all other areas (indicated in gray in panel A). Inset shows location of enlarged area in Taiwan. C) Age pyramid of confirmed cases specified by known severity status or death. Age and spatial distribution of fatalities is shown in Appendix Figure 4 (https://wwwnc.cdc.gov/EID/article/28/10/22-0456-App1.pdf)

Table. Demographic and clinical characteristics of persons with confirmed COVID-19 cases, by geographic region, Taiwan, April 23, 2021–August 25, 2021*

Characteristic	No. (%)			
	Taiwan	Taipei	New Taipei City	Other counties
Age group				
<17	845 (5.9)	225 (4.6)	410 (6.0)	210 (7.7)
17–34	2,660 (18.4)	642 (13.2)	1,168 (17.0)	850 (31.0)
15–64	7,489 (51.9)	2,629 (54.2)	3,656 (53.3)	1,204 (44.0)
>64	3,448 (23.9)	1,354 (27.9)	1,620 (23.6)	474 (17.3)
Sex				
F	7,149 (49.5)	2,502 (51.6)	3,387 (49.4)	1,260 (46.0)
M	7,293 (50.5)	2,348 (51.6)	3,467 (49.4)	1,478 (54.0)
Severity				
Mild/asymptomatic	11,349 (78.6)	3,807 (78.5)	5,309 (77.5)	2,233 (81.6)
Severe	3,093 (21.4)	1,043 (21.5)	1,545 (22.5)	505 (18.4)
Known to be symptomatic				
No	5,037 (34.9)	1,710 (35.3)	2,193 (32.0)	1,134 (41.4)
Yes	9,405 (65.1)	3,140 (64.7)	4,661 (68.0)	1,604 (58.6)
Total	14,442	4,850 [33.6]	6,854 [47.5]	2,738 [19.0]

*Parentheses indicate a columnwise fraction of cases within each group. Brackets indicate a rowwise proportion of cases.

These estimates prompted our further investigation into why the initial set of level 3 measures implemented on May 15 for Taipei and New Taipei City and on May 19 nationwide were insufficient to bring R_t substantially below 1. We estimated R_t by infection date using 2 different functions of time. First, R_t was modeled by a piecewise constant function of time with equidistant time windows (e.g., 5 or 7 days). Second, the change in R_t was correlated with the observed change in community mobility across 6 different community metrics (see Methods).

When we modeled R_t using a piecewise constant function of time, we observed a pattern similar to that of R_t by date of symptom onset, except that the pattern was time-lagged (compare Figure 3, panel A, and Figure 2, panel A). The temporal pattern also resembled the change in various mobility metrics over time (compare Figure 3, panel A, and Figure 3, panel B). However, the posterior mean of R_t did not increase after July 12, even though some mobility metrics previously recognized as important for explaining the transmission potential of COVID-19 (*17*) (e.g., retail and recreation, transit stations, and workplaces) continued to increase over time. To address this contradiction, we theorized that the basic reproduction number (R_0) changed over time. The time-variability of R_0 represented the proxy measure of changing contact rate of infected and susceptible individuals over time and served as an indicator of PHSMs, including the voluntary changes in public behavior (*33*). When we defined it by a monotonically decreasing sigmoidal function over time, the corresponding model fit the data better. We compared a model with a time-varied R_0 with a model with a constant R_0 using a "leave-one-out" information criteria (LOOIC), which is used in Bayesian frameworks for model selection (*34*). The model with a time-varied R_0 had a lower median LOOIC value (884.2) compared with that of the model that used a constant R_0 (899.6) (Appendix Figure 5). The fit resulted in the change point of R_0 on approximately July 19, and R_0 decreased from a median of 3.17 at the beginning of the epidemic to 1.72 at the end of the epidemic (defined as August 14), a 46% reduction.

We additionally investigated the association of different mobility metrics with R_t. The model with only 3 mobility metrics showed a fairly indistinguishable data fit compared to models with 4 to 6 mobility metrics, and the difference in LOOIC values was <2 (ΔLOOIC ≤1.56). By sequentially fitting the models with 1, 2, and 3 metrics, we identified that the most significant metrics describing the individual mobility were transit stations, workplaces, and grocery stores and pharmacies (Figure 3, panel D).

We investigated counterfactual scenarios wherein level 3 measures had been implemented either earlier or later than the actual May 15 date (Figure 4). If the level 3 measures had been delayed by just 3 days, the size of the epidemic on August 14 likely would have been double that of the baseline scenario (23,900 cases [95% CI 7,900–61,500)] vs. 12,500 cases [95% CI 4,000–29,800]) or the actual case count (14,400). Beginning level 3 measures 3 days earlier likely would have resulted in only 6,400 cases (95% CI 2,200–15,600) (Appendix Figure 6). Varying the date of level 3 implementation revealed a nonlinear, exponential-like relationship whereby a longer delay would accelerate the increase in the final epidemic size.

Discussion

In this study, we analyzed the spread of SARS-CoV-2 in Taiwan during April–August 2021 and quantified

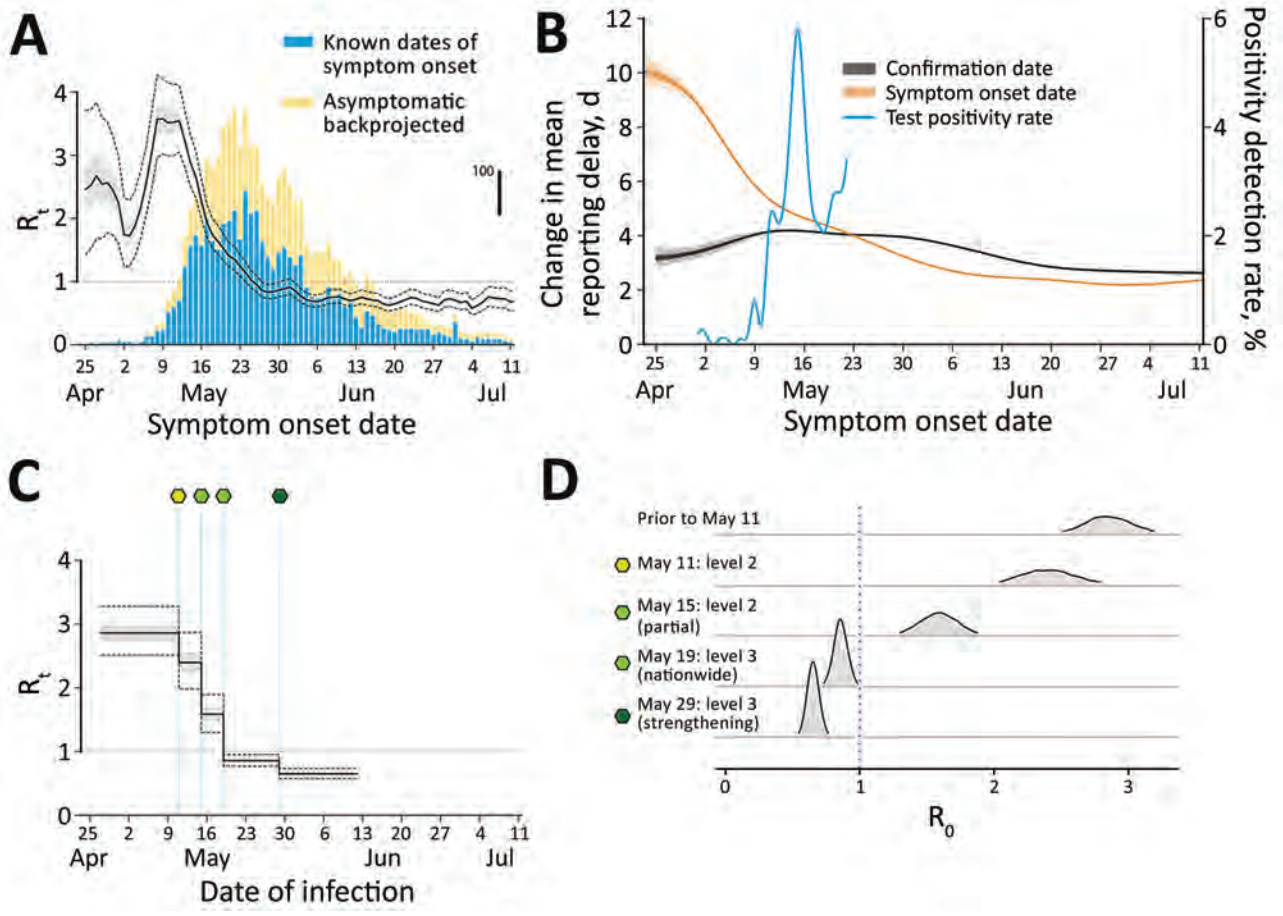

Figure 2. Comparison of Rt inferred by infection date with Rt by symptom onset date during epidemic wave of COVID-19 in Taiwan, April–August 2021. A) Rt by infection date (overlay) is notably shifted to the left compared with symptom onset date. Black line indicates mean; light gray shading indicates interquartile range; dotted lines indicate 95% CI. Bars indicate the nowcasted daily incidence of COVID-19 cases; vertical scale is indicated by thick black line on the right. B) Change in the mean reporting delay, which is the time between symptom onset date and confirmation date, over time, characterized by either the date of symptom onset (orange) or by confirmation date (black). Dark gray shading indicates IQR; light gray shading indicates 95% CI. The blue line indicates the test positivity rate that peaked around May 16 (axis on the right). C, D) The estimated Rt by date of infection, linked to public health and social measures (green-shaded hexagons, as defined in panel D). Rt, effective reproduction number.

the effectiveness of PHSMs implemented by the government. Initial COVID-19 cases had longer reporting delays, and there was a higher test-positivity rate at the beginning of the outbreak (Figure 1). Shortening of the reporting delay over time (Figure 2, panel B) indicated better management of the outbreak in later periods. Our results also showed that implementing stricter PHSMs on May 29, 2021 (Appendix Table 2), was followed by R_t falling below 1. We conclude that the timing of introduction of PHSMs by the government was judicious, and postponement by ≥3 days would have likely more than doubled the final size of the outbreak.

Because the number of cases grows exponentially at the beginning of an outbreak, delaying PHSMs by just 3 days can lead to a significant increase in the disease burden and can double the final epidemic size. Given the indications that the healthcare system of Taiwan was close to being overwhelmed with COVID-19 patients in mid-May, the actual timing of level 3 measures on May 15 likely prevented an even larger healthcare crisis. Although an earlier introduction of PHSMs could have substantially improved the situation, the low case numbers might have caused some public misunderstanding regarding the necessity of strict prevention measures when there was no evidence of escalating case counts. It is fortunate that the government of Taiwan acted in accordance with the country's 4-level COVID-19 alert system criteria by implementing stricter PHSMs as soon as possible (Appendix Table 2).

The April–August 2021 epidemic wave was the first such large-scale wave seen in Taiwan. Using

Bayesian statistical inference of the effective reproduction number by date of infection, we were able to attribute reductions in R_t to the implementation of PHSMs and estimate their effectiveness. The value of R_t only fell below 1 (95% CI 0.57–0.74) consistently after the PHSMs were further strengthened. We base this result, however, largely on model assumptions, so the association might be confounded by behaviors not accounted for in the models.

Even assuming only 1 in 5 COVID-19 cases was confirmed, the cumulative number of cases would have reached fewer than 100,000 cases, according to our models. In 2022, however, Taiwan experienced a much larger outbreak associated with the Omicron variant, during which the total number of confirmed cases exceeded 4 million. Given Omicron's higher transmissibility and greater capacity for evading immunity, coupled with pandemic fatigue and high vaccination coverage of the Taiwanese population (80.2% for the second dose and 60.1% for the booster dose as of May 2, 2022), the government chose to relax PHSMs such as proactive case finding and contact tracing in mid-May 2022. As a result, a direct comparison between the pandemic situation in 2021 we have described and the 2022 Omicron wave is not possible.

Using mobility metrics, which are the proxies of contact rates in different settings, was unable to completely capture the temporal change in R_t. However, the additional assumption of a simultaneous decrease in R_0 at later stages of the epidemic adequately explained the observed dynamics. This decrease could likely be a result of higher efficiency in terms of case finding and contact tracing when the number of cases was significantly lower compared with the efficiency in gathering that information at the peak of the epidemic wave.

In regard to study limitations, we did not distinguish fully asymptomatic infections from those that were asymptomatic at the time of testing but became

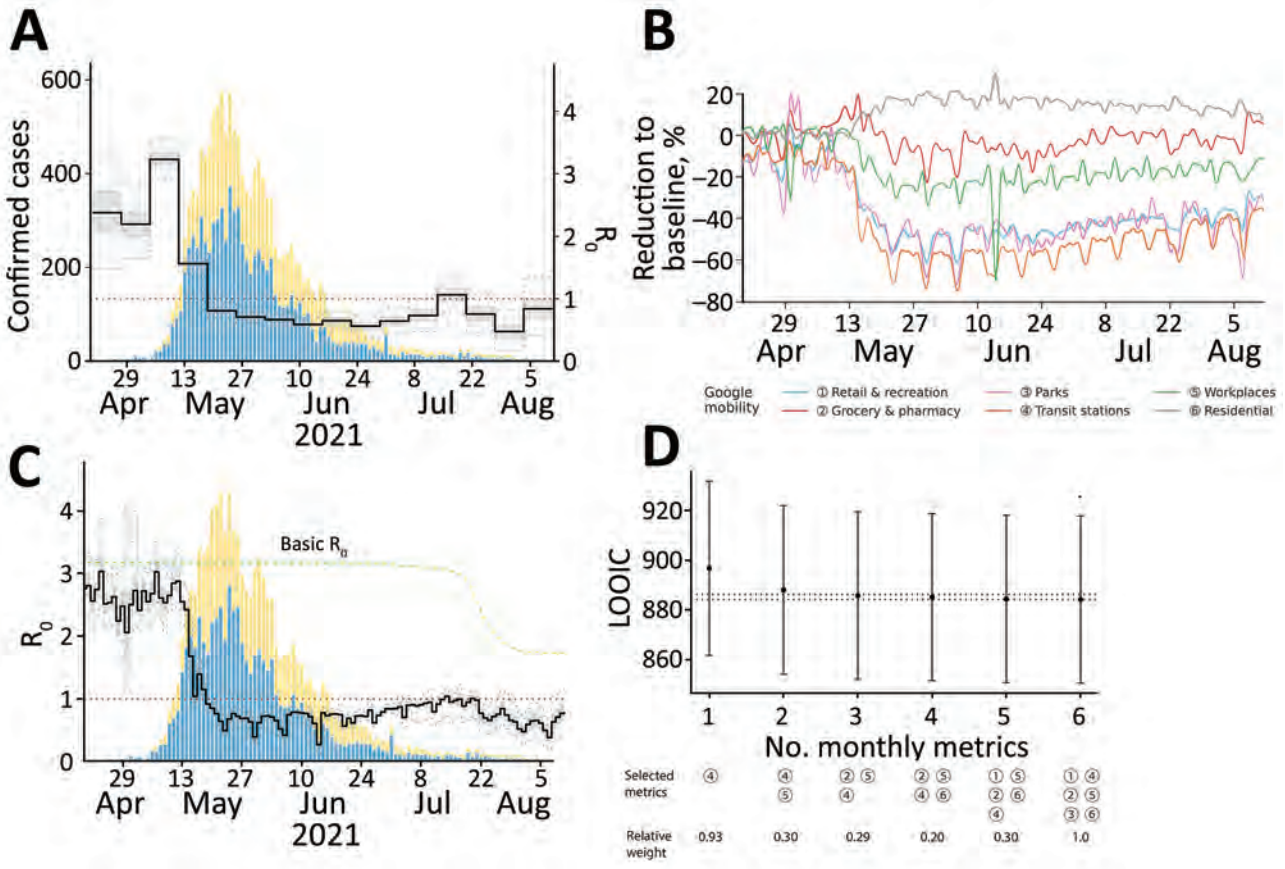

Figure 3. . Rt by infection date and its link to mobility patterns for epidemic wave of COVID-19 in Taiwan, April–August 2021. A) The change in Rt modeled by a piecewise constant function with a 7-day time window. B) The Rt inferred based on monotonically decreasing basic reproduction number (green) and 6 mobility metrics. C) The temporal dynamics of mobility metrics. D) Comparison of different models based on LOOIC values under a restricted number of mobility metrics (numbers defined in panel B). The legend indicates the set of metrics with highest probability of selection shown by relative weight. Dashed lines contain the region where the change in LOOIC values does not exceed 2 from the minimum, implying a relatively equivalent fit to the data; error bars indicate SD. The blue and yellow bars in A and C are the same as in Figure 2, panel A. LOOIC, leave-one-out information criteria; Rt, effective reproduction number.

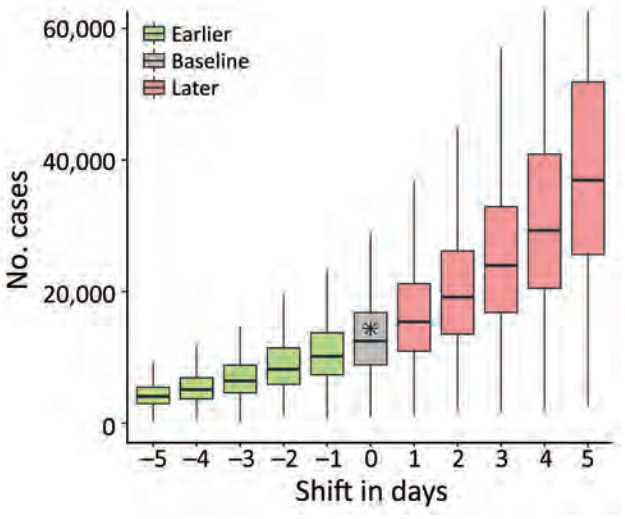

Figure 4. Epidemic wave of COVID-19 in Taiwan, April–August 2021. Model shows impact on epidemic size (by August 14, 2021) of a delay in implementing level 3 prevention measures (Appendix Figure 2, https://wwwnc.cdc.gov/EID/article/28/10/22-0456-App1.pdf) or of implementing them earlier. Horizontal line within boxes indicate medians; box tops and bottoms indicate interquartile ranges; whiskers indicate 95% CIs. Gray box indicates baseline scenario; asterisk indicates observed data.

symptomatic later. We also did not account for age, sex, and spatial structures in our framework for estimating R_t; including those factors could have provided more insight into the transmission dynamics. We also did not distinguish high-risk and low-risk transmission venues in our statistical model, nor did we account for the contribution of superspreading events. We noted, with interest, that the Alpha variant was not the only variant detected among the locally acquired infections during the investigation period. An outbreak associated with the Delta variant also was reported in June 2021, which surfaced in Pingtung County in the south of Taiwan and was contained within 2 weeks. The cluster originated from 2 travelers who returned to Taiwan from Peru and involved a total of 17 cases.

In 2021, Taiwan's pandemic response demonstrated that, despite low levels of vaccine coverage, containment and elimination of COVID-19 remained feasible. The timely introduction of PHSMs helped Taiwan to avoid healthcare system collapse, and the PHSM strategies employed serve as an example for future outbreaks of emerging and re-emerging infectious diseases. In the case of SARS-CoV-2, the continued evolution of the virus toward higher transmissibility and immune evasion poses a continued threat. It is clear from the 2022 Omicron waves in Taiwan and elsewhere that high levels of vaccine coverage, although offering protection against severe disease, are insufficient in preventing transmission. PHSMs beyond vaccination might become necessary again for future SARS-CoV-2 epidemic waves.

Acknowledgments

The authors are grateful to Jenny Wu, Chih-Chan Lan, and Tzu-You Lin for helpful discussions and assistance in data collection and Taiwan public health authorities and institutions for surveillance, laboratory testing, epidemiological investigations, and data collection. A.R.A. thanks Katherine Thieltges for editing the first draft of this manuscript.

This study was approved by the Research Ethics Committee of National Taiwan University (202203HM021). A.R.A. was supported by the National Science and Technology Council, Taiwan (NSTC #111-2314-B-002-289).

About the Author

Dr. Akhmetzhanov is an assistant professor in the Global Health Program and Institute of Epidemiology and Preventive Medicine of the College of Public Health, National Taiwan University, Taiwan. His research interests include the epidemiology and prevention of infectious disease outbreaks.

References

1. Kang CR, Lee JY, Park Y, Huh IS, Ham HJ, Han JK, et al.; Seoul Metropolitan Government COVID-19 Rapid Response Team (SCoRR Team). Coronavirus disease exposure and spread from nightclubs, South Korea. Emerg Infect Dis. 2020;26:2499–501. https://doi.org/10.3201/eid2610.202573
2. Takaya S, Tsuzuki S, Hayakawa K, Kawashima A, Okuhama A, Kanda K, et al. Nightlife clusters of coronavirus disease in Tokyo between March and April 2020. Epidemiol Infect. 2020;148:e250. https://doi.org/10.1017/S0950268820002496
3. Oshitani H; Expert Members of The National COVID-19 Cluster Taskforce at The Ministry of Health, Labour and Welfare, Japan. Cluster-based approach to coronavirus disease 2019 (COVID-19) response in Japan—February–April 2020. Jpn J Infect Dis. 2020;73:491–3. https://doi.org/10.7883/yoken.JJID.2020.363
4. Pan A, Liu L, Wang C, Guo H, Hao X, Wang Q, et al. Association of public health interventions with the epidemiology of the COVID-19 outbreak in Wuhan, China. JAMA. 2020;323:1915–23. https://doi.org/10.1001/jama.2020.6130
5. Flaxman S, Mishra S, Gandy A, Unwin HJT, Mellan TA, Coupland H, et al.; Imperial College COVID-19 Response Team. Estimating the effects of non-pharmaceutical interventions on COVID-19 in Europe. Nature. 2020;584:257–61. https://doi.org/10.1038/s41586-020-2405-7
6. Di Domenico L, Sabbatini CE, Boëlle PY, Poletto C, Crépey P, Paireau J, et al. Adherence and sustainability of interventions informing optimal control against the COVID-19 pandemic. Commun Med (Lond). 2021;1:57. https://doi.org/10.1038/s43856-021-00057-5
7. Li Y, Campbell H, Kulkarni D, Harpur A, Nundy M,

Wang X, et al.; Usher Network for COVID-19 Evidence Reviews (UNCOVER) group. The temporal association of introducing and lifting non-pharmaceutical interventions with the time-varying reproduction number (*R*) of SARS-CoV-2: a modelling study across 131 countries. Lancet Infect Dis. 2021;21:193–202. https://doi.org/10.1016/S1473-3099(20)30785-4
8. Brauner JM, Mindermann S, Sharma M, Johnston D, Salvatier J, Gavenčiak T, et al. Inferring the effectiveness of government interventions against COVID-19. Science. 2021;371:eabd9338. https://doi.org/10.1126/science.abd9338
9. Yang B, Huang AT, Garcia-Carreras B, Hart WE, Staid A, Hitchings MDT, et al.; UFCOVID Interventions Team. Effect of specific non-pharmaceutical intervention policies on SARS-CoV-2 transmission in the counties of the United States. Nat Commun. 2021;12:3560. https://doi.org/10.1038/s41467-021-23865-8
10. Chernozhukov V, Kasahara H, Schrimpf P. The association of opening K-12 schools with the spread of COVID-19 in the United States: County-level panel data analysis. Proc Natl Acad Sci U S A. 2021;118:e2103420118. https://doi.org/10.1073/pnas.2103420118
11. Dighe A, Cattarino L, Cuomo-Dannenburg G, Skarp J, Imai N, Bhatia S, et al. Response to COVID-19 in South Korea and implications for lifting stringent interventions. BMC Med. 2020;18:321. https://doi.org/10.1186/s12916-020-01791-8
12. Ku D, Yeon C, Lee S, Lee K, Hwang K, Li YC, et al. Safe traveling in public transport amid COVID-19. Sci Adv. 2021;7:eabg3691. https://doi.org/10.1126/sciadv.abg3691
13. Cori A, Ferguson NM, Fraser C, Cauchemez S. A new framework and software to estimate time-varying reproduction numbers during epidemics. Am J Epidemiol. 2013;178:1505–12. https://doi.org/10.1093/aje/kwt133
14. Abbott S, Hellewell J, Thompson RN, Sherratt K, Gibbs HP, Bosse NI, et al. Estimating the time-varying reproduction number of SARS-CoV-2 using national and subnational case counts [version 2, peer review: 1 approved with reservations]. Wellcome Open Res. 2020;5:112. https://doi.org/10.12688/wellcomeopenres.16006.2
15. Röst G, Bartha FA, Bogya N, Boldog P, Dénes A, Ferenci T, et al. Early phase of the COVID-19 outbreak in Hungary and post-lockdown scenarios. Viruses. 2020;12:708. https://doi.org/10.3390/v12070708
16. Abbott S, Hellewell J, Sherratt K, Gostic K, Hickson J, Badr HS, et al. EpiNow2: estimate real-time case counts and time-varying epidemiological parameters. 2020 [cited 2022 Jul 15]. https://zenodo.org/record/4088545
17. Jung SM, Endo A, Akhmetzhanov AR, Nishiura H. Predicting the effective reproduction number of COVID-19: inference using human mobility, temperature, and risk awareness. Int J Infect Dis. 2021;113:47–54. https://doi.org/10.1016/j.ijid.2021.10.007
18. Knock ES, Whittles LK, Lees JA, Perez-Guzman PN, Verity R, FitzJohn RG, et al. Key epidemiological drivers and impact of interventions in the 2020 SARS-CoV-2 epidemic in England. Sci Transl Med. 2021;13:eabg4262. https://doi.org/10.1126/scitranslmed.abg4262
19. Leung K, Wu JT, Leung GM. Real-time tracking and prediction of COVID-19 infection using digital proxies of population mobility and mixing. Nat Commun. 2021;12:1501. https://doi.org/10.1038/s41467-021-21776-2
20. Lin Y, Yang B, Cobey S, Lau EHY, Adam DC, Wong JY, et al. Incorporating temporal distribution of population-level viral load enables real-time estimation of COVID-19 transmission. Nat Commun. 2022;13:1155. https://doi.org/10.1038/s41467-022-28812-9
21. Rüdiger S, Konigorski S, Rakowski A, Edelman JA, Zernick D, Thieme A, et al. Predicting the SARS-CoV-2 effective reproduction number using bulk contact data from mobile phones. Proc Natl Acad Sci U S A. 2021;118:e2026731118. https://doi.org/10.1073/pnas.2026731118
22. Summers J, Cheng HY, Lin HH, Barnard LT, Kvalsvig A, Wilson N, et al. Potential lessons from the Taiwan and New Zealand health responses to the COVID-19 pandemic. Lancet Reg Health West Pac. 2020;4:100044. https://doi.org/10.1016/j.lanwpc.2020.100044
23. Akhmetzhanov AR, Jung SM, Cheng HY, Thompson RN. A hospital-related outbreak of SARS-CoV-2 associated with variant Epsilon (B.1.429) in Taiwan: transmission potential and outbreak containment under intensified contact tracing, January–February 2021. Int J Infect Dis. 2021;110:15–20. https://doi.org/10.1016/j.ijid.2021.06.028
24. Wang CJ, Ng CY, Brook RH. Response to COVID-19 in Taiwan: big data analytics, new technology, and proactive testing. JAMA. 2020;323:1341–2. https://doi.org/10.1001/jama.2020.3151
25. Taiwan Centers for Disease Control. COVID-19 (SARS-CoV-2 Infection) [cited 2022 Jul 11]. https://www.cdc.gov.tw
26. World Health Organization. COVID-19 clinical management: living guidance. 2021 Jan 25 [cited 2022 Jul 15]. https://www.who.int/publications/i/item/WHO-2019-nCoV-clinical-2021-1
27. Google Inc. COVID-19 community mobility reports. [cited 2022 Jul 15]. https://www.google.com/covid19/mobility/Taiwan
28. Reich NG, Lessler J, Cummings DAT, Brookmeyer R. Estimating incubation period distributions with coarse data. Stat Med. 2009;28:2769–84. https://doi.org/10.1002/sim.3659
29. Linton NM, Kobayashi T, Yang Y, Hayashi K, Akhmetzhanov AR, Jung SM, et al. Incubation period and other epidemiological characteristics of 2019 novel coronavirus infections with right truncation: a statistical analysis of publicly available case data. J Clin Med. 2020;9:538. https://doi.org/10.3390/jcm9020538
30. van de Kassteele J, Eilers PHC, Wallinga J. Nowcasting the number of new symptomatic cases during infectious disease outbreaks using constrained P-spline smoothing. Epidemiology. 2019;30:737–45. https://doi.org/10.1097/EDE.0000000000001050
31. Nakajo K, Nishiura H. Estimation of R(t) based on illness onset data: An analysis of 1907–1908 smallpox epidemic in Tokyo. Epidemics. 2022;38:100545. https://doi.org/10.1016/j.epidem.2022.100545
32. He X, Lau EHY, Wu P, Deng X, Wang J, Hao X, et al. Temporal dynamics in viral shedding and transmissibility of COVID-19. Nat Med. 2020;26:672–5. https://doi.org/10.1038/s41591-020-0869-5
33. Delamater PL, Street EJ, Leslie TF, Yang YT, Jacobsen KH. Complexity of the basic reproduction number (R_0). Emerg Infect Dis. 2019;25:1–4. https://doi.org/10.3201/eid2501.171901
34. Vehtari A, Gelman A, Gabry J. Practical Bayesian model evaluation using leave-one-out cross-validation and WAIC. Stat Comput. 2017;27:1413–32. https://doi.org/10.1007/s11222-016-9696-4

Address for correspondence: A.R. Akhmetzhanov, National Taiwan University, College of Public Health, No. 17 Xuzhou Rd. Zhongzheng District, Taipei 10055, Taiwan; email: akhmetzhanov@ntu.edu.tw

Two Cases of Lassa Fever Successfully Treated with Ribavirin and Adjunct Dexamethasone for Concomitant Infections

Sylvanus Okogbenin, Cyril Erameh, Joseph Okoeguale, Osahogie Edeawe, Esele Ekuaze, Kelly Iraoyah, John Agho, Mirjam Groger, Benno Kreuels, Lisa Oestereich, Femi O. Babatunde, Peter Akhideno, Stephan Günther, Michael Ramharter, Till Omansen

Lassa fever is a viral hemorrhagic fever treated with supportive care and the broad-spectrum antiviral drug ribavirin. The pathophysiology, especially the role of hyperinflammation, of this disease is unknown. We report successful remission of complicated Lassa fever in 2 patients in Nigeria who received the antiinflammatory agent dexamethasone and standard ribavirin.

Lassa fever is a viral hemorrhagic fever endemic to West Africa; an estimated 300,000 cases of Lassa fever and 5,000 deaths occur annually (*1*). Lassa fever is currently treated with ribavirin, a nucleoside analog that has broad-spectrum antiviral properties (*2*). Despite being recommended in most national treatment guidelines (*3*,*4*), ribavirin is not formally approved for treatment of Lassa fever. Evidence supporting a beneficial effect of ribavirin for treatment of Lassa fever is scarce, and the pivotal landmark study (*2*) showed a high risk for bias (*5*,*6*). A study focused on evaluation of pharmacokinetics of ribavirin to better characterize its role in treatment for Lassa fever (*7*). Severe Lassa fever with lethal outcome is associated with encephalopathy, acute kidney injury, and respiratory failure (*8*). Lassa virus (LASV) has been observed in the cerebrospinal fluid of patients exhibiting clinical symptoms of encephalitis (*9*,*10*). However, it is insufficiently understood how LASV causes pathology; in severely ill patients, mediators of coagulation, as well as inflammatory markers, were found to be dysregulated (*11*).

Because of the epidemic potential of Lassa fever and its high case-fatality rates in hospitalized patients, Lassa fever was added to the World Health Organization blueprint priority list of diseases for research and development, urging intensified research, including improved treatments. Based on the excess in inflammatory response observed in severe Lassa fever patients (*12*), host directed antiinflammatory treatment has been discussed as adjunct therapy. This therapy has been found to be beneficial, as indicated by expert's opinion in LASV-infected adults and pregnant women.

We report 2 patients, 1 who had severe Lassa fever complicated by COVID-19 and acute kidney injury (patient A), and 1 who had acute kidney injury and neurologic complications (patient B) who, in addition to intravenous ribavirin and supportive care, received dexamethasone. Dexamethasone is a glucocorticoid agent also successfully used for other severe viral infections, such as COVID-19, to reduce damage conferred by systemic hyperinflammation (*13*).

The Study

Patient A was a 72-year-old man who came to Irrua Specialist Teaching Hospital (ISTH) in Irrua, Nigeria,

Author affiliations: Irrua Specialist Teaching Hospital, Irrua, Nigeria (S. Okogbenin, C. Erameh, J. Okoeguale, O. Edeawe, E. Ekuaze, K. Iraoyah, J. Agho, F.O. Babatunde, P. Akhideno); Bernhard Nocht Institute for Tropical Medicine, Hamburg, Germany (M. Groger, B. Kreuels, M. Ramharter, L. Oestereich, S. Günther, T. Omansen); University Medical Center, Hamburg-Eppenforf, Germany (M. Groger, B. Kreuels, M. Ramharter, T. Omansen); German Center for Infection Research, Partner Sites Hamburg-Lübeck-Borstel-Riems, Germany (M. Groger, B. Kreuels, L. Oestereich, S. Günther, M. Ramharter, T. Omansen)

DOI: https://doi.org/10.3201/eid1810.220625

on January 15, 2021, because of reported weakness and poor appetite. He had previously been given artemether/lumefantrine for suspected malaria for 4 consecutive days. However, his symptoms persisted. His medical history included diabetes mellitus type 2 and arterial hypertension. At examination, the patient was in apparent good clinical condition, afebrile, and had normal vital signs and adequate peripheral oxygenation at ambient air.

A molecular test of an oropharyngeal swab specimen for SARS-CoV-2 showed a positive result (reverse transcription PCR [RT-PCR] cycle threshold [Ct] 14.97 for betacoronavirus] and Ct 12.3 for SARS-CoV-2). Oral dexamethasone therapy was initiated, and the patient was referred to domestic quarantine, according to standard local practice. Two days later, the patient came again to the hospital and reported progressive worsening of body weakness; he appeared pale and in a markedly reduced clinical condition.

He had a body temperature of 38.0°C, heart rate 105 bpm, blood pressure 115/75 mm Hg, respiratory rate 24/min, and 95% oxygen saturation in ambient air. Auscultation of the chest and further physical examination showed no abnormalities.

The patient was admitted to the isolation ward and tested for Lassa fever because of persistent fever and worsening condition in a zone to which Lassa fever is endemic. The result was positive (Ct 33.33, by RealStar Lassa Virus RT-PCR Kit; Altona Diagnostics, https://www.altona-diagnostics.com).

During hospitalization, the patient required 2–4 L/min of supplemental oxygen by nasal cannula, received intravenous ribavirin according to the Irrua regimen (*3*) and continued therapy with dexamethasone (8 mg orally every 8 h). Laboratory diagnosis showed anemia and acute renal failure (Table). An initial treatment with prophylactic low molecular weight heparin was discontinued once Lassa fever was diagnosed to avoid exacerbation of risk for bleeding in viral hemorrhagic fever. The patient had progressive normocytic anemia and received 2 blood transfusions. Stool for occult blood was negative, and there were no further clinical signs of external or internal bleeding.

Over time, the condition of the patient improved, and the creatinine level returned to within the reference range. The patient had sufficient urinary output and did not require dialysis. On day 21 after admission, repeat PCR testing results for SARS-CoV-2 and LASV were negative, and all vital signs were stable. The patient was discharged in good health.

Patient B was a 40-year-old woman who was referred by a peripheral healthcare center to ISTH on March 15, 2021. She came to the hospital because of fever, headache, and loss of appetite. She was empiri-

Table. Laboratory parameters of 2 patients in Nigeria at admission who had Lassa fever, were given ribavirin and dexamethasone, and showed favorable outcomes*

Parameter	Patient A	Patient B
Hematology		
Hemoglobin, g/dL	9.8	9.2
Packed cell volume, %	26.40	31.40
Erythrocytes, × 10^9 cells/L	3.04	3.77
Mean corpuscular volume, fL	88.5	83.3
Mean corpuscular hemoglobin, pg	32.2	24.4
Mean corpuscular hemoglobin concentration, g/dL	36.4	29.3
Red cell distribution width, %	29.2	27.4
Platelets/mm^3	155,000	140,000
Mean platelet volume, fL	12.4	10.3
Platelet distribution width, %	28.1	27.4
Total leukocytes, x 10^9 cells/L	7,800	14,400
Neutrophils, %	66.40	NA
Lymphocytes, %	18.50	NA
Monocytes, %	12.40	NA
Eosinophils, %	2.40	NA
Basophils, %	0.30	NA
Clinical chemistry		
Creatinine, mg/dL	2.8	1.1
Urea, mg/dL	81	57
Bilirubin, mg/dL	0.8	0.6
Total protein, g/dL	6.8	7.8
Alanine aminotransferase, IU/L	6	11
Aspartate aminotransferase, IU/L	19	14
Electrolytes		
Sodium, mmol/L	136	NA
Potassium, mmol/L	5	NA

*NA, not available.

cally given artemether/lumefantrine but symptoms persisted. This finding prompted testing for LASV at ISTH; result was positive (Ct 31.80, by RealStar Lassa Virus RT-PCR Kit).

She had a body temperature of 37.8°C, heart rate (tachycardia) 118 bpm/min, blood pressure 89/69 mm Hg, regular respiration, and 99% oxygen saturation in ambient air. Physical examination showed no additional major pathologic findings.

Antiviral therapy with intravenous ribavirin according to the Irrua regimen was initiated. On day 3 of admission, the patient reported intense headaches and had persistent fever of 38.3°C. Examination showed pronounced neck stiffness that was interpreted as a sign of meningeal irritation. Lumbar puncture was not performed to minimize risk for bleeding in the context of a viral hemorrhagic fever with unknown mechanisms of bleeding and lacking availability for coagulation testing.

Based on a clinical diagnosis of meningitis, the patient was empirically given intravenous ceftriaxone (2 g every 12 h) and intravenous dexamethasone (4 mg every 12 h). Over the next few days, fever and other complaints subsided gradually and vital signs returned to reference ranges. Ceftriaxone and dexamethasone were discontinued after 7 days of treatment. On day 13 of admission, headache and neck stiffness were markedly reduced, and ribavirin was switched to oral therapy. PCR for LASV on day 14 of admission was negative. Ribavirin was then discontinued, and the patient was discharged.

Both patients were seen for follow-up. They appeared to be in good health and recovered without sequelae.

Conclusions

Improved treatment options for Lassa fever are urgently needed because convincing evidence for use of ribavirin is lacking (*5*,*6*). Hyperinflammation is a consistent feature in severe Lassa fever (*11*,*12*), as well as in other severe viral infections. Because corticosteroids in general, and dexamethasone as a particularly potent derivative, rapidly reduce hyperinflammation, their use might address this pathophysiologic process. Fear of exacerbation of viral replication and thus worsening the outcome of Lassa fever has so far prevented its routine use for Lassa fever.

In the 2 cases reported, dexamethasone was initiated for treatment of concomitant infections, rather than for indication of Lassa fever. No apparent detrimental effects on the clinical course of disease or virologic or laboratory features were observed. Both patients were severely ill, yet recovered after receiving dexamethasone and ribavirin therapy and showed no sequelae. Patient A had considerable risk factors for poor disease outcome of Lassa fever, such as preexisting chronic concurrent conditions and co-infection with COVID-19. The disease course was complicated by anemia and acute kidney injury. Treatment with dexamethasone might have also contributed to reducing hyperinflammation causing or contributing to these pathologies and similarly to the clinical signs of meningeal inflammation in patient B.

Although these 2 cases of severe Lassa fever cannot be interpreted as proven evidence of the benefit of dexamethasone in Lassa fever therapy, we have not observed any considerable side effects, which provides reassurance for safe assessment in future interventional clinical trials. We suggest that future systematic research into the exact pathophysiology of Lassa fever and a systematic clinical investigation of antiinflammatory and immune-modulatory drugs, such as dexamethasone, for ancillary therapy for Lassa fever are warranted.

About the Author

Dr. Okogbenin is the chief medical director of the Irrua Specialist Teaching Hospital, Irrua, Edo State, Nigeria. His primary research interests are antiviral therapy for Lassa fever, including pregnant women.

References

1. Kenmoe S, Tchatchouang S, Ebogo-Belobo JT, Ka'e AC, Mahamat G, Guiamdjo Simo RE, et al. Systematic review and meta-analysis of the epidemiology of Lassa virus in humans, rodents and other mammals in sub-Saharan Africa. PLoS Negl Trop Dis. 2020;14:e0008589. https://doi.org/10.1371/journal.pntd.0008589
2. McCormick JB, King IJ, Webb PA, Scribner CL, Craven RB, Johnson KM, et al. Lassa fever. Effective therapy with ribavirin. N Engl J Med. 1986;314:20–6. https://doi.org/10.1056/NEJM198601023140104
3. Nigeria Center for Disease Control. National Guideline for Lassa Fever Case Management. 2018 [cited 2022 Feb 2]. https://ncdc.gov.ng/themes/common/docs/protocols/92_1547068532.pdf
4. World Health Organization. Clinical management of patients with viral haemorrhagic fever: a pocket guide for front-line health workers: interim emergency guidance for country adaptation. 2016 [cited 2022 Feb 2]. https://apps.who.int/iris/bitstream/handle/10665/205570/9789241549608_eng.pdf
5. Eberhardt KA, Mischlinger J, Jordan S, Groger M, Günther S, Ramharter M. Ribavirin for the treatment of Lassa fever: a systematic review and meta-analysis. Int J Infect Dis. 2019;87:15–20. https://doi.org/10.1016/j.ijid.2019.07.015
6. Salam AP, Cheng V, Edwards T, Olliaro P, Sterne J, Horby P. Time to reconsider the role of ribavirin in Lassa fever. PLoS

Negl Trop Dis. 2021;15:e0009522. https://doi.org/10.1371/journal.pntd.0009522
7. Erameh C, Edeawe O, Akhideno P, Eifediyi G, Omansen TF, Wagner C, et al. Prospective observational study on the pharmacokinetic properties of the Irrua ribavirin regimen used in routine clinical practice in patients with Lassa fever in Nigeria. BMJ Open. 2020; 10:e036936. https://doi.org/10.1136/bmjopen-2020-036936
8. Duvignaud A, Jaspard M, Etafo IC, Gabillard D, Serra B, Abejegah C, et al.; LASCOPE study group. Lassa fever outcomes and prognostic factors in Nigeria (LASCOPE): a prospective cohort study. Lancet Glob Health. 2021;9:e469–78. https://doi.org/10.1016/S2214-109X(20)30518-0
9. Okokhere PO, Erameh CO, Alikah F, Akhideno PE, Iruolagbe CO, Osazuwa OO, et al. Acute Lassa virus encephalitis with Lassa virus in the cerebrospinal fluid but absent in the blood: a case report with a positive outcome. Case Rep Neurol. 2018;10:150–8. https://doi.org/10.1159/000490374
10. Günther S, Weisner B, Roth A, Grewing T, Asper M, Drosten C, et al. Lassa fever encephalopathy: Lassa virus in cerebrospinal fluid but not in serum. J Infect Dis. 2001;184: 345–9. https://doi.org/10.1086/322033
11. Strampe J, Asogun DA, Speranza E, Pahlmann M, Soucy A, Bockholt S, et al. Factors associated with progression to death in patients with Lassa fever in Nigeria: an observational study. Lancet Infect Dis. 2021;21:876–86. https://doi.org/10.1016/S1473-3099(20)30737-4
12. Port JR, Wozniak DM, Oestereich L, Pallasch E, Becker-Ziaja B, Müller J, et al. Severe human Lassa fever is characterized by nonspecific T-cell activation and lymphocyte homing to inflamed tissues. J Virol. 2020;94:e01367-20. https://doi.org/10.1128/JVI.01367-20
13. Horby P, Lim WS, Emberson JR, Mafham M, Bell JL, Linsell L, et al.; RECOVERY Collaborative Group. Dexamethasone in hospitalized patients with COVID-19. N Engl J Med. 2021;384:693–704. https://doi.org/10.1056/NEJMoa2021436

Address for correspondence: Till Omansen, Department of Tropical Medicine, Bernhard Nocht Institute for Tropical Medicine and I. Dept. of Medicine, University Medical Center Hamburg-Eppendorf, Hamburg, Germany; email: till.omansen@bnitm.de

Ophidiomyces ophiodiicola, Etiologic Agent of Snake Fungal Disease, in Europe since Late 1950s

Francesco C. Origgi, Simone R.R. Pisano, Olivier Glaizot, Stefan T. Hertwig, Andreas Schmitz, Sylvain Ursenbacher

The fungus *Ophidiomyces ophiodiicola* is the etiologic agent of snake fungal disease. Recent findings date US occurrence at least as far back as 1945. We analyzed 22 free-ranging snakes with gross lesions consistent with snake fungal disease from museum collections from Europe. We found 5 positive samples, the oldest collected in 1959.

In the past few decades, fungal agents have surfaced as relevant threats to conservation and biodiversity among both ectotherms and endotherms (*1*–*3*). The emerging fungal agent *Ophidiomyces ophiodiicola* has been detected in both captive and free-ranging snakes in the United States in the past 16 years (*4*–*7*) and more recently in the United Kingdom and Czech Republic (*8*). *O. ophiodiicola* fungus has been associated with a variably severe dermatitis but also multisystemic disease (*9*). Experimental infections (*10*) demonstrated the causative association between *O. ophiodiicola* infection and snake fungal disease (SFD), the common name attributed to the disease caused by this fungus. The effect on free-ranging populations of snakes is not completely understood, but many species of snakes appear to be susceptible and different populations appear to have been negatively affected (*9*,*11*).

A recent article showed that the earliest evidence of *O. ophiodiicola* infection in North America dates back to 1945 (*12*). However, records of *O. ophiodiicola* fungi in Europe date back only to 2010–2016 (*8*). Detection of 2 phylogenetically distinct lineages in the United States and Europe consistent with genetic differences between the clades, presumably reflects independent evolution of the lineages. To acquire additional data about the origins of this agent in Europe, we obtained skin samples from free-ranging snake collections from multiple natural history museums in Switzerland.

Author affiliations: University of Bern, Bern, Switzerland (F.C. Origgi, S.R.R. Pisano, S.T. Hertwig); Museum of Zoology, Lausanne, Switzerland (O. Glaizot); University of Lausanne, Lausanne (O. Glaizot); Naturhistorisches Museum Burgergemeinde Bern, Bern (S.T. Hertwig); Natural History Museum of Geneva, Geneva, Switzerland (A. Schmitz); University of Basel, Basel, Switzerland (S. Ursenbacher); info fauna CSCF & karch, Neuchâtel, Switzerland (S. Ursenbacher).

DOI: https://doi.org/10.3201/eid2810.220564

The Study

We selected 22 skin samples with macroscopic lesions consistent with SFD out of 1,100 free ranging snakes examined from the collections of 3 natural history museums in Switzerland (Table 1; Appendix, https://wwwnc.cdc.gov/EID/article/28/10/22-0564-App1.pdf). We collected tissue samples from the integument of snakes showing obvious macroscopic lesions consistent with dermatitis (Appendix Figure 1). Snake specimens were preserved in 100% ethanol. We collected tissue samples using sterile instrumentation changed between each sampling. We placed each tissue sample in a cryotube containing an aliquot of absolute ethanol. Upon delivery at the laboratory, tissue samples were split into 2 portions for processing for DNA extraction and histopathology (Appendix).

We performed PCR according to various protocols aiming to detect multiple gene targets belonging to the *O. ophiodiicola* genome. Initial screening for the presence of *O. ophiodiicola* fungi was performed by applying a modified PCR protocol (an original protocol performed in a conventional PCR setting) (*13*) targeting the partial sequence of the intergenic spacer (IGS). We then tested positive samples and, later, negative samples to rule out false-negative results

Table 1. Museum tissue samples from snakes of genuses *Natrix* and *Vipera* used in investigation of snake fungal disease in Europe*

Sample	Museum	Species	ID	Sex	Year	Location (country)
1	**NMBE**	***Natrix helvetica***	**1049780**	**F**	**2001**	**Erlach (Switzerland)**
2†	NMBE	*N. helvetica*	1056184	NA	2007	Tavannes (Switzerland)
3‡	NMBE	*Vipera aspis*	1072979	NA	2015	Grandvillars (Switzerland)
4	MHNG	*N. tessellata*	1402.040	F	1972	Lake Geneva (Switzerland)
5‡	MHNG	*N. natrix*	851.077	NA	NA	NS (Czech Republic)
6	**MHNG**	***N. natrix***	**1342.87**	**NA**	**1963**	**Thurgau (Switzerland)**
7	**MHNG**	***N. helvetica***	**1137.18**	**NA**	**1967**	**NS (Italy)**
8†	MHNG	*N. tessellata*	1386.55	F	1969	Tessin (Switzerland)
9	**MHNG**	***N. helvetica***	**1397.21**	**NA**	**1959**	**NS (Italy)**
10	MHNG	*N. helvetica*	2430.91	NA	1986	Zurich (Switzerland)
11†	MHNG	*N. maura*	1199.084	F	1971	Haute-Savoie (France)
12	**MHNG**	***N. tessellata***	**1387.60**	**F**	**1961**	**Maggia (Switzerland)**
13	MZL	*N. tessellata*	MZL41123	F	2008	Lake Geneva (Switzerland)
14†	MZL	*N. tessellata*	MZL30407	F	2007	Lake Geneva (Switzerland)
15‡	MZL	*N. tessellata*	MZL41142	M	2009	Lake Geneva (Switzerland)
16	MZL	*N. tessellata*	MZL30508	F	2007	Lake Geneva (Switzerland)
17‡	MZL	*N. tessellata*	MZL40905	F	2012	Lake Geneva (Switzerland)
18	MZL	*N. tessellata*	MZL31837	F	2010	Lake Geneva (Switzerland)
19	MZL	*N. tessellata*	MZL30505	NA	2007	Lake Geneva (Switzerland)
20	MZL	*N. tessellata*	MZL41144	F	2009	Lake Geneva (Switzerland)
21†	MZL	*N. tessellata*	MZL40911	F	2013	Lake Geneva (Switzerland)
22	MZL	*N. tessellata*	MZL31839	M	2010	Lake Geneva (Switzerland)

*Bold indicated PCR-positive samples with presence of fungal hyphae. MZL, Museum of Zoology, Lausanne; NMBE, Natural History Museum of Bern; MHNG, Natural History Museum of Geneva; NA, not available; NS, not specified.
†PCR-negative samples with presence of fungal hyphae and with histological lesions similar to those observed in the PCR-positive samples.
‡PCR-negative samples with presence of fungal hyphae and with histological lesions dissimilar to those observed in the PCR-positive samples.

by IGS PCR by using 3 additional newly developed protocols targeting distinct genome sequences: the 5.8–28s RNA internal transcribed spacer (ITS) 2, the transcription elongation factor (TEF), and the actin genes (Appendix). We used nucleotide sequences obtained from each of the readable PCR amplicons for phylogenetic analysis. We used partial sequences from the amplified ITS, TEF, and actin targets to build up a maximum-likelihood phylogenetic tree for each of the amplified genomic sequences (Appendix). All 22 samples examined for the presence of *O. ophiodiicola* genomic DNA were characterized by gross and microscopic lesions consistent with dermatitis (Table 2; Appendix Figures 1–3).

Overall, we observed fungal elements in 14/22 examined tissue sections. All samples positive for SFD by PCR were characterized by the presence of intralesional fungal hyphae and heterophilic granulomas or microabscesses (Appendix Figures 2, 3); we observed intradermal granulomas in 1 sample, in which we could not histologically detect any fungal elements. When we used the original IGS-PCR protocol (*13*), 5/22 samples yielded a detectable band (sample numbers 1, 6, 7, 9, and 12). Samples 6, 7, 9, and 12 were also confirmed positive when we used the ITS primer set. Four of 22 samples (6, 7, 9, and 12) yielded a detectable band when we used the actin primer set. Two of 22 samples (9 and 12) yielded a detectable band when we used the TEF primer set. Despite positive IGS amplification, we could not amplify sample 1 with either the actin or the TEF primer sets. We obtained a nonspecific amplification with the ITS primer set and consequently did not further consider sample 1 for sequence comparison and phylogenetic analysis (Appendix, Figure 4).

Sequence alignments, reflected in the phylogenetic trees (Appendix Figure 4), showed unique single-nucleotide polymorphisms clearly separating the museum samples from Switzerland into either the clade circulating in Europe or the one circulating in North America (Figure) (*8*). Results were consistent across the partial sequences of the targeted ITS, TEF, and actin genomic regions. Specifically, samples 7 and 9 from Italy always clustered within the clade from Europe, whereas 6 and 12 from Switzerland clustered within the clade from North America (Appendix Figure 4).

Conclusions

Our research, conducted similarly to an investigation performed in North America, provided evidence of the presence of *O. ophiodiicola* infection in free-ranging snakes in Europe at least since 1959 (*12*). Our findings were supported by test results for 4 distinct molecular targets and consistent histological findings. Furthermore, all PCR-positive samples confirmed by sequencing were also associated with the presence of intralesional fungal structures consistent with *O. ophiodiicola* and associated with an obvious inflammatory reaction.

Of note, supporting data are consistent with the surprising finding that the proposed clades from both North America and Europe (*8*) have been present at least since the early 1960s. Furthermore, because our dataset spanned only 1959–2012, *O. ophiodiicola* fungi might have been present in Europe even before 1959. The significance of both clades existing in Europe will require further investigations. In spite of the absence in the United States of any strain proven to belong to the clade from Europe, introduction cannot be completely ruled out (*14*). In an alternative scenario, the clade from North America might have been introduced into Europe before the 1950s. At the moment, the colonization of *O. ophiodiicola* fungi on the European continent appears to have occurred several decades before proposed (*8*).

Detection of *O. ophiodiicola* fungi in Italy and Switzerland north of the Alps, further expands its known distribution in Europe. Curiously, Switzerland appears to be the only country in Europe where the clade of *O. ophiodiicola* fungi from North America has to date been identified. However, sampling bias secondary to the restricted sampling area selected cannot be ruled out. Finally, although the 2 samples from Switzerland that clustered with the clade from North America were from different regions, the regions are located relatively close geographically to one another (160 km or ≈100 miles).

In summary, this investigation supports the presence of *O. ophiodiicola* fungi in Europe since at least 1959 with genomic sequences compatible with the 2 known lineages. These results provide critical elements for helping to rethink disease ecology and global distribution of *O. ophiodiicola* fungi and reconstructing its natural history.

Table 2. Histologic findings from investigation of snake fungal disease in Europe*

Sample	Light microscopy descriptions	PAS findings	Score†
1	Epidermal hyperplasia with serocellular crusts and histiocytic granulomas; mononuclear to heterophilic dermatitis	Septate fungal hyphae, 3 μm thick, branching both at 90 and 45 degrees	3
2	Epidermal hyperplasia with serocellular crusts and microabscesses	Rare, septate fungal hyphae, 2–3 μm thick, branching at 90 degrees	2
3	Epidermal ulceration with heterophilic infiltration and histiocytic dermatitis, intralesional bacteria and foreign material	Septate fungal hyphae, 3 μm thick, branching at 90 degrees	1
4	Ulcerative dermatitis with serocellular crusts and hyperkeratosis	No evidence of fungal hyphae	0
5	Hyperkeratosis	Septate fungal hyphae, embedded in the keratin, 2–3 μm thick, branching at 90 degrees and acute angle	1
6	Hyperkeratosis with histiocytic (granulomatous) dermatitis	Septate fungal hyphae, 3–4 μm thick, branching at acute angle	3
7	Heterophilic granulomas and microabscesses in the epidermis	Rare fungal hyphae, 3 μm thick embedded or associated with the microgranulomas	3
8	Hyperkeratosis with serocellular crusts, epidermal microgranulomas and lymphocytic dermatitis	Septate fungal hyphae, 3 μm thick, branching at 90 degrees and acute angle	2
9	Large crusts surrounded by histiocytic to heterophilic infiltrate and multifocal microgranulomas	Fungal hyphae in the crusts, 2–3 μm thick	3
10	Few crust fragments admixed with bacteria	No detectable fungal hyphae	0
11	Lympho-histiocytic dermatitis with dermal heterophilic granulomas	Rare fragmented hyphae in the heterophilic granulomas	2
12	Serocellular crusts together with large heterophilic granulomas and more diffused histiocytic infiltration; lympho-histiocytic dermatitis	Septate fungal hyphae, 3 μm thick, branching at 90 degrees or acute angle	3
13	Small serocellular crusts	No evidence of fungal hyphae	0
14	Small and rare heterophilic granulomas	Fragments of fungal hyphae in microgranulomas	2
15	A small serocellular crust	Few fungal septate hyphae, 2–3 μm thick, branching at 90 degrees	1
16	Severe dermal edema with isolated inflammatory cells	No obvious fungal elements	0
17	Serocellular crusts with intralesional bacteria	Fragments of non-septate hyphae	1
18	Hyperkeratosis with upper keratin heterophilic to histiocytic infiltration	No obvious fungal elements	0
19	Serocellular crust	No obvious fungal elements	0
20	Intradermal heterophilic granulomas	No obvious fungal elements	0
21	Epidermal heterophilic granulomas with serocellular crusts	Septate fungal hyphae, 2–3 μm thick, branching at 90 degrees	2
22	Intraepidermal crusts with heterophilic granulomas and intralesional bacteria	No obvious fungal elements	0

*PAS, periodic acid–Schiff.
†Subjective scoring system complementing morphologic and molecular data; 0, PCR-negative with no histologic evidence of fungi; 1, PCR-negative with presence of fungi but without lesions consistent with those observed in PCR-positive samples (absence of heterophilic granulomas); 2, PCR-negative with presence of fungi and lesions consistent with snake fungal disease; 3, PCR-positive with presence of fungi consistent with *Ophidiomyces ophiodiicola*.

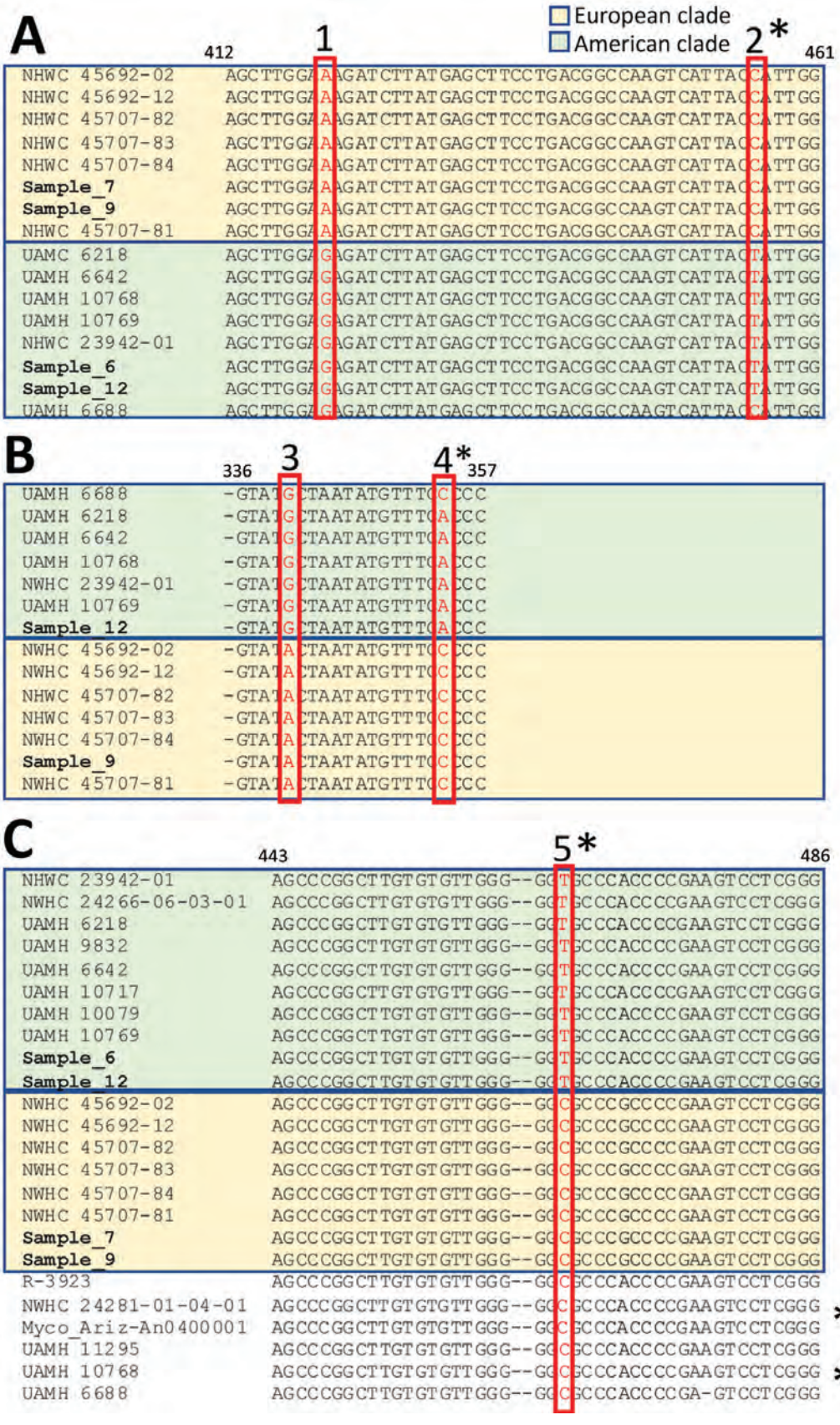

Figure. Nucleotide sequence alignment of selected sections of *Ophidiomyces ophiodiicola* from free-ranging snake collections from multiple natural history museums in Switzerland (bold) compared with reference sequences. Amplicons obtained with different PCR primer sets highlight single-nucleotide polymorphisms (SNPs, red boxes) unique to either the European (pastel gold) or American (pastel green) clades. PCR primer results: A) actin; B) transcription elongation factor; and C) internal transcribed spacer. The isolate UAMH 6688 (UK strain) shares 2/5 unique SNPs with the members of the clade from North America, whereas 3 of them (single asterisks) are shared with strains from Europe. These differences match the divergent branching of this strain in the clades from both North America and Europe. Similarly, 5 others fungal isolates (double asterisks)—R-3923; NWHC 24281-01-04-01, Myco_Ariz-An0400001, UAMH 11295, and UAMH 10768, in addition to UAMH 6688, originating from the United States, Australia, and the United Kingdom—shared the internal transcribed spacer SNP of the clade from Europe and clustered consistently in an intermediate group in the corresponding phylogenetic tree (Appendix Figure 4, https://wwwnc.cdc.gov/EID/article/28/10/22-0564-App1.pdf).

Acknowledgments

We thank the Natural History Museum of Bern, the Natural History Museum of Geneva, the Museum of Zoology of Lausanne, and David Guerra for help during the sampling.

This work was partially financed by the Swiss Federal Office for the Environment (grant no. 05.0040.PZ/R413-2016).

About the Author

Dr. Origgi is a veterinary microbiologist and pathologist with strong interest in infectious diseases and associated pathogenesis in wildlife and nondomestic animals.

References

1. Hoyt JR, Kilpatrick AM, Langwig KE. Ecology and impacts of white-nose syndrome on bats. Nat Rev Microbiol. 2021;19:196–210. https://doi.org/10.1038/s41579-020-00493-5
2. Martel A, Spitzen-van der Sluijs A, Blooi M, Bert W, Ducatelle R, Fisher MC, et al. *Batrachochytrium salamandrivorans* sp. nov. causes lethal chytridiomycosis in amphibians. Proc Natl Acad Sci U S A. 2013;110:15325–9. https://doi.org/10.1073/pnas.1307356110
3. O'Hanlon SJ, Rieux A, Farrer RA, Rosa GM, Waldman B, Bataille A, et al. Recent Asian origin of chytrid fungi causing global amphibian declines. Science. 2018;360:621–7. https://doi.org/10.1126/science.aar1965
4. Clark RW, Marchand MN, Clifford BJ, Stechert R, Stephens S. Decline of an isolated timber rattlesnake (*Crotalus horridus*) population: interactions between climate change, disease, and loss of genetic diversity. Biol Conserv. 2011;144:886–91. https://doi.org/10.1016/j.biocon.2010.12.001
5. Allender MC, Dreslik M, Wylie S, Phillips C, Wylie DB, Maddox C, et al. *Chrysosporium* sp. infection in eastern massasauga rattlesnakes. Emerg Infect Dis. 2011;17:2383–4. https://doi.org/10.3201/eid1712.110240
6. Sigler L, Hambleton S, Paré JA. Molecular characterization of reptile pathogens currently known as members of the *Chrysosporium* anamorph of *Nannizziopsis vriesii* complex and relationship with some human-associated isolates. J Clin Microbiol. 2013;51:3338–57. https://doi.org/10.1128/JCM.01465-13
7. McKenzie CM, Oesterle PT, Stevens B, Shirose L, Lillie BN, Davy CM, et al. Pathology associated with ophidiomycosis in wild snakes in Ontario, Canada. Can Vet J. 2020;61:957–62.
8. Franklinos LHV, Lorch JM, Bohuski E, Rodriguez-Ramos Fernandez J, Wright ON, Fitzpatrick L, et al. Emerging fungal pathogen *Ophidiomyces ophiodiicola* in wild European snakes. Sci Rep. 2017;7:3844. https://doi.org/10.1038/s41598-017-03352-1
9. Lorch JM, Knowles S, Lankton JS, Michell K, Edwards JL, Kapfer JM, et al. Snake fungal disease: an emerging threat to wild snakes. Philos Trans R Soc Lond B Biol Sci. 2016;371:20150457.
10. Lorch JM, Lankton J, Werner K, Falendysz EA, McCurley K, Blehert DS. Experimental infection of snakes with *Ophidiomyces ophiodiicola* causes pathological changes that typify snake fungal disease. mBio, 2015;6:e01534–15. https://doi.org/10.1128/mBio.01534-15
11. Davy CM, Shirose L, Campbell D, Dillon R, McKenzie C, Nemeth N, et al. Revisiting Ophidiomycosis (snake fungal disease) after a decade of targeted research. Front Vet Sci. 2021;8:665805. https://doi.org/10.3389/fvets.2021.665805
12. Lorch JM, Price SJ, Lankton JS, Drayer AN. Confirmed cases of ophidiomycosis in museum specimens from as early as 1945, United States. Emerg Infect Dis. 2021;27:1986–9. https://doi.org/10.3201/eid2707.204864
13. Bohuski E, Lorch JM, Griffin KM, Blehert DS. TaqMan real-time polymerase chain reaction for detection of *Ophidiomyces ophiodiicola*, the fungus associated with snake fungal disease. BMC Vet Res. 2015;11:95. https://doi.org/10.1186/s12917-015-0407-8
14. Ladner JT, Palmer JM, Ettinger CL, Stajich JE, Farrell TM, Glorioso BM, et al. The population genetics of the causative agent of snake fungal disease indicate recent introductions to the USA. PLoS Biol. 2022;20:e3001676. https://doi.org/10.1371/journal.pbio.3001676

Address for correspondence: Francesco C. Origgi, Institute of Animal Pathology (ITPA), Vetsuisse Faculty, University of Bern, Länggassstrasse 122, CH-3012, Bern, Switzerland; email: francesco.origgi@vetsuisse.unibe.ch

Dialysis Water Supply Faucet as Reservoir for Carbapenemase-Producing *Pseudomonas aeruginosa*

Christopher Prestel, Heather Moulton-Meissner, Paige Gable, Richard A. Stanton, Janet Glowicz, Lauren Franco, Mary McConnell, Tiffany Torres, Dijo John, Gillian Blackwell, Renae Yates, Chavela Brown, Kristina Reyes, Gillian A. McAllister, Jasen Kunz, Erin E. Conners, Katharine M. Benedict, Amy Kirby, Mia Mattioli, Kerui Xu, Nicole Gualandi, Stephanie Booth, Shannon Novosad, Matthew Arduino, Alison Laufer Halpin, Katherine Wells, Maroya Spalding Walters

During June 2017–November 2019, a total of 36 patients with carbapenem-resistant *Pseudomonas aeruginosa* harboring Verona-integron–encoded metallo-β-lactamase were identified in a city in western Texas, USA. A faucet contaminated with the organism, identified through environmental sampling, in a specialty care room was the likely source for infection in a subset of patients.

Verona-integron–encoded metallo-β-lactamase–producing carbapenem-resistant *Pseudomonas aeruginosa* (VIM-CRPA) and other carbapenemase-producing organisms (CPOs) are emerging public health threats. CPOs cause infections that are often extensively drug-resistant and associated with substantial rates of illness and death. By colonizing faucet aerators and wastewater plumbing systems, CPOs can spread rapidly within healthcare facilities, including to patients (*1*–*9*). VIM is a carbapenemase, a type of enzyme that inactivates carbapenems and other β-lactam antimicrobial drugs that are frequently encoded on mobile genetic elements, which in turn can lead to horizontal spread.

Author affiliations: Centers for Disease Control and Prevention, Atlanta, Georgia, USA (C. Prestel, H. Moulton-Meissner, P. Gable, R.A. Stanton, J. Glowicz, L. Franco, G.A. McAllister, J. Kunz, E.E. Conners, K.M. Benedict, A. Kirby, M. Mattioli, K. Xu, N. Gualandi, S. Booth, S. Novosad, M. Arduino, A. Laufer Halpin, M.S. Walters); City of Lubbock Health Department, Lubbock, Texas, USA (M. McConnell, T. Torres, D. John, K. Wells); Texas Department of State Health Services, Austin, Texas (G. Blackwell); University Medical Centers, Lubbock (R. Yates, C. Brown, K. Reyes)

DOI: https://doi.org/10.3201/eid2810.220371

VIM-CRPA is uncommon in the United States; <150 isolates are reported to CDC annually (*10*). During June 2017–November 2019, in a city of 250,000 residents in western Texas, USA (city A), 36 patients with VIM-CRPA were identified. Most were hospitalized for ≥1 night at an acute-care hospital (hospital A) in the 6 months before VIM-CRPA was isolated, but patients did not have overlapping hospital stays or common procedures. We assessed water sources and plumbing in hospital A to identify potential VIM-CRPA reservoirs.

Beginning in June 2017, the Texas Department of State Health Services asked clinical laboratories to voluntarily submit clinical *P. aeruginosa* isolates resistant to imipenem, meropenem, or doripenem to the Texas Department of State Health Services Laboratory for mechanism testing through the Antibiotic Resistance Laboratory Network (https://www.cdc.gov/drugresistance/ar-lab-networks/domestic.html). The 2 clinical laboratories that served hospitals in city A began submitting all CRPA for mechanism testing in June 2017 (hospital A) and April 2018 (hospital B). During July 2017–January 2019, a total of 36 patients with VIM-CRPA isolated from clinical cultures were identified from city laboratories; 21 (58%) had been admitted to hospital A for ≥1 night in the 6 months before culture collection.

We reviewed medical records from hospital A of patients with VIM-CRPA. Median patient age was 57 (range 9–84) years; 57% were male. VIM-CRPA was isolated from wounds in 9 (43%) patients, respiratory sources in 7 (33%), and urine in 5 (24%). Most patients primarily received care on

either medical/surgical units (n = 13, 62%) or intensive care units (ICU 1 or ICU 2; n = 6, 29%). Among persons who had been hospitalized at hospital A in the previous 6 months, VIM-CRPA–positive specimens collected by hospital day 2 were classified as healthcare-associated, community-onset (n = 11, 52%); those collected on or after the third hospitalization day were considered hospital-onset (n = 10, 48%). No patients overlapped on the same unit at the same time, but 3 were placed in the same room in ICU 1, room A, over the 2-year period. A single point-prevalence screening of patients in ICU 1 in October 2018 did not identify additional *P. aeruginosa*–colonized patients. On the basis of common exposure to room A, we considered the potential for an environmental reservoir.

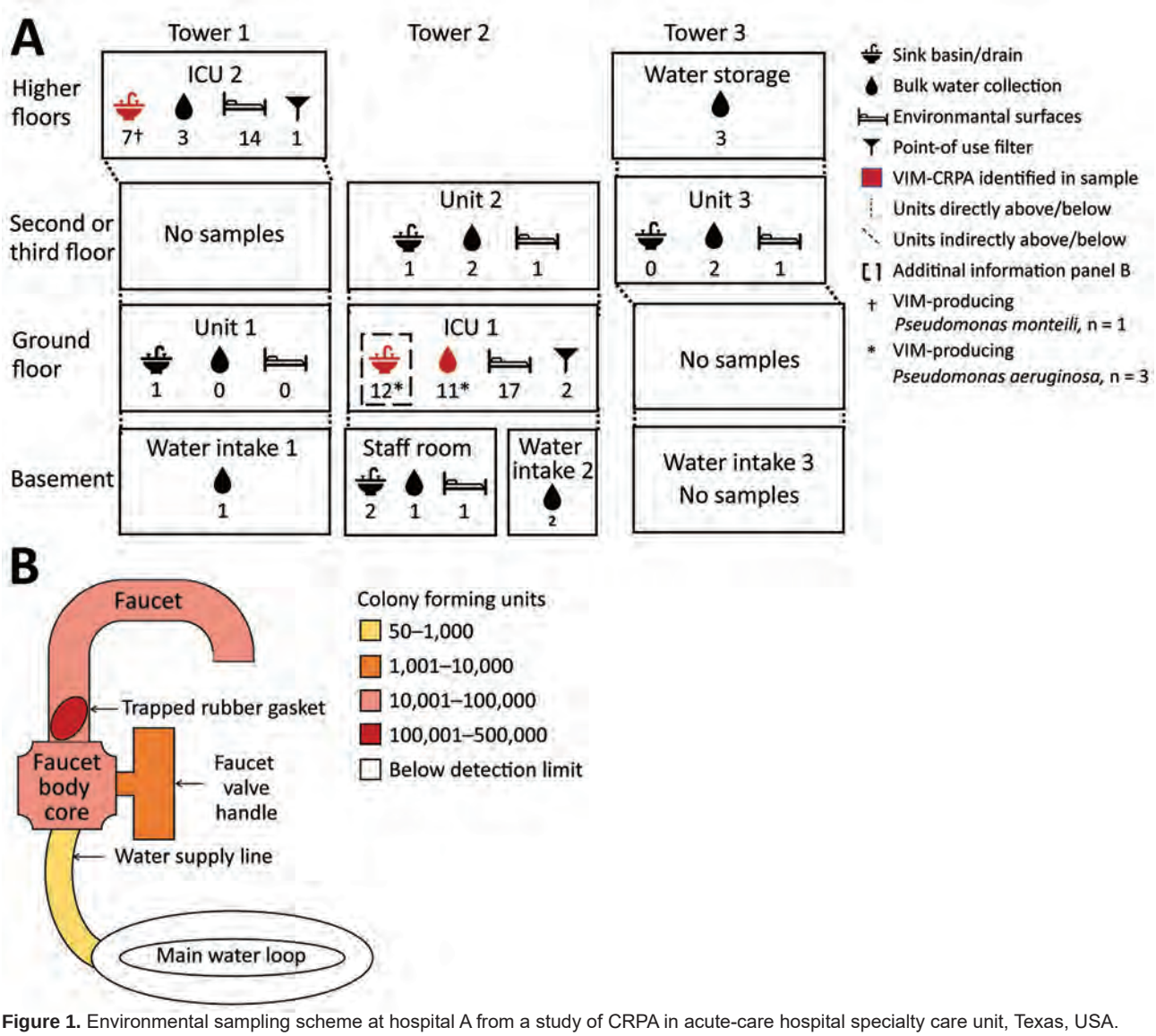

Figure 1. Environmental sampling scheme at hospital A from a study of CRPA in acute-care hospital specialty care unit, Texas, USA. A) Collection location in hospital and number of each sample type (icons with numbers underneath) collected (N = 85). We selected units and rooms for environmental sampling on the basis of chart review, focusing on where patients who developed clinical infections were located; patient rooms were those where patients with VIM-CRPA had been previously located. Three patients developed clinical infections while in ICU 1 and 3 while in ICU 2. Thirteen other patients from several medical or surgical units also developed clinical infections. Samples from which we recovered ≥1 VIM-producing isolate are indicated in red. We identified VIM-CRPA from 3 sites related to a single sink in room A of ICU 1: the sink drain, the interior surface of the dialysis faucet, and bulk water from a dialysis faucet used as the water source for the reverse osmosis unit of portable dialysis machines. We identified VIM-producing *Pseudomonas monteilii* (†) in a single sink basin sample of 1 room in ICU 2. B) Schematic view and heatmap of colony forming units identified by culture at selected internal surface locations within the faucet and water supply used for portable dialysis in ICU 1, room A. CRPA, carbapenem-resistant *Pseudomonas aeruginosa*; ICU, intensive care unit; VIM, Verona-integron-encoded metallo-β-lactamase.

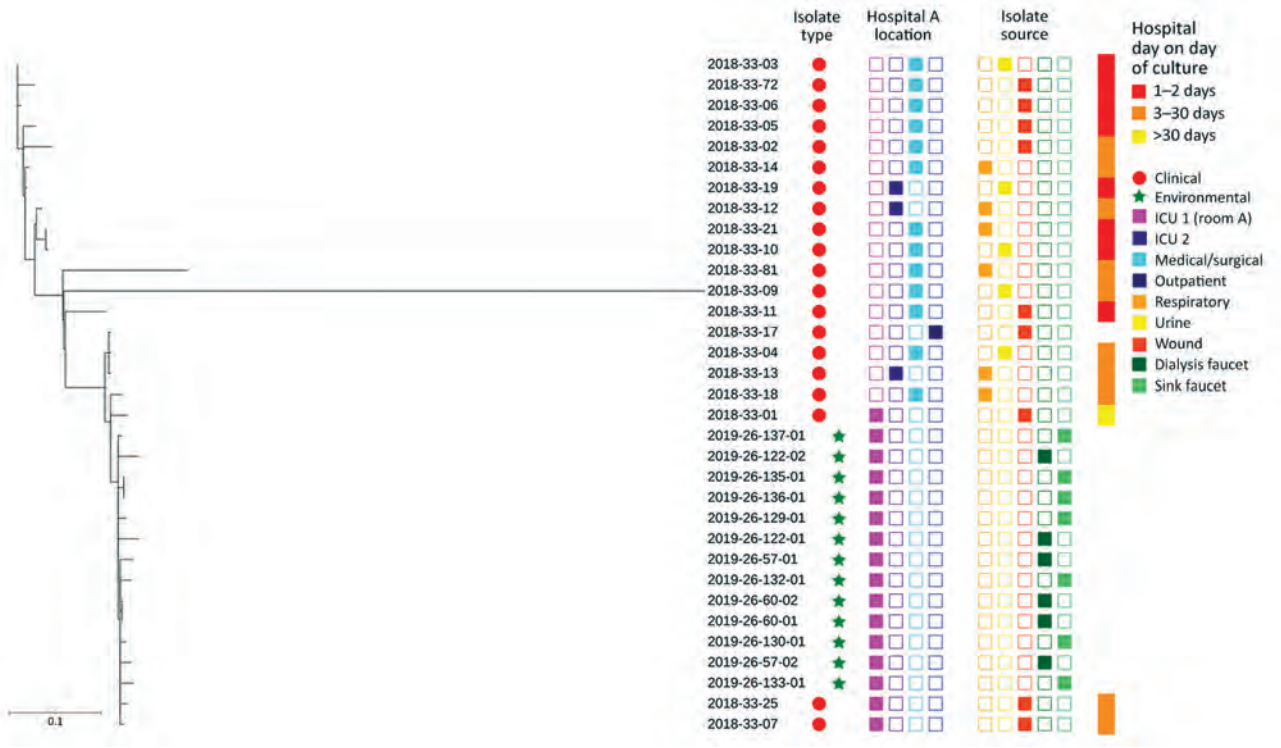

Figure 2. Whole-genome sequencing dendrogram of VIM-CRPA clinical (N = 20) and environmental (N = 13) isolates from hospital A, Texas, USA. Location of culture collection, isolate source, and patient hospital day when clinical culture was obtained are shown. All isolates were sequence type 308 and harbored a VIM-2 allele. No hospital day is provided for isolate 2018-33-17 because it was collected during an emergency department encounter; patient had had an overnight hospitalization in hospital A 2 weeks earlier. ICU, intensive care unit.

The Study

We conducted an environmental investigation focused on water supplies and other sites conducive to biofilm formation. We collected 85 samples from plumbing fixtures and environmental surfaces in patient care areas as well as from water intake and storage areas, and evaluated for the presence of VIM-CRPA (Appendix, https://wwwnc.cdc.gov/EID/article/28/10/22-0731-App1.pdf).

We identified VIM-CRPA in 3 sites in room A related to a sink: the drain, bulk water (1 L of tap water), and the interior surface of a faucet serving as the water source for the reverse osmosis unit of portable dialysis machines (Figure 1, panel A). Of note, this faucet did not have an aerator, which has been implicated as a source of contamination in prior outbreaks. We did not recover VIM-CRPA from the interior of a second faucet intended for hand hygiene, the bulk water or point-of-use filter from that faucet, surface samples of the sink basin, or nearby areas.

The dialysis faucet in room A was installed in October 2017. After we identified VIM-CRPA from associated samples, it was disassembled, revealing a rubber gasket trapped in the gooseneck. We collected swab samples from the interior of the disassembled faucet, valve, and core; we then instilled water into the fixture, agitated it using a sonic device, and filtered it onto culture medium with 4 rinses from the faucet, connection supply line, core, and gasket. We cultured VIM-CRPA from the gasket, faucet, and water supply line (Figure 1, panel B). Three patients with VIM-CRPA infections received care in room A over a 6-month period; 1 had an infection identified on hospital day 46 and was discharged 1 month before the dialysis faucet was installed. None of the infected patients received dialysis.

We considered that portable dialysis machines attachable to the contaminated faucet could spread VIM-CRPA to other dialysis hook-ups and sink drains where effluent reverse osmosis water was discharged. We cultured bulk water and swab samples from the sink in the biomedical room where dialysis machines were cleaned, the dialysis machine connector, and the tubing from the reverse osmosis unit of the dialysis machine connected to the contaminated faucet to test for CPOs, but identified no VIM-CRPA. After removing the dialysis faucet and adopting measures intended to mitigate spread of organisms from

premise plumbing (*11*), we identified no additional VIM-CRPA clinical cultures in patients admitted to the specialty unit.

We performed whole-genome sequencing on 33 VIM-CRPA clinical isolates from 20 patients at multiple locations in hospital A and 13 environmental isolates from room A (Figure 2; Appendix); sequences are available at the National Center for Biotechnology Information (BioProject ID PRJNA288601). All 33 isolates were sequence type 308 and harbored VIM-2; clinical isolates varied by 3–255 (median 54, mean 60.3) high-quality single-nucleotide variants (hqSNVs) (*12*–*14*). Environmental isolates from the faucet and clinical isolates from 3 patients admitted to room A varied from 0–24 (median 10, mean 11.8) hqSNVs. The hqSNVs were derived from a conserved core of 6.5 Mb, which covered on average 91% of the assembled genome for the 33 isolates in the analysis.

The mechanism by which the faucet became contaminated is unknown. We considered it might have been through the water supply, considering a recent report of carbapenemase-producing organisms, although not VIM-producing, in US municipal water systems (*15*); however, none of the 24 water samples collected from other hospital locations grew any CPOs in cultures. Given the stay in room A of a patient with VIM-CRPA before the faucet was installed, we hypothesize that the sink drain became contaminated first, followed by retrograde contamination from the sink drain to the faucet, either during installation or through patient care activities. Although the misplaced rubber gasket provided a nidus for contamination, whether that was necessary for persistent faucet contamination is unclear.

We could not ascertain relative contributions of the faucet interior and upper part of the sink drain toward patients acquiring VIM-CRPA. Although none of the patients underwent dialysis, the faucet was not labeled for dialysis use and may have been used for hand hygiene and other purposes. Infection prevention efforts at hospital A focused on improving sink hygiene, including removing patient care supplies from sink splash zones and regularly cleaning splash zones to prevent future transmission to patients from wastewater plumbing. During the 18-month period after the sink hygiene interventions began in October 2018, another 2 cases were identified, but in units unrelated to the specialty care unit.

Conclusions

We identified VIM-CRPA from a dialysis faucet, in water from that faucet, and from the associated sink drain in an ICU room where VIM-CRPA infections of the same strain developed in 3 patients. Although healthcare facility wastewater plumbing and faucet aerators are well-documented reservoirs of CPOs, our findings highlight the importance of considering other plumbing sources as well.

About the Author

Dr. Prestel is a medical officer with the Prevention and Response Branch, Division of Healthcare Quality Promotion, Centers for Disease Control and Prevention in Atlanta. This work was completed while he was an Epidemic Intelligence Service officer in that branch. His research interests include pediatrics, infectious diseases, and infection prevention and control within healthcare settings.

References

1. Decraene V, Phan HTT, George R, Wyllie DH, Akinremi O, Aiken Z, et al.; TRACE Investigators' Group. A large, refractory nosocomial outbreak of *Klebsiella pneumoni*ae carbapenemase-producing *Escherichia coli* demonstrates carbapenemase gene outbreaks involving sink sites require novel approaches to infection control. Antimicrob Agents Chemother. 2018;62:e01689-18. https://doi.org/10.1128/AAC.01689-18
2. Salm F, Deja M, Gastmeier P, Kola A, Hansen S, Behnke M, et al. Prolonged outbreak of clonal MDR *Pseudomonas aeruginosa* on an intensive care unit: contaminated sinks and contamination of ultra-filtrate bags as possible route of transmission? Antimicrob Resist Infect Control. 2016;5:53. https://doi.org/10.1186/s13756-016-0157-9
3. Kanamori H, Weber DJ, Rutala WA. Healthcare outbreaks associated with a water reservoir and infection prevention strategies. Clin Infect Dis. 2016;62:1423–35. https://doi.org/10.1093/cid/ciw122
4. Hopman J, Meijer C, Kenters N, Coolen JPM, Ghamati MR, Mehtar S, et al. Risk assessment after a severe hospital-acquired infection associated with carbapenemase-producing *Pseudomonas aeruginosa*. JAMA Netw Open. 2019;2:e187665. https://doi.org/10.1001/jamanetworkopen.2018.7665
5. Hajar Z, Mana TSC, Cadnum JL, Donskey CJ. Dispersal of gram-negative bacilli from contaminated sink drains to cover gowns and hands during hand washing. Infect Control Hosp Epidemiol. 2019;40:460–2. https://doi.org/10.1017/ice.2019.25
6. Knoester M, de Boer MG, Maarleveld JJ, Claas EC, Bernards AT, de Jonge E, et al. An integrated approach to control a prolonged outbreak of multidrug-resistant *Pseudomonas aeruginosa* in an intensive care unit. Clin Microbiol Infect. 2014;20:O207–15. https://doi.org/10.1111/1469-0691.12372
7. Aranega-Bou P, George RP, Verlander NQ, Paton S, Bennett A, Moore G, et al.; TRACE Investigators' Group. Carbapenem-resistant *Enterobacteriaceae* dispersal from sinks is linked to drain position and drainage rates in a laboratory model system. J Hosp Infect. 2019;102:63–9.
8. Kotay S, Chai W, Guilford W, Barry K, Mathers AJ. Spread from the sink to the patient: *in situ* study using green fluorescent protein (GFP)–expressing *Escherichia coli* to model bacterial dispersion from hand-washing sink-trap reservoirs. Appl Environ Microbiol. 2017;83:e033270-16. https://doi.org/10.1128/AEM.03327-16

9. Chia PY, Sengupta S, Kukreja A, S L Ponnampalavanar S, Ng OT, Marimuthu K. The role of hospital environment in transmissions of multidrug-resistant gram-negative organisms. Antimicrob Resist Infect Control. 2020;9:29. https://doi.org/10.1186/s13756-020-0685-1
10. Centers for Disease Control and Prevention. Antibiotic resistance [cited 2021 Sep 19]. https://arpsp.cdc.gov/profile/antibiotic-resistance
11. Centers for Disease Control and Prevention. Healthcare-associated infections: reduce risk from water: from plumbing to patients [cited 2022 Feb 8]. https://www.cdc.gov/hai/prevent/environment/water.html
12. Stanton RA, Vlachos N, Laufer Halpin A. GAMMA: a tool for the rapid identification, classification, and annotation of translated gene matches from sequencing data. Bioinformatics. 2022;38:546–8.
13. Petkau A, Mabon P, Sieffert C, Knox NC, Cabral J, Iskander M, et al. SNVPhyl: a single nucleotide variant phylogenomics pipeline for microbial genomic epidemiology. Microb Genom. 2017;3:e000116. https://doi.org/10.1099/mgen.0.000116
14. Letunic I, Bork P. Interactive Tree Of Life (iTOL) v5: an online tool for phylogenetic tree display and annotation. Nucleic Acids Res. 2021;49(W1):W293–6. https://doi.org/10.1093/nar/gkab301
15. Tanner WD, VanDerslice JA, Goel RK, Leecaster MK, Fisher MA, Olstadt J, et al. Multi-state study of *Enterobacteriaceae* harboring extended-spectrum beta-lactamase and carbapenemase genes in U.S. drinking water. Sci Rep. 2019;9:3938.

Address for correspondence: Christopher Prestel, Centers for Disease Control and Prevention, 1600 Clifton Rd NE, Mailstop H16-3, Atlanta, GA 30329-4027, USA; email: okn0@cdc.gov

Ten-Week Follow-Up of Monkeypox Case-Patient, Sweden, 2022

Aleksandra Pettke, Finn Filén, Katarina Widgren, Andreas Jacks, Hedvig Glans, Sofia Andreasson, Shaman Muradrasoli, Sofia Helgesson, Elenor Hauzenberger, Maria Lind Karlberg, Noura Walai, Annelie Bjerkner, Hadrien Gourlé, Sara Gredmark-Russ, Oskar Karlsson Lindsjö, Klara Sondén,[1] Hilmir Asgeirsson[1]

A previously healthy male patient had detectable monkeypox virus DNA in saliva 76 days after laboratory confirmation of infection. A comprehensive characterization of viral kinetics and a detailed follow-up indicated a declining risk for transmission during the weeks after monkeypox symptoms appeared.

Monkeypox is a zoonotic infection caused by monkeypox virus (MPXV), belonging to the *Orthopoxvirus* genus of the Poxviridae family. Monkeypox outbreaks have historically been described mainly in central and west Africa (*1*). Cases outside Africa are rare and, until 2022, consisted mostly of imported cases, patients' household contacts, and, in some cases, nosocomial infections (*2*,*3*). One outbreak in 2003 outside Africa was linked to importing exotic pets (*4*).

In May 2022, a multinational monkeypox outbreak surfaced; cases were reported from Europe, the Americas, Israel, and Australia. Compared with those in previous outbreaks, these reported patients show a different clinical manifestation of localized rashes and mucosal lesions predominantly in the genital area. Common systemic symptoms included fever and lymphadenopathy. The cases clustered in men who have sex with men (*5*).

Author affiliations: Public Health Agency of Sweden, Solna, Sweden (A. Pettke, S. Muradrasoli, S. Helgesson, E. Hauzenberger, M.L. Karlberg, N. Walai, A. Bjerkner, H. Gourlé, O. Karsson Lindsjö, K. Sondén); Stockholm South General Hospital Skin and Venereology Clinics, Stockholm, Sweden (F. Filén); Stockholm County Council, Stockholm (K. Widgren, A. Jacks); Karolinska Institutet, Stockholm (K. Widgren, H. Glans, S. Gredmark-Russ, K. Sondén, H. Ásgeirsson); Karolinska University Hospital, Stockholm (H. Glans, S. Andreasson, S. Gredmark-Russ, H. Ásgeirsson); Laboratory for Molecular Infection Medicine Sweden, Umeå, Sweden (S. Gredmark-Russ)

DOI: https://doi.org/10.3201/eid2810.221107

We report a monkeypox case detected in Sweden during the multinational outbreak, focusing on the clinical symptoms, microbial diagnostic findings, and viral kinetics in different sample types over time. Moreover, we report a fast and robust bioinformatics analysis of sequencing data for characterizing cases. We obtained consent from the patient for our study.

The Study

The patient, a previously healthy man with no history of smallpox vaccination, first noticed an inguinal swelling (day 0). The next day, he observed a small skin change on his foreskin, progressing over the next days to a deeper, well-circumscribed lesion with local lymphadenopathy. Fever developed on day 5 and 6, peaking at 39°C. One week after symptom onset, the patient sought care at an outpatient clinic. By then, the fever had subsided. No new lesions appeared. He reported a history of receiving oral sex from several male partners within the 3 weeks before symptom onset. At a follow-up visit on day 11, the lesion had increased in size to 2 cm in diameter. Microbiologic analyses for herpes simplex virus, syphilis, and *Haemophilus ducreyi* returned negative results; because of reports of monkeypox cases in Europe manifesting as unusual genital skin lesions, we initiated analysis for MPXV at the Public Health Agency of Sweden. We performed real-time PCRs for orthopoxvirus DNA and MPXV DNA on the genital lesion swab; results were positive and confirmed by Sanger sequencing of an orthopox-specific PCR product.

The genital lesion slowly healed but with increasing local lymphadenopathy; on day 25, the patient had a ruptured local lymph node with discharge. At a follow-up visit on day 53, the patient was feeling

[1]These authors contributed equally to this work.

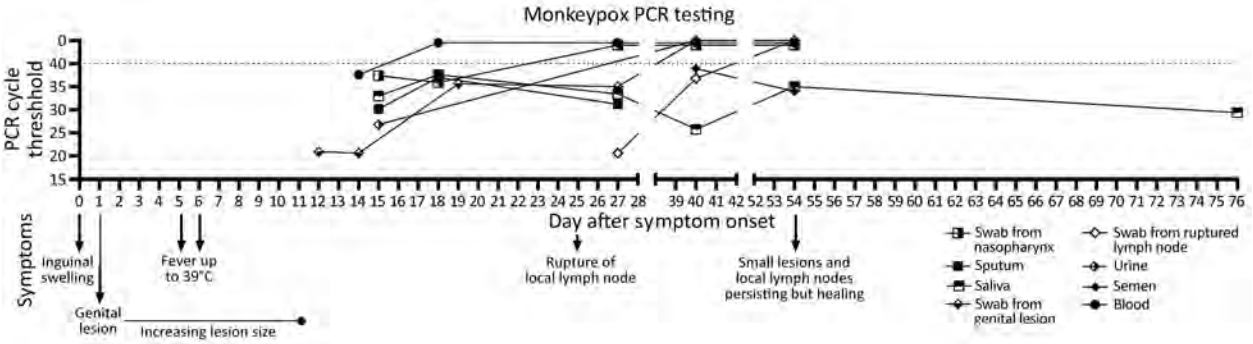

Figure 1. Overview of clinical and laboratory findings in a patient with monkeypox, Sweden, 2022**.** Timeline depicts clinical symptom evolution and PCR testing results. Dotted line indicates cycle threshold for detection of monkeypox virus by real-time PCR.

well but still had enlarged lymph nodes. The original genital lesion had diminished to 5 mm in diameter and bled slightly when touched. The wound from the ruptured lymph node had healed.

We took repeated samples from the patient during the 10-week follow-up period from the genital lesion, the ruptured local lymph node, urine, semen, blood and the respiratory tract. We detected MPXV DNA in most samples (Figure 1; Appendix Table 1, https://wwwnc.cdc.gov/EID/article/28/10/22-1107-App1.pdf). Although tests of all genital samples were initially positive, all showed a rapid decline in viral DNA content. Of note, MPXV DNA was detected in swabs from the ruptured lymph node 40 days after symptom onset, in semen and saliva after 54 days, and in saliva after 76 days (Figure 1; Appendix Table 1).

We performed electron microscopy on skin lesion material and observed viral particles characteristic for orthopoxviruses (Appendix Figure). The particles were 220–450-nm long and 140–260-nm wide. We extracted DNA from the first genital-

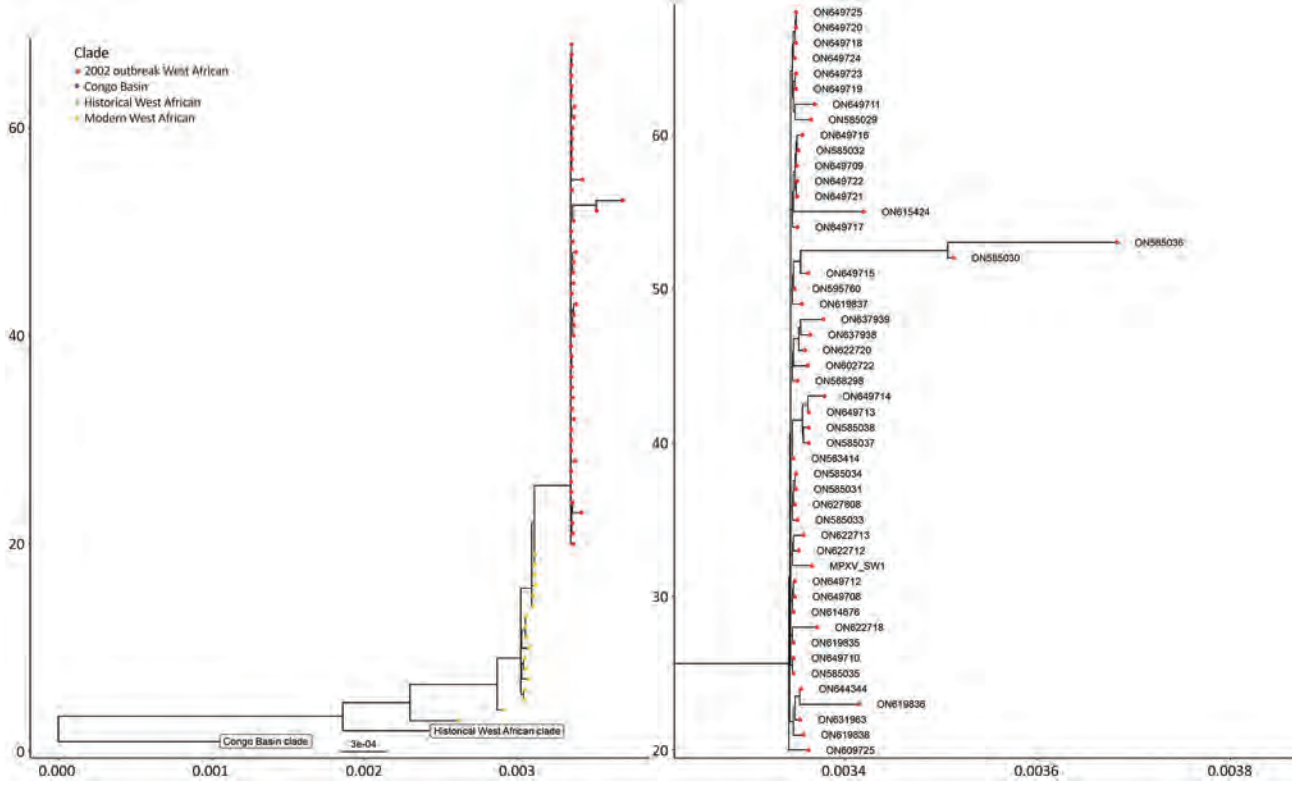

Figure 2. Phylogenetic tree depicting the relationship of the monkeypox virus strain detected in a genital lesion sample from a patient in Sweden to previously published isolates and the strain repsonsible for the 2022 multinational outbreak. The x-axis represents the branch lengths, interpreted as the number of nucleotide substitutions per site. The y-axis represents the tree cardinality (e.g. the amount of sequences represented in the tree) of each clade.

lesion sample and subjected it to metagenomics sequencing using both short-read and long-read technologies. We reconstructed the viral genome from metagenomics data using a long-read first assembly approach. In brief, reads were cleaned from human sequences using Kraken 2 (https://github.com/DerrickWood/kraken2), followed by assembly of the nanopore reads using Flye (http://github.com/fenderglass/Flye), resulting in a single contig representing MPXV. The contig was polished using medaka (https://github.com/nanoporetech/medaka) for the long reads and then ntEdit (https://github.com/bcgsc/ntedit) for the short reads, which produced a nearly complete genome sequence. We compared this genome sequence by whole-genome alignment and tree construction using publicly available sequences (Appendix). The analysis suggested that the case virus belongs to the West Africa clade. Furthermore, the case is closely related with sequences reported from the current outbreak; genome alignment using ViralMSA (https://github.com/niemasd/ViralMSA) showed a single-nucleotide polymorphism distance of 4 nt (Figure 2).

Conclusions

As of August 2022, the multinational monkeypox outbreak is still unfolding; new cases are being reported in an increasing number of countries. Many aspects of monkeypox infection in the ongoing outbreak differ from previous endemic and imported monkeypox cases, including clinical manifestations and route of transmission (*6*,*7*). The new aspects of the infection have implications for clinical case management and behavioral recommendations for the patient, infection control measures, and public health. More knowledge is urgently needed to control the outbreak at an early stage and prevent virus transmission in previously non–monkeypox-endemic regions.

This report highlights several aspects of monkeypox as an emerging infectious disease. First, the case manifested as a single genital lesion accompanied by enlarged local lymph nodes, leading to lymph node rupture. The appearance of localized genital lesions was consistent with recent reports from other countries in Europe (*8*) and clearly demonstrated an alternative clinical manifestation of the strain of MPXV associated with the 2022 multinational outbreak, causing localized lesions rather than the classic generalized rash or vesicles spread over the body. Lymph node rupture is an unusual manifestation.

Second, we presented viral kinetics in different sample materials over time and show that, despite the localized lesion in this patient, viral DNA could also be found in urine, blood, and the respiratory tract. So far, this type of data has been published for few cases (*9*) within the current multinational outbreak, connected to sexual transmission of MPXV, but this finding is consistent with previous reports from classical monkeypox imported from Africa (*2*). The persistent detection of MPXV DNA in samples from semen and the respiratory tract in this case could have implications for transmissibility. Prolonged infectivity of bodily fluids such as semen has been described for viral infections like Zika and Ebola (*10*). However, knowledge gaps include whether a positive PCR result indicates the presence of live virus.

Third, phylogenetic analysis revealed that the virus belongs to the Western Africa clade of monkeypox, which has been associated with lower mortality rates than the Central Africa clade (*7*,*11*). Consistent with this classification, the case-patient described had noncritical illness. Furthermore, the sequence showed high degree of similarity to recently published MPXV sequences from Portugal and other countries (*12*,*13*).

Within the context of the emerging outbreak of monkeypox, we present comprehensive clinical and microbiologic data with long follow-up times revealing persistent PCR positivity. Previous reports have provided PCR data from single timepoints or short follow-up periods of ≤8 days (*9*,*14*). Moreover, we present a strategy for adequate sequencing, highlighting a fast but accurate bioinformatics analysis, combining long reads and short reads, that achieves a near-complete genome assembly (Appendix). This analysis will enable other researchers to reliably classify viruses' phylogenetic relationships, which will lead to rapid and accurate epidemiologic case tracing and phylogenetic network analyses at a relatively low cost.

About the Author

Dr. Pettke is a medical doctor working with diagnostics of high-consequence pathogens at the Public Health Agency of Sweden. She has a strong passion and interest for emerging viruses and global health.

References

1. World Health Organization. Monkeypox. 2022 [cited 2022 May 30]. https://www.who.int/news-room/fact-sheets/detail/monkeypox
2. Adler H, Gould S, Hine P, Snell LB, Wong W, Houlihan CF, et al.; NHS England High Consequence Infectious Diseases (Airborne) Network. Clinical features and management of

human monkeypox: a retrospective observational study in the UK. Lancet Infect Dis. 2022;22:1153–62. https://doi.org/10.1016/S1473-3099(22)00228-6
3. Vaughan A, Aarons E, Astbury J, Brooks T, Chand M, Flegg P, et al. Human-to-human transmission of monkeypox virus, United Kingdom, October 2018. Emerg Infect Dis. 2020;26:782–5. https://doi.org/10.3201/eid2604.191164
4. Centers for Disease Control and Prevention. Update: multistate outbreak of monkeypox—Illinois, Indiana, Kansas, Missouri, Ohio, and Wisconsin, 2003. MMWR Morb Mortal Wkly Rep. 2003;52:642–6.
5. Thornhill JP, Barkati S, Walmsley S, Rockstroh J, Antinori A, Harrison LB, et al.; SHARE-net Clinical Group. Monkeypox virus infection in humans across 16 countries—April–June 2022. N Engl J Med. 2022;NEJMoa2207323. https://doi.org/10.1056/NEJMoa2207323
6. Brown K, Leggat PA. Human monkeypox: current state of knowledge and implications for the future. Trop Med Infect Dis. 2016;1:8. https://doi.org/10.3390/tropicalmed1010008
7. Bunge EM, Hoet B, Chen L, Lienert F, Weidenthaler H, Baer LR, et al. The changing epidemiology of human monkeypox—a potential threat? A systematic review. PLoS Negl Trop Dis. 2022;16:e0010141. https://doi.org/10.1371/journal.pntd.0010141
8. European Centre for Disease Prevention and Control. Epidemiological update: monkeypox multi-country outbreak. 2022 [cited 2022 May 30]. https://www.ecdc.europa.eu/en/news-events/epidemiological-update-monkeypox-multi-country-outbreak
9. Antinori A, Mazzotta V, Vita S, Carletti F, Tacconi D, Lapini LE, et al.; INMI Monkeypox Group. Epidemiological, clinical and virological characteristics of four cases of monkeypox support transmission through sexual contact, Italy, May 2022. Euro Surveill. 2022;27. https://doi.org/10.2807/1560-7917.ES.2022.27.22.2200421
10. Thorson AE, Deen GF, Bernstein KT, Liu WJ, Yamba F, Habib N, et al.; Sierra Leone Ebola Virus Persistence Study Group. Persistence of Ebola virus in semen among Ebola virus disease survivors in Sierra Leone: a cohort study of frequency, duration, and risk factors. PLoS Med. 2021;18:e1003273. https://doi.org/10.1371/journal.pmed.1003273
11. Likos AM, Sammons SA, Olson VA, Frace AM, Li Y, Olsen-Rasmussen M, et al. A tale of two clades: monkeypox viruses. J Gen Virol. 2005;86:2661–72. https://doi.org/10.1099/vir.0.81215-0
12. Isidro J, Borges V, Pinto M, Ferreira R, Sobral D, Nunes A, et al. First draft genome sequence of monkeypox virus associated with the suspected multi-country outbreak, May 2022. 2022 [cited 2022 May 30]. https://virological.org/t/first-draft-genome-sequence-of-monkeypox-virus-associated-with-the-suspected-multi-country-outbreak-may-2022-confirmed-case-in-portugal/799
13. GenBank. Monkeypox virus isolate MPXV-BY-IMB25241, complete genome. 2022 [cited 2022 Aug 23]. https://www.ncbi.nlm.nih.gov/nuccore/ON568298
14. Tutu van Furth AM, van der Kuip M, van Els AL, Fievez LC, van Rijckevorsel GG, van den Ouden A, et al. Paediatric monkeypox patient with unknown source of infection, the Netherlands, June 2022. Euro Surveill. 2022;27. https://doi.org/10.2807/1560-7917.ES.2022.27.29.2200552

Address for correspondence: Klara Sondén, Public Health Agency of Sweden, Department of Microbiology, 171 65 Solna, Sweden; email: klara.sonden@folkhalsomyndigheten.se

Early Estimates of Monkeypox Incubation Period, Generation Time, and Reproduction Number, Italy, May–June 2022

Giorgio Guzzetta, Alessia Mammone, Federica Ferraro, Anna Caraglia, Alessia Rapiti, Valentina Marziano, Piero Poletti, Danilo Cereda, Francesco Vairo, Giovanna Mattei, Francesco Maraglino, Giovanni Rezza,[1] Stefano Merler[1]

We analyzed the first 255 PCR-confirmed cases of monkeypox in Italy in 2022. Preliminary estimates indicate mean incubation period of 9.1 (95% CI 6.5–10.9) days, mean generation time of 12.5 (95% CI 7.5–17.3) days, and reproduction number among men who have sex with men of 2.43 (95% CI 1.82–3.26).

After the first reports of autochthonous cases of monkeypox (MPX) in Europe at the beginning of May, the World Health Organization (WHO) and the European Centre for Disease Prevention and Control alerted member states to report suspected and confirmed cases. Apart from early cases reported in the United Kingdom, most cases were identified in men who have sex with men (MSM) (*1*–*4*). We analyzed characteristics of the first 255 PCR-confirmed cases of monkeypox in Italy in 2022.

The Study

In Italy, suspected MPX cases fitting the criteria of the World Health Organization case-definition (*5*) are reported to the surveillance system of the Ministry of Health. Only those cases testing positive by MPX-specific PCR were considered confirmed. Information on main patient characteristics (age, sex, earliest date of symptom onset, presence of rash and other signs, exposure modality, and travel abroad) were collected.

As of July 8, 2022, a total of 255 PCR-confirmed cases had been reported in Italy (Figure). All except 2 were men, and 190/200 (95%) men who disclosed information reported having sex with men; median age was 37 (range 20–71) years.

For 139/184 cases for which information was available, rash was localized at the genital or perianal area. Fever was reported in 151/222 cases for which information was available.

Information about travel was available for 228 case-patients; 86 (37.7%) had traveled abroad, and 25 (29.1%) of those had vacationed in the Canary Islands, suggesting a major amplifying event had occurred (Table). Only 1 case-patient had traveled to West Africa and was symptomatic upon arrival in Italy.

We estimated the incubation period for 30 cases with known date of symptom onset and for which epidemiologic investigations enabled the identification of the likely period of exposure (exact date for 15 cases and dates of visit to Canary Islands for 15 cases). We estimated the generation time (time elapsed between date of exposure of a confirmed case and those of secondary cases) by considering 16 infector-infectee pairs identified during contact tracing operations. We assumed the 2 periods were distributed as gamma functions and estimated them using a Bayesian approach similar to that adopted by F. Miura et al. (*6*). We considered likely dates of exposure for each confirmed case within a Markov chain Monte Carlo procedure. For estimating generation time, we assumed no presymptomatic transmission. Therefore, s ampling of candidate dates of exposure was repeated

Author affiliations: Center for Health Emergencies, Fondazione Bruno Kessler, Trento, Italy (G. Guzzetta, V. Marziano, P. Poletti, S. Merler); Directorate General of Health Prevention, Ministry of Health, Rome, Italy (A. Mammone, F. Ferraro, A. Caraglia, A. Rapiti, F. Maraglino, G. Rezza); Directorate General for Health, Lombardy Region, Milano, Italy (D. Cereda); National Institute of Infectious Diseases Lazzaro Spallanzani, Rome (F. Vairo); General Directorate for Personal Care, Health and Welfare, Emilia Romagna Region, Bologna, Italy (G. Mattei)

DOI: https://doi.org/10.3201/eid2810.221126

[1]These senior authors contributed equally to this article.

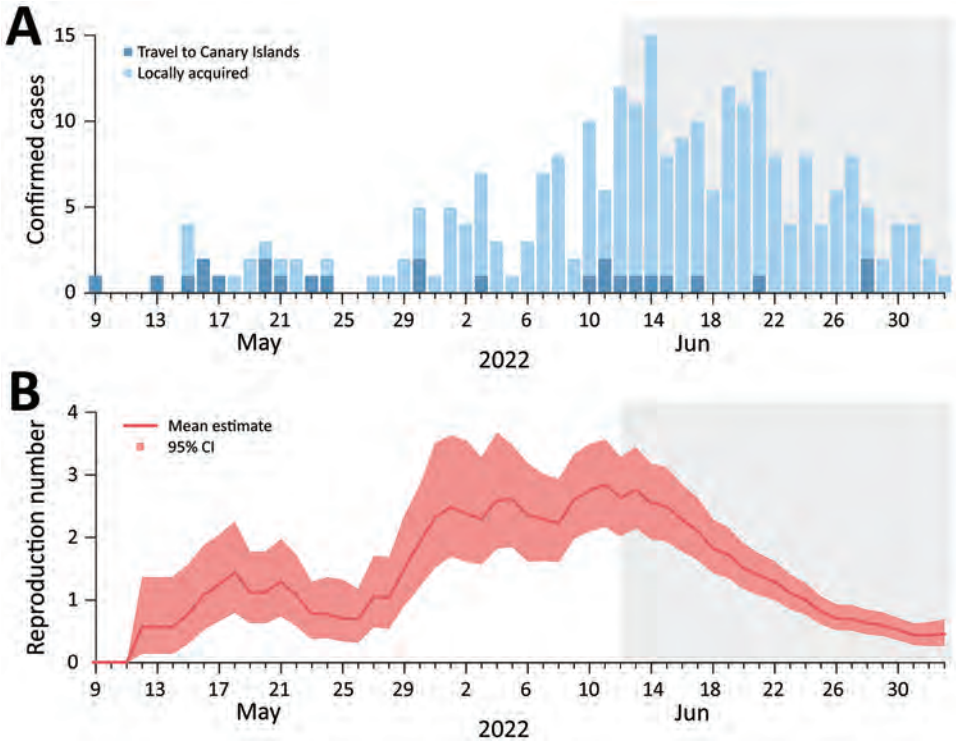

Figure. Epidemic curve and reproduction number of monkeypox cases in Italy through July 8, 2022. A) Number of cases by date of symptom onset and history of travel in Canary Islands. For 4 persons, the date of symptom onset was unknown. B) Estimate of the net reproduction number over time from the epidemic curve by date of symptom onset. We assumed that all cases with a history of travel to Canary Islands were imported and that all the others were locally transmitted, and we used a generation time distribution with mean 12.5 days. Gray shading indicates the part of the epidemic curve that is possibly incomplete because of diagnostic and reporting delays.

if the date of exposure for the infectee was earlier than the date of symptom onset for the infector. We used estimates of the generation time to compute the net reproduction number and used individual anonymized data to estimate the incubation period and generation time (Appendix, https://wwwnc.cdc.gov/EID/article/28/10/22-1126-App1.pdf).

The mean incubation period was estimated to be 9.1 days (95% CI 6.5–10.9 days; 5th and 95th percentiles of the distribution 2–20 days). The mean generation time was estimated to be 12.5 days (95% CI 7.5–17.3 days; 5th and 95th percentiles of the distribution, 5–23 days). By assuming a mean generation time of 12.5 days and importation from Canary Islands, we estimate the mean net reproduction number (mean number of cases generated by a single index case) at 2.43 (95% CI 1.82–3.26) during the first week of June (i.e., when the net reproduction number had stabilized so that the growth of the epidemic curve could be approximated as exponential). A similar estimate was obtained under the assumption of exponential growth in the first week of June (Appendix). After June 12, 2022, we estimated a progressive decrease of the reproduction number.

Table. Characteristics of 255 confirmed monkeypox cases reported in Italy through July 8, 2022

Characteristic	Value
Sex	
M	253 (99.2)
F	2 (0.8)
Median age, y (range)	37 (20–71)
Clinical symptoms†	
Fever	151/222 (68.0)
Rash	248/251 (98.8)
Genital/perianal rash	139/184 (75.5)
Travels†	
Travel abroad in previous 21 d	86/228 (37.7)
Travel to Canary Islands in previous 21 d	25/142 (17.6)

*Values are no. (%) patients except as indicated.
†Denominators indicate the total number of available answers.

Conclusions

The first large outbreak of MPX outside Africa is to some extent unique. The analysis of virus genome strongly suggests that the epidemic is caused by the West African clade of the MPX virus (*7*); however, with the exception of 1 case-patient who reported travels to West Africa (*8*), ≥60% of cases diagnosed in Italy were autochthonous. Retrospective investigations in Portugal and United Kingdom indicated that the first case-patients had symptoms in April 2022. The presence of skin lesions at the point of sexual contact is suggestive of sexual transmission (*9*).

After early reports of this multicountry outbreak, the Ministry of Health of Italy issued recommendations consisting of case notification, protective measures to reduce contacts and possible exposure for healthcare workers, tracing of close contacts with monitoring of symptom onset, and the possibility of implementing quarantine measures at the discretion of

local health authorities in particular epidemiologic or environmental contexts (*10*). After the first 4 cases in MSM in Italy who had traveled abroad (*4*), cases were increasingly notified (*8*), mostly in the Lombardy and Lazio regions, where Milan and Rome are located; 11 of 21 regional health authorities reported cases. Almost all cases were among MSM. Travel abroad occurred in a substantial fraction of cases (38.9%) identified in Italy, and direct or sexual contact is still likely to be the main transmission mode. Whether the infection was transmitted through direct contact with skin lesions or body fluids remains undefined. The link to different geographic areas (Europe and West Africa) underlines the possibility of multiple independent introductions of the virus, suggesting widespread infection in West Africa before the COVID-19 pandemic (*3*,*11*).

Using a limited number of MPX cases, we provided estimates of the mean incubation period (≈9 days; n = 15 persons with known date of exposure and 15 persons with known travel dates in Canary Islands) and of the mean generation time (≈12 days; n = 16 infector-infectee pairs). Based on the estimated mean generation time, we found that the reproduction number for this outbreak is ≈2.4, although with a broad uncertainty (95% CI 1.82–3.26) because of the limited number of locally acquired confirmed cases. We found small variations in the estimated reproduction number (mean values ranging from 2.08 to 2.70) when considering different distributions of the generation time (mean 7.5 or 17.3 days) and when exploring alternative assumptions on the importation of cases (Appendix). Our estimates of the reproduction number refer to the community of MSM in which MPX is spreading and not to the general population. The extent to which the decrease of the reproduction number estimated after June 12, 2022, is a result of reduced transmission (e.g., led by increasing awareness about the risk of infection) or from the analysis of incomplete data because of diagnostic and reporting delays is unclear. However, considering that most cases seem to have been transmitted by sexual contact, the reproduction number is likely below threshold in the general population. Besides the limited number of cases, our estimates might be biased by several factors: the assumption that case-patients returning from Canary Islands acquired the infection there, possible recall bias for the dates of exposure, and selection bias in the reconstructed infector-infectee pairs (e.g., a recent sexual partner might be more likely to be identified). Finally, the observed reproduction number might have been inflated by the potential occurrence of superspreading events.

Maintaining a high level of public attention and providing nonstigmatizing information to at-risk population groups are key to contain the spread of MPX virus, in addition to considering the seasonal intensity of aggregation events and recreational activities. Our estimates provide useful indications to assist with outbreak surveillance and containment. The distribution of the incubation period identifies the period over which symptoms should be monitored among identified contacts, and the generation time provides insight on the recommended duration of isolation for confirmed cases and the timeframe for contact tracing. The generation time is also necessary for computing the net reproduction number, which is critical to monitoring the spread of disease over time.

Acknowledgments

We thank Corrado Cenci, Arianna Bruscolotti, Andreina Pagini, Ivana Raccio, Francesca Zanella, Francesca Russo, Chiara Pasqualini, Marcello Tirani, Federica Attanasi, Marino Faccini, Gian Luigi Belloli, Giulio Matteo, Gabriella De Carli, Emanuela Balocchini, Daniela Senatore, Cristina Zappetti, Maria Grazia Zuccali, Domenico Martinelli, the Directorate General of Health Prevention, Ministry of Health, and the Regional Health authorities for their collaboration. We also thank all healthcare workers in the regions who notified the cases.

About the Author

Dr. Guzzetta is a researcher at the Bruno Kessler Foundation in Trento, Italy. His primary research interests are epidemiology and mathematical models of infectious disease transmission dynamics with a focus on public health applications, assessments of potential risks, and evaluation of effectiveness of interventions.

References

1. Vivancos R, Anderson C, Blomquist P, Balasegaram S, Bell A, Bishop L, et al.; UKHSA Monkeypox Incident Management team; Monkeypox Incident Management Team. Community transmission of monkeypox in the United Kingdom, April to May 2022. Euro Surveill. 2022;27:2200422. https://doi.org/10.2807/1560-7917.ES.2022.27.22.2200422
2. Perez Duque M, Ribeiro S, Martins JV, Casaca P, Leite PP, Tavares M, et al. Ongoing monkeypox virus outbreak, Portugal, 29 April to 23 May 2022. Euro Surveill. 2022;27:2200424. https://doi.org/10.2807/1560-7917.ES.2022.27.22.2200424
3. European Centre for Disease Prevention and Control (ECDC). Monkeypox multicountry outbreak—23 May 2022. Stockholm: The Centre; 2022.
4. Antinori A, Mazzotta V, Vita S, Carletti F, Tacconi D, Lapini LE, et al.; INMI Monkeypox Group. Epidemiological, clinical and virological characteristics of four cases of monkeypox support transmission through sexual contact,

Italy, May 2022. Euro Surveill. 2022;27:2200421. https://doi.org/10.2807/1560-7917.ES.2022.27.22.2200421
5. World Health Organization. Disease Outbreak News, 21 May 2022. Multi-country monkeypox outbreak in non-endemic countries [cited 2022 Aug 5]. https://www.who.int/emergencies/disease-outbreak-news/item/2022-DON385
6. Miura F, van Ewijk CE, Backer JA, Xiridou M, Franz E, Op de Coul E, et al. Estimated incubation period for monkeypox cases confirmed in the Netherlands, May 2022. Euro Surveill. 2022;27:2200448. https://doi.org/10.2807/1560-7917.ES.2022.27.24.2200448
7. Isidro J, Borges V, Pinto M, Ferreira R, Sobral D, Nunes A, et al. First draft genome sequence of monkeypox virus associated the suspected multi-country outbreak, May 2022 [cited 2022 Aug 5]. https://virological.org/t/first-draft-genome-sequence-of-monkeypox-virus-associated-with-the-suspected-multi-country-outbreak-may-2022-confirmed-case-in-portugal/799
8. Ferraro F, Caraglia A, Rapiti A, Cereda D, Vairo F, Mattei G, et al. Letter to the editor: multiple introductions of MPX in Italy from different geographic areas. Euro Surveill. 2022;27:2200456. https://doi.org/10.2807/1560-7917.ES.2022.27.23.2200456
9. Otu A, Ebenso B, Walley J, Barceló JM, Ochu CL. Global human monkeypox outbreak: atypical presentation demanding urgent public health action. Lancet Microbe. 2022;3:e554–5. https://doi.org/10.1016/S2666-5247(22)00153-7
10. Minister of Health, Italy. Moneypox [in Italian] [cited 2022 Aug 5]. https://www.salute.gov.it/portale/news/p3_2_1_1_1.jsp?lingua=italiano&menu=notizie&p=dalministero&id=5907
11. Rezza G. Emergence of human monkeypox in west Africa. Lancet Infect Dis. 2019;19:797–9. https://doi.org/10.1016/S1473-3099(19)30281-6

Address for correspondence: Stefano Merler, Fondazione Bruno Kessler, via Sommarive 18, 38123, Povo (Trento), Italy; email: merler@fbk.eu

Epidemiology of Early Monkeypox Virus Transmission in Sexual Networks of Gay and Bisexual Men, England, 2022

Amoolya Vusirikala,[1] Hannah Charles,[1] Sooria Balasegaram, Neil Macdonald, Deepti Kumar, Ceri Barker-Burnside, Kerry Cumiskey, Michelle Dickinson, Michelle Watson, Oluwakemi Olufon, Katie Thorley, Paula Blomquist, Charlotte Anderson, Thomas Ma, Hamish Mohammed, Samantha Perkins, Karthik Paranthaman, Petra Manley, Obaghe Edeghere, Katy Sinka, Mateo Prochazka

After community transmission of monkeypox virus was identified in Europe, interviews of 45 case-patients from England indicated transmission in international sexual networks of gay and bisexual men since April 2022. Interventions targeting sex-on-premises venues, geospatial dating applications, and sexual health services are likely to be critical for outbreak control.

Monkeypox is a zoonotic viral infection endemic to West and Central Africa. Human-to-human transmission of monkeypox virus (MPXV) is thought to be primarily through close skin-to-skin contact; other transmission routes include respiratory secretions and fomites (*1*). MPXV incubation period is 5–21 days (*1*). Before 2022, sporadic cases reported in England had been directly linked to travel from monkeypox-endemic areas or were identified as household or healthcare contacts of case-patients (*2*–*4*). However, in May 2022, several countries in Europe reported sustained human-to-human transmission of MPXV, primarily in sexual networks of gay, bisexual, and other men who have sex with men (GBMSM) (*5*–*7*).

By May 25, 2022, in England, 85 PCR-confirmed monkeypox cases were reported, 82 with known or suspected links to transmission in GBMSM sexual networks (*7*). Sexual networks are social networks in which persons are connected by sexual activity. An urgent need for information about the epidemiology of this unusual pattern of MPXV transmission led the UK Health Security Agency (UKHSA) to deploy rapid sexual health questionnaires to persons with confirmed MPXV infection. We analyzed the findings and implications for public health action.

This study was undertaken for health protection purposes under permissions granted to UKHSA to collect and process confidential patient data under Regulation 3 of The Health Service (Control of Patient Information) Regulations 2020 and Section 251 of the National Health Service Act 2006. All data were anonymized during analysis, and records were stored securely.

The Study

Persons with confirmed MPXV infection were identified by PCR at the Rare and Imported Pathogens Laboratory at UKHSA, according to standard procedure, and reported to local health protection teams, who were responsible for public health management. Case-patients with known or suspected links to transmission in GBMSM sexual networks were invited for follow-up interviews focused on their sexual health; phone interviews were conducted during May 25–30, 2022, and followed a structured questionnaire. Participation in the follow-up interviews was voluntary, and verbal consent was obtained after the context and rationale for the additional interview was explained. The questionnaire information was similar to that captured in previous outbreaks: demographics (sex, age, sexual orientation, ethnicity, country of birth); potential exposures in the 21 days before symptom onset (travel history, exposure events, sexual behavior); markers of sexual behavior associated with higher risk of acquiring sexually transmitted infections (STIs) (previous STI, number

Author affiliation: UK Health Security Agency, London, UK

DOI: https://doi.org/10.3201/eid2810.220960

[1]These authors contributed equally to this article.

of sex partners in past 3 months); and HIV prevention and care (status, HIV preexposure prophylaxis [PrEP], HIV treatment) (*8*,*9*).

Sexual activity was defined as any direct contact of a sexual nature, including kissing, oral, and penetrative sex. Group sex was defined as sexual activity with >1 person at a time. Chemsex was defined as use of drugs such as GHB (gamma-hydroxybutyrate), crystal methamphetamine, or mephedrone during sex. Exposure sites/events included sex-on-premises venues (commercial venues where sexual activity occurs), private sex parties, cruising, and international events/festivals. Cruising was defined as sexual activity with anonymous partners in public outdoor spaces. Private sex parties were defined as group sex in a household, and when not explicitly mentioned, private sex parties were inferred if a person reported group sex and chemsex outside sex-on-premises venues.

We securely recorded data by using the online questionnaire tool Snap 11 Professional (https://www.snapsurverys.com) and extracted data for analysis on May 30, 2022. We used Stata 17.0 (https://www.stata.com) to clean and summarize the data to provide descriptive statistics. To assess participation bias, we used Mann-Whitney U, χ^2, and Fisher exact tests to compare case-patients by age, region of residence, and travel history; data were sourced from the public health case management system (HPZone, https://hpzone.phe.gov.uk). To identify time when community transmission started and potential routes of importation, we plotted onset of first symptoms (prodrome or rash), travel, and venue attendance dates on timelines.

Of 82 case-patients with known or suspected links to transmission in GBMSM sexual networks identified up to May 25, 2022 (*7*), we re-interviewed 45 (55%) for this specific detailed questionnaire (Figure). Reasons for not interviewing included lack of contact details (n = 11), declining to participate (n = 4), and inability to re-establish phone contact (n = 22). We found no significant differences between interviewed and noninterviewed case-patients in terms of age, region of residence, or travel history (p>0.05).

Symptom onset dates were April 8–May 20, 2022. All cases were diagnosed in May; because of suspected community transmission, some persons with ulcerative and vesicular rashes were re-called for MPXV testing and retrospectively identified as early confirmed case-patients (*7*). Of 31 interviewed case-patients who did not travel abroad in the 21 days before symptom onset, symptom onset began in April 2022, including for 1 case-patient who subsequently traveled to an international event. Throughout May 2022, symptoms developed in several case-patients who returned to the United Kingdom after traveling in Europe (Figure).

Nearly all interviewed case-patients self-identified as either gay or bisexual (98%, 44/45). HIV status was reported by 43 case-patients: 74% (32/43) were HIV negative, of which 91% (29/32) were receiving PrEP; 11/43 (26%) reported living with HIV and all were receiving HIV treatment. Although most (29/45, 64%) case-patients reported attending sex-on-premises

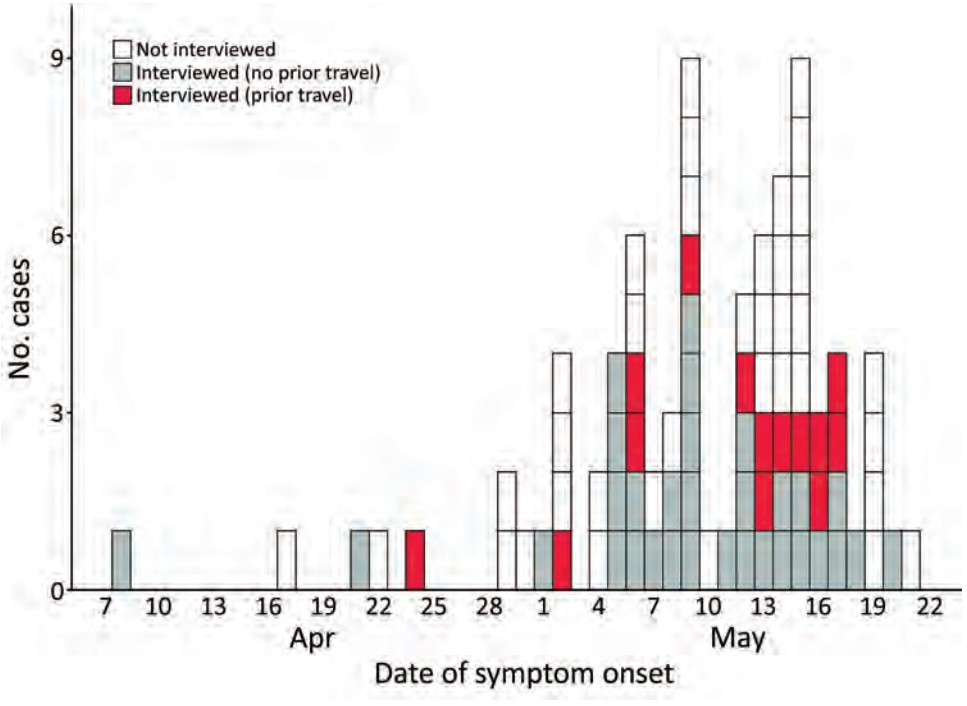

Figure. Epidemic curve of monkeypox cases, by symptom onset date and patient travel status within 21 days before symptom onset, England, 2022.

Table. Characteristics and exposures of 45 interviewed persons with confirmed monkeypox, England, 2022*

Variables	No. (%)
Cisgender men	45 (100)
Ethnicity	
White	35 (78)
Black	1 (2)
Asian	3 (7)
Mixed	3 (7)
Other	3 (7)
Place of birth	
United Kingdom	19 (43)
Europe, not including United Kingdom	12 (27)
South America	5 (11)
Other	8 (18)
Unknown	1 (2)
Region of residence	
London	39 (87)
Other regions in the United Kingdom	6 (13)
Sexual orientation	
Gay	40 (89)
Bisexual	4 (9)
Heterosexual	0
Other	1 (2)
No. sexual contacts in past 3 mo	
1	4 (9)
2–3	6 (14)
4–9	13 (30)
≥10	20 (47)
Prefer not to say/unknown	2 (3)
HIV prevention and care	
HIV negative	32 (71)
Receiving PrEP	29 (91)
Living with diagnosed HIV	11 (24)
Receiving HIV treatment	11 (100)
Undetectable viral load	10 (91)
Prefer not to say/unknown HIV status	2 (4)
History of STI in past year	
Yes	27 (60)
No	18 (40)
Travel abroad within 21 d before symptom onset	
Yes, reported sexual activity	9 (20)
Yes, but no sexual activity	5 (11)
No	31 (69)
Exposure events within 21 d before symptom onset†	
Festivals outside of the United Kingdom	5 (11)
Sex-on-premises venues	20 (44)
Private sex parties	9 (20)
Cruising grounds	7 (16)
None of the above	16 (36)
Sexual activity within 21 d before symptom onset‡	
Sexual activity with new partners	37 (82)
Sexual activity with one-time partners	34 (76)
Sexual activity with occasional partners	24 (53)
Sexual activity with established partners	12 (27)
Sexual activity with women	2 (5)
Group sexual activity	20 (44)
Chemsex	10 (22)
Sexual activity with partners who are not regular UK residents	11 (24)
Sexual activity in locations different from city/town of residence	13 (30)
Sexual activity with partners met via geospatial dating apps	28 (64)
No sexual activity reported	2 (4)

*Sexual activity was defined as direct contact of a sexual nature, such as kissing, oral sex, and penetrative (vaginal, anal) sex. Some categories in this table were collapsed to avoid deductive disclosure. Median (interquartile range) age, 40 (32–43) y. PrEP, pre-exposure prophylaxis; STI, sexually transmitted infection.
†Sex-on-premises venues, private sex parties and cruising grounds are activities that took place either in the United Kingdom or abroad.
‡New partner, person with whom the index case-patient is likely to have had sex on >1 occasion; one-time partner, person with whom the index case-patient has had sex on 1 occasion only; occasional partner, person with whom the index case-patient has had sex on >1 occasion and with whom there is an expectation of sex again on a sporadic or regular basis; established partner, primary partner or secondary partner (e.g., a long-term affair) (*10*); chemsex, use of drugs such as GHB (gamma-hydroxybutyrate), crystal methamphetamine, or mephedrone during sex.

venues, festivals, private sex parties, or cruising grounds in the 21 days before symptom onset, 16/45 (36%) did not report such exposures (Table). Of those, 12/16 (75%) reported sexual activity with new partners; 10/12 (83%) met via geospatial dating applications.

Conclusions

Our findings suggest that sustained domestic MPXV transmission in sexual networks of GBMSM in England has been occurring since at least April 2022, with potential importations and exportations from other countries in Europe. MPXV transmission in sexual networks has been suggested for outbreak investigations in Nigeria (*11*). The origin and prevalence of MPXV infection among GBMSM is unknown, but international dissemination was probably catalyzed by travel and resumption of events after lifting of restrictions associated with the COVID-19 pandemic.

Our findings show that domestic transmission seems to be sustained by sexual contact in dense sexual networks of GBMSM, often between multiple new partners who are probably difficult to contact trace because of one-time contacts. Similar to previous outbreaks of other STIs among GBMSM (*12*,*13*), contact tracing alone might not be effective as the primary control intervention to stop transmission.

Our findings also suggest that a substantial element of MPXV transmission in England occurs within sex-on-premises venues. To achieve outbreak control, targeted interventions for venues and their users are vital, including supporting enhanced cleaning of venues to prevent transmission via fomites, targeted health promotion to build awareness and inform risk management, and innovative approaches to support contact tracing of venue attendees (*14*). Designing and implementing these interventions requires community and stakeholder engagement.

Persons with a monkeypox diagnosis were in frequent contact with sexual health services and linked to care for HIV medication or PrEP. This link to existing services and programs provides an opportunity for policymakers to implement other interventions to reach those with highest need, including using smallpox Modified Vaccinia Ankara vaccine (Bavarian Nordic, https://www.bavarian-nordic.com) as PrEP for MPXV (*15*).

A substantial proportion of case-patients did not report specific exposure settings, stressing the need for wider interventions to reach all GBMSM in these sexual networks. The high use of geospatial dating applications highlights their utility as a platform for health promotion.

Limitations of this study include social desirability bias, participation bias, and evolving patterns of transmission, affecting their generalizability. Nonetheless, these analyses may provide information for the initial outbreak response in countries with similar transmission patterns. Because of the high interconnectivity of sexual networks, urgent multilateral action is needed to stop human-to-human transmission and avoid global endemicity.

Acknowledgments

We thank all persons who took part in the interviews. This report would not have been possible without the contribution of many colleagues across the healthcare system in the United Kingdom, including health protection teams in the UKHSA, the London Coordination and Response Cell, and the Sexual Health Liaison Group. We gratefully acknowledge all those across UKHSA, National Health Service, the British Association for Sexual Health and HIV, the British HIV Association, sexual health services, and Devolved Administrations in the United Kingdom involved in the response and the advice and support from third sector organizations, including the Terrence Higgins Trust, The Love Tank, and Stonewall.

M.P., S.B., A.V., H.C., N.M., D.K., C.B.B., K.C., M.D., M.W., O.O., P.B., C.A., K.P., T.M., and O.E. were involved in epidemiologic investigations. M.P., H.C., S.B., K.T., H.M., K.P., N.M., S.P., D.K., and P.M. contributed to questionnaire design. M.P., A.V., H.C., S.B., N.M., and P.B. drafted the manuscript. All authors read, revised, and approved the final manuscript.

About the Author

Dr. Vusirikala is a UK Field Epidemiology Training Fellow and a specialist registrar in public health, working in the UK Health Security Agency. Her research interests include infectious disease epidemiology and outbreak investigations.

References

1. World Health Organization. Monkeypox [cited 2022 Jul 13]. https://www.who.int/news-room/fact-sheets/detail/monkeypox
2. Vaughan A, Aarons E, Astbury J, Balasegaram S, Beadsworth M, Beck CR, et al. Two cases of monkeypox imported to the United Kingdom, September 2018. Euro Surveill. 2018;23. https://doi.org/10.2807/1560-7917.ES.2018.23.38.1800509
3. Vaughan A, Aarons E, Astbury J, Brooks T, Chand M, Flegg P, et al. Human-to-human transmission of monkeypox virus, United Kingdom, October 2018. Emerg Infect Dis. 2020;26:782–5. https://doi.org/10.3201/eid2604.191164
4. Hobson G, Adamson J, Adler H, Firth R, Gould S, Houlihan C, et al. Family cluster of three cases of monkeypox imported from Nigeria to the United Kingdom, May 2021.

Euro Surveill. 2021;26. https://doi.org/10.2807/1560-7917.ES.2021.26.32.2100745
5. Perez Duque M, Ribeiro S, Martins JV, Casaca P, Leite PP, Tavares M, et al. Ongoing monkeypox virus outbreak, Portugal, 29 April to 23 May 2022. Euro Surveill. 2022; 27: 2200424 https://doi.org/10.2807/1560-7917.ES.2022.27.22.2200424
6. Antinori A, Mazzotta V, Vita S, Carletti F, Tacconi D, Lapini LE, et al.; INMI Monkeypox Group. Epidemiological, clinical and virological characteristics of four cases of monkeypox support transmission through sexual contact, Italy, May 2022. Euro Surveill. 2022;27:2200421. https://doi.org/10.2807/1560-7917.ES.2022.27.22.2200421
7. Vivancos R, Anderson C, Blomquist P, Balasegaram S, Bell A, Bishop L, et al.; UKHSA Monkeypox Incident Management Team. Community transmission of monkeypox in the United Kingdom, April to May 2022. Euro Surveill. 2022;27:2200422. https://doi.org/10.2807/1560-7917.ES.2022.27.22.2200422
8. Gilbart VL, Simms I, Jenkins C, Furegato M, Gobin M, Oliver I, et al. Sex, drugs and smart phone applications: findings from semistructured interviews with men who have sex with men diagnosed with *Shigella flexneri* 3a in England and Wales. Sex Transm Infect. 2015;91:598–602. https://doi.org/10.1136/sextrans-2015-052014
9. Charles H, Prochazka M, Thorley K, Crewdson A, Greig DR, Jenkins C, et al.; Outbreak Control Team. Outbreak of sexually transmitted, extensively drug-resistant *Shigella sonnei* in the UK, 2021–22: a descriptive epidemiological study. Lancet Infect Dis. 2022;S1473-3099(22)00370-X. https://doi.org/10.1016/S1473-3099(22)00370-X
10. Estcourt CS, Flowers P, Cassell JA, Pothoulaki M, Vojt G, Mapp F, et al. Going beyond 'regular and casual': development of a classification of sexual partner types to enhance partner notification for STIs. Sex Transm Infect. 2022;98:108–14. https://doi.org/10.1136/sextrans-2020-054846
11. Ogoina D, Izibewule JH, Ogunleye A, Ederiane E, Anebonam U, Neni A, et al. The 2017 human monkeypox outbreak in Nigeria—report of outbreak experience and response in the Niger Delta University Teaching Hospital, Bayelsa State, Nigeria. PLoS One. 2019;14:e0214229. https://doi.org/10.1371/journal.pone.0214229
12. Beebeejaun K, Degala S, Balogun K, Simms I, Woodhall SC, Heinsbroek E, et al. Outbreak of hepatitis A associated with men who have sex with men (MSM), England, July 2016 to January 2017. Euro Surveill. 2017;22. https://doi.org/10.2807/1560-7917.ES.2017.22.5.30454
13. Simms I, Field N, Jenkins C, Childs T, Gilbart VL, Dallman TJ, et al. Intensified shigellosis epidemic associated with sexual transmission in men who have sex with men—*Shigella flexneri* and *S. sonnei* in England, 2004 to end of February 2015. Euro Surveill. 2015;20:21097. https://doi.org/10.2807/1560-7917.ES2015.20.15.21097
14. UK Health Security Agency, Public Health Scotland, Public Health Wales, Public Health Agency Northern Ireland. Principles for monkeypox control in the UK: 4 nations consensus statement [cited 2022 Jul 13]. https://www.gov.uk/government/publications/principles-for-monkeypox-control-in-the-uk-4-nations-consensus-statement/principles-for-monkeypox-control-in-the-uk-4-nations-consensus-statement
15. UK Health Security Agency. Monkeypox outbreak: vaccination strategy [cited 2022 Jul 13]. https://www.gov.uk/guidance/monkeypox-outbreak-vaccination-strategy

Address for correspondence: Mateo Prochazka, UK Health Security Agency, 61 Colindale Ave, London NW9 5EQ, UK; email: mateo.prochazka@ukhsa.gov.uk

Nosocomial COVID-19 Incidence and Secondary Attack Rates among Patients of Tertiary Care Center, Zurich, Switzerland

Aline Wolfensberger, Verena Kufner, Maryam Zaheri, Marius Zeeb, Isabelle Nortes, Peter W. Schreiber, Miriam Vazquez, Verena Schärer, Thomas Scheier, Stefan Schmutz, Elisabeth Probst, Dirk Saleschus, Michael Huber, Silvana K. Rampini, Walter Zingg

Of 1,118 patients with COVID-19 at a university hospital in Switzerland during October 2020–June 2021, we found 83 (7.4%) had probable or definite healthcare-associated COVID-19. After in-hospital exposure, we estimated secondary attack rate at 23.3%. Transmission was associated with longer contact times and with lower cycle threshold values among index patients.

Since the beginning of the COVID-19 pandemic, hospitals have introduced infection prevention and control (IPC) measures to protect inpatients from SARS-CoV-2. Despite these precautions, healthcare-associated COVID-19 has affected a notable proportion of hospitalized patients (*1*–*3*). During the second and third waves of COVID-19 in Switzerland, an increasing number of patients with presymptomatic or asymptomatic COVID-19 exposed hospital roommates to SARS-CoV-2. We estimated the secondary attack rate (SAR) after exposure in a hospital in Zurich and identified risk factors for SARS-CoV-2 transmission.

The Study

University Hospital Zurich, a 900-bed tertiary care center, implemented intensified standard precaution measures during the COVID-19 pandemic (Appendix, https://wwwnc.cdc.gov/EID/article/28/10/22-0321-App1.pdf). We included in our analysis all patients with COVID-19 admitted during the second and third COVID-19 waves, weeks 40 of 2020 through 25 of 2021; a small percentage were also included in a study investigating transmission to healthcare workers (*4*). We stratified COVID-19 sources as community-associated, healthcare-associated (definite and probable), or indeterminate according to European Centre for Disease Prevention and Control criteria (*5*). We defined index patients as those who, during the 48 hours before onset of signs and symptoms or a positive SARS-CoV-2 test, had contact with an exposed patient. We defined exposed patients as those sharing a room with an index patient for ≥6 hours in an intermediate care unit (IMC) or intensive care unit (ICU) (*1*), any time on the general ward, or when the index patient underwent an aerosol-generating procedure (*2*). We initiated droplet isolation precaution measures for exposed patients and tested them upon symptom onset or, beginning week 47 of 2020, systematically at 2, 5, and 10 days after exposure. We contacted discharged patients by phone and offered testing in the outpatient clinic. Patients with up-to-date vaccination or known COVID-19 during the previous 6 months were considered unexposed.

We assessed transmission pathways between patients by in-depth reviews of symptom onset and dynamics of cycle threshold (Ct) values. If sequencing results were available, evidence of transmission was defined as ≤1 single-nucleotide polymorphism (SNP). Exposed patients with >1 SNP difference from the index patient were excluded from the main analysis, but patients without sequencing data were included. For association with SARS-CoV-2 transmission, we assessed index patient age, sex, aerosol generating

Author affiliations: University Hospital Zürich and University of Zürich Division of Infectious Diseases and Hospital Epidemiology, Zurich, Switzerland (A. Wolfensberger, M. Zeeb, P.W. Schreiber, M. Vazquez, V. Schärer, T. Scheier, D. Saleschus, W. Zingg); University of Zürich Institute of Medical Virology, Zurich (V. Kufner, M. Zaheri, M. Zeeb, S. Schmutz, M. Huber); University Hospital Zürich and University of Zürich Department for Internal Medicine, Zurich (I. Nortes, S.K. Rampini); University Hospital Zürich Clinic of Immunology, Zurich (E. Probst)

DOI: https://doi.org/10.3201/eid2810.220321

procedures, and Ct values from first positive PCR test, duration of contact between an index patient and exposed patient, ward type, and pandemic week.

Routine SARS-CoV-2 PCR testing was conducted in 3 laboratories and whole-genome sequencing performed according to nCoV-2019 sequencing protocol v3 (LoCost) V.3 (https://www.protocols.io/view/ncov-2019-sequencing-protocol-v3-locost-bp2l6n26rgqe/v3) (Appendix 2). To estimate SAR, we calculated cumulative incidence using the Kaplan-Meier estimator. We assessed risk factors for transmission in univariate and multivariable logistic regression models. We conducted sensitivity analyses on patients with ≥10 days clinical or laboratory follow-up (Appendix Table 1), on all patients irrespective of phylogenetic results (Appendix Table 2), and on patients with phylogenetically proven transmission (Appendix Table 3). We conducted analyses using Stata statistical software release 16 (StataCorp LLC, https://www.stata.com) and R version 4.0.2 (https://cran.r-project.org/bin/windows/base). The Zurich Cantonal Ethics Commission waived formal ethics evaluation because our analysis was part of an outbreak investigation for quality control and infection prevention (Req 2021-00560).

Of 1,118 patients with COVID-19, a total of 1,012 (90.5%) cases were community-associated, 40 (3.6%) probable healthcare-associated, 43 (3.8%) definite healthcare-associated, and 23 (2.1%) indeterminate (Figure 1). In total, we found 127 index patients for 303 exposed patients. Phylogenetic data supported transmission in 14/23 pairs of index–exposed patients with epidemiologic links for whom we had available data (Appendix Figure 1). In addition, we confirmed 4 transmissions indirectly by data from transmission chains (Figure 2). We excluded 5 exposed patients from the analysis because of >1 SNP difference between index and exposed patient. Among exposed patients in the analysis, 42/298 (14.1%) tested positive for SARS-CoV-2 and 179/298 (69.9%) had a follow-up time <10 days. Cumulative incidence for COVID-19 as an estimator of the SAR was 23.3% (95% CI 16%–30%) (Appendix Figure 2). Clusters were small, with only 2 multigeneration transmissions (Figure 2). We found links to identified index patients for 26 (65%) patients with probable and 15 (34.9%) patients with definite healthcare-associated COVID-19.

We performed univariable and multivariable analyses to explore factors associated with transmission of SARS-CoV-2 from patients to roommates (Table). We found similar results for 2 of the 3 sensitivity analyses (Appendix Tables 2, 3). However, in analysis of patients with a follow-up ≥10 days (Appendix Table 1), exposure on IMC/ICUs and higher number of weeks into the COVID-19 pandemic were associated with a lower risk for transmission, likely because of greater physical distance between immobile patients on the IMC/ICU and increased IPC standards.

In a mostly unvaccinated population in which most infections were caused by pre-Alpha variant SARS-CoV-2 (6), we found that 7.4% of all COVID-19 patients had probable or definite healthcare-associated COVID-19. This finding is comparable to that from the second wave in Brazil (8.6%) (*7*) but lower than that from the first wave in the United Kingdom (9%–15%) (*2*,*3*). We were able to link only half of the healthcare-associated cases in our hospital to an identified index patient. Despite all the IPC measures in place, high population incidence probably contributed to an increased risk for healthcare-associated transmissions from other patients but also from visitors and HCWs.

We identified ≈11% of all COVID-19 patients as index patients and estimated a 23% SAR in exposed

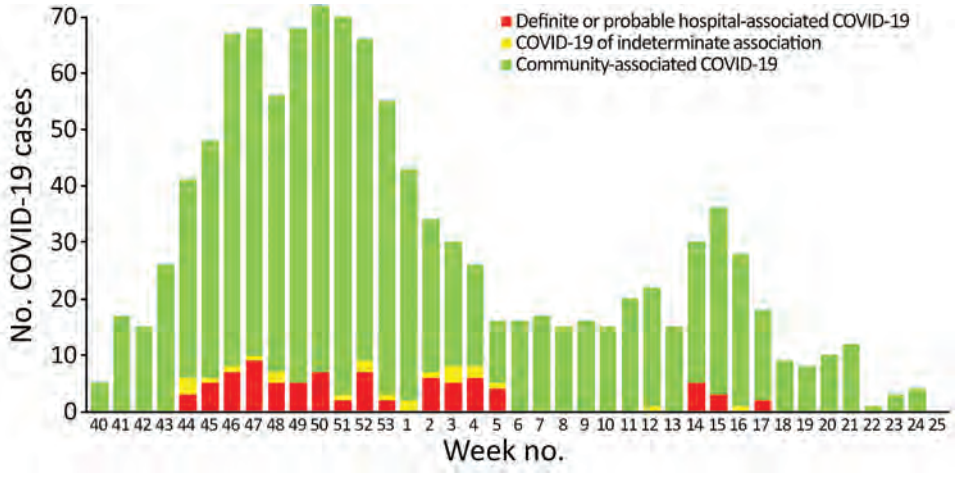

Figure 1. Incidence of admitted patients with positive SARS-CoV-2-PCR per week, including categorization hospital-associated versus community-associated, temporal trend of incidence of SARS-CoV-2 positive patients from week 40 of 2020 through week 25 of 2021. Incident cases were stratified according to European Centre for Disease Prevention and Control definitions of healthcare-associated COVID-19.

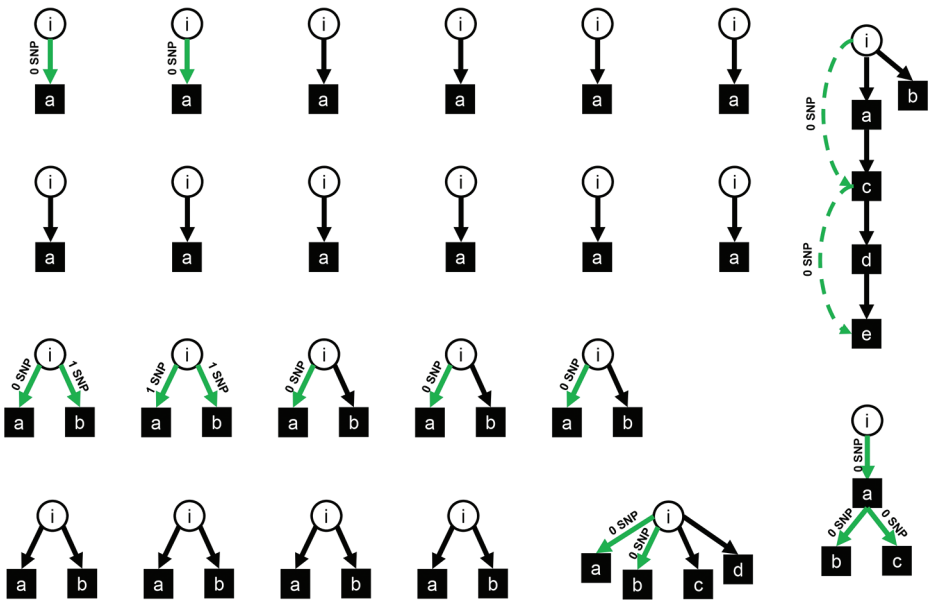

Figure 2. Transmission clusters of patients after exclusion of 5 exposed patients in whom phylogenetic data did not support transmission. Circles are index patients, squares are infected contact patients. Green arrows represent phylogenetically confirmed transmissions, with the labels "0 SNP" and "1 SNP" indicating 0 or 1 SNP difference between index and exposed patient. Green dashed arrows represent phylogenetic proof of second-generation transmission. Black arrows represent assumed transmissions without phylogenetic proof. i, index patient; a–d, exposed.

patients. From the 23 epidemiologically linked pairs with available phylogenetic data, transmission was endorsed in only 18, suggesting that the overall index-to-contact patient transmission rate may have been overestimated. SARs among hospital roommates in a study from a tertiary care center in Iowa, USA, was 21.6% (*8*); from a tertiary care center in New York, New York, USA, 18.9% (*9*); and from a hospital in Boston, Massachusetts, USA, 39% (*10*). These SAR numbers are comparable to those in households (*11*), implying either that distancing and masking are of limited effectiveness for preventing transmission while sharing accommodations (supporting an aerosol transmission pathway between patients) (*13*) or that adherence to distancing and masking were low. Unsurprisingly, as also demonstrated elsewhere (*8*,*10*), the 2 parameters most strongly associated with SARS-CoV-2 were longer contact time between index and exposed patients and low Ct values (i.e., high viral loads) among index patients; Ct values <21 were shown to be associated with transmission.

Among limitations in our study, phylogenetic results were available for only half of the patients, laboratory follow-up with inpatients was only 10 days, and discharged patients were often not available for further follow-up. We also limited contact time on IMC/ICUs to >6 hours, which might have excluded relevant contacts, and we might have missed superinfection. Finally, we were unable to model potential drivers for transmission, such as patient nonadherence to IPC-measures, distance between index and exposed patients, or respiratory signs or symptoms of index patients.

Table. Univariable and multivariable analysis of factors associated with SARS-CoV-2 transmission to exposed patients in a hospital in Zurich, Switzerland, October 2020–June 2021*

Exposure	Exposed patients positive for SARS-CoV-2, n = 42	Exposed patients not testing for SARS-CoV-2, n = 256	OR (95%CI) Univariable analysis	OR (95%CI) Multivariable analysis
Contact time of index and exposed patient in hours, median (IQR)	54 (28–96)	17 (8–29)	1.03 (1.02–1.03)	1.02 (1.01–1.03)
Ct value of index patient in units, median (IQR)	19 (18–26)	28 (19–33)	0.91 (0.87–0.96)	0.93 (0.87–0.98)
AGP in index patient, mean (SD)	0.26 (0.44)	0.25 (0.43)	1.04 (0.50–2.19)	NA
Exposure on IMC/ICU, mean (SD)	0.14 (0.35)	0.31 (0.46)	0.37 (0.15–0.92)	0.70 (0.27–1.87)
Male sex of index patient, mean (SD)	0.55 (0.50)	0.52 (0.50)	1.08 (0.56–2.09)	NA
Age of index patient, y, median (IQR)	71 (58–77)	72 (58–78)	1.00 (0.98–1.02	NA
Exposure before mandatory patient masking at bed place, mean (SD)	0.09 (0.28)	0.11 (0.32)	1.41 (0.50–3.96	NA
Calendar week into second and third waves, median (IQR)	13 (9–17)	13 (8–18)	0.96 (0.91–1.01)	0.95 (0.90–1.01)

*AGP, aerosol-generating procedures; Ct, cycle threshold; IQR, interquartile range; IMC, intermediate care units; ICU, intensive care units; NA, not available; OR, odds ratio.

Conclusions

High viral loads among index patients and prolonged contact time in shared hospital rooms play critical roles in healthcare-associated SARS-CoV2-transmission. Although based on data from a time when pre-Alpha and Alpha variants circulated in a nonvaccinated population, our findings might be relevant in the context of more recently emerged and future variants of concern (*13*,*14*) and waning immunity (*15*). The findings in our study and other studies of substantial SARs in hospitals support early adoption strategies to prevent healthcare-associated transmission during times of high population COVID-19 incidence. Those strategies include identifying contagious patients early (e.g., by performing systematic and repetitive SARS-CoV-2 testing), improving mask-wearing adherence in patients, and frequently replacing air in shared patient rooms.

P.W.S. is supported by the Filling the Gap academic career program of the medical faculty of the University of Zürich. This study was supported by the clinical research priority Comprehensive Genomic Pathogen Detection Program of the University of Zurich.

A.W., S.K.R., and W.Z. designed the study. V.K., M.Za., I.N., P.W.S., M.V., V.S., T.S., and D.S. acquired the data, and A.W., M. Ze., and P.W.S. performed statistical analysis. V.K., M.Za., E.P., and S.S. performed laboratory analyses. A.W., V.K., M.Za., M. Ze., and W.Z. analyzed and interpreted the data. A.W. and V.K. drafted the manuscript, and M.Za., M. Ze., I.N., P.W.S., M.V., V.S., T.S., S.S., E.P., D.S., M.H., S.K.R., and W.Z. provided critical review of the manuscript for intellectual content.

About the Author

Dr. Wolfensberger is an infectious disease physician and hospital epidemiologist at the University Hospital Zürich. Her primary research interests include outbreak investigations and hospital-acquired pneumonia.

References

1. Luong-Nguyen M, Hermand H, Abdalla S, Cabrit N, Hobeika C, Brouquet A, et al. Nosocomial infection with SARS-Cov-2 within departments of digestive surgery [in French]. J Chir Visc Surg. 2020;157:S13–9.
2. Rickman HM, Rampling T, Shaw K, Martinez-Garcia G, Hail L, Coen P, et al. Nosocomial transmission of coronavirus disease 2019: a retrospective study of 66 hospital-acquired cases in a London teaching hospital. Clin Infect Dis. 2021;72:690–3. https://doi.org/10.1093/cid/ciaa816
3. Taylor J, Rangaiah J, Narasimhan S, Clark J, Alexander Z, Manuel R, et al. Nosocomial COVID-19: experience from a large acute NHS trust in south-west London. J Hosp Infect. 2020;106:621–5. https://doi.org/10.1016/j.jhin.2020.08.018
4. Zeeb M, Weissberg D, Rampini SR, Müller R, Scheier T, Zingg W, et al. Identifying risk contacts for SARS-CoV-2 transmission to healthcare-workers during a COVID-19 ward outbreak. Emerg Infect Dis. In press 2022.
5. European Centre for Disease Prevention and Control. Surveillance definitions for COVID-19: source of infection: healthcare (nosocomial) vs community transmission [cited 2022 Aug 16] https://www.ecdc.europa.eu/en/covid-19/surveillance/surveillance-definitions
6. Federal Office of Public Health Switzerland. COVID-19 Switzerland information on the current situation [cited 2022 Aug 16]. https://www.covid19.admin.ch/en
7. Tauffer J, Roma de Oliveira Konstantyner TC, Stockler de Almeida MC, Ferreira DB, Antonelli TS, Souza Fram D, et al. Impact of in-hospital infection with SARS-CoV-2 among inpatients at a university hospital. Am J Infect Control. 2021;49:1464–8. https://doi.org/10.1016/j.ajic.2021.09.015
8. Trannel AM, Kobayashi T, Dains A, Abosi OJ, Jenn KE, Meacham H, et al. Coronavirus disease 2019 (COVID-19) incidence after exposures in shared patient rooms in a tertiary-care center in Iowa, July 2020–May 2021. Infect Control Hosp Epidemiol. 2021:1–4. https://doi.org/10.1017/ice.2021.313
9. Chow K, Aslam A, McClure T, Singh J, Burns J, McMillen T, et al. Risk of healthcare-associated transmission of SARS-CoV-2 in hospitalized cancer patients. Clin Infect Dis. 2022;74:1579–85.
10. Karan A, Klompas M, Tucker R, Baker M, Vaidya V, Rhee C. The risk of SARS-CoV-2 transmission from patients with undiagnosed Covid-19 to roommates in a large academic medical center. Clin Infect Dis. 2022;74:1097–100.
11. Fung HF, Martinez L, Alarid-Escudero F, Salomon JA, Studdert DM, Andrews JR, et al.; Stanford-CIDE Coronavirus Simulation Model (SC-COSMO) Modeling Group. The household secondary attack rate of severe acute respiratory syndrome coronavirus 2 (SARS-CoV-2): a rapid review. Clin Infect Dis. 2021;73(Suppl 2):S138–45. https://doi.org/10.1093/cid/ciaa1558
12. Greenhalgh T, Jimenez JL, Prather KA, Tufekci Z, Fisman D, Schooley R. Ten scientific reasons in support of airborne transmission of SARS-CoV-2. Lancet. 2021;397:1603–5. [Erratum in Lancet. 2021;397:1808.] https://doi.org/10.1016/S0140-6736(21)00869-2
13. Ai J, Zhang H, Zhang Y, Lin K, Zhang Y, Wu J, et al. Omicron variant showed lower neutralizing sensitivity than other SARS-CoV-2 variants to immune sera elicited by vaccines after boost. Emerg Microbes Infect. 2022;11:337–43.
14. Zhang L, Li Q, Liang Z, Li T, Liu S, Cui Q, et al. The significant immune escape of pseudotyped SARS-CoV-2 variant Omicron. Emerg Microbes Infect. 2022;11:1–5. https://doi.org/10.1080/22221751.2021.2017757
15. Poukka E, Baum U, Palmu AA, Lehtonen TO, Salo H, Nohynek H, et al. Cohort study of Covid-19 vaccine effectiveness among healthcare workers in Finland, December 2020–October 2021. Vaccine. 2022;40:701–5.

Address for correspondence: Aline Wolfensberger, Division of Infectious Diseases and Hospital Epidemiology, University Hospital Zürich, University of Zürich, Rämistrasse 100, CH-8091 Zurich, Switzerland; email: aline.wolfensberger@usz.ch

Endofungal *Mycetohabitans rhizoxinica* Bacteremia Associated with *Rhizopus microsporus* Respiratory Tract Infection

Shangxin Yang, Victoria Anikst, Paul C. Adamson

We report *Mycetohabitans rhizoxinica* bacteremia in a 65-year-old woman in California, USA, who was undergoing chimeric antigen receptor T-cell therapy for multiple myeloma. Acute brain infarction and pneumonia developed; *Rhizopus microsporus* mold was isolated from tracheal suction. Whole-genome sequencing confirmed bacteria in blood as genetically identical to endofungal bacteria inside the mold.

Mycetohabitans rhizoxinica (previously *Burkholderia rhizoxinica*) and *M. endofungorum* are endofungal bacteria inhabiting *Rhizopus microsporus* mold. These bacteria form symbiosis to help the mold infect plants and produce mycotoxins, such as rhizoxin, that cause rice seedling blight (*1*,*2*). Genetically, *Mycetohabitans* species are highly similar to *Burkholderia* species but with significantly smaller genome sizes (3.3–3.8 Mb vs. 5.8–11 Mb), reflecting their endosymbiotic nature (*3*). *R. microsporus* causes mucormycosis, a devastating invasive fungal infection seen most prevalently in immunocompromised patients, but no strong evidence has suggested that the symbiont bacteria contribute to the pathogenicity of *R. microsporus* mold in humans (*1*,*4*). Isolation of endofungal bacteria have seldom been reported in clinical settings, most likely because of limitations in identification methods. In a study performed by the Centers for Disease Control and Prevention, *M. rhizoxinica* and *M. endofungorum* isolated from blood and wounds were characterized as oxidase-positive, gram-negative coccobacilli and could be reliably identified only by sequencing; no clinical information was provided to characterize the clinical presentation nor did researchers describe any link to *R. microsporus* (*4*). We report *M. rhizoxinica* bacteremia associated with multifocal pneumonia presumptively caused by *R. microsporus* mold in a severely immunocompromised patient.

Author affiliation: David Geffen School of Medicine at University of California–Los Angeles, Los Angeles, California, USA

DOI: https://doi.org/10.3201/eid2810.220507

The Study

A 65-year-old woman in California, USA, with a history of relapsed and refractory multiple myeloma visited a hospital to receive chimeric antigen receptor (CAR) T-cell therapy. She previously had received 3 doses of the COVID-19 mRNA vaccine. On the day after CAR T-cell therapy, she experienced a rapid decline in mental status, accompanied by fever and hypotension, and was transferred to the intensive care unit. At that time, her total leukocyte count was 0.09 $\times 10^3$ cells/uL. Nasopharyngeal testing for COVID-19 by PCR was negative. She was diagnosed with immune effector cell-associated neurotoxicity syndrome and cytokine release syndrome. She received high doses of dexamethasone and 4 doses of tocilizumab, as well as anakinra, which was tapered over 7 days. The patient's symptoms improved, and she was discharged after a 15-day hospital stay, with plans for a prolonged taper of orally administered dexamethasone (8 mg 2×/d). On discharge, the patient's leukocyte count was 1.4 $\times 10^3$ cells/uL (87% neutrophils, 7% lymphocytes); the next day, her outpatient blood work showed mild lactic acidosis.

Four days after leaving the hospital, the patient sought treatment at an outpatient oncology clinic, reporting generalized weakness and fatigue. We performed blood and urine analyses and began a regimen of oral levofloxacin (500 mg daily). On day 6 after discharge, we noted a positive blood culture result, with a gram-negative rod. The urine culture grew 30,000 CFU/mL of *Klebsiella pneumoniae*. When evaluating the patient during clinical rounds, we

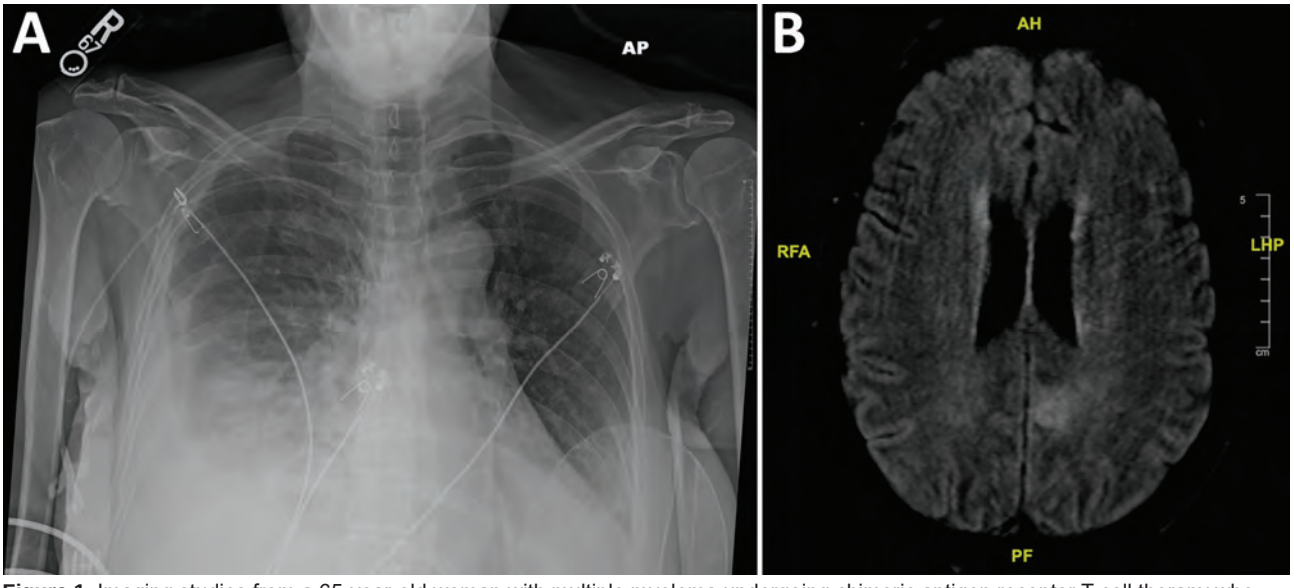

Figure 1. Imaging studies from a 65-year-old woman with multiple myeloma undergoing chimeric antigen receptor T-cell therapy who was admitted to the hospital for worsening foot and ankle pain, California, USA. A) Chest radiograph image, showing a moderate right-sided pleural effusion and adjacent pulmonary opacities indicative of pneumonia. B) Magnetic resonance imaging of the patient's brain, showing the infarct involving the left medial parietal lobe.

performed repeat blood and urine cultures and recommended inpatient management, which was refused. We administered 1 intravenous dose of meropenem (1 g) at that visit and 1 dose of intravenous ceftriaxone (2 g) the next day.

On day 8 after discharge, the patient sought emergency treatment for worsening foot and ankle pain. Her leukocyte count was 0.44×10^3 cells/uL. Bacterial identification of the positive blood culture was still pending. Results of repeat blood and urine cultures and COVID-19 PCR testing (nasopharyngeal) were negative; chest radiograph showed right-, middle-, and lower-lobe airspace opacification (Figure 1, panel A). We began piperacillin/tazobactam and performed an arthrocentesis, which showed crystals but revealed a negative Gram stain. Shortly thereafter, the patient reported acute numbness and weakness of her right leg. She subsequently developed dyspnea, respiratory distress, and altered mental status. We intubated her and conducted magnetic resonance imaging, which showed an acute infarct of the left medial parietal lobe, with hemorrhagic transformation (Figure 1, panel B). We transferred the patient to the intensive care unit, where she was febrile (38.2°C) and required 2 vasopressors. We administered vancomycin, caspofungin, and isavuconazole. The next day, hypotension worsened, requiring 3 vasopressors. Leukocyte was 0.16×10^3 cells/uL. On hospital day 3, we obtained a tracheal aspirate for cultural analysis. Later that day, pulseless electrical activity occurred; the patient suffered cardiac arrest and died.

The day after her death, results of analysis of tracheal aspirate obtained on hospital day 3 revealed a mold. The bacteria from the initial positive blood culture were gram-negative, oxidase-positive coccobacilli not identifiable by the Vitek MS system (bioMérieux, https://www.biomerieux.com). The specimen was automatically reflexed to a laboratory-developed whole-genome sequencing (WGS) identification test

Table. Antibiotic susceptibility results for *Mycetohabitans rhizoxinica* isolate from a 65-year-old woman with multiple myeloma undergoing chimeric antigen receptor T-cell therapy admitted to the hospital for worsening foot and ankle pain, California, USA*

Antibiotic	MIC, µg/mL*
Amoxicillin/clavulanate	≤2
Ceftriaxone	≤1
Ceftazidime	≤0.5
Ceftolozane/tazobactam	≤0.5
Cefepime	≤0.5
Ceftazidime/avibactam	≤2
Ertapenem	≤0.25
Imipenem	≤1
Meropenem	≤0.25
Piperacillin/tazobactam	≤8
Amikacin	8
Gentamicin	≤1
Tobramycin	≤1
Ciprofloxacin	0.5
Levofloxacin	≤0.5
Trimethoprim/sulfamethoxazole	≤1/20

*Susceptibility testing was performed on broth-microdilution panels prepared in-house in accordance with CLSI guidelines from the Clinical and Laboratory Standards Institute (https://www.clsi.org).

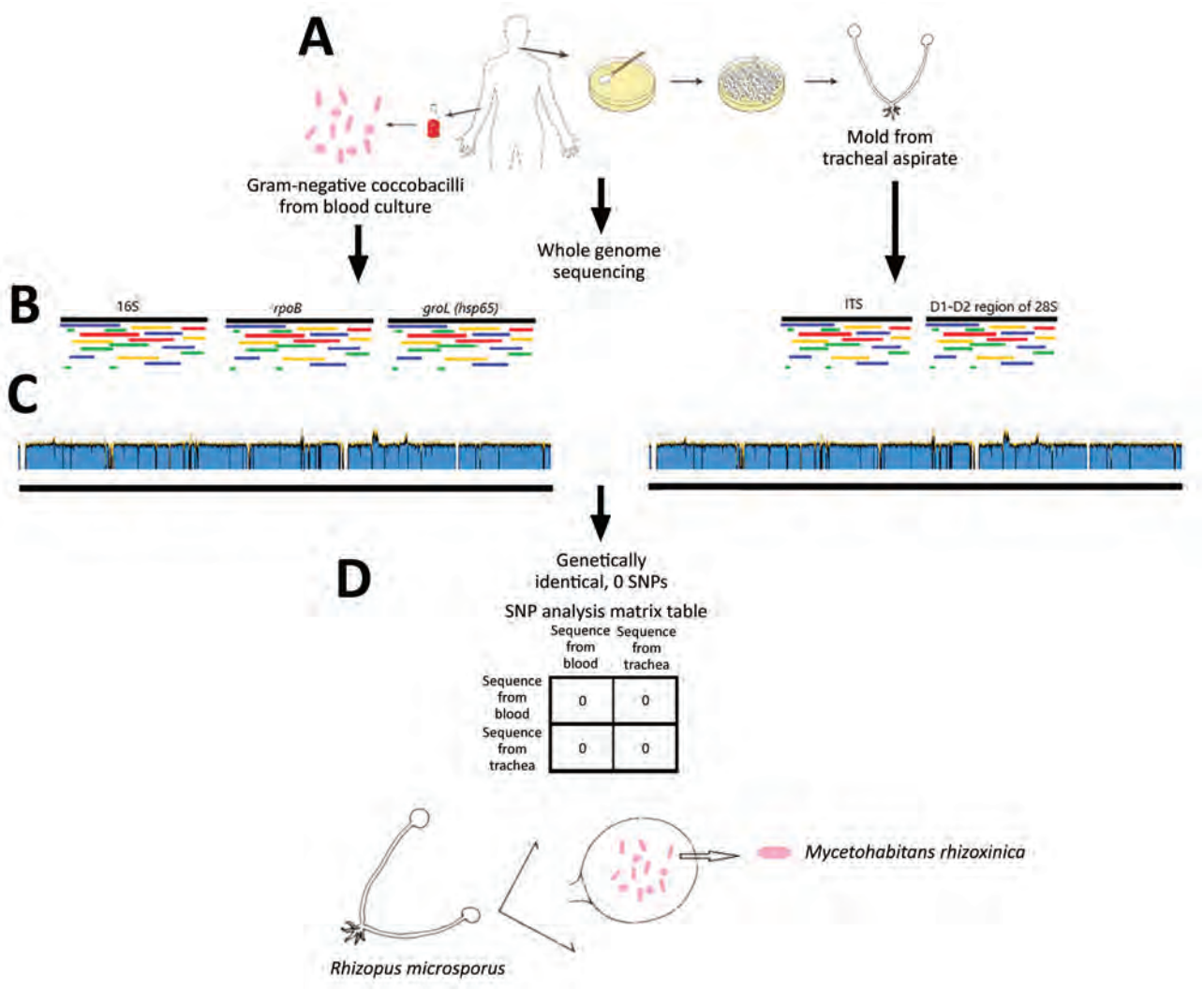

Figure 2. Whole-genome sequencing analysis of bacterial and fungal isolates (A) in a 65-year-old woman with multiple myeloma undergoing chimeric antigen receptor T-cell therapy, California, USA. The bacteria were identified as *Mycetohabitans rhizoxinica* with >99% identity in all 3 full-length marker genes compared with the reference organism (B, left side). The mold was identified as *Rhizopus microsporus* with >99% identity in the ITS gene and the D1–D2 region of the 28S gene compared with a reference organism (B, right side). Whole-genome sequences of the bacteria from blood (C, left side) revealed whole-genome coverage 94.0% and pairwise identity 95.5% with sufficient mean coverage of 298×. Whole-genome sequence of the mold from tracheal aspirate (C, right side) aligned to reference bacterial whole-genome sequence showed whole-genome coverage 94.1% and pairwise identity 95.8%, with sufficient mean coverage of 75×. The bacteria inside the mold from the trachea were genetically identical to the bacteria from the blood, as shown by the SNP analysis (D). ITS, internal transcribed spacer; SNP, single nucleotide polymorphism.

(*5*). Drug-susceptibility testing showed presumptive (due to lack of breakpoint) susceptibility to most drugs tested, including amoxicillin/clavulanate, ceftriaxone, piperacillin/tazobactam, carbapenems, gentamicin, ciprofloxacin, and trimethoprim/sulfamethoxazole (Table).

We performed WGS on the bacteria from both the blood and the mold obtained from tracheal suction using Illumina MiSeq (Illumina, https://www.illumina.com) (*5*) (Figure 2). We identified the bacteria as *M. rhizoxinica*, with >99% identity in all 3 full-length marker genes, including 16S, *rpo*B, and *gro*L (*hsp65*) compared with the type strain *M. rhizoxinica* HKI 454 (GenBank accession no. NC_014722.1). We identified the mold as *R. microsporus*, with >99% identity in the internal transcribed spacer (ITS) gene and the D1–D2 region of the 28S gene compared with *R. microsporus* var. chinensis CBS 631.82 (accession no. NR_149337.1 for ITS and HM849668.1 for D1–D2). We mapped the whole genome sequences of the bacteria and mold isolates (Genbank Sequence Read Archive data: PRJNA857096) to the *M. rhizoxinica* HKI 454 complete

genome using Geneious Prime (Geneious, https://www.geneious.com) and achieved similar whole-genome coverage (bacteria, 94.0%; mold, 94.1%) and pairwise identity (bacteria, 95.5%; mold, 95.8%), with sufficient mean coverage (bacteria, 298×; mold, 75×). We used the mapped sequence reads from the bacteria and the mold for single-nucleotide polymorphism analyses using CLC Genomics Workbench (QIAGEN, https://www.qiagen.com) as previously described (*6*). Results showed no single-nucleotide polymorphism between the sequences in the bacteria from blood and the bacteria within the mold, indicating the bacteria in the blood was derived from the mold (Figure 2). Further genomic analysis confirmed the presence of a gene cluster (*rhi*A–*rhi*I) that encodes the biosynthesis of rhizoxin in both bacterial and mold isolates (*7*).

Conclusions

Using WGS, we present clear evidence linking the endofungal bacteria *M. rhizoxinica*, isolated from a patient's blood, to the bacteria residing within the *R. microsporus* mold isolated from the patient's respiratory sample. The bacteria were isolated in the blood culture before initiating antibiotics were pansusceptible to the antibiotics tested, and cleared quickly after treatment. However, it is not clear whether the antibiotics retained activity against the bacteria within the fungal cytoplasm or whether activity was preserved for only bacteria outside the fungi. We hypothesize that the bacteria were most likely inside the mold in vivo and freed only after sample collection and then grew in the blood culture bottle during the incubation, when the fungus became degraded or lysed. Blood culture has low yield for Mucorales species (*8*), indicating those molds often die during the blood culture process. Because of the clinical manifestation, we believe the bacteria did not contribute to sepsis but rather served as a signal for a developing invasive mold infection that manifested during the immune suppression related to the patient's CAR T-cell therapy. Unfortunately, the patient decompensated rapidly and died before the mold was identified and before we could initiate aggressive antifungal treatment.

Infarction and necrosis of infected tissues are hallmarks of mucormycosis (*9*). Disseminated mucormycosis, the presumptive diagnosis in this case based on the pulmonary findings and hemorrhagic brain infarction, is a rapidly progressive infection associated with a mortality rate >90% (*10*). This patient was at risk for disseminated mucormycosis because of profound immune suppression. Early diagnosis and prompt treatment of mucormycosis are key to improving clinical outcomes. Disseminated mucormycosis appears to be the underlying infectious process in this case, but this report lacks autopsy examination to confirm the presumptive diagnosis.

In conclusion, we found that isolation of endofungal bacteria *M. rhizoxinica* in the clinical setting might indicate invasive *Rhizopus* infection. Because identification methods used in most clinical laboratories are limited, endofungal bacteria may be underrecognized and require sequencing to identify.

Acknowledgement

We thank the University of California–Los Angeles Clinical Microbiology Laboratory for technical support.

This work was supported by the National Institutes of Health (K01TW012170 to PCA).

About the Author

Dr. Yang is a clinical microbiologist and assistant clinical professor at the University of California–Los Angeles Department of Pathology and Medicine. Dr. Yang's main research interests include molecular diagnostics and innovation, clinical virology, transplant-related infectious diseases testing, genomic epidemiology, and antimicrobial resistance mechanisms.

References

1. Frey-Klett P, Burlinson P, Deveau A, Barret M, Tarkka M, Sarniguet A. Bacterial-fungal interactions: hyphens between agricultural, clinical, environmental, and food microbiologists. Microbiol Mol Biol Rev. 2011;75:583–609. https://doi.org/10.1128/MMBR.00020-11
2. Lackner G, Hertweck C. Impact of endofungal bacteria on infection biology, food safety, and drug development. PLoS Pathog. 2011;7:e1002096. https://doi.org/10.1371/journal.ppat.1002096
3. Estrada-de los Santos P, Palmer M, Chávez-Ramírez B, Beukes C, Steenkamp ET, Briscoe L, et al. Whole genome analyses suggests that *Burkholderia* sensu lato contains two additional novel genera (*Mycetohabitans* gen. nov., and *Trinickia* gen. nov.): implications for the evolution of diazotrophy and nodulation in the *Burkholderiaceae*. Genes (Basel). 2018;9:389. https://doi.org/10.3390/genes9080389
4. Gee JE, Glass MB, Lackner G, Helsel LO, Daneshvar M, Hollis DG, et al. Characterization of *Burkholderia rhizoxinica* and *B. endofungorum* isolated from clinical specimens. PLoS One. 2011;6:e15731. https://doi.org/10.1371/journal.pone.0015731
5. Price TK, Realegeno S, Mirasol R, Tsan A, Chandrasekaran S, Garner OB, et al. Validation, implementation, and clinical utility of whole genome sequence-based bacterial identification in the clinical microbiology laboratory. J Mol Diagn. 2021;23:1468–77. https://doi.org/10.1016/j.jmoldx.2021.07.020
6. Price TK, Mirasol R, Ward KW, Dayo AJ, Hilt EE, Chandrasekaran S, et al. Genomic characterizations of clade

iii lineage of *Candida auris*, California, USA. Emerg Infect Dis. 2021;27:1223–7. https://doi.org/10.3201/eid2704.204361
7. Partida-Martinez LP, Hertweck C. A gene cluster encoding rhizoxin biosynthesis in "*Burkholderia rhizoxina*", the bacterial endosymbiont of the fungus *Rhizopus microsporus*. ChemBioChem. 2007;8:41–5. https://doi.org/10.1002/cbic.200600393
8. Walsh TJ, Gamaletsou MN, McGinnis MR, Hayden RT, Kontoyiannis DP. Early clinical and laboratory diagnosis of invasive pulmonary, extrapulmonary, and disseminated mucormycosis (zygomycosis). Clin Infect Dis. 2012;54 (Suppl 1):S55–60. https://doi.org/10.1093/cid/cir868
9. Petrikkos G, Skiada A, Lortholary O, Roilides E, Walsh TJ, Kontoyiannis DP. Epidemiology and clinical manifestations of mucormycosis. Clin Infect Dis. 2012;54(Suppl 1):S23–34. https://doi.org/10.1093/cid/cir866
10. Roden MM, Zaoutis TE, Buchanan WL, Knudsen TA, Sarkisova TA, Schaufele RL, et al. Epidemiology and outcome of zygomycosis: a review of 929 reported cases. Clin Infect Dis. 2005;41:634–53. https://doi.org/10.1086/432579

Address for correspondence: Shangxin Yang, UCLA Clinical Microbiology Laboratory, 11633 San Vicente Blvd, Los Angeles, CA 90049, USA; email: shangxinyang@mednet.ucla.edu

Non–SARS-CoV-2 Respiratory Viruses in Athletes at Major Winter Sport Events, 2021 and 2022

Maarit Valtonen, Matti Waris, Raakel Luoto, Katja Mjøsund, Mira Kaikkonen, Olli J. Heinonen, Olli Ruuskanen

We performed prospective studies on respiratory viral infections among Team Finland participants during the 2021 Oberstdorf World Ski Championships and the 2022 Beijing Olympic Games. We enrolled 73 athletes and 110 staff members. Compared with similar studies we conducted before the COVID-19 pandemic, illnesses and virus detections dropped by 10-fold.

Elite athletes have an increased risk for contracting acute respiratory infections (ARIs) during major winter sport events (*1*–*5*), which often occur during viral peaks in the community. Many of the athletes' behavioral factors during events, such as using public transportation, crowding, using group accommodation, and close socializing activities, may all increase an athlete's susceptibility to acute respiratory viral infection (*6*).

The aim of our study was to investigate the occurrence of respiratory viruses in sport teams during 2 major winter sport events that implemented public and individual COVID-19 prevention procedures. For comparison, we used observations from 2 previous studies in corresponding competitions conducted before the COVID-19 pandemic (*3*,*5*).

The Study

We conducted the studies at the Nordic World Ski Championships in Oberstdorf, Germany, during February 18–March 7, 2021, and at the Olympic Winter Games in Beijing, China, during January 27–February 21, 2022. In Oberstdorf, 633 athletes from 65 countries participated, and in Beijing, 2,871 athletes from 91 countries participated. Our study included 73 Team Finland members in Oberstdorf (26 athletes and 47 staff) and 110 in Beijing (47 athletes and 63 staff); we excluded the ice hockey teams. We monitored team members for the duration of their trip, starting from their arrival at the event location and finishing with their departure from the hotel. At arrival at both events, all team members were asymptomatic. ARI (i.e., the common cold) was defined as the acute onset of any of the following signs and symptoms: sore throat, rhinorrhea, nasal congestion, hoarseness, cough, and fever (≥37.8°C) (*7*).

In addition to the SARS-CoV-2 testing conducted by the event organizers (every other day in Oberstdorf and every day in Beijing), we collected flocked nasal swab specimens from the team in Oberstdorf on days 1, 7, and 13 with minor variations. In Beijing, nasal swab specimens were taken only from participants with acute onset of a respiratory symptom or symptoms.

We conducted all study-related activities according to Guideline for Good Clinical Practice (https://www.ema.europa.eu/en/documents/scientific-guideline/ich-e-6-r2-guideline-good-clinical-practice-step-5_en.pdf), which includes the provisions in the Declaration of Helsinki. The protocol was approved by the Ethics Committee of the Hospital District of Southwest Finland (Oberstdorf) and the Ethics Committee, Central Finland Health Care District (Beijing).

COVID-19 countermeasures included relative quarantine of the team members before traveling (i.e., use of masks and physical distancing); having a negative SARS-CoV-2 test before departure; using masks during travel and at the games; traveling by chartered flights; following enhanced hand hygiene and environmental disinfection; maintaining physical distance; housing in single or double rooms; limiting use of indoor public facilities; and allowing no

Author affiliations: Finnish Institute of High Performance Sport KIHU, Jyväskylä, Finland (M. Valtonen, M. Kaikkonen); University of Turku and Turku University Hospital, Turku, Finland (M. Waris, R. Luoto, O. Ruuskanen); University of Turku, Turku, Finland (K. Mjøsund, O.J. Heinonen)

DOI: https://doi.org/10.3201/eid2810.220478

spectators in Oberstdorf and a limited number in Beijing. The team in Beijing was fully vaccinated against COVID-19; the team in Oberstdorf was unvaccinated.

We performed laboratory testing at the site in Beijing using a BioFire FilmArray Respiratory Panel 2.1 Plus (BioFire, https://www.biofiredx.com). The panel detects the following viruses: respiratory syncytial virus; adenovirus; influenza A and B viruses; rhinovirus/enterovirus; parainfluenza type 1–4 viruses; human coronaviruses 229E, OC43, HKU1, and NL63; SARS-CoV-2; Middle East respiratory syndrome coronavirus; and human metapneumovirus. We retrospectively tested the Oberstdorf samples in Turku, Finland, using Allplex Respiratory Panels 1–3 (Seegene, https://www.seegene.com). This panel detects 16 viruses that are otherwise the same as FilmArray except that it differentiates between rhinoviruses and enteroviruses and detects human bocavirus but does not detect coronavirus HKU1, SARS-CoV-2, and MERS-CoV. Furthermore, we tested these samples with a laboratory-designed PCR for rhinoviruses, enteroviruses, and respiratory syncytial virus (*8*). The event organizers screened for SARS-CoV-2 using PCR assays in Oberstdorf and in Beijing.

In Oberstdorf, no cases of symptomatic ARIs were verified among the 73 sport team members. All 357 PCR tests for SARS-CoV-2 performed by the organizers were negative. Of a total of 203 nasal mucus samples, we detected rhinovirus in 2 samples, both collected on day 1 of the event from 1 athlete and 1 staff member.

At arrival at the airport in Beijing, 1 asymptomatic athlete tested positive for SARS-CoV-2. However, retesting in the Olympic Village proved negative. We recorded 6 cases of symptomatic ARIs, and we identified a virus in 4 of them. We detected 1 respiratory syncytial virus in 1 athlete on day 1, 1 metapneumovirus in 1 staff member on day 2, and 1 coronavirus 229E in 1 athlete on day 3. In 1 staff member, an ARI was evident on return to Finland and was identified as coronavirus OC43.

Conclusions

We found only 6 cases of symptomatic ARI among 183 (3%) members of Team Finland during 2 major winter sports events (the 2021 World Ski Championships and the 2022 Beijing Olympic Winter Games). The difference between these events and the historical comparison groups before COVID-19 is dramatic. At the January 26–February 28, 2018, Olympic Winter Games in PyeongChang, South Korea, and the February 18–March 3, 2019, World Ski Championships in Seefeld, Austria, ARIs were recorded in 58 (33%) of the 174 members of Team Finland (*3*,*5*) (Table). Clinically, all the ARIs were mild common colds.

In the Oberstdorf and Beijing winter sport events, we detected only 3 (4%) non–SARS-CoV-2 infections (caused by 3 different viruses) in 73 athletes, and those infections did not spread further. Symptom onset was 1–3 days after arrival in Beijing, which suggests that the infections were acquired in Finland. We recorded no SARS-CoV-2–positive results among

Table. ARIs among Team Finland during 4 major winter sport events before and during the COVID-19 pandemic, 2018–2022*

Event	2022 Winter Olympic Games	2021 Nordic World Ski Championships	2019 Nordic World Ski Championships	2018 Winter Olympic Games
Location	Beijing, China	Oberstdorf, Germany	Seefeld, Austria	PyeongChang, South Korea
Study period	Jan 27–Feb 21	Feb 18–Mar 7	Feb 18–Mar 3	Jan 26–Feb 28
Median length of stay, d	21	14	14	21
Local viral season	Not known	Low	Medium/high	High
Team members, no.	110	73	62	112
Athletes	47	26	26	44
Staff	63	47	36	68
ARIs, no. (%)	6 (5)	0	16 (26)	42 (38)
Athletes	3 (6)	0	10 (38)	20 (45)
Staff	3 (5)	0	6 (17)	22 (32)
Virus detections,† no. (%)	4 (67)	0	14 (90)	30 (71)
Athletes	2 (67)	0	8 (80)	15 (75)
Staff	2 (67)	0	6 (100)	15 (68)
Asymptomatic persons tested,† no. (no. tests)	0	73 (203 tests)‡	62 (158 tests)‡	34 (34 tests)§
Virus detections	0	2 (3)	10 (16)	6 (18)
SARS-CoV-2 testing#				
Total no. tests at event	≈1,800,000	≈20,000	NA	NA
No. positive	437	9	NA	NA
Reference	This study	This study	(*3*)	(*5*)

*ARI, acute respiratory infection; NA, not applicable.
†Analyses of the study for other than SARS-CoV-2 respiratory viruses.
‡Active surveillance of asymptomatic infections.
§Only high-risk contacts of symptomatic case-patients were tested.
#Surveillance conducted by event organizers.

Team Finland at either event, although COVID-19 cases were detected among other teams at both events (Table). In contrast, in our 2 earlier studies, conducted amid limited mitigation strategies (e.g., enhanced hand hygiene and disinfection and isolation of symptomatic persons), we detected respiratory viral infections (caused by 9 different viruses) in 30 (50%) of the 60 athletes (Table). Those infections spread readily among the team members (*3*,*5*,*6*).

Control measures during the COVID-19 pandemic markedly reduced the global occurrence of non–SARS-CoV-2 respiratory viruses (*9*–*12*). For example, a 98%–99% decrease in the detection of respiratory syncytial and influenza virus infections throughout the winter of 2020 was reported in Australia (*11*). During the 2021 Championships in Obertsdorf, low prevalences of only rhinoviruses and seasonal coronaviruses (no influenza) were observed in the community (https://www.rki.de/EN/Home/homepage.html). Furthermore, no or only a few spectators attended the events. Minimal environmental viral pressure is most probably the major explanation for our observations, and individual prevention procedures inhibited transmission of detected viruses among the team.

Limitations of our study include the fact that the number of team members was low and the methods for viral diagnostics varied, but neither of these factors should affect the overall results. We carefully recorded occurrence of ARIs in each study, but comprehensive testing of all participants for asymptomatic infections might have increased the numbers of viruses detected in some of the studies.

In summary, our observations suggest that multilayered mitigation strategies effectively prevented respiratory viral infections during 2 major winter sport events that occurred during the COVID-19 pandemic. Sport events may be held without an increased risk for respiratory viral infections (*13*). ARIs are now returning, concurrent with relaxed control measures (*14*,*15*). It remains to be clarified what mitigation procedures will be sufficiently effective in preventing respiratory viral infections during major sports events after the COVID-19 pandemic while, at the same time, minimally affecting the well-being of the athletes.

Acknowledgments

The authors acknowledge the collaboration of the members of Team Finland and the many other persons who demonstrated their willingness to help during the development of this research.

This work was supported by the Jenny and Antti Wihuri Foundation.

About the Author

Dr. Valtonen is the chief physician of the Finnish Olympic Committee with the Finnish Institute of High Performance Sport KIHU in Jyväskylä, Finland. Her primary research interests are the surveillance and characterization of r espiratory viral infections in elite athletes.

References

1. Gundlapalli AV, Rubin MA, Samore MH, Lopansri B, Lahey T, McGuire HL, et al. Influenza, winter Olympiad, 2002. Emerg Infect Dis. 2006;12:144–6. https://doi.org/10.3201/eid1201.050645
2. Svendsen IS, Gleeson M, Haugen TA, Tønnessen E. Effect of an intense period of competition on race performance and self-reported illness in elite cross-country skiers. Scand J Med Sci Sports. 2015;25:846–53. https://doi.org/10.1111/sms.12452
3. Valtonen M, Waris M, Vuorinen T, Eerola E, Hakanen AJ, Mjøsund K, et al. Common cold in Team Finland during 2018 Winter Olympic Games (PyeongChang): epidemiology, diagnosis including molecular point-of-care testing (POCT) and treatment. Br J Sports Med. 2019;53:1093–8. https://doi.org/10.1136/bjsports-2018-100487
4. Nabhan D, Windt J, Taylor D, Moreau W. Close encounters of the US kind: illness and injury among US athletes at the PyeongChang 2018 Winter Olympic Games. Br J Sports Med. 2020;54:997–1002. https://doi.org/10.1136/bjsports-2018-100015
5. Valtonen M, Grönroos W, Luoto R, Waris M, Uhari M, Heinonen OJ, et al. Increased risk of respiratory viral infections in elite athletes: a controlled study. PLoS One. 2021; 16:e0250907. https://doi.org/10.1371/journal.pone.0250907
6. Ruuskanen O, Luoto R, Valtonen M, Heinonen OJ, Waris M. Respiratory viral infections in athletes: many unanswered questions. Sports Med. 2022;52:2013–21. https://doi.org/10.1007/s40279-022-01660-9
7. Puhakka T, Mäkelä MJ, Malmström K, Uhari M, Savolainen J, Terho EO, et al. The common cold: effects of intranasal fluticasone propionate treatment. J Allergy Clin Immunol. 1998;101:726–31. https://doi.org/10.1016/S0091-6749(98)70301-X
8. Österback R, Tevaluoto T, Ylinen T, Peltola V, Susi P, Hyypiä T, et al. Simultaneous detection and differentiation of human rhino- and enteroviruses in clinical specimens by real-time PCR with locked nucleic Acid probes. J Clin Microbiol. 2013;51:3960–7. https://doi.org/10.1128/JCM.01646-13
9. Groves HE, Piché-Renaud PP, Peci A, Farrar DS, Buckrell S, Bancej C, et al. The impact of the COVID-19 pandemic on influenza, respiratory syncytial virus, and other seasonal respiratory virus circulation in Canada: a population-based study. Lancet Reg Health Am. 2021;1:100015. https://doi.org/10.1016/j.lana.2021.100015
10. Olsen SJ, Winn AK, Budd AP, Prill MM, Steel J, Midgley CM, et al. Changes in influenza and other respiratory virus activity during the COVID-19 pandemic—United States, 2020–2021. MMWR Morb Mortal Wkly Rep. 2021;70:1013–9. https://doi.org/10.15585/mmwr.mm7029a1
11. Yeoh DK, Foley DA, Minney-Smith CA, Martin AC, Mace AO, Sikazwe CT, et al. Impact of coronavirus disease 2019 public health measures on detection of influenza and respiratory syncytial virus in children during the 2020

Australian winter. Clin Infect Dis. 2021;72:2199–202. https://doi.org/10.1093/cid/ciaa1475
12. Oh DY, Buda S, Biere B, Reiche J, Schlosser F, Duwe S, et al. Trends in respiratory virus circulation following COVID-19-targeted nonpharmaceutical interventions in Germany, January–September 2020: analysis of national surveillance data. Lancet Reg Health Eur. 2021;6:100112. https://doi.org/10.1016/j.lanepe.2021.100112
13. Schultz EA, Kussman A, Jerome A, Abrams GD, Hwang CE. Comparison of SARS-CoV-2 test positivity in NCAA Division I student athletes vs nonathletes at 12 institutions. JAMA Netw Open. 2022;5:e2147805. https://doi.org/10.1001/jamanetworkopen.2021.47805
14. Chan HC, Tambyah PA, Tee NWS, Somani J. Return of other respiratory viruses despite the disappearance of influenza during COVID-19 control measures in Singapore. J Clin Virol. 2021;144:104992. https://doi.org/10.1016/j.jcv.2021.104992
15. Haapanen M, Renko M, Artama M, Kuitunen I. The impact of the lockdown and the re-opening of schools and day cares on the epidemiology of SARS-CoV-2 and other respiratory infections in children—a nationwide register study in Finland. EClinicalMedicine. 2021 34:100807.https://doi.org/10.1016/j.eclinm.2021.100807

Address for correspondence: Maarit Valtonen, Finnish Institute of High Performance Sport KIHU, Rautpohjankatu 6, 40700 Jyväskylä, Finland; email: maarit.valtonen@kihu.fi

Molecular Detection of *Histoplasma capsulatum* in Antarctica

Lucas Machado Moreira, Wieland Meyer, Márcia Chame, Martha Lima Brandão, Adriana Marcos Vivoni, Juana Portugal, Bodo Wanke, Luciana Trilles

We detected *Histoplasma capsulatum* in soil and penguin excreta in the Antarctic Peninsula by sequencing after performing species-specific PCR, confirming previous observations that this pathogen occurs more broadly than suspected. This finding highlights the need for surveillance of emerging agents of systemic mycoses and their transmission among regions, animals, and humans in Antarctica.

Histoplasma capsulatum is a dimorphic fungus of the order Onygenales, which can cause systemic mycosis when inhaled (*1*). The filamentous phase of the fungus usually inhabits environments rich in phosphate and nitrogenous compounds, typically coming primarily from bird or bat droppings. Human intervention and other disturbances to those environments promote dispersion of fungal propagules (spores) in the air, which enables the inhalation of infectious particles (*2*). This pathogen has a wide variety of hosts in addition to humans, and its close relationship with vertebrates suggests that birds and mammals can play a crucial role in the dispersal of the members of this species complex (*3*).

Histoplasmosis occurs worldwide; prevalence varies from low in Europe and Oceania to moderate in Africa and South Asia to high in North America, Central America, and South America. Among areas where it is most prevalent, Latin America is the region with the largest number of cases (*3*).

The genus *Histoplasma* is composed of multiple genetically distinct clades, which differ in geographic distribution, virulence, and progression of pathology (*4*). Kasuga et al. (*4*) evaluated the population genetic diversity of isolates from different countries and continents by using 4 partial protein coding regions and suggested dividing *H. capsulatum* into 7 phylogenetic species (*4*). Those results initiated a whole-genome study to evaluate the species complex, proposing 4 genetically different species: *H. capsulatum* (Panamanian linage), *H. mississippiense* (NAm1), *H. ohiense* (NAm2), and *H. suramericanum* (LAmA) (*5*).

Antarctica is the most isolated and inhospitable continent on the planet. Over the past 2 decades, however, the intensity of human activity has continued to increase, driven by not just explorers but also scientific researchers, station support personnel, fishers, whalers, and, more recently, tourists. These increased human activities have a substantial effect on all life forms in Antarctica, transporting nonindigenous species to the continent and exporting endemic and autochthones species to other continents, including human, animal and plant pathogenic fungi (*6*,*7*). However, pathogenic fungi are rarely explored in the Antarctic setting (*8*), and their effect on visitors to Antarctica and on the human populations in other continents is underinvestigated. This study describes the molecular detection of *H. capsulatum* in soil and penguin excreta in the Antarctic Peninsula.

The Study

We collected environmental samples in the Potter Peninsula, an Antarctic Special Protected Area located in King George Island, during the summer of 2020 (Figure 1). In total, we collected 9 samples of penguin excreta, 3 samples of fur seal feces, and 8 samples of superficial soil using sterile material and kept them at 2°C–8°C until analysis.

We extracted DNA from the environmental samples and monitored crossover contamination by including 1 sterile water sample at every set (Appendix, https://wwwnc.cdc.gov/EID/article/28/10/22-0046-App1.pdf). We performed nested PCR twice for all samples, using methods specific for the detection

Author affiliations: Oswaldo Cruz Foundation, Rio de Janeiro, Brazil (L.M. Moreira, M. Chame, M.L. Brandão, A.M. Vivoni, J. Portugal, B. Wanke, L. Trilles); Sydney University, Sydney, New South Wales, Australia (W. Meyer); Curtin University, Perth, Western Australia, Australia (W. Meyer)

DOI: https://doi.org/10.3201/eid2810.220046

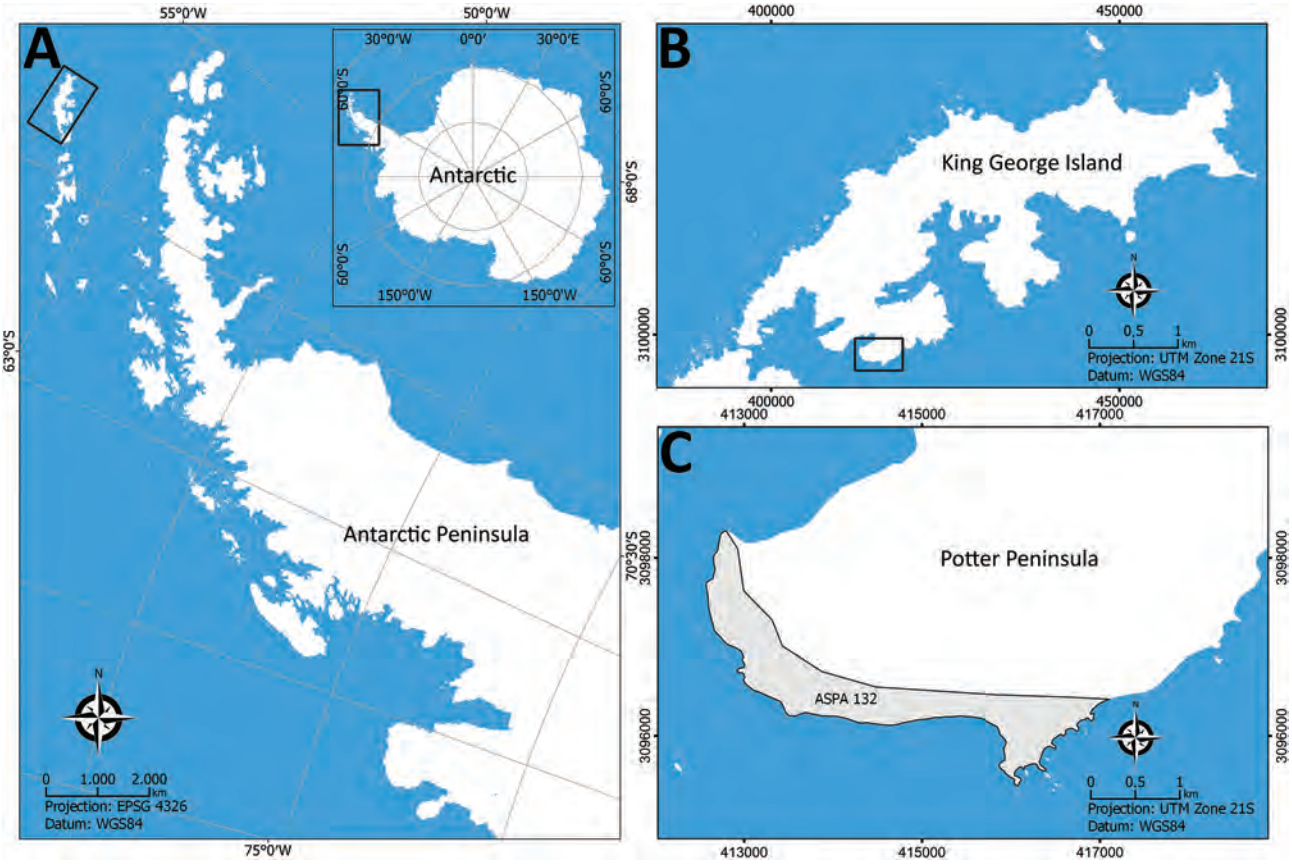

Figure 1. Sampling locations for study of *Histoplasma capsulatum* in Antarctica. A) Location of the Antarctic Peninsula in the Antarctica continent; B) King George Island; C) Potter Island and the Antarctic Specially Protected Area ASPA N°132. Source: SCAR Antarctic Digital Database (https://www.scar.org/resources/antarctic-digital-database).

and identification of *H. capsulatum* DNA according to Bialek et al. (*9*). To check for the presence of PCR inhibitors and to avoid false-negative results, we used *H. capsulatum* reference strain G217B as positive control. Sequence analysis detected *H. capsulatum* in 2 of 8 soil samples and in 3 of 9 samples from penguin excreta (Appendix Figure).

We submitted the 5 sequences we detected to GenBank (accession nos. MZ713369–73) and compared them with other *H. capsulatum* sequences. This comparison generated an identity of >98.56% (100% cover) with the deposited sequences of the 100-kDa-like protein gene from *H. capsulatum* and 85% similarity with the sequence of a transcription factor of *Blastomyces dermatitidis* SLH14081 and *B. gilchristii* SLH14081 (GenBank accession nos. XM_045419905 and XM_002628281.2).

Alignment with GenBank sequences from strains representing the different genetic lineages (Table) demonstrated a difference of up to 14 bp with the 3 haplotypes from Antarctica. The phylogenetic tree formed different groups corresponding to different geographic lineages. Two excreta samples and 1 soil sample grouped with representative strains of the Latin American lineage LAmB1, and 1 soil and 1 excreta sample grouped with a representative strain of LAmA2 lineage. No sample from Antarctica grouped with representative strains of the North America or Panama lineages (Figure 2), indicating a closer association of the newly discovered *Histoplasma* from Antarctica to the South America lineages.

Conclusions

Moderate temperatures (18°C–28°C), constant humidity (>60%), and a low light environment are thought to characterize suitable ecologic conditions for *H. capsulatum* growth (*10*). Despite the average temperature in Antarctica being below that recognized as ideal for the growth of the fungus, the molecular identification of *H. capsulatum* in 5 of 20 samples collected in Antarctica suggests this species complex could survive at lower temperatures.

Although molecular detection of the fungus does not guarantee its viability, this area of Antarctica

is part of an Antarctic Special Protected Area and experiences strong influence of avifauna during the summer period, as well as being host to bird colonies, sea mammal breeding areas, and diverse plant species. Consequently, the soil has high levels of potassium, nitrogen, calcium, and total organic carbon (*11*), which are good conditions for fungal growth. Ideally, *H. capsulatum* should be isolated for complete phenotypic and genotypic study, but it is a slow-growth fungus, and its growth is overtaken by fast-growing fungi. Animal inoculation is often used to recover *H. capsulatum*, but it demands a Biosafety Level 3 facility, which was not available to us.

The molecular detection of *H. capsulatum* in penguin excreta and ornithogenic soil samples leads us to consider the possibility that the fungus could have been imported from outside the continent by migratory birds. Birds are the only terrestrial vertebrates that share with humans the peculiarity of traveling in a few hours across national and intercontinental borders (*12*). During migration, birds have the

Table. List of fungal isolates used in study of *Histoplasma capsulatum* in Antarctica*

Identification	Other names	Source	Location	Phylogenetic species	Accession no.
1001	1001†	Human	Washington, USA	NAm1	KC990358.1
H18	4745‡/1019†/5-1MD	Human	Missouri, USA	NAm2	KC990359.1
H59	2349†/H-0057-I-10	Human	Bogota, Colombia	LAmB1	KC990362.1
H60	2350†/H-0057-I-11	Human	Bogota, Colombia	LAmA1	KC990360.1
H66	2357†/13594/GH	Human	Medellin, Colombia	LAmB2	KC990365.1
H67	2358†/30177/JE	Human	Medellin, Colombia	LAmA2	KC990361.1
H69	2360†/21402/JVM	Human	Medellin, Colombia	LAmB2	KC990366.1
H81	26028‡/2431†	Human	Panamá	Panama	KC990367.1
H91	24295/2444†/8123	Human	Guinea–Liberia border, Africa	Africa/H140 clade	KC990363.1
H176	4741†/CBS 243.69	Human	Netherlands	Netherlands	KC990364.1
COL_S_1	NI	Soil	Colombia	LAmA1	MH122835.1
COL_S_2	NI	Soil	Colombia	LAmA1	MH122836.1
COL_S_3	NI	Soil	Colombia	LAmA1	MH122837.1
COL_H_001	NI	Human	Colombia	NAm2	MH122818.1
COL_H_004	NI	Human	Colombia	LAmA1	MH122816.1
COL_H_005	NI	Human	Colombia	NAm2	MH122819.1
COL_H_013	NI	Human	Colombia	LAmA2	MH122821.1
COL_H_014	NI	Human	Colombia	LAmA2	MH122813.1
COL_H_015	NI	Human	Colombia	LAmA1	MH122814.1
COL_H_024	NI	Human	Colombia	LAmA1	MH122815.1
COL_H_025	NI	Human	Colombia	LAmA2	MH122822.1
COL_H_029	NI	Human	Colombia	LAmB1	MH122807.1
COL_H_032	NI	Human	Colombia	LAmB1	MH122808.1
COL_H_035	NI	Human	Colombia	LAmB1	MH122809.1
COL_H_038	NI	Human	Colombia	NAm2	MH122820.1
COL_H_039	NI	Human	Colombia	LAmA1	MH122828.1
COL_H_040	NI	Human	Colombia	LAmB1	MH122810.1
COL_H_041	NI	Human	Colombia	LAmA2	MH122825.1
COL_H_042	NI	Human	Colombia	LAmB1	MH122812.1
COL_H_044	NI	Human	Colombia	LAmA1	MH122832.1
COL_H_048	NI	Human	Colombia	LAmA1	MH122817.1
COL_H_053	NI	Human	Colombia	LAmA2	MH122829.1
COL_H_055	NI	Human	Colombia	LAmA2	MH122826.1
COL_H_056	NI	Human	Colombia	LAmB1	MH122811.1
COL_H_062	NI	Human	Colombia	LAmA2	MH122827.1
COL_H_068	NI	Human	Colombia	LAmA2	MH122838.1
G184A	H81 lineage	Human	Panamá	Panama	MZ713378.1
G217B	26032‡/1000†/H8	Human	Louisiana, USA	NAm2	MZ713379.1
01.16	INI_01.16	Human	Rio de Janeiro, Brazil	Northeast	MZ713380.1
24.11	IPEC_24.11	Human	Rio de Janeiro, Brazil	RJ	MZ713375.1
39942	NI	Human	Rio de Janeiro, Brazil	Panama	MZ713377.1
S268B	S268	Soil	Potter Peninsula, Antarctic	LAmA2	MZ713373.1
S269	NI	Soil	Potter Peninsula, Antarctic	LAmB1	MZ713371.1
F47	NI	Penguin excreta	Potter Peninsula, Antarctic	LAmA2	MZ713372.1
F49	NI	Penguin excreta	Potter Peninsula, Antarctic	LAmB1	MZ713369.1
F54	NI	Penguin excreta	Potter Peninsula, Antarctic	LAmB1	MZ713370.1

*CBS, Centraalbureau voor Schimmelcultures (Baarn, The Netherlands); INI, Instituto Nacional de Infectologia Evandro Chagas (Rio de Janeiro, Brazil); IPEC, Instituto de Pesquisa Clínica Evandro Chagas (Rio de Janeiro, Brazil); NI, no information.
†Roche Molecular Systems Culture Collection, Alameda, CA, USA.
‡American Type Culture Collection, Rockville, MD, USA.

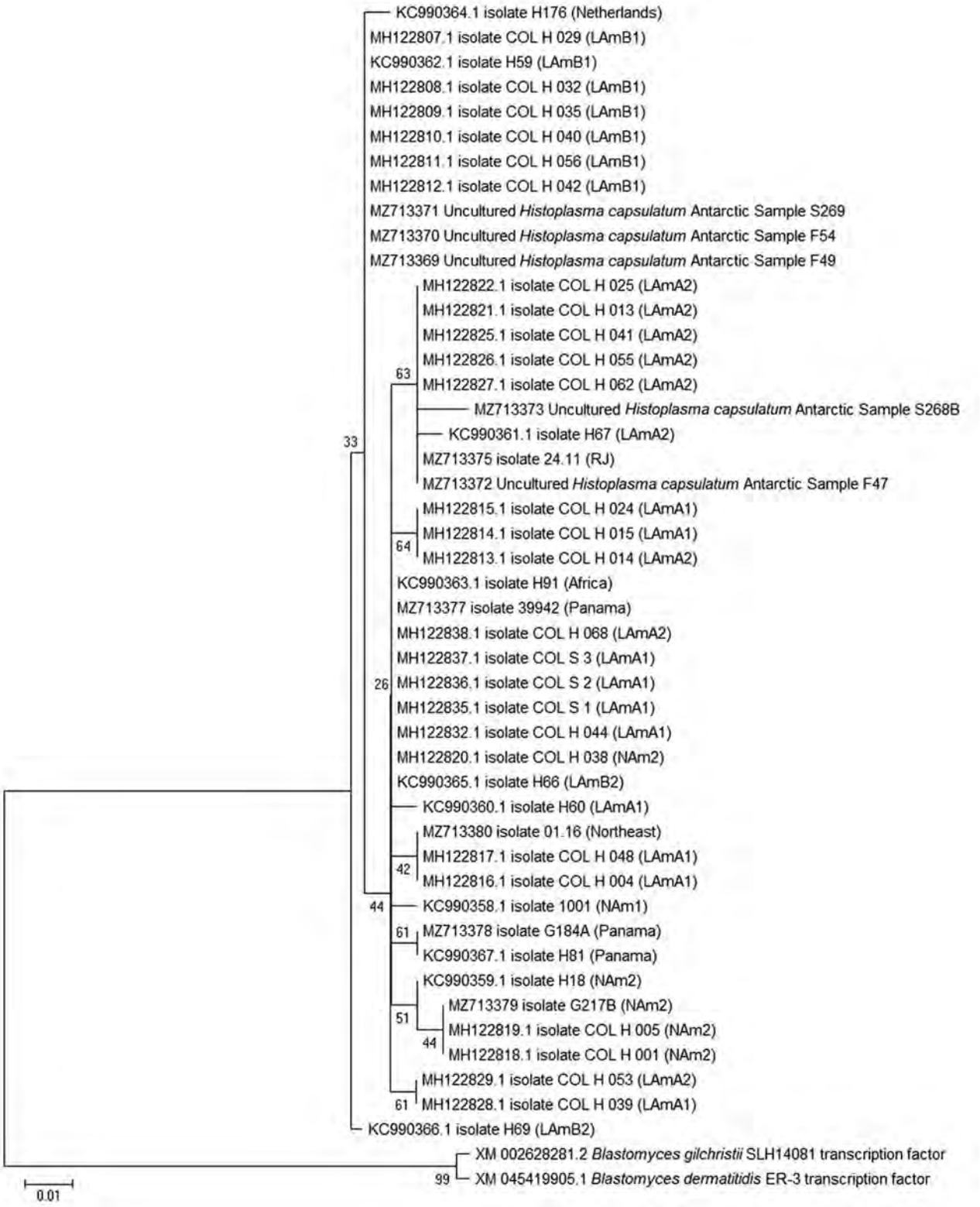

Figure 2. Phylogenetic tree based on the 100-kDa–like protein partial gene sequences of *Histoplasma capsulatum* from Antarctica. The evolutionary history was inferred by using the maximum-likelihood method in in MEGA X software (https://www.megasoftware.net). This analysis involved 46 sequences: 5 from Antarctica samples and 41 representing geographic lineages of *H. capsulatum* in addition to the closest non-*Histoplasma* sequences (*Blastomyces* spp.) downloaded from GenBank (accession numbers shown). The bootstrap percentage of trees in which the associated taxa clustered together is shown next to the branches. Scale bar indicates the number of substitutions per site.

potential to disperse microorganisms that can be dangerous to humans and a threat to animals (*13*). The fact that high densities of cosmopolitan fungi were found in winter seasonal snow suggests those fungi might be present in air arriving at the Antarctica Peninsula (*14*). Another possibility could be human intervention in the region. Alien microbes, fungi, plants, and animals have arrived over approximately the previous 2 centuries, coinciding with human activity in Antarctica (*6*).

The differentiation of the 7 phylogenetic species in the complex could not be performed with the genetic marker used in this study. However, we detected different haplotypes that grouped with some of those geographically distinct phylogenetic species, suggesting dispersion of the fungus on multiple occasions and, perhaps, indicating adaptation on its way to becoming endemic to the Antarctic Peninsula. The detection of *H. capsulatum* genetically close to representative strains of the Latin American lineages (LAmA2/LAmB1) in Antarctica represents not only the geological history of the continent with South America but the complex dynamics of soil formation and presence of fauna and flora that enable adequate conditions for its maintenance.

This study evaluated a small geographic area of the peninsula, but it has already demonstrated that *H. capsulatum* occurs more broadly than previously suspected (*15*). Considering the capacity of the species to cause life-threatening epidemics and the intensifying human presence on the continent, identifying and monitoring fungi in various Antarctic habitats and animals becomes a fundamental strategy for surveilling emerging systemic mycoses and the flow of these agents between regions, animals, and humans.

This project was partially funded by CNPQ/MCTIC/CAPES/FNDCT Nº 21/2018–PROANTAR (442646/2018-6) and Inova Fiocruz/Fundação Oswaldo Cruz (project no. 4720463444). The funders had no role in study design, data collection and interpretation, or the decision to submit the work for publication.

We are eternally grateful to the late Dr. Bodo Wanke for the opportunity to start this project, for his help on designing the study, and mentoring. He will be missed.

About the Author

Mr. Machado Moreira is a PhD student in the postgraduate program in Tropical Medicine at Instituto Oswaldo Cruz, Fiocruz. His primary research interests are polyphasic taxonomy, phylogeny, and diagnosis of invasive fungal infections.

References

1. Deepe GS Jr. Outbreaks of histoplasmosis: the spores set sail. PLoS Pathog. 2018;14:e1007213. https://doi.org/10.1371/journal.ppat.1007213
2. Knox KS, Hage CA. Histoplasmosis. Proc Am Thorac Soc. 2010;7:169–72. https://doi.org/10.1513/pats.200907-069AL
3. Teixeira MM, Patané JS, Taylor ML, Gómez BL, Theodoro RC, de Hoog S, et al. Worldwide phylogenetic distributions and population dynamics of the genus *Histoplasma*. PLoS Negl Trop Dis. 2016;10:e0004732. https://doi.org/10.1371/journal.pntd.0004732
4. Kasuga T, White TJ, Koenig G, McEwen J, Restrepo A, Castañeda E, et al. Phylogeography of the fungal pathogen *Histoplasma capsulatum*. Mol Ecol. 2003;12:3383–401. https://doi.org/10.1046/j.1365-294X.2003.01995.x
5. Sepúlveda VE, Márquez R, Turissini DA, Goldman WE, Matute DR. Genome sequences reveal cryptic speciation in the human pathogen *Histoplasma capsulatum*. MBio. 2017;8:8. https://doi.org/10.1128/mBio.01339-17
6. Frenot Y, Chown SL, Whinam J, Selkirk PM, Convey P, Skotnicki M, et al. Biological invasions in the Antarctic: extent, impacts and implications. Biol Rev Camb Philos Soc. 2005;80:45–72. https://doi.org/10.1017/S1464793104006542
7. Tin T, Fleming ZL, Hughes KA, Ainley DG, Convey P, Moreno CA, et al. Impacts of local human activities on the Antarctic environment. Antarct Sci. 2009;21:3–33. https://doi.org/10.1017/S0954102009001722
8. de Sousa JRP, Gonçalves VN, de Holanda RA, Santos DA, Bueloni CFLG, Costa AO, et al. Pathogenic potential of environmental resident fungi from ornithogenic soils of Antarctica. Fungal Biol. 2017;121:991–1000. https://doi.org/10.1016/j.funbio.2017.09.005
9. Bialek R, Feucht A, Aepinus C, Just-Nübling G, Robertson VJ, Knobloch J, et al. Evaluation of two nested PCR assays for detection of *Histoplasma capsulatum* DNA in human tissue. J Clin Microbiol. 2002;40:1644–7. https://doi.org/10.1128/JCM.40.5.1644-1647.2002
10. Kwon-Chung KJ, Bennett JE. Medical mycology. 2nd ed. Philadelphia: Lea & Febiger; 1992.
11. Poelking EL. Solos, ambiente e dinâmica climática da camada na Península Potter, Antártica Marítima [dissertation]. Viçosa, Brazil: Federal University of Viçosa; 1978.
12. Jourdain E, Gauthier-Clerc M, Bicout DJ, Sabatier P. Bird migration routes and risk for pathogen dispersion into western Mediterranean wetlands. Emerg Infect Dis. 2007;13:365–72. https://doi.org/10.3201/eid1303.060301
13. Reed KD, Meece JK, Henkel JS, Shukla SK. Birds, migration and emerging zoonoses: West Nile virus, Lyme disease, influenza A and enteropathogens. Clin Med Res. 2003;1:5–12. https://doi.org/10.3121/cmr.1.1.5
14. de Menezes GCA, Amorim SS, Gonçalves VN, Godinho VM, Simões JC, Rosa CA, et al. Diversity, distribution, and ecology of fungi in the seasonal snow of Antarctica. Microorganisms. 2019;7:445. https://doi.org/10.3390/microorganisms7100445
15. Ashraf N, Kubat RC, Poplin V, Adenis AA, Denning DW, Wright L, et al. Re-drawing the maps for endemic mycoses. Mycopathologia. 2020;185:843–65. https://doi.org/10.1007/s11046-020-00431-2

Address for correspondence: Luciana Trilles, Instituto Nacional de Infectologia Evandro Chagas–INI/FIOCRUZ, Pavilhão Maria Deane Av. Brasil, 4365, 21040-900 Rio de Janeiro, Brazil; email: luciana.trilles@ini.fiocruz.br

Anisakiasis Annual Incidence and Causative Species, Japan, 2018–2019

Hiromu Sugiyama, Mitsuko Shiroyama, Ikuyo Yamamoto, Takashi Ishikawa, Yasuyuki Morishima

Using data from 2018–2019 health insurance claims, we estimated the average annual incidence of anisakiasis in Japan to be 19,737 cases. Molecular identification of larvae revealed that most (88.4%) patients were infected with the species *Anisakis simplex* sensu stricto. Further insights into the pathogenesis of various anisakiasis forms are needed.

Anisakiasis is a foodborne zoonosis caused by ingestion of raw or undercooked fish and cephalopods parasitized by anisakid nematode larvae. As seafood consumption has increased globally (*1*), the incidence of anisakiasis has also increased worldwide (*2*,*3*). The population of Japan traditionally consumes large quantities of seafood (*4*), and consuming raw seafood, such as sushi and sashimi, is common.

In response to the large number of annual cases, the government of Japan added anisakiasis under food poisoning in its Ordinance for Enforcement of the Food Sanitation Act to strengthen countermeasures in 1999, when food poisoning statistics included a case of anisakiasis (*5*). In 2012, the government amended the ordinance and registered anisakid nematodes, comprising *Anisakis* spp. and *Pseudoterranova* spp., as a single disease agent, *Anisakis*, in the list of food poisoning agents (*6*). These measures enabled the government to aggregate the number of *Anisakis* food poisoning cases, which showed a near-constant increase. However, epidemiologic studies have indicated that the number of food poisoning cases in Japan is considerably higher than those officially reported (*7*). For anisakiasis, the discrepancy between food poisoning statistics and the actual incidence is unclear because no nationwide investigation into anisakiasis incidence has been conducted since the 2012 amendment.

Author affiliations: National Institute of Infectious Diseases, Tokyo, Japan (H. Sugiyama, I. Yamamoto, Y. Morishima); Azabu University, Kanagawa, Japan (M. Shiroyama); BML, Inc., Saitama, Japan (T. Ishikawa)

DOI: https://doi.org/10.3201/eid2810.220627

We analyzed a large database of health insurance claim data (*8*) to estimate the national incidence of anisakiasis and determine the degree of discrepancy between foodborne statistics and actual incidence. Furthermore, we performed molecular identification of anisakid larvae isolated from infected patients to clarify the causative agent and adduce reasons for the high incidence of anisakiasis in Japan.

The Study

To estimate the number of anisakiasis patients, we used an anonymized health insurance claim database from JMDC, Inc. (https://www.jmdc.co.jp), a commercial medical database provider in Japan. The nation has a universal health insurance system wherein medical institutions prepare health insurance claims that list the name of the disease or injury on a service basis. Medical expenses, other than a portion directly paid by patients, are reimbursed from taxes and mandatory insurance fees. In this process, medical institutions first submit health insurance claims to a specialized organization that assesses the appropriateness of treatment and amount of reimbursement. In this study, we used a database covering ≈8.43 million persons annually, accounting for >6% of the total population of Japan, during January 2018–December 2019. We extracted health insurance claims with the diagnosis code B81.0 in the International Classification of Diseases, 10th Revision (ICD-10), indicating *Anisakis* and *Pseudoterranova* infections.

The number of patients with anisakiasis registered in the target database was 991 in 2018 and 766 in 2019. However, the data revealed a male-biased sex ratio and a workforce-biased distribution for persons 20–39 years of age. Therefore, we adjusted the value in each group for estimation by stratifying the population of Japan by sex and age by using a previously described expanded estimate method (*9*), and data from the national census conducted by the Ministry of Internal Affairs and Communications in 2015

(https://www.stat.go.jp/english/data/kokusei/2015/final_en/final_en.html). On the basis of our adjustment, we estimate the number of patients in Japan with anisakiasis was 21,511 in 2018 and 17,962 in 2019. The number of patients with anisakiasis recorded in the food poisoning statistics during the same period was considerably lower, <1/40, in our estimation (Table 1).

For molecular identification, we obtained 189 larvae of anisakid nematodes from BML, Inc. (http://www.bml.co.jp/eng), a privately-owned clinical testing laboratory in Japan. The larvae were isolated from 181 anisakiasis patients in 30 of 47 prefectures in Japan during 2018–2019 (Figure 1). We extracted DNA samples from individual larvae, used PCR to amplify the internal transcribed spacer 1 region, and sequenced the amplicons to distinguish between nematode genera and identify the *Anisakis* species. For *Pseudoterranova* larvae, we further amplified a portion of the NADH dehydrogenase subunit 1 gene in mitochondrial DNA and sequenced to discriminate between species of this genus (Appendix, https://wwwnc.cdc.gov/EID/article/28/10/22-0627-App1.pdf).

Consequently, we identified 168 (88.9%) *Anisakis simplex* sensu stricto larvae, 10 (5.3%) *A. pegreffii* larvae, and 11 (5.8%) *Pseudoterranova azarasi* larvae (Table 2). These findings represent perfect sequence identity with the respective species, regardless of the targets. We deposited the obtained sequences in GenBank under accession nos. LC684518–21 (Appendix Table 1).

Table 1. Reported and estimated number of patients with anisakiasis, Japan, 2018–2019

Year	Food poisoning cases*	Health insurance claims	
		No. in database†	Nationwide estimates‡
2018	478	991	21,511
2019	336	766	17,962
Average	407	878.5	19,737

*Data collected from Ministry of Health, Labour and Welfare.
†Data extracted from JMDC Inc. (https://www.jmdc.co.jp) health insurance claim database, which covers ≈8.43 million persons annually.
‡Estimates calculated by stratifying the population of Japan by sex and age, as previously described (*9*).

Conclusions

A recent study estimated 7,700–8,320 annual anisakiasis cases in Spain, a country with a high incidence of anisakiasis in Europe (*10*). Although our survey methods differed, we demonstrated that Japan had an average of 19,737 anisakiasis cases per year during 2018–2019. As preventive measures, the government of Japan has repeatedly instructed local establishments (e.g., restaurants, fish mongers, and grocery stores) and consumers to freeze seafood at −20°C for at least 24 hours before consuming it raw or

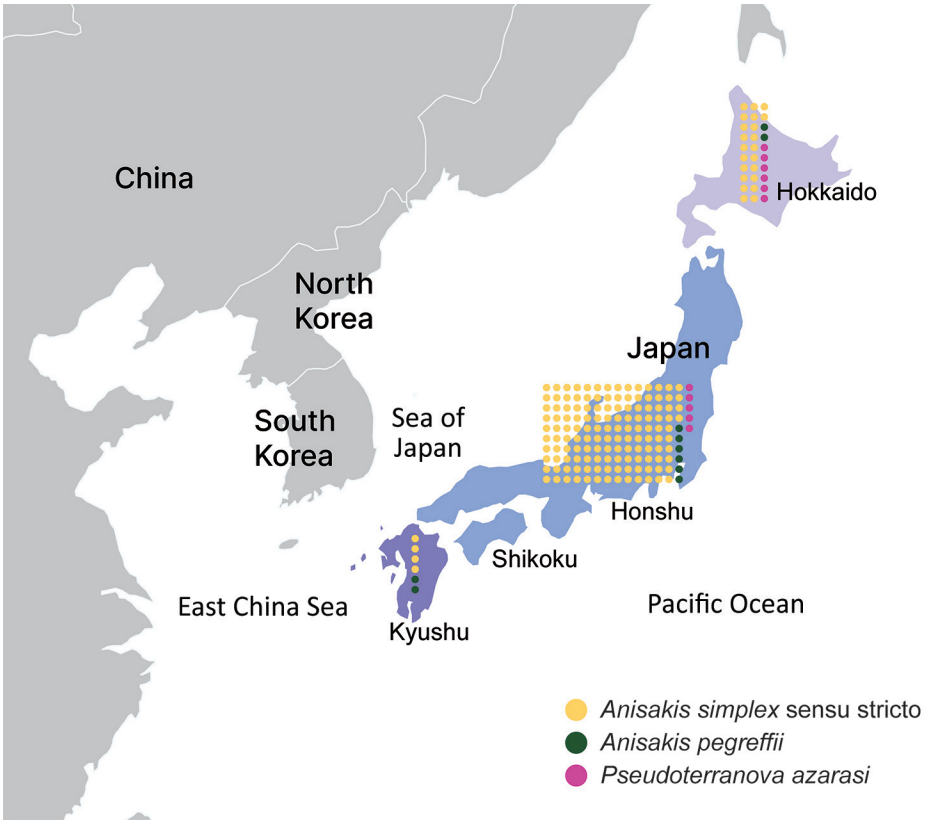

Figure 1. Anisakiasis patient number and causative species analyzed in study of anisakiasis in Japan, 2018–2019. Three geographic locations in Japan are noted: Hokkaido Island (North Japan), Honshu and Shikoku Islands (Central Japan), and Kyushu Island (Southwest Japan). Each dot indicates 1 patient, and color indicates the anisakiasis-causing species. Identifications were made at the sibling species level by using PCR and sequencing.

Table 2. Molecular identification of anisakid larvae isolated from patients, Japan, 2018–2019

Species, isolation site	Symptomatic cases, no.		Asymptomatic cases, no.		Total cases, no.		Overall, no. (%)	
	Patients	Larvae	Patients	Larvae	Patients	Larvae	Patients	Larvae
Anisakis simplex sensu stricto							160 (88.4)	168 (88.9)
Stomach	139	146*†	18	19‡§	157	165		
Intestine	0	0	3	3‡	3	3		
Anisakis pegreffii							10 (5.5)	10 (5.3)
Stomach	9	9*	0	0	9	9		
Intestine	0	0	1	1‡	1	1		
Pseudoterranova azarasi							11 (6.1)	11 (5.8)
Oral cavity	0	0	4	4¶	4	4		
Stomach	6	6*#	1	1‡	7	7		
Total	154	161	27	28	181	189	181 (100)	189 (100)

*Abdominal pain.
†Two larvae were isolated from 5 patients and 3 larvae were isolated from 1 patient.
‡Larvae were incidentally detected endoscopically during health check-ups or routine follow-up cancer screening.
§Two larvae were isolated from 1 patient.
¶*P. azarasi* larvae were spontaneously expelled from the mouth.
#Of 6 *P. azarasi* patients, 1 showed urticaria in addition to abdominal pain.

to remove anisakid nematodes during cooking. The Ministry of Health, Labour and Welfare of Japan provides web-based food poisoning statistics with information regarding fish species reported by anisakiasis patients and preparation procedures associated with infections in Japanese to help consumers and fishmongers avoid anisakiasis.

In Japan, *A. simplex* s.s. nematodes are responsible for the highest incidence of anisakiasis, whereas the species *A. pegreffii* is the leading cause of anisakiasis in Europe and South Korea (*2*). *A. simplex* s.s. nematodes penetrate the muscles of various fish species at a higher rate than *A. pegreffii* (*11*), which could

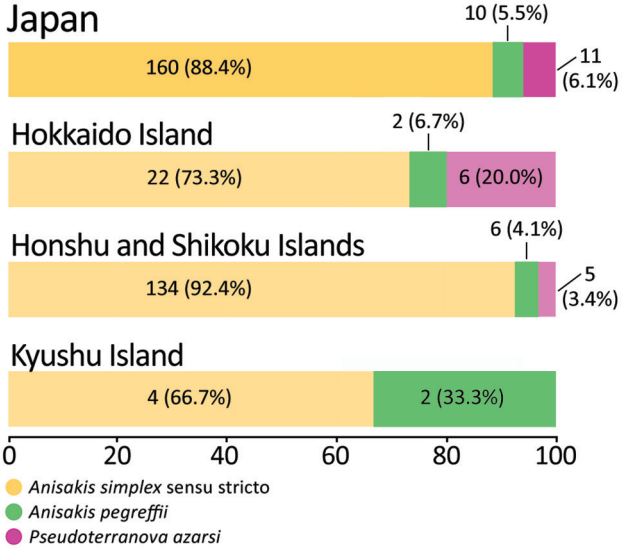

Figure 2. Analyzed number and percentage of anisakiasis patients and causative species, Japan, 2018–2019.One third (2/6) of patients in the Kyushu Island had *Anisakis pegreffii* infections. *A. pegreffii*–carrying fish are predominant in the Sea of Japan and the East China Sea, located between South Korea and Japan (*11*). Over 50% (6/11) of the patients with *Pseudoterranova azarasi* infection were from Hokkaido.

partly explain the smaller proportion of *A. pegreffii* anisakiasis cases in Japan because *A. pegreffii* nematodes are often removed with fish viscera during the preparation of sushi and sashimi. Furthermore, fish habitat can corroborate the difference in predominant anisakid nematode species between South Korea and Japan; *A. simplex* s.s.–carrying fish are predominant in the Pacific side of Japan, whereas *A. pegreffii*–carrying fish are more common in the Sea of Japan and the East China Sea, located between South Korea and Japan (*11*) (Figure 1).

In this study, we identified 11 *P. azarasi* larvae (5.8%) from 11 patients, 6 of whom lived in Hokkaido, the northernmost insular prefecture of Japan, where cold water fish, such as Pacific cod (*Gadus macrocephalus*), are commonly consumed (Figures 1,2) (*12*). Although patients have been reported to orally expel *Pseudoterranova* larvae that have developed to the fourth stage (*13*), most (7/11 cases) *P. azarasi* larvae detected in this study were in the stomach.

Anisakid larvae were isolated from the stomach or intestines of 177 patients, 23 (13%) of whom were asymptomatic. These asymptomatic cases were found incidentally during health check-ups or routine follow-up cancer screening. Some studies have already reported asymptomatic gastrointestinal cases (*14*,*15*), but our findings revealed a varied and greater number of anisakid species associated with asymptomatic infections: *A. simplex* s.s. (91.3%), *A. pegreffii* (4.3%), and *P. azarasi* (4.3%). One urticaria case was associated with symptomatic *P. azarasi* gastric infection. Numerous cases of *Anisakis* allergy, including cases of urticaria, angioedema, and anaphylaxis, have been reported in Europe (*10*). In healthcare claims from Japan, *Anisakis* allergy was not registered as a disease name until 2021. Thus, the database did not include anisakiasis patients with allergic symptoms alone, which is a limitation of this study.

In conclusion, *Anisakis* infection is currently drawing more attention in Japan. Elucidating the immunopathological mechanisms behind asymptomatic and symptomatic anisakiasis is imperative and can provide insights into the pathogenesis of gastrointestinal anisakiasis.

Acknowledgments

We thank Chisato Kagawa for her support. We also thank the members of Inspection and Safety Division, Department of Food Safety, Ministry of Health, Labour and Welfare, Japan, for their assistance in re-confirming the cases of anisakiasis in the food poisoning statistics of Japan.

This study was supported by a grant from the Japan Agency for Medical Research and Development (grant no. 21fk0108136 to H.S.).

About the Author

Dr. Sugiyama is the former chief of the Laboratory of Helminthology, Department of Parasitology at the National Institute of Infectious Diseases in Tokyo, Japan, and currently continues his research in this institution as a guest researcher. His primary research interests are epidemiology and laboratory diagnosis of foodborne helminthic zoonoses, including anisakiasis and paragonimiasis.

References

1. Naylor RL, Kishore A, Sumaila UR, Issifu I, Hunter BP, Belton B, et al. Blue food demand across geographic and temporal scales. Nat Commun. 2021;12:5413. https://doi.org/10.1038/s41467-021-25516-4
2. Lim H, Jung BK, Cho J, Yooyen T, Shin EH, Chai JY. Molecular diagnosis of cause of anisakiasis in humans, South Korea. Emerg Infect Dis. 2015;21:342–4. https://doi.org/10.3201/eid2102.140798
3. Shamsi S, Butcher AR. First report of human anisakidosis in Australia. Med J Aust. 2011;194:199–200. https://doi.org/10.5694/j.1326-5377.2011.tb03772.x
4. Food and Agriculture Organization of the United Nations. FAO yearbook. Fishery and aquaculture statistics 2019. Rome: The Organization; 2021. https://doi.org/10.4060/cb7574t
5. Sugiyama H. Food and parasitic infections [in Japanese]. Shokuhin Eiseigaku Zasshi. 2010;51:285–91. https://doi.org/10.3358/shokueishi.51.285
6. Director-General, Department of Food Safety, Pharmaceutical and Food Safety Bureau, Ministry of Health, Labour and Welfare. Partial revision of the ordinance for enforcement of the Food Sanitation Act [in Japanese]. 2012 Dec 28; Notification shokuan no. 1228–7 [cited 2022 Apr 11]. https://www.mhlw.go.jp/topics/bukyoku/iyaku/syoku-anzen/gyousei/dl/121228_2.pdf
7. Kubota K, Kasuga F, Iwasaki E, Inagaki S, Sakurai Y, Komatsu M, et al. Estimating the burden of acute gastroenteritis and foodborne illness caused by *Campylobacter, Salmonella*, and *Vibrio parahaemolyticus* by using population-based telephone survey data, Miyagi Prefecture, Japan, 2005 to 2006. J Food Prot. 2011;74:1592–8. https://doi.org/10.4315/0362-028X.JFP-10-387
8. Kimura S, Sato T, Ikeda S, Noda M, Nakayama T. Development of a database of health insurance claims: standardization of disease classifications and anonymous record linkage. J Epidemiol. 2010;20:413–9. https://doi.org/10.2188/jea.JE20090066
9. Ohisa M, Kimura Y, Matsuo J, Akita T, Sato T, Matsuoka T, et al. Estimated numbers of patients with liver disease related to hepatitis B or C virus infection based on the database reconstructed from medical claims from 2008 to 2010 in Japan. Hepatol Res. 2015;45:1228–40. https://doi.org/10.1111/hepr.12497
10. Bao M, Pierce GJ, Pascual S, González-Muñoz M, Mattiucci S, Mladineo I, et al. Assessing the risk of an emerging zoonosis of worldwide concern: anisakiasis. Sci Rep. 2017;7:43699. https://doi.org/10.1038/srep43699
11. Suzuki J, Murata R, Kodo Y. Current status of anisakiasis and *Anisakis* larvae in Tokyo, Japan. Food Saf (Tokyo). 2021;9:89–100. https://doi.org/10.14252/foodsafetyfscj.D-21-00004
12. Arizono N, Miura T, Yamada M, Tegoshi T, Onishi K. Human infection with *Pseudoterranova azarasi* roundworm. Emerg Infect Dis. 2011;17:555–6. https://doi.org/10.3201/eid1703.101350
13. Torres P, Jercic MI, Weitz JC, Dobrew EK, Mercado RA. Human pseudoterranovosis, an emerging infection in Chile. J Parasitol. 2007;93:440–3. https://doi.org/10.1645/GE-946R.1
14. Nakaji K, Kumamoto M, Wada Y, Nakae Y. Asymptomatic gastric and colonic anisakiasis detected simultaneously. Intern Med. 2019;58:2263–4. https://doi.org/10.2169/internalmedicine.2657-19
15. Song H, Jung BK, Cho J, Chang T, Huh S, Chai JY. Molecular identification of *Anisakis* larvae extracted by gastrointestinal endoscopy from health check-up patients in Korea. Korean J Parasitol. 2019;57:207–11. https://doi.org/10.3347/kjp.2019.57.2.207

Address for correspondence: Hiromu Sugiyama, Department of Parasitology, National Institute of Infectious Diseases, Toyama 1-23-1, Shinjuku, Tokyo, 162-8640, Japan; email: hsugi@niid.go.jp

Emerging Tickborne Bacteria in Cattle from Colombia

Alejandro Ramírez-Hernández, Esteban Arroyave, Álvaro A. Faccini-Martínez, Heidy C. Martínez-Diaz, Paola Betancourt-Ruiz, Luz-Adriana Olaya-M, Elkin G. Forero-Becerra, Marylin Hidalgo, Lucas S. Blanton, David H. Walker

Author affiliations: Universidad de La Salle, Bogotá, Colombia (A. Ramírez-Hernández); University of Texas Medical Branch, Galveston, Texas, USA (A. Ramírez-Hernández, E. Arroyave, Á.A. Faccini-Martínez, L.S. Blanton, D.H. Walker); Fundación Universitaria de Ciencias de la Salud, Bogotá (Á.A. Faccini-Martínez); Servicios y Asesorías en Infectología Sai S.A.S., Bogotá (Á.A. Faccini-Martínez); Pontificia Universidad Javeriana, Bogotá (H.C. Martínez-Diaz, P. Betancourt-Ruiz, E.G. Forero-Becerra, M. Hidalgo); Universidad Libre, Cali, Colombia (L.-A. Olaya-M)

DOI: https://doi.org/10.3201/eid2810.220657

Ehrlichia minasensis is a new pathogenic bacterial species that infects cattle, and *Borrelia theileri* causes bovine borreliosis. We detected *E. minasensis* and *B. theileri* DNA in cattle from southwestern Colombia by using PCR. *E. minasensis* and *B. theileri* should be considered potential etiologies of febrile syndrome in cattle from Colombia.

Ehrlichia spp. are tickborne obligate intracellular bacteria and comprise different pathogenic species that affect both veterinary and public health (*1*). *Ehrlichia minasensis* was first detected in cattle and deer in Canada and later in cattle and *Rhipicephalus microplus* ticks from Brazil (*2*–*4*). Infected cattle manifest signs that include fever, lethargy, depression, and anorexia (*3*,*4*). *Borrelia theileri* belongs to the relapsing fever group of borreliae and causes bovine borreliosis, which is a mild febrile disease associated with lethargy, hemoglobinuria, and anemia (*5*). This spirochete is transmitted by *Rhipicephalus* (formerly *Boophilus*) sp. ticks and has been documented in Africa, Europe, Oceania, and South America (*5*,*6*). To our knowledge, *E. minasensis* or *B. theileri* infections have not been reported in cattle from Colombia.

During September and October 2017, we collected blood samples from 30 bovids with tick parasitism in El Tambo and Santander de Quilichao municipalities, Cauca department, Colombia (Appendix Figure, https://wwwnc.cdc.gov/EID/article/28/10/22-0657-App1.pdf). We extracted DNA from blood using the QIAGEN DNeasy Blood & Tissue Kit (https://www.qiagen.com), according to the manufacturer's instructions. We verified DNA quality using PCR amplification of the vertebrate cytochrome B gene *CYTB*. We subsequently performed PCR to detect *dsb* and *trp36* genes for *Ehrlichia* spp.; *flaB* and 16S rRNA genes for *Borrelia* spp.; and *rpoB*, *msp4*, and *msp1a* genes for *Anaplasma* spp. (Appendix Table). DNA samples that produced strong PCR bands underwent sequencing on an Applied Biosystems 3130/3130xl Genetic Analyzer (Thermo Fisher Scientific, https://www.thermofisher.com). The *msp1a* PCR products were poor quality and did not undergo sequencing. We aligned sequences using GeneStudio (GeneStudio, Inc., https://genestudio-pro.software.informer.com) and performed multiple sequence alignments using the EMBL-European Bioinformatics Institute tools MUSCLE (for *Ehrlichia* spp.) and ClustalW (for *Borrelia* and *Anaplasma* spp.) (https://www.clustal.org). Phylogenetic analyses were performed with MEGA X software (https://www.megasoftware.net). We generated phylogenetic trees for *dsb*, *flaB*, and 16S rRNA genes and Trp36 protein using the maximum-likelihood estimation method. All procedures were approved by the Pontificia Universidad Javeriana Ethics Committee in Colombia.

We detected *CYTB* in all samples. We detected the *dsb* gene in 10% (3/30) and *trp36* in 20% (6/30) of samples. The *flaB* gene was detected in 13.3% (4/30), and the 16S rRNA gene was detected in 10% (3/30) of samples. The *rpoB* gene was amplified in 90% (27/30), *msp4* was amplified in 83.3% (25/30), and *msp1a* was amplified in 83.3% (25/30) of samples. We performed phylogenetic analyses of 3 sequences for *dsb* (GenBank accession nos. ON209405–7), 6 sequences for Trp36 protein (inferred from GenBank accession nos. OL513405–10), 3 sequences for the 16S rRNA gene (GenBank accession nos. ON112216–8), 4 sequences for *flaB* (GenBank accession nos. ON135431–4); 6 sequences for *rpoB* (GenBank accession nos. ON209412–7), and 4 sequences for *msp4* (GenBank accession nos. ON209408–11).

Phylogenetic analyses showed that our *dsb* gene sequences clustered with *E. minasensis dsb* sequences from Brazil, Australia, and Colombia (Figure, panel A). The greater genetic diversity of Trp36 protein compared with *dsb* provided more detailed characterization of *Ehrlichia* sp. genotypes. Our Trp36 sequences clustered with 3 sequences from Brazil and a recently described *E. minasensis* strain from China isolated from *Haemaphysalis hystricis* ticks (Figure, panel B). The *flaB* and 16S rRNA genes clustered with *B. theileri* sequences (Figure, panels C, D).

Bootstrap values were 86% for *flaB* and 72% for the 16S rRNA gene. The *flaB* sequences grouped with sequences from Argentina, Republic of the Congo, Egypt, and Israel (Figure, panel C). The 16S rRNA gene sequences grouped independently but close to sequences from Egypt and the United States (Figure,

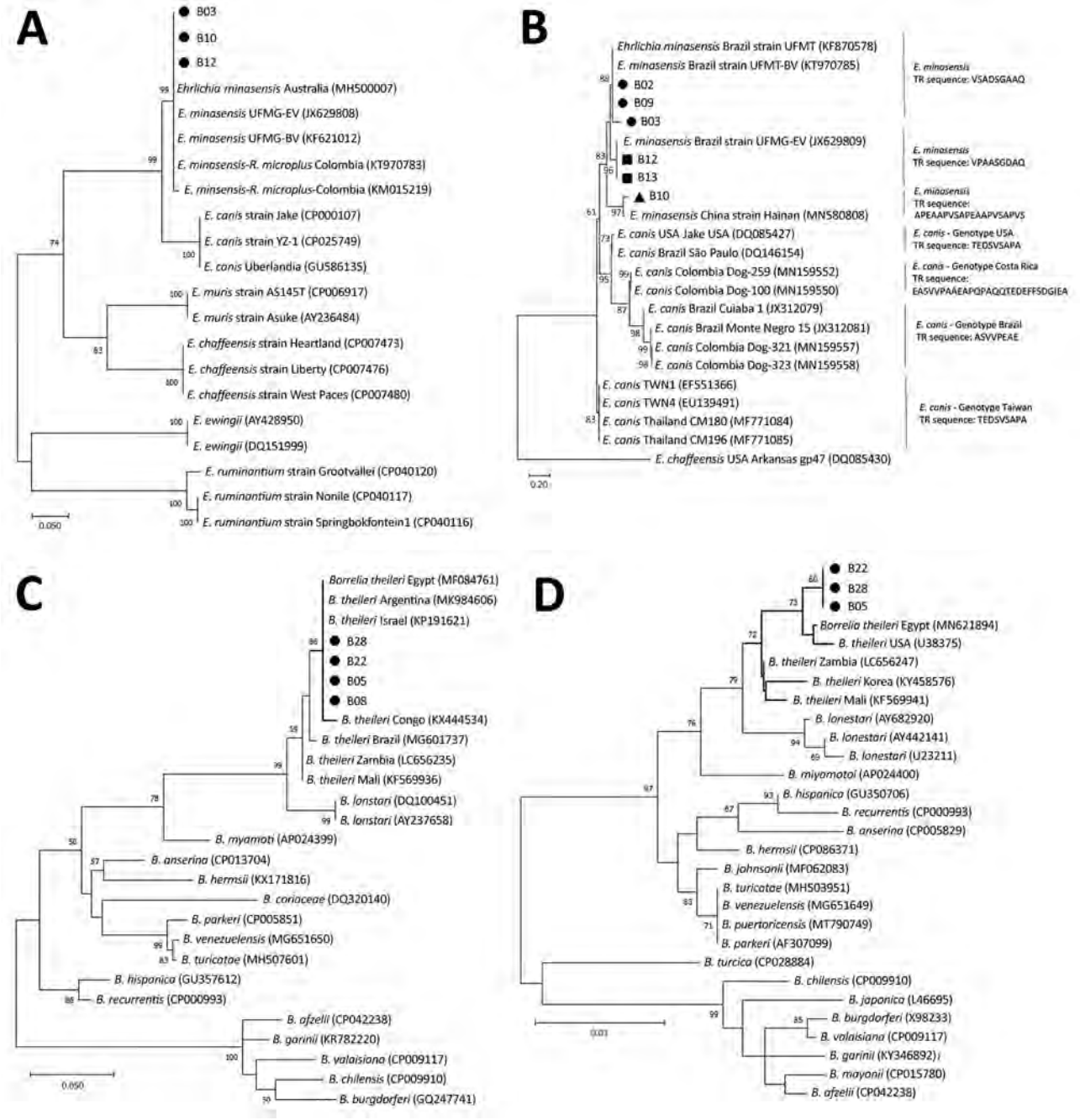

Figure. Phylogenetic analysis of emerging tickborne bacteria in cattle from Colombia. Phylogenetic trees are shown for *dsb* genes (A), Trp36 proteins (amino acid sequences) (B), *flaB* genes (C), and 16S rRNA genes (D). We performed PCR on blood samples from cattle in El Tambo and Santander de Quilichao, Cauca department, Colombia to detect *dsb* and *trp36* genes for *Ehrlichia* sp.; *flaB* and 16S rRNA genes for *Borrelia* sp.; and *rpoB*, *msp4*, and *msp1a* genes for *Anaplasma* sp. We generated phylogenetic trees using the maximum-likelihood method and Tamura 3-parameter model with a gamma distribution parameter of 0.28 to compare evolutionary relationships between our sequences and publicly available sequences from Genbank (accession numbers indicated on trees). We applied bootstrap tests using 1,000 replicates; bootstrap values are shown at key nodes. The ●, ■, and ▲ symbols represent the differential clustering of sequences obtained in this study. Scale bars indicate nucleotide substitutions per site.

panel D). We confirmed *A. marginale* using identity analysis (100% identical to GenBank sequences; accession nos. CP023731, CP006846, CP001079, CP000030, and AF428086) of *rpoB* and *msp4* genes. Co-infection with *E. minasensis* and *A. marginale* was confirmed in 6 animals from El Tambo. Co-infection with *B. theileri* and *A. marginale* was documented in 1 animal from El Tambo and 1 animal from Santander de Quilichao.

These results showed the simultaneous circulation of *E. minasensis*, *B. theileri*, and *A. marginale* in bovids from Cauca department, Colombia. In Latin America, *E. minasensis* has been identified in Brazil (*7*) and Colombia (found in *R. microplus* ticks) (*8*), and *B. theileri* has been found in Argentina (*6*), Mexico (*9*), and Brazil (*10*). The *R. microplus* tick is likely the main vector for both pathogens in these regions and has been confirmed by molecular detection of *E. minasensis* in tick specimens collected from the same animals (H.C. Martínez-Diaz, unpub. data) and various reports in Latin America for *B. theileri* (*9*,*10*). Despite the lack of clinical signs in these animals, tick-borne infections caused by these pathogenic bacteria often occur as subclinical infections or with intermittent clinical manifestations. *E. minasensis* and *B. theileri* infections, either separately or as co-infections, may be more frequent than previously recognized and should be considered potential etiologies of febrile syndrome in cattle from this and other regions of Colombia.

Acknowledgments

We thank all personnel involved in sample collection in Cauca, Colombia.

This research was supported by COLCIENCIAS, Colombia (code no. 120374455209) and the Fogarty International Center, National Institute of Allergy and Infectious Diseases, National Institutes of Health (award no. 5D43TW010331-05). Content is solely the responsibility of the authors and does not necessarily represent the official views of the National Institutes of Health.

About the Author

Dr. Ramírez-Hernández is a researcher at Universidad de La Salle, Bogotá D.C., Colombia. His research interests focus on ticks, fleas, and ecoepidemiology of tickborne and fleaborne diseases.

References

1. Ismail N, McBride JW. Tick-borne emerging infections: ehrlichiosis and anaplasmosis. Clin Lab Med. 2017;37:317–40. https://doi.org/10.1016/j.cll.2017.01.006
2. Cabezas-Cruz A, Zweygarth E, Vancová M, Broniszewska M, Grubhoffer L, Passos LMF, et al. *Ehrlichia minasensis* sp. nov., isolated from the tick *Rhipicephalus microplus*. Int J Syst Evol Microbiol. 2016;66:1426–30. https://doi.org/10.1099/ijsem.0.000895
3. Moura de Aguiar D, Pessoa Araújo Junior J, Nakazato L, Bard E, Aguilar-Bultet L, Vorimore F, et al. Isolation and characterization of a novel pathogenic strain of *Ehrlichia minasensis*. Microorganisms. 2019;7:528. https://doi.org/10.3390/microorganisms7110528
4. Aguiar DM, Ziliani TF, Zhang X, Melo AL, Braga IA, Witter R, et al. A novel *Ehrlichia* genotype strain distinguished by the TRP36 gene naturally infects cattle in Brazil and causes clinical manifestations associated with ehrlichiosis. Ticks Tick Borne Dis. 2014;5:537–44. https://doi.org/10.1016/j.ttbdis.2014.03.010
5. Elelu N. Tick-borne relapsing fever as a potential veterinary medical problem. Vet Med Sci. 2018;4:271–9. https://doi.org/10.1002/vms3.108
6. Morel N, De Salvo MN, Cicuttin G, Rossner V, Thompson CS, Mangold AJ, et al. The presence of *Borrelia theileri* in Argentina. Vet Parasitol Reg Stud Rep. 2019;17:100314. https://doi.org/10.1016/j.vprsr.2019.100314
7. Cabezas-Cruz A, Zweygarth E, Aguiar DM. *Ehrlichia minasensis*, an old demon with a new name. Ticks Tick Borne Dis. 2019;10:828–9. https://doi.org/10.1016/j.ttbdis.2019.03.018
8. Miranda J, Mattar S. Molecular detection of *Anaplasma* sp. and *Ehrlichia* sp. in ticks collected in domestical animals, Colombia. Trop Biomed. 2015;32:726–35.
9. Smith RD, Brener J, Osorno M, Ristic M. Pathobiology of *Borrelia theileri* in the tropical cattle tick, *Boophilus microplus*. J Invertebr Pathol. 1978;32:182–90. https://doi.org/10.1016/0022-2011(78)90028-9
10. Martins JR, Ceresér VH, Corrêa BL, Smith RD. *Borrelia theileri*: observação em carrapatos do gênero *Boophilus microplus* no município de Guaíba, RS, Brasil. Ciência Rural, Santa Maria. 1996;26:447–50. https://doi.org/10.1590/S0103-84781996000300018

Address for correspondence: David H. Walker, Department of Pathology, University of Texas Medical Branch, 301 University Blvd, Galveston, TX, 77555-0609, USA; email: dwalker@utmb.edu

Cluster of Donor-Derived Cryptococcosis after Liver and Kidney Transplantation

Meng Sha,[1] Chuan Shen,[1] Ying Tong, Qiang Xia

Author affiliation: Shanghai Jiao Tong University, Shanghai, China

DOI: https://doi.org/10.3201eid2810.220522

Cryptococcosis infection after transplantation is easily overlooked or misdiagnosed. We report a cluster of donor-derived cryptococcosis infection in liver and kidney transplant recipients from the same donor in China. Infections occurred within 1 month after transplantation, and were confirmed by using biopsies and blood tests.

Cryptococcosis is the third most common invasive fungal infection in solid-organ transplants (*1*,*2*). The incidence of cryptococcosis in transplant recipients was estimated to be 0.76% in mainland China, and the *Cryptococcus neoformans* variant *grubii* genotype was the predominant species (*3*–*5*).

Cryptococcosis after transplantation is easily overlooked because of high diversity of clinical symptoms, which leads to mortality rates as high as 20% (*6*). Another feature of recipient-acquired cryptococcosis is the late onset of infection, which usually is 15–21 months posttransplant (*7*). However, donor-derived transmission should be considered if disease is found within 1 month posttransplant or if multiple recipients from the same donor become ill (*8*,*9*). We report a cluster of donor-derived cryptococcosis after liver and kidney transplantation in China.

This study was approved by the Administration Committee of Shanghai Jiao Tong University, China. Written informed consent was obtained from the patient for the anonymized information to be published in this article.

The transplant donor was a 60-year-old man who had severe cerebral infarction, which progressed to brain death. Chest computed tomography (CT) scan showed clear lung fields and no infiltration. At organ procuring, the liver and kidney grafts looked grossly normal. Routine donor biopsy did not show any histopathologic abnormality. However, retrospective testing of donor serum for cryptococcal antigen (CrAg; Lateral Flow Assay; Immuno-Mycologics, Inc., https://www.immy.com) showed a titer of 1:8 seven days after grafts had been transplanted. One of 2 blood cultures at the time of organ procurement became positive after 8 days of incubation. *C. neoformans* was subsequently identified.

The first recipient was a 64-year-old man who had hepatocellular carcinoma and underwent liver transplantation. The transplant was successful, and there were no immediate complications. Postoperative aminotransferase levels decreased gradually. However, the recipient had progressive jaundice. The total bilirubin level increased from 103.6 μmol/L on postoperative day (POD) 1 to 704.3 μmol/L on POD 15. The patient had no fevers, cough, or dizziness.

Liver biopsy on POD 7 showed no evidence of rejection, biliary complications or drug-induced liver injury. The unexpected jaundice persisted and showed no major decrease. Liver biopsy was performed on POD 30. Large numbers of encapsulated yeasts were found inside the liver. Microscopically, the colonized organism had an oval shape and a loose surrounding histiocytic response (Figure). A subsequent recipient serum sample was positive for CrAg (titer >1:2,560) on POD 32.

The recipient received amphotericin B lipid complex plus 5-flucytosine for 4 weeks. A gradual decrease in bilirubin was observed. The antifungal treatment was changed to oral fluconazole after he was discharged. Follow-up of CrAg showed a decrease from 1:2,560 to 1:32 at 1 year after transplant. Fluconazole was discontinued 15 months after transplant. The recipient showed good liver function for 30 months without active infection (Table). Hepatocellular carcinoma did not recur.

The second recipient was a 65-year-old man who had end-stage renal disease and received a kidney transplant from the same donor. The graft function recovered uneventfully. The recipient was discharged on POD 6 and received an immunosuppression regimen of tacrolimus and mycophenolate. However, the recipient had a low fever and cough on POD 21. Chest CT showed pulmonary consolidations and infiltration. Bronchoalveolar lavage was not performed because intubation was not conducted; there were no signs of hypoxia. However, a CrAg titer of 1:1,280 and positive blood culture resulted in a diagnosis of cryptococcal pneumonia. Antifungal therapy was given for 4 weeks, and oral fluconazole maintenance therapy was given subsequently. The recipient recovered and showed standard graft function and no signs of infection.

The third recipient was a 50-year-old woman who received a kidney transplant from the same donor. She was discharged on POD 6 and had no

[1]These authors contributed equally to this article.

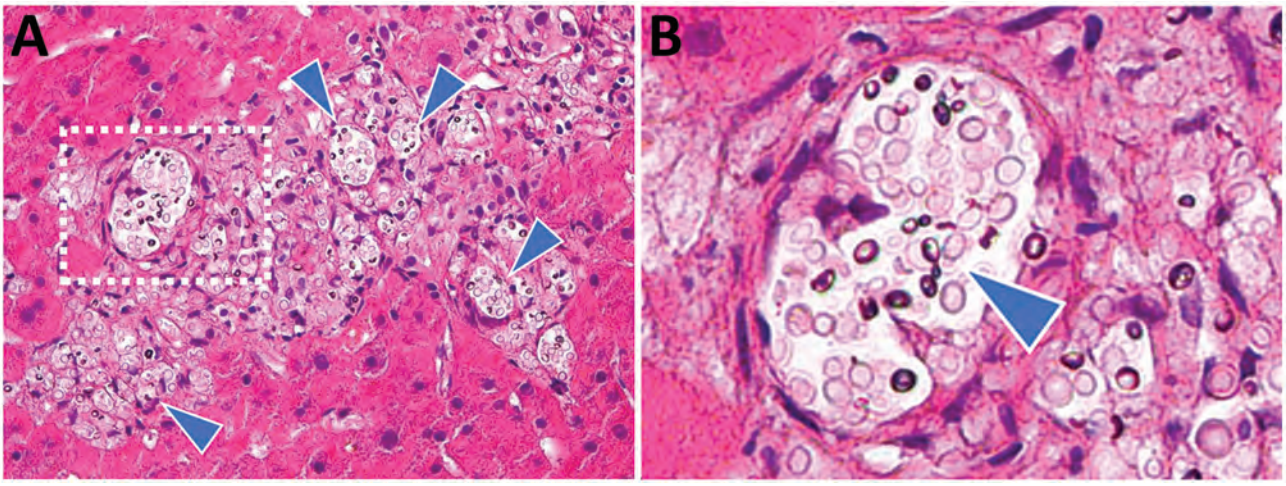

Figure. Transplanted liver tissue biopsy specimen on postoperative day 30 from donor in cluster of donor-derived cryptococcosis, China. A) Hematoxylin and eosin stain shows cryptococcal yeast liver (arrowheads). Original magnification ×200. B) Enlarged view of boxed area from panel A. Original magnification ×400.

specific complaints. On POD 26, she reported dizziness, diplopia, and severe headache and was readmitted to the hospital. Fluid from a lumbar puncture culture showed *C. neoformans*. The serum CrAg titer was >1:2,560. The recipient was given amphotericin B lipid complex and 5-flucytosine. However, loss of consciousness and a convulsion occurred on POD 31. Further brain CT showed serious cerebral hemorrhage and compression of the brainstem. Her family withdrew care at that point, and the recipient died. Autopsy showed that the glomeruli of the transplanted kidney and spinal cord were infiltrated with oval-shaped yeast consistent with *C. neoformans*.

The recipients had negative clinical signs and no CrAg pretransplantation. However, the liver and kidney recipients who received organs from the same donor all showed development of cryptococcosis. *Cryptococcus* sp. in the blood culture and biopsies makes donor-derived transmission the most likely means of infection. Communication gaps between the microbiology laboratories and transplant team were associated with the donor-derived infection of our case. Positive blood culture results should be communicated immediately to initiate antifungal treatment promptly.

Although illnesses and deaths from donor-derived cryptococcosis remain high, results for these case-patients emphasize an increased pretransplant clinical awareness of donor-derived infection. Serum CrAg might identify infected donors and enable effective prophylaxis. In addition, timely communication of suspected results is critical to improve outcomes.

This study was supported by the National Natural Science Foundation of China (grant 81902379) and National Key Research on Precision Medicine of China (grants 2017YFC0908102 and 2018ZX10723204).

M.S. and C.S. designed the methods, Y.T. and Q.X. conducted the study, M.S. and C.S. wrote the article, and Q.X. supervised the study.

About the Author

Dr. Sha is a transplant surgeon at Renji Hospital, School of Medicine, Shanghai Jiao Tong University, Shanghai, China. His primary research interests are transplant infection and immunity.

Table. Postoperative cryptococcal antigen titer change and antifungal treatment regimen for transplant donor in cluster of donor-derived cryptococcosis, China

Postoperative day	Cryptococcal antigen titer	Treatment
30	>1:2,560	Amphotericin B lipid complex and 5-flucytosine
60	>1:1,280	Oral fluconazole, 400 mg/d
90	>1:640	Oral fluconazole, 400 mg/d
120	1:640	Oral fluconazole, 400 mg/d
180	1:128	Oral fluconazole, 400 mg/d
270	1:128	Oral fluconazole, 400 mg/d
360	1:32	Oral fluconazole, 400 mg/d
450	Negative result	Discontinued

References

1. Penumarthi LR, La Hoz RM, Wolfe CR, Jackson BR, Mehta AK, Malinis M, et al. *Cryptococcus* transmission through solid organ transplantation in the United States: a report from the Ad Hoc Disease Transmission Advisory Committee. Am J Transplant. 2021;21:1911–23. https://doi.org/10.1111/ajt.16433
2. Singh N, Sifri CD, Silveira FP, Miller R, Gregg KS, Huprikar S, et al. Cryptococcosis in patients with cirrhosis of the liver and posttransplant outcomes. Transplantation.2015;99:2132–41. https://doi.org/10.1097/TP.0000000000000690
3. Wang Y, Gu Y, Shen K, Cui X, Min R, Sun S, et al. Clinical features of cryptococcosis in patients with different immune statuses: a multicenter study in Jiangsu Province, China. BMC Infect Dis. 2021;21:1043. https://doi.org/10.1186/s12879-021-06752-x
4. Yuchong C, Fubin C, Jianghan C, Fenglian W, Nan X, Minghui Y, et al. Cryptococcosis in China (1985–2010): review of cases from Chinese database. Mycopathologia. 2012;173:329–35. https://doi.org/10.1007/s11046-011-9471-1
5. Chen M, Xu Y, Hong N, Yang Y, Lei W, Du L, et al. Epidemiology of fungal infections in China. Front Med. 2018;12:58–75. https://doi.org/10.1007/s11684-017-0601-0
6. Baddley JW, Forrest GN; AST Infectious Diseases Community of Practice. Cryptococcosis in solid organ transplantation: guidelines from the American Society of Transplantation Infectious Diseases Community of Practice. Clin Transplant. 2019;33:e13543. https://doi.org/10.1111/ctr.13543
7. Camargo JF, Simkins J, Schain DC, Gonzalez AA, Alcaide ML, Anjan S, et al. A cluster of donor-derived *Cryptococcus neoformans* infection affecting lung, liver, and kidney transplant recipients: Case report and review of literature. Transpl Infect Dis. 2018;20:e12836. https://doi.org/10.1111/tid.12836
8. Natarajan P, Lockhart SR, Basavaraju SV, Anjan S, Lindsley MD, McGrath MM, et al. Donor-derived *Cryptococcus gattii* sensu stricto infection in two kidney transplant recipients, southeastern United States. Am J Transplant. 2021;21:3780–4. https://doi.org/10.1111/ajt.16729
9. Malinis M, Boucher HW; AST Infectious Diseases Community of Practice. Screening of donor and candidate prior to solid organ transplantation: guidelines from the American Society of Transplantation Infectious Diseases Community of Practice. Clin Transplant. 2019;33:e13548. https://doi.org/10.1111/ctr.13548

Address for correspondence: Ying Tong, Department of Liver Surgery, Renji Hospital, School of Medicine, Shanghai Jiao Tong University, Shanghai 200127, China; email: tongyingsjtu@163.com

Pulmonary Paragonimiasis in Native Community, Esmeraldas Province, Ecuador, 2022

José C.N. Diaz, Mariella Anselmi, Manuel Calvopiña, Mayra E.P. Vera, Yuvy L.C. Cabrera, Javier J. Perlaza, Luz A.O. Cabezas, Christian O.R. Gaspar, Dora Buonfrate

Author affiliations: Distrito de Salud 08D05 San Lorenzo, San Lorenzo, Ecuador (J.C.N. Diaz, Y.L.C. Cabrera, J.J. Perlaza, L.A.O. Cabezas, C.O.R. Gaspar); Centro de Epidemiologia Comunitaria y Medicina Tropical, Esmeraldas, Ecuador (M. Anselmi); Universidad de las Americas, Quito, Ecuador (M. Calvopiña); Energy e Palma Energypalma SA, Montecristi, Ecuador (M.E.P. Vera); Istituto di Ricovero e Cura a Carattere Scientifico Sacro IRCCS Cuore Don Calabria Hospital, Negrar, Verona, Italy (D. Buonfrate)

DOI: https://doi.org/10.3201/eid2810.220927

Paragonimiasis is a food-borne infection caused by several species of the *Paragonimus* fluke. Clinical manifestations can mimic tuberculosis and contribute to diagnostic delay. We report a cluster of paragonimiasis in a community in Ecuador, where active surveillance was set up after detection of the first 2 cases.

Human paragonimiasis is a foodborne disease caused by trematode worms of the genus *Paragonimus* (*1*). Several species that have different geographic distributions have been associated with human infection (*2*). Paragonimiasis is caused by ingestion of raw/undercooked freshwater crabs or crayfish infested by metacercariae of *Paragonimus* species. Thus, it is frequently reported in Asia because of cultural dietary customs (*1*,*3*). Clusters are occasionally reported in Africa (*4*) and the Americas, where cases are observed mostly in countries in Latin America (*5*). Localized infection with *P. kellicotti* trematode occurs in the United States (*1*,*5*).

In Ecuador, cases have been reported from almost all provinces, but lack of official recording by the Ministry of Health and few active surveillance surveys probably cause an underestimation of the incidence (*5*). Nevertheless, Ecuador is considered the country with the highest incidence of paragonimiasis in South America (*5*). The main trematode species known to cause paragonimiasis in Ecuador is *P. mexicanus*, although molecular characterization has not been performed extensively. Thus, information about circulating species might be incomplete (*5*,*6*).

Symptoms include fever and respiratory involvement, and most persons have a productive cough with rusty sputum or chest pain that can last from a few months to years. Thus, tuberculosis is the main condition to be ruled out in differential diagnosis (*6*,*7*). We report a public health intervention for a cluster of paragonimiasis observed during the end of 2021–May 2022, in San Lorenzo, Ecuador.

The first 2 cases were diagnosed in laborers working on the same palm oil farm. They both reported productive cough with rusty sputum and dyspnea lasting for about 4 months (first case-patient) and for at least 4 years (second case-patient). The second patient had been tested several times for tuberculosis but was not previously tested for other causes of respiratory symptoms. Microscopic examination of acid-fast–stained smears of sputum ruled out tuberculosis, but directly observed microscopic examination showed parasite eggs (Figure). Specimens were then sent to the Laboratory of Parasitology of the Universidad de las Americas in Quito, where diagnosis of paragonimiasis was made. Both patients confirmed the habit of eating raw freshwater crustaceans.

After the first 2 cases, the Department of Epidemiology of San Lorenzo Health District organized a meeting with the community where the 2 case-patients lived. Aims of the intervention were to ascertain whether the infection was spreading in the community and evaluate possible control strategies. Healthcare workers collected 3 sputum samples from each of 22 persons who had compatible respiratory symptoms and 1 fecal sample from each of 36 asymptomatic persons, including family members of the positive case-patients.

Paragonimus eggs were found in samples from 8 persons, all from the same community (La Ceiba), except for 1 person (who lived in Balsareño but worked on the same palm oil farm as the first case-patient) (Table). Symptoms lasted for months in all persons reporting them.

Praziquantel was donated by the Istituto di Ricovero e Cura a Carattere Scientifico Sacro Cuore Don Calabria to the Centro de Epidemiologia Comunitaria y Medicina Tropical. This drug was administered by the physician at the local health center to infected persons at a dose of 25 mg/kg, 3 times/day for 2 days.

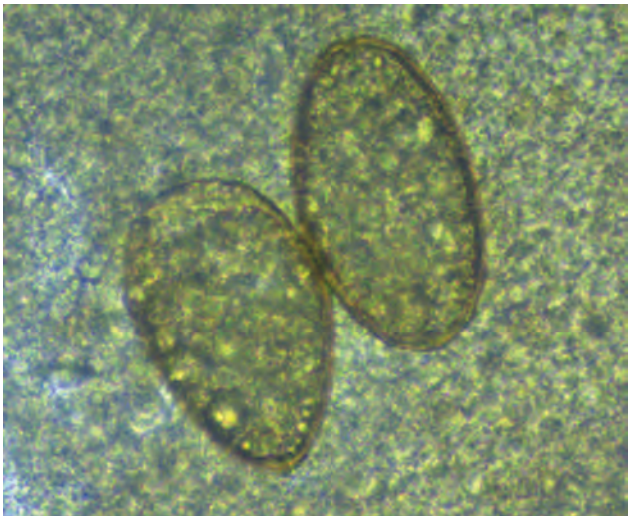

Figure. *Paragonimus* eggs from sputum from a patient in Ecuador. Eggs are yellow, elongated, have a thick shell, and are asymmetric with 1 end slightly flattened. The operculum is clearly visible at the large end and is thickened at the abopercular end. Original magnification ×40, size 80–90 μm × 45–50 μm.

Our study highlights some limitations that hampered estimation of incidence of paragonimiasis in Ecuador. The first limitation is delay in diagnosis. Because knowledge about this parasite is scarce, local physicians seldom prescribe diagnostic tests that could help diagnosis, and misdiagnosis as tuberculosis can be frequent. Limited diagnostic capacity can contribute to the underestimation because the sensitivity of microscopic examination is low, in particular for persons who have mild-to-moderate disease: 30%–40% for a sputum sample and 11%–15% for a stool sample (*1*). Multiple sampling increases sensitivity (*1*), but collection of a series of specimens over time can be difficult in remote settings for cultural and logistic issues.

Although stool microscopy has low sensitivity, it can detect *Paragonimus* eggs in persons who do not have respiratory symptoms. Other diagnostic tests,

Table. Demographic and clinical characteristics of 10 persons infected with *Paragonimus* eggs, Ecuador

Case-patient	Age, y/sex	Sample positive for eggs	Symptoms
1	24/M	Sputum	Rusty sputum and dyspnea while working, episodes of productive cough
2	32/M	Sputum	Rusty sputum and mild dyspnea, episodes of productive cough
3	27/F	Stool	None
4	20/M	Sputum	Rusty sputum
5	29/F	Stool	None
6	32/M	Sputum	Rusty sputum
7	8/M	Stool	None
8	10/M	Stool	None
9	31/F	Sputum	Rusty sputum
10	22/F	Sputum	Rusty sputum

such as serologic or molecular methods, are not available in Ecuador, and have been seldom used there, for research purposes (*5*,*8*). Moreover, serologic assays have been implemented mostly for other species, such as *P. westermani* and *P. kellicotti* worms (*8*,*9*), and clinical validation for *P. mexicanus* worms is lacking (*9*,*10*). Limited access to healthcare services in some remote communities can further cause late diagnosis.

Control strategies to limit human infection are hampered by the wide presence of the parasite in many domestic and wild mammals, and the complex life cycle involving 2 intermediate hosts (snail and crustacean) (*5*). Thus, health education on proper food preparation is the main intervention to reduce infections (*1*).

Acknowledgments

We thank Alvaro Santiago Guerrero Moscoso, Adela Boboy Porozo, and Joel Adrian Mendoza Alarcon for providing excellent support for screening and management and Teresa Zuppini for organizing drug donation.

This study was partially supported by the Italian Ministry of Health Fondi Ricerca Corrente to Istituto di Ricovero e Cura a Carattere Scientifico Sacro Cuore Don Calabria Hospital, Linea 2.

About the Author

Dr. Diaz is a physician at the Distrito de Salud 08D05 San Lorenzo in San Lorenzo, Ecuador and coordinator of the epidemiology surveillance service of the San Lorenzo Health District. His primary resesarch interests are epidemiology and hygiene.

References

1. Diaz JH. Paragonimiasis acquired in the United States: native and nonnative species. Clin Microbiol Rev. 2013;26:493–504. https://doi.org/10.1128/CMR.00103-12
2. Blair D. Lung flukes of the genus *Paragonimus*: ancient and re-emerging pathogens. Parasitology. 2022;16:1–36. https://doi.org/10.1017/S0031182022000300
3. Lane MA, Marcos LA, Onen NF, Demertzis LM, Hayes EV, Davila SZ, et al. *Paragonimus kellicotti* flukes in Missouri, USA. Emerg Infect Dis. 2012;18:1263–7. https://doi.org/10.3201/eid1808.120335
4. Rabone M, Wiethase J, Clark PF, Rollinson D, Cumberlidge N, Emery AM. Endemicity of *Paragonimus* and paragonimiasis in sub-Saharan Africa: a systematic review and mapping reveals stability of transmission in endemic foci for a multi-host parasite system. PLoS Negl Trop Dis. 2021;15:e0009120. https://doi.org/10.1371/journal.pntd.0009120
5. Calvopiña M, Romero D, Castañeda B, Hashiguchi Y, Sugiyama H. Current status of *Paragonimus* and paragonimiasis in Ecuador. Mem Inst Oswaldo Cruz. 2014;109:849–55. https://doi.org/10.1590/0074-0276140042
6. Calvopina M, Romero-Alvarez D, Macias R, Sugiyama H. Severe pleuropulmonary paragonimiasis caused by *Paragonimus mexicanus* treated as tuberculosis in Ecuador. Am J Trop Med Hyg. 2017;96:97–9. https://doi.org/10.4269/ajtmh.16-0351
7. Lane MA, Barsanti MC, Santos CA, Yeung M, Lubner SJ, Weil GJ. Human paragonimiasis in North America following ingestion of raw crayfish. Clin Infect Dis. 2009;49:e55–61. https://doi.org/10.1086/605534
8. Xunhui Z, Qingming K, Qunbo T, Haojie D, Lesheng Z, Di L, et al. DNA detection of *Paragonimus westermani*: diagnostic validity of a new assay based on loop-mediated isothermal amplification (LAMP) combined with a lateral flow dipstick. Acta Trop. 2019;200:105185. https://doi.org/10.1016/j.actatropica.2019.105185
9. Fischer PU, Weil GJ. North American paragonimiasis: epidemiology and diagnostic strategies. Expert Rev Anti Infect Ther. 2015;13:779–86. https://doi.org/10.1586/14787210.2015.1031745
10. Procop GW. North American paragonimiasis (caused by *Paragonimus kellicotti*) in the context of global paragonimiasis. Clin Microbiol Rev. 2009;22:415–46. https://doi.org/10.1128/CMR.00005-08

Address for correspondence: Dora Buonfrate, Department of Infectious, Tropical Diseases, and Microbiology, Istituto di Ricovero e Cura a Carattere Scientifico Sacro Cuore Don Calabria Hospital, Via Sempreboni 7, Negrar, Verona 37024 Italy; email: dora.buonfrate@sacrocuore.it

Haematospirillum jordaniae Cellulitis and Bacteremia

Emil Pal, Iztok Štrumbelj, Tjaša Cerar Kišek, Marko Kolenc, Mateja Pirš, Katarina Resman Rus, Tina Triglav, Tatjana Avšič-Županc

Author affiliations: Murska Sobota General Hospital Department of Infectious Diseases, Murska Sobota, Slovenia (E. Pal); National Laboratory of Health, Environment and Food, Murska Sobota (I. Štrumbelj); Institute of Microbiology and Immunology, Ljubljana, Slovenia (T. Cerar Kišek, M. Kolenc, M. Pirš, K. Resman Rus, T. Triglav, T. Avšič-Županc)

DOI: https://doi.org/10.3201/eid2810.220326

We isolated *Haematospirillum jordaniae* from a positive blood culture from a 57-year-old man in Slovenia who had bacteremia and bullous cellulitis of lower extremities. The infection was successfully treated with ciprofloxacin. Our findings signal the need for increased awareness about the clinical course of *H. jordaniae* and its potential effects as a human pathogen.

A 57-year-old man living near Lendava, Slovenia, with a medical history of type 2 diabetes, varicose veins in his legs, obesity, and arterial hypertension, sought treatment for a 1-day history of bilateral swelling, redness, warmness, and pain in his lower extremities. The day before, he had pricked himself on his left shin and the sole of his right foot with a reed in the Pacsa Fishing Lake in Hungary. At hospital admission, the patient was febrile (38.5°C) but with vital signs within reference ranges.

Physical examination revealed painful, indurated, erythematous lower extremities, with edema and warmth. Clinically relevant results from blood analysis demonstrated leukocytosis (16.5 × 10^9 cells/L) with neutrophilia (14.0 × 10^9 cells/L) and elevated C-reactive protein (CRP; 189 mg/L), suggesting bacterial etiology; procalcitonin (PCT) level was within reference range (0.1 μg/L). We empirically introduced therapy with intravenous flucloxacillin (2 g/6 h) for coverage of cellulitis.

On day 2 of hospitalization, extensive bullous changes appeared in the lower extremities. Because of unusual bilateral presentation, we added intravenous therapy with ciprofloxacin. Two days later, fever subsided, and blood leukocyte count returned to normal (10.5 × 10^9 cells/L). CRP had mildly increased to 204 mg/L; PCT remained within reference range (0.4 μg/L). On day 7 of hospitalization, we observed major improvement in the patient's laboratory parameters (leukocyte count 6.4 × 10^9 cells/L, CRP 35 mg/L). We continued treatment with intravenous flucloxacillin and ciprofloxacin until discharge on day 13. Signs of bullous cellulitis in the lower extremities had subsided.

Aerobic blood culture bottle was positive after 3 days of incubation. We observed small, slender, pleomorphic bacilli and coccobacilli in Gram stain. After subcultivation onto solid media, we detected growth on blood and chocolate agar (Figure, panels B, C) on the third day, with no growth observed on MacConkey or TCBS (Thiosulfate-citrate-bile salts-sucrose) agar or in microaerophilic atmosphere. However, we could not identify the causative agent using Gram stain from culture (Figure 1, panel A), colony morphology, growth characteristics, or MALDI-TOF (matrix-assisted laser desorption/ionization time-of-flight) mass spectrometry. We suspected *Francisella tularensis* on the basis of clinical manifestations and local epidemiology. We sent blood agar and chocolate agar plates to the reference Biosafety Level 3 laboratory at the Institute of Microbiology and

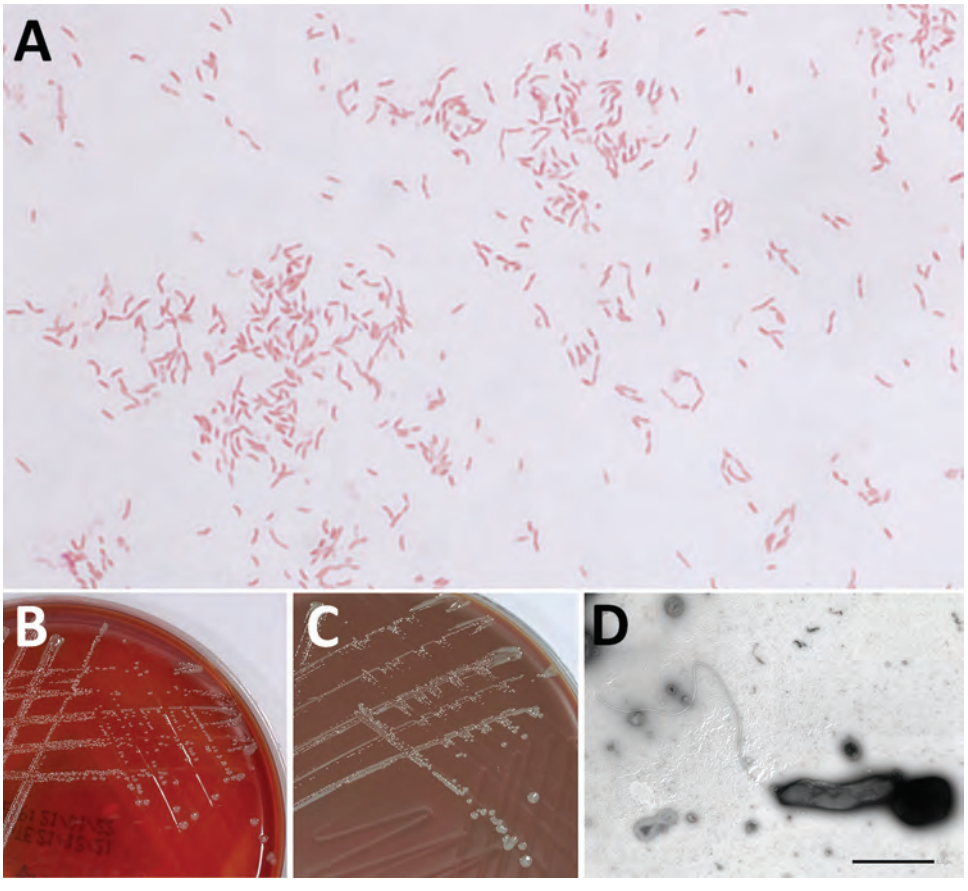

Figure. Detection of *Haematospirillum jordaniae* in a male patient in Slovenia. A) Gram stain of *H. jordaniae*; original magnification ×1,000. B) Colonies on blood agar after 3-day incubation. C) Colonies on chocolate agar after 3-day incubation. D) Transmission electron micrograph image of negatively stained cell of *H. jordaniae* exhibiting flagellum. Scale bar indicates 1 μm.

Table. Antimicrobial susceptibility of *Haematospirillum jordaniae* from a male patient in Slovenia, interpreted according to non–species-related EUCAST PK/PD breakpoints*

Antimicrobial	MIC, mg/L	Susceptibility category
Benzylpenicillin	8	R
Ampicillin	2	S
Amoxicillin/clavulanic acid	0.125	S
Cefuroxime Iv	16	R
Cefotaxime	0.25	S
Imipenem	>32	R
Meropenem	1	S
Ciprofloxacin	<0.002	S
Levofloxacin	<0.002	S
Tigecycline	<0.016	S

*EUCAST, https://www.eucast.org. PK/PD, pharmacokinetics/pharmacodynamics; R, resistant; S, susceptible

Immunology (Ljubljana, Slovenia) for further analysis. We isolated DNA using QiaAmp DNA Mini Kit (QIAGEN, https://www.qiagen.com) and tested it, including dilutions from 1:10 to 1:1,000, by specific real-time PCR, which ruled out *F. tularensis* (*1*). We performed standard tube extraction protocol for MALDI-TOF mass spectrometry identification using the latest MALDI Biotyper sirius (Bruker Daltonics, https://www.bruker.com) and SR library according to manufacturer instructions but could not identify the organism because scores fell below genus cutoff values. We undertook further molecular analyses, included amplifying the 16S V3/V4 region using Mastermix 16S Complete (Molzym, https://www.molzym.com). We purified amplicons using QIAquick PCR purification kit (QIAGEN) and sequenced them on a ABI3500 genetic analyzer (Applied Biosystems, https://www.thermofisher.com). We analyzed 16S rDNA sequences using the CLC Main Workbench 21.0.5 (QIAGEN) and compared those sequences with others available in the rRNA databases: GenBank BLAST (https://blast.ncbi.nlm.nih.gov/Blast.cgi), Ribosomal Database Project (https://rdp.cme.msu.edu), and MicrobeNet (https://microbenet.cdc.gov). Our isolate most closely matched *Haematospirillum jordaniae* isolate Acr132, H5569 and H2509, with 100% sequence identity. By sequencing a longer, 1,462 bp 16S rRNA region (*2*), we observed 99.93% identity to *H. jordaniae* H2509 (GenBank accession no. OM075117). After successful molecular identification, we created *H. jordaniae* main spectra profiles according to manufacturer standard procedures and added them to a custom main spectra profile library because the pathogen was not part of any commercial mass spectra library (Appendix Figure, https://wwwnc.cdc.gov/EID/article/28/10/22-0326-App1.pdf).

H. jordaniae is a slow-growing, gram-negative rod bacterium that is difficult to identify because it is not included in standard identification databases. Molecular analysis is necessary for definite identification (*3*,*4*). *H. jordaniae*, which belongs to the alphaproteobacteria family *Rhodospirillaceae* (*5*), was first identified as a potential human pathogen in 2016, when the new genus and species were described from an isolate obtained from a human blood sample in 2010 (*3*,*4*). An additional 13 isolates from human blood samples with identical or very similar 16S rRNA sequences, all from men (average age: 60), were later identified at the CDC Special Bacteriology Reference Laboratory (https://www.cdc.gov/ncezid/dhcpp/bacterial_special/special_lab.html).

We determined the antimicrobial susceptibility of *H. jordaniae* using gradient diffusion E-test strips (bioMérieux, https://www.biomerieux.com) and Liofilchem MTS (MIC test strips) for amoxicillin/clavulanic acid (https://www.liofilchem.com) on Muller-Hinton Fastidious agar (CO_2, 48-h incubation). We interpreted results according to non–species-related EUCAST (https://www.eucast.org) PK/PD (pharmacokinetics/pharmacodynamics) antimicrobial susceptibility breakpoints (Table). According to the results of susceptibility testing, fluoroquinolones had the most favorable breakpoint-to-MIC ratios: ciprofloxacin and levofloxacin had MIC <0.002 mg/L (both) and PK/PD breakpoints of 0.25 mg/L (ciprofloxacin) and 0.5 mg/L (levofloxacin).

Molecular evidence of *H. jordaniae* in the blood of any vertebrate other than humans was described only in a bird species, the reed warbler, *Acrocephalus scirpaceus* (*6*). Possible routes of infection are through environmental contact, mostly following skin injury (*4*). Current knowledge about *H. jordaniae* is limited; therefore, our findings signal the need for increased awareness about its clinical course and potential effects as a human pathogen.

Acknowledgments

The authors thank our colleagues Meta Kodre, Kitty Žnidar, and Ivana Velimirović for excellent laboratory assistance.

This work was supported by the Slovenian Research Agency (grant P3-0083) and by the network of research infrastructure centers of the University of Ljubljana (MRIC UL, ICBSL3+; grant I0-0510).

About the Author

Dr. Pal works at Murska Sobota General Hospital in Murska Sobota, Slovenia. His research focuses on infectious diseases.

References

1. Versage JL, Severin DDM, Chu MC, Petersen JM. Development of a multitarget real-time TaqMan PCR assay for enhanced detection of *Francisella tularensis* in complex specimens. J Clin Microbiol. 2003;41:5492–9. https://doi.org/10.1128/JCM.41.12.5492-5499.2003
2. Kawahara M, Rikihisa Y, Lin Q, Isogai E, Tahara K, Itagaki A, et al. Novel genetic variants of *Anaplasma phagocytophilum*, *Anaplasma bovis*, *Anaplasma centrale*, and a novel *Ehrlichia* sp. in wild deer and ticks on two major islands in Japan. Appl Environ Microbiol. 2006;72:1102–9. https://doi.org/10.1128/AEM.72.2.1102-1109.2006
3. Humrighouse BW, Emery BD, Kelly AJ, Metcalfe MG, Mbizo J, McQuiston JR. Haematospirillum jordaniae gen. nov., sp. nov., isolated from human blood samples. Antonie van Leeuwenhoek. 2016;109:493–500. https://doi.org/10.1007/s10482-016-0654-0
4. Hovan G, Hollinger A. Clinical isolation and identification of *Haematospirillum jordaniae*. Emerg Infect Dis. 2018;24:1955–6. https://doi.org/10.3201/eid2410.180548
5. Degli Esposti M, Lozano L, Martínez-Romero E. Current phylogeny of Rhodospirillaceae: a multi-approach study. Mol Phylogenet Evol. 2019;139:106546. https://doi.org/10.1016/j.ympev.2019.106546
6. Hornok S, Ágh N, Takács N, Kontschán J, Hofmann-Lehmann R. *Haematospirillum* and insect Wolbachia DNA in avian blood. Antonie van Leeuwenhoek. 2018;111:479–83. https://doi.org/10.1007/s10482-017-0961-0

Address for correspondence: Tatjana Avšič-Županc, Institute of Microbiology and Immunology, Faculty of Medicine, Zaloška 4, SI-1000 Ljubljana, Slovenia; email: tatjana.avsic@mf.uni-lj.si

Infection Rate of SARS-CoV-2 in Asymptomatic Healthcare Workers, Sweden, June 2022

Kim Blom, Sebastian Havervall, Ulrika Marking, Nina Greilert Norin, Philip Bacchus, Ramona Groenheit, Andreas Bråve, Charlotte Thålin, Jonas Klingström

Author affiliations: Karolinska Institutet, Stockholm, Sweden (K. Blom, S. Havervall, U. Marking, N. Greilert Norin, C. Thålin, J. Klingström); Public Health Agency of Sweden, Solna, Sweden (K. Blom, R. Groenheit, A. Bråve, J. Klingström); Karolinska Institutet Danderyd Hospital, Stockholm (S. Havervall, U. Marking, N. Greilert Norin, C. Thålin); Swedish Armed Forces, Umeå, Sweden (P. Bacchus)

DOI: http://doi.org/10.3201/eid2810.221093

Given the recent surge in SARS-CoV-2 Omicron infections, we performed a quantitative PCR screening survey during June 28–29, 2022, in Stockholm, Sweden, to investigate SARS-CoV-2 point prevalence in a group with high exposure risk. Results showed SARS-CoV-2 infection in 2.3% of healthcare workers who were asymptomatic at time of sampling.

Emerging data show a rapid increase in the prevalence of SARS-CoV-2 infection linked to an increase in COVID-19 cases, which is being driven by the SARS-CoV-2 Omicron variant. Compared with previous variants, Omicron has shown superior capacity for transmission and less sensitivity to neutralizing antibodies induced by vaccination or prior infection with other variants of the virus (*1*). Initially, the Omicron sublineages BA.1 (including BA.1.1) and BA.2 spread globally at a rapid pace, infecting a large proportion of the population, including vaccinated persons. Nonetheless, vaccines have been shown to provide good protection against severe disease (*2*). Recently, 2 new sublineages of Omicron, BA.4 and BA.5, have emerged (*3*). These variants show an even stronger capacity to elude infection- and vaccine-induced immune responses, even evading antibodies in serum from BA.1-infected persons (*4*,*5*). Such findings raise concerns that a high community spread might lead to an increasing number of severe cases and a subsequent surge in global hospitalization rates. We performed a quantitative real-time PCR (qPCR) screening survey to estimate the point prevalence of SARS-CoV-2 infection among asymptomatic (defined as having no symptoms at time of sampling) healthcare workers at Danderyd Hospital, Stockholm, Sweden, during June 28–June 29, 2022.

In April and May of 2020, the COMMUNITY study enrolled 2,149 healthcare workers employed at Danderyd Hospital (*6*). Once enrolled, study participants provided blood samples every 4 months for SARS-CoV-2 serologic assessment (*7*). Information regarding vaccination status was obtained through the Swedish vaccination register (VAL Vaccinera), and SARS-CoV-2 infection was determined by either seroconversion before vaccination or positive PCR test results obtained from the national communicable diseases register, SmiNet (Public Health Agency of Sweden).

We conducted a qPCR screening survey during June 28–June 29, 2022. We invited all COMMUNITY-study participants who had provided a blood sample in January 2022 (n = 1,412) to participate in the screening survey via a mobile application program. We restricted participation in the survey to

Table. Characteristics of 259 asymptomatic HCWs who participated in a quantitative real-time PCR screening survey, Stockholm, Sweden, June 28–29, 2022*

Characteristic	All HCWs	Infected HCWs
Total	259 (100)	6 (2.3)
Sex		
M	26 (60)	1 (17)
F	233 (40)	5 (83)
Median age, y	51	48
Vaccination status		
No vaccination	5 (2)	1 (17)
1 vaccine dose	2 (1)	0
2 vaccine doses	24 (9)	0
3 vaccine doses	228 (88)	5 (83)
Previous Infections		
1 infection	119 (46)	2 (33)
2 infections	11 (4)	0

*Values are no. (%) except as indicated. HCW, healthcare worker.

healthcare workers who were actively working and who had been asymptomatic for ≥5 days before screening. We gathered self-administered naso-oropharyngeal/saliva swab specimens (*8*), which were collected at Danderyd Hospital during work hours, and transported those samples to the National Pandemic Center in Stockholm for assessment by qPCR. The screening survey was approved by the Swedish Ethical Review Authority (dnr 2020–01653) and conducted in accordance with the declaration of Helsinki. We obtained written informed consent from all survey participants.

A total of 259 healthcare workers (18.3% of all invited participants) with no symptoms at the time of inclusion underwent qPCR screening. A large proportion (88%) of participants had received 3 vaccine doses, and 50% had been confirmed as having 1 (46%) or 2 (4%) prior SARS-CoV-2 infection(s) (Table). In total, 6 participants (2.3% [95% CI 1.1%–5.0%]) tested positive by qPCR screening; 5 had received 3 vaccine doses, and 2 had a confirmed previous SARS-CoV-2 infection (Table). Just 1 of the 6 participants who tested positive was unvaccinated and previously uninfected. Five samples could be successfully sequenced, revealing 1 infection traced to the BA.2.9.2 sublineage and 4 infections traced to BA.5 (BA.5.1 [2 cases], BA.5.2, and BA.5.3), suggesting community spread of several variants of Omicron. Isolation on A549-ACE2 cells was successfully accomplished for 2 samples.

A 2.3% point prevalence of SARS-CoV-2 infection among asymptomatic healthcare workers indicates widespread transmission of SARS-CoV-2. This prevalence aligns with estimates from the United Kingdom (*9*), where ≈1 in 30 persons was estimated to be infected by SARS-CoV-2 on July 1, 2022. A recent survey conducted in March 2022 during the BA.1/BA.2 wave estimated an overall prevalence of SARS-CoV-2 infection in Sweden of 1.4% (*10*). Although our survey differs in design from that earlier survey, results of both indicate a trend of increased circulation of variants in the population of Sweden, despite the summer season, high vaccine coverage, and a high rate of prior infection.

Additional PCR screenings of our cohort, conducted before the survey we report, revealed that ≈10% of SARS-CoV-2-infected participants remained asymptomatic over the course of the infection (*8*). In parallel with the testing on June 28–29, we performed a substudy using the same cohort during the same days to attempt to isolate the BA.5 sublineage from participants diagnosed with COVID-19 within the previous 5 days. Ten participants were included, and the BA.5 variant of the virus could be isolated on A549-ACE2 cells in 5 samples. Ten people is likely an underrepresentation of true cases in this cohort, but these findings show nonetheless that at least 0.7% of the healthcare workers were diagnosed with COVID-19 at the same time as an additional 2.3% of the healthcare workers had an asymptomatic infection.

We theorize that the latest surge in SARS-CoV-2 infection, in Sweden and elsewhere, can be likely explained by the emergence of the BA.5 variant. The observed prevalence of 2.3% in asymptomatic healthcare workers in Sweden implies a need to take precautions to protect this high-risk population, in hospitals and all other vulnerable settings.

Acknowledgments

This study was funded by grants from the Knut and Alice Wallenberg Foundation (to C.T. and J.K.), the Center for Innovative Medicine (to K.B. and J.K.), Jonas and Kristina of the Jochnick Foundation (to C.T.), the Leif Lundblad Family Foundation (to C.T.), and Region Stockholm (to C.T.).

About the Author

Dr. Blom is a researcher at the Public Health Agency of Sweden. Her research interests include acute viral infections and vaccines, with a focus on human immunology.

References

1. Dejnirattisai W, Shaw RH, Supasa P, Liu C, Stuart AS, Pollard AJ, et al.; Com-COV2 study group. Reduced neutralisation of SARS-CoV-2 omicron B.1.1.529 variant by post-immunisation serum. Lancet. 2022;399:234–6. https://doi.org/10.1016/S0140-6736(21)02844-0
2. Altarawneh HN, Chemaitelly H, Ayoub HH, Tang P, Hasan MR, Yassine HM, et al. Effects of Previous Infection and Vaccination on Symptomatic Omicron Infections.

N Engl J Med. 2022;387:21–34. https://doi.org/10.1056/NEJMoa2203965
3. Tegally H, Moir M, Everatt J, Giovanetti M, Scheepers C, Wilkinson E, et al. Emergence of SARS-CoV-2 Omicron lineages BA.4 and BA.5 in South Africa. Nat Med. 2022; preprint June 27. https://doi.org/10.1038/s41591-022-01911-2
4. Tuekprakhon A, Nutalai R, Dijokaite-Guraliuc A, Zhou D, Ginn HM, Selvaraj M, et al.; OPTIC Consortium; ISARIC4C Consortium. Antibody escape of SARS-CoV-2 Omicron BA.4 and BA.5 from vaccine and BA.1 serum. Cell. 2022;185:2422–2433.e13. https://doi.org/10.1016/j.cell.2022.06.005
5. Cao Y, Yisimayi A, Jian F, Song W, Xiao T, Wang L, et al. BA.2.12.1, BA.4 and BA.5 escape antibodies elicited by Omicron infection. Nature. 2022; preprint June 17. https://doi.org/10.1038/s41586-022-04980-y
6. Rudberg AS, Havervall S, Månberg A, Jernbom Falk A, Aguilera K, Ng H, et al. SARS-CoV-2 exposure, symptoms and seroprevalence in healthcare workers in Sweden. Nat Commun. 2020;11:5064. https://doi.org/10.1038/s41467-020-18848-0
7. Havervall S, Marking U, Greilert-Norin N, Gordon M, Ng H, Christ W, et al. Impact of SARS-CoV-2 infection on vaccine-induced immune responses over time. Clin Transl Immunology. 2022;11:e1388. https://doi.org/10.1002/cti2.1388
8. Blom K, Marking U, Havervall S, Norin NG, Gordon M, García M, et al. Immune responses after omicron infection in triple-vaccinated health-care workers with and without previous SARS-CoV-2 infection. Lancet Infect Dis. 2022;22:943–5. https://doi.org/10.1016/S1473-3099(22)00362-0
9. Office for National Statistics. Coronavirus (COVID-19): latest data and analysis on coronavirus (COVID-19) in the UK and its effect on the economy and society [cited July 1, 2022] https://www.ons.gov.uk/peoplepopulationandcommunity/healthandsocialcare/conditionsanddiseases
10. Public Health Agency of Sweden. The presence of COVID-19 and antibodies against SARS-CoV-2 in Sweden 21–25 March 202. [cited July 1, 2022] https://www.folkhalsomyndigheten.se/publicerat-material/publikationsarkiv/f/forekomsten-av-covid-19-och-antikroppar-mot-sars-cov-2-i-sverige-21-25-mars-2022

Address for correspondence: Jonas Klingström, Center for Infectious Medicine, Department of Medicine Huddinge, Karolinska Institutet, 141 86 Stockholm, Sweden; email: jonas.klingstrom@ki.se

Human Monkeypox without Viral Prodrome or Sexual Exposure, California, USA, 2022

Abraar Karan, Ashley R. Styczynski, ChunHong Huang, Malaya K. Sahoo, Krithika Srinivasan, Benjamin A. Pinsky, Jorge L. Salinas

Author affiliation: Stanford University School of Medicine, Stanford, California, USA

DOI: https://doi.org/10.3201/eid2810.221191

We report human monkeypox in a man who returned to the United States from the United Kingdom and reported no sexual contact. He had vesicular and pustular skin lesions but no anogenital involvement. The potential modes of transmission may have implications for the risk of spread and for epidemic control.

The 2022 multicountry monkeypox outbreak has been linked primarily to intimate contact among men who have sex with men (*1*,*2*). We describe a case of monkeypox in a traveler who returned from the United Kingdom to the United States who did not report recent sexual contact.

A man in his 20s sought care at an emergency department in Stanford, California, USA, on day 7 of an asynchronous, diffuse vesicular rash following travel to the United Kingdom. The first lesion appeared ≈14 days after he attended a large, crowded outdoor event at which he had close contact with others, including close dancing, for a few hours. He said that many attendees were in sleeveless tops and shorts. He wore pants and a short-sleeved top. He did not notice any skin lesions on anyone present, nor did he notice anyone who seemed sick. He shared an e-cigarette with a woman that he met while there. The event was not a rave and was not attended specifically or mostly by persons identifying as gay or bisexual. He attended other similar outdoor events over 4 days. He reported consuming alcohol but no other drug use at these events. He did not wear a mask at these events. He had contact with domestic dogs that he petted.

He took 2 flights to return to the United States; masks were worn on 1 flight. He identifies as bisexual but reported no recent sexual contacts during his travels or in the preceding 3 months. He reported no close indoor activities, although he traveled on crowded public trains. He reported no close contacts

Table. Monkeypox virus DNA levels in clinical specimens from a man with monkeypox. California, USA, 2022*

Specimen type	Days since symptom onset	Viral copies/mL	log_{10} copies/mL	Ct value
Lesion swab	7	65,647,690	7.82	12.7
Nasopharyngeal swab	7	1,200	3.08	27.6
Saliva	10	3,030	3.48	26.3
Rectal swab	10	Detected, unable to quantitate	NA	30.2
Conjunctival swab	10	Detected, unable to quantitate	NA	32.6
Oropharyngeal swab	10	Not detected	NA	NA
Semen	10	Not detected	NA	NA

*The concentrations of the lesion, and self-collected rectal and conjunctival swab specimens are expressed in copies/mL phosphate-buffered saline (PBS). These samples, as well as the self-collected oropharyngeal swab, were collected dry and rehydrated with 1 mL PBS. The nasopharyngeal swab was healthcare worker–collected in 3 mL viral transport media. Cycle threshold values and estimated concentrations are based on the results from the non-variola orthopoxvirus quantitative PCR. All samples with values in copies/mL or reported as detected, unable to quantitate, were positive by both the non-variola orthopoxvirus qPCR and the clade 2/3 monkeypox qPCR. Ct, cycle threshold; NA, not applicable.

since his return. He lives with 1 roommate who did not manifest any symptoms. He had a history of syphilis treated 3 months earlier and was taking HIV preexposure prophylaxis. He denied preceding fevers, chills, headache, lymph node swelling, cough, fatigue, or anorectal pain.

We noted multiple nondraining skin lesions at different stages of appearance, including a centrally umbilicated vesicle on his left palm, a crusting flat lesion on his lip, and pustules on his right and left knuckles and on his lateral torso and back. He had no penile, testicular, or anal lesions and no cervical, axillary, or inguinal lymphadenopathy (Appendix, https://wwwnc.cdc.gov/EID/article/28/10/22-1191-App1.pdf).

Results of complete blood count and basic metabolic panel results were unremarkable. Results of rapid HIV-1 antibody/antigen test was negative, as was urine testing for *N. gonorrhoeae* and *C. trachomatis*. Rapid plasma reagin test results were positive (titer of 1:1). The palmar vesicle was unroofed; a swab of the expressed clear fluid tested positive for nonvariola orthopoxvirus DNA by quantitative PCR (qPCR) and was confirmed as monkeypox virus DNA by qPCR specific for clade 2/3 (West Africa) monkeypox (Table; Appendix). A nasopharyngeal swab specimen that tested negative for SARS-CoV-2 was positive for monkeypox virus DNA using this 2-step testing algorithm. We did not prescribe specific monkeypox treatment because the patient did not have complications or risk factors for severe disease.

We performed follow-up monkeypox virus testing with patient consent 3 days after initial evaluation (day 10 after symptom onset) to clarify viral shedding. We detected virus DNA in a saliva sample, as well as from patient-collected conjunctival and rectal swabs using both the non-variola orthopoxvirus and clade 2/3 monkeypox virus qPCRs. Lesions resolved by day 26 after symptom onset.

This patient tested positive for monkeypox virus DNA from several nonlesion samples. The nasopharyngeal and saliva findings are noteworthy because the patient did not report respiratory symptoms. In addition, the detectable viral DNA in the rectal swab specimen in the absence of visible anal lesions or pain indicates a potential for sustained sexual transmission, although the viral DNA levels were low; contamination during self-collection cannot be ruled out. We were unable to assess whether internal rectal lesions were present.

This case highlighted the distinctiveness of clinical manifestations as they indicated potential routes of transmission during the 2022 multicountry outbreak of monkeypox. This patient did not report recent sexual contact, did not have evidence of genital lesions or inguinal lymphadenopathy (*3*), and did not report a viral prodrome. His primary risk factor was close, nonsexual contact with numerous unknown persons at a crowded outdoor event. His case highlights the potential for spread at such gatherings, which may have implications for epidemic control. The lack of both sexual exposure and anogenital involvement indicates that mode of transmission may be associated with clinical symptoms; fomites (hotel bedding and sheets, high-touch areas in public settings) may be alternative modes of transmission. Overall, the viral inoculum required for all possible modes of transmission remains an area of active investigation.

This case also demonstrates the importance of local monkeypox virus testing, rather than centralized testing in public health or commercial reference laboratories. Local testing enabled diagnosis in <12 hours and immediate notification to local and state public health authorities for isolation and contact tracing.

About the Author

Dr. Karan is an infectious disease physician and postdoctoral researcher at Stanford University. His research focuses on infectious disease epidemiology and interventions to slow epidemic spread.

References

1. Vivancos R, Anderson C, Blomquist P, Balasegaram S, Bell A, Bishop L, et al.; UKHSA Monkeypox Incident Management team; Monkeypox Incident Management Team. Community transmission of monkeypox in the United Kingdom, April to May 2022. Euro Surveill. 2022;27. https://doi.org/10.2807/1560-7917.ES.2022.27.22.2200422
2. Antinori A, Mazzotta V, Vita S, Carletti F, Tacconi D, Lapini LE, et al.; INMI Monkeypox Group. Epidemiological, clinical and virological characteristics of four cases of monkeypox support transmission through sexual contact, Italy, May 2022. Euro Surveill. 2022;27. https://doi.org/10.2807/1560-7917.ES.2022.27.22.2200421
3. Patrocinio-Jesus R, Peruzzu F. Monkeypox genital lesions. N Engl J Med. 2022;387:66. https://doi.org/10.1056/NEJMicm2206893

Address for correspondence: Abraar Karan, Stanford University School of Medicine, 300 Pasteur Dr, Lane 134, Stanford, CA 94304, USA; email: abraar@stanford.edu

Introduction and Differential Diagnosis of Monkeypox in Argentina, 2022

Adrian Lewis, Alejandro Josiowicz, Stella Maris Hirmas Riade, Monica Tous, Gustavo Palacios,[1] Daniel M. Cisterna[1]

Author affiliations: Instituto Nacional de Enfermedades Infecciosas, ANLIS Dr. Carlos G. Malbran, Buenos Aires, Argentina (A. Lewis, A. Josiowicz, S.M.H. Riade, M. Tous, D.M. Cisterna); Icahn School of Medicine at Mount Sinai, New York, New York, USA (G.P.)

We report detection of cases of monkeypox virus infection in Argentina in the context of a marked increase in confounding cases of atypical hand-foot-and-mouth syndrome caused by enterovirus coxsackie A6. We recommend performing an accurate differential virological diagnosis for exanthematous disease in suspected monkeypox cases.

DOI: https://doi.org/10.3201/eid2810.221075

Global surveillance of monkeypox cases has resulted in the detection of an increasing number of suspected cases in countries to which the disease is not endemic (*1*). We report the results of a virological investigation of 9 suspected cases of monkeypox from Argentina (n = 6) and Bolivia (n = 3) detected during May 22–June 8, 2022. The investigation was conducted using World Health Organization case definitions (*2*).

We attempted laboratory diagnosis for all 9 cases by using classical and molecular methods such as electron microscopy (EM) and conventional orthopoxvirus PCR. We analyzed swab samples collected from the skin, genital lesions, or both for monkeypox screening. We performed negative staining electron microscopy using direct absorption for 10 minutes of a 10-μL sample volume on fomvar-coated 400 mesh grids. We performed staining with 1% phosphotungstic acid (*3*) and examined samples using a Zeiss EM-109 transmission electron microscope.

We extracted viral nucleic acid by using the High Pure Viral RNA kit (Roche Molecular Biochemicals, https://www.roche.com) according to the manufacturer's instructions. We performed end-point PCR amplification by using primers EACP1 and EACP2 targeting the complete viral hemagglutinin gene, as done previously (*4*). We sequenced amplicon PCR fragments by using BigDye Terminator version 3.1 reagent in an ABI3500 Genetic Analyzer automatic sequencer (both ThermoFisher Scientific, https://www.thermofisher.com). We performed phylogenetic analysis by using the maximum-likelihood method and Tamuka 3-parameter model according to Modeltest using MEGA software (https://www.megasoftware.net). We produced bootstraps using 500 replicates. For differential diagnosis, we analyzed negative monkeypox virus (MPXV) samples by molecular methods for the detection of herpes simplex virus, varicella zoster virus, and enterovirus. We performed molecular typing of enteroviruses as previously reported (*5*).

The images obtained by EM in cases 1–3, all from Argentina, showed the presence of viral particles compatible with a member of the genus *Orthopoxvirus* (Appendix Figure 1, https://wwwnc.cdc.gov/EID/article/28/10/22-1075-App1.pdf). The phylogenetic analysis of the complete hemagglutinin genes for these viruses confirmed the identification of MPXV (West African clade) (Appendix Figure 2). Enterovirus was identified by PCR in 4 (66.7%) of the remaining 6 cases (2 from Argentina and 2 from Bolivia). Coxsackievirus A6 (CV-A6) was identified in 3 of these 4 cases. CV-A6 is usually associated with atypical hand-foot-mouth syndrome. Finally, the 6 samples analyzed were negative for herpes simplex virus and varicella zoster virus. In summary, of the 9

[1]These authors were co–principal investigators.

cases from South America with exanthematic disease that fit the definition of suspected cases, 3 (33%) cases were confirmed for MPXV and 4 (44%) cases were differentially diagnosed as CV-A6 infections.

We evaluated the clinical manifestations of all 9 cases. In the 3 laboratory-confirmed cases of MPXV, clinical manifestations included pustular lesions of heterogeneous distribution in the body, multiple painful intergluteal and perianal lesions, and genital ulcers (Table). All 3 patients reported multiple sexual partners during the previous few weeks, 2 during international travel to Spain and 1 with international travelers from countries reporting cases. No patients experienced lymphadenopathy. Patients 1 and 3 were hospitalized briefly for pain management related to their symptoms.

The remaining 6 patients who were negative for orthopoxvirus displayed vesicular lesions in various stages on the palms, soles, and genital locations. Some reported travel from the Dominican Republic, Colombia, Paraguay, or Spain.

The epidemiologic information we collected on these monkeypox cases, together with genetic analysis, confirm that they are directly related to outbreaks in several countries in Europe (*6*) and are not linked to previous introductions in the United States (*7*; C.M. Gigante et al., unpub. data, https://www.biorxiv.org/content/10.1101/2022.06.10.495526v1). Although 1 patient did not travel, he reported direct physical contact with persons who had traveled to countries with reported cases, revealing local community transmission.

Of note, South America is experiencing a marked increase in cases of atypical hand-foot-mouth syndrome caused by CV-A6 (*8*,*9*). Unlike the classic syndrome, this atypical variant also affects young adults and occurs in unusual regions of the body, including the genital areas, and could easily be confused with monkeypox. A wide case definition makes surveillance easier, but it also emphasizes the need to perform precise differential virological diagnosis for exanthematic disease in suspected cases.

In summary, we report 3 cases of monkeypox in patients in Argentina. Six additional patients in Argentina and Bolivia had monkeypox ruled out by differential diagnosis; 4 of those cases were atypical hand-foot-mouth syndrome caused by CV-A6. We recommend considering virological diagnosis of this

Table. Characteristics of suspected cases of monkeypox in Argentina and Bolivia*

Patient no.	Age, y/sex	Clinical manifestations	Country	Travel history	Hospital admission	Background	MPXV PCR	EV PCR/EV type	HSV PCR	VZV PCR
1	40/M	Pustular lesions on the left shoulder, sternal, cervical, right scapula, left lower limb, multiple painful intergluteal and perianal lesions	Argentina	Spain	Yes	Multiple sexual partners, HIV+	+	ND	ND	ND
2	40/M	Genital ulcer	Argentina	Spain	No	Multiple sexual partners	+	ND	ND	ND
3	36/M	Fever, headache, myalgia, back pain, maculopapular lesions and pustules	Argentina	No reported travel	Yes	Multiple sexual partners	+	ND	ND	ND
4	36/M	Vesicular lesions on the palms, soles, and perineum	Argentina	Dominican Republic	No	3-year-old son with blistering lesion on the perineum	–	–	–	–
5	43/M	Fever, maculopapular lesions and pustules	Argentina	Paraguay	No	No data	–	+/CV-A6	–	–
6	39/F	Vesicular lesions on hand, mouth, and groin area	Argentina	Dominican Republic and Colombia	No	No data	–	+/CV-A6	–	–
7	53/F	Exanthematous lesions of unspecified distribution, lymphadenopathy	Bolivia	No reported travel	No	No data	–	–	–	–
8	22/F	Exanthematous lesions of unspecified distribution, lymphadenopathy	Bolivia	Spain	No	No data	–	+/CV-A6	–	–
9	27/M	Exanthematous lesions of unspecified distribution, lymphadenopathy	Bolivia	No reported travel	No	HIV+	–	+/ND	–	–

*CV-A6, coxsackievirus A6; EV, enterovirus; HSV, herpes simplex virus; MPXV, monkeypox virus; ND, not done; VZV, varicella zoster virus; +, positive; –, negative.

disease in suspected cases of monkeypox. Clinicians should be aware of the possibility for misdiagnosis related to these viral infections.

This work was supported by the Ministry of Health of Argentina as part of the surveillance program for monkeypox virus.

About the Author

Dr. Lewis is head of the Electron Microscopy Laboratory in the Virology Department, INEI- ANLIS "Dr. Carlos G. Malbran." His primary research focus is poxvirus virology and emerging virus surveillance.

References

1. Bunge EM, Hoet B, Chen L, Lienert F, Weidenthaler H, Baer LR, et al. The changing epidemiology of human monkeypox—a potential threat? A systematic review. PLoS Negl Trop Dis. 2022;16:e0010141. https://doi.org/10.1371/journal.pntd.0010141
2. Argentina Ministry of Health. Data collection tabs for notification [in Spanish]. 2022 [cited 2022 Jun 22]. https://www.argentina.gob.ar/salud/epidemiologia/fichas
3. Laue M, Bannert N. Detection limit of negative staining electron microscopy for the diagnosis of bioterrorism-related micro-organisms. J Appl Microbiol. 2010;109:1159–68. https://doi.org/10.1111/j.1365-2672.2010.04737.x
4. Ropp SL, Jin Q, Knight JC, Massung RF, Esposito JJ. PCR strategy for identification and differentiation of small pox and other orthopoxviruses. J Clin Microbiol. 1995;33:2069–76. https://doi.org/10.1128/jcm.33.8.2069-2076.1995
5. Cisterna DM, Lema CL, Martinez LM, Verón E, Contarino LP, Acosta D, et al. Atypical hand, foot, and mouth disease caused by Coxsackievirus A6 in Argentina in 2015. Rev Argent Microbiol. 2019;51:140–3. https://doi.org/10.1016/j.ram.2018.05.003
6. Perez Duque M, Ribeiro S, Martins JV, Casaca P, Leite PP, Tavares M, et al. Ongoing monkeypox virus outbreak, Portugal, 29 April to 23 May 2022. Euro Surveill. 2022;27. https://doi.org/10.2807/1560-7917.ES.2022.27.22.2200424
7. Antinori A, Mazzotta V, Vita S, Carletti F, Tacconi D, Lapini LE, et al.; INMI Monkeypox Group. Epidemiological, clinical and virological characteristics of four cases of monkeypox support transmission through sexual contact, Italy, May 2022. Euro Surveill. 2022;27. https://doi.org/10.2807/1560-7917.ES.2022.27.22.2200421
8. Lizasoain A, Piegas S, Victoria M, Da Silva EE, Colina R. Hand-foot-and-mouth disease in uruguay: coxsackievirus A6 identified as causative of an outbreak in a rural childcare center. J Med Virol. 2020;92:167–73. https://doi.org/10.1002/jmv.25590
9. Luchs A, Azevedo LS, Souza EV, Medeiros RS, Souza YFVP, Teixeira DLF, et al. Coxsackievirus A6 strains causing an outbreak of hand-foot-and-mouth disease in Northeastern Brazil in 2018. Rev Inst Med Trop São Paulo. 2022;64:e16. https://doi.org/10.1590/s1678-9946202264016

Address for correspondence: Daniel M. Cisterna, Instituto Nacional de Enfermedades Infecciosas, ANLIS, "Dr. Carlos G. Malbran," Av. Velez Sarsfield 563 (1282AFF), Buenos Aires, Argentina; email: dcisterna@anlis.gob.ar

Renewed Risk for Epidemic Typhus Related to War and Massive Population Displacement, Ukraine

Paul N. Newton, Pierre-Edouard Fournier, Dennis Tappe, Allen L. Richards

Author affiliations: University of Oxford, Oxford, UK (P.N. Newton); Mahidol–Oxford Tropical Medicine Research Unit, Bangkok, Thailand (P.N. Newton), Institut Hospitalo-Universitaire Méditerranée Infection, Marseille, France (P.-E. Fournier), Bernhard-Nocht-Institut für Tropenmedizin, Hamburg, Germany (D. Tappe); Allen L. Richards Consulting, Damascus, Maryland, USA (A.L. Richards)

DOI: https://doi.org/10.3201/eid2810.220776

Epidemic typhus, caused by *Rickettsia prowazekii* bacteria and transmitted through body lice (*Pediculus humanus corporis*), was a major public health threat in Eastern Europe as a consequence of World War II. In 2022, war and the resulting population displacement in Ukraine risks the return of this serious disease.

The war in Ukraine has produced devastation in the region unseen since World War II. Epidemic typhus, one of the diseases that ravaged Europe during that period and before, but nearly forgotten in 2022, risks returning because of war and massive population displacement. History suggests that planning is needed to prevent this disease from aggravating the current war-induced public health crisis. Epidemic typhus (also called louse-borne typhus) is caused by *Rickettsia prowazekii* bacteria and is transmitted through the feces of body lice (*Pediculus humanus corporis*) that live in clothes. Before the advent of antibiotics, mortality rates from epidemic typhus reached 60%, especially in persons who were elderly and malnourished. The disease can be reactivated, in the absence of lice, after many decades as Brill–Zinsser disease, which can lead rapidly to further epidemics if patients become infested with body lice (*1*).

Epidemic typhus is associated with war, poverty, homelessness, cold weather, crowding, unsanitary conditions, and refugee camps. The disease has generated very little recent public awareness; the most recent regional outbreak reported in the public domain in English occurred in Russia in 1997 (*2*).

During World War II, Ukraine and adjacent countries were ravaged by epidemic typhus, especially the Jewish populations who were forced

into ghettos. The city of Lviv in western Ukraine was a center for typhus vaccine research, especially through the work of Fleck and Weigl (*3*). Ukraine now has an estimated 1.8 million persons ≥80 years of age (*4*), some of whom may have contracted *R. prowazekii* infection during the 1940s and are at risk for Brill–Zinsser disease. Body louse infestations among refugee and sheltering populations, living in overcrowded and unsanitary conditions because of war, may trigger epidemics of *R. prowazekii* infection. A further risk for these populations is infection with *Bartonella quintana* bacteria, the cause of trench fever, that is also transmitted by body lice.

The public health services of Ukraine and the Eastern Europe region face multiple threats. Does the current epidemic typhus risk warrant timely surveillance to curtail outbreaks? Public health organizations, including and organizations caring for refugees, might consider sending body lice specimens collected from patients for *R. prowazekii* PCR testing (a list of laboratories that can perform this test is available from the authors) to give early warning of outbreaks. When body lice are detected, these organizations could consider community treatment, including delousing and the administration of ivermectin (*1*,*5*) and doxycycline, while assays are performed.

Because PCR testing and tetracycline drugs are now available, we can respond in such dire circumstances to prevent *R. prowazekii* outbreaks before they occur. Public health officials could institute a system analogous to that for surveillance and control of plague and fleas. We now have the tools and treatments that can make it possible to avert and mitigate epidemic typhus outbreaks.

P.N. Newton is funded by the Wellcome Trust.

About the Author

Dr. Newton is an infectious disease research doctor and founding director of the Lao–Oxford–Mahosot Hospital Wellcome Trust Research Unit, Mahosot Hospital, Vientiane, Laos, now based in Center for Tropical Medicine and Global Health, Oxford, UK.

References

1. Bechah Y, Capo C, Mege JL, Raoult D. Epidemic typhus. Lancet Infect Dis. 2008;8:417–26. https://doi.org/10.1016/S1473-3099(08)70150-6
2. Tarasevich I, Rydkina E, Raoult D. Outbreak of epidemic typhus in Russia. Lancet. 1998;352:1151. https://doi.org/10.1016/S0140-6736(05)79799-3
3. Allen A. The fantastic laboratory of Dr. Weigl. New York: WW Norton; 2014.
4. Knoema. World data atlas. Ukraine—total population aged 75 years and over [cited 2022 Aug 24]. https://knoema.com/atlas/Ukraine/topics/Demographics/Age/Population-aged-75-years
5. Foucault C, Ranque S, Badiaga S, Rovery C, Raoult D, Brouqui P. Oral ivermectin in the treatment of body lice. J Infect Dis. 2006;193:474–6. https://doi.org/10.1086/499279

Address for correspondence: Paul Newton, Center for Tropical Medicine and Global Health, Nuffield Department of Medicine, Oxford University, Oxford OX3 7LG, UK; email: paul.newton@ndm.ox.ac.uk

Effectiveness of Booster and Influenza Vaccines against COVID-19 among Healthcare Workers, Taiwan

Jun Yi Sim, Ping-Sheng Wu, Ching-Feng Cheng, You-Chen Chao, Chun-Hsien Yu

Author affiliations: Taipei Tzu Chi Hospital, Buddhist Tzu Chi Medical Foundation, Taipei, Taiwan; and Tzu Chi University, Hualien, Taiwan

DOI: https://doi.org/10.3201/eid2810.221134

Among previously uninfected healthcare workers in Taiwan, mRNA COVID-19 booster vaccine was associated with lower odds of COVID-19 after primary recombinant vaccine. Symptom-triggered testing revealed that tetravalent influenza vaccine was associated with higher odds of SARS-CoV-2 infection. COVID-19 vaccination continues to be most effective against SARS-CoV-2.

Border control, contact tracing, and adherence to nonpharmaceutical interventions enabled Taiwan to contain COVID-19 for >2 years (*1*). From the beginning of the pandemic in 2020 through March 31, 2022, Taiwan had just 16,224 domestic COVID-19 cases, an incidence of 0.07% for a population of 23.6 million (*2*). In this backdrop, we found no COVID-19 cases among healthcare workers (HCWs) at Taipei Tzu Chi Hospital, Taipei,

Taiwan, through April 10, 2022, despite symptom monitoring and surveillance.

Meanwhile, to overcome vaccine shortages and hesitancy among adults in Taiwan, homologous and heterologous regimens of the adenoviral vector vaccine ChAdOx1-S/nCoV-19 (AstraZeneca, https://www.astrazeneca.com), the adjuvanted subunit protein vaccine MVC-COV1901 (Medigen, https://www.medigenvac.com), and the mRNA vaccines mRNA-1273 (Moderna, https://www.modernatx.com) and BNT162b2 (Pfizer-BioNTech, https://www.pfizer.com) were used widely. All vaccines were given in a 2-dose primary series and for a 1-dose booster, except for ChAdOx-S/nCoV-19 (*3*).

To evaluate effectiveness of COVID-19 booster vaccines and the 2021–22 tetravalent seasonal influenza vaccine against COVID-19 during an Omicron variant–predominant surge, we conducted a retrospective study of HCW vaccination at Taipei Tzu Chi Hospital. We obtained an employee list with vaccination data and COVID-19 surveillance reports from the hospital for April 10–June 10, 2022. During this period, the hospital tested HCWs in 2 groups: the routine testing group comprised emergency department and COVID-19 ward staff who received regular, weekly testing; the symptom-triggered group comprised staff who were tested whenever symptoms developed or after a high-risk exposure. Nasopharyngeal swab samples were collected by professionals and tested for SARS-CoV-2 by reverse transcription PCR (RT-PCR) using a previously described RT-PCR protocol (*4*) or by Panbio rapid antigen test (Abbott, https://www.abbott.com). This study received approval from the Taipei Tzu Chi Hospital institutional review board with waiver for informed consent because the study used previously collected data (approval no. 11-X-106).

We compared data by using 2-tailed χ^2 and Kruskal-Wallis tests and considered $p<0.05$ statistically significant. We used a multivariate logistic regression model to assess the relationship between SARS-CoV-2 infection during April 10–June 10,

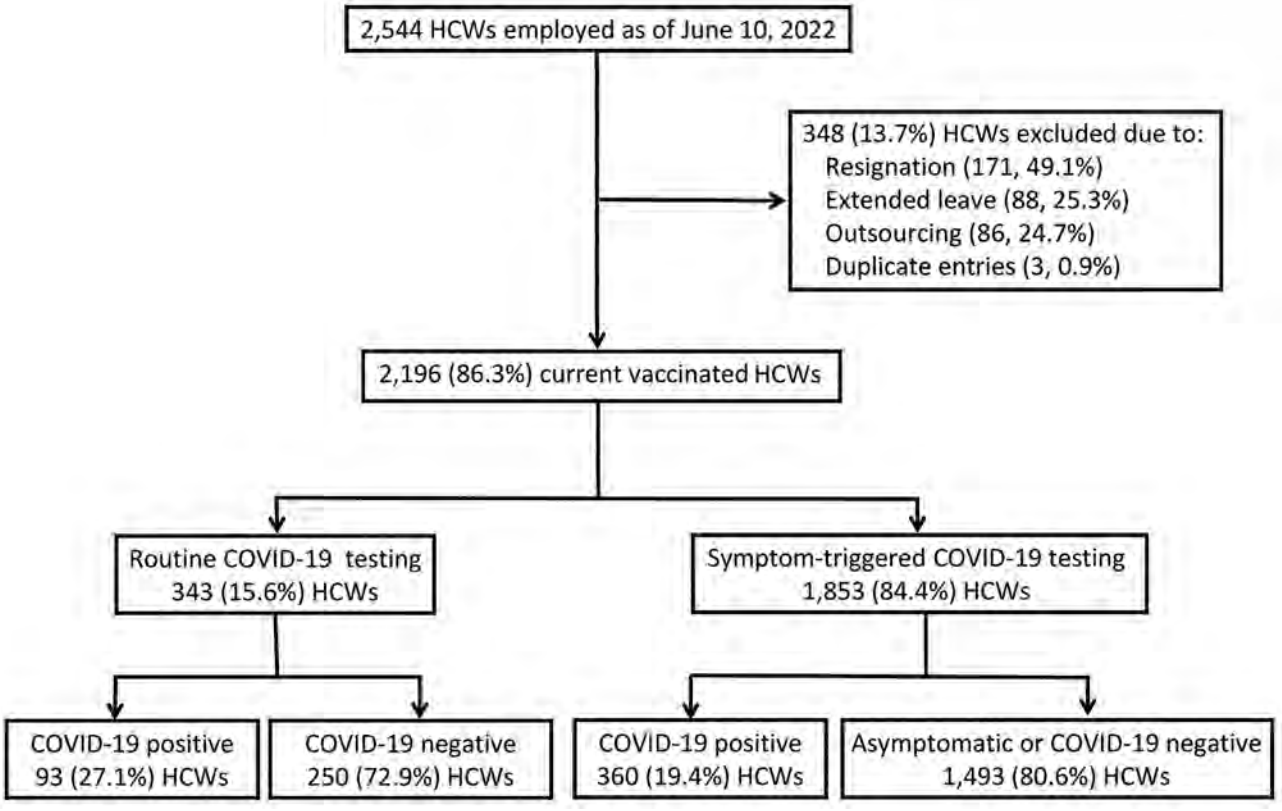

Figure. Worker exclusion and testing in a study of the effectiveness of booster and influenza vaccines against COVID-19 among healthcare workers, Taipei Tzu Chi Hospital, Taipei, Taiwan. Employment, vaccination, and testing data for April 10–June 10, 2022, were provided by the hospital's Human Resource Office and corroborated by the Occupational Safety and Health Administration Office and the hospital's Center for Infection Control. Workers in the routine testing group were tested weekly by reverse transcription PCR or rapid antigen test; workers in the symptom-triggered testing group were tested if COVID-19 symptoms developed or after they were exposed to COVID-19 cases. HCW, healthcare worker.

2022, and age, sex, work sector, COVID-19 booster vaccine, and seasonal influenza vaccination. We performed all analyses in SPSS Statistics 25.0 (IBM, https://www.ibm.com).

The employment list included a total of 2,544 HCWs; we excluded 348 (13.7%) staff who were outsourced, who were on extended leave, or who had resigned. Of the remaining 2,196 HCWs, 453 (20.6%) tested SARS-CoV-2 positive during the study period (Figure). COVID-19 incidence was highest (35.3%) among housekeeping staff and lowest (13.5%) among medical staff (Table). All COVID-19–positive HCWs experienced mild symptoms; none required intensive care.

Table. Characteristics of 2,196 healthcare workers tested for SARS-CoV-2 after receiving COVID-19 booster and influenza vaccines, Taipei Tzu Chi Hospital, Taipei, Taiwan*

	Regular testing, n = 343†				Symptom-triggered testing, n = 1,853			
Characteristics	Positive, no. (%)	Negative, no. (%)	p value	OR (95% CI)	Positive, no. (%)	Negative or no symptom, no. (%)	p value	OR (95% CI)
Total	93 (100)	250 (100)	NA	NA	360 (100)	1,493 (100)	NA	NA
Sex			0.051				0.084	
F	67 (72.0)	205 (82.0)	NA	1.4 (0.7–3.1)	278 (77.2)	1,085 (72.7)	NA	1.0 (0.7–1.4)
M	26 (28.0)	45 (18.0)	NA	Referent	82 (22.8)	408 (27.3)	NA	Referent
Age range, y			0.377				0.345	
71–80	1 (1.1)	0	NA	NA	1 (0.3)	8 (0.5)	NA	0.7 (0.1–6.0)
61–70	1 (1.1)	4 (1.6)	NA	0.7 (0.1–6.6)	6 (1.7)	55 (3.7)	NA	0.5 (0.2–1.3)
51–60	3 (3.2)	18 (7.2)	NA	0.5 (0.1–2.0)	33 (9.2)	160 (10.7)	NA	0.9 (0.6–1.3)
41–50	15 (16.1)	39 (15.6)	NA	0.9 (0.4–1.9)	93 (25.8)	362 (24.2)	NA	1.0 (0.7–1.4)
31–40	29 (31.2)	63 (25.2)	NA	1.1 (0.6–2.1)	92 (25.6)	391 (26.2)	NA	1.0 (0.7–1.3)
21–30	44 (47.3)	126 (50.4)	NA	Referent	135 (37.5)	517 (34.6)	NA	Referent
Work sector			<0.001				<0.001	
Nursing	52 (55.9)	175 (70.0)	NA	0.1 (0.1–0.4)	170 (47.2)	641 (42.9)	NA	0.9 (0.6–1.2)
Medical	15 (11.3)	37 (14.8)	NA	0.2 (0.1–0.5)	39 (10.8)	309 (20.7)	NA	0.5 (0.3–0.8)
Technical	6 (6.5)	9 (3.6)	NA	0.3 (0.1–1.1)	43 (11.9)	197 (13.2)	NA	0.8 (0.5–1.2)
Laboratory, pharmacy	3 (3.2)	20 (8.0)	NA	0.1 (0.0–0.3)	32 (8.9)	100 (6.7)	NA	1.1 (0.7–1.8)
Housekeeping	0	2 (0.8)	NA	NA	6 (1.7)	9 (0.6)	NA	2.8 (0.9–8.6)
Administration	17 (18.3)	7 (2.8)	NA	Referent	70 (19.4)	237 (15.9)	NA	Referent
No. COVID-19 vaccine doses			0.065				<0.001	
3	88 (94.6)	246 (98.4)	NA	0.2 (0.0–0.8)	319 (88.6)	1,416 (94.8)	NA	0.4 (0.2–0.6)
2	5 (5.4)	4 (1.6)	NA	Referent	38 (10.6)	73 (4.9)	NA	Referent
1	0	0	NA	NA	0	0	NA	NA
0	0	0	NA	NA	3 (0.8)	4 (0.3)	NA	NA
COVID-19 primary series‡			0.442				0.348	
Viral vector + viral vector	70 (75.3)	193 (77.2)	NA	NA	270 (75.0)	1,091 (73.1)	NA	NA
Viral vector + mRNA	7 (7.5)	27 (10.8)	NA	NA	45 (12.5)	189 (12.7)	NA	NA
mRNA + mRNA	15 (16.1)	30 (12.0)	NA	NA	41 (11.4)	206 (13.8)	NA	NA
Protein subunit + protein subunit	0	0	NA	NA	0	2 (0.1)	NA	NA
COVID-19 booster§			1.00				0.145	
mRNA	86 (92.5)	243 (97.2)	NA	NA	317 (88.1)	1,387 (92.9)	NA	NA
Protein subunit	0	2 (0.8)	NA	NA	2 (0.5)	27 (1.8)	NA	NA
Booster vaccine date¶			0.111				<0.001	
December 2021	23 (24.7)	68 (27.2)	NA	NA	70 (19.4)	319 (21.4)	NA	NA
January 2022	55 (59.1)	164 (65.6)	NA	NA	219 (60.8)	999 (66.9)	NA	NA
February 2022	4 (4.3)	4 (1.6)	NA	NA	17 (4.7)	35 (2.3)	NA	NA
March 2022	3 (3.2)	7 (2.8)	NA	NA	5 (1.4)	32 (2.1)	NA	NA
April 2022	0	3 (1.2)	NA	NA	6 (1.7)	24 (1.6)	NA	NA
May 2022	1 (1.1)	0	NA	NA	0	4 (0.3)	NA	NA
Tetravalent influenza vaccine, 2021–22 season			0.297				0.016	
Vaccinated	68 (73.1)	167 (66.8)	NA	1.5 (0.8–2.7)	265 (73.6)	1,001 (67.0)	NA	1.5 (1.1–2.0)
Not vaccinated	25 (26.9)	83 (33.2)	NA	Referent	95 (26.4)	492 (33.0)	NA	Referent

*p values calculated by using χ^2 test; OR and 95% CI calculated by using multinomial logistic regression. NA, not applicable; OR, odds ratio.
†For age 71–80 y and housekeepers of the regularly tested subgroup, estimates were not shown because the groups were too small.
‡Excluding 7 unvaccinated workers and 3 workers who did not report vaccine type. Data available for a total of 2,186 healthcare workers; regular testing subgroup included 92 positive cases and 250 negative cases; symptom-triggered testing subgroup included 356 positive cases and 1,488 negative cases; thus, percentages do not add up to 100%.
§Excluding 7 unvaccinated workers, 120 workers who did not receive a booster vaccine, and 5 workers who did not report booster vaccine type. Data available for a total of 2,064 healthcare workers; regular testing subgroup included 86 positive cases and 245 negative cases; symptom-triggered testing subgroup included 319 positive cases and 1,414 negative cases; thus, percentages do not add up to 100%.
¶Excluding 7 unvaccinated workers, 120 workers who did not receive a booster vaccine, and 7 workers who did not report month of booster vaccine. Data available for a total of 2,062 healthcare workers; regular testing subgroup included 86 positive cases and 246 negative cases; symptom-triggered testing subgroup included 317 positive cases and 1,413 negative cases; thus, percentages do not add up to 100%.

COVID-19 vaccine uptake was 99.7% for primary series and 94.5% for booster doses; booster uptake was highest (94.9%) among technicians and lowest (92.7%) among administrators. Influenza vaccine uptake was 68.4%, highest (74.3%) among nurses and lowest (52.9%) among housekeeping staff.

Compared with HCWs who had symptom-triggered testing, regularly tested HCWs were younger (median age 31.0 years, interquartile range [IQR] 26.0–40.0 years, vs. 36.0 years, IQR 28.0–45.5 years; p<0.001). Regularly tested HCWs also were more likely to be female (79.3% vs. 73.6%; p = 0.026), have had received booster vaccination (97.4% vs. 93.7%; p = 0.005), and have tested COVID-19–positive (27.1% vs. 19.4%; p = 0.002). Influenza vaccine uptake and types of primary and booster regimens were not greatly different for either subgroup (Table).

Regression analyses identified receiving booster vaccination and being medical staff were also associated with lower odds of COVID-19 for both testing subgroups. Tetravalent influenza vaccination was associated with higher odds of COVID-19, although we observed statistically significant results only for HCWs who underwent symptom-triggered testing (Table).

Effectiveness of primary ChAdOx-S/nCoV-19 series coupled with mRNA booster is limited because some countries suspended use of ChAdOx-S/nCoV-19 because of thromboembolic concerns (*5*,*6*). However, our study provides real-world insights into effectiveness of mRNA booster after primary homologous and heterologous ChAdOx-s/nCoV-19 regimens. Our results showed a booster dose was associated with much lower odds of COVID-19 among HCWs in both the routine and symptom-triggered testing subgroups compared with HCWs having no booster. These findings are similar to observations of fewer COVID-19 infections among BNT162b2-boosted HCWs (*7*) and observed effectiveness of mRNA-1273 (47.3%) and BNT162b2 (49.4%) boosters against symptomatic Omicron infection (*8*).

A meta-analysis suggested reduced COVID-19 susceptibility with influenza vaccination for the general population but not HCWs (*9*). However, we observed a statistically significant increase in odds for COVID-19 among HCWs in the symptom-triggered testing group but not the routine testing group (p<0.001). The effect of influenza vaccines against COVID-19 among HCWs remains to be elucidated.

Study limitations include lack of universal testing and use of self-reported symptoms, which might have missed some cases. Also, vaccinated HCWs can be asymptomatically infected (*10*); hence, COVID-19 infections might be underreported in our study. Causality could not be inferred due to the study's observational nature. We also did not account for individual behaviors and household exposures. Nevertheless, our study highlights the benefits of booster COVID-19 vaccination and its effectiveness against SARS-CoV-2 among HCWs.

Acknowledgments

We thank all hospital staff for their unwavering dedication and determination during a period of hardship. We also thank Ming-Yieh Peng, Sheg-Kang Chiu, and Ming-Chin Chan for their contributions to this effort.

This study was partially supported by grants to C.-H.Y. from the Ministry of Science and Technology, Taiwan (grant no. MOST 108-2314-B-303 -019 -MY2), and Taipei Tzu Chi Hospital (grant no. TCRD-TPE-110-019).

About the Author

Dr. Sim is a pediatric infectious disease physician at Taipei Tzu Chi Hospital, Taipei, and an adjunct professor of pediatrics at Tzu Chi University, Hualien, Taiwan. His primary research interests include vaccine-preventable diseases, respiratory viruses, and adolescent mental health and well-being.

References

1. Ng TC, Cheng HY, Chang HH, Liu CC, Yang CC, Jian SW, et al. Comparison of estimated effectiveness of case-based and population-based interventions on COVID-19 containment in Taiwan. JAMA Intern Med. 2021;181:913–21. https://doi.org/10.1001/jamainternmed.2021.1644
2. Taiwan Centers for Disease Control. Taiwan national infectious disease statistics system [cited 2022 Jul 16]. https://nidss.cdc.gov.tw
3. Sheng WH, Chang SY, Lin PH, Hsieh MJ, Chang HH, Cheng CY, et al. Immune response and safety of heterologous ChAdOx1-nCoV-19/mRNA-1273 vaccination compared with homologous ChAdOx1-nCoV-19 or homologous mRNA-1273 vaccination. J Formos Med Assoc. 2022;121:766–77. https://doi.org/10.1016/j.jfma.2022.02.020
4. Su WL, Lin CP, Huang HC, Wu YK, Yang MC, Chiu SK, et al. Clinical application of 222 nm wavelength ultraviolet C irradiation on SARS CoV-2 contaminated environments. J Microbiol Immunol Infect. 2022;55:166–9. https://doi.org/10.1016/j.jmii.2021.12.005
5. del Cura-Bilbao A, López-Mendoza H, Chaure-Pardos A, Vergara-Ugarriza A, Guimbao-Bescós J. Effectiveness of 3 COVID-19 vaccines in preventing SARS-CoV-2 infections, January–May 2021, Aragon, Spain. Emerg Infect Dis. 2022;28:591–8. https://doi.org/10.3201/eid2803.212027
6. Nordström P, Ballin M, Nordström A. Effectiveness of heterologous ChAdOx1 nCoV-19 and mRNA prime-boost vaccination against symptomatic Covid-19 infection in Sweden: a nationwide cohort study. Lancet Reg Health Eur. 2021;11:100249. https://doi.org/10.1016/j.lanepe.2021.100249

7. Spitzer A, Angel Y, Marudi O, Zeltser D, Saiag E, Goldshmidt H, et al. Association of a third dose of BNT162b2 vaccine with incidence of SARS-CoV-2 infection among health care workers in Israel. JAMA. 2022;327:341–9. https://doi.org/10.1001/jama.2021.23641
8. Abu-Raddad LJ, Chemaitelly H, Ayoub HH, AlMukdad S, Yassine HM, Al-Khatib HA, et al. Effect of mRNA vaccine boosters against SARS-CoV-2 Omicron infection in Qatar. N Engl J Med. 2022;386:1804–16. https://doi.org/10.1056/NEJMoa2200797
9. Su W, Wang H, Sun C, Li N, Guo X, Song Q, et al. The association between previous influenza vaccination and COVID-19 infection risk and severity: a systematic review and meta-analysis. Am J Prev Med. 2022;63:121–30. https://doi.org/10.1016/j.amepre.2022.02.008
10. Laing ED, Weiss CD, Samuels EC, Coggins SA, Wang W, Wang R, et al. Durability of antibody response and frequency of SARS-CoV-2 infection 6 months after COVID-19 vaccination in healthcare workers. Emerg Infect Dis. 2022;28:828–32. https://doi.org/10.3201/eid2804.212037

Address for correspondence: Chun-Hsien Yu, Department of Pediatrics, Taipei Tzu Chi Hospital, Buddhist Tzu Chi Medical Foundation, 289 Jianguo Rd, Xindian District, New Taipei City 23142, Taiwan; email: chryu@mail.tcu.edu.tw

Three-Dose Primary Series of Inactivated COVID-19 Vaccine for Persons Living with HIV, Hong Kong

Denise Pui Chung Chan, Ngai Sze Wong, Bonnie C.K. Wong, Jacky M.C. Chan, Shui Shan Lee

Author affiliations: The Chinese University of Hong Kong, Hong Kong, China (D.P.C. Chan, N.S. Wong, S.S. Lee); Department of Health, Hong Kong (B.C.K. Wong); Princess Margaret Hospital, Hong Kong (J.M.C. Chan)

DOI: https://doi.org/10.3201/eid2810.220691

In a cohort of persons living with HIV in Hong Kong, surrogate virus neutralization testing for COVID-19 yielded a median level of 89% after the third dose of an inactivated COVID-19 vaccine, compared with 37% after the second dose. These results support using a 3-dose primary series for enhanced immune protection.

Worldwide, inactivated vaccines are most widely used to prevent SARS-CoV-2 infection and severe COVID-19 disease (*1*). Vaccination effectiveness is of particular importance for protecting persons at increased risk for severe diseases, notably immunocompromised patients, including persons living with HIV (PLHIV). As recently reported in a prospective study in Brazil (*2*), immunogenicity of inactivated vaccine is lower in PLHIV than in healthy adults. This lower protection is a cause for concern, especially in populations with high burden of HIV/AIDS and COVID-19. In Hong Kong, both inactivated and mRNA vaccines are available free for all eligible healthy and immunocompromised citizens. Immunocompromised persons have been prioritized for receiving a third, booster, dose, 3 months after completion of a 2-dose series of any COVID-19 vaccine. In a real-world study conducted prospectively on PLHIV in Hong Kong, we measured vaccine immunogenicity by the surrogate virus neutralization test (sVNT) to compare the responses after completion of 2 versus 3 doses of CoronaVac (Sinovac, https://www.sinovac.com), the same inactivated vaccine used in the Brazil study (*2*). Based on antibody-mediated blockage of ACE2-spike receptor binding domain (RBD) interaction, the sVNT results were used to assess the amplitude of neutralizing antibody responses against SARS-CoV-2 (*3*,*4*).

During April 2021–March 2022, a total of 122 PLHIV who had received CoronaVac were enrolled at 2 major HIV specialist clinics providing comprehensive HIV care, including antiretroviral therapy, in Hong Kong. Participants provided informed consent. We measured sVNT after completion of 2 or 3 doses of CoronaVac, in addition to transcribing demographic and clinical data collected during routine clinical follow-up appointments (Appendix, https://wwwnc.cdc.gov/EID/article/28/10/22-0691-App1.pdf). The median age of recruited PLHIV was 49 (IQR 40–56.5) years of age; most (86%) were male, all were receiving antiretroviral therapy, and the median latest CD4 count was 564.5/μL (IQR 394–733/μL) (Appendix Table 1). We included in the analyses a total of 132 sVNT measurements made within 90 days (median 48 days, IQR 24–70 days) of the second and within 90 days (median 33 days, IQR 28–53 days) of the third dose. We expressed results as percentage inhibition, using a cutoff of 30% for positive neutralizing response.

The median sVNT level was 37% (IQR 24%–53%); 64% of participants tested positive (sVNT ≥30%) after the second dose. After the third dose, the median sVNT rose to 89% (IQR 58%–95%; Mann-Whitney U = 648.5;

p<0.001), paralleling a significantly higher percentage with sVNT positivity (91%; OR 5.67, 95% CI 1.86–17.33) (Figure). In multivariable linear regression, third-dose vaccination (B = 33.61; p<0.001), days past respective dose (B = −0.17; p = 0.047), and latest CD4 count (B = 0.02; p = 0.02) were significant factors associated with high sVNT, whereas viral load suppression (<200/mL) and age were not significant (Appendix Table 2).

Our immunogenicity results on the completion of a 2-dose schedule of CoronaVac in PLHIV were remarkably similar to those reported in Brazil (*2*). After 2 doses of CoronaVac, 28 PLHIV in Hong Kong had a median sVNT of 48% (IQR 30%–58%) after 27–55 days, compared with median sVNT of 46.2% (IQR 26.9%–69.7%) in Brazil after 41 days. The corresponding proportion of PLHIV with sVNT positivity (≥30%) was 79% after 27–55 days in our study and 71% after 41 days in the Brazil study.

Although effectiveness of inactivated COVID-19 vaccines has previously been shown in PLHIV (*5*), their moderate efficacy and waning immunogenicity after a standard 2-dose schedule pose challenges in developing vaccination strategy (*1*). Recent studies have demonstrated effectiveness and safety of 3 doses of inactivated COVID-19 vaccine in healthy adults (*6*). In this study, we have shown a stronger sVNT response after the third dose than the second dose, as has been reported for inactivated vaccines in healthy adults, including elderly persons (*6,7*). Our results provide data support for the effectiveness of a 3-dose primary series of inactivated COVID-19 vaccine for all vaccinees, including PLHIV and immunocompromised hosts.

The anticipated suboptimal clinical outcome for PLHIV after COVID-19 has been shown in population-level studies (*8*) that called for prioritizing PLHIV for vaccination. With a high proportion of the global population receiving inactivated COVID-19 vaccines, we note a need to strategically adjust the regimen to attain a sustained and enhanced response in PLHIV. Routine administration of a 3-dose primary series of inactivated vaccines is a possible approach for reducing virus transmission and associated severe disease in healthy adults and PLHIV alike, as highlighted in guidance from the World Health Organization Strategic Advisory Group of Experts on Immunization (https://www.who.int/publications/i/item/WHO-2019-nCoV-vaccines-SAGE_recommendation-Sinovac-CoronaVac-2021.1) and the Centers for Disease Control and Prevention (https://www.cdc.gov/hiv/basics/covid-19.html). Recent studies have shown that the effectiveness of current COVID-19 vaccines against new variants, such as Omicron, could be reduced; immunogenicity was lower after 2 doses of inactivated vaccines than of mRNA vaccines (*9*). Further research is needed as the COVID-19 pandemic continues to evolve; in particular, the ongoing Ubuntu trial (https://www.coronavirusprevention network.org) may provide evidence for enhancing vaccination strategy for PLHIV amid the emergence of new variants.

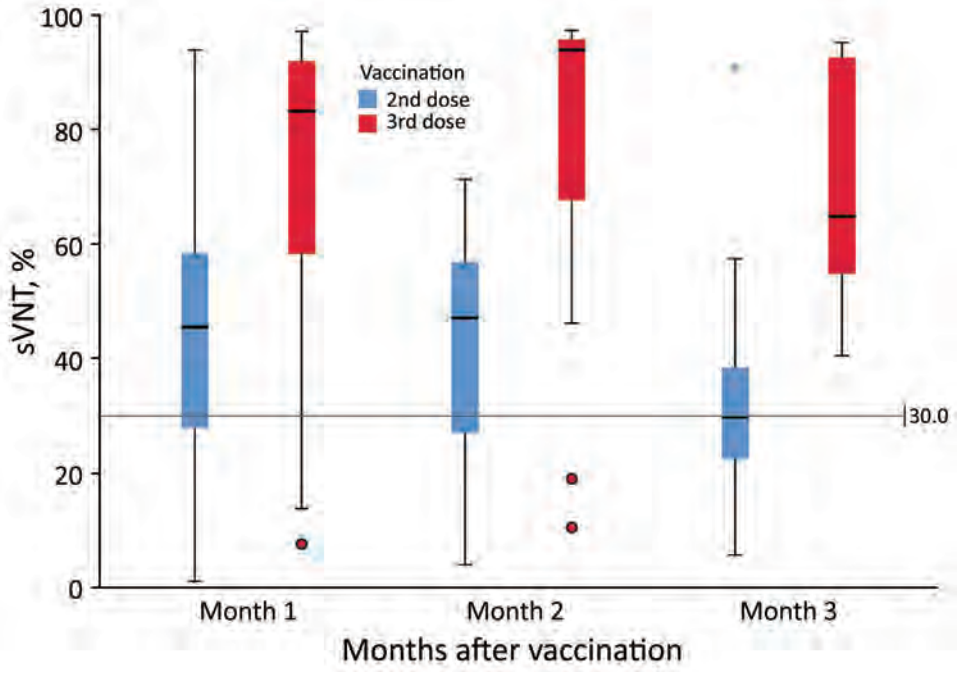

Figure. Distribution of sVNT by month after second and third doses of CoronaVac vaccine (Sinovac, https://www.sinovac.com) among persons living with HIV, Hong Kong. Horizontal lines inside boxes indicate medians, box tops and bottoms indicate 25th and 75th percentiles, and error bars indicate high and low values excluding outliers. Blue asterisk and red dots indicate outliers. Gray line indicates cutoff of 30% for positive neutralizing response. sVNT, surrogate virus neutralization test.

Acknowledgments

We thank the clinical team for assistance in recruitment, blood sampling, and data management. We thank Eric Poon and Samantha So for laboratory assistance.

This work was supported by Health and Medical Research Fund Commissioned Research on the Novel Coronavirus Disease (grant COVID1903008-Project A) and Council for the AIDS Trust Fund (grant MSS358R).

About the Author

Dr. Chan is a research fellow at the Chinese University of Hong Kong, Hong Kong, China. Her research interests include emerging viral infections and vaccine studies.

References

1. Mallapaty S. China's COVID vaccines have been crucial—now immunity is waning. Nature. 2021;598:398–9. https://doi.org/10.1038/d41586-021-02796-w
2. Netto LC, Ibrahim KY, Picone CM, Alves APPS, Aniceto EV, Santiago MR, et al. Safety and immunogenicity of CoronaVac in people living with HIV: a prospective cohort study. Lancet HIV. 2022; 9:e323–31. https://doi.org/10.1016/S2352-3018(22)00033-9
3. Tan CW, Chia WN, Qin X, Liu P, Chen MI, Tiu C, et al. A SARS-CoV-2 surrogate virus neutralization test based on antibody-mediated blockage of ACE2-spike protein-protein interaction. Nat Biotechnol. 2020;38:1073–8. https://doi.org/10.1038/s41587-020-0631-z
4. Wong NS, Wong BCK, Chan JMC, Wong KH, Tsang OTY, Mok CKP, et al. Surrogate neutralization responses following severe acute respiratory syndrome coronavirus 2 vaccination in people with HIV: comparison between inactivated and mRNA vaccine. AIDS. 2022;36:1255–64. https://doi.org/10.1097/QAD.0000000000003237
5. Feng Y, Zhang Y, He Z, Huang H, Tian X, Wang G, et al. Immunogenicity of an inactivated SARS-CoV-2 vaccine in people living with HIV-1: a non-randomized cohort study. EClinicalMedicine. 2022;43:101226. https://doi.org/10.1016/j.eclinm.2021.101226
6. Zeng G, Wu Q, Pan H, Li M, Yang J, Wang L, et al. Immunogenicity and safety of a third dose of CoronaVac, and immune persistence of a two-dose schedule, in healthy adults: interim results from two single-centre, double-blind, randomised, placebo-controlled phase 2 clinical trials. Lancet Infect Dis. 2022;22:483–95. https://doi.org/10.1016/S1473-3099(21)00681-2
7. Liang XM, Xu QY, Jia ZJ, Wu MJ, Liu YY, Lin LR, et al. A third dose of an inactivated vaccine dramatically increased the levels and decay times of anti-SARS-CoV-2 antibodies, but disappointingly declined again: a prospective, longitudinal, cohort study at 18 serial time points over 368 days. Front Immunol. 2022;13:876037. https://doi.org/10.3389/fimmu.2022.876037
8. Boffito M, Waters L. More evidence for worse COVID-19 outcomes in people with HIV. Lancet HIV. 2021;8:e661–2. PubMed https://doi.org/10.1016/S2352-3018(21)00272-1
9. Cheng SMS, Mok CKP, Leung YWY, Ng SS, Chan KCK, Ko FW, et al. Neutralizing antibodies against the SARS-CoV-2 Omicron variant BA.1 following homologous and heterologous CoronaVac or BNT162b2 vaccination. Nat Med. 2022;28:486–9. PubMed https://doi.org/10.1038/s41591-022-01704-7

Address for correspondence: Shui Shan Lee, Stanley Ho Centre for Emerging Infectious Diseases, Postgraduate Education Centre, Prince of Wales Hospital, Shatin, Hong Kong, China; email: sslee@cuhk.edu.hk

Rickettsial Infections Causing Acute Febrile Illness in Urban Slums, Brazil

John B. Fournier,[1] Lucas S. Blanton,[1] Nivison Nery Jr., Elsio A. Wunder Jr., Federico Costa, Mitermayer G. Reis, Guilherme S. Ribeiro, David H. Walker, Albert I. Ko

Author affiliations: Yale School of Public Health, New Haven, Connecticut, USA (J.B. Fournier, E.A. Wunder Jr., F. Costa, M.G. Reis, A.I. Ko); University of Texas Medical Branch, Galveston, Texas, USA (L.S. Blanton, D.H. Walker); Fundação Oswaldo Cruz, Salvador, Brazil (N. Nery Jr., F. Costa, M.G. Reis, G.S. Ribeiro, A.I. Ko); Universidade Federal da Bahia, Salvador (N. Nery Jr., F. Costa, M.G. Reis, G.S. Ribeiro)

DOI: https://doi.org/10.3201/eid2810.220497

We conducted enhanced acute febrile illness surveillance in an urban slum community in Salvador, Brazil. We found that rickettsial infection accounted for 3.5% of urgent care visits for acute fever. Our results suggest that rickettsiae might be an underrecognized, treatable cause of acute febrile illness in impoverished urban populations in Brazil.

Rickettsia spp. are small, obligately intracellular, gram-negative bacilli. The genus includes the spotted fever group rickettsiae (SFGR) and typhus group rickettsiae (TGR). SFGR and TGR are underrecognized causes of acute febrile illness (AFI) worldwide, particularly in the tropics, because clinical manifestations of rickettsial infections are often indistinguishable from those of other endemic infections (*1*). Recent studies have suggested that SFGR profiles in Brazil might be shifting toward

[1]These authors contributed equally to this article.

an increasing number of cases in urban areas (*2*). However, knowledge of whether rickettsiae cause AFI in urban settings is limited, especially in informal settlements where social determinants and the presence of potential vectors and reservoirs might favor transmission. Rickettsiae-mediated AFI has considerable public health and therapeutic implications because prompt administration of targeted antimicrobial therapy can reduce illness and death associated with rickettsioses (*3*).

To evaluate whether rickettsial infections might be a potential cause of AFI in an urban slum setting, we performed enhanced surveillance from April 1, 2009, through October 31, 2012, in a public sector urgent care facility that served a community of ≈55,000 inhabitants in Salvador, Brazil (*4*). We identified and enrolled eligible outpatients who were ≥5 years of age and had a measured (>37.8°C) or reported fever of <21 days duration. We collected blood samples during the acute phase at the time of enrollment and during the convalescent phase ≥15 days later. We screened serum samples at an initial dilution of 1:64 using a rickettsial immunofluorescence assay in which the *Rickettsia rickettsii* Sheila Smith strain was used to determine SFGR IgG reactivity, and *R. typhi* Wilmington strain was used to determine TGR IgG reactivity. Laboratory-confirmed rickettsial infections were defined as seroconversion (negative acute-phase titer and convalescent-phase titer of ≥128) or a 4-fold increase in titer between acute- and convalescent-phase samples. We detected dengue viral infections using DENV reverse transcription PCR, Panbio Dengue Early ELISA (NS1 antigen-capture), and Bioline Dengue IgM-capture ELISA (Abbott Laboratories, https://www.abbott.com) (*5*,*6*) and leptospirosis using the microscopic agglutination test (*7*). The study was approved by the Oswaldo Cruz Foundation Committee on Ethics in Research, Brazilian National Council for Ethics in Research, and Yale University Institutional Review Board.

Among 5,035 enrolled patients with AFI, 1,016 (20.2%, 95% CI 19.1%–21.3%) had confirmed dengue and 137 (2.7%, 95% CI 2.3%–3.2%) had confirmed leptospirosis. Among the 3,882 patients who did not have dengue or leptospirosis, 1,016 (26.2%) did not fulfill criteria for an influenza-like illness (temperature ≥37.8°C, reported fever and cough, or sore throat for ≤7 days), and these patients provided acute- and convalescent-phase serum samples. We used a random number generator to select 200 patients from the 1,016 participants whose samples were evaluated in the rickettsial immunofluorescence assay. Of those 200 patients, we identified 6 (3.0%, 95% CI 1.4%–6.4%) patients who had SFGR-positive serum samples and 1 (0.5%, 95% CI 0.0%–2.8%) patient who had a TGR-positive serum sample (Table).

Patients who had SFGR- and TGR-positive samples were 6–42 years of age, and 5 of the 7 patients were women. All 7 patients had measured (>37.8°C) or reported fever, 6 of 7 patients reported headaches, and 5 of 7 patients reported myalgia. Patients did not report a rash (Table). The 7 patients attended the urgent care facility 1–10 days after the onset of symptoms and had mild self-limiting illnesses. Those patients did not receive antimicrobial therapy or require hospitalization; symptoms resolved within 30 days of onset.

Identifying rickettsial infections among patients attending an urgent care facility in an urban center in Brazil is noteworthy because rickettsiae have not previously been described as a substantial cause of AFI in urban populations in this country. Of note, the immunofluorescence assay used is unable to differentiate among *Rickettsia* spp. *R. rickettsii* is a well-described

Table. Clinical characteristics of 7 patients and IFA serum titers for SFGR or TGR IgG reactivity in study of rickettsial infections causing acute febrile illness in urban slums, Brazil*

Patient no.	Age, y/sex	Symptoms	Duration of illness, d†	Antigen (group)	IFA titers	
					Acute phase‡	Convalescent phase§
1	10/F	Fever, headache, myalgia	6	*R. rickettsii* (SFGR)	0	256
2	21/F	Fever, headache, myalgia	1	*R. rickettsii* (SFGR)	0	256
3	42/F	Fever, headache, myalgia, lethargy, diarrhea	3	*R. rickettsii* (SFGR)	0	256
4	6/M	Fever, headache, myalgia, lethargy, vomiting, diarrhea	10	*R. rickettsii* (SFGR)	0	128
5	8/F	Fever, headache, myalgia, fatigue, vomiting, diarrhea	6	*R. rickettsii* (SFGR)	0	256
6	12/M	Fever, headache	1	*R. rickettsii* (SFGR)	128	512
7	6/F	Fever, lethargy, diarrhea	5	*R. typhi* (TGR)	0	256

**Rickettsia rickettsii* Sheila Smith strain was used to determine SFGR IgG reactivity and *R. typhi* Wilmington strain was used to determine TGR IgG reactivity. IFA, immunofluorescence assay; SFGR, spotted fever group rickettsiae; TGR, typhus group rickettsiae.
†Number of days of illness before attending urgent care facility in Salvador, Brazil.
‡Acute-phase serum samples were obtained at the time of enrollment when the patient arrived initially at the urgent care facility.
§Convalescent-phase serum samples were obtained ≥15 d after enrollment in the study.

cause of spotted fever in Brazil in rural settings, and *R. parkeri* is an emerging cause of infection (*8*–*10*). Antibodies that are cross-reactive with *R. rickettsii* can be stimulated by *R. parkeri*, *R. akari*, and other SFGR. *R. typhi* has been rarely reported as a cause of AFI in urban settings. Other rickettsial species identified in Brazil are *R. felis*, *R. rhipicephali*, *R. bellii*, *R. amblyommatis*, *R. andeanae*, and *R. monteiroi*, although their pathogenicity is unclear (*10*).

Although all causative rickettsial species, potential vectors, and reservoirs have yet to be identified, this study suggests that rickettsiae might be a cause of AFI in urban slum settings in Brazil. A limitation of this study is that it was performed in a single urban center; further studies will be needed to confirm the generalizability of these findings. However, these findings raise clinical awareness for rickettsiae as a potential cause of AFI in urban slum populations in the tropics and the possible need for empiric antimicrobial therapy in suspected cases, especially because diagnostic testing is often lacking in these urban environments.

This work was supported by the National Institutes of Health (grant nos. T32 AI007517, R01 AI121207, R25 TW009338, U01 AI088752, and R01 AI052473), the Brazilian National Council for Scientific and Technological Development (CNPq nos. 550160/2010-8, 307450/2017-1, and 311365/2021-3), and the Bahia Foundation for Research Support (FAPESB no. PNX0010/2011).

About the Author

Dr. Fournier is a 4th-year clinical and research infectious disease fellow at Yale University. His primary research interests focus on emerging tropical infections.

References

1. Blanton LS. The rickettsioses: a practical update. Infect Dis Clin North Am. 2019;33:213–29. https://doi.org/10.1016/j.idc.2018.10.010
2. Montenegro DC, Bitencourth K, de Oliveira SV, Borsoi AP, Cardoso KM, Sousa MSB, et al. Spotted fever: epidemiology and vector-*Rickettsia*-host relationship in Rio de Janeiro state. Front Microbiol. 2017;8:505. https://doi.org/10.3389/fmicb.2017.00505
3. Gudiol F, Pallares R, Carratala J, Bolao F, Ariza J, Rufi G, et al. Randomized double-blind evaluation of ciprofloxacin and doxycycline for Mediterranean spotted fever. Antimicrob Agents Chemother. 1989;33:987–8. https://doi.org/10.1128/AAC.33.6.987
4. Hagan JE, Moraga P, Costa F, Capian N, Ribeiro GS, Wunder EA Jr, et al. Spatiotemporal determinants of urban leptospirosis transmission: four-year prospective cohort study of slum residents in Brazil. PLoS Negl Trop Dis. 2016;10:e0004275. https://doi.org/10.1371/journal.pntd.0004275
5. Silva MMO, Tauro LB, Kikuti M, Anjos RO, Santos VC, Gonçalves TSF, et al. Concomitant transmission of dengue, chikungunya, and Zika viruses in Brazil: clinical and epidemiological findings from surveillance for acute febrile illness. Clin Infect Dis. 2019;69:1353–9. https://doi.org/10.1093/cid/ciy1083
6. Silva MMO, Rodrigues MS, Paploski IAD, Kikuti M, Kasper AM, Cruz JS, et al. Accuracy of dengue reporting by national surveillance system, Brazil. Emerg Infect Dis. 2016;22:336–9. https://doi.org/10.3201/eid2202.150495
7. Ko AI, Galvão Reis M, Ribeiro Dourado CM, Johnson WD Jr, Riley LW; Salvador Leptospirosis Study Group. Urban epidemic of severe leptospirosis in Brazil. Lancet. 1999;354:820–5. https://doi.org/10.1016/S0140-6736(99)80012-9
8. Silva N, Eremeeva ME, Rozental T, Ribeiro GS, Paddock CD, Ramos EAG, et al. Eschar-associated spotted fever rickettsiosis, Bahia, Brazil. Emerg Infect Dis. 2011;17:275–8. https://doi.org/10.3201/eid1702.100859
9. Weck B, Dall'Agnol B, Souza U, Webster A, Stenzel B, Klafke G, et al. Spotted fever group *Rickettsia* in the Pampa biome, Brazil, 2015–2016. Emerg Infect Dis. 2016;22:2014–6. https://doi.org/10.3201/eid2211.160859
10. Labruna MB, Mattar V S, Nava S, Bermudez S, Venzal JM, Dolz G, et al. Rickettsioses in Latin America, Caribbean, Spain and Portugal. Rev MVZ Córdoba. 2011;16:2435–57. https://doi.org/10.21897/rmvz.282

Address for correspondence: Albert I. Ko, Yale School of Public Health, 60 College St, New Haven, CT 06510, USA; email: albert.ko@yale.edu

Identifying Contact Risks for SARS-CoV-2 Transmission to Healthcare Workers during Outbreak on COVID-19 Ward

Marius Zeeb,[1] Dana Weissberg,[1] Silvana K. Rampini, Rouven Müller, Thomas Scheier, Walter Zingg, Roger D. Kouyos,[2] Aline Wolfensberger[2]

Author affiliations: University Hospital Zurich and University of Zurich, Zurich, Switzerland (M. Zeeb, D. Weissberg, S.K. Rampini, R. Müller, T. Scheier, W. Zingg, R.D. Kouyos, A. Wolfensberger); Institute of Medical Virology, Zurich, Switzerland (M. Zeeb, R.D. Kouyos)

DOI: https://doi.org/10.3201/eid2810.220266

[1]These first authors contributed equally to this article.
[2]These senior authors contributed equally to this article.

We assessed the risk for different exposures to SARS-CoV-2 during a COVID-19 outbreak among healthcare workers on a hospital ward in late 2020. We found working with isolated COVID-19 patients did not increase the risk of COVID-19 among workers, but working shifts with presymptomatic healthcare coworkers did.

One study found SARS-CoV-2 seroprevalence to be higher among healthcare workers (HCWs) with patient contact than among those without (*1*), but another study found that HCWs were less likely to acquire SARS-CoV-2 from patients than from coworkers or someone outside the hospital (*2*). We investigated a COVID-19 outbreak in a 26-bed hospital ward with 50 HCWs in Switzerland during October–November 2020, the peak of the second COVID-19 wave. During the 43-day outbreak period, transmission chains could not be reconstructed epidemiologically or phylogenetically. Instead, we used statistical modeling to assess and compare patients and coworkers as potential sources for COVID-19 among HCWs.

At all times, HCWs were to observe universal masking and social distancing protocols and regularly disinfect mutually used surfaces. HCWs also were to observe standard precaution measures (SPMs) for all patient contacts: wearing surgical masks at all times, eyewear when approaching a patient, and FFP2 (filtering facepiece) respirator masks during aerosol-generating procedures or prolonged contact with a patient with respiratory symptoms. For contact with patients with confirmed COVID-19, HCWs were to observe isolation precaution measures (IPMs), which, in addition to SPMs, meant wearing single-use gowns and disposing of personal protective equipment immediately after use. All patients were to wear masks when leaving bed and, starting in November 2020, when in contact with HCWs.

We assessed 3 possible risk factors as routes of exposure for HCWs: caring for contagious patients, stratified by whether using IPM or SPM when in contact with contagious patients, and working shifts during the contagious period of coworkers later found to have COVID-19. We defined the contagious period of a person with COVID-19 as the 48 hours before symptom onset, or a positive test if asymptomatic, until at least 14 days after sign/symptom onset or 2 days after signs/symptoms ended, whichever was later. HCWs were tested if symptomatic or during a staff screening on day 31 of the outbreak.

We assumed that transmission occurred 2–10 days before symptom onset or a positive test and calculated exposure risk scores for a given day and contact type. Exposure risk scores per contact type equaled mean numbers of patient contacts when using IPM, patient contacts when using SPM, and contacts with contagious HCWs per day (Appendix Figure 1, https://wwwnc.cdc.gov/EID/article/28/10/22-0266-App1.pdf). We included all HCW workdays during the outbreak except days worked after HCWs recovered from COVID-19. To calculate hazard ratios, we used time-updated univariable and multivariable Cox proportional-hazards models with time to COVID-19 as the outcome and exposure risk scores as predictors. We also performed a sensitivity analysis for presence or absence on the ward.

Because our analyses were part of an outbreak investigation, the Zurich Cantonal Ethics Commission waived formal ethical evaluation (Req 2021–00098). The 12 COVID-positive patients in the hospital ward were also part of a 1,118-patient study about nosocomial COVID-19 incidence in a tertiary care center (*3*).

We found that 18/50 (38%) HCWs had COVID-19 during the study period. For the 12 patients with COVID-19 on the ward, IPM were used for 11, SPM were used for 7 of those patients until diagnosis was made; 1 patient was diagnosed only after being discharged (Table). Univariable and multivariable models indicated that COVID-19 infection among HCWs working on the ward was associated with shifts worked with coworkers subsequently found to be ill (Figure), supporting results of other studies (*4*–*6*).

Our results suggested no strong association between COVID-19 in HCWs and using IPM during patient contact. Sufficiently available personal protective equipment, intensive training, and routine safety practices in handling COVID-19 patients may explain this finding. Caring for COVID-19 patients when using SPM was associated with SARS-CoV-2 infection,

Table. Number of different exposures to SARS-CoV-2 for total HCW population, HCW who tested positive, and HCW who tested negative during outbreak in hospital ward, Switzerland, October–November 2020*

Type of contact	No. (%) HCWs		
	All	SARS-CoV-2–positive	SARS-CoV-2–negative
All contacts	50 (100)	18 (36)	32 (64)
Shifts with patient contact using SPM	69 (13.9)	24 (20.2)	45 (11.9)
Shifts with patient contact using IPM	143 (28.8)	31 (26.1)	112 (29.7)
Shifts with HCW contact	284 (57.3)	64 (53.8)	220 (58.4)

*IPM, isolation precaution measure; SPM, standard precaution measure; HCW, healthcare worker.

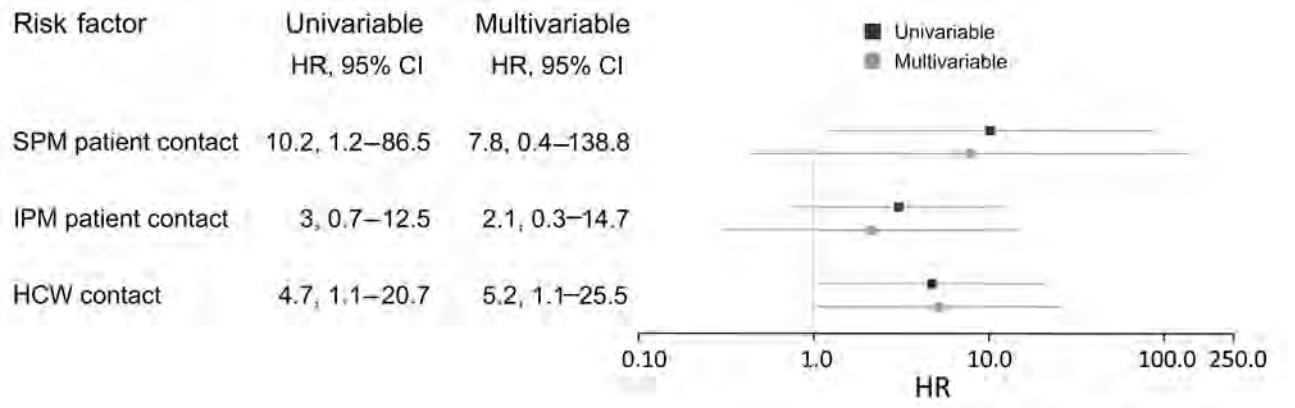

Figure. Hazard ratios and the 95% CIs for HCWs to acquire SARS-CoV-2 after using SPM and IPM for patient contact and HCW contact (i.e., contact with positive HCWs) during COVID-19 outbreak in hospital ward, Switzerland, October–November 2020. The multivariable model combined patient contact using SPM and IPM and HCW contact. HCW, healthcare worker; HR, hazard ratio; IPM, isolation precaution measures; SPM, standard precaution measures.

although only in the univariable model, pointing to a potential risk (*7*). However, we could only speculate whether our finding of increased risk resulted from the concept of SPM or as it was implemented. IPM might add extra layers of safety not only through its added protective elements but also by sensitizing HCWs to the heightened need to take precautionary measures; further investigation is needed. Ward contact, accounting for social work interactions including but not limited to those previously mentioned, showed increased SARS-CoV-2 transmission risk (Appendix Figure 2). HCWs were to wear masks, keep distance, and disinfect mutually used surfaces, but we assume full compliance at all times is unlikely. Also, social contact among peers before and after work, which might favor SARS-CoV-2 transmission, was unknown.

Two study limitations were small sample size and lack of data from exposures outside the hospital. However, applied statistical methods enabled us to investigate and identify transmission risks. Like others (*8*), we are confident that these findings provide critical information for design and adjustment of SPM and IPM during the COVID-19 pandemic. In addition, applying our methods to larger, nonoutbreak settings might be worthwhile. More detailed weighting of specific risks taking into account distribution of incubation time (*9*) might improve estimates of transmission risk in larger studies.

In conclusion, we provide additional evidence for SARS-CoV-2 infection risk for HCWs in contact with contagious coworkers and patients using SPM. Our findings highlight the importance of choosing protective equipment wisely and strictly adhering to safety protocols, including SPM.

About the Author

Mr. Zeeb is working on his PhD degree at the University of Zurich. His primary research interests are the epidemiology and genomics of infectious diseases, in particular HIV. Ms. Weissberg is a fellow in the Division of Infectious Diseases and Hospital Epidemiology at the University Hospital of Zurich, Switzerland. Her research focuses on infection control and prevention.

References

1. Rudberg AS, Havervall S, Månberg A, Jernbom Falk A, Aguilera K, Ng H, et al. SARS-CoV-2 exposure, symptoms and seroprevalence in healthcare workers in Sweden. Nat Commun. 2020;11:5064. https://doi.org/10.1038/s41467-020-18848-0
2. Braun KM, Moreno GK, Buys A, Somsen ED, Bobholz M, Accola MA, et al. Viral sequencing to investigate sources of SARS-CoV-2 infection in US healthcare personnel. Clin Infect Dis. 2021;73:e1329–36. PubMed https://doi.org/10.1093/cid/ciab281
3. Wolfensberger A, Kufner V, Zaheri M, Zeeb M, Nortes I, Schreiber PW, et al. Nosocomial COVID-19 in a tertiary care center—incidence and secondary attack rates in patients after in-hospital exposure. Emerg Infect Dis. In press 2022.
4. Çelebi G, Pişkin N, Çelik Bekleviç A, Altunay Y, Salcı Keleş A, Tüz MA, et al. Specific risk factors for SARS-CoV-2 transmission among health care workers in a university hospital. Am J Infect Control. 2020;48:1225–30. https://doi.org/10.1016/j.ajic.2020.07.039
5. Ariza-Heredia EJ, Frenzel E, Cantu S, Carlson M, Thomas G, Khawaja F, et al. Surveillance and identification of clusters of healthcare workers with coronavirus disease 2019 (COVID-19): multidimensional interventions at a comprehensive cancer center. Infect Control Hosp Epidemiol. 2021;42:797–802. https://doi.org/10.1017/ice.2020.1315
6. Gordon CL, Trubiano JA, Holmes NE, Chua KYL, Feldman J, Young G, et al. Staff to staff transmission as a driver of healthcare worker infections with COVID-19. Infect Dis Health. 2021;26:276–83. https://doi.org/10.1016/j.idh.2021.06.003

7. He X, Lau EHY, Wu P, Deng X, Wang J, Hao X, et al. Temporal dynamics in viral shedding and transmissibility of COVID-19. Nat Med. 2020;26:672–5. https://doi.org/10.1038/s41591-020-0869-5
8. Abbas M, Robalo Nunes T, Martischang R, Zingg W, Iten A, Pittet D, et al. Nosocomial transmission and outbreaks of coronavirus disease 2019: the need to protect both patients and healthcare workers. Antimicrob Resist Infect Control. 2021;10:7. https://doi.org/10.1186/s13756-020-00875-7
9. McAloon CG, Wall P, Griffin J, Casey M, Barber A, Codd M, et al. Estimation of the serial interval and proportion of pre-symptomatic transmission events of COVID-19 in Ireland using contact tracing data. BMC Public Health. 2021;21:805. https://doi.org/10.1186/s12889-021-10868-9

Address for correspondence: Marius Zeeb, Division of Infectious Diseases and Hospital Epidemiology, University Hospital Zurich, University of Zurich, Rämistrasse 100 CH-8091 Zurich, Switzerland; email: marius.zeeb@usz.ch

Sindbis Virus Antibody Seroprevalence in Central Plateau Populations, South Africa

Nicole Kennedy, Dominique Goedhals, Sabeehah Vawda, Philip Armand Bester, Felicity Burt

Author affiliations: University of the Free State, Bloemfontein, South Africa (N. Kennedy, D. Goedhals, S. Vawda, P.A. Bester, F. Burt); National Health Laboratory Service, Bloemfontein, South Africa (D. Goedhals, S. Vawda, P.A. Bester, F. Burt)

DOI: https://doi.org/10.3201/eid2810.211798

We report a higher percentage of Sindbis virus-specific IgG in serum from patients attending a rheumatology clinic (18.8%) compared with healthy residents (9.6%) and patients with acute febrile illness (9.4%) in Free State Province, South Africa. Sindbis virus infection should be considered a potential cause of arthritis in South Africa.

Sindbis virus (SINV) is a mosquitoborne virus that belongs to the Togaviridae family; SINV is considered an arthritogenic alphavirus, which is known to cause self-limiting acute febrile illness (AFI) in Africa, Australia, Asia, and Europe and occasional debilitating arthritis that can persist for years after infection (*1*). Outbreaks are associated with heavy rainfall and temperature changes that favor mosquito breeding. Associations between SINV infection and acute or chronic arthralgia and myalgia have been described in Finland and Sweden (*2*,*3*). The extent of chronic debilitating disease caused by SINV in South Africa remains largely unknown.

SINV was identified as a cause of human disease in South Africa in 1963, and subsequent studies confirmed that the virus was present in mosquito populations in the central plateau region, which includes Free State Province (*4*). We investigated the seroprevalence of SINV in selected human populations of Free State Province. We used an in-house ELISA to detect SINV-specific IgG in serum and confirmed positive serum samples using neutralization assays (Appendix, https://wwwnc.cdc.gov/EID/article/28/10/21-1798-App1.pdf). We screened a total of 568 stored serum samples retrospectively and anonymously. All available stored samples were tested and included 165 serum specimens submitted to the Division of Virology, National Health Laboratory Service, for routine clinical pathology tests from patients who attended the rheumatology clinic at the Universitas Hospital, Bloemfontein, South Africa, during 2013–2017 and 267 serum samples submitted to the National Health Laboratory Service during 2008–2010 from patients with AFI and no confirmed diagnosis. No clinical data were available; however, most attendees at the rheumatology clinic had chronic arthritis. We also included 136 serum samples from healthy volunteers that were collected during 2016–2017 for seroepidemiology studies of Crimean-Congo hemorrhagic fever virus and other vectorborne diseases.

We confirmed 11 serum samples were negative for SINV antibodies using a commercial immunofluorescence assay (EuroImmun, https://www.euroimmun.com); these samples were used to determine ELISA cutoff values. Positive control serum was obtained from 1 patient who had a laboratory-confirmed SINV infection. We obtained institutional ethics approval for this study from the Health Sciences Research Ethics Committee, University of the Free State (HSREC approval no. 95/2016C), and informed consent was available for samples collected for the seroepidemiology study (HSREC approval no. 34/2016), negative control serum panel (approval no. ETOVS 152/06), and positive control (approval no. ETOVS 118/06).

We determined optimal reagent dilutions for the ELISA using checkerboard titrations. We diluted serum samples 1:100 and tested for reactions to SINV-

Table. Sindbis virus–specific IgG and neutralizing antibodies in patient serum samples in study of Sindbis virus antibody seroprevalence in central plateau populations, South Africa*

Patient group	Collection period, y	Patient samples			
		No. IgG+/no. tested per group (%)	% IgG+ of total tested	No. IgG+/total IgG+ (%)	No. NA+/no. IgG+ tested
Patients attending rheumatology clinic	2013–2017	31/165 (18.8)	5.5	31/69 (44.9)	29/31
High-risk populations†	2016–2017	13/136 (9.6)	2.3	13/69 (18.8)	13/13
Patients with AFI, no diagnosis	2007– 2010	25/267 (9.4)	4.4	25/69 (36.2)	23/25
Total no. patients		69/568	12.2		65/69

*We used an in-house ELISA to measure Sindbis virus–specific IgG and a 50% tissue culture infectious dose serum neutralization assay to measure Sindbis virus neutralizing antibodies in patient serum samples. AFI, acute febrile illness; NA, neutralizing antibody; +, positive.
†Residents of Sindbis virus-endemic regions.

specific and mock antigens (Appendix). We detected reactions using horse radish peroxidase-conjugated antihuman IgG (1:8000) and 2,2′-azino-di-3-ethylbenzthiazoline-6-sulfonate (SeraCare Life Sciences, https://www.seracare.com). We measured optical density (OD) values at 405 nm and calculated net OD values by subtracting each sample OD obtained with mock antigen from the OD value obtained with SINV antigen. To normalize data, percent positivity (PP) for each sample was calculated as PP = (mean net sample OD ÷ mean net OD of the positive control) × 100.

We used the mean PP value ±2 SD for 11 SINV-negative serum samples derived from a total of 83 replicates to determine the cutoff value between positive and negative samples (Appendix). We tested SINV antibody-positive serum samples for neutralizing antibodies using a 50% tissue culture infectious dose serum neutralization assay; samples were considered positive for neutralizing antibodies if the titer was $\geq \log_{10}$ 1.0, equal to a serum dilution ≥1:10 (*5*).

We detected SINV antibodies in 31/165 (18.8%) serum samples from patients who attended the rheumatology clinic, 13/136 (9.6%) samples from residents of SINV-endemic regions (high risk), and 25/267 (9.4%) samples from patients with AFI but no diagnosis (Table). Of the total number of SINV-positive samples, ≈45% of the samples were from patients who attended the rheumatology clinic (Table). We detected neutralizing antibodies with endpoint titers ranging from 1:20 to ≥1:640 in 65 of 69 SINV antibody-positive serum samples; 4 samples showed discordant results.

SINV seroprevalence in South Africa for 2006–2009 was 5.4% and increased to 12% after heavy rainfalls in 2010 (*6*). A 9.4%–9.6% seroprevalence in persons at high risk and for febrile patients is within an expected range, considering that the samples were collected over a 10-year period during which substantial rainfall in Free State Province was associated with arbovirus outbreaks (*7*,*8*). Rheumatology clinic attendees had the highest percentage (18.8%) of samples with SINV-specific IgG, compared with 9.4% for residents from SINV-endemic regions and 9.6% for patients with AFI. However, limitations exist when comparing cohorts collected at different time points, and undetected outbreaks might have been responsible for higher seroprevalence among the rheumatology clinic patients. Prospective studies in national tertiary or specialist healthcare clinics should elucidate the contribution of viral infections to chronic arthritis. Our results suggest that associations between SINV infections and arthritis have been underreported in South Africa, and SINV infection should be considered a potential cause of arthritis in this country.

This study was supported by funds from the South African Research Chair in Vectorborne and Zoonotic Diseases (grant no. 98346), which was hosted by the University of the Free State, funded by the Department of Science and Technology, and administered by the National Research Foundation.

About the Author

Ms. Kennedy is a postgraduate student in the Division of Virology, University of the Free State, Bloemfontein, South Africa. Her research interests focus on arboviruses and the public health implications of arboviral infections.

References

1. Adams MJ, Lefkowitz EJ, King AMQ, Harrach B, Harrison RL, Knowles NJ, et al. Changes to taxonomy and the International Code of Virus Classification and Nomenclature ratified by the International Committee on Taxonomy of Viruses (2017). Arch Virol. 2017;162:2505–38. https://doi.org/10.1007/s00705-017-3358-5
2. Kurkela S, Helve T, Vaheri A, Vapalahti O. Arthritis and arthralgia three years after Sindbis virus infection: clinical follow-up of a cohort of 49 patients. Scand J Infect Dis. 2008;40:167–73. https://doi.org/10.1080/00365540701586996
3. Gylfe Å, Ribers Å, Forsman O, Bucht G, Alenius GM, Wållberg-Jonsson S, et al. Mosquitoborne Sindbis virus infection and long-term illness. Emerg Infect Dis. 2018;24:1141–2. https://doi.org/10.3201/eid2406.170892
4. Jupp PG, Blackburn NK, Thompson DL, Meenehan GM. Sindbis and West Nile virus infections in the Witwatersrand-Pretoria region. S Afr Med J. 1986;70:218–20.
5. Pearce MC, Venter M, Schouwstra T, Van Eeden C, Jansen van Vuren P, Paweska J, et al. Serum neutralising antibody response of seronegative horses against lineage 1 and lineage 2 West Nile virus following vaccination with an

inactivated lineage 1 West Nile virus vaccine. J S Afr Vet Assoc. 2013;84:1–4. https://doi.org/10.4102/jsava.v84i1.1052
6. Storm N, Weyer J, Markotter W, Kemp A, Leman PA, Dermaux-Msimang V, et al. Human cases of Sindbis fever in South Africa, 2006–2010. Epidemiol Infect. 2014;142:234–8. https://doi.org/10.1017/S0950268813000964
7. Archer BN, Thomas J, Weyer J, Cengimbo A, Landoh DE, Jacobs C, et al. Epidemiologic investigations into outbreaks of Rift Valley fever in humans, South Africa, 2008–2011. Emerg Infect Dis. 2013;19:1918–25. https://doi.org/10.3201/eid1912.121527
8. Weyer J, Thomas J, Leman PA, Grobbelaar AA, Kemp A, Paweska JT. Human cases of Wesselsbron disease, South Africa 2010–2011. Vector Borne Zoonotic Dis. 2013;13:330–6. https://doi.org/10.1089/vbz.2012.1181

Address for correspondence: Felicity Burt, Division of Virology, Faculty of Health Sciences, National Health Laboratory Service and University of the Free State, Bloemfontein, 9301, South Africa; email: burtfj@ufs.ac.za

Corrections

Vol. 27, No. 3

The name of author Tróndur Høgnason Mohr was misspelled in Epidemiology and Clinical Course of First Wave Coronavirus Disease Cases, Faroe Islands (M.F. Kristiansen et al.). The article has been corrected online (https://wwwnc.cdc.gov/EID/article/27/3/20-2589_article).

Vol. 28, No. 8

The Figure legend has been corrected to refer to case counts by category in Incidence of Nontuberculous Mycobacterial Pulmonary Infection, by Ethnic Group, Hawaii, USA, 2005–2019 (R.A. Blakney et al.). The article has been corrected online (https://wwwnc.cdc.gov/EID/article/28/8/21-2375_article).

Vol. 26, No. 9

The descriptions in the Acknowledgments have been expanded and updated for Sequestration and Destruction of Rinderpest Virus–Containing Material 10 Years after Eradication (C.M. Budke et al.). The article has been corrected online (https://wwwnc.cdc.gov/EID/article/28/9/22-0297_article).

Forgotten People, Forgotten Diseases: The Neglected Tropical Diseases and Their Impact on Global Health and Development

Peter J. Hotez

John Wiley & Sons, Hoboken, NJ, USA, 2021;ISBN: 9781683673897 (eBook); ISBN: 9781683673873 (print); ISBN-10: 9781555818746; ISBN-13: 978-1555818746; Pages: 256; Price: US $38.00 (eBook), US $46.99 (paperback)

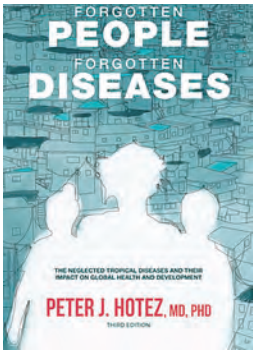

Forgotten People, Forgotten Diseases by Peter J. Hotez provides an overview of neglected tropical diseases (NTDs) that affect marginalized communities. NTDs are major global burdens but receive limited attention from researchers, policymakers, and funding agencies. Dr. Hotez is working to change this paradigm. He is a professor in the Departments of Pediatrics and Molecular Virology and Microbiology at Baylor College of Medicine, Houston, Texas; founding dean of the National School of Tropical Medicine at Baylor; and former president of the American Society for Tropical Medicine and Hygiene. Dr. Hotez shares his expertise in this clear and accessible text.

This book begins by introducing the geographic distribution of NTDs and features that make these diseases stigmatizing, poverty-promoting, chronic, and often disabling. In subsequent chapters, Dr. Hotez addresses groups of related tropical diseases, such as soil transmitted helminths (Chapter 2) and mycobacterial infections (Chapter 6). Using vivid descriptions, he demonstrates vital reasons for treating these diseases, such as "each adult hookworm has the ability to fasten deeply to the inner lining of the intestine and extract blood… hookworms essentially rob growing children of their daily iron" (Chapter 2). Each chapter discusses morbidity and mortality (where known), essential features of biology and epidemiology, treatments, and public health control measures. Also included are current research, policy initiatives, economics of public health programs, and on-going global eradication efforts, including mass drug administration for lymphatic filariasis. He states, "In 2019 alone, more than 500 million people received [mass drug administration], representing almost two-thirds of the global population at risk" (Chapter 4).

The final chapters discuss current trends in NTD research and control. Although obstacles exist for validating and implementing treatments, Dr. Hotez praises pharmaceutical companies for donating albendazole and creating new facilities for NTD research (Chapter 11). This book concludes with a plea for tikkun olam, a Hebrew phrase for "repairing the world." Dr. Hotez's main objective is to inspire well-optimized interventions, such as including NTD control measures in US foreign policy, financial innovations, or government–academic–industrial enterprises devoted to NTDs (Chapter 12).

As a pioneer and global leader in NTD research and vaccine development, Dr. Hotez uses this book to highlight his unique perspective and research conducted with a large and diverse number of collaborators. As a clinician, he describes his experiences working with patients with NTDs. For example, he writes about patients who are concurrently affected by malnutrition and Chagas disease (Chapter 7).

The book could be improved by expanding discussion of the challenges to NTD elimination, such as the discovery of new paratenic hosts for dracunculiasis and ongoing effects of COVID-19. In addition, details provided for NTDs vary substantially. Almost an entire chapter is dedicated to schistosomiasis, but a single paragraph is dedicated to foodborne trematodes (Chapter 3). Additional information on the most neglected diseases would strengthen this text.

This book is useful for persons who are familiar with biology but have limited knowledge of NTDs, especially health economists, students, early-career global health researchers, and policymakers involved with NTD prevention, treatment, and elimination. Although the extent of NTDs is vast and diverse, Dr. Hotez conveys optimism throughout the text and projects a positive outlook toward ongoing research and elimination initiatives.

Estee Y. Cramer, Andrew A. Lover

Author affiliations: University of Massachusetts, Amherst, Massachusetts, USA

DOI: https://doi.org/10.3201/eid2810.220740

Address for correspondence: Estee Cramer, School of Public Health and Health Sciences, University of Massachusetts, 715 N Pleasant St, Amherst, MA 01003, USA; email: ecramer@umass.edu

Timothy Ivanov (1729–1802), *Inoculation of Catherine II and Her Son Paul against Smallpox* (c. 1770–1800). Copper, 2.5 in/64.7 mm, 6.1 oz/173 gm. Louvre Museum, Department of Art Objects of the Middle Ages, Renaissance and Modern Times. Permalink: https://collections.louvre.fr/en/ark:/53355/cl010366995

A Head of State Leading by Example

Terence Chorba, José Esparza

Before the introduction of smallpox vaccine, variolation was practiced as a preventive measure (i.e., deliberate infection with smallpox to provide immunity), most commonly by inserting or rubbing material from smallpox lesions into the skin of uninfected persons. Most persons thus infected would get a milder case of smallpox as the virus was generally introduced via the skin rather than via the respiratory route, as in the case of natural exposure. Infection occurring in this manner could still be transmitted by droplets to others who could develop a full-blown case of smallpox. Variolation developed over several centuries in many different sites including China, India, Sudan, Asia Minor, and Britain. Because variolation was reputed to have risk of inducing severe disease, variolation hesitancy existed long before the smallpox vaccine and its associated vaccine hesitancy. Inoculation with materials putatively derived from cowpox lesions (vaccination) or from horsepox lesions (equination) was a welcomed advance because it was safer and did not present the hazard of onward transmission of smallpox to the contacts of recipients.

Author affiliation: Centers for Disease Control and Prevention, Atlanta, Georgia, USA (T. Chorba); University of Maryland School of Medicine, Baltimore, Maryland, USA (J. Esparza)

DOI: https://doi.org/10.3201/eid2810.AC2810

Figure. Obverse of medal featured on the cover art. **Timothy Ivanov (1729−1802), *Bust of Catherine II*, (c. 1770−1800).** Copper, 2.5 in/64.7 mm, 6.1 oz/173 gm. Louvre Museum, Department of Art Objects of the Middle Ages, Renaissance and Modern Times. Permalink: https://collections.louvre.fr/en/ark:/53355/cl010366995 .

On the cover of this month's journal is an image of a copper medal, executed by the Russian sculptor Timothy Ivanov (1729–1802). Ivanov created several medals celebrating the contributions of Catherine II (1729–1796), also known as Catherine the Great, whose reign (1762–1796) was that of Russia's longest-ruling female leader. This medal was struck to honor those most distinguished in Russia's mass immunization efforts against smallpox at the turn of the 18th into the 19th centuries. On the obverse (Figure), a crowned right-facing bust of Catherine is surrounded by a legend that reads *Б[ОЖИЕЮ] · М[ИЛОСТЬЮ] · ЕКАТЕРИНА II ИМПЕРАТ[РИЦА] · И САМОДЕРЖ[ИЦА] · ВСЕРОСС[ИЙСКАЯ]* (By the grace of God, Catherine II, Empress and absolute ruler of all Russia). Underneath the bust is inscribed *ТИМОѲЕИ. ЇВАН[ОВЬ]* (Timothy Ivan[ov]). On the reverse (featured on the cover) is a female figure, presumably Catherine herself, holding the hand of her son, Paul Petrovich (later Tsar Paul I), encountering another female figure, perhaps Russia itself, and two small children. Representing disease, a dead hydra lies in the background below the colonnade and pediment of a classical-style building; these figures are surrounded by a legend: *СОБОЮ ПОДАЛА ПРИМѢРЪ* (She herself set the example). Beneath is the Russian lettering for "October 12 in the year 1768," the date on which Catherine was inoculated with smallpox material.

Catherine's efforts focused on the high endemicity of smallpox in Russia after the death of one of her ministers and after corresponding with Voltaire, another proponent of variolation. In 1768, Catherine recruited Thomas Dimsdale, an English physician who had published on inoculation methods and on variolation. On October 12, the empress was variolated in great secrecy. She then developed a mild case of smallpox, from which she recovered in 2 weeks. Her son, Paul, was variolated with material from one of her own smallpox pustules. However, as a precaution, in case her subjects were to hold Dimsdale accountable if she were to become gravely ill or die after variolation, Catherine had arranged for a yacht to be stationed temporarily in the Gulf of Finland to convey Dimsdale to a site out of danger, if needed. News of the success of Catherine's procedure was then widely disseminated and Dimsdale inoculated more than 140 members of her court. The response to Catherine's successful experiment was widespread uptake of the procedure elsewhere in Russia, and a burst of interest in funding hospitals and training programs and improving healthcare in general.

The use of medals as a decorative form of jewelry dates to the 4th century BCE, but from the Renaissance into the 19th century, the portrait medal flourished as a distinct art form to honor public figures. Medals have also been commonly used to commemorate public events or to reward worthy individuals. More than 20,000 medals are in the domain of medical numismatics, many of which commemorate discoveries in infectious diseases and the ends of epidemics. What sets Catherine's medal apart is its uniqueness as a tool of public health advocacy.

In 1796, English physician Edward Jenner inoculated a child with fluid extracted from human cowpox lesions. After the same child was later inoculated with material obtained from a human smallpox lesion, the child exhibited no clinical symptoms of smallpox, demonstrating that receipt of cowpox inoculation was protective against smallpox. The procedure was successful because cowpox virus and smallpox virus both belong to the same family (*Poxviridae*) and genus (*Orthopoxvirus*) of viruses; some *Orthopoxvirus* species generate cross-immunity in humans against subsequent infection with certain other *Orthopoxvirus* species. Another example of cross-immunity was observed after monkeypox, another *Orthopoxvirus* species, was identified in human populations. In the 1980s, when greater numbers of persons in Zaire (now the Democratic Republic of the Congo) had received smallpox vaccine, its prior receipt was found to confer considerable

protection in close contacts of persons with monkeypox and in reducing the severity of disease associated with monkeypox. This phenomenon has been noted in considerations of vaccine development and risk in the current monkeypox outbreak.

The work of Dimsdale in pursuing variolation, the work of Catherine II in mobilizing the support of influential nobles to overcome inoculation hesitancy, and the work of Jenner in developing the first vaccine against smallpox all took place many decades before the germ theory of disease was conceived of and demonstrated by Edwin Klebs, Louis Pasteur, Robert Koch, and their disciples. As public recognition of the science and its success increased, variolation was replaced by the less risky practice of vaccination and inoculation hesitancy decreased with the concomitant decrease in associated adverse events.

Bibliography

1. Boylston A. The origins of inoculation. J R Soc Med. 2012;105:309–13. https://doi.org/10.1258/jrsm.2012.12k044
2. Clendenning PH. Dr. Thomas Dimsdale and smallpox inoculation in Russia. J Hist Med Allied Sci. 1973;28:109–25. https://doi.org/10.1093/jhmas/XXVIII.2.109
3. Damon IK. Poxviruses. In: Knipe DM, Howley PM, editors. Fields virology. 6th ed. Philadelphia: Lippincott, Williams & Wilkins; 2013. p. 2160–84.
4. Esparza J. Early vaccine advocacy: medals honoring Edward Jenner issued during the 19th century. Vaccine. 2020;38:1450–6. https://doi.org/10.1016/j.vaccine.2019.11.077
5. Esparza J, Schrick L, Damaso CR, Nitsche A. Equination (inoculation of horsepox): an early alternative to vaccination (inoculation of cowpox) and the potential role of horsepox virus in the origin of the smallpox vaccine. Vaccine. 2017;35:7222–30. https://doi.org/10.1016/j.vaccine.2017.11.003
6. Fine PE, Jezek Z, Grab B, Dixon H. The transmission potential of monkeypox virus in human populations. Int J Epidemiol. 1988;17:643–50. https://doi.org/10.1093/ije/17.3.643
7. Griffiths J. Doctor Thomas Dimsdale, and smallpox in Russia. The variolation of the Empress Catherine the Great. Bristol Med Chir J. 1984;99:14–6.
8 Proskurina, V. Creating the empress: politics and poetry in the age of Catherine II. Boston: Academic Studies Press; 2011. p. 89 [cited 2022 Aug 2]. https://www.academicstudiespress.com/arsrossica/creating-the-empress-politics-and-poetry-in-the-age-of-catherine-ii
9. Razzell P. The conquest of smallpox. London: Caliban; 1977.
10. Ward L. The empress and the English doctor: how Catherine the Great defied a deadly virus. London: Oneworld Publications; 2022.
11. Williams G. Angel of death. Basingstoke (UK): Palgrave Macmillan, 2010.

Address for correspondence: Terence Chorba, Division of Tuberculosis Elimination, Centers for Disease Control and Prevention, 1600 Clifton Rd NE, Mailstop US12-4, Atlanta, GA 30329-4027, USA; email: tlc2@cdc.gov

EMERGING INFECTIOUS DISEASES®

Upcoming Issue

- Severe Pneumonia Caused by Corynebacterium striatum in Adults, Seoul, South Korea, 2014–2019
- Invasive Infections Caused by Lancefield Groups C/G and A Streptococci, Western Australia, Australia, 2000–2018
- Ascertaining Current Prevalence of Histoplasmosis among Persons with AIDS, Nigeria
- Age-Stratified Seroprevalence of SARS-CoV-2 Antibodies in the Pre- and Post-Vaccination Era, Japan, February 2020–March 2022
- Polyclonal Dissemination of OXA-232 Carbapenemase-Producing Klebsiella pneumoniae, France, 2013–2021
- Crimean-Congo Hemorrhagic Fever Outbreak in Refugee Settlement during COVID-19 Pandemic, Uganda, April 2021
- Rift Valley Fever Outbreak during COVID-19 Surge, Uganda, 2021
- Molecular Diagnosis of Haplorchis pumilio Eggs from Schoolchildren on Kome Island, Lake Victoria, Tanzania
- Cluster of Norovirus Genogroup IX Outbreaks in Long-Term Care Facilities, Utah, USA, 2021
- Imported Haycocknema perplexum Infection, United States
- Reinfections with Different SARS-CoV-2 Omicron Subvariants, France
- Human Parainfluenza Virus in Homeless Shelters Before and During COVID-19 Pandemic, Washington, USA
- Serologic Evidence of Human Exposure to Ehrlichiosis Agents in Japan
- SARS-CoV-2 Omicron BA.1 Challenge after Ancestral or Delta Infection in Mice
- Vaccine Effectiveness Against SARS-CoV-2 Variant P.1 in Nursing-Facility Residents, Washington State, April 2021

Complete list of articles in the November issue at

https://wwwnc.cdc.gov/eid/#issue-293

Earning CME Credit

To obtain credit, you should first read the journal article. After reading the article, you should be able to answer the following, related, multiple-choice questions. To complete the questions (with a minimum 75% passing score) and earn continuing medical education (CME) credit, please go to http://www.medscape.org/journal/eid. Credit cannot be obtained for tests completed on paper, although you may use the worksheet below to keep a record of your answers.

You must be a registered user on http://www.medscape.org. If you are not registered on http://www.medscape.org, please click on the "Register" link on the right hand side of the website.

Only one answer is correct for each question. Once you successfully answer all post-test questions, you will be able to view and/or print your certificate. For questions regarding this activity, contact the accredited provider, CME@medscape.net. For technical assistance, contact CME@medscape.net. American Medical Association's Physician's Recognition Award (AMA PRA) credits are accepted in the US as evidence of participation in CME activities. For further information on this award, please go to https://www.ama-assn.org. The AMA has determined that physicians not licensed in the US who participate in this CME activity are eligible for AMA PRA Category 1 Credits™. Through agreements that the AMA has made with agencies in some countries, AMA PRA credit may be acceptable as evidence of participation in CME activities. If you are not licensed in the US, please complete the questions online, print the AMA PRA CME credit certificate, and present it to your national medical association for review.

Article Title

Systematic Review and Meta-analysis of Foodborne Tick-Borne Encephalitis, Europe, 1980–2021

CME Questions

1. You are advising a public health department in Europe about the prevention and detection of foodborne tick-borne encephalitis (FB-TBE). On the basis of the systematic review and meta-analysis by Elbaz and colleagues, which one of the following statements about epidemiological characteristics of FB-TBE in Europe in the last 4 decades is correct?

A. Most cases were reported during fall and winter
B. Most cases were associated with ingestion of unpasteurized dairy products from cows
C. Approximately 10% of cases were vaccinated
D. Incubation period was short

2. On the basis of the systematic review and meta-analysis by Elbaz and colleagues, which one of the following statements about clinical characteristics and estimated attack rate of FB-TBE in Europe in the last 4 decades is correct?

A. Biphasic disease occurred in 49 (77%) of 64 patients for whom the disease course was described
B. Skin rash was the most prominent symptom of the first phase of disease
C. In studies specifically reporting on central nervous system (CNS) disease, the rate of probable/proven neuroinvasive disease was 26%
D. Overall clinical attack rate for outbreaks occurring after 2012 was 8%, mostly consistent among outbreaks

3. According to the systematic review and meta-analysis by Elbaz and colleagues, which one of the following statements about clinical and public health implications of FB-TBE in Europe in the last 4 decades is correct?

A. Most reported cases of FB-TBE occurred in months different from the tick season in Europe
B. Vaccination programs and public awareness campaigns have the potential to reduce the number of patients with this potentially severe CNS infection
C. TBE is currently not a reportable disease in Europe
D. Cases of FB-TBE and attack rate are unlikely to be underestimated

Earning CME Credit

To obtain credit, you should first read the journal article. After reading the article, you should be able to answer the following, related, multiple-choice questions. To complete the questions (with a minimum 75% passing score) and earn continuing medical education (CME) credit, please go to http://www.medscape.org/journal/eid. Credit cannot be obtained for tests completed on paper, although you may use the worksheet below to keep a record of your answers.

You must be a registered user on http://www.medscape.org. If you are not registered on http://www.medscape.org, please click on the "Register" link on the right hand side of the website.

Only one answer is correct for each question. Once you successfully answer all post-test questions, you will be able to view and/or print your certificate. For questions regarding this activity, contact the accredited provider, CME@medscape.net. For technical assistance, contact CME@medscape.net. American Medical Association's Physician's Recognition Award (AMA PRA) credits are accepted in the US as evidence of participation in CME activities. For further information on this award, please go to https://www.ama-assn.org. The AMA has determined that physicians not licensed in the US who participate in this CME activity are eligible for AMA PRA Category 1 Credits™. Through agreements that the AMA has made with agencies in some countries, AMA PRA credit may be acceptable as evidence of participation in CME activities. If you are not licensed in the US, please complete the questions online, print the AMA PRA CME credit certificate, and present it to your national medical association for review.

Article Title

Demographic and Socioeconomic Factors Associated with Fungal Infection Risk, United States, 2019

CME Questions

1. All the following fungal infections were more common among men vs women in the current study of hospitalized patients except:

A. Candidiasis
B. Pneumocystis
C. Coccidiomycosis
D. Cryptococcus

2. Which one of the following sociodemographic risk factors was most associated with a higher risk for aspergillosis infections in the current study?

A. Non-Hispanic White race and higher income
B. Low income and rural location
C. Hispanic ethnicity and being a woman
D. Medicare insurance and Black race

3. Which of the following types of fungal infection were more common among Black and Hispanic patients in the current study?

A. Histoplasmosis and mucormycosis
B. Coccidiomycosis and candidiasis
C. Aspergillosis and mucormycosis
D. Cryptococcus and pneumocystis

4. Which one of the following fungal infections was significantly more common among adults at age 65 years and older compared with younger adults in the current study?

A. Histoplasmosis
B. Candidiasis
C. Mucormycosis
D. Cryptococcus